SCOPE 57

PARTICLE FLUX IN THE OCEAN

Edited by
V. Ittekkot
P. Schäfer
S. Honjo
P. J. Depetris

WILEY

SCOPE 1: Global Environment Monitoring, 1971, 68 pp (out of print)
SCOPE 2: Man-Made Lakes as Modified Ecosystems, 1972, 76 pp (out of print)
SCOPE 3: Global Environmental Monitoring Systems (GEMS): Action Plan for Phase I, 1973, 132 pp (out of print)
SCOPE 4: Environmental Sciences in Developing Countries, 1974, 72 pp (out of print)

Environmental and Development, proceedings of SCOPE/UNEP Symposium on Environmental Sciences in Developing Countries, Nairobi, February 11–23, 1974, 418 pp (out of print)

SCOPE 5: Environmental Impact Assessment: Principles and Procedures, Second Edition, 1979, 208 pp (out of print)
SCOPE 6: Environmental Pollutants: Selected Analytical Methods, 1975, 277 pp (out of print)
SCOPE 7: Nitrogen, Phosphorus and Sulphur: Global Cycles, 1975, 129 pp (out of print)
SCOPE 8: Risk Assessment of Environmental Hazard, 1978, 132 pp (out of print)
SCOPE 9: Simulation Modelling of Environmental Problems, 1978, 128 pp (out of print)
SCOPE 10: Environmental Issues: 1977, 242 pp (out of print)
SCOPE 11: Shelter Provision in Developing Countries, 1978, 112 pp (out of print)
SCOPE 12: Principles of Ecotoxicology, 1978, 372 pp (out of print)
SCOPE 13: The Global Carbon Cycle, 1979, 491 pp (out of print)
SCOPE 14: Saharan Dust: Mobilization, Transport, Deposition, 1979, 320 pp (out of print)
SCOPE 15: Environmental Risk Assessment, 1980, 176 pp (out of print)
SCOPE 16: Carbon Cycle Modelling, 1981, 404 pp (out of print)
SCOPE 17: Some Perspectives of the Major Biogeochemical Cycles, 1981, 175 pp (out of print)
SCOPE 18: The Role of Fire in Northern Circumpolar Ecosystems, 1983, 344 pp (out of print)
SCOPE 19: The Global Biogeochemical Sulphur Cycle, 1983, 495 pp (out of print)
SCOPE 20: Methods for Assessing the Effects of Chemicals on Reproductive Functions, SGOMSEC 1, 1983, 568 pp (out of print)
SCOPE 21: The Major Biogeochemical Cycles and Their Interactions, 1983, 554 pp (out of print)
SCOPE 22: Effects of Pollutants at the Ecosystem Level, 1984, 460 pp (out of print)
SCOPE 23: The Role of Terrestrial Vegetation in the Global Carbon Cycle: Measurement by Remote Sensing, 1984, 272 pp (out of print)
SCOPE 24: Noise Pollution, 1986, 466 pp (out of print)
SCOPE 25: Appraisal of Tests to Predict the Environmental Behaviour of Chemicals, 1985, 400 pp (out of print)
SCOPE 26: Methods for Estimating Risks of Chemical Injury: Human and Non- Human Biota and Ecosystems, SGOMSEC 2, 1985, 712 pp (out of print)
SCOPE 27: Climate Impact Assessment: Studies of the Interaction of Climate and Society 1985, 650 pp
SCOPE 28: Environmental Consequences of Nuclear War
Volume I Physical and Atmospheric Effects, 1986, 400 pp
Volume II Ecological and Agricultural Effects, 1985, 563 pp
SCOPE 29: The Greenhouse Effect, Climatic Change and Ecosystems, 1986, 574 pp
SCOPE 30: Methods for Assessing the Effects of Mixtures of Chemicals, SGOMSEC 3, 1987, 928 pp (out of print)
SCOPE 31: Lead, Mercury, Cadmium and Arsenic in the Environment, 1987, 384 pp
SCOPE 32: Land Transformation in Agriculture, 1987, 552 pp
SCOPE 33: Nitrogen Cycling in Coastal Marine Environments, 1988, 478 pp
SCOPE 34: Practitioner's Handbook on the Modelling of Dynamic Change in Ecosystems, 1988, 196 pp
SCOPE 35: Scales and Global Change: Spatial and Temporal Variability in Biospheric and Geospheric Processes, 1988, 376 pp

SCOPE 57

Particle Flux in the Ocean

SCOPE 57

Particle Flux in the Ocean

Edited by

VENUGOPALAN ITTEKKOT
PETRA SCHÄFER
SCOPE/UNEP International Carbon Unit
Universität Hamburg, Germany

SUSUMU HONJO
Woods Hole Oceanographic Institution
Woods Hole, MA, USA

PEDRO J. DEPETRIS
Universidad Nacional de Córdoba
Córdoba, Republica Argentina

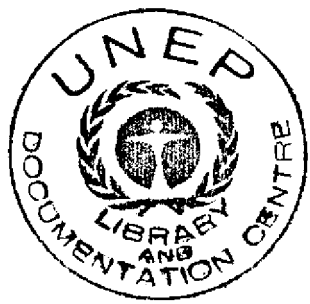

Published on behalf of the
Scientific Committee on Problems of the Environment (SCOPE)
of the International Council of Scientific Unions (ICSU),
and the United Nations Environment Programme (UNEP)

ICSU UNEP

by
JOHN WILEY & SONS
Chichester • New York • Brisbane • Toronto • Singapore

Published in 1996 by John Wiley & Sons Ltd,
Baffins Lane, Chichester,
West Sussex PO19 1UD, England

National 01243 779777
International (+44) 1243 779777
e-mail (for orders and customer service enquiries): cs-books@wiley.co.uk
Visit our Home Page on http://www.wiley.co.uk
or http://www.wiley.com

Other Wiley Editorial Offices

John Wiley & Sons, Inc., 605 Third Avenue,
New York, NY 10158-0012, USA

Jacaranda Wiley Ltd, 33 Park Road, Milton,
Queensland 4064, Australia

John Wiley & Sons (Canada) Ltd, 22 Worcester Road,
Rexdale, Ontario M9W 1L1, Canada

John Wiley & Sons (Asia) Pte Ltd, 2 Clementi Loop #02-01,
Jin Xing Distripark, Singapore 0512

British Library Cataloguing in Publication Data

A catalogue record for this book is available from the British Library

ISBN 0-471-96073-X

Produced from camera-ready copy supplied by the editors.
Printed and bound in Great Britain by Bookcraft (Bath) Ltd., Midsomer Norton, Somerset
This book is printed on acid-free paper responsibly manufactured from sustainable forestation, for which at least two trees are planted for each one used for paper production.

International Council of Scientific Unions (ICSU)
Scientific Committee on Problems of the Environment (SCOPE)

SCOPE is one of a number of committees established by a non-governmental scientific organization, the International Council of Scientific Unions (ICSU). The membership of ICSU includes representatives of 94 academies of science, 23 scientific unions and 30 scientific associates. ICSU has established 26 interdisciplinary bodies to bring together activities which include the interests of several unions.

SCOPE was established by ICSU in 1969 as one such interdisciplinary body. Its attention and scientific programme are directed to existing and potential environmental issues – either global or shared by several nations – which are in urgent need of interdisciplinary syntheses.

The mandate of SCOPE is to assemble, review, and assess the information available on human-made environmental changes and the effects of these changes on people; to assess and evaluate the methodologies of measurement of environmental parameters; to provide an intelligence service on current research; and by the recruitment of the best available scientific information and constructive thinking to establish itself as a corpus of informed advice for the benefit of centres of fundamental research and of organizations and agencies operationally engaged in studies of the environment. It acts at the interface between the science and decision-making spheres, providing advisors, policy-planners and decision-makers with analytical tools to promote sound management and policy practices.

At present, representatives of 38 member countries and 22 international unions and scientific committees participate in the work of SCOPE, with scientists from around the world contributing their time and expertise to the projects in the scientific programme. SCOPE is governed by a General Assembly, which meets every three years. Between such meetings its activities are directed by the Executive Committee.

R.E. MUNN
Editor-in-Chief
SCOPE Publications

Executive Director: V. Plocq-Fichelet

Secretariat: 51 boulevard de Montmorency
75016 Paris, France

Contents

Foreword

The global balance of water, CO_2 and radiation regulate the climate of our planet. The involved fluxes of matter and energy are conditioned by the pressure of life on Earth. Hence, it is the existence of living organisms - unicellular in the first place - to whom the Earth's surface owe its shape and habitability. Biogeochemical element cycles are a manifestation of the permanent material exchange between the living and the non-living world. There is variability in the fluxes on a continuous spectrum of space and time scales covering several orders of magnitude.

In this context, particle flux in the ocean is a unique phenomenon in that it encompasses a wealth of mechanisms that operate on the whole range of space and time scales, that involve innumerable interactions between the living and the non-living world and that provide a link between the ocean-atmosphere boundary, the deep sea and the sediments. Its relevance on the climate system ranges from the seasonal cycle of pCO_2 to the deposition of sediment on geologic time scales.

The papers in the present SCOPE volume provide information collected over several years by scientists world-wide which will eventually provide the answer. The pattern that emerges is that particle flux in the ocean responds to many geophysical parameters: Wind speeds and aerosol deposition over the oceans, nutrient levels, CO_2 levels in the mixed layer, the availability of trace elements such as iron, and volcanic emissions, all affect particle flux in the oceans. Many of the parameters have been anthropogenically perturbed. Thus the present particle flux measurements - even in open ocean areas - must no longer give natural background values. Since fertilizer, CO_2 and trace element input to the sea have increased, one is tempted to claim a particle flux increase in the ocean as well, but this would be a premature statement. Some of the basic questions therefore are: Is particle flux in the ocean on a secular steady state or anthropogenically perturbed? Would the perturbation influence the long term CO_2 uptake of the ocean? With what sign?

Several years of experience in fruitful international cooperation was gathered during the execution of projects sponsored by SCOPE and UNEP. I urge scientists to build on this and on similar experience of other global projects such as JGOFS and TOGA, which both lead to an understanding of the seasonal and interannual features and to combine forces for a joint WCRP (World Climate Research Programme)/IGBP study of the Global Ocean Euphotic Zone. This seems to me to be the right step forward.

Hartmut Grassl
Director, WCRP

Preface

For more than two decades SCOPE's Projects on Biogeochemical Cycles has synthesized scientific information of the complex and dynamic network of flows and interactions of carbon, nitrogen, sulfur and phosphorus between various compartments of the global environment. The *modus operandi* of these projects has been to ask leading scientists working on mechanisms, sources, sinks and fluxes of the various cycles to review current knowledge and to subject these literature studies to critical review in interdisciplinary workshops. After several such workshops the accumulated information is synthesized, edited and published as SCOPE reports in the Wiley series.

The publication of this volume on *Particle Flux in the Ocean* brings to a close a phase of the Global Carbon Cycle project which has concentrated on understanding the flow, interaction and fate of carbon and other nutrients from land via rivers to lakes and to deep oceans. In 1977 SCOPE, following a meeting in Ratzeburg, Germany, decided to launch a large program on various aspects of carbon cycling. Initially five Units and Subunits were established. These were:

- Carbon Unit in Stockholm (Bert Bolin) to deal with *atmospheric carbon cycle and modeling aspects*. This unit was to concentrate on interactions with other cycles and later, on increased CO_2 and other greenhouse gases. It was to have a profound effect on global environmental policy.
- Subunit in Woods Hole (George Woodwell) dealing with the *role of vegetation* in the carbon cycle;
- Subunit in Brussels (Paul Duvigneaud) dealing with *mapping issues*;
- Subunit in Germany (K. Meyer-Abich) dealing with *socioeconomic aspects*. These Subunits each produced one workshop and one book and dissolved at their own call.
- Last, but not least, was the establishment of the Carbon Unit in Hamburg (Egon Degens). It was given the task of dealing more specifically with *carbon in seas* and the important task of the coordination of the carbon network, especially the establishment of an international documentation center on the biogeochemical carbon cycle.

Thus, in December 1978 a contract was signed between SCOPE, UNEP and Hamburg University for the establishment of the SCOPE/UNEP Carbon Unit. Prof. Egon Degens headed a team of researchers initially composed of Stephan Kempe, Venugopalan Ittekkot, Alejandro Spitzy, Walter Michaelis and How Kin Wong, and attracted a large number of graduate students, visiting scholars and academics.

The first workshop held by his group in March 1979 in Hamburg dealt with *carbon in the sea*. It established priorities for further research emphasizing that

data on the sources, sinks and fluxes of carbon in major world river systems was urgently needed and beyond that *a study of carbon transport from land to sea.* In contrast to many other SCOPE projects the Carbon Unit had an active research arm and thus Egon Degens set about creating a vast network in developed and developing countries for the collection and analysis of data on these systems. During 1980–82 the first project on *carbon cycle in major world rivers* was prepared through a review of existing knowledge, establishment of main research issues and delineation of an agenda and also methodologies for a world-wide research effort. Between 1982–88 their work concentrated on *Carbon and Nutrient Transport in Major World Rivers*, this was followed in 1987–89 with *Carbon and Nutrient Transport in Lakes and Estuaries*, and finally in 1991–95 by *Particle Flux in the Ocean.*

During most of this time the Carbon Unit was directed, inspired and sustained by Egon Theodor Degens, a scientist of immense productivity and creativity. He and his research group focused on the biogeochemical cycling of elements and on anthropogenic effects in these processes. In this capacity and through the Carbon project they have trained and inspired many biogeochemists who continue this work around the world. Degens greatly enjoyed interdisciplinary meetings where ideas were traded and explored. His special interest was in creating active functioning research institutions in developing countries and this may be his greatest legacy. Unfortunately he died in 1989 just as the synthesis of the first two parts of the program were completed. His colleagues in the unit, notably Venugopalan Ittekkot and Stephan Kempe continued the project and worked to ensure that the task was completed.

The productivity of this unit has been prodigious (see Bibliography - Carbon Unit). This alone would ensure that their work was successful but the main legacy of the Hamburg C unit will be the manner in which they provided inspiration and allowed hands on experience in interdisciplinary data collection and synthesis to many young scientists from all over the world.

John W. B. Stewart
Past-President, SCOPE

Bibliography - Carbon Unit

Title	Editors	Year	ISSN/ISBN
Transport of Carbon and Minerals in Major World Rivers - 1	E. T. Degens	1982	0072-1115
Transport of Carbon and Minerals in Major World Rivers - 2	E. T. Degens, S. Kempe & H. Soliman	1983	0072-1115
Transport of Carbon and Minerals in Major World Rivers - 3	E. T. Degens S. Kempe & R. Herrera	1985	0072-1115
Biogeochemistry of Black Shales	E. T. Degens, P. A. Meyers & S. C. Brassell	1986	0072-1115
Transport of Carbon and Minerals in Major World Rivers - 4	E. T. Degens, S. Kempe & Gan Weibin	1987	0072-1115
Particle Flux in the Ocean	E. T. Degens, E. Izdar & S. Honjo	1987	0072-1115
Biogeochemistry and Distribution of Suspended Matter in the North Sea and Implications to Fisheries Biology	S. Kempe, G. Liebezeit, V. Dethlefsen & U. Harms	1988	0072-1115

Transport of Carbon and Minerals in Major World Rivers - 5	E. T. Degens, S. Kempe & A. S. Naidu	1988	0072-1115
The Sea off Mount Tambora	E. T. Degens, H. K. Wong & M. T. Zen	1992	0072-1115
Interactions of Biogeochemical Cycles in Aqueous Ecosystems	E. T. Degens, S. Kempe, A. Lein & Y. Sorokin	1992	0072-1115
Monsoon Biogeochemistry	V. Ittekkot & R. R. Nair	1993	0072-1115
Transport of Carbon and Nutrients in Lakes and Estuaries	S. Kempe, D. Eisma & E. T. Degens	1993	0072-1115
SCOPE 13 - The Global Carbon Cycle	B. Bolin, E. T. Degens, S. Kempe & P. Ketner	1979	0471 997102
SCOPE 42 - Biogeochemistry of Major World Rivers	E. T. Degens, S. Kempe & J. E. Richey	1991	0471 926760

List of Contributors

Mark A. Altabet
Chemistry Department, University of Massachusetts, Dartmouth, N. Dartmouth, MA 02747-2300, U.S.A.

Vernon L. Asper
University of Southern Mississippi, Center for Marine Science, Building 1105, Room 102, Stennis Space Center, MS 39529, U.S.A.

Michael P. Bacon
Dept. of Marine Chemistry and Geochemistry, Woods Hole Oceanographic Institution, Woods Hole, MA 02543, U.S.A.

Martin Bartsch
Institute of Biogeochemistry and Marine Chemistry, University of Hamburg, Bundesstr. 55, D-20146 Hamburg, Germany

Ulrich V. Bathmann
Alfred-Wegener-Institute for Polar and Marine Research, D-27515 Bremerhaven, Germany

Roselyne Buscail
Université de Perpignan, Laboratoire de Sédimentologie et Géochemie Marines, CNRS URA 715, 52 avenue de Villeneuve, 66860 Perpignan, France

Carlos E. V. Carvalho
Universidade Estadual do Norte Fluminense, Centro de Biociências e Biotecnologia, Lab. de Ciências Ambientais, Av. Alberto Lamego 2000, 28015-620 Campos dos Goitacazes, RJ, Brazil

Wenbin Chen
Second Institute of Oceanography, State Oceanic Administration, P.O. Box 1207, Hangzhou 310012, P.R. China

Pedro J. Depetris
F.C.E.F. y N., Universidad Nacional de Córdoba, Avda. Vélez Sársfield 299, 5000 Córdoba, Argentina

Werner G. Deuser
Dept. of Marine Chemistry and Geochemistry, Woods Hole Oceanographic Institution, Woods Hole, MA 02543, U.S.A.

Alain Dinet
Observatoire Océanologique de Banyuls, Laboratoire Arago, 66650 Banyuls/Mer, France

Xavier Durrieu de Madron
Université de Perpignan, Laboratoire de Sédimentologie et Géochemie Marines, CNRS URA 715, 52 avenue de Villeneuve, 66860 Perpignan, France

Henri Etcheber
Université de Bordeaux 1, Département de Géologie et Océanographie - URA CNRS 197, Avenue des Facultés, 33405 Talence Cédex, France

Gerhard Fischer
University of Bremen, FB Geowissenschaften, Postfach 330440, D-28334 Bremen, Germany

Birgit Haake
Institute of Biogeochemistry and Marine Chemistry, University of Hamburg, Bundesstr. 55, D-20146 Hamburg, Germany

Serge Heussner
Université de Perpignan, Laboratoire de Sédimentologie et Géochemie Marines, CNRS URA 715, 52 avenue de Villeneuve, 66860 Perpignan, France

Susumu Honjo
Dept. of Geology and Geophysics, Woods Hole Oceanographic Institution, Woods Hole, MA 02543, U.S.A.

Venugopalan Ittekkot
Institute of Biogeochemistry and Marine Chemistry, University of Hamburg, Bundesstr. 55, D-20146 Hamburg, Germany

Tim C. Jennerjahn
Institute of Biogeochemistry and Marine Chemistry, University of Hamburg, Bundesstr. 55, D-20146 Hamburg, Germany

Stephan Kempe
Geological-Paleontological Institute, Technische Hochschule Darmstadt, Schnittspahnstr. 9, D-64287 Darmstadt, Germany

Heiko Knaack
Institute of Biogeochemistry and Marine Chemistry, University of Hamburg, Bundesstr. 55, D-20146 Hamburg, Germany

Jean Christophe Miquel
AIEA, Marine Environment Laboratory, BP 800MC, 98012 Monaco

André Monaco
Université de Perpignan, Laboratoire de Sédimentologie et Géochemie Marines, CNRS URA 715, 52 avenue de Villeneuve, 66860 Perpignan, France

R. R. Nair
National Institute of Oceanography, Dona Paula, Goa 403004, India

Joseph M. Prospero
University of Miami, Rosenstiel School of Marine and Atmospheric Science, 4600 Rickenbacker Causeway, Miami, FL 33149-1098, U.S.A.

V. Ramaswamy
National Institute of Oceanography, Dona Paula, Goa 403004, India

Thorsten Reemtsma
Institute of Biogeochemistry and Marine Chemistry, University of Hamburg, Bundesstr. 55, D-20146 Hamburg, Germany

Tim Rixen
Institute of Biogeochemistry and Marine Chemistry, University of Hamburg, Bundesstr. 55, D-20146 Hamburg, Germany

Petra Schäfer
Institute of Biogeochemistry and Marine Chemistry, University of Hamburg, Bundesstr. 55, D-20146 Hamburg, Germany

Martina Schaumburg
Institute of Biogeochemistry and Marine Chemistry, University of Hamburg, Bundesstr. 55, D-20146 Hamburg, Germany

Peter Schlüssel
University of Colorado at Boulder, Colorado Center for Astrodynamics Research, Boulder, CO 80309-0431, U.S.A.

Jörg Tiemann
Institute of Biogeochemistry and Marine Chemistry, University of Hamburg, Bundesstr. 55, D-20146 Hamburg, Germany

Yubo Wang
Institute of Biogeochemistry and Marine Chemistry, University of Hamburg, Bundesstr. 55, D-20146 Hamburg, Germany

Olivier Weber
Université de Bordeaux I, Départment de Géologie et Océanographie, CNRS URA 197, Avenue des Facultés, 33405 Talence, France

Gerold Wefer
University of Bremen, FB Geowissenschaften, Postfach 330440, D-28334 Bremen, Germany

Martin G. Wiesner
Institute of Biogeochemistry and Marine Chemistry, University of Hamburg, Bundesstr. 55, D-20146 Hamburg, Germany

How Kin Wong
Institute of Biogeochemistry and Marine Chemistry, University of Hamburg, Bundesstr. 55, D-20146 Hamburg, Germany

Lianfu Zheng
Second Institute of Oceanography, State Oceanic Administration, P.O. Box 1207, Hangzhou 310012, P.R. China

1 Particle Flux in the Ocean: Introduction

V. ITTEKKOT

1.1 BACKGROUND

For more than a decade the SCOPE/UNEP Carbon Unit at the Hamburg University has initiated and coordinated projects on global carbon cycle. The three projects conducted by the Unit are: *Carbon and Mineral Transport in Major World Rivers, Carbon and Nutrient Cycling in Lakes and Estuaries* and *Particle Flux in the Ocean*. A large number of scientists from developing, threshold and developed countries actively participated in the projects. Within the framework of these projects ten international workshops were organized by the Unit in: Hamburg, Germany (1982); Assuit, Egypt (1983); Caracas, Venezuela (1984), Tianjin, People's Republic of China (1985); Fairbanks, USA (1986), Texel, The Netherlands (1987), Irkutsk, Russia (1988), Istanbul, Turkey (1989), Goa, India (1991) and Hamburg, Germany (1993). These workshops provided a state of the art assessment in the respective fields and formulated future research needs. The proceedings of these workshops have been published in a series of special monographs from the Hamburg Carbon Unit. *SCOPE Report 42: Biogeochemistry of Major World Rivers* provides a summary of information collected within the framework of the first two projects mentioned above.

The present volume is an outcome of the final workshop on *Particle Flux in the Ocean*, which was held in Hamburg, Germany in September 1993. Scientists from several countries, including Argentina, Brazil, Chile, the People's Republic of China, France, Germany, India, Japan, Romania, Russia, Turkey, Ukraine and the USA, participated in the Workshop to review progress made in the field. The following is a brief introduction to the role of particle flux in the marine carbon cycle.

Particle Flux in the Ocean.
Edited by V. Ittekkot, P. Schäfer, S. Honjo and P. J. Depetris

1.2 PARTICLE FLUX AND THE MARINE CARBON CYCLE

The production of biogenic particles in the upper ocean and their fractional removal to the deep sea determines the distribution of the biogeochemical elements in seawater. The rain of particles from the sea surface is the source of sediments accumulating at the ocean floor and fuels benthic life in the deep sea. Their fractional decay and remineralization as they sink through the water column controls - together with water circulation - the balances of oxygen, nutrients and other trace constituents. The settling particles carry with them indicators of biogeochemical processes at the ocean surface whose distribution in sediments can hence be used to reconstruct palaeoenvironmental conditions.

With regard to the global carbon cycle, particle flux in the ocean is one mechanism for the transfer of carbon derived from atmospheric CO_2 to the deep sea. The two relevant biological processes in this context ("the biological pump") are the formation of organic matter during photosynthesis (organic carbon pump) and the formation of carbonate during calcification (carbonate pump) (Heinze et al., 1991). These processes affect the surface ocean CO_2-balance in different ways. Photosynthesis consumes CO_2, calcification releases CO_2 (it is the dissolution of carbonate by CO_2 that effectively takes up CO_2 in the long run). Thus, changes in the initial production ratio of calcium carbonate to organic carbon can be expected to effect changes in atmospheric CO_2 (Berger and Keir, 1984). This ratio is controlled by the upper ocean community structure; e.g., the relative abundances of diatoms and coccolithophorids, which are the major respresentatives of primary producers in the ocean.

The efficiency of the marine biological pump does not depend on the gross uptake of atmospheric CO_2 via the formation of organic matter in the upper ocean (much of the organic matter is quickly mineralized back to CO_2 within the surface layers, which exchange gas with the atmosphere) but on the net export to the ocean's interior which is isolated from the atmosphere. It is only this fraction of organic matter that ultimately removes CO_2 from the atmosphere.

The importance of organic matter degradation within the water column in the modern ocean is also evident from a comparison of the carbon inputs at the ocean surface (Figure 1.1) with the amount of organic carbon being buried in the underlying sediments (Figure 1.2). The ocean's water volume and its carbon input at the surface are grouped according to depth intervals in Figure 1.1.

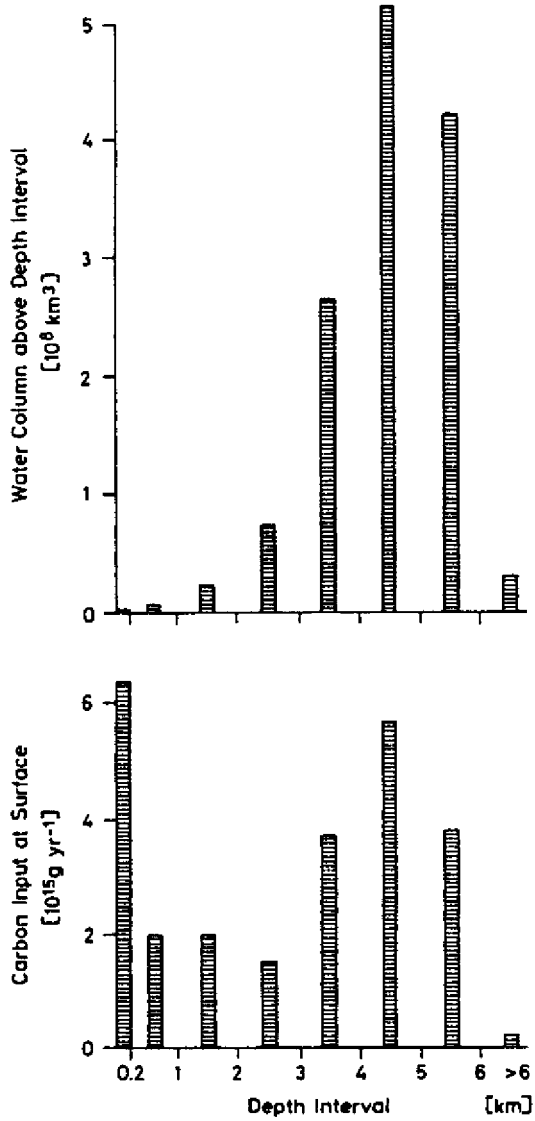

Figure 1.1 Water volume distribution above the various depth intervals in the modern ocean (top) and their respective carbon inputs at the surface (bottom) (after Deuser, 1979).

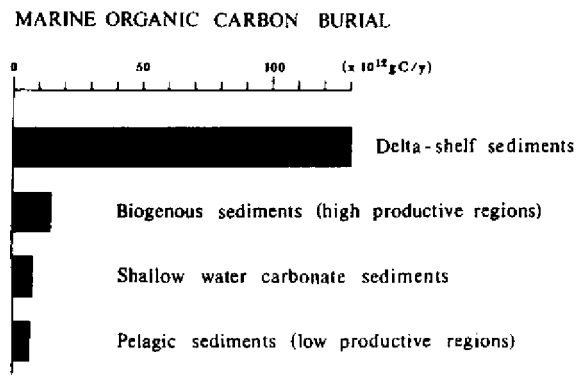

Figure 1.2 Distribution of organic carbon burial in the modern ocean according to sediment types (after Berner, 1982). Total burial rates 157 x 10^{12} g y^{-1} of which 85% occurs in deltaic and shelf sediments. Note that biogenic sediments underlying highly productive areas contribute less than 10%.

It is of note that the shallow regions (< 200 m) with their relatively small volumes of water receive comparatively large amount of carbon input at the surface. Also, oceanic regions with water depths > 3000 m obtain significant quantities of carbon input at the surface. Surprisingly, in modern marine sediments, 83% of the annual carbon burial (total burial 157 x 10^{12} g y^{-1}) occurs in deltaic-shelf sediments (Figure 1.2), and no more than 4% is buried in the deep-sea sediments. Apparently, organic matter recycling within the water column is a major process in the open ocean environment, effectively limiting the quantity of carbon being fixed in deep-sea sediments. The similar quantities of refractory organic carbon brought by the rivers to the sea (e.g., Ittekkot, 1988) and of organic carbon buried in modern marine sediments annually also suggest that the bulk of carbon fixed during marine photosynthesis is recycled within the water column, leaving very little for burial in sediments. The vertical distribution of this recycled carbon flux determines how much of the photosynthetically fixed CO_2 remains in exchange with the atmosphere on a given time scale, in a given water circulation regime. It is on this aspect of the global carbon cycle that particle flux studies provide invaluable information.

Vertical particle flux in the ocean is mediated by biological processes occuring in the upper ocean (Figure 1.3). Thus, aeolian and riverine particles entering the oceans are rapidly removed from the upper ocean together with biogenic particles produced *in situ* (e.g., Honjo, 1982; Deuser et al., 1983). Biological processes mediate in the formation of large particle aggregates such as fecal pellets, macroaggregates and marine snow which subsequently act as vehicles for particle

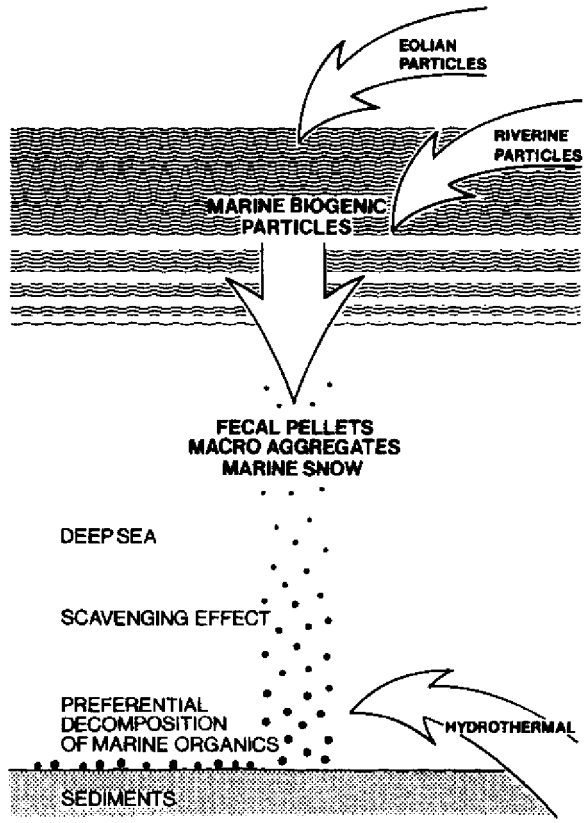

Figure 1.3 A scheme of particle sources and vertical transport in the ocean (from Ittekkot and Haake, 1990).

transport. During descent through the water column and at the seafloor the metabolizable fraction becomes decomposed leaving the refractory fraction to accumulate in sediments alongwith biogenic hard parts.

The present volume contains a series of review articles and case studies on these and other aspects of particle flux in the ocean contributed by scientists actively involved in research in the field. They cover results from particle flux experiments using time-series sediment traps in the Nordic Seas, the Northern and Equatorial Atlantic, the Southern Ocean, the Mediterranean, the Black Sea, the Arabian Sea, the Bay of Bengal, the South China Sea and the Pacific Ocean. They include results from some of the longest running ocean particle flux studies in the world. Included in the report is also a contribution on particle flux in Lake Baikal, the largest fresh water lake in the world. Large lakes and oceans have many traits in

common, and also the controlling factors of vertical particle flux are similar. These contributions show the considerable effort being put in by groups of scientists in various countries on ocean particle studies and we hope that they will add significantly to our understanding of processes controlling material cycling in the ocean.

1.3 ACKNOWLEDGMENTS

The transfer of know-how and the training of young scientists from developing countries have been landmarks of the three projects undertaken by the Carbon Unit in Hamburg over the last decade. Through its activities the Unit has been able to establish an international network which has served to catalyze research in the field of biogeochemistry. Interested groups in developing countries were provided with information and the necessary training to initiate national programs in the field. The United Nation's Environment Programme (UNEP) and SCOPE have jointly encouraged and generously supported these activities throughout the years and we express our sincere gratitude to both organizations. We gratefully acknowledge the support by the national SCOPE Committees, universities and research organizations in the various countries. Dr. E. Duursma provided a review of the manuscript on behalf of SCOPE. The comments and suggestions by Dr. J. Thornton on behalf of UNEP helped considerably in improving the manuscript. We thank Mrs. Veronique Plocq-Fichelet and her team at the SCOPE Secretariat, Paris, who have been a constant source of encouragement and help throughout the years.

1.4 REFERENCES

Berger, W. H. and R. S. Keir (1984) "Glacial-Holocene changes in atmospheric CO_2 and the deep-sea record", in J. E. Hansen and T. Takahashi (eds) *Climate Processes and Climate Sensitivity*, Geophys. Monogr., 29, Am. Geophys. Union, Washington, 337-351.

Berner, R. A. (1982) "Burial of organic carbon and pyrite sulfur in the modern ocean: Its geochemical and environmental significance", *Am. J. Sci.*, **282**, 451–473.

Deuser, W. G. (1979) "Marine biota, nearshore sediments, and the global carbon balance", *Org. Geochem.*", **1**, 243–247.

Deuser, W. G., P. G. Brewer, T. D. Jickells and R. F. Commeau (1983) "Biological control of the removal of abiogenic particles from the surface ocean", *Science*, **219**, 388–391.

Heinze, C., E. Maier-Reimer and K. Winn (1991) "Glacial pCO_2 reduction by the world ocean: Experiments with the Hamburg Carbon Cycle model", *Paleoceanography*, **6**, 395–430.

Honjo, S. (1982) "Seasonality of biogenic and lithogenic fluxes in the Panama Basin", *Science*, **218**, 883–884.

Ittekkot, V. (1988) "Global trends in the nature of organic matter in river suspensions", *Nature*, **332**, 436–438.

Ittekkot, V. and B. Haake (1990) "The terrestrial link in the removal of organic carbon in the sea", in V. Ittekkot, S. Kempe, W. Michaelis and A. Spitzy (eds) *Facets of Modern Biogeochemistry*, Springer-Verlag, Heidelberg, 318–325.

2 Remote Sensing of Parameters Relevant to the Particle Flux in the Ocean Using Meteorological Satellites

PETER SCHLÜSSEL

2.1 INTRODUCTION

Knowledge of meteorological oceanographic parameters is crucial for the interpretation of particle flux measurements in the oceans. *In situ* measurements, however, are sparse over the sea and simply not available in large areas like the southern oceans away from ship routes. Satellite-borne Earth observation instruments are the only tools capable of acquiring information about environmental parameters in those areas. Although there are no satellites in orbit so far which are dedicated to particle flux studies, operational meteorological and experimental oceanographic satellites can be used to derive a variety of relevant parameters over the global ocean. Furthermore, the satellite measurements have advantages over the common *in situ* observations in that they provide continuous, reliable, and convenient information.

The Earth-observation instruments can be broadly classified in two groups. Radars and lidars measure actively by emitting own radiation into the atmosphere which is attenuated and backscattered to the satellite. The modified signal has to be interpreted with respect to geophysical parameters. Radiometers passively measure the radiation that is emitted from the Earth-atmosphere system in the infrared and microwave spectral domains or radiation emitted from the Sun at ultraviolet, visible and near-infrared wavelengths which has interacted with the Earth's surface and atmosphere. Depending on the geophysical parameter of interest one or other method has to be utilized. For example, sea surface temperatures are measured passively at infrared wavelengths near 3.7 or 11 μm where the clear atmosphere is transparent and the sea surface has a high emissivity. Otherwise, the surface wind speed over sea is measured by observing the wind-induced surface roughness which alters the surface reflectivity. This is best done at centimeter wavelengths with both, passive and active instruments.

Particle Flux in the Ocean
Edited by V. Ittekkot, P. Schäfer, S. Honjo and P. J. Depetris

The measurement of this surface parameter also requires the use of spectral regions where the radiation passes the atmosphere without strong attenuation. These regions are called atmospheric windows.

The interpretation of radiation measurements obtained from satellite observations requires the inversion of integral equations, hence, the development of retrieval methods which are outlined in Figure 2.1. Unless a retrieval technique for use with single radiometers or synergistic combinations of several instruments is available the measurements are rather useless and the extracted information will remain qualitative only.

Operational meteorological satellites currently flying are the polar orbiting satellites of the NOAA (National Oceanographic and Atmospheric Administration) and the DMSP (Defense Meteorological Satellite Program) series as well as geostationary satellites like METEOSAT, GOES, GMS and INSAT. While the latter carry imaging instruments scanning the visible disk of the Earth every 30 minutes the instruments on polar orbiters scan the Earth's surface and the

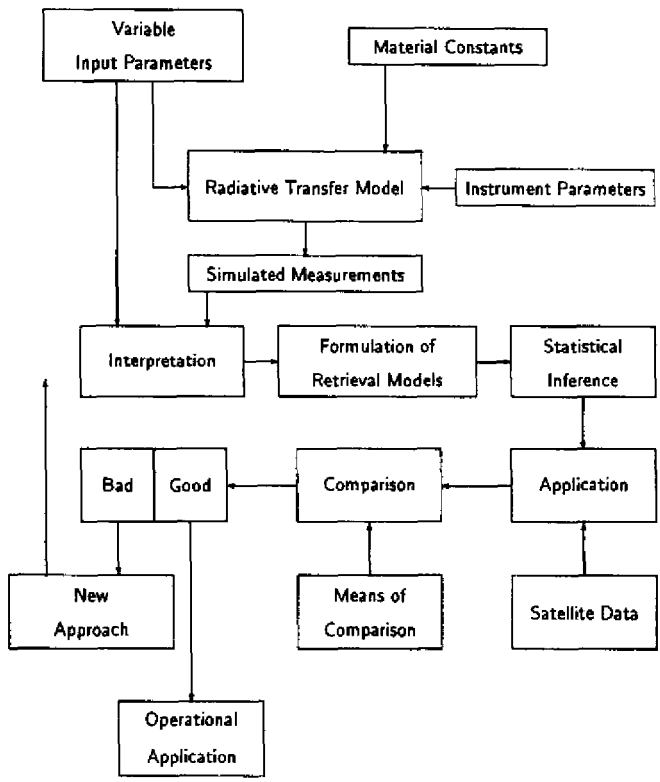

Figure 2.1 Development of a retrieval scheme.

atmosphere on cross-track swaths of 1400 to 3000 km width. Sunsynchronous satellites allow the measurement of most areas two times per day as shown in Figure 2.2 for the Special Sensor Microwave/Imager (SSM/I) which is flown on the DMSP satellites since July 1987. Only 85% of the Earth is seen every day, the remaining diamond shaped areas are monitored within the following three days.

2.2 METEOROLOGICAL PARAMETERS INFLUENCING THE ENVIRONMENT OF PHYTOPLANKTON BLOOMS

The origin of more than 80% of particulate matter reaching the deep ocean is due to phytoplankton blooms. The meteorological parameters influencing the environment of phytoplankton blooms are sea surface temperature (SST), cloud cover, sea ice thickness and distribution, as well as the precipitation.

Sea surface temperature is an indicator of upwelling, entrainment or advection of cooler waters which often are accompanied by higher concentrations of nutrients. Infrared sensors like the AVHRR (Advanced Very High Resolution Radiometer) and the ATSR (Along Track Scanning Radiometer) allow the best retrieval of SST in cloud-free areas utilizing measurements at 3.7, 11, and 12 μm. Observations at two or three wavelengths are combined in order to correct for atmospheric attenuation due to water vapor and aerosols (e.g., McClain et al., 1983; Llewellyn-Jones et al.; 1984, Schlüssel et al., 1987; Minnett, 1990). These methods reach accuracies of about 1 K. More recently, the SST retrieval from AVHRR measurements has been amended by the inclusion of water-vapor information from SSM/I observations in order to allow for higher accuracies close to 0.5 K (Emery et al., 1994). Further improvements of SST measurements from space have been demonstrated with the ATSR (flying on the ERS-1 satellite) which contains actively cooled detectors providing measurements with less noise than the AVHRR (0.02 K instead of 0.12 K at 11 μm). Additionally, a two-angle view at the same surface elements further enhances the correction of atmospheric effects and thus the measurement errors. Current SST retrievals are believed to be better than 0.5 K (Barton et al., 1992). Unfortunately, when using infrared radiometry the surface temperature retrievals are restricted to cloud-free areas only. Depending on the actual cloud cover a global mapping of SST is possible within one to four weeks.

The cloud cover and cloud thickness control the solar illumination of the ocean. Various methods utilizing satellite imagery in the infrared and visible spectral domains have been developed. A summary and intercomparison was done in the frame of the International Satellite Cloud Climatology Project (ISCCP) as described by Rossow et al. (1985). As a result a unified cloud analysis algorithm has been retrieved from this project and applied to global satellite imagery from geostationary and polar orbiting spacecraft. Figure 2.3 shows the zonal

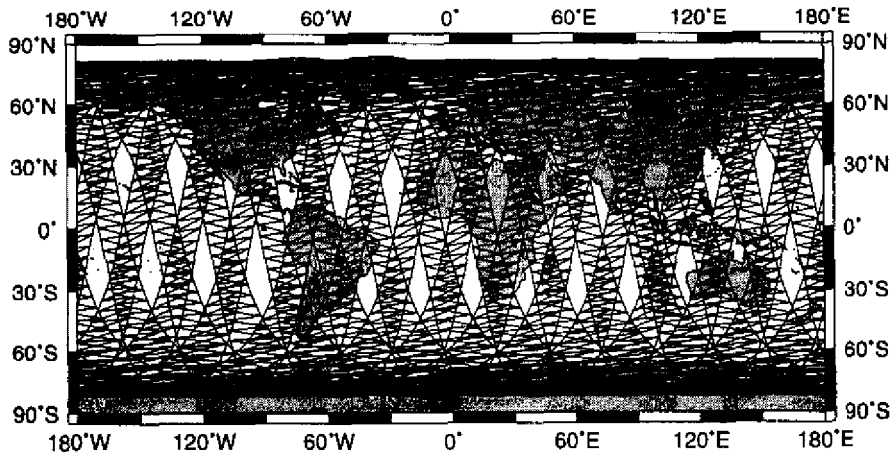

Figure 2.2 Daily coverage of the Earth by the Special Sensor Microwave/Imager.

distribution of average cloud frequencies and optical depths of various cloud types over oceans in 1990 as calculated from the ISCCP data set. The knowledge of these quantities is necessary in order to compute the solar radiation budget at the sea surface which determines the photosynthetically active radiation (PAR) and, hence, the primary productivity in the ocean. Using the ISCCP data together with a retrieval model based on radiative transfer theory Pinker and Laszlo (1992a, b) derive the downwelling solar irradiance at the surface and from that the photosynthetically active radiation. Their results have been mapped globally and presented as time series demonstrating the seasonal and interannual variability. A validation with ground-based pyranometric measurements shows the good performance of their satellite retrievals (Pinker et al., 1993).

Sea ice strongly influences the solar radiation field that is transmitted into the ocean. The photosynthetically active radiation that is available in the upper ocean is determined by the sea ice extent, the type and the thickness of the sea ice. Microwave radiometry is the most valuable tool for the detection and classification of sea ice. It is largely independent from cloud coverage. By partly penetrating into the ice the microwaves allow discrimination between young, first year, and multi-year sea ice (e.g., Comiso, 1986; Cavalieri et al., 1991). The sea ice fields derived from SSM/I measurements agree with aircraft observations within 15%. New methods go even further in classifying new sea ice also using SSM/I observations (Steffen and Schweiger, 1991; Martin and Taurat, 1992). The distribution of different sea ice types is shown in Plate 2.1 for the Arctic and Antarctic areas on *February 1, 1988, and August, 1 1988*, respectively, as derived from SSM/I vertically polarized measurements at 19.35 and 85.5 Ghz. Measurements from a single satellite have been used to map the sea ice. Only small areas could not be

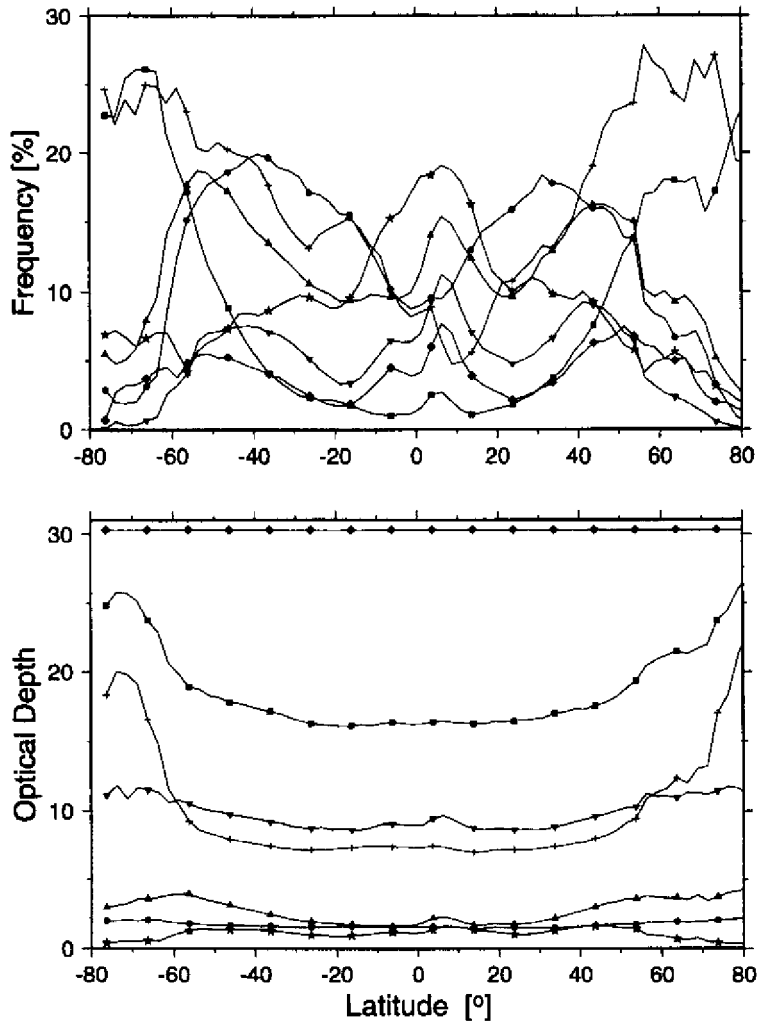

Figure 2.3 Zonal distribution of cloud types (top) and optical depths (bottom) over oceans as derived from ISCCP-C1 data; (●) cumulus, (+) stratus, (▲) altocumulus, (■) nimbostratus, (★) cirrus, (▼) cirrostratus, and (◆) deep convective clouds.

covered because of precipitation or wet ice conditions. A disadvantage of the passive microwave methods is their rather coarse horizontal resolution of a few tens of kilometers. Higher resolution can be achieved with infrared and visible imagery in cloud-free areas as obtained from AVHRR and the Landsat-Thematic Mapper, with resolutions of 1–5 km and 30–100 m respectively (Emery et al.,

1991b; Steffen and Schweiger, 1991; Martin, 1993). SAR (Synthetic Aperture Radar) measurements allow an all-weather monitoring of sea ice with a resolution of 10 m. However, the coverage of large areas is hardly achieved by SAR or the Thematic Mapper because of the narrow swath widths of about 100 km and 185 km, respectively, compared with the separation of adjacent orbits of up to 1400 km in polar regions.

The interaction of wind and oceanic currents with the sea ice can cause strong migrations of the marginal ice zone and alter the sea ice coverage which is reflected in the plankton and particle concentrations in the near surface water. Dense phytoplankton blooms have been found below sea ice where they were not grown and clear, almost phytoplankton-free water has been observed in the open water adjacent to the ice edge where one would have expected phytoplankton blooms. Tracking of sea ice movement with the aid of successive AVHRR images allows identification of areas with such unexpected distributions of phytoplankton (Emery et al., 1986, Emery et al., 1991a).

Recently, Garrity (1992) has shown that utilization of microwave radiometry allows characterization of the depth, wetness, and stratification of the snow pack on floating ice. This information also could be used for computation of the radiation field below the sea ice.

Precipitation over the ocean can drastically change the salinity of the near surface water body within short time periods. Thus, precipitation can directly alter the environment of phytoplankton. Satellite measurements of precipitation reaching the surface, however, are largely indirect. Only during light rain is the microwave radiation interacting with rain drops transmitted to the top of the atmosphere (Wilheit et al., 1977). For moderate and heavy precipitation one has to measure the rain conditions at higher atmospheric levels or to observe the brightness of clouds in order to draw conclusions on the surface rain rates (Spencer et al., 1989). The latter technique is used at infrared wavelengths, too, as demonstrated by Arkin and Meisner (1987). Methods utilizing passive microwave measurements combining direct and indirect observations have been developed and successfully applied to SSM/I measurements over the global ocean (Bauer and Schlüssel, 1993). Plate 2.2 shows the monthly average rainfall over the sea for five months in the time period August 1987 through August 1988 as derived from SSM/I measurements. The strong seasonal and regional variation covers a range from no precipitation in subtropical areas to maxima greater than 1000 mm in the tropical convergence zone. The images also reveal the strong interannual variation. In August 1987 the tropical rainfall was higher than in August 1988 while the precipitation in the storm tracks in the middle latitudes of both hemispheres was less pronounced. This was likely to be an effect of the El Niño 1987. The application shown demonstrates that the use of climatological mean values instead of actual observations of precipitation certainly would lead to wrong estimates of local rainfall.

2.3 QUANTITIES DRIVING THE VERTICAL EXCHANGE IN THE UPPER OCEAN

The wind dynamically couples the atmosphere to the ocean. While acting on the sea surface the wind transfers momentum from the atmosphere to the ocean which leads to the formation of oceanic currents and to vertical mixing of the near-surface water. The vertical mixing determines the transport of particles from the upper waters to the deep sea. Remote sensing of the near-surface wind speed is achieved by observing the emissivity changes or variations of the radar backscatter of the wind-roughened sea surface. A variety of retrieval schemes have been developed for the use with passive and active satellite measurements. (e.g., Miller et al., 1982; Wentz et al., 1986; Guymer et al., 1981; Wentz et al., 1984). So far the techniques rely on semi-empirical approaches relating wind speed to emissivity changes (Pandey and Kakar, 1982). Theories based on first principles which can describe the relationships between wind and surface optical parameters are still premature for use with remote sensing methods.

The flight of the SSM/I, a well calibrated in-flight microwave radiometer, allowed for the first time retrieval of surface wind speeds with an accuracy better than 2 m s^{-1} when compared to co-located in-situ measurements (Goodberlet et al., 1989; Schlüssel and Luthardt, 1991). Monthly mean oceanic wind speeds derived from SSM/I measurements are shown in Plate 2.3 for five months as in Plate 2.2. Highest values of wind speed are found, as expected, in the Southern Ocean with means up to 15 m s^{-1}. A strong variability, related to the monsoon circulation, is seen in the northern Indian Ocean with lowest values near 1 m s^{-1} in November and February and highest wind speeds in the Somali or Findlater Jet showing wind speeds greater than 10 m s^{-1} in August 1988. According to Figure 2.2 the wind-speed fields are available almost daily in most regions which allows not only for the computation of monthly average fields but also for detailed process studies.

The existence of sea ice strongly affects the momentum exchange at the sea surface and, hence, the vertical mixing. Knowledge of the ice type and extent is necessary to delineate areas with decreased mixing in order to study details of the oceanic particle flux.

Precipitation also might affect the vertical mixing in the upper ocean in two ways. The momentum transferred by falling rain drops impinging on the surface causes vertical mixing of the uppermost layer of the ocean (Guymer et al., 1981). On the other hand, fresh rain water is less dense than sea water, hence, the precipitation leads to a stabilized upper ocean with reduced vertical mixing (Ostapoff et al., 1973). While the density stratification can cover the uppermost ten meters after a heavy rainfall, that lasts for several hours, it seems that this effect is more important than the mixing induced by the impact of drops on the sea surface. Therefore, the joint observation of precipitation and surface wind

speed with passive microwave measurements is indicated when the particle flux in the uppermost ocean is studied.

2.4 PARAMETERS RELEVANT TO TRANSPORT AND DEPOSITION OF LITHOGENIC PARTICLES

The long-range transport of lithogenic particles from the continents to the ocean is effected by the three-dimensional atmospheric wind-vector field and its temporal evolution which determines the trajectories along which the particles are carried from their originating areas. Currently, there are no satellite instruments available which allow the complete measurement of the atmospheric wind field. Tracking of clouds and water-vapor structures in successive images from geostationary satellites allows the determination of wind vectors at single levels (Leese et al., 1971; Endlich and Wolf, 1981; Eigenwillig and Fischer, 1982). These satellite winds are useful in areas where no other measurements are available, but, they do not give a complete coverage. The thermal wind which is the vertical variation of the geostrophic wind due to horizontal temperature gradients can be obtained from temperature profiles retrieved from the TIROS (Television Infra Red Observational Satellite) Operational Vertical Sounder (TOVS) which is flown operationally on the NOAA spacecraft. Chedin et al. (1985) have demonstrated the retrieval of three-dimensional fields of the thermal wind from such temperature soundings. Although the thermal wind is the major component of the wind field in the upper troposphere an absolute wind field at an arbitrary level has to be known in order to calculate the complete wind field. This can currently only be achieved with the help of other observations and numerical weather forecast models.

The deposition of lithogenic particles on to the sea surface is most effectively done by precipitation processes. Thus, the observation of rain events must accompany the study of trajectories carrying the aerosols.

2.5 FUTURE PERSPECTIVES

Observations from space provide extensive global data that can be used to study meteorological parameters relevant to the oceanic particle flux. These data are the only source of information about large parts of the global atmosphere and ocean. Interdisciplinary research within the earth sciences has begun to exploit these data in order to understand coupled processes among atmosphere, ocean and cryosphere. Within the next decade the current operational Earth observation satellites will be amended and replaced by a series of orbiters carrying advanced as well as newly developed instruments which inter alia will be of great benefit for

particle flux studies. An overview has been given by Dozier (1994). Obviously, the key instruments related to oceanic particle flux will be those directly dedicated to the marine biogeochemistry. However, instruments observing the atmosphere and the sea surface are complementary to those and the synergistic use of all data will certainly provide the most valuable insight.

2.6 REFERENCES

Arkin, P. A. and B. N. Meisner (1987) "The relationship between large-scale convective rainfall and cold cloud cover over the western hemisphere during 1982–1984", *Mon. Wea. Rev.*, **115**, 51–74.

Barton, I. J., A. M. Zavody, A. J. Prata, D. T. Llewellyn-Jones, P. Bailey, R. P. Cechet, M. R. Gorman, P. Kent, D. J. Lee, C. T. Mutlow and C. S. Nilsson (1992) "Intercomparison of satellite-derived sea surface temperatures", Proceedings of the Central Symposium of the 'International Space Year' Conference, held in Munich, Germany, 30 March - 4 April 1992, ESA SP-341, 367–372.

Bauer, P. and P. Schlüssel (1993) "Rainfall, total water, ice water and water vapour over sea from polarized microwave simulations and SSM/I data", *J. Geophys. Res.*, **98**, 20737–20760.

Cavalieri, D. J., J. P. Crawford, M. R. Drinkwater, D. T. Eppler, L. D. Farmer, R. R. Jentz and C. C. Wackerman (1991) "Aircraft active and passive microwave validation of sea ice concentration from the Defense Meteorological Satellite Program Special Sensor Microwave Imager", *J. Geophys. Res.*, **96**, 21989–22008.

Chedin, A., N. A. Scott, C. Wahiche and P. Moulinier (1985) "The improved initialization inversion method: A high resolution physical method for temperature retrievals from satellites of the TIROS-N series", *J. Climate Appl. Meteorol.*, **24**, 128–143.

Comiso, J. C. (1986) "Characteristics of Arctic winter sea ice from satellite multispectral microwave observations", *J. Geophys. Res.*, **91**, 975–995.

Dozier, J. (1994) "Planned EOS observations of the land, ocean and atmosphere", *Atmos. Res.*, **31**, 329–357.

Eigenwillig, N. and H. Fischer (1982) "Determination of midtropospheric wind vectors by tracking pure water vapor structures in METEOSAT water vapor image sequences", *Bull. Am. Meteorol. Soc.*, **63**, 44–58.

Emery, W. J., C. Fowler, J. Hawkins and R. H. Preller (1991a) "Fram Strait satellite image-derived ice motions", *J. Geophys. Res.*, **96**, 4751–4768.

Emery, W. J., M. Radebaugh, C. W. Fowler, D. J. Cavalieri and K. Steffen (1991b) "A comparison of sea ice parameters computed from Advanced Very High Resolution Radiometer and Landsat satellite imagery and from airborne passive microwave radiometry", *J. Geophys. Res.*, **96**, 22075–22085.

Emery, W. J., A. C. Thomas, M. J. Collins, W. R. Crawford and D. L. Mackas (1986) "An objective method for computing advective surface velocities from sequential infrared satellite images", *J. Geophys. Res.*, **91**, 12865–12878.

Emery, W. J., Y. Yu, G. A. Wick, P. Schlüssel and R. Reynolds (1994) "Improving satellite infrared sea surface temperature estimates by including independent water-vapor observations", *J. Geophys. Res.*, **99**, 5219–5236.

Endlich, R. M. and D. Wolf (1981) "Automatic cloud tracking applied to GOES and Meteosat applications", *J. Appl. Meteorol.*, **20**, 309–319.

Garrity, C. (1992) "Characterization of snow on floating ice and case studies of brightness temperature changes during the onset of melt", in *Microwave Remote Sensing of Sea Ice*, Geophys. Monogr., 68, American Geophysical Union, 313–328.

Goodberlet, M. A., C. T Swift and J. C. Wilkerson (1989) "Remote sensing of ocean surface winds with the Special Sensor Microwave/Imager", *J. Geophys. Res.*, **94**, 14547–14555.

Guymer, T. H., J. H. Businger, W. L. Jones and R. H. Stewart (1981) "Anomalous wind estimates from the Seasat scatterometer", *Nature*, **294**, 735–737.

Leese, J., C. S. Novak and B. B. Clark (1971) "An automated technique for obtaining cloud motion from geosynchronous satellite data using cross correlation", *J. Appl. Meteorol.*, **10**, 118–132.

Llewellyn-Jones, D. T., P. J. Minnett, R. W. Saunders and A. M. Zavody (1984) "Satellite multichannel infrared measurement of sea surface temperature of the N.E. Atlantic Ocean using AVHRR/2", *Quart. J. Roy. Meteorol. Soc.*, **110**, 613–631.

Martin, T. (1993) "Multispektrale Mehreisklassifikation mit passiven Satelliten-radiometern", *Berichte aus dem Zentrum für Meeres- und Klimaforschung, Universität Hamburg*, **A7**, 110 pp.

Martin, T. and D. Taurat (1992) "Detecting new ice in the Arctic from multispectral satellite data", Proceedings of the Central Symposium of the 'International Space Year' Conference, held in Munich, Germany, 30 March - 4 April 1992, ESA SP-341, July 1992, 135–140.

McClain, E. P., W. G. Pichel, C. C. Walton, Z. Ahmad and J. Sutton (1983) "Multi-channel improvements to satellite derived global sea surface temperatures", *Adv. Space Res.*, **2**, 43–47.

Miller, J. R., J. E. Geyser, A. T. C. Chang and T. T. Wilheit, Jr. (1982) "Observations of oceanic surface-wind fields from the Nimbus-7 microwave radiometer", *IEEE Trans. Geosci. and Remote Sens.*, 549–554.

Minnett, P. J. (1990) "The regional optimization of infrared measurements of sea surface temperature from space", *J. Geophys. Res.*, **95**, 13497–13510.

Ostapoff, F., Y. Tarbeyev and S. Worthem (1973) "Heat flux and precipitation estimates from oceanographic observations", *Science*, **180**, 960–962.

Pandey, P. C. and R. K. Kakar (1982) "An empirical microwaves emissivity model for a foam-covered sea", *IEEE J. Ocean Engin.*, **7**, 135–140.

Pinker, R. T. and I. Laszlo (1992a) "Modeling surface solar irradiance for satellite applications on a global scale", *J. Appl. Meteorol.*, **31**, 194–211.

Pinker, R. T. and I. Laszlo (1992b) "Global distribution of photo-synthetically active radiation as observed from satellites", *J. Climate*, **5**, 56–65.

Pinker, R. T., I. Laszlo and F. Miskolczi (1993) "Photosynthetically active radiation from satellite observations", in S. Keevallik and O. Kärner (eds) *IRS'92 Current Problems in Atmospheric Radiation*, A. Deepak Publishing, Hampton VA, USA, 202–206.

Rossow, W. B., F. Mosher, E. Kinsella, A. Arking, M. Desbois, E. Harrison, P. Minnis, E. Ruprecht, G. Seze, C. Simmer and E. Smith (1985) "ISCCP cloud algorithm intercomparison", *J. Climate Appl. Meteorol.*, **24**, 877–903.

Schlüssel, P. and H. Luthard (1991) "Surface wind speeds over the North Sea from Special Sensor Microwave/Imager Observations", *J. Geophys. Res.*, **96**, 4845–4853.

Schlüssel, P., H.-Y. Shin, W. J. Emery and H. Grassl (1987) "Comparison of satellite-derived sea surface temperatures with in situ skin measurements", *J. Geophys. Res.*, **92**, 2859–2874.

Spencer, E. W., H. W. Goodman, R. E. Hood (1989) "Precipitation retrieval over land and ocean with the SSM/I: Identification and characteristics of the scattering signal", *J. Atmos. Ocean. Techn.*, **6**, 254–274.

Steffen, K. and A. Schweiger (1991) "NASA team algorithm for sea ice concentration retrieval from Defense Meteorological Satellite Program Special Sensor Microwave Imager: Comparison with Landsat satellite imagery", *J. Geophys. Res.*, **96**, 21971–21987.

Wentz, F. J., L. A. Mattox and S. Peteherych (1986) "New algorithms for microwave measurements of ocean winds: Applications to Seasat and the Special Sensor Microwave Imager", *J. Geophys. Res.*, **91**, 2289–2307.

Wentz, F. J., S. Peteherych and L. A. Thomas (1984) "A model function for ocean radar cross section at 14.6 GHz", *J. Geophys. Res.*, **89**, 3689–3704.

Wilheit, T. T., A. T. C. Chang, M. S. V. Rao, E. B. Rodgers, J. S. Theon (1977) "A satellite technique for quantitatively mapping rainfall rates over oceans", *J. Appl. Meteorol.*, **16**, 551–560.

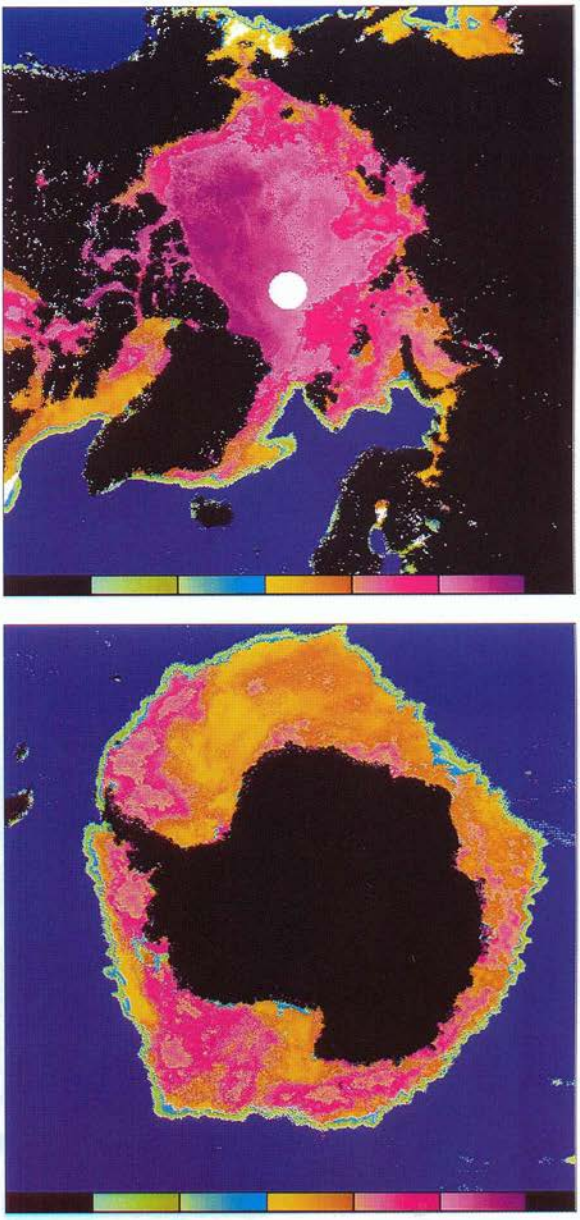

Plate 2.1 Distribution of sea ice as derived from SSM/I in the Arctic on 1 February 1988 and around Antarctica on 1 August 1988. The colour bars indicate different ice types and ice concentrations, from left to right: new ice, mainly new ice, young ice, first year ice, multi-year ice.

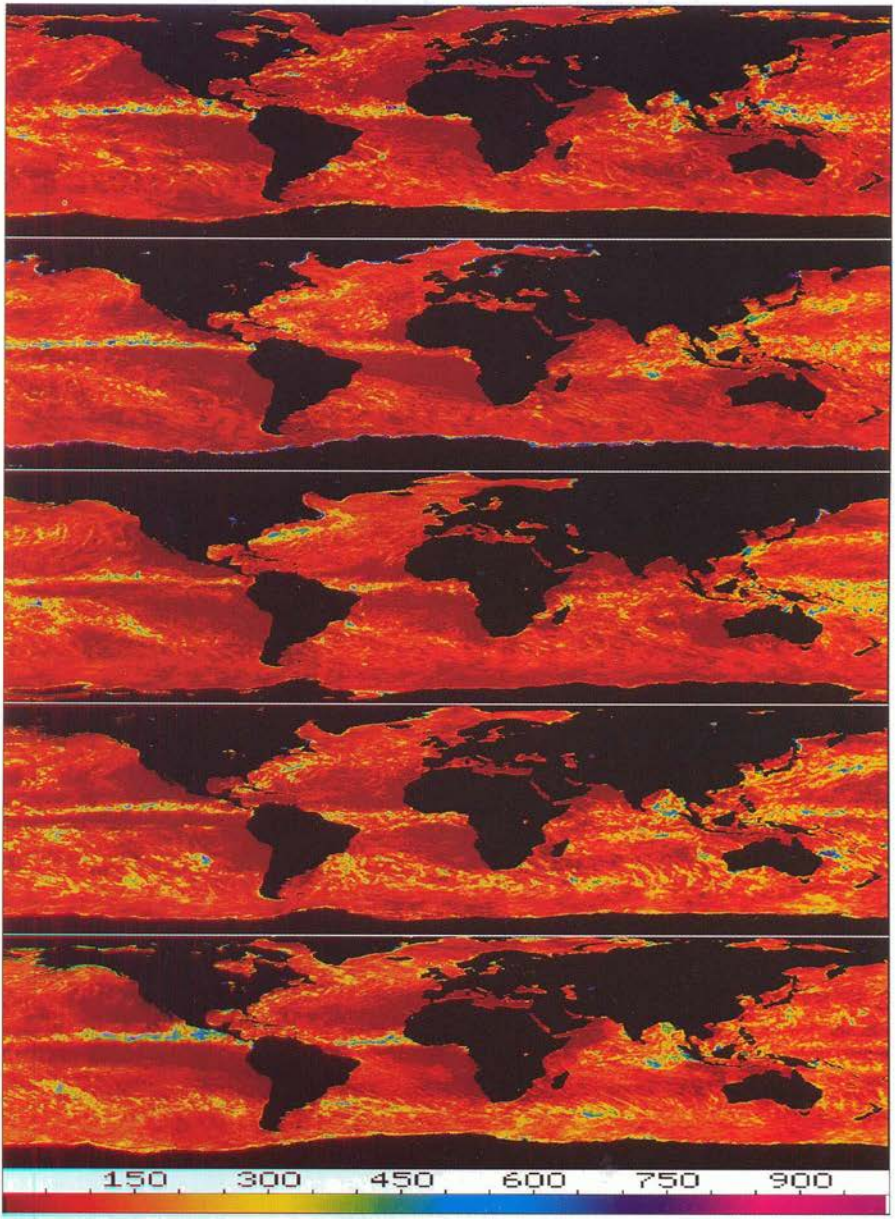

Plate 2.2 Monthly average rainfall over oceans in mm as derived from SSM/I for August 1987, November 1987, February 1988, May 1988, and August 1988 (top to bottom).

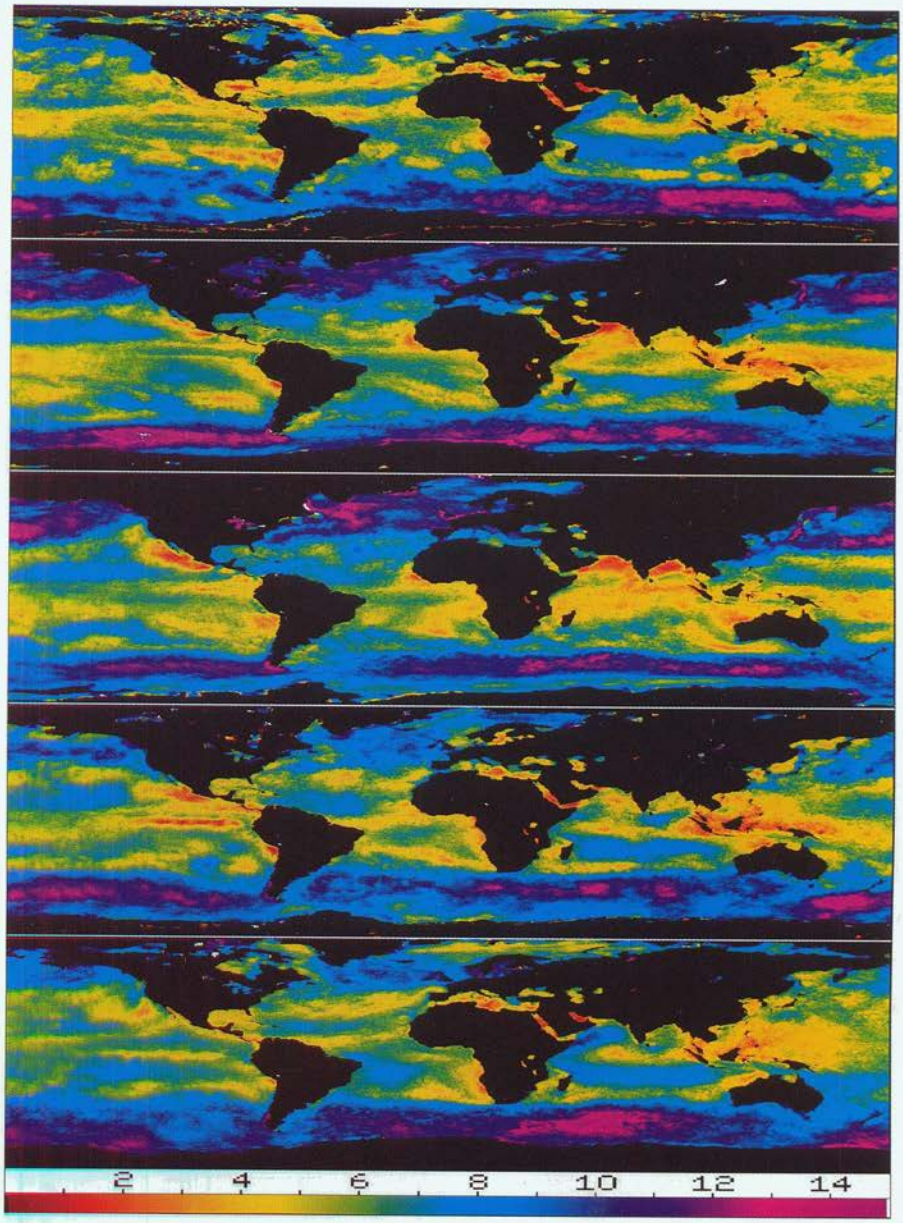

Plate 2.3 Monthly mean surface wind speed over oceans in m/s as derived from SSM/I for August 1987, November 1987, February 1988, May 1988, and August 1988 (top to bottom).

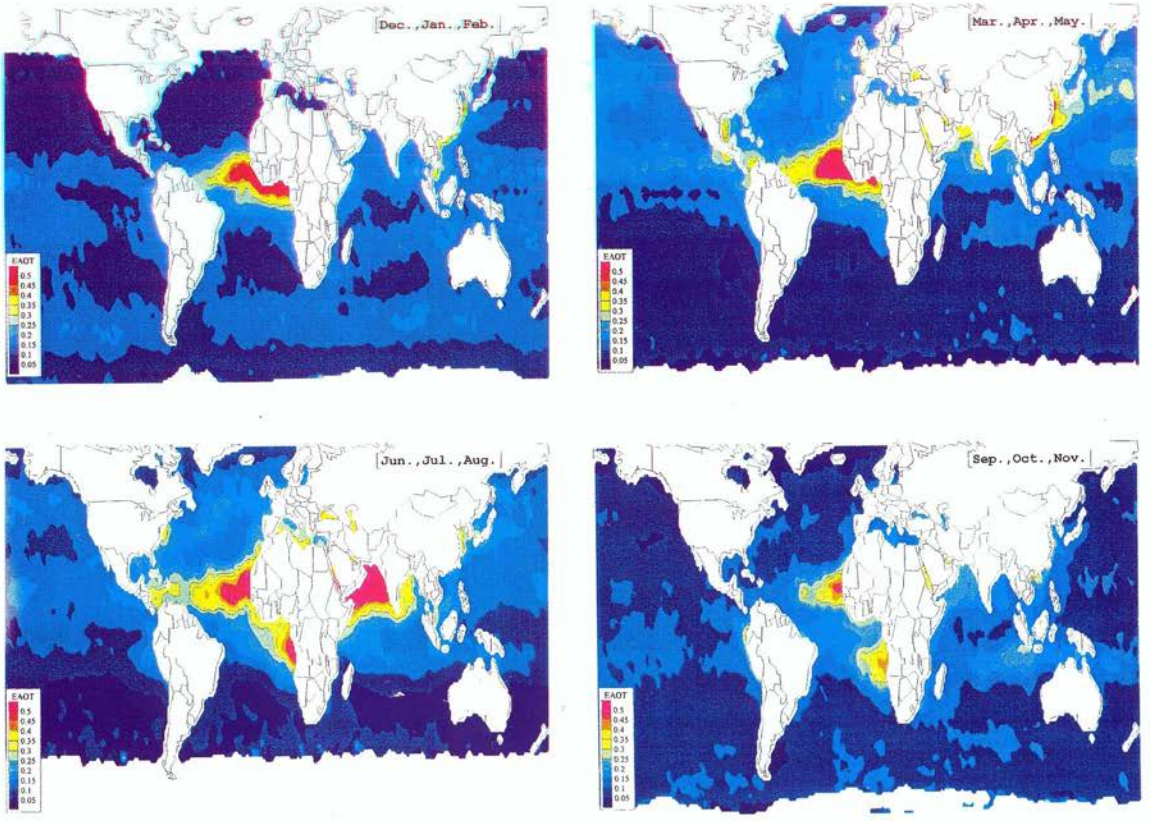

Plate 3.1 AVHRR aerosol optical depth, four seasons (R. Husar and L. Stowe, personal communication 1995). The Figure incorporates data for the period July 1989 to June 1991; consequently, it avoids the biasing effects of the Mt. Pinatubo eruption.

3 The Atmospheric Transport of Particles to the Ocean

JOSEPH M. PROSPERO

3.1 INTRODUCTION

The atmosphere is an important pathway for the transport of materials from the continents to the oceans. Although the magnitude of these wind-borne fluxes is not accurately known, there is evidence that some could be large enough to have a significant impact on chemical and biological processes in the oceans. The concentration, composition and physical properties of particles in the marine atmosphere can vary greatly, depending on the distribution of sources, the controlling meteorological processes in the source regions, the large scale circulation systems that subsequently control long-range transport and, finally, the various removal processes that act on the particles and cause them to be deposited in the ocean. In order to assess the transport of continental materials to the oceans, we must have a good understanding of all these processes.

The emphasis in this chapter is on mineral aerosol transport. Mineral dust is a substantial, at times major, component in the marine aerosol over many ocean regions. The principal sources of mineral dust are found in the arid and semi-arid regions of the world, especially those in North Africa, eastern Asia and the Middle East. These sources have a major impact on the mineral flux to the North Atlantic, the North Pacific and the northern Indian Ocean. This result is evident in the mineral assemblage distributions in the ocean sediments and it should also be reflected in the suspended particle distributions in these waters.

In this chapter I will characterize the distributions of mineral dust over the oceans and discuss some of the factors that affect the transport and deposition of dust to the oceans. An important consideration is the short-term (i.e., days to weeks) temporal and spatial variability of dust deposition; because of the highly episodic character of dust events, the concentration of dust (and associated materials) in sea water can be highly variable. Dust fluxes also appear to be highly variable on longer time scales (i.e., decades and longer); some of the climatic factors that might affect this variability will be discussed.

Particle Flux in the Ocean
Edited by V. Ittekkot, P. Schäfer, S. Honjo and P. J. Depetris

3.2 AEROSOL DISTRIBUTIONS OVER THE OCEANS

Our knowledge of aerosol transport over the oceans rests on a variety of sources. The quantitative understanding of this transport is based on actual measurements of aerosol concentrations; some of these measurements will be discussed in later sections. However, there are relatively few data for most ocean regions because of the difficulties in sampling on the spatial scale of the ocean; also much of the data are derived from short time-scale field studies that provide little information about seasonal variability which can be very large. Furthermore, the vast majority of such measurements are made at the surface, either at island stations or on ships. There are relatively few data from the free troposphere because such measurements must be made from aircraft and, as a result, are very expensive.

As a result of the dearth of *in situ* measurements, much of our understanding of the large scale features of aerosol transport over the oceans is derived from satellite imagery. Dust events are readily observable in visible spectrum satellite imagery such as GOES and METEOSAT. For example, individual dust storms can be tracked across the Atlantic from the time they emerge from the west coast of Africa until they reach the western Atlantic and the east coast of the United States (Ott et al., 1991). Similar events have been observed off the coast of Asia (Iwasaka et al., 1983; Takayama and Takashima, 1986). Over land surfaces, dust can best be tracked in the infrared bands (Tanre and Legrand, 1991; Jankowiak and Tanre, 1992).

NOAA issues a routine operational satellite product (Advanced Very High Resolution Radiometer (AVHRR)) that provides mapped distributions of aerosol optical depth (AOD) over the oceans on a weekly and monthly basis (National Climatic Data Center, Asheville, NC). The AOD provides a semi-quantitative indication of the geographical distribution of the vertically integrated loading of aerosols (Rao et al., 1988) over the oceans on a weekly basis. Plate 3.1 shows a color composite of the mean AVHRR AOD for four seasons (R. Husar and L. Stowe, personal communication). The AOD distributions in Plate 3.1 clearly show that areas of increased AOD are associated with continental sources. The continents are often fringed by regions of high AOD and in some regions the continents appear, in effect, to emit long "plumes" of enhanced AOD. The following paragraphs present an overview of the major features in Plate 3.1; later sections present a more detailed examination in terms of actual aerosol measurements.

The most prominent areas of high AOD values (red, indicating an optical depth greater than 0.5) are found in the tropical North Atlantic Ocean (NAO) and Indian Ocean (IO), especially the Arabian Sea. The plume in the low-latitude NAO is associated with mineral dust that is transported out of North Africa. The African AOD plume is by far the largest, the most persistent, and the most dense to be found over any ocean region. Plate 3.1 shows large seasonal changes in the

location and density of the AOD plumes over the NAO. These patterns are due to seasonal changes in the distribution of dust storm activity (which is related in part to seasonal rainfall patterns) and also to the seasonal shift of the large scale circulation. For example, the relatively steep gradient of the southern dust boundary of the NAO dust plume roughly corresponds to the seasonal climatological position of the northern boundary of the intertropical convergence zone (ITCZ). Large seasonal changes are also found in the Arabian Sea (and, to a lesser extent, the Bay of Bengal). The extremely high AOD values (greater than 0.5) are attributable to dust transport from the Arabian peninsula and from sources in the Middle East and northern India. The seasonal progression of the monsoon circulation system exerts a strong control over dust distributions, especially over the Arabian Sea.

Pollution plumes are also evident over the mid-latitude NAO. During the spring and summer, a large AOD plume emerges from the east coast of the U.S.A. and extends to the central NAO. There is also a substantial transport of pollutants out of Europe, to the west. During the summer, the North American plume merges with that from Europe, effectively bridging the NAO. The large area of relatively low AOD values in the central NAO coincides with the mean position of the Bermuda-Azores high pressure center. While the pollution plumes are obviously major features, both their areal extent and the magnitude of the AOD values are considerably less than those associated with dust transport region to the south.

In the North Pacific, a large plume emerges from the east coast of Asia in the spring. This plume is associated with the transport of mineral dust and pollution aerosols from sources in Asia. While the areal extent of this plume is quite large, the AOD values are considerably lower than those observed in the tropical NAO and the Arabian Sea. Although there is considerable evidence of a substantial continental influence in the coastal regions of Asia in the other seasons, there is no indication of a major plume comparable to that in the spring.

There are many other interesting AOD features in Plate 3.1, but the ones described above are the most obvious cases. It should be noted that these large-scale plumes are all located in the northern hemisphere. Prominent areas of enhanced AOD are visible in the southern hemisphere, but they are small. Plumes off the west coast of South Africa could be associated with arid regions in Angola and South Africa (e.g., the Kalahari desert); these plumes could also be related to biomass burning in these latitudes (Crutzen and Andreae, 1990). One of the most interesting features of the southern ocean AOD distributions is that there is no evidence of major dust plumes emerging from Australia despite the fact that it is the largest expanse of arid and desert land in the southern hemisphere (Pye, 1987).

There are other interesting features in Plate 3.1 which cannot be readily explained. A particularly striking one appears in the March-May composite, the large band of increased AOD that extends from Central America westward, almost reaching the Philippines. There are no known major sources of aerosol in

Central America and, even if there were, it is difficult to understand how substantial amounts of material could be carried over such great distances (10000–12000 km).

Satellite imagery makes a persuasive case for the prominence of mineral dust aerosols over the oceans and the presence of pollutant aerosols. In the following sections, I will discuss the quantitative measurements of aerosols and use the satellite imagery to generalize to the larger ocean.

3.3 MINERAL DUST

3.3.1 INTRODUCTION

The importance of aeolian transport to oceanic processes was first suggested by studies of the mineral distributions in pelagic ocean sediments. The concentration patterns of certain minerals (e.g., quartz, kaolinite, illite) in sediments off the coasts of some continents (e.g., the west coast of North Africa and North America, the east coast of Asia) were not related to fluvial sources but rather to the pattern of large scale wind fields (Prospero, 1981a). Various aspects of dust transport and effects have been extensively studied during the past two decades (for reviews, see for example: Andreae, 1995; Chester, 1986; Buat-Menard, 1986; Chester and Murphy, 1990; Prospero, 1981a; Prospero 1981b; Prospero, 1990; Pye, 1987; Middleton, 1990; Duce et al., 1991; Duce, 1995; Goudie and Middleton, 1992; Pèwè, 1981; Leinen and Sarnthein, 1982; Schütz et al., 1990; Morales, 1985; Golytsin and Gillette, 1993).

The following sections focus largely on dust transport out of Africa and Asia, the two regions that have been most extensively studied. Table 3.1 summarizes the annual mean concentrations of mineral dust at selected stations in the Atlantic and Pacific. These data are from samples collected with identical systems in continuous sampling programs that extend over a period of about one year or more. In Table 3.1 (Savoie et al., 1995), the aluminum values are converted to equivalent mineral dust concentrations based on the average concentration of Al in crustal materials (6–8%, Taylor and McLennan, 1985). Duce (1995) presents a much more extensive compilation of mineral aerosol measurements over the oceans although many of the measurements are for relatively limited time spans and some were made using semiquantitative techniques; Duce also provides an excellent review of aerosol physical properties.

Table 3.1 Aerosol concentrations from selected stations in the North Atlantic and the North and South Pacific.

Station	Lat. °N	Long. °E	Months #	Al ng m^{-3}	Dust* µg m^{-3}	NO_3^- µg m^{-3}	nss-$SO_4^=$ µg m^{-3}	NH_4^+ µg m^{-3}
NORTH PACIFIC								
Western Pacific								
Cheju, Korea	33.52	126.48	11	1650.7	20.63	5.07	9.32	3.76
Okinawa	26.92	128.25	18	1119.1	13.99	1.86	4.16	1.08
Hong Kong	22.55	114.30	18	967.0	12.09	2.61	6.69	2.74
Taiwan	21.87	120.87	2	317.0	3.96	2.06	5.40	1.45
Central Pacific								
Shemya	52.92	174.06	132	107.3	1.34	0.22	0.37	0.13
Midway	28.22	-177.35	144	62.6	0.78	0.27	0.53	0.06
Oahu	21.33	-157.70	144	54.6	0.68	0.35	0.50	0.04
SOUTH PACIFIC								
American Samoa	-14.25	-170.58	110	1.5	0.02	0.11	0.37	-
NORTH ATLANTIC								
Mace Head, Ireland	53.32	-9.85	32	37.8	0.47	1.49	2.03	0.91
Bermuda	32.27	-64.87	51	447.4	5.59	1.06	2.19	0.31
Izaña, Tenerife	28.30	-16.50	84	1782.6	22.28	0.77	0.92	0.33
Barbados	13.17	-59.43	108	1163.8	14.55	0.53	0.78	0.11

* Dust concentration computed from Al based on a crustal abundance of 8%.

3.3.2 NORTH AFRICA AND THE NORTH ATLANTIC

3.3.2.1 Concentrations and seasonal trends

Large quantities of mineral dust are transported from sources in North Africa across large areas of the tropical Atlantic during much of the year. The most extensive long term record of African dust transport are the measurements that have been made almost continuously at Barbados since 1965 (Delany et al., 1967; Prospero and Nees, 1986). These data show that the dust transport in the trade winds in this region is extremely variable on time scales of hours to decades. The short term variability is shown in the daily dust concentrations for 1989–1992 (Figure 3.1, Arimoto et al., 1995a). Although it is not readily seen in Figure 3.1, the dust concentrations at Barbados typically rise and fall in a coherent manner over the period of several days; this pattern can usually be associated with identifiable weather phenomena such as the passage of easterly waves that emerge from Africa in the summer months and move across the Atlantic (Carlson and Prospero, 1972; Prospero and Carlson, 1972; Karyampudi and Carlson, 1988). The time required for a specific dust-laden air mass to be carried past Barbados by the trade winds is usually several days; this suggests that the dimensions of the dust clouds along the transport trajectory range from hundreds of km to over a thousand km. This is substantiated by satellite imagery (principally GOES and AVHRR) which also show that it takes about one week for dust outbreaks to cross the tropical NAO from the coast of Africa to the Caribbean (Ott et al., 1991).

Although dust transport takes place during much of the year in the tropical North Atlantic, the maximum at Barbados occurs in the summer when monthly mean concentrations typically fall in the range of about 10–30 $\mu g\ m^{-3}$. The African dust transport affects a very large area of the NAO, producing a similar seasonal pattern of aerosol Al concentrations at Barbados, Bermuda and Izaña (Tenerife) - a summer maximum and a winter minimum (Figure 3.1). Saharan dust is also carried into the Miami area, at times producing dense hazes; in Miami, dust concentrations follow the same seasonal cycle as that at Barbados (Prospero et al., 1987) although mean concentrations are only about half those at Barbados (Prospero et al., 1993). Bermuda Al concentrations are only about a third of those in Barbados (Table 3.1). It is significant that major dust events in Bermuda are always associated with the advection of dust from African sources (which are at least 4500 km distant) whereas dust sources in North America (1000 km distant) appear to have relatively little effect.

Dust concentrations are high in the eastern tropical NAO. Note, however, that the concentrations at Tenerife are only about 50% greater than at Barbados despite the fact that Tenerife is only 300 km from the coast of Africa. While major dust events are often observed in this region (Bergametti et al., 1989a), the relatively low values at Tenerife are due to the fact that much of the dust transport takes place in the latitudes south of the Canary Islands (see Plate 3.1). As a result

of the large north-south gradient in the dust concentration in this region, small shifts in the large scale wind systems or in the dust sources in Africa could result in very large changes in dust transport and in the related deposition to the oceans. The factors affecting the Tenerife dust record can be generalized to dust transport over the oceans in general: because of the large gradients in the plumes, small

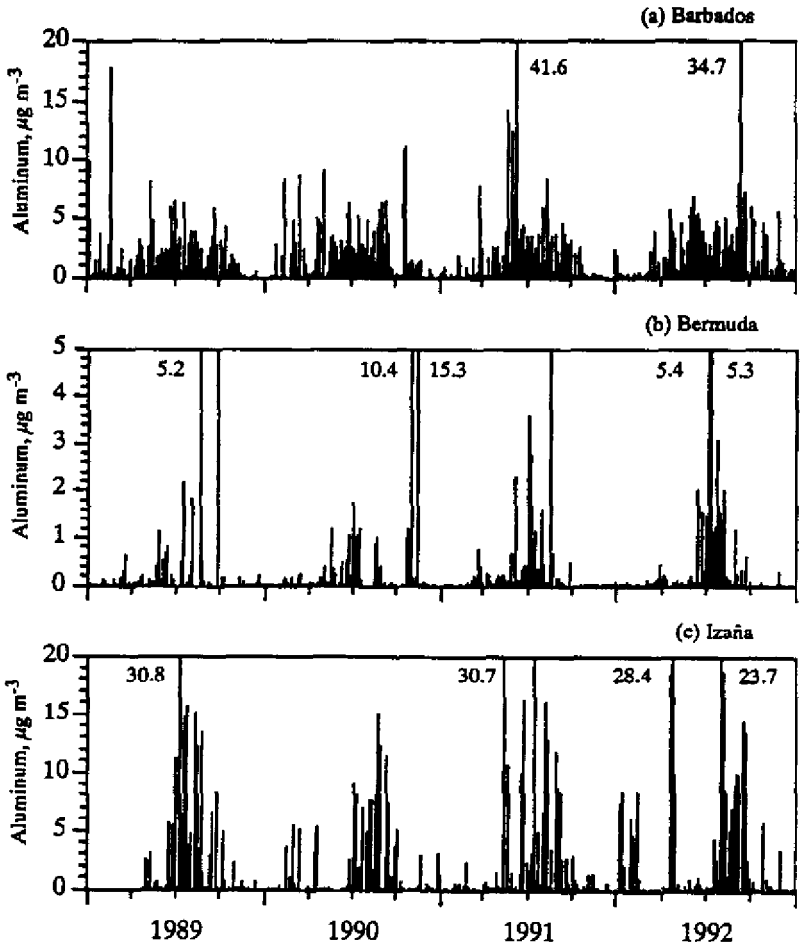

Figure 3.1 Aluminum concentrations at Barbados, Bermuda and Izaña (Tenerife, Canary Islands) from 1989 to 1992 (Arimoto et al., 1995a; reproduced by permission of the authors). Each bar represents a one-day sample. Note that the ordinate for the Bermuda graph is only 25% of those for Barbados and Izaña. The numbers in the Figure represent off-scale values. To convert the aluminum concen-tration to an equivalent mineral dust concentration, multiply by 12.5, a value that assumes an average Al crustal abundance of 8% (Taylor and McLennan, 1985).

changes in sources distributions and transport conditions can result in very large changes in concentrations at specific locations. This applies to the day-to-day changes in dust concentrations (which are subject to the winds associated with the controlling large-scale meteorological situation) and also to longer term concentrations (which are related to climatological factors and the associated long-term changes in meteorology).

During the northern hemisphere winter the large scale circulation systems shift southward; consequently, dust concentrations at Barbados and the other NAO stations are at a seasonal low. Large amounts of dust continue to be transported out of North Africa but the trajectories lie further to the south, including the Gulf of Guinea. Much dust is transported across the Atlantic in the low latitudes and into South America (Prospero et al., 1981; Talbot et al., 1986) and over the Amazon basin where they are believed to serve as a significant and important source of nutrients for the soils (Swap et al., 1992).

Large quantities of dust are carried over the Mediterranean and into Europe (Bergametti et al., 1989b, Bergametti et al., 1989c). Studies of dust accumulation in Alpine snows have provided an excellent quantitative record of Saharan dust transport over the past few decades (De Angelis and Gaudichet, 1991; Dessens and Van Dinh, 1990). These studies show that dust transport to Europe increased markedly during the past two decades, in agreement with the observations in the trade winds. Whatever the cause of the increased emissions of dust from Africa, they have had a widespread effect.

The seasonal pattern of dust concentrations measured at the various stations in the NAO are consistent with the AVHRR satellite observations shown in Plate 3.1. The dust distributions and satellite imagery are also consistent with records of haze distributions at sea prior to the 1930's as recorded from ships observations (McDonald, 1938; see also, Prospero, 1981a). All evidence suggests that the North African dust outbreaks are large, synoptic scale events that fill much of the lower troposphere, and that they are frequent occurrences. Historical records show that they have been taking place for at least hundreds of years (Prospero, 1981a).

3.3.2.2 Aerosol chemical properties

In addition to carrying large quantities of dust, the winds over the NAO often bring high concentrations of pollutants. The pulses of increased dust concentrations are accompanied by sharply increased concentrations of nss-$SO_4^=$ and NO_3^- which are largely attributed to pollutant sources (Table 3.1). At Barbados, the pollutants appear to be derived mostly from Europe (Savoie et al, 1989a; Savoie et al., 1992), a conclusion that is supported by the lead isotope ratios in Barbados aerosols (Hamelin et al., 1989). Similarly, the aerosols collected at Bermuda are strongly affected by North American pollution sources (Arimoto et al., 1992; Arimoto et al., 1995a; Ellis et al., 1993). A recent study used tracers to quantitatively assess the relative impact of natural and

anthropogenic sources of sulfate aerosol over the NAO (Savoie et al., 1995); the annual mean anthropogenic component of aerosol nss-$SO_4^=$ was 50% at Barbados, 70% at Bermuda and 80–90% at Mace Head, Ireland. A number of studies suggest that many aspects of the particle and elemental distributions in ocean waters can be interpreted in terms of atmospheric transport (see, for example: Helmers and Rutgers van der Loeff, 1993; Duce and Tindale, 1991; Donaghay et al., 1991; Fanning, 1989; Owens et al., 1992; Kremling and Streu, 1993; Veron et al., 1992; Veron et al., 1993; Carder et al., 1986).

These studies show the pervasive effects of the long range transport of natural and pollutant materials over the NAO. Nonetheless, on a mass basis, dust is the major component. Indeed, at Barbados during the past decade, the mean concentration of mineral dust is almost an order of magnitude greater than that of the other major non-sea-salt aerosol components (i.e., NO_3^-, nss-$SO_4^=$, and NH_4^+); even at Bermuda, the mean mineral dust mass is about 50% greater than other components despite the fact that dust concentrations are lower and pollutant concentrations higher than at Barbados.

3.3.2.3 Relationship of dust transport to rainfall in Africa

The long-term record of dust concentrations at Barbados (Figure 3.2; Prospero and Nees, 1986; Prospero et al., 1993) shows the long-term consistency of the pattern of annual dust transport in the trade winds. Dust concentrations increased sharply beginning in 1970 when a persistent drought began in the sub-Saharan (Sahel) regions of Africa. Prior to 1970, the annual average dust concentration was 3.9 μg m^{-3} (range 3.2–4.5 μg m^{-3}); from 1970 to 1992, the average was 11.0 μg m^{-3} (5.4–18.7 μg m^{-3}). The highest dust concentrations at Barbados occurred in the mid 1980's when the drought was especially severe; during 1983–87 (excepting 1986), the June to August average dust concentrations exceeded 25 μg m^{-3}; the maximum June-August mean concentration for the entire 27 year record occurred in 1984, 37.8 μg m^{-3}.

The Barbados dust concentrations for 1965–1992 are inversely related to the prior year rainfall in sub-Saharan (Sahel) Africa (Lamb and Peppler, 1991; Figure 3.2). A similar relationship is obtained using rainfall data (Gray et al., 1992) from West Africa that incorporates more stations closer to the coast (Prospero et al., 1993). Mean summer dust concentrations at Barbados increase by about 10 μg m^{-3} for every standard deviation of rainfall deficit. The relationship between dust concentrations and rainfall is less evident during the winter when the transport of dust to Barbados is more sporadic. While the dust and drought data can be interpreted as supporting a direct drought-related cause for increased dust, there are other mechanisms that could effect the same result (see below, 3.4.4, Long Range Dust Transport and Climate).

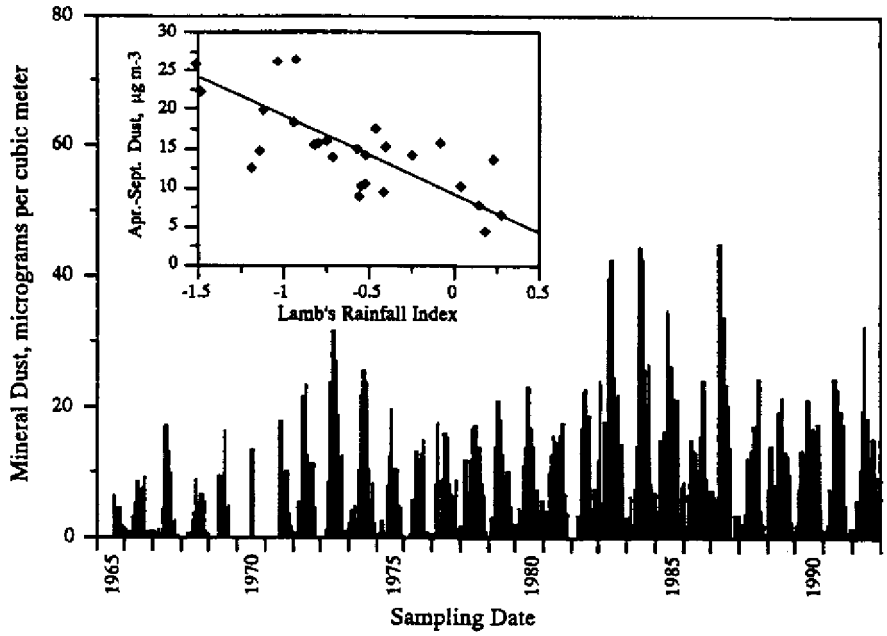

Figure 3.2 Long-term (1965–1992) record of monthly average atmospheric dust concentrations at Barbados (Prospero and Nees, 1986. The inset shows the relationship of Barbados dust concentrations to rainfall deficits in the Sahel as expressed by the Lamb rainfall index (Lamb and Peppler, 1991) which is a measure of rainfall departures (in standard deviations) from the mean. The rainfall data are from 20 sub-Saharan stations. The index uses as a reference base rainfall from 1941 to 1982. Lower index numbers correspond to drier conditions.

3.3.2.4 Meteorology of long range African dust transport

Large scale dust outbreaks are usually associated with complex meteorological processes; our understanding of them is poor because there has never been a major field experiment that focussed on synoptic-scale dust mobilization processes in the areas where the mobilization of long-range dust transport is greatest (West Africa, Asia and the Middle East). Much of our current understanding about African dust events was obtained incidentally during a large-scale meteorological program off the west coast of North Africa (the GARP Atlantic Tropical Experiment - GATE) during the summer of 1974 (Karyampudi and Carlson, 1988). Large dust outbreaks were associated with strong convective disturbances that developed deep in West Africa at about 15°–20°N and moved to the west. Over the ocean, the dust outbreaks events were usually associated with easterly waves which emerge from the coast of Africa every 3–4 days. Easterly waves have a complex dynamic structure which produces complex distribution patterns for the dust. The areal

distributions are plainly visible in satellite imagery as stated earlier. A consistent feature is that the main transport occurs at higher altitudes in a layer that typically reaches to several km and often to 5–6 km (Prospero and Carlson, 1972; Talbot et al., 1986; Karyampudi and Carlson, 1988); concentrations aloft are usually several times greater than in the marine boundary layer. Because of the unusually high temperature and low relative humidity of the dust layer, it can be identified in routine meteorological soundings as far west as the Caribbean, Miami (Carlson and Prospero, 1972; Ott et al., 1991) and over the Amazon basin in eastern Brazil (Swap et al., 1992).

Because of the complexity of the meteorological events associated with African dust transport, it is very difficult to assess dust transport in a comprehensive and quantitative way. Indeed, the fundamental meteorological processes themselves are poorly understood and it has not been possible to understand the evolution of the layered structure even in terms of the dynamics of the systems (Westphal et al., 1987; Westphal et al., 1988).

3.3.3 PACIFIC STUDIES

There are many dust sources in Asia, most notably the large deserts in the People's Republic of China especially the Gobi and the Takla Makan. In addition, China has extremely large loess deposits (Pye, 1987) much of which is used for agriculture; because of their fine texture, these soils are easily deflated by winds. Dust storms are quite frequent in these regions (Littmann, 1991; Middleton, 1989; Middleton, 1991), especially in the spring when there is wide-spread dust which can be carried great distances (Gao et al., 1992a). In Japan and Korea during the spring, they often experience extensive dust hazes that are caused by yellow dust (Kosa) that can be traced to sources in Asia (Gao et al., 1992b; Chung, 1992; Iwasaka et al., 1983; Takayama and Takashima, 1986; Tsunogai et al., 1985).

Dust transport across the North Pacific has been most extensively measured in the Sea/Air Exchange (SEAREX) Program (Prospero et al., 1989). Continuous measurements were begun in the early 1980's when a network of stations was established in the North and South Pacific (Prospero et al., 1989; Uematsu et al., 1983; Uematsu et al., 1985; Uematsu, 1987). Subsequent measurements were made as a part of the NASA Pacific Exploratory Mission (PEM, Arimoto et al., 1995b). The stations in the North Pacific show a well-defined seasonal pattern of dust transport with a maximum in the spring months and a minimum in the summer. The seasonal cycle is best illustrated by the data from Midway (Figure 3.3) where the record is longest. The dust maximum corresponds to the seasonal cycle of dust storm activity in Asia (Duce, 1995). There are often large year-to-year variations in the seasonal cycle; these can be related to changes in dust storm frequencies in Asia and to changes in the large-scale wind systems (Duce, 1995; Merrill, 1989).

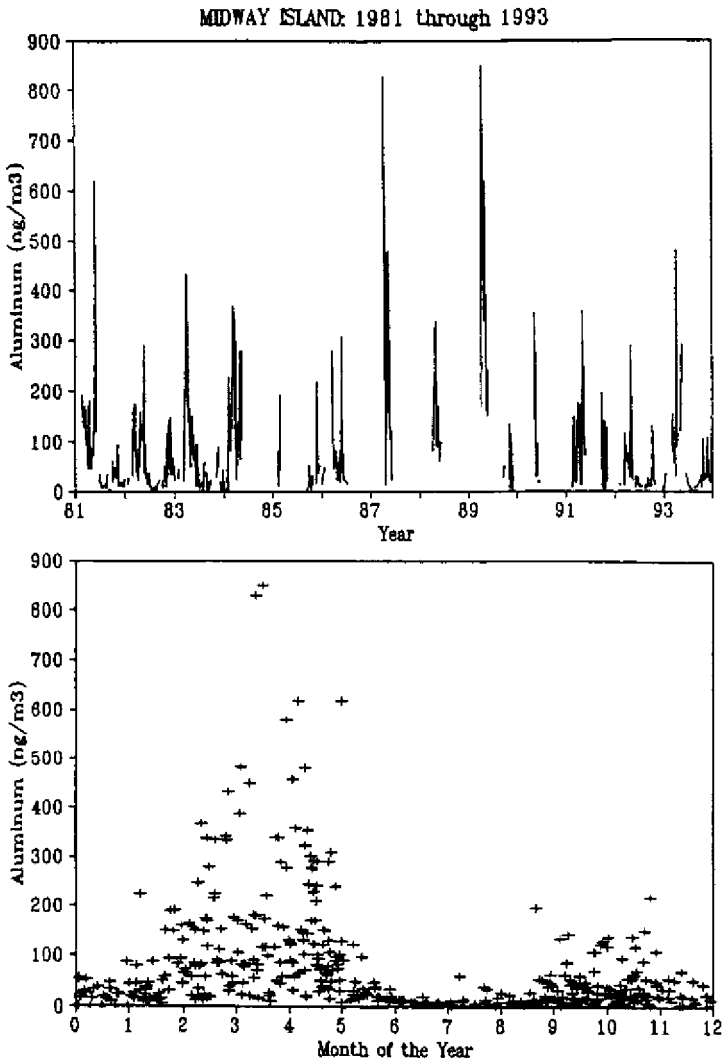

Figure 3.3 Aluminum concentration in aerosols collected in oceanic air at Midway island: 1981 – 1993. Top: 12 year time series. Bottom: same data as in the time series but plotted on an annual basis. (Arimoto et al., 1995b; R. Arimoto, personal communication).

The mineral characteristics of aerosols over the North Pacific Ocean (NPO) reflect many of the characteristics of the underlying sediments (Blank et al., 1985, Leinen et al., 1994). The mineral composition of the aerosols changes with the

transport trajectories and can be associated with sources in Asia and North America (Merrill et al., 1994).

Over the North Pacific, continental sources strongly affect the concentration of several other species: aerosol NO_3^- and nss-$SO_4^=$ (Savoie et al., 1989a) and ^{210}Pb (Turekian et. al., 1989). ^{210}Pb is a daughter product of ^{222}Rn that is emitted from soils and, as such, it serves as a tracer for air masses that have recently been in convective contact with soils. All have a seasonal cycle similar to that for dust. The spring-time maximum of nss-$SO_4^=$ and NO_3^- is attributed to the transport of pollutants along with dust; concentrations are substantially higher than would be expected from natural sources (Savoie et al., 1989a).

The monthly mean Al concentrations at all the major NPO stations are shown in Figure 3.4. The highest monthly means are observed at the stations on the western NPO, Okinawa, Cheju (Korea) and Hong Kong (Arimoto et al., 1995b). Okinawa and Cheju show a springtime maximum similar to that at the central Pacific sites (Oahu, Midway and Shemya). The Hong Kong data show a bimodal distribution with a small peak in the spring and a larger, broader one in the winter; the winter peak is associated with transport from the North. Thus, all stations show a consistent picture of large scale dust transport in the spring as depicted in the AVHRR imagery (Plate 3.1).

The effects of continental transport are much greater over the NPO than the SPO. Figure 3.5 shows the annual arithmetic mean mineral aerosol concentrations over the NPO and SPO as measured in the SEAREX network (Prospero et al., 1989). Dust concentrations are highest in the mid-latitude of the NPO and lowest in the equatorial Pacific and central SPO. The relatively high concentrations at Funafuti compared to the other equatorial stations is attributed to Asian dust transport. New Caledonia and Norfolk Island are affected by dust transport from Australia (Prospero et al., 1989). Nonetheless, considering the distance from Australia and comparing concentrations with those at stations off the coast of Asia and Africa, the concentrations of dust and other trace species (Arimoto et al., 1990) are quite low. The low concentrations are consistent with the AVHRR imagery which shows very low AOD in this region in all seasons. Collectively these data suggest that Australia is a poor source of dust. The lowest dust concentrations are observed at American Samoa; the concentrations of other continental sources species (nss-$SO_4^=$, NO_3^- and ^{210}Pb) are also extremely low (Savoie et al., 1989b).

The meteorological setting for long-range dust transport events over the NPO is quite complex. Major dust storms are most frequent in the spring because of the combined effects of low rainfall (and, hence, dry soils), large expanses of soils freshly plowed for spring planting, and the frequent occurrence of high winds that are usually associated with cold fronts that move out of central Asia (see Prospero et al., 1989; Merrill et al., 1985, Merrill et al., 1989); dust is typically lifted to 5–6 km (Merrill et al., 1985; Kotamarthi and Carmichael, 1993). Because of the extremely dynamic character of cold fronts, dust is often lifted from widely diverse

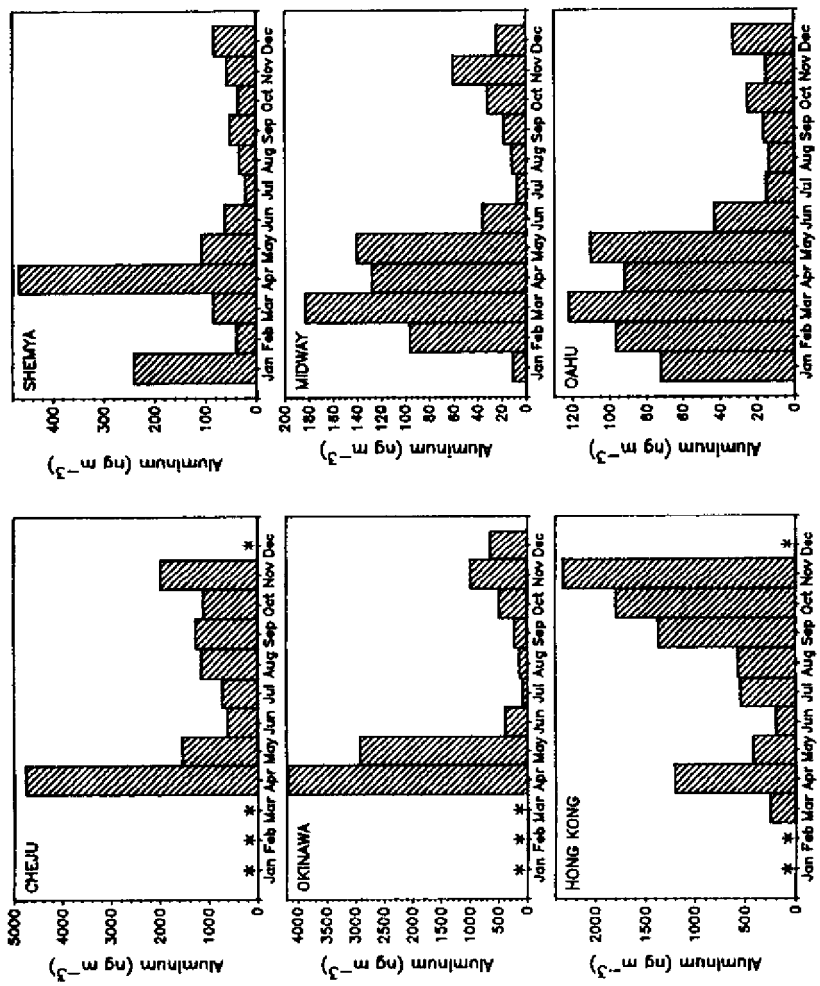

Figure 3.4 Monthly mean Al aerosol concentrations in the North Pacific PEM-West network (Arimoto et al., 1995b).

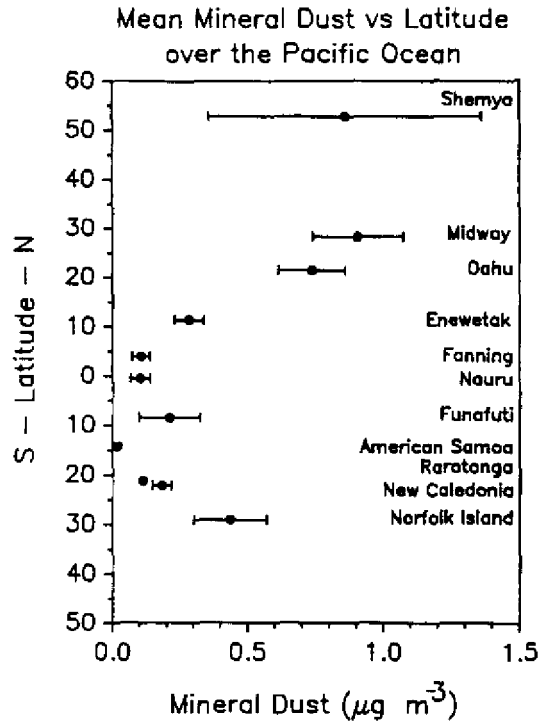

Figure 3.5 Annual arithmetic mean mineral aerosol concentrations over the Pacific Ocean as measured in the SEAREX network (Prospero et al., 1989). This figure contains only the data from relatively remote stations; it does not contain the data from the stations in the western North Pacific which are more heavily impacted by dust transport because of their proximity to sources in Asia. Dust concentrations are based on measurements of Al concentration multiplied by 12.5, assuming an average Al crustal abundance of 8% (Taylor and McLennan, 1985).

regions; plumes from distant sources are lofted and interleaved in the atmosphere, producing a strongly layered structure (Kotamarthi and Carmichael, 1993). The larger-scale meteorological setting will control the trajectories that transport the dust over the ocean (Merrill, 1989). These factors combine to yield the highly episodic dust events that are observed in the NPO.

3.3.4 INDIAN OCEAN AND THE ARABIAN SEA

There are very few data for the Indian Ocean and most are for short periods during cruises. Nonetheless, these data clearly show that dust concentrations are very large over the Arabian Sea and the NW IO close to Africa; values are comparable to those along the west coast of Africa (Savoie et al., 1987; Prodi et

al., 1983). These values and the seasonality of the concentrations are consistent with the dust transport distributions shown in AVHRR (Plate 3.1) and with the monsoon circulation (Ackerman and Cox, 1989). Soils in the Tigris and Euphrates River basin appear to be major source of dust that is transported to the Arabian Sea (Ackerman and Cox, 1989; Prospero, 1981a; Prospero, 1981b); the transport takes place in deep, well-defined layers that extend to 4–7 km, similar to those observed with Saharan dust outbreaks (Ackerman and Cox, 1989).

There is even less quantitative data from the central and southern IO. The few data that exist suggest that concentrations are extremely low. Measurements (a total of 3 samples!) at Amsterdam Island (34°47'S, 77°31'E), yield concentrations in the range of those observed at American Samoa (Table 3.1) (Gaudichet et al., 1989). The dearth of measurements makes it extremely difficult to characterize deposition to this vast region but it would appear that mineral dust concentrations across much of the southern oceans are extremely low.

3.3.5 SUMMARY

Figure 3.6 presents graphically the Al data from Table 3.1. The Al values range over three orders of magnitude. It is not surprising that the highest values are found close to the continents (e.g., the western North Pacific stations; Tenerife). It is notable that the concentrations at Barbados (which is 4500 km from the coast of Africa) are comparable to those in coastal regions. Indeed, the distance from Barbados (and also Bermuda) to the coast of Africa is about the same as that between Midway and the coast of Asia; yet the mean dust concentration at Barbados is about 20 times that at Midway. These data illustrate once again that

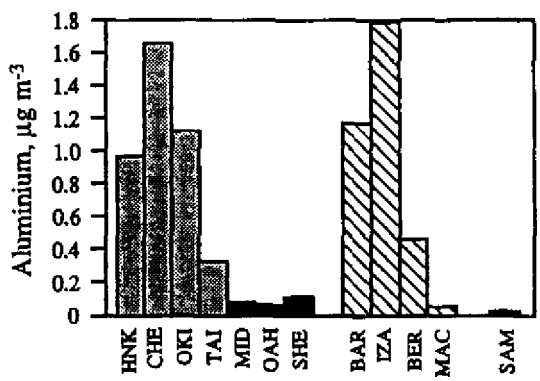

Figure 3.6 Annual mean aluminum concentrations at sites in the Atlantic and Pacific Oceans based on measurements in the PEM-West, SEAREX, and AEROCE networks. HNK: Hong Kong; CHE: Cheju, Korea; OKI: Okinawa; TAI: Taiwan; MID: Midway; OAH: Oahu; SHE: Shemya; BAR: Barbados; IZA: Izaña, Tenerife, Canary Islands; BER: Bermuda; MAC: Mace Head, Ireland; SAM: American Samoa.

the efficiency with which materials are transported by winds from the continents to the oceans is a function of many factors (Merrill 1989; Whelpdale and Moody, 1990), and that distance alone is not necessarily important. Indeed, the intensity and year-round persistence of the dust transport in the tropical NAO seems to be unique: it appears to be the result of the coupling of the strong dust sources in North Africa with an extremely efficient transport system - the trade wind regime. Finally, the fact that pulses of dust are usually accompanied by increased levels of pollutants must be considered when assessing the effects of dust deposition on ocean processes.

3.4 MINERAL PARTICLE DEPOSITION TO THE OCEANS

3.4.1 SOURCE STRENGTHS

The quantitative estimation of dust transport is extremely difficult for a number of reasons, one of which is the difficulty in defining what is meant by "transport". Vast amounts of soil material are moved by winds each year especially in regions of sand dunes and in eroding agricultural areas (Pye, 1987). However, close to the source regions, much of the transported mass consists of large particles (i.e., diameters of tens of microns; d'Almeida and Schütz, 1983; Duce, 1995) which have a very short residence time in the atmosphere because of their high Stokes settling velocity; therefore, such large particles will not be carried very far by winds. For this reason, flux estimates are usually based on that portion of the mass that is below 10–20 μm diameter. During transport, the size distribution rapidly shifts to smaller particles because of the rapid fallout of large particles (i.e., 5–10 μm diameter and greater); at distances of a few hundreds of kilometers or more from the source, the dust attains a relatively stable size distribution with a mass median diameter of one-to-several μm (e.g., Duce, 1995) although some very large particles can be carried great distances (Betzer et al., 1988; Carder et al., 1986). Thus, the properties of the "long-range" dust will be those of the clay-silt fraction in soils (Gomes et al., 1990). Consequently the physical, mineralogical and chemical properties of this component of soils are relevant to understanding the properties of deflated dust and long range transport.

Because of the uncertainties about sources, dust deflation processes and the subsequent transport and removal dynamics, estimates of the source strength of dust are probably the poorest of any major aerosol species. Duce (1995) has recently reviewed and summarized the dust estimates made over the past 25 years. Early estimates yielded global input rates on the order of several hundreds of Tg y^{-1}. In contrast, estimates made since the mid 1980's are an order of magnitude higher, ranging from 1000 to 3000 Tg y^{-1}. Some of the recent estimates are based on process studies in North Africa and, consequently, they may be biased by the

increased deflation associated with the drought. Nonetheless the agreement of the recent estimates is surprising because, for the most part, they are generated on the basis of different models.

3.4.2 DUST DEPOSITION RATES

Over the open ocean, where the mass median diameter is only a few microns at most, the dominant deposition mechanism is generally removal by precipitation (e.g., "wet" removal). Removal by "dry" processes (principally by sedimentation and impaction) could be important in coastal regions close to sources (such as along the west coast of North Africa) where the dust size distribution is skewed towards large particles. Unfortunately, there have been very few efforts to make direct measurements of dust deposition to the oceans for extended time periods. Consequently, estimates of wet deposition rates must be based on calculations using scavenging ratios (defined as the concentration of a substance in rain divided by the corresponding concentration in air, e.g., Scott, 1981; Galloway et al., 1993). Scavenging ratios are empirically derived from measurements made with co-located precipitation and aerosol samplers. However, because of the dearth of long-term measurements of dust in precipitation and aerosols (Prospero et al., 1987; Uematsu et al., 1985), it has been necessary to extrapolate scavenging ratios to the world ocean. The most recent and most comprehensive estimate of dust deposition to the oceans is presented in Duce et al. (1991). For various reasons, Duce et al. (1991), use a scavenging ratio of 200 for the NAO; for the remainder of the world ocean, they used a ratio of 1000 (which, all other things being equal, will yield a deposition flux that is five times that obtained with the 200 value). The Duce et al. dust deposition rates for various ocean regions are shown in table 3.2. The largest basin rates (per unit area) are, in order, the North Indian Ocean, the NPO and the northern NAO.

The high fluxes in the IO and NAO are consistent with the patterns of dust seen in AVHRR (Plate 3.1). In contrast, the very large values for the NPO seem high in light of the indicated transport from AVHRR. The calculated deposition flux fields in the western NPO are comparable to those in the eastern tropical NAO. Yet the AVHRR data suggest that aerosol concentrations are never as high as those in the tropical NAO and that the transport takes place only during the spring; in contrast dust is carried out of North Africa all year long. It is possible that this discrepancy is due to a sampling bias by AVHRR which only can measure aerosols in cloud-free regions. Consequently, if dust transport in Asia takes place under cloudy conditions (for example, with persistent high stratus), the transport would not be recorded in the AVHRR data base. Nonetheless the previously cited measurements of aluminum (and other) aerosols over the NPO do support the seasonality implied by AVHRR.

Table 3.2 Dust deposition rates to various ocean regions (After Duce et al., 1991).

Ocean	Mean Basin Flux, g m^{-2} y^{-1} *	Total Basin Deposition, Tg y^{-1}	
		Duce et al., 1991*	SR = 200+
North Pacific	5.3	480	96
South Pacific	0.35	39	8
North Atlantic	4.0	220	220
South Atlantic	0.47	24	5
North Indian	7.1	100	20
South Indian	0.82	44	9
Global	2.5	910	358

* Duce et al. (1991) SR = 1000 except for North Atlantic where SR = 200
+ Duce et al. (1991) Modified using SR = 200 globally

The total estimated deposition to the world ocean is 910 Tg y^{-1} (Table 3.2). Compared to the estimates of dust production (Duce, 1995), the estimated total ocean deposition rate is equal to 100% of the lowest production estimate and about a third of the highest estimate. This suggests that the estimated transport (i.e., 910 Tg y^{-1}) may be too high or that the lower-range estimates of dust source strength might be too low. The mean global ocean accumulation rate is 250 mg cm^{-2} ky^{-1}. Basin means range from 35 to 710 mg cm^{-2} ky^{-1} but there are very large gradients across basins.

In some basins the deposition rates reported in Duce et al. (1991; Table 3.2) are remarkably high and are comparable to those measured on the continents or near major source regions. For example, the mean deposition rate for the entire North Pacific (about 500 mg cm^{-2} ky^{-1} is about half that measured for the deposition of Saharan dust in the Alps (about 1000 mg cm^{-2} ky^{-1}, De Angelis and Gaudichet, 1991) and on Corsica (about 800 mg cm^{-2} ky^{-1}, Bergametti, 1989b; Bergametti, 1989c); these measurements were made in the 1980's when dust transport from the Sahara was unusually high. The Duce et al. values are even high compared to measured continental deposition rates. The most extensive continental program (Reheis and Kihl, 1995) was a five year study at 55 sites in southern Nevada and California. The average silt-clay deposition rate (both wet and dry) over most of this relatively arid region was in the range of 430–1570 mg cm^{-2} ky^{-1}. Reheis and Kihl summarize dust deposition rates from various continental regions (their Table 8); the rates are generally consistent with those that they obtained (excluding the values that included sand). At the very least the Reheis and Kihl data emphasize the fact that arid regions are not necessarily good sources of dust

compared to the major sources that we see today in North Africa, Asia and the Middle East.

3.4.3 COMPARISON WITH AEOLIAN DEPOSITION RATES

Recently Rea (1994) has reviewed aeolian deposition rates to the oceans based on the analysis of pelagic sediment cores. Rea's measured accumulation rates for aeolian materials in Holocene sediments in the NPO, where he has a relatively high data density, seem to be in reasonable agreement with the estimates by Duce et al. (1991). Data in the Atlantic are quite sparse and concentrated in the eastern equatorial regions; but here too, the agreement seems acceptable. Rea has much less data in the low sedimentation rate regions, especially in the southern oceans but most notably in the IO. Rea states that the Duce et al. deposition rates to the southern oceans are too high by a factor of 5 to 10; however Rea's data density in these regions is very sparse and does not warrant a strong conclusion in this regard.

Recent data (Duce, 1995) seem to suggest that the scavenging ratio of 1000 (which was used in the Duce et al. (1991) estimate for every ocean region except the NAO) may be too high and that a value of 200 (which was used for the NAO) might be appropriate. If true, this would lower the estimated deposition fluxes by a factor of five, all other factors being equal. In Table 3.2, the deposition rates are also shown for this lower rate which yields a global rate of 360 Tg y^{-1}. A scavenging ratio of 200 will yield deposition rates in the southern oceans that are more in line with Rea's (sparse) data; however the resulting values in the NPO would be substantially lower than Rea's.

There are a number of possible explanations for discrepancies between the estimated deposition rates and the measured accumulation rates. First, the scavenging ratios used in the estimates could be wrong; it is possible that scavenging could vary regionally or even temporally with changes in climate and that large scale extrapolations of scavenging ratios are not appropriate. There are so few data on the dust scavenging that it is impossible to assess these effects. Second, the accumulation rates in sediments are in effect long-term averages, typically thousands of years, whereas the dust deposition estimates are based on current measurements. Differences could be due to relatively recent changes in climate that could affect dust transport. Third, only recently have humans had the capability to strongly alter the landscape; land-use practices, especially cultivation and intense grazing of livestock, can lead to greatly increased rates of deflation. Fourth, the sediment accumulation rates could be wrong or the material could have been transported by mechanisms other than aeolian. At this time, it is not possible to resolve these issues.

3.4.4 LONG RANGE DUST TRANSPORT AND CLIMATE

3.4.4.1 Wind erosion and climate

Aeolian particles in pelagic sediments can provide a long-term record of the transport of mineral dust to the oceans. On the basis of our knowledge (and assumptions) about the relationship between dust transport, weather and climate, the aeolian sediment component can be interpreted in terms of past climate on the continents. Changes in the accumulation rates and grain-size distributions of aeolian dust in deep-sea sediments have been used as indicators of past aridity and as a measure of the "vigor" of the atmospheric circulation (Rea, 1994). Many studies have suggested that the aeolian dust in sediments might serve as a useful indicator of paleoclimate (Sarnthein et al., 1982; Leinen, 1989; Hovan et al., 1991; Rea, 1994). These studies show that there have been large changes (factors of ten) in the transport of dust to the oceans in the past. Changes have been related in a general way with glacial cycles, suggesting that the major glaciations were associated with greatly increased dust transport and more vigorous wind systems. The association of cold cycles with enhanced dust transport has also been noted in ice core studies, especially in the northern hemisphere.

There is an extensive literature on large scale wind erosion (Middleton, 1985; Middleton, 1990; Goudie, 1983; Goudie and Middleton, 1992; Pye, 1987; Golitsyn and Gillette, 1993). This shows that major sources are associated with arid and semi arid regions. But deserts (and arid lands) are not necessarily good sources; for example, as shown above, Australia is a very weak source of dust despite the fact that it is largely arid and desert. High rates of emission are generally associated with semi-arid regions where marginal lands are used for agriculture and herding (Middleton, 1990; Littmann, 1991); during periods of drought, the denuded and broken soil surface is easily carried away. The periodic creation of "dust bowl" conditions in the midwestern United States is a good example.

It is difficult to relate the sedimentary dust record with climate in an unambiguous way. Indeed, the physical basis for the interpretation of the sedimentary record (Rea, 1994) has never been established by measurements of dust/transport relationships in the present day world (Prospero, 1985; Duce, 1995). For example, the Barbados data (Figures 3.2 and 3.3) certainly appear to suggest that there is a relationship between dust transport and rainfall. Yet, if dust were strictly related to rainfall, then we would expect that the dominant source in North Africa would be the Sahara. We do know that the Sahara is an important source, especially for dust that is transported northward, across the Mediterranean to Europe (De Angelis and Gaudichet, 1991). But if the Sahara is the major source for the trans-Atlantic dust, then why should dust transport from this source be modulated in such a way as to correlate with rainfall in the Sahel and West Africa? Is "drought" occurring in the Sahara as well? One could argue that the

meteorological factors that produced the drought in the Sahel were accompanied by other changes (for example, changes in wind speed and gustiness) that could have deflated more dust in the Sahara itself. Because there is a threshold wind velocity for deflating soils (e.g., Gillette et al., 1980; Gillette, 1981; Gillette, 1984), dust generation and transport are linked to the wind speed distribution spectrum.

There is evidence that the variability of rainfall in the Sahel is linked to changes in meteorological features on a hemispheric or even global scale. Consequently, concurrent variations in other meteorological variables over and downwind of North Africa may influence the dust concentrations measured at Barbados as much as, or more than, the variation in the Sahelian rainfall. Indeed, Gray et al. (1992) have developed a predictive model for North Atlantic hurricanes that is based on African rainfall statistics. The frequency and intensity of hurricanes has diminished greatly since the beginning of the African drought (Gray et al., 1992). Both the Hadley circulation and the mid-tropospheric easterly jet are more intense during the Sahelian dry spells (Nicholson, 1986; Newell and Kidson, 1984). The intensification of these two features could cause greater dust generation and transport even in the absence of drought. Moreover, the overall meteorological changes may result in variations in the intensities of dust storms associated with strong winds over the Sahara as well as those associated with squall lines in the Sahel. Episodic disturbances (Nickling and Gillies, 1989) and the seasonality of climate in the source regions (Leinen, 1989) also may influence dust fluxes. The "Sahara vs. Sahel" argument may eventually be resolved by remote sensing. Unfortunately it is not easy to use satellites to identify sources of dust storms in a systematic way; although Saharan storms are relatively easy to identify, squall-line clouds tend to obscure those that occur in the Sahel. Indeed, it may be significant that the season of greatest dust transport in the tropical NAO coincides with the greatest frequency of squalls in the sub-Saharan region.

3.4.4.2 The role of humans

A further complicating factor is the role of humans in augmenting the deflation of soils. The vastly increased dust transport out of North Africa during the past 25 years seems to be associated with marginal lands in the Sahel that were brought into cultivation during a relatively moist climate phase in the 1950's and 1960's. Cash crops were introduced into this region and the raising of livestock was greatly increased due to the availability of water at natural sources and also from bore-holes that became widely available as a result of development programs. As a result of these activities, the soil surface was greatly disturbed over wide areas; these soils were highly susceptible to wind erosion once the drought began in the late 1960's. If the increased dust amounts that we have seen over the North Atlantic in the past few decades are due to the effects of drought augmented by land use practices, then the dust/drought relationship that we observe may not be

applicable to "natural" processes. Under such conditions, the dust that we seen in this region could be regarded as an anthropogenic pollutant. The same statement may be applicable to Asian dust sources. Thus, the present-day dust transport may not be representative of the transport over the geological record. This could explain some of the discrepancies between the present day measurements of dust transport and the aeolian record in the sediments.

3.4.4.3 Modeling dust generation and transport

In the preceding sections, we have seen that large scale dust events are associated with intense meteorological events: traveling disturbances in West Africa; severe frontal passages in Asia and monsoon events over the Arabian Sea. In this regard, dust transport is different from that of other "pollutants" which are emitted essentially continuously and transported according to the prevailing meteorological conditions. In contrast dust generation is a highly non-linear process and it occurs under meteorological conditions that are quite complex.

The complexity of the dust deflation processes is reflected in the difficulty that models have in replicating the global distribution of dust sources and the temporal and spatial distribution of dust transport (e.g., Joussaume, 1990; Tegen and Fung, 1994; Genthon, 1992; G. Rau, personal communication). The dust generation algorithms give heavy weight to rainfall and soil moisture conditions; consequently, they tend to show plumes emerging from deserts. For example, the present day dust transport (as indicated by AVHRR AOD) off west Africa is located much further south than the plumes produced in models. Also, in the models, the dust plume emerging from west Africa does not move much from season to season whereas in AVHRR the plume, in addition to being much further south of the model plume, undergoes a very large seasonal north-south migration, tracking the movement of the equatorial circulation and the ITCZ.

These comments are not intended to denigrate modeling in general or any model in particular, but rather to emphasize that it is a much more difficult task to model dust sources than other continental aerosol materials because of the many complex factors that are involved in dust generation. Furthermore, it will be difficult for modelers to incorporate the human factors such as land use in their algorithms. Yet humans may be the chief factor affecting present-day dust emission rates.

3.5 EFFECTS OF AEOLIAN INPUTS TO THE OCEANS

Wind transported dust has a significant impact on a number of sedimentary processes on geological time scales. As stated previously, the distribution of minerals in the oceans is clearly related to aeolian inputs. Saharan dust is also a major contributor to the soils on Barbados (Muhs et al., 1987, Muhs et al., 1990) and possibly the soils on Bermuda (Bricker and McKenzie, 1970) and other

islands in the Caribbean and the Bahamas (Muhs et al., 1990). Over the past decade, there has been increased interest in the role of aeolian transport to present-day ocean processes. Much of this interest was stimulated by the possible role of aeolian inputs as nutrients (Duce, 1986), especially the role of Fe (Martin, 1990; DiTullio et al., 1993; Donaghay et al., 1991; Duce and Tindale, 1991; Morel et al., 1991; Young et al, 1991).

The impact of mineral dust nutrient inputs to the oceans will depend on a number of factors including the composition of the particles and the solubility of the species of interest. The gross elemental composition of dust is close to that of average crustal material (see for example, Prospero, 1981a). The dust generation process does result in a fractionation of some elemental species (Schütz and Sebert, 1987; Eltayeb et al., 1993) but for many elements the fractionation factors are relatively minor in the small-particle size range that is important in long-range transport. There is evidence of some significant regional differences in some species such as the rare earths (Sholkovitz et al., 1993). A major consideration is the solubility of the aerosol species in sea water since this will affect the availability to biological processes. Solubility is a complex property that depends on the weathering history of the soil particle in the source environment, the chemical and physical processes that occur during the particle's lifetime in the atmosphere (especially the cycling of the particle through clouds), and subsequent processing in sea water. There are many aspects about particle solubility that are poorly understood (Lim and Jickells, 1990; Kersten et al., 1991; Maring and Duce, 1989; Maring and Duce, 1990; Zhou et al., 1992; Zhu et al., 1992; Zhu et al., 1993; Zhuang et al., 1992; Giusti et al., 1993). Nonetheless, aeolian inputs do seem to have a discernible impact on some particle and elemental distributions in the oceans (Helmers and Rutgers van der Loeff, 1993; Jickells et al., 1990; Kremling and Streu, 1993; Maring et al., 1989; Veron et al., 1993; Veron et al., 1994). Given the large temporal and spatial variability of dust inputs, especially the sensitivity to climate, we might expect the aeolian-related processes in ocean waters to vary accordingly. Also, to the extent that erosional processes are human-induced, the impact of aeolian inputs on surface water processes may have changed dramatically during the past century.

Based on budget estimates for ocean surface waters and estimates of atmospheric deposition, Duce (1986) suggested that atmospheric NO_3^- (principally in aerosols and precipitation) could serve as a nutrient and enhance primary productivity. A number of studies have supported this conclusion although the magnitude and importance of the effect is still debated (Fanning, 1989; Michaels et al., 1993; Owens et al., 1992; Willey and Paerl, 1993). If atmospheric NO_3^- inputs are important, then we must be concerned about anthropogenic impacts. Various estimates indicate that about half or more of the oxidized nitrogen compounds in the atmosphere are derived from anthropogenic emissions (Hameed and Dignon, 1992). Because most of the world's population is located in the northern hemisphere, pollutant effects will be much greater in the northern hemisphere

where over 90% of the global anthropogenic emissions of sulfur and nitrogen occur (Hameed and Dignon, 1992); we would expect the effects to be greatest over the NAO because of the density and proximity of sources on the surrounding continents.

3.6 CONCLUSIONS

Aerosol studies, coupled with satellite imagery, have established that mineral dust is a major aerosol component over many ocean areas; they show that the concentration of the dust is highly variable with time and with geographical location. Unfortunately, there have been very few studies of dust deposition processes to the ocean. Consequently, the estimates of input rates to the oceans are highly uncertain. In order to improve these estimates, it will be necessary to carry out an extensive program of deposition studies in many ocean regions. This will be difficult because of the highly sporadic nature of the dust deposition fluxes; a large fraction of the annual deposition takes place in a very small fraction of the precipitation events. In a one-year study of Saharan dust deposition in Miami (Prospero et al., 1987), 22% of the annual deposition occurred in one day and 68% in rain events that occurred during two dust episodes spread over a total of four days. In a study at Midway Island (Uematsu et al., 1985), about half of the annual deposition of dust occurred during a two week period. Because of the highly sporadic nature of these events, the concentration of mineral dust (or any other atmospheric component that is principally removed by precipitation) in ocean surface waters will be highly variable in time and space. Thus, in ocean regions where there is active dust transport, the mean concentration of dust in the underlying ocean could be relatively high but the concentration distribution could be highly non-uniform. To the extent that atmospheric deposition provides nutrients such as NO_3^- or iron, these inputs will occur as brief and infrequent pulses.

In the absence of actual deposition measurements, we must rely on estimates based on aerosol data; such estimates are crude because of the dearth of aerosol data from many ocean regions. This problem is especially severe for the southern oceans where there are huge regions for which there are essentially no measurements. Nonetheless, we would expect that the concentrations of mineral dust and other pollution-related species in these regions (and the associated deposition to the ocean) would be quite low.

While the measurement of dust deposition rates in precipitation is relatively easy (aside from the logistical problems of making the measurements in remote sites), the measurement of dry deposition rates is fundamentally difficult (Slinn, 1983; Hicks, 1986; Holsen and Noll, 1992; Nicholson, 1988). At present there is no generally accepted method for making quantitative estimates of the dry deposition

of dust to water surfaces under ambient conditions. This is a severe problem close to sources where the dust-laden air contains a relatively high concentration of large particles that have a high settling rate. At greater distances, as stated earlier, the dry deposition rate is believed to be a relatively small compared to wet deposition. However, this statement is based on the extrapolation of data from other types of aerosols and it has never been satisfactorily substantiated.

Studies of aeolian components in pelagic sediment cores have provided interesting and provocative results concerning the paleoclimate of the earth. However these interpretations are handicapped by a lack of physical substantiation for the underlying hypothesis. There is a critical need to study the physical processes involved in present day dust transport so that we can more accurately assess the paleoclimatic record in the sediments. In particular there is a major concern about the relationship of modern day dust transport conditions to those that obtained in the past. There is evidence that soil dust deflation has been greatly increased in modern times due to agriculture and poor land use practices. Consequently, if we wish to interpret the past climatic record in the ocean sediments, we must study soil deflation for conditions where soils are in an undisturbed state. In addition, if we are to assess the future trend in dust emissions and the possible impact on climate, it will be necessary to assess the deflation processes that apply to disturbed soils.

If the present-day deflation rates of soils are strongly impacted by human activities, then they must be regarded as a pollutant. There is evidence that dust can play a significant role in climate (Andreae, 1995; Duce, 1995) In order to assess the climate affects of dust, it will be necessary to model the dust distribution and properties. Further, if we are to anticipate future trends, it will be necessary to model the changes in dust transport that we might expect as a consequence of different climate, population and land use scenarios. As pointed out earlier, dust generation is a highly nonlinear process that is very sensitive to the energetics of meteorological processes and to site-specific soil properties. Consequently this modeling task will be much more difficult than for other atmospheric pollutants.

Finally, if dust, pollutants and other continental emissions are having an impact on processes in the oceans, then the effects should be most readily observable over the northern hemisphere oceans, especially the North Atlantic.

3.7 ACKNOWLEDGMENTS

This work was supported by the National Science Foundation, Atmosphere/Ocean Chemistry Experiments (AEROCE) grants - ATM-8703411, ATM-9013125, ATM-8701292 and ATM-9012950.

3.8 REFERENCES

Ackerman, S. A. and S. K. Cox (1989) "Surface weather observations of atmospheric dust over the southeast summer monsoon region", *Meteorol. Atmos. Phys.*, **41**, 19–34.

Andreae, M. O. (1995) "Climatic effects of changing atmospheric aerosol levels", in A. Henderson-Sellers (ed) *World Survey of Climatology, Vol. 16, Future Climates of the World*, Elsevier, Amsterdam, (in press).

Arimoto, R., R. A. Duce, D. L. Savoie and J. M. Prospero (1992) "Trace elements in aerosol particles from Bermuda and Barbados: Concentrations, sources, and relationships to aerosol sulfate", *J. Atmos. Chem.*, **14**, 439–457.

Arimoto, R., B. J. Ray, R. A. Duce, A. D. Hewitt, R. Boldi and A. Hudson (1990) "Concentrations, sources, and fluxes of trace elements in the atmosphere of New Zealand", *J. Geophys. Res.*, **95**, 22,389–22,405.

Arimoto, R., R. A. Duce, B. J. Ray, J. D. Cullen, J. T. Merrill and W. G. Ellis Jr. (1995a) "Trace elements in the atmosphere over the North Atlantic", *J. Geophys. Res.*, **100**, 1199–1213.

Arimoto, R., R. A. Duce, D. L. Savoie, J. M. Prospero, R. Talbot, J. D. Cullen, U. Tomza, N. F. Lewis and B. J. Ray (1995b) "Relationship among aerosol constituents from Asia and the North Pacific during PEM-West (A)", *J. Geophys. Res.*, (accepted).

Bergametti, G., L. Gomes, G. Coude-Gaussen, P. Rognon and M. Le Coustumer (1989a) "African dust observed over Canary Islands: Source-regions identification and transport pattern for some summer situations", *J. Geophys. Res.*, **94**, 14,855–14,864.

Bergametti, G., A.-L. Dutot, P. Buat-Menard, R. Losno and E. Remoudaki (1989b) "Seasonal variability of the elemental composition of atmospheric aerosol particles over the northwestern Mediterranean", *Tellus*, **41B**, 353–361.

Bergametti, G., L. Gomes, E. Remoudaki, M. Desbois, D. Martin and P. Buat-Menard (1989c) "Present transport and deposition patterns of African dusts to the North Western Mediterranean", in M. Leinen and M. Sarnthein (eds) *Paleoclimatology and Paleometeorology: Modern and Past Patterns of Global Atmospheric Transport*, Kluwer Acad. Publ., Dordrecht, 227–252.

Betzer, P. R., K. L. Carder, R. A. Duce, J. T. Merrill, N. W. Tindale, M. Uematsu, D. K. Costello, R. W. Young, R. A. Feely, J. A. Breland, R. E. Bernstein and A. M. Greco (1988) "Long-range transport of giant mineral aerosol particles", *Nature*, **336**, 568–571.

Blank, M., M. Leinen and J. M. Prospero (1985) "Major Asian aeolian inputs indicated by the mineralogy of aerosols and sediments in the western North Pacific", *Nature*, **314**, 84–86.

Bricker, O. P. and F. T. Mackenzie (1970) "Limestones and red soils of Bermuda: Discussion", *Geol. Soc. Am. Bull.*, **81**, 2523–2524.

Buat-Menard, P. (1986) "The ocean as a sink for atmospheric particles", in P. Buat-Menard (ed) *The Role of Air-Sea Exchange in Geochemical Cycling*, D. Reidel, Norwell, MA., 165–183.

Carder, K. L., R. G. Steward, P. R. Betzer, D. L. Johnson and J. M. Prospero (1986) "Dynamics and composition of particles from an aeolian input event to the Sargasso Sea", *J. Geophys. Res.*, **D91**, 1055–1066.

Carlson, T. N. and J. M. Prospero (1972) "The large-scale movement of Saharan air outbreaks over the northern equatorial Atlantic", *J. Appl. Meteorol.*, **11**, 283–297.

Chester, R. (1986) "The marine mineral aerosol", in P. Buat-Menard (ed) *The Role of Air-Sea Exchange in Geochemical Cycling*, Reidel, 443–476.

Chester, R. and K. J. T. Murphy (1990) "Metals in the marine atmosphere", in R. W. Furness and P. S. Rainbow (eds) *Heavy Metals in the Marine Environment*, CRC Press, Boca Raton, 27–49.

Chung, Y.-S. (1992) "On the observation of yellow sand (dust storms) in Korea", *Atmos. Environ.*, **26A**, 2743–2749.

Crutzen, P. J. and M. O. Andreae (1990) "Biomass burning in the tropics: Impact on atmospheric chemistry and biogeochemical cycles", *Science*, **250**, 1669–1678.

d'Almeida, G. A. and L. Schütz (1983) "Number, mass and volume distributions of mineral aerosols and soils of the Sahara", *J. Clim. Appl. Meteorol.*, **22**, 233–243.

De Angelis, M. D. and A. Gaudichet (1991) "Saharan dust deposition over Mont Blanc (French Alps) during the last 30 years", *Tellus*, **43B**, 61–75.

Delany, A. C., A. C. Delany, D. W. Parkin, J. J. Griffin, E. D. Goldberg and B. E. F. Reimann (1967) "Airborne dust collected at Barbados", *Geochim. Cosmochim. Acta*, **31**, 885–909.

Dessens, J. and P. Van Dinh (1990) "Frequent Saharan dust outbreaks north of the Pyrenees: A sign of climatic change?", *Weather*, **45**, 327–333.

DiTullio, G. R., D. A. Hutchins and K. W. Bruland (1993) "Interaction of iron and major nutrients controls phytoplankton growth and species composition in the tropical North Pacific Ocean", *Limnol. Oceanogr.*, **38**, 495–508.

Donaghay, P. L., P. S. Liss, R. A. Duce, D. R. Kester, A. K. Hanson, T. Villareal, N. W. Tindale and D. J. Gifford (1991) "The role of episodic atmospheric nutrient inputs in the chemical and biological dynamics of oceanic ecosystems", *Oceanography*, **4**, 62–70.

Duce, R. A. (1986) "The impact of atmospheric nitrogen, phosphorus, and iron species on marine biological productivity", in P. Buat-Manard (ed) *The Role of Air-Sea Exchange in Geochemical Cycling*, Reidel, Dordrecht, 497–528.

Duce, R. A. (1995) "Sources, distributions, and fluxes of mineral aerosols and their relationship to climate", in R. J. Charlson and J. Heintzenberg (eds) *Dahlem Workshop on Aerosol Forcing of Climate*, May, 1994, Berlin, 43–72.

Duce, R. A. and N. W. Tindale (1991) "Atmospheric transport of iron and its deposition in the ocean", *Limnol. Oceanogr.*, **36**, 1715–1726.

Duce, R. A., P. S. Liss, J. T. Merrill, E. L. Atlas, P. Buat-Menard, B. B. Hicks, J. M. Miller, J. M. Prospero, R. Arimoto, T. M. Church, W. Ellis, J. N. Galloway, L. Hansen, T. D. Jickells, A. H. Knap, K. H. Reinhardt, B. Schneider, A. Soudine, J. J. Tokos, S. Tsunogai, R. Wollast and M. Zhou (1991) "The atmospheric input of trace species to the world ocean", *Glob. Biogeochem. Cycles*, **5**, 193–259.

Ellis, W. G., Jr., R. Arimoto, D. L. Savoie, J. T. Merrill, R. A. Duce and J. M. Prospero (1993) "Aerosol selenium at Bermuda and Barbados", *J. Geophys. Res.*, **98**, 12,673–12,685.

Eltayeb, M. A. H., R. E. Van Grieken, W. Maenhaut and H. J. Annegarn (1993) "Aerosol-soil fractionation for Namib Desert samples", *Atmos. Environ.*, **27A**, 669–678.

Fanning, K. A. (1989) "Influence of atmospheric pollution on nutrient limitation in the ocean", *Nature*, **339**, 460–463.

Galloway, J. N., D. L. Savoie, W. C. Keene, and J. M. Prospero (1993) "The temporal and spatial variability of scavenging ratios for nss sulfate, nitrate, methanesulfonate and sodium in the atmosphere over the North Atlantic Ocean", *Atmos. Environ.*, **27A**, 235–250.

Gao, Y., R. Arimoto, M. Y. Zhou, J. T. Merrill and R. A. Duce (1992a) "Relationships between the dust concentrations over Eastern Asia and the remote North Pacific", *J. Geophys. Res.*, **97**, 9867–9872.

Gao, Y., R. Arimoto, R. A. Duce, D. S. Lee and M. Y. Zhou (1992b) "Input of atmospheric trace elements and mineral matter to the Yellow Sea during the spring of a low-dust year", *J. Geophys. Res.*, **97**, 3767–3777.

Gaudichet, A., R. Lefevre, A. Gaudry, B. Ardouin, G. Lambert and J. M. Miller (1989) "Mineralogical composition of aerosols at Amsterdam Island", *Tellus*, **41B**, 344–352.

Genthon, C. (1992) "Simulations of the long range transport of desert dust and sea-salt in a general circulation model", in S. E. Schwartz and W. G. N. Slinn (eds) *Precipitation Scavenging and Atmospheric-Surface Exchange, Vol. 3, Hemisphere*, Washington, 1783–1794.

Giusti, L., Y.-L. Yang, C. N. Hewitt, J. Hamilton-Taylor and W. Davison (1993) "The solubility an partitioning of atmospherically derived trace metals in artificial and natural waters: A review", *Atmos. Environ.*, **27A**, 1567–1578.

Golitsyn, G. and D. A. Gillette (1993) "Introduction: A joint Soviet-American experiment for the study of Asian desert dust and its impact on local meteorological conditions and climate", *Atmos. Environ.*, **27A**, 2467–2470.

Gomes, L., G. Bergametti, G. Coude-Gaussen and P. Rognon (1990) "Submicron desert dusts: A sandblasting process", *J. Geophys. Res.*, **95**, 13,927–13,935.

Goudie, A. S. (1983) "Dust storms in space and time", *Prog. Phys. Geog.*, **7**, 502–530.

Goudie, A. S. and N. J. Middleton (1992) "The changing frequency of dust storms through time", *Climatic Change*, **20**, 197–225.

Gray, W. M., C. W. Landsea, P. W. Mielke Jr. and K. J. Berry (1992) "Predicting Atlantic seasonal hurricane activity 6–11 months in advance", *Weather and Forecasting*, **7**, 440–455.

Hameed, S. and J. Dignon (1992) "Global emissions of nitrogen and sulfur oxides in fossil fuel combustion 1970–1986", *J. Air Waste Manage. Assoc.*, **42**, 159–163.

Hamelin, B., F. E. Grousett, P. E. Biscaye, A. Zindler and J. M. Prospero (1989) "Lead isotopes in trade wind aerosols at Barbados: The influence of European emissions", *J. Geophys. Res.*, **94**, 16,243–16,250.

Helmers, E. and M. M. Rutgers van der Loeff (1993) "Lead and aluminium in Atlantic surface waters (50°N to 50°S) reflecting anthropogenic and natural sources in aeolian transport", *J. Geophys. Res.*, **98**, 20,261–20,273.

Hicks, B. B. (1986) "Measuring dry deposition: A re-assessment of the state of the art", *Water Air Soil Pollut.*, **30**, 75–90.

Holsen, T. M. and K. E. Noll (1992) "Dry deposition of atmospheric Particles: Application of current models to ambient data", *Environ. Sci. Tech.*, **26**, 1807–1815.

Iwasaka, Y., H. Minoura and K. Nagaya (1983) "The transport and spacial scale of Asian dust-storm cloud: A case study of the dust-storm event of April 1979", *Tellus*, **35B**, 189–196.

Jankowiak, I. and D. Tanre (1992) "Satellite climatology of Saharan dust outbreaks: Method and preliminary results", *J. Climate*, **5**, 646–656.

Jickells, T. D., W. G. Deuser, A. Fleer and C. Hemleben (1990) "Variability of some elemental fluxes in the western tropical Atlantic Ocean", *Oceanologica Acta*, **13**, 291–298.

Joussaume, S. (1990) "Three-dimensional simulations of the atmospheric cycle of desert dust particles using a general circulation model", *J. Geophys. Res.*, **95**, 1909–1941.

Karyampudi, V. M. and T. N. Carlson (1988) "Analysis and numerical simulations of the Saharan air layer and its effects on easterly wave disturbances", *J. Atmos. Sci.*, **45**, 3102–3136.

Kersten, M., M. Kriews and U. Förstner (1991) "Partitioning of trace metals released from polluted marine aerosols in coastal seawater", *Mar. Chem.*, **36**, 165–182.

Kotamarthi, V. R. and G. R. Carmichael (1993) "A modelling study of the long range transport of Kosa using particle trajectory methods", *Tellus*, **45B**, 426–441.

Kremling, K. and P. Streu (1993) "Saharan dust influenced trace element fluxes in deep North Atlantic subtropical waters", *Deep Sea Res.*, **40**, 1155–1168.

Lamb, P. J. and R. A. Peppler (1991) "West Africa", Chapter 5 in M. Glantz, R. W. Katz and N. Nicholls (eds) *Teleconnections Linking Worldwide Climate Anomalies*, Cambridge Univ. Press, London, 121–189.

Leinen, M. (1989) "The late Quaternary record of atmospheric transport to the northwest Pacific from Asia", in M. Leinen and M. Sarnthein (eds) *Paleoclimatology and Paleometeorology: Modern and Past Patterns of Global Atmospheric Transport*, Kluwer Acad. Publ., Dordrecht, 693–732.

Leinen, M. and M. Sarnthein (eds) (1989) *Paleoclimatology and Paleometeorology: Modern and Past Patterns of Global Atmospheric Transport*, Kluwer Acad. Publ., Dordrecht, 909 pp.

Leinen, M., J. M. Prospero, E. Arnold and M. Blank (1994) "Mineralogy of aeolian dust reaching the North Pacific Ocean, I. Sampling and Analysis", *J. Geophys. Res.*, **99**, 21,017–21,024.

Lim, B. and T. D. Jickells (1990) "Dissolved, particulate and acid-leachable trace metal concentrations in North Atlantic precipitation collected on the global change expedition", *Glob. Biogeochem. Cycles*, **4**, 445–458.

Littmann, T. (1991) "Dust storm frequency in Asia: Climatic control and variability", *Int. J. Climatology*, **11**, 393–412.

McDonald, W. F. (1938) *Atlas of Climatic Charts of the Oceans*, Weather Bureau, Department of Agriculture, Washington, DC., 60 pp.

Maring, H. B. and R. A. Duce (1989) "The impact of atmospheric aerosols on trace metal chemistry in open ocean surface waters, II, Copper", *J. Geophys. Res.*, **C94**, 1039–1045.

Maring, H. B. and R. A. Duce (1990) "The impact of atmospheric aerosols on trace metal chemistry in open ocean surface waters, III, Lead", *J. Geophys. Res.*, **C95**, 5341–5347.

Maring, H., C. Patterson and D. Settle (1989) "Atmospheric input fluxes of industrial and natural Pb from the westerlies to the mid-North Pacific", in J. P. Riley, R. Chester and R. A. Duce (eds) *Chemical Oceanography, Vol. 10*, Academic Press., London, 84–105.

Martin, J. H. (1990) "Glacial-interglacial CO_2 change: The iron hypothesis", *Paleoceanography*, **5**, 1–13.

Merrill, J. T. (1989) "Atmospheric long-range transport to the Pacific Ocean", in J. P. Riley, R. Chester and R. A. Duce (eds) *Chemical Oceanography*, Vol. 10, Academic Press, London, 15–50.

Merrill, J. T., R. Bleck and L. Avila (1985) "Modeling atmospheric transport to the Marshall Islands", *J. Geophys. Res.*, **90**, 12,927–12,936.

Merrill, J. T., M. Uematsu and R. Bleck (1980) "Meteorological analyses of long range transport of mineral aerosol over the North Pacific", *J. Geophys. Res.*, **94**, 8584–8598.

Merrill, J. T., E. Arnold, M. Leinen and C. J. Weaver (1994) "Mineralogy of aeolian dust reaching the North Pacific, II: Relationship of mineral assemblages to atmospheric transport patterns", *J. Geophys. Res.*, **99**, 21,025–21,032.

Michaels, A. F., D. A. Siegel, R. J. Johnson, A. H. Knap and J. N. Galloway (1993) "Episodic inputs of atmospheric nitrogen to the Sargasso Sea: Contributions to new production and phytoplankton blooms", *Glob. Biogeochem. Cycles*, **7**, 339–351.

Middleton, J. J. (1985) "Effect of drought on dust production in the Sahel", *Nature*, **316**, 431–434.

Middleton, N. J. (1989) "Desert dust", in D. S. G. Thomas (ed) *Arid-Zone Geomorphology*, Belhaven Press, London, 262–283.

Middleton, N. J. (1990) "Wind erosion and dust-storm control", in A. S. Goudie (ed) *Techniques for Desert Reclamation*, John Wiley & Sons, New York, 87–108.

Middleton, N. J. (1991) "Dust storms in the Mongolian People's Republic", *J. Arid Environ.*, **20**, 287–297.

Morales, C. (1985) "The airborne transport of Saharan dust: A review", *Climate Change*, **9**, 219–241.

Morel, F. M. M., J. G. Reuter and N. M. Price (1991) "Iron nutrition of phytoplankton and its possible importance in the ecology of ocean regions with high nutrient and low biomass", *Oceanography*, **4**, 56–61.

Muhs, D. R., C. A. Bush, K. C. Stewart, T. R. Rowland and R. C. Crittenden (1990) "Geochemical evidence of Saharan dust parent material for soils developed on quaternary limestones of Caribbean and western Atlantic islands", *Quaternary Res.*, **33**, 157–177.

Muhs, D. R., R. C. Crittenden, J. H. Rosholt, C. A. Bush and K. C. Stewart (1987) "Genesis of marine terrace soils, Barbados, West Indies: evidence from mineralogy and geochemistry", *Earth Surface Processes and Landform*, **12**, 605–618.

Newell, R. E. and J. W. Kidson (1984) "African mean wind changes between Sahelian wet and dry periods", *J. Climatol.*, **4**, 27–33.

Nicholson, K. W. (1988) "The dry deposition of small particles: a review of experimental measurements", *Atmos. Environ.*, **22**, 2653–266.

Nicholson, S. E. (1985) "The spatial coherence of African rainfall anomalies: Interhemispheric teleconnections", *J. Clim. Appl. Meteorol.*, **25**, 1365–1381.

Ott, S.-T., A. Ott, D. W. Martin and J. A. Young (1991) "Analysis of a trans-Atlantic Saharan dust outbreak based on satellite and GATE data", *Mon. Weather Rev.*, 1832–1850.

Owens, N. J. P., J. N. Galloway and R. A. Duce (1992) "Episodic atmospheric nitrogen deposition to oligotrophic oceans", *Nature*, **357**, 397–399.

Pèwè, T. L. (ed) (1981) "Desert dust: Origin, characteristics and effect on man", *Spec. Pap. Geol. Soc. Am.*, **186**, 303 pp.

Prodi, F., G. Santachiara and F. Olioski (1983) "Characterization of aerosols in marine environments (Mediterranean, Red Sea, and Indian Ocean)", *J. Geophys. Res.*, **88**, 10,957–10,968.

Prospero, J. M. (1981a) "Aeolian transport to the World Ocean", in C. Emiliani (ed) *The Sea, Vol. 7, The Oceanic Lithosphere*, Wiley Interscience, New York, 801–974.

Prospero, J. M. (1981b) "Arid regions as sources of mineral aerosols in the marine atmosphere", in T. L. Pewe (ed) *Geological Society of America Special Paper 186*, Boulder, Colorado, 11–26.

Prospero, J. M. (1985) "Records of past climates in deep sea sediments", *Nature*, **315**, 279–280.

Prospero, J. M. (1990) "Mineral aerosol transport to the North Atlantic and North Pacific: the impact of African and Asian sources", in A. H. Knap (ed) *The Long-Range Atmospheric Transport of Natural and Contaminant Substances*, Kluwer Acad. Publ., Dordrecht, 59–86.

Prospero, J. M. and T. N. Carlson (1972) "Vertical and areal distribution of Saharan dust over the western equatorial North Atlantic Ocean", *J. Geophys. Res.*, 77, 5255–5265.

Prospero, J. M. and R. T. Nees (1986) "Impact of the North African drought and El Niño on mineral dust in the Barbados trade wind", *Nature*, **320**, 735–738.

Prospero, J. M., R. A. Glaccum and R. T. Nees (1981) "Atmospheric transport of soil dust from Africa to South America", *Nature*, **289**, 570–572.

Prospero, J. M., R. T. Nees and M. Uematsu (1987) "Deposition rate of particulate and dissolved aluminum derived from Saharan dust in precipitation at Miami, Florida", *J. Geophys. Res.*, **92**, 14,723–14,731.

Prospero, J. M., M. Uematsu and D. L. Savoie (1989) "Mineral aerosol transport to the Pacific Ocean", in J. P. Riley, R. Chester, and R. A. Duce (eds) *Chemical Oceanography, Vol. 10*, Academic Press, London, 187–218.

Prospero, J. M., D. L. Savoie, R. Arimoto and F. Huang (1993) "Long-term trends in African mineral dust concentrations over the western North Atlantic: Relationship to North African rainfall", *Eos Trans. AGU*, 74(43), 146. Fall Meeting of the American Geophysical Union, San Francisco, CA, December 6–10, 1993.

Pye, K. (1987) *Aeolian Dust and Dust Deposits*, Academic Press, London, 334 pp.

Rao, C. R. N., L. L. Stowe, E. P. McClain and J. Sapper (1988) "Development and application of aerosol remote sensing with AVHRR data from the NOAA Satellites", in P. V Hobbs and M. P. McCormick (eds) *Aerosols and Climate*, A. Deepak Publishing, Hampton, Virginia, 69–79.

Rea, D. K. (1994) "The paleoclimatic record provided by aeolian deposition in the deep sea - The geologic history of wind", *Rev. Geophysics*, **32**, 159–195.

Reheis, M. C. and R. Kihl (1995) "Dust deposition in southern Nevada and California 1984–1989: Relations to climate, source area and source lithology", *J. Geophys. Res.*, **100**, 8893–8918.

Samthein, M., J. Thiede, U. Pflaumann, H. Erkenkeuser, D. Fütterer, B. Koopmann, H. Lange and E. Seibold (1982) "Atmospheric and oceanic patterns off Northwest Africa during the past 25 million years", in U. Von Rad, K. Linz, M. Samthein and E. Seibold (eds) *Geology of the Northwest African Continental Margin*, 545–604.

Savoie, D. L., J. M. Prospero and R. T. Nees (1987) "Nitrate, non-sea-salt sulfate, and mineral aerosol over the northwestern Indian Ocean", *J. Geophys. Res.*, **92**, 933–942.

Savoie, D. L., J. M. Prospero and E. S. Saltzman (1989a) "Non-sea-salt sulfate and nitrate in trade wind aerosols at Barbados: Evidence for long-range transport", *J. Geophys. Res.*, **94**, 5069–5080.

Savoie, D. L., J. M. Prospero and E. S. Saltzman (1989b) "Nitrate, non-sea-salt sulfate and methanesulfonate over the Pacific Ocean", in J. P. Riley, R. Chester and R. A. Duce (eds) *Chemical Oceanography, Vol. 10*, Academic Press, London, 219–250

Savoie, D. L., J. M. Prospero, S. J. Oltmans, W. C. Graustein, K. K. Turekian, J. T. Merrill and H. Levy II (1992) "Sources of nitrate and ozone in the marine boundary layer of the tropical North Atlantic", *J. Geophys. Res.*, **97**, 11,575–11,589.

Savoie, D. L., R. Arimoto, J. M. Prospero, R. A. Duce, W. C. Graustein, K. K. Turekian, J. N. Galloway and W. C. Keene (1995) "Marine biogenic and anthropogenic contributions to non-sea-salt sulfate in the marine boundary layer over the North Atlantic Ocean, *J. Geophys. Res.*, (in review).

Schütz, L. and M. Sebert (1987) "Mineral aerosols and source identification", *J. Aerosol Sci.*, **18**, 1–10.

Schütz, L. W., J. M. Prospero, P. Buat-Menard, R. A. C. Carvalho, A. Cruzado, R. Harriss, N. Z. Heidam and R. Jaenicke (1990) "The long-range transport of mineral aerosols: Group report", in A. H. Knap (ed) *The Large-Scale Atmospheric Transport of Natural and Contaminant Substances*, Chapter 10, Kluwer Acad. Publ., Dordrecht, 197–229.

Scott, B. C. (1981) "Modeling of atmospheric wet deposition", in S. J. Eisenreich (ed) *Atmospheric Pollutants in Natural Waters*, Butterworth, Stoneham, MA., 3–22.

Sholkovitz, E. R., T. M. Church and R. Arimoto (1993) "Rare earth element composition of precipitation, precipitation particles, and aerosols", *J. Geophys. Res.*, **98**, 20,587–20,599.

Slinn, W. G. N. (1983) "Air-to-sea transfer of particles", in P. S. Liss and W. G. N. Slinn (eds) *Air-Sea Exchange of Gases and Particles*, D. Reidel, Hingham, Mass., 299–405.

Swap, R., M. Garstang, S. Graco, R. Talbot and P. Kallberg (1992) "Sahara dust in the Amazon basin", *Tellus*, **44B**, 133–149.

Takayama, Y. and T. Takashima (1986) "Aerosol optical thickness of yellow sand over the Yellow Sea derived from NOAA satellite data", *Atmos. Environ.*, **20**, 631–638.

Talbot, R. W., R. C. Harriss, V. Browell, G. L. Gregory, D. I. Sebacher and S. M. Beck (1986) "Distribution and geochemistry of aerosols in the tropical North Atlantic troposphere: Relationship to Saharan dust", *J. Geophys. Res.*, **91**, 5173–5182.

Tanre, D. and M. Legrand (1991) "On the satellite retrieval of Saharan dust optical thickness over land: Two different approaches", *J. Geophys. Res.*, **96**, 5221–5227.

Taylor, S. R. and S. M. McLennan (1985) *The Continental Crust: Its Composition and Evolution*, Blackwells, Oxford, England, 312 pp.

Tegen, I. and I. Fung (1994) "Modeling of mineral dust in the atmosphere: Sources, transport, and optical thickness", *J. Geophys. Res.*, **99**, 22,897–22,914.

Tsunogai, S., T. Suzuki, T. Kurata and M. Uematsu (1985) "Seasonal and areal variation of continental aerosol in the surface air over the western North Pacific region", *J. Oceanogr. Soc. Japan*, **41**, 427–434.

Uematsu, M. (1987) "Study of the continental material transported through the atmosphere to the ocean", *J. Oceanogr. Soc. Japan*, **43**, 395–401.

Uematsu, M., R. A. Duce and J. M. Prospero (1985) "Deposition of atmospheric mineral particles to the North Pacific", *J. Atmos. Chem.*, **3**, 123–138.

Uematsu, M., R. A. Duce, J. M. Prospero, L. Chen, J. T. Merrill and R. L. McDonald (1983) "Transport of mineral aerosol from Asia over the North Pacific Ocean", *J. Geophys. Res.*, **88**, 5343–5352.

Veron, A., T. M. Church, C. C. Patterson and A. R. Flegal (1994) "Distribution and use of stable lead isotopes to characterize the sources and circulation of lead in North Atlantic surface waters", *Geochim. Cosmochim. Acta*, **58**, 3199–3206.

Veron, A., T. M. Church, C. C. Patterson, Y. Erel and J. T. Merrill (1992) "Continental origin and industrial sources of trace metals in the northwest Atlantic troposphere", *J. Atmos. Chem.*, **14**, 339–351

Veron, A. J., T. M. Church, A. R. Flegal, C. C. Patterson and Y. Erel (1993) "Response of lead cycling in the surface Sargasso Sea to changes in tropospheric input", *J. Geophys. Res.*, **98**, 18,269–18,276.

Westphal, D. L., O. B. Toon and T. N. Carlson (1987) "A two-dimensional numerical investigation of the dynamics and microphysics of Saharan dust storms", *J. Geophys. Res.*, **92**, 3027–3049.

Westphal, D. L., O. B. Toon and T. N. Carlson (1988) "A case study of mobilization and transport of Saharan dust", *J. Atmos. Sci.*, **45**, 2145–2175.

Whelpdale, D. M. and J. L. Moody (1990) "Large-scale meteorological regimes and transport process", in A. H. Knap and M. S. Marston (eds) *The Large-Scale Atmospheric Transport of Natural and Contaminant Substances*, D. Reidel, Dordrecht, Holland, 3–36.

Willey, J. D. and H. W. Paerl (1993) "Enhancement of chlorophyll a production in Gulf Stream surface seawater by synthetic versus natural rain", *Mar. Biol.*, **116**, 329–334.

Young, R. W., K. L. Carder, P. R. Betzer, D. K. Costello, R. A. Duce, G. R. DiTullio, N. W. Tindale, E. A. Laws, M. Uematsu, J. T. Merrill and R. A. Feely (1991) "Atmospheric iron inputs and primary productivity: Phytoplankton responses in the North Pacific", *Glob. Biogeochem. Cycles*, **5**, 119–134.

Zhou, M., N. Lu, J. Miller, F. Parungo, C. Nagamoto and S. Yang (1992) "Characterization of atmospheric aerosols and of suspended particles in seawater in the western Pacific Ocean, *J. Geophys. Res.*, **97**, 7553–7567.

Zhu, X. R., J. M. Prospero, F. J. Millero, D. L. Savoie and G. W. Brass (1992) "The solubility of ferric ion in marine mineral aerosol solutions at ambient relative humidities", *Mar. Chem.*, **38**, 91–107.

Zhu, X., J. M. Prospero, D. L. Savoie, F. J. Millero, R. G. Zika and E. S. Saltzman (1993) "Photoreduction of Fe(III) in marine mineral aerosol solutions", *J. Geophys. Res.*, **98**, 9039–9046.

Zhuang, G., Z. Yi, R. A. Duce and P. R. Brown (1992) "Link between iron and sulfur cycles suggested by detection of Fe(II) in remote marine aerosols", *Nature*, **355**, 537–539.

4 Riverine Transfer of Particulate Matter to Ocean Systems

PEDRO J. DEPETRIS

4.1 INTRODUCTION

A few transport modes deliver particulate phases from the continents to world oceans: riverine, wind-borne, and glacial. Although the magnitude of the mass of sediments thus transferred is largely open to speculation, earth scientists have proposed for many years now that rivers are undoubtedly the major suppliers of sediments to world oceans. But only in terms of geological time scales is it correct to assume that the sediment load of world rivers reach deep pelagic plains. Floodplains, coastal marshlands, estuaries, and continental shelves temporarily store most of the detrital load discharged by rivers. Exceptions are those instances where a particular river mouth is close to the shelf break, or where currents (e.g., tidal, longshore) are strong enough to displace suspended particles into submarine canyons. From there, by means of gravity-controlled mass flows (i.e., slumps, slides, turbidity currents), particles are episodically carried down, towards the deep sea platform.

The difficulties inherent to the assessment of global mass transport of sediment are such that estimates on world riverine transport are at best tentative, and subjected to permanent revision (e.g., Clarke and Washington, 1924; Livingstone, 1963; Holeman, 1968; Garrels and Mackenzie, 1971; Martin et al., 1980; Meybeck, 1982; Milliman and Meade, 1983; Degens et al., 1984; Degens et al., 1991; Milliman and Syvitski, 1992). In spite of its debatable nature, riverine sediment transport is presently considered as the best known one of the three modes mentioned above.

Several years ago, scientific evidence indicated that wind-borne dust was effectively transported across oceans, presumably from arid land areas in the jet stream (e.g., Delany et al., 1967; Ferguson et al., 1970). The implications relative to marine sedimentation were obvious, and Windom (1969) suggested that the North and South Pacific, and the Central Atlantic presently receive as much as 25 to 75% of their detrital phases from atmospheric dust fallout. Aeolian transport also determines, for instance, a quartz-rich (> 10%) band in the sediments of the eastern Atlantic, which is unequivocally linked to the expanded arid region

Particle Flux in the Ocean
Edited by V. Ittekkot, P. Schäfer, S. Honjo and P. J. Depetris

formed by the Sahara Desert and the Sahel (Kolla et al., 1979). Hence, despite uncertainties, the preponderance of wind-borne input of various elements and compounds to certain oceanic regions is now clearly established, being particularly important in shelf areas and in semi-enclosed seas, such as the Mediterranean (Martin et al., 1989). Additionally, with obvious implications on the global cycling of carbon, recent research stresses the likely significance of dust fallout on the wind-driven biological pump, which sequesters fresh organic matter from the upper ocean to the deep sea (Ittekkot, 1993). A detailed treatment on the biogeochemical significance of the wind-borne flux of particles to world oceans can be found in elsewhere in this volume (this volume, Chapter 3).

Although ice-rafting has been a significant mode of sediment transport in the geological past (e.g., during the last glacial maximum 18 ky B.P.) minera-logical evidence of its present-day effect is limited to high-latitude sea-floor sediments (e.g., Biscaye, 1965; Griffin et al., 1968; Kolla et al., 1979). Bottom current winnowing of relict glacial detritus turns difficult the present-day quantitative assessment of the significance of ice-rafting as a mechanism of sediment transport.

Beyond the fact that there are certain oceanic areas where wind-borne material and ice-rafting attain relevance, in terms of global mass transport rate, rivers are surely the major sediment suppliers to the world ocean. So far, Garrels and Mackenzie's (1971) rough estimate, that rivers supply 90%, ice-rafting an additional 7%, and desert winds and submarine discharges less than 1% of the global sediment transport, still stands essentially unmodified.

4.2 RIVERINE TRANSPORT OF CARBON AND MINERALS

Sediments transported to ocean systems are derived from rocks exposed at the Earth's surface, subjected to ceaseless alteration. Chemical, physical, and biological processes are involved in the weathering of rocks, the first of which has been identified as the most significant (e.g., Garrels and Mackenzie, 1971; Drever, 1988). Continental runoff consists not only of water and inorganic particulate and dissolved phases. It includes the end products of the destruction and decomposition of the vegetation cover, as well as organic matter produced within the boundaries of continental aquatic systems.

Continental denudation is now understood as occurring between two extreme regimes: *transport-limited* and *weathering-limited* (Stallard and Edmond, 1983). In a transport-limited regime, mechanical erosion is less intense, all weatherable minerals would contribute to the dissolved load in proportion to their abundance, and the end-products of weathering would accumulate. In opposition, denudation in a weathering-limited regime is highly selective, with the majority of dissolved phases contributed by the most reactive minerals while the less reactive ones are

transported away by physical erosion (e.g., Drever and Zobrist, 1992). Chemical reactions involved in rock-water interactions, however, are now perceived as complex processes, with implications of biogeochemical significance, such as the CO_2 consumption during the global cycling of carbon (e.g., Kempe, 1984; Probst et al., 1994). But weathering will not be treated here beyond these remarks. The following considerations are restricted to the solid residues which, from the moment of their formation, endure dissemination by the main agent of erosion: flowing water.

Rivers transport sediment as bed load and in suspension. The significance of the former is deficiently known at present, mainly due to difficulties inherent to its quantification. It is commonly assumed that most large rivers transport sediment along the river bed in subordinate amounts (typically, < 10% of their total load), although there are indications that some rivers may transport a significantly higher proportion. Not only is the contribution made by bed load to the total sediment load of rivers open to conjecture but also its occurrence, whether bed load transport takes place continuously or primarily during flooding events.

The bed load of large rivers is made up of coarse-fraction sediment, which is deposited in the lower reaches of rivers, in beaches, off the mouths of estuaries, and in continental platforms. Quartz, feldspar, and rock fragments constitute, for example, most of South America's modern sands (from rivers and beaches). Their quantitative study has allowed Potter (1994) to distinguish three major families of South American sands which, ultimately, are the result of the interaction of climate and the distribution and activity of major continental tectonic elements. Despite wide geomorphic dissimilarities three large groups or families were defined: a) a group of immature lithic arenites that covers about 30% of South America, mostly supplied by Andean volcanic and metamorphic sources; b) a quartz-rich cratonic association that covers about 62% of the eastern side of the continent; and c) a molasse association, reportedly of a transitional nature, which covers about 8% of the continent and occurs as a separation of the previous two groups. Eventually, coarse sediments bypass continental shelves carrying along the signature of their source: the plate tectonic significance of the light mineral fraction found in offshore studies has been put forward by Maynard (1984), and Yerino and Maynard (1984).

Whereas the coarse end product of weathering is mostly retained on or near continents, the fine-grained particles of the suspended load (silt- and clay-size sediments) comprise the bulk of the sediment mass entering the coastal zone. Subjected to very specific processes (Eisma and Cadeé, 1991), these fine-grained particles normally coagulate upon encountering the low salinities of the upper estuary (Kranck, 1981). The resulting flocs are then transported and settled in the middle and lower estuary (e.g., Gibbs et al., 1989). Once river sediment has been deposited in an estuary, it may remain there for hundreds and even thousands of years. Meade (1982) estimated that probably less than 5% of the sediment

reaching the coastal zone in the Atlantic seaboard of the United States, is transferred to the continental shelf or to the deep sea.

In the Arabian Sea, where sediment sources were identified several years ago (Goldberg and Griffin, 1970), most of the annual input of lithogenic material of ca. 0.2×10^{15} g remains in estuaries, deltas, and continental shelves. Trap measurements have shown that only 2 to 3% of such flux reaches the deeper parts of the sea (Ramaswamy et al., 1991). At any rate, the transfer of sediments from continents to the deep sea appears to occur mostly in a pulse-like mode. Currents and climatic events (sometimes exceptional) are the main factors ruling such transfer of fine sediments from the continental platform to the continental rise and, eventually, in episodic fashion, to the deep sea platform (e.g., Ittekkot et al., 1991). The sediments thus accumulated in the sea-floor, carry along the distinct biogeochemical signature of their source (e.g., Reemtsma et al., 1990, 1993).

Milliman and Meade (1983) calculated an annual global riverine discharge of 13.5×10^{15} g, by extrapolating average sediment yields over large regions with similar relief. More recently, the international project "Transport of Carbon and Minerals in Major World Rivers" which, with the assistance of SCOPE and UNEP, was carried out under the leadership of Prof. Egon T. Degens (Degens et al., 1991), put forth a global annual figure of ca. 16.0×10^{15} g. A more recent analysis suggests that before the propagation of dam construction which the world has witnessed since the beginning of the second half of this century, rivers probably discharged about 20.0×10^{15} g (Milliman and Syvitski, 1992).

Data gathered in many world rivers, representing most of the global runoff reaching the seas and oceans (Degens et al., 1991), support the estimation that about 0.23×10^{15} g are particulate organic carbon (POC) (Ittekkot and Laane, 1991). Figure 4.1 shows the continental contributions of total suspended solids (TSS) and POC loads. Asiatic rivers are the main TSS and POC suppliers to world oceans whereas African rivers are the least significant sources.

4.3 FACTORS CONTROLLING SEDIMENT YIELD

The sediment load of a river is dependent upon its drainage area (Figure 4.2). Clearly, larger drainage basins deliver higher sediment loads to world oceans. Also, as it has been known for some time, sediment yields exhibit an inverse relationship with drainage areas, with the smaller mountainous basins being the sources of highest yields (Meybeck et al., 1989).

Recently, Milliman and Syvitski (1992) have analyzed data from 280 rivers discharging to the ocean, and have concluded that sediment loads/yields are a log-linear function of basin area and maximum elevation of the river basin. These major controlling variables are followed in order of importance by precipitation and runoff, which affect sediment discharge to a lesser extent.

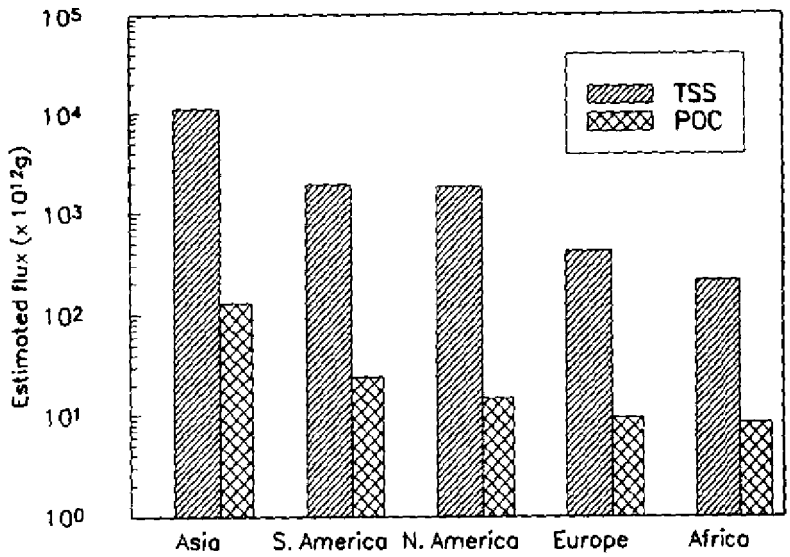

Figure 4.1 Estimated continental flux of total suspended sediments (TSS) and particulate organic carbon (POC). Basic data from Degens et al. (1991).

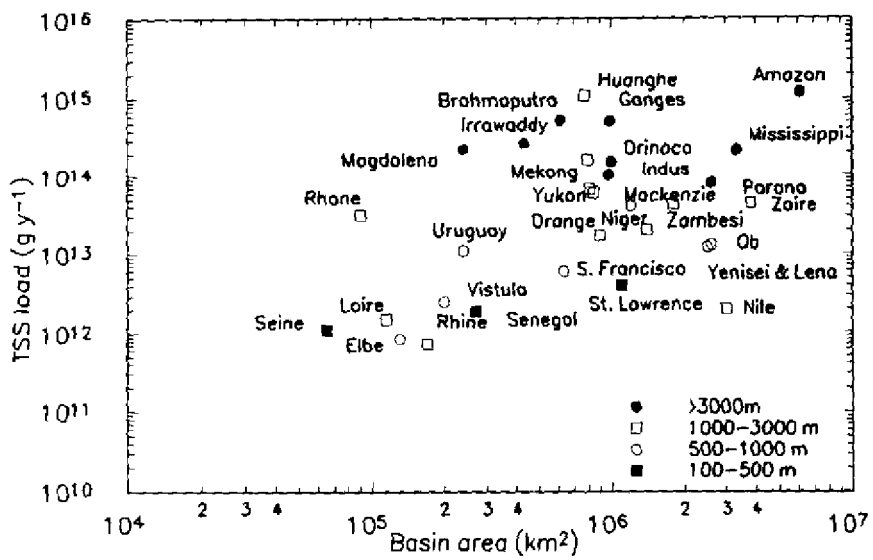

Figure 4.2 Plot of basin area vs. TSS load of some major world rivers. Rivers have been divided into classes according to their relief, following the criteria used by Milliman and Syvitski (1992). Most basic data from Degens et al. (1991).

The total specific exporting capacity of river systems (i.e., sediment yield plus dissolved solids yield) is more difficult to evaluate inasmuch other factors (e.g., geology, climate) attain relevance in the control of the specific yield of dissolved phases. Figure 4.3 shows that some world rivers, whose total specific export is dominated by the dissolved fraction, occur in a wide variety of climates (runoff) and reliefs. Also, it implies that mechanical denudation is not only dominant in high-relief basins (e.g., Ganges, Brahmaputra, Paraná) but also in lowland (e.g., Senegal) or upland drainage basins (e.g., Uruguay).

Milliman and Syvitski (1992) have also stressed the importance of small mountainous rivers, many placed in active continental margins (e.g., western South and North America), whose sediment fluxes may have been grossly underestimated. By virtue of a greater impact of episodic events (i.e., flash floods and earthquakes) during high stands of sea level, and due to the narrow shelves associated with these active margins, the sediment loads from such drainage basins are likely to be transferred to the deep sea. Moreover, a recent study indicated that an ephemeral desert river in Israel (a stream-type which, incidentally, abounds along most of the North and South America active margins) is, on average, as much as 400 times more efficient at transporting very high rates

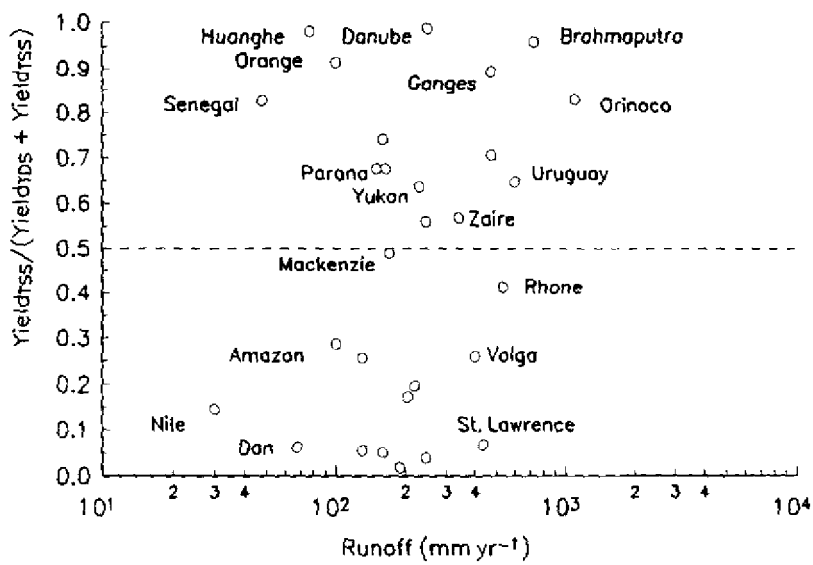

Figure 4.3 Variation of $Yield_{TSS}/(Yield_{TDS} + Yield_{TSS})$ as a function of runoff (discharge/basin area) in a group (some labeled) of world rivers. The broken line separates the fields of mechanical denudation dominance (upper) and chemical denudation dominance (lower). Most basic data from Degens et al. (1991).

of coarse sediment bed load than its perennial counterparts in humid zones (Laronne and Reid, 1993).

Obviously climate, along with other factors, such as geology, and human activity have also been identified as important variables controlling sediment load, particularly in certain areas (e.g., southern Asia) where high erosion rates also reflect deforestation and over-farming (Milliman and Syvitski, 1992).

Particulate organic matter in world rivers appears to vary between 1 and 8% of the total suspended matter. Rivers with low TSS concentrations (< 15 mg l^{-1}) exhibit the highest relative POC contents, whereas rivers with a high TSS concentration (500–1500 mg l^{-1}) display the lowest relative POC contents (ca. 1.6 mgC l^{-1}) (Ittekkot and Laane, 1991). It is still difficult to interpret, however, the factors controlling POC yield in world rivers inasmuch as those rivers with a high TSS yield are likely to transport mostly carbon from allochtonous sources (e.g., soil-derived), whereas rivers with a low TSS yield are exporting organic matter which may be mainly produced by autochtonous sources. This can be inferred from the results gathered by the SCOPE/UNEP International Carbon Project, which show that rivers with moderate TSS concentrations have a higher proportion of the so-called labile particulate organic carbon (carbohydrates and proteins) in their POC load than rivers with high TSS concentrations (Ittekkot and Laane, 1991). Turbid waters limit light penetration and thus may hinder primary production, a riverine source of labile particulate carbon.

Although significant progress has been accomplished in the last decade, more research is needed to fully appraise the factors controlling erosion and sediment routing within drainage basins under various climatic conditions and on various rock substrata.

4.4 THE ROLE OF EXCEPTIONAL CLIMATIC EVENTS

In contrast with what appears to be a relatively continuous chemical denudation, the removal of sedimentary materials from the continents is often perceived as mostly occurring in a pulse-like manner. In other words, discrete events, such as earthquakes or unusually intense climatic anomalies may play a major role in removing the bulk of the sediment load from the continents to the oceans. Many references in the scientific literature indicate that this is decidedly the case in small to medium-size drainage basins, where there is unequivocal evidence that occasional, intense events, transport more sediments than years or even decades of normal functioning of the erosive processes.

The response of large river systems to short-lived intense phenomena is more difficult to interpret. The Amazon, for one, being the largest river on Earth, exhibits a peculiar behavior in connection with the yearly flood (Meade et al., 1985). The mean slope of the flood wave on the river surface is smaller during the

rising stages than during the falling ones. As a result, the Amazon stores sediment in its lower reaches during rising stages and actually resuspends the previously stored sediment during falling ones. Superimposed on its highly regular hydrograph (Richey et al., 1989), the pattern of storage and remobilization damps out the extreme values of high and low sediment discharge, keeping the mean annual discharge of suspended sediment in the lower Amazon between 1.1×10^{15} and 1.3×10^{15} g. If this mechanism also applies during exceptional positive flow departures from the mean is open to verification. In the Amazon, such deviations mostly occur on a 2- to 3-year time scale and are coupled to the positive phase of the El Niño-Southern Oscillation (ENSO) phenomenon (Richey et al., 1989), the so-called La Niña or cold event (Philander, 1990; Díaz and Kiladis, 1992).

The Paraná River is also coupled to the ENSO phenomenon but, in opposition to the Amazon, its positive discharge anomalies appear to be correlated with ENSO negative (or warm) phases. This teleconnection was originally described by Mossman (1924), and then by Bliss (1928), at the onset of the studies on the general characteristics and mechanisms of remote atmospheric and oceanic responses associated with sea level pressure and sea surface temperature fluctuations in the equatorial Pacific.

The 1982 ENSO event was specially persistent, had an exceptionally large amplitude, and its effects appeared in an unusually large area (e.g., Quiroz, 1983). Heavy rainfall in the upper Paraná drainage basin triggered an exceptional flood which significantly altered the biogeochemical functioning of the River (Depetris and Kempe, 1990). Despite the fact that during the once-in-a-century flood of 1982/83, the Paraná River reached record peak discharges of over 60000 $m^3 s^{-1}$ at Corrientes (the long-term mean is ca. 15700 $m^3 s^{-1}$), TSS transport did not increase significantly and POC transport even seemed to decrease during the ENSO-triggered flood. Although TDS appeared to be subjected to dilution in inverse proportion to the additional discharge, dissolved inorganic and organic carbon (DIC and DOC) experienced marked increases in transport rates which were probably linked to increased remineralization of organic matter in the floodplain, and mobilization of refractory material from the floodplain and from soils upstream.

However, during the receding stage of the 1982/83 flood, TSS concentration increased markedly (Depetris and Kempe, 1993), suggesting remobilization of TSS similar to that described for the Amazon (Meade et al., 1985); i.e., due to changes in the water-surface slope, suspended sediment was apparently stored during the rising stages of the river and resuspended during the falling river stage.

The mean surface slope of the Paraná mainstream in the lower 200 km is ca. 1.2×10^{-5} m m^{-1}. The effect of the flood wave on water surface slope of the Paraná during the 1982/83 ENSO-triggered flood was investigated in a 320 km-stretch of the lower Paraná River (Figure 4.4). The graph represents the variability of the gage height at Paraná (600 km from the mouth) during 1983, and the variation in

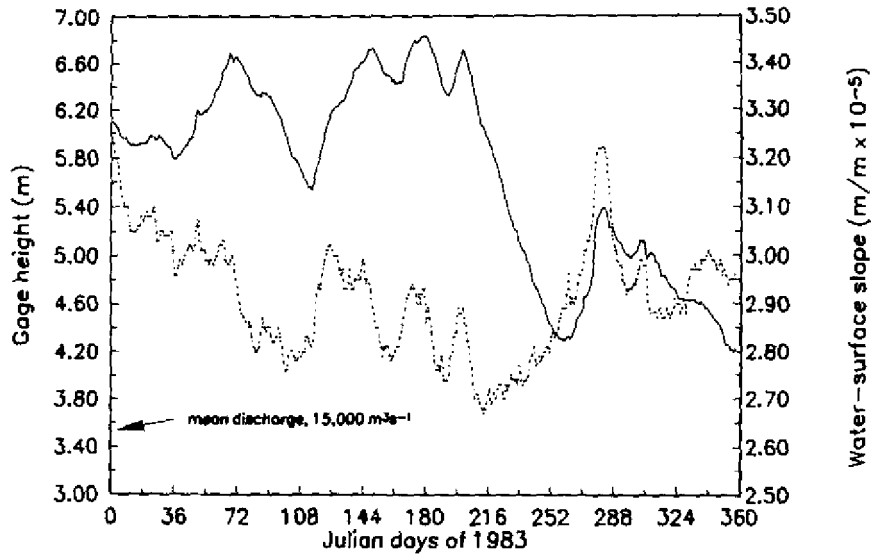

Figure 4.4 Time-dependent variation of gage height (discharge) and water-surface slope (broken line) in the Paraná River during the ENSO-triggered flood of 1982/83. Water-surface slopes were calculated between the cities of Paraná (600 km upstream from the mouth) and San Pedro (280 km upstream from the mouth). The arrow indicates the gage height value corresponding to mean river discharge.

water-surface slopes in the reach comprised between the cities of Paraná and San Pedro (280 km upstream from the mouth). Clearly, increasing discharges (gage heights) generate a decreasing trend in the water-surface slopes and, conversely, decreasing discharges result in higher water-surface slopes. However, the process appears as a complex one, with a clear hysteretic condition (Figure 4.5) which implies that the Paraná River deposits and resuspends sediments in pulses. Lower slopes mean decreasing water velocities and, possibly, sedimentation, whereas slightly steeper slopes denote higher water velocities and resuspension.

In addition to this effect, which is probably common to a number of large world rivers, the Paraná receives most of its water discharge from the upper Paraná drainage basin, which normally contributes a subordinate proportion of the TSS load. Figure 4.6 shows results of TSS load measurements performed in the upper Paraná River, the Paraguay River, in the receiving section of the Paraná which joins both rivers at the City of Corrientes, and at the Paraná-Santa Fe cross-section. The trends of the individual rating curves in the graph suggest that under conditions of high runoff, the TSS flux could in fact decrease with increasing discharge. Such would be the case when the upper Paraná dilutes the Paraguay's

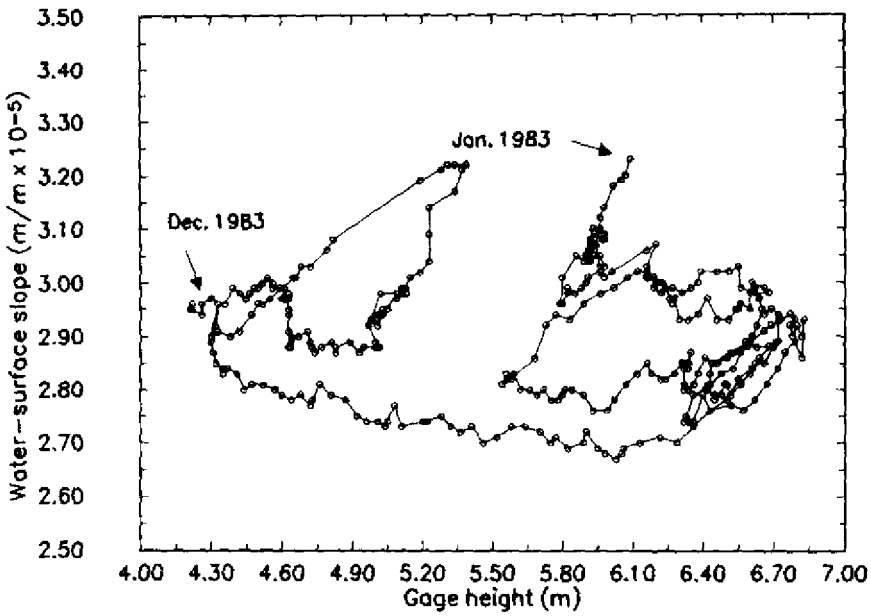

Figure 4.5 Variation of gage height and water-surface slope in the Paraná River during the ENSO-triggered flood of 1982/83 (see Figure 4.4). The hysteretic loop on the right side corresponds to an inverse relationship (sediment deposition?), whereas the one on the left depicts the direct relationship between both variables (sediment resuspension?).

TSS flux by supplying most of the water discharge (e.g., 70 – 80%) entering the Río de la Plata.

Continental sediment fluxes are controlled by global runoff. Discharge fluctuations during this century have been largely related to surface air temperature anomalies (Probst and Tardy, 1989). At any rate, evidence from the recent geological past (a 7000-year geological record for Mississippi River tributaries), indicates that extreme flooding is not necessarily associated to profound changes in climate. Rather, it has been parallel to moderate climatic changes (ca. 1 – 2 °C, and changes in mean annual precipitation of ca. 10 – 20%), which have caused adjustments in both, magnitudes and frequencies of floods (Knox, 1993).

The forecast for a doubled CO_2 climate scenario anticipates significant discharge increases in 25 out of 33 of the world's major rivers (Miller and Russell, 1992) and, most likely, a substantial alteration of the global sediment flux from continents to world oceans.

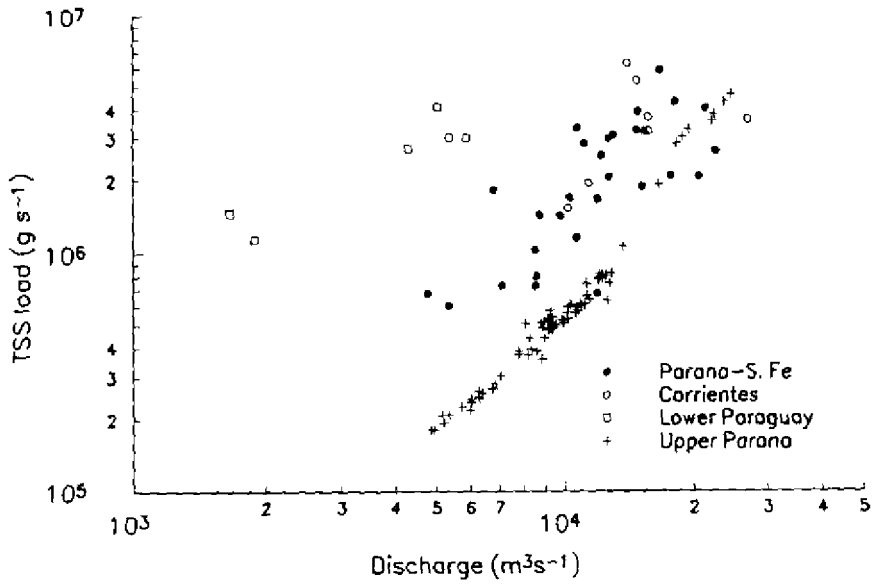

Figure 4.6 TSS depth-integrated measurements at different cross-sections of the Paraná River drainage basin. Note the agreement between the measurements performed at Corrientes (ca. 1200 km upstream from mouth) and those at Paraná-Santa Fe (ca. 500 km upstream from mouth). Also worthy of attention are the high TSS fluxes delivered by the Paraguay River. Data produced by the UNDP/Argentine Government ARG. 31 Project.

4.5 AN ASSESSMENT OF SEDIMENT INPUTS INTO THE SW ATLANTIC: A CASE STUDY

Both, the advent of the revolutionary idea of sea-floor spreading in the early 1960's, and the birth of the broader concept of global plate tectonics by the end of that decade, stimulated studies on the sediment distribution in world oceans (e.g., Ewing and Ewing, 1967). From the onset, the SW Atlantic was particularly amenable to such studies, partly due to the clear climatic signal (Stevenson and Cheng, 1969) exhibited by the carbonate-free, carbon-rich sediments being accumulated in nearly horizontal layers at a significant rate in the abyssal plain of the Argentine Basin (3 to 7 cm ky^{-1}, Turekian and Stuiver, 1964). But mainly because the sedimentary deposits in this region attain thicknesses exceeding 3000 m, and appear as markedly current-controlled (Ewing et al., 1964).

Biscaye (1965) studied the mineralogy and sedimentation of Recent deep-sea sediments in the Atlantic Ocean and concluded that most deep-sea clay is unequivocally detritus from the continents, and a useful indicator of sediment provenance, inasmuch as the component mineral species exhibit relatively restricted loci of continental origin. *In situ* mineral formation on the ocean bottom was qualified as unimportant in the Atlantic.

Among other several meaningful and interesting conclusions, Biscaye (1965) clearly proposed that the fine-fraction mineralogy of the surface sediment of the Argentine Basin, in the western South Atlantic Ocean, was sufficiently diverse from the sediment contiguous to the mouth of the Río de la Plata to eliminate it as a major Recent sediment source for that basin. Further, he proposed the southern Argentine continental shelf, the Scotia Ridge, and the Weddell Sea as more likely sources of fine-fraction sediment transported into the abyssal plain. Moreover, he identified the Antarctic Bottom Water (AABW) as the probable agent transporting fine-fraction sediment from the Weddell Sea, perhaps as far north as the Brazil Basin.

Griffin et al. (1968) studied the distribution of clay minerals in the world Oceans. Using Biscaye's (1965) data they reached essentially the same conclusions for the southwestern Atlantic: the clay-size fraction (illite 40 – 50%, smectite 20 – 30%, kaolinite < 5 – 10%, and chlorite 10 – 30%) appears to be controlled to a large extent by the Antarctic continent, with its chlorite and illite-rich sediments, which are the source of ice rafted material to the southern Atlantic.

More than 20 years passed until the studies performed by Klaus and Ledbetter (1988) in the Argentine Basin by means of high-resolution seismic records (3.5 kHz echograms) revealed that sediment is supplied to the Argentine Basin principally by gravity-controlled mass flows off the mouth of the Río de la Plata, and that the sediment transported by the AABW from higher latitudes is, in fact, a secondary source. Sedimentary material from both sources is winnowed by strong AABW flow along the Argentine continental rise. Earlier works (Ewing et al., 1973) had already suggested that giant ripples and channels are the confirmation of the strong dependence of Argentine Basin sedimentation on moving water masses. As the AABW flow decreases, the fine-grained sediment fraction is deposited in the central abyssal plain as large, migrating mud waves. Klaus and Ledbetter (1988) also found evidence that most land-derived coarse sediment bypasses the continental shelf and rise by means of slides, turbidity currents, etc., and is finally deposited in the adjoining plain. A very extensive mass flow placed east of the Río de la Plata finally suggested that it was a major sediment source to the Argentine Basin.

A comparison is now possible, in light of the above mentioned findings, between the clay-size mineralogy determined in the Argentine Basin, and adjacent areas by Biscaye (1965) and Griffin et al.(1968), with that of possible riverine sediment sources to the SW Atlantic.

Conceivable sources include the Patagonian rivers, and the Antarctic Peninsula and adjacent islands. Along the Patagonian margin, a number of smaller rivers (Colorado, Negro, Chubut, Deseado, Shehuén-Chico, Santa Cruz, Coyle, and Gallegos) supply an additional 63 $km^3\ y^{-1}$ of water and an estimated sediment mass of ca. 40.0 x 10^{12} g y^{-1}. The Colorado River supplies a smectite-rich fine-fraction suite, with subordinate proportions of illite, chlorite, and kaolinite, whereas the Negro River delivers an illite-rich clay-size mineralogy, with lower proportions of smectite and chlorite + kaolinite (Irion and Depetris, unpublished data). Recent studies (Yoon et al., 1992) have confirmed the Antarctic Peninsula as a major source of illite-rich sediments. However, other Antarctic sources such as the South Shetland Islands, exhibit ample mineralogical variability in their weathering products.

Through the Río de la Plata, the Paraná and Uruguay drainage basins deliver water and sediment to the SW Atlantic, directly into the Confluence zone where the Brazil and Malvinas currents meet and intense mixing occurs, along the western boundary of the SW Atlantic Ocean. The Río de la Plata discharges ca. 615 $km^3\ y^{-1}$ of water and over 90.0 x 10^{12} g y^{-1} of sediment to the adjacent continental shelf (Depetris and Paolini, 1991).

Figure 4.7 compares the mean clay mineralogy for the SW Atlantic as reported by Biscaye (1965) and Griffin et al. (1968), with the mineral suite determined for

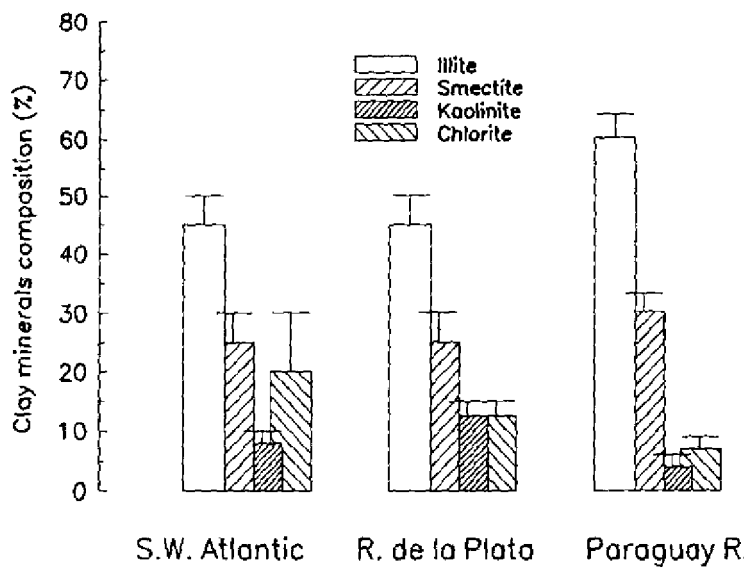

Figure 4.7 Mean clay mineralogy in the SW Atlantic (Biscaye, 1965; Griffin et al., 1968), the Río de la Plata (Depetris and Griffin, 1968), and the Paraguay River (Bertolino and Depetris, 1992). Bars depict estimated variability.

the Rio de la Plata and the Paraguay River. The latter, mainly by means of the effect of its Andean tributary, the Bermejo, reportedly supplies about 60% of the Paraná TSS load (i.e., ca. 48 x 10^{12} g y^{-1}). Aside from differences in the chlorite and kaolinite content, it is possible to conclude that the clay mineralogy of the fine fraction of surface sediments from the Argentine Basin and adjacent areas, is closely related to the material supplied by the Rio de la Plata, thus adding to the geophysical evidence supplied by Klaus and Ledbetter (1988) in the sense that the Rio de la Plata is a major sediment source to the SW Atlantic. The importance of wind-borne particles transported from arid Patagonia to the SW Atlantic remains to be investigated, but may be anticipated as also significant, provided the intense dominant westerlies that sweep the southern portion of South America are considered.

4.6 CONCLUDING REMARKS

Rivers are prominent sources of particles, which transfer their solid load from continents to world oceans. Since most large rivers are located along passive continental margins, a dominant portion of their sediment fluxes is retained at or near continental boundaries. However, there are indications that, subjected to the influence of exceptional events, rivers depart from their "usual" functioning and possibly modify their effect upon coastal seas. These pulses are probably effective ways, accessible to large riverine systems, to increase the transfer of particulate material to deep basins.

Milliman and Syvitski (1992) have pointed out that smaller mountainous rivers, along active margins, are far more likely to by-pass the associated narrow shelves and deliver a larger percentage of their fluxes to deeper ocean basins during both high and low stands of sea level.

Future research directed towards the assessment of the role of world rivers in the transfer of particulate material to the deep sea should address these aspects in more detail.

4.7 REFERENCES

Bertolino, S. R. A. and P. J. Depetris (1992) "Mineralogy of the clay-sized suspended load from headwater tributaries of the Paraná River: Bermejo, Pilcomayo, and Paraguay rivers", in E. T. Degens, S. Kempe, A. Lein, and Y. Sorokin (eds) *Interactions of Biogeochemical Cycles in Aqueous Systems, Part 7*, Mitt. Geol.-Paläont. Inst. Univ. Hamburg, 72, 19–31.

Biscaye, P. E. (1965) "Mineralogy and sedimentation of recent deep-sea clay in the Atlantic Ocean and adjacent seas and oceans", *Geol. Soc. America Bull.*, 76, 803–832.

Bliss, E. W. (1928) "Correlations of world weather and a formula for forecasting the height of the Paraná River", *Mem. Royal Meteor. Soc.*, **II**, 39–45.

Clarke, F. W., and H. W. Washington (1924) "The composition of the Earth's crust", *US Geol. Surv. Prof. Paper*, **127**, 117.

Degens, E. T., S. Kempe and V. Ittekkot (1984) "Monitoring carbon in world rivers", *Environment*, **26**, 29–33.

Degens, E. T., S. Kempe and J. E. Richey (1991) "Summary: Biogeochemistry of major world rivers", in E. T. Degens, S. Kempe, and J. E. Richey (eds) *Biogeochemistry of Major World Rivers*, SCOPE 42, Wiley, Chichester, 323–347.

Delany, A. C., A. C. Delany, D. W. Parkin, J. J. Griffin, E. D. Goldberg and B. E. F. Reimann (1967) "Airborne dust collected at Barbados", *Geochim. Cosmochim. Acta*, **31**, 885–909.

Depetris, P. J. and J. J. Griffin (1968) "Suspended load in the Río de la Plata drainage basin", *Sedimentology*, **11**, 53–60.

Depetris, P. J. and S. Kempe (1990) "The impact of the El Niño 1982 event on the Paraná River, its discharge and carbon transport", *Palaeogeogr., Palaeoclim., Palaeoecol. (Global Planet. Change Sect.)*, **89**, 239–244.

Depetris, P. J. and S. Kempe, S. (1993) "Carbon dynamics and sources in the Paraná River", *Limnol. Oceanogr.*, **38**, 382–395.

Depetris, P. J. and J. E. Paolini (1991) "Biogeochemical aspects of South American rivers: The Paraná and the Orinoco", in E. T. Degens, S. Kempe, and J. E. Richey (eds) *Biogeochemistry of Major World Rivers*, SCOPE 42, Wiley & Sons, Chichester, 105–125.

Díaz, H. F. and G. N. Kiladis (1992) "Atmospheric teleconnections associated with the extreme phases of the Southern Oscillation", in H. F. Díaz and V. Markgraf (eds) *El Niño. Historical and Paleoclimatic Aspects of the Southern Oscillation*, Cambridge University Press, Cambridge, 7–28.

Drever, J. I. (1988) *The Geochemistry of Natural Waters*, 2nd. ed., Prentice Hall, Englewood Cliffs, 437 pp.

Drever, J. I. and J. Zobrist (1992) "Chemical weathering of silicate rocks as a function of elevation in the southern Swiss Alps", *Geochim. Cosmochim. Acta*, **56**, 3209–3216.

Eisma, D. and G. C. Cadeé (1991) "Particulate matter processes in estuaries", in E. T. Degens, S. Kempe, and J. E. Richey (eds) *Biogeochemistry of Major World Rivers*, SCOPE 42, Wiley & Sons, Chichester, 283–296.

Ewing, M., G. Carpenter, C. Windisch and J. I. Ewing (1973) "Sediment distribution in the oceans: the Atlantic", *Geol. Soc. Amer. Bull.*, **84**, 71–88.

Ewing, J. I. and M. Ewing (1967) "Sediment distribution on the mid-ocean ridges with respect to spreading of the sea floor", *Science*, **156**, 1590–1591.

Ewing, M., W. J. Ludwig and J. L. Ewing (1964) "Sediment distribution in the oceans: the Argentine basin", *J. Geophys. Res.*, **69**, 2003–2032.

Ferguson, W. S., J. J. Griffin and E. D. Goldberg (1970) "Atmospheric dust from the North Pacific - A short note on a long-range eolian transport", *J. Geophys. Res.*, **75**, 1137–1139.

Garrels, R. M. and F. T. Mackenzie (1971) *Evolution of Sedimentary Rocks*, W. W. Norton & Co., New York, 397 pp.

Gibbs, R. J., D. M. Tshudy, L. Konwar and J. M. Martin (1989) "Coagulation and transport of sediments in the Gironde Estuary", *Sedimentology*, **36**, 987–999.

Goldberg, E. D. and J. J. Griffin (1970) "The sediments of the northern Indian Ocean", *Deep-Sea Res.*, **17**, 513–537.

Griffin, J. J., H. Windom and E. D. Goldberg (1968) "The distribution of clay minerals in the World Ocean", *Deep-Sea Res.*, **15**, 433–459.

Holeman, J. N. (1968) "Sediment yield of major rivers of the world", *Water Resour. Res.*, **4**, 737–747.

Ittekkot, V. (1993) "The abiotically driven biological pump in the ocean and short-term fluctuations in atmospheric CO_2 contents", *Glob. Planet. Change.*, **8**, 17–25.

Ittekkot, V., and R. W. P. M. Laane (1991) "Fate of riverine particulate organic matter", in E. T. Degens, S. Kempe, and J. E. Richey (eds) *Biogeochemistry of Major World Rivers*, SCOPE 42, Wiley & Sons, Chichester, 233–243.

Ittekkot, V., R. R. Nair, S. Honjo, V. Ramaswamy, M. Bartsch, S. Manganini and B. N. Desai (1991) "Enhanced particle fluxes in Bay of Bengal induced by injection of fresh water", *Nature*, **351**, 385–387.

Kempe, S. (1984) "Sinks of the anthropogenically enhanced carbon cycle in surface fresh waters", *J. Geophys. Res.*, **89**, 4657–4676.

Klaus, A. and M. T. Ledbetter (1988) "Deep-sea sedimentary processes in the Argentine Basin revealed by high-resolution seismic records (3.5 kHz echograms), *Deep-Sea Res.*, **35**, 899–917.

Knox, J. C. (1993) "Large increases in flood magnitude in response to modest changes in climate", *Nature*, **361**, 430–432.

Kolla, V., P. E. Biscaye and A. F. Hanley (1979) "Distribution of quartz in Late Quaternary Atlantic sediments in relation to climate", *Quaternary Res.*, **11**, 261–277.

Kranck, K. (1981) "Particulate matter grain-size characteristics and flocculation in a partially mixed estuary", *Sedimentology*, **28**, 107–114.

Laronne, J. B. and I. Reid (1993) "Very high rates of bed load sediment transport by ephemeral desert rivers", *Nature*, **336**, 148–150.

Livingstone, D. A. (1963) "Chemical composition of rivers and lakes", *US Geol. Surv. Prof. Paper*, **440-G**, p. 64.

Martin, J.-M., D. Burton and D. Eisma (1980) *River Inputs to Ocean Systems*, UNEP-UNESCO, Switzerland, 384 pp.

Martin, J.-M., F. Elbaz-Poulichet, C. Guieu, M.-D. Loye-Pilot and G. Han (1989) "River versus atmospheric input of material to the Mediterranean sea: an overview", *Mar. Chem.*, **28**, 159–182.

Maynard, J. B. (1984) "Composition of plagioclase feldspar in modern deep sea sands: relationship to tectonic setting", *Sedimentology*, **31**, 493–502.

Meade, R. H. (1982) "Sources, sinks, and storage of river sediment in the Atlantic drainage of the United States", *Jour. Geol.*, **90**, 235–252.

Meade, R. H., T. Dunne, J. E. Richey, U. Santos and E. Salati (1985) "Storage and remobilization of suspended sediment in the lower Amazon River of Brazil", *Science*, **228**, 488–490.

Meybeck, M. (1982) "Carbon, nitrogen and phosphorous transport by major world rivers", *Am. Jour. Sci.*, **282**, 401–501.

Meybeck, M., D. V. Chapman and R. Helmer, R. (eds) (1989) *Global Freshwater Quality. A First Assessment*, WHO/UNEP, Blackwell Reference, Oxford, 306 pp.

Miller, J. R., and G. L. Russell (1992) "The impact of global warming on river runoff", *J. Geophys. Res.*, **97**, 2757–2764.

Milliman, J. D. and R. H. Meade (1983) "World-wide delivery of river sediments to the oceans", *Jour. Geol.*, **91**, 1–21.

Milliman, J. D. and J. P. M. Syvitski (1992) "Geomorphic/tectonic control of sediment discharge to the ocean: The importance of small mountainous rivers", *Jour. Geol.*, **100**, 525–544.

Mossman, R. C. (1924) "Indian monsoon rainfall in relation to South American weather, 1875-1914", *Mem. Ind. Meteor. Dept.*, **23**, 157–242.

Philander, S. G. (1990) *El Niño, La Niña, and the Southern Oscillation*, Academic Press, San Diego, 289 pp.

Potter, P. E. (1994) "Modern sands of South America: Composition, provenance and global significance" *Geol. Rundsch.*, **83**, 212–232.

Probst, J. L., J. Mortatti and Y. Tardy (1994) "Carbon river fluxes and weathering CO_2 consumption in the Congo and Amazon river basins", *Applied Geochem.*, **9**, 1–13.

Probst, J. L. and Y. Tardy (1989) "Global runoff fluctuations during the last 80 years in relation to world temperature change", *Am. Jour. Sci.*, **289**, 267–285.

Quiroz, R. S. (1983) "The climate of the "El Niño" winter of 1982–83 - A season of extraordinary climatic anomalies", *Month. Weather Rev.*, **111**, 1685–1706.

Ramaswamy, V., R. R. Nair, S. Manganini, B. Haake and V. Ittekkot (1991) "Lithogenic fluxes to the deep Arabian Sea measured by sediment traps", *Deep-Sea Res.*, **38**, 169–184.

Reemtsma, T., B. Haake, V. Ittekkot, R. R. Nair and U. H. Brockmann (1990) "Downward flux of particulate fatty acids in the central Arabian Sea", *Mar. Chem.*, **29**, 183–202.

Reemtsma, T., V. Ittekkot, M. Bartsch and R. R. Nair (1993) "River inputs and organic matter fluxes in the northern Bay of Bengal: fatty acids", *Chem. Geol.*, **103**, 55–71.

Richey, J. E., C. Nobre and C. Deser (1989) "Amazon River discharge and climate variability: 1903 to 1985", *Science*, **246**, 101–103.

Stallard, R. F. and J. M. Edmond (1983) "Geochemistry of the Amazon: 2. The influence of geology and weathering environment on the dissolved load", *J. Geophys. Res.*, **88**, 9671–9688.

Stevenson, F. J. and C. N. Cheng (1969) "Amino acid levels in the Argentine Basin sediments: Correlation with Quaternary climatic changes", *Jour. Sed. Petrol.*, **39**, 345–349.

Turekian, K. K. and M. Stuiver (1964) "Clay- and carbonate-accumulation rates in three South Atlantic deep-sea cores", *Science*, **146**, 55–56.

Windom, H. L. (1969) "Atmospheric dust records in permanent snowfields: Implications to marine sedimentation", *Geol. Soc. Amer. Bull.*, **80**, 761–782.

Yerino, L. N. and J. B. Maynard (1984) "Petrography of modern marine sands from the Perú-Chile Trench and adjacent seas", *Sedimentology*, **31**, 83–89.

Yoon, H. I., M. W. Han, B. K. Park, S. J. Han and J. K. Oh (1992) "Distribution, provenance, and dispersal pattern of clay minerals in the surface sediments, Bransfield Strait, Antarctica", *Geo-Marine Letters*, **12**, 223–227.

5 Particle Flux in the Ocean: Oceanographic Tools

VERNON L. ASPER

5.1 INTRODUCTION

The flux of particles at any point in the ocean can be considered to be a product of their abundance and sinking speed. Therefore, to fully understand the dynamics of particle flux, it is important to also investigate these other parameters. In some cases where it is impractical to measure flux directly, it may be possible to estimate flux by determining size-specific abundances and sinking speeds and calculating flux as a product of these two parameters. In this chapter, the factors determining particle flux will be discussed, including technologies in use to measure each of the three parameters directly and the limitations associated with each.

5.2 DIRECT FLUX MEASUREMENTS

Conceptually, particle flux at a given point can be determined by simply placing a receptacle (sediment trap) in the water column to intercept the particles as they settle. Flux is then calculated by the mass collected divided by the collecting area and the time over which the collection was made. These devices have been in use for several decades and have provided valuable insight into the rates, timing and mechanisms of material and energy transfer in the oceans (Staresinic et al., 1978; 1982; Knauer et al., 1979; Reynolds et al., 1980; Bruland et al., 1981; Baker and Milburn, 1982; Simoneit et al., 1986; Deuser et al., 1988; Honjo and Doherty, 1988; Kempe and Jennerjahn, 1988; Wassmann and Heiskanen, 1988; Knauer and Asper, 1989; Ittekkot et al., 1991; Wefer and Fischer, 1991; Asper et al., 1992; Hargrave et al., 1994). Two of the most popular designs in common use today are the time-series trap designed by Honjo (Honjo and Doherty, 1988, Figure 5.1) and the MULTITRAP designed by Knauer and Martin (Knauer et al., 1979, Figure 5.2). These two designs illustrate the range of complexity in designs available to address a broad spectrum of research questions.

Particle Flux in the Ocean
Edited by V. Ittekkot, P. Schäfer, S. Honjo and P. J. Depetris

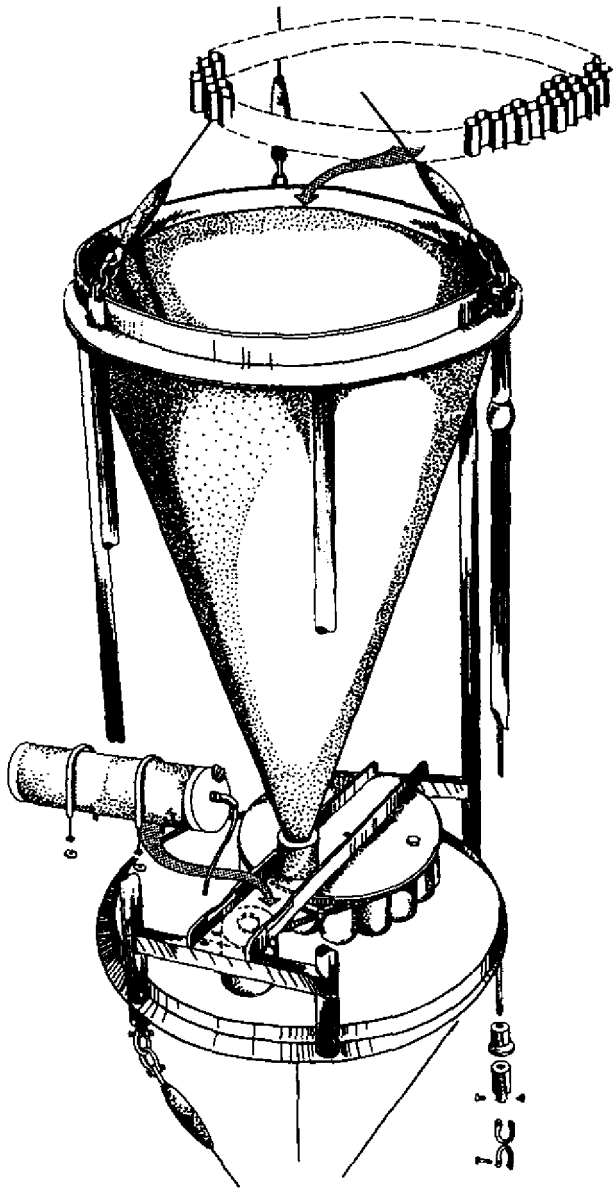

Figure 5.1 Drawing of the PARFLUX Mark V time-series sediment trap showing the collecting funnel, rotating sample collector, baffle and computerized controller. The trap opening of this model is 1.2 m^2, but more recent versions have been reduced to 0.5 m^2 (reproduced from Honjo and Doherty, 1988; reproduced by permission of the authors).

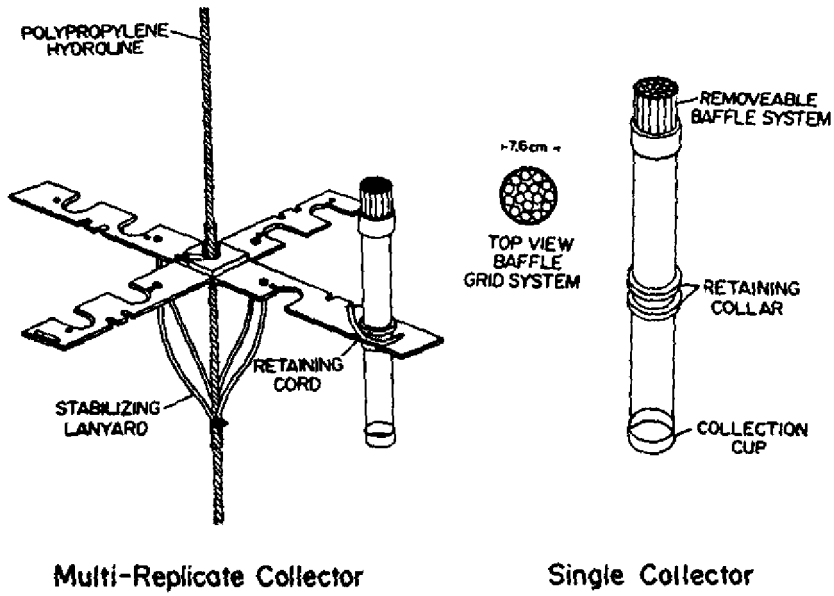

Figure 5.2 Drawing of the VERTEX MULTITRAP system showing an individual collector, support structure and baffle system. The simple design of this system assures high reliability and has gained it wide acceptance in a variety of applications (from Knauer et al., 1979; reproduced by permission of the authors).

In practice, expectations of accurate interception of the rain of particles are complicated by several factors which, in some cases, threaten to invalidate the results (Knauer and Asper, 1989). The three most important considerations are: 1) hydrodynamic bias in collection efficiency caused by the flow of water relative to the trap opening, 2) contamination of the sample by organisms which settle into the trap and die (referred to as swimmers), thus artificially enhancing the collection, and 3) remineralization or degradation of the particles during the interval of time between their arrival in the trap and retrieval of the sample. Investigators intent on collecting the most accurate samples possible must deal with each of these effects in turn and address them either in the design of the deployment or with specific technologies.

5.2.1 HYDRODYNAMIC BIAS

The most direct means of minimizing bias due to hydrodynamic effects are those which reduce the flow of water relative to the trap opening (Asper, 1988; Knauer and Asper, 1989). This can be accomplished by designing the deployment so that the trap is positioned in relatively tranquil water, in environments such as the deep-sea, trenches or restricted basins such as the Black Sea (Honjo et al., 1987).

In cases where this is possible, it represents the best solution to minimizing this effect. In other cases, the choice of either a surface- or seafloor-tethered array can be made so as to minimize current shear between the trap and the surrounding water (Staresinic et al., 1978; 1982). For example, if a sample from 40 meters' depth below the surface in a 500 meter water column is desired, it would generally be better to deploy the trap from a surface rather than a bottom array because the difference in flow vectors between the surface and 40m can be expected to be less than that between 40m and 500m.

Numerous attempts have been made to calibrate or otherwise characterize the accuracy of trap collections, including studies performed in flumes (Gardner, 1980; Butman, 1986; Butman et al., 1986) and in the ocean (Bruland et al., 1981; Lorenzen et al., 1981; Jickells et al., 1987; Siegel et al., 1990; Buesseler, 1991; Asper et al., 1992; Gust et al., 1992; 1994). These studies show that traps appear to be collecting samples which are accurate to within a factor of two when deployed conservatively (Buesseler, 1991). Without some kind of absolute standard against which to compare trap results, however, most of these studies provide intercomparisons of the traps rather than actual calibrations (Knauer and Asper, 1989).

The only way to eliminate hydrodynamic bias is to remove any connection between the trap and any water stratum other than that which is to be sampled. Diercks and Asper (1993) describe a Neutrally Buoyant Sediment Trap (NBST) which consists of a platform with a buoyancy regulating system capable of maintaining the trap at a given depth and thus allowing it to drift freely with the current (Figure 5.3). This approach is similar to that of a hot-air balloon which is buoyed by the surrounding air, is not tethered to the ground, and which experiences no wind (Swallow, 1955; Davis, et al., 1992). Their approach to achieving neutral buoyancy is to use compressed air purge or flood a ballast tank in response to depth inputs from a pressure transducer. These inputs are processed by a microcomputer (Tattletale 5) which monitors the actual depth and the trend and compensates the trap's position accordingly.

While this solution addresses the hydrodynamic problem, it poses other problems including the need to track the platform continuously during its deployment and to recall it to the surface and locate it after the collection is complete. The Diercks and Asper (1993) solution to these problems was to install an acoustic release and ballast weight onto the platform to allow it to be tracked acoustically and to provide a backup recovery system in the event the on-board computer should fail. These requirements and the additional complexity of this system require an extra level of effort and cost which may not be warranted for routine use, but in cases where a calibration or uncompromised sample is required, the effort may be warranted (Knauer and Asper, 1989).

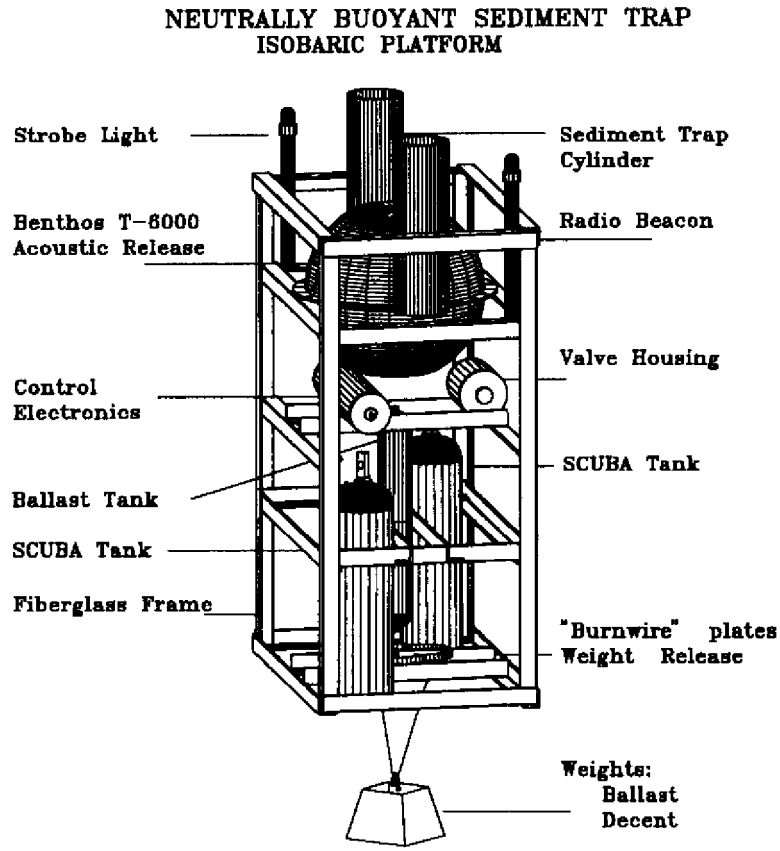

Figure 5.3 The neutrally buoyant sediment trap is intended to minimize hydrodynamic biases by reducing the flow of water relative to the trap opening. This is accomplished by having the trap float freely in the water with no attachments to either the sea surface or the sea floor. Neutral buoyancy is maintained by a microcomputer which varies the amount of water or air in a stainless steel ballast tank (Figure supplied by the authors, Diercks and Asper, 1993).

5.2.2 SWIMMERS

Because of the scarcity of solid surfaces in the ocean and because of the presence of the collected particles, plankton and nekton are often attracted to sediment traps. Once inside they may be killed through contact with the poison and thus contribute their remains to the sediment sample and artificially enhance its

contents (Lee et al., 1988; Karl and Knauer, 1989; Michaels et al., 1990). Most investigators deal with this problem by simply picking the remains of these organisms out of the sample (Karl and Knauer, 1989). This straightforward approach is complicated by the somewhat subjective judgement of which remains are those of swimmers and which are those of organisms which died a natural death and should be included in a sample of downward flux of particulate matter (Michaels et al., 1990). Most visible particles in these samples are the remains of organisms, many of which are known to naturally associate with settling particles, so these evaluations are not clearcut (Michaels et al., 1990). Another approach is to use a screen over the trap mouth to prevent swimmers from entering the trap interior (Karl and Knauer, 1989). These screens, however, are thought to provide an artificial "bottom" to the trap and thus reduce its aspect ratio (ratio of height to diameter) and therefore alter its hydrodynamic response to flow and allow particles to be scoured from sample by even weak currents. They may also break up large, settling aggregates and alter their sinking characteristics to the extent that they fail to contribute to the sample. For these reasons, screens have not seen widespread use although some investigators continue to use them in parallel with non-screened traps.

An elegant solution to the swimmer problem has been suggested by Peterson et al. (1993) who built a mechanical device to exclude swimmers from the sample without affecting the sample (Figure 5.4). This device consists of a dimpled sphere located at the base of the trap and just above the sample receptacle. Particles entering the trap accumulate on the upper surface of this sphere and are periodically transferred to the underlying sample cup by rotating the sphere. This device has been shown to be very effective in eliminating most large swimmers from the samples, but smaller organisms, whose abundance can be substantial, continue to be included. Also, portions of the sample are often retained by the sphere and returned to the upper, non-preserved portion of the trap as the sphere rotates, presenting them to the organisms residing there.

5.2.3 REMINERALIZATION/DECOMPOSITION OF THE SAMPLE

Many attempts have been made to find the ideal preservative to prevent microbial decomposition while not interfering with the analyses of interest (Manganini and Honjo, 1985; Lee et al., 1988). The most popular are mercuric chloride (Manganini and Honjo, 1985) and formalin, but others have been used with some success as well. In addition to reducing microbial activity, formalin has the advantage of preserving and hardening the chitinous portions of crustacean carapaces, which facilitates their removal. Regardless of the preservative, most investigators recover the supernatant fluid and analyze it for additions of substances from the particles.

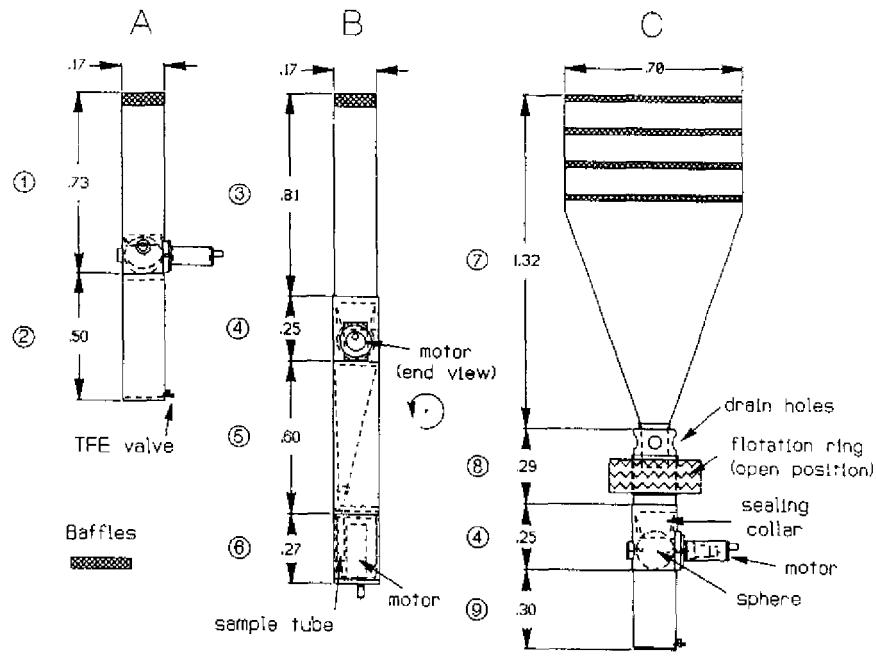

Figure 5.4 Schematic of indented rotating sphere (IRS) sediment traps. A. Prototype IRS valved trap. B. Narrowmouth valved trap with carousel subsampler. C. Widemouth valved trap which collects a single composite sample. Component key: 1 - combination baffled narrowmouth collector/IRS valve; 2 - single-sample accumulator; 3 - baffled, narrowmouth interceptor; 4 - IRS valve and motor; 5 - skewed funnel; 6 – 12 - sample carousel; 7 - baffled, widemouth collector; 8 - flush valve/adapter; 9 - short, single-sample accumulator (from Peterson et al., 1993; reproduced by permission of the authors).

5.3 PARTICLE ABUNDANCES

Determinations of total suspended mass can be made by filtration of large volumes of water, but when size-specific particle abundances are required, optical methods are generally employed (Costin, 1970; Sternberg et al., 1974; Bartz et al., 1978; Spinrad, 1986; Eisma et al., 1990; Agrawal and Pottsmith, 1994). Even the relatively straightforward task of water filtration requires attention to detail because of the possible artifacts. The most accurate determinations are those performed at low vacuum pressures, with the final rinsing and filter recovery operations performed on a laminar flow bench to minimize airborne contamination. Accurate recovery of particulate organic carbon (POC) remains elusive because the accepted practice of rinsing the filters with distilled water to remove sea salts

has been shown to result in the lysis of cells and the loss of intracellular components. Transmissometers are useful in determining relative abundances of particles in a given water column, but must be carefully calibrated against known particle concentrations to give quantitative but not size-specific results.

Optical methods for size-specific determinations are characterized by the size range of interest and are capable of ranges from microns to centimeters. On the low end of this range, traditional techniques have employed ship or laboratory-based instruments such as the Coulter counter, but new technology has recently been introduced which will allow *in situ* determinations of particle sizes (Agrawal and Pottsmith, 1993; 1994). These instruments use the near-forward scattering of laser light and are applicable to sizes from 5 to 500 microns.

In natural seawater, many particles exist as aggregates of smaller constituents in a loose and highly porous organic matrix (Suzuki and Kato, 1953; Shanks and Trent, 1980; Alldredge and Cox, 1982; Asper, 1986; Alldredge and Gottschalk, 1988; Alldredge et al., 1990). The challenge of determining the abundance of these large aggregates (often referred to as "marine snow") lies in their fragile construction. Attempts to sample aggregates using water bottles or nets usually result in their dis-aggregation, and intact aggregates have been observed to settle quickly inside the bottle and escape recovery by falling below the level of the spigot (Gardner, 1977).

Because of these characteristics, marine snow aggregate concentrations are usually monitored using photographic techniques which image a large volume of water, but make no physical contact with the particles (Eisma et al., 1983; 1990; Honjo et al., 1984; Lampitt, 1985; Asper, 1987; Davis and Pilskaln, 1993). This technique was pioneered by Honjo et al (1984), but has been adapted and improved by many investigators since its inception, including incorporation of multiple cameras, video imaging and deployment on a remotely operated vehicle (ROV) (Davis and Pilskaln, 1993). While this technique produces excellent results, time-consuming analyses of many images are required to produce the data.

5.3 SINKING SPEEDS

By far the most difficult characteristic to assess is the rate at which particles settle through the water column. This measurement is complicated by ambient turbulence, shear and advection in the water as well as the difficulty inherent in establishing a stable frame of reference (Kajihara, 1971; McCave, 1975; Shanks and Trent, 1980; Alldredge and Gotschalk, 1988; Kineke and Sternberg, 1989). Sinking speed measurements made from free vehicles are likely to result in determinations of the relative motions of the particle and vehicle rather than an absolute sinking speed. Determinations made from a mooring or floating array are

complicated by the motion of the water relative to the instrument. Asper (1987) and Asper et al. (1992) used a semi-enclosed volume of water in a sediment trap to photographically time aggregates falling through a known distance. This technique produced excellent results, but is capable of detecting only those particles which are within the resolution limits of the cameras, and is only able to assess those particles which actually settled into the trap. Particles or aggregates settling at very slow speeds (less than ca. 1 m d^{-1}) do not enter the trap in significant quantities and are therefore not incorporated into the measurements.

New techniques on the horizon which promise to enhance our ability to monitor particle dynamics include a multi-aperture detector and a dual-purpose imaging and sending device known as MOPAR (Moored Optical PARticle). The multiple aperture device uses several photodiodes in an array to follow the trajectories of particles in a manner patterned after an insect's compound eye (Figure 5.5), and has the advantage of simplicity of components. This system is in the final test and software development stage at this time, and its inventors are optimistic that it will ultimately be capable of providing three-dimensional trajectories of multiple particles simultaneously. The MOPAR (Figure 5.6) is designed to be installed on a mooring and will enclose a volume of water in a delicate manner chosen to minimize aggregate breakup. Once the volume is sealed, it will be imaged by both a shadowgraph technique and a laser diffraction instrument. Together, these will provide the means to determine size-specific particle abundances and sinking speeds.

5.4 SUMMARY

Determination of the vertical flux of mass and energy through the water column continues to be a major goal of oceanographic research. As such, attempts will continue to be made to improve the technology with which we approach this problem so that the most accurate assessments possible are obtained in a cost effective manner. Along with the sophisticated equipment which has recently been introduced, the simple sediment traps and optical devices which have been used for decades will continue to provide the basic flux measurements scientists depend on. The potential for biases with all such samplers is great, however, and scientists should be aware of the potential impacts of these effects on their samples and should continue to interpret their results cautiously. Minimal environmental data should be acquired in all cases, including flow and sea state if surface-tethered, so that the samples can be qualitatively assessed and results discarded if the potential for bias is too great. This conservative approach to the application of the data, along with new technologies and approaches to looking at the phenomenon of particle flux, will allow us to monitor these processes to the level of accuracy which we desire.

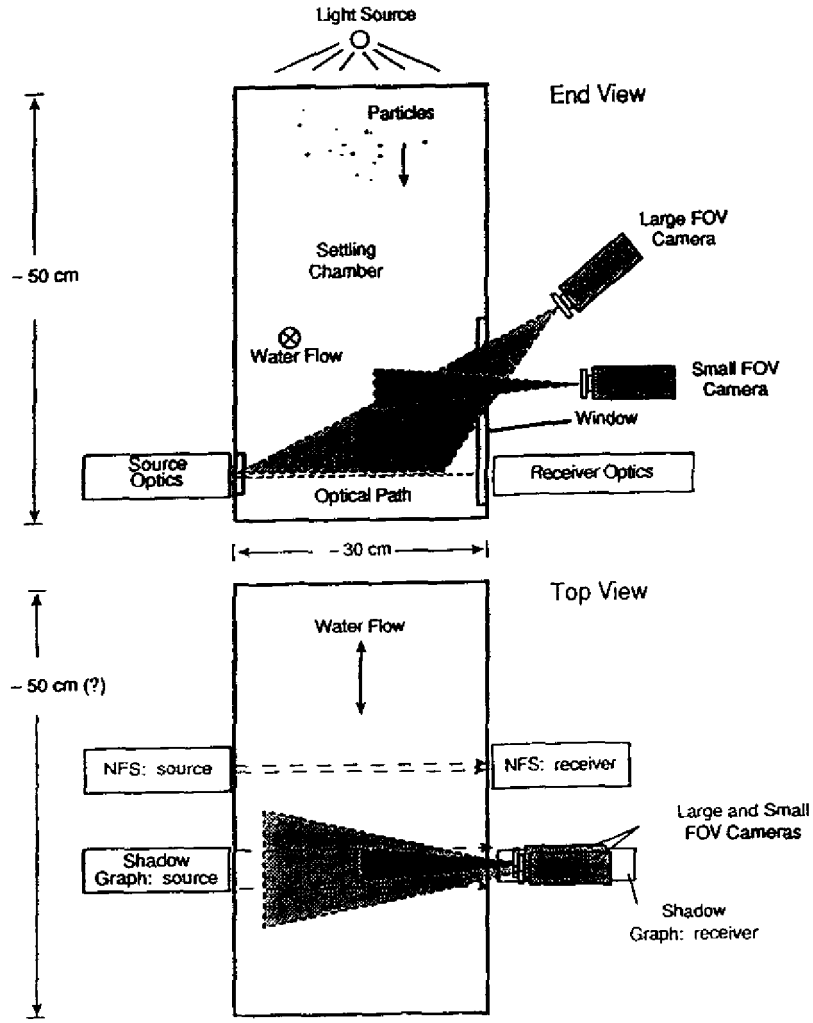

Figure 5.5 Schematic of the MOPAR instrument which is under development at Dynamics Technology in California. The sizes and sinking speeds of particles entering the system will be determined by both shadograph (cameras) and laser diffraction techniques (Near Forward Scattering, NFS; from Patton and Chang, 1992; reproduced by permission of the authors).

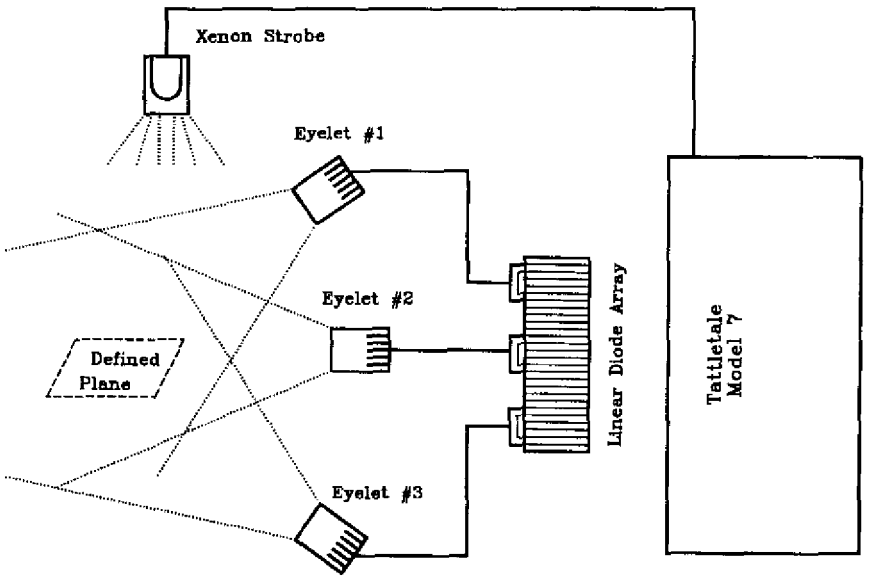

Figure 5.6 Drawing of Multi-Aperture Sensor System (MASS) showing the principal components. Signals from each of the 7 eyelets are processed to provide particle motion information in a manner analogous to an insect's compound eye (Figure provided by Ocean Optics).

5.5 REFERENCES

Agrawal, Y. C. and H. C. Pottsmith (1993) "Optimizing the kernel for laser diffraction particle sizing", *Applied Optics*, **32**, 4285–4286.

Agrawal, Y. C. and H. C. Pottsmith (1994) "Laser diffraction and particle sizing in STRESS", *Continent. Shelf Res.*, **14**, 1101–1121.

Alldredge, A. L. and J. L. Cox (1982) "Primary productivity and chemical composition of marine snow in surface waters of the Southern California Bight", *J. Mar. Res.*, **40**, 517–527.

Alldredge A. L. and C. Gotschalk (1988) "In situ settling behavior of marine snow", *Limnol. Oceanogr.*, **33**, 339–351.

Alldredge, A. L., T. C. Granata, C. C. Gotschalk and T. D. Dickey (1990) "The physical strength of marine snow and its implications for particle disaggregation in the ocean", *Limnol. Oceanogr.*, **35**, 1415–1428.

Asper, V. L. (1986) "Accelerated settling of particulate matter by 'marine snow' aggregates", Ph.D. Thesis, Woods Hole Oceanographic Institution/Massachusetts Institute of Technology, 189 pp.

Asper, V. L. (1987) "Measuring the flux and sinking speed of marine snow aggregates", *Deep-Sea Res.*, **34**, 1–17.

Asper, V. L. (1988) "A review of sediment trap technique", *Mar. Technol. Soc. J.*, **21**, 18–25.

Asper, V. L., W. G. Deuser, G. A. Knauer and S. E. Lohrenz (1992) "Rapid coupling of sinking particle fluxes between surface and deep ocean waters", *Nature*, **357**, 670–672.

Baker, E. T. and H. B. Milburn (1982) "An instrument system for the investigation of particle fluxes", *Continent. Shelf Res.*, **1**, 1–11.

Bartz, R., J. R. V. Zaneveld and H. Pak (1978) "A transmissometer for profiling and moored observations in water", *Society of Photo-Optical Instrumentation Engineers*, **160**, 102–108.

Bruland, K. W., R. P. Franks, W. M. Landing and A. Soutar (1981) "Southern California inner basin sediment trap calibration", *Earth Planet. Sci. Let.*, **53**, 400–408.

Buesseler, K. O. (1991) "Do upper-ocean sediment traps provide an accurate record of particle flux?", *Nature*, **353**, 420–423.

Butman, C. A. (1986) "Sediment trap biases in turbulent flows: results from a laboratory flume study", *J. Mar. Res.*, **44**, 645–693.

Butman, C. A., W. D. Grant and K. D. Stolzenbach (1986) "Predictions of sediment trap biases in turbulent flows: A theoretical analysis based on observations from the literature", *J. Mar. Res.*, **44**, 601–644.

Costin, J. M. (1970) "Visual observations of suspended-particle distribution at three sites in the Caribbean Sea", *J. Geophys. Res.*, **75**, 4144–4150.

Davis, D. L. and C. H. Pilskaln (1993) "Measurements with underwater video: camera field width calibration and structured lighting", *J. Mar. Technol. Soc.*, **26**, 13–19.

Davis, R. E., D. C. Webb, L. A. Regier and J. Dufour (1992) "The Autonomous Lagrangian Circulation Explorer (ALACE) ", *J. Atmosph. Oceanic Technol.*, **9**, 264–285.

Deuser, W. G., F. E. Muller-Karger and C. Hemleben (1988) "Temporal variations of particle fluxes in the deep subtropical and tropical North Atlantic: Eulerian and Lagrangian effects", *J. Geophys. Res.*, **93**, 6857–6862.

Diercks, A.-R. and V. L. Asper (1993) "A neutrally buoyant sediment trap for marine particle flux studies", Presented to the Scientific Committee on Problems of the Environment/United Nations Environmental Program, Workshop on Particle Flux in the Ocean, September 20–23, 1993, Hamburg, Germany

Eisma, D., J. Boon, R. Groenewegen, V. Ittekkot, J. Kalf and W. G. Mook (1983) "Observations on macro-aggregates, particle size and organic composition of suspended matter in the Ems estuary", in E. T. Degens, S. Kempe and H. Soliman (eds) *Transport of Carbon and Minerals in Major World Rivers*, Mitt. Geol.-Paläont. Inst. Univ. Hamburg No. 55, 295–314.

Eisma, D., T. Schuhmacher, H. Boekel, J. Van Heerwaarden, H. Franken, M. Laan, A. Vaars, F. Aijgenraam and J. Kalf (1990) "A camera and image-analysis system for In Situ observation of flocs in natural waters", *Netherl. J. Sea Res.*, **27**, 43–56.

Gardner, W. D. (1977) "Incomplete extraction of rapidly settling particles from water samplers", *Limnol. Oceanogr.*, **22**, 764–768.

Gardner, W. D. (1980) "Sediment trap dynamics and calibration: a laboratory evaluation", *J. Mar. Res.*, **38**, 17–39.

Gust, G., R. H. Byrne, R. E. Bernstein, P. R. Betzer and W. Bowles (1992) "Particle fluxes and moving fluids: experience from synchronous trap collections in the Sargasso Sea", *Deep-Sea Res.*, **39**, 1071–1083.

Gust, G., A. F. Michaels, R. Johnson, W. G. Deuser and W. Bowles (1994) "Mooring line motions and sediment trap hydromechanics: in situ intercomparison of three common deployment designs", *Deep-Sea Res.*, **41**, 831–857.

Hargrave, B., G. Siddall, G. Steeves and G. Awalt (1994) "A current-activated sediment trap", *Limnol. Oceanogr.*, **39**, 383–390.

Honjo, S. and K. W. Doherty (1988) "Large aperture time-series oceanic sediment traps: Design objectives, construction and application", *Deep-Sea Res.*, **35**, 133–149.

Honjo, S., K. W. Doherty, Y. C. Agrawal and V. L. Asper (1984) "Direct optical assessment of large amorphous aggregates (marine snow) in the deep ocean", *Deep-Sea Res.*, **31**, 67–76.

Honjo, S., B. J. Hay, S. J. Manganini, V. L. Asper, E. T. Degens, S. Kempe, V. Ittekkot, E. Izdar, Y. T. Konuk and H. A. Benli (1987) "Seasonal cyclicity of lithogenic particle fluxes at a southern Black Sea sediment trap station", in E. T. Degens, E. Izdar and S. Honjo (eds) *Particle flux in the Ocean*, Mitt. Geol.-Paläont. Inst. Univ. Hamburg No. 62, 19–39.

Ittekkot, V., R. R. Nair, S. Honjo, V. Ramaswamy, M. Bartsch, S. Manganini and B. N. Desai (1991) "Enhanced particle fluxes in Bay of Bengal induced by injection of fresh water", *Nature*, **351**, 385–387.

Jickells, T. D., T. M. Church and W. G. Deuser (1987) "A comparison of atmospheric inputs and deep-ocean particle fluxes for the Sargasso Sea", *Glob. Biogeochem. Cycles*, **1**, 117–130.

Kajihara, M. (1971) "Settling velocity and porosity of large suspended particle", *J. Oceanograph. Soc. Japan*, **27**, 158–162.

Karl, D. M. and G. A. Knauer (1989) "Swimmers: a recapitulation of the problem and a potential solution", *Oceanography*, **2**, 23–25.

Kempe, S. and T. C. Jennerjahn (1988) "The vertical particle flux in the northern North Sea, its seasonality and composition", in S. Kempe, G. Liebezeit, V. Dethlefsen and U. Harms (eds) *Biogeochemistry and Distribution of Suspended Matter in the North Sea and Implications to Fisheries Biology*, Mitt. Geol.-Paläont. Inst. Univ. Hamburg No. 65, 229–268.

Kineke, G. C. and R. W. Sternberg (1989) "The effect of particle settling velocity on computed suspended sediment concentration profiles", *Mar. Geol.*, **90**, 159–174.

Knauer, G. A. and V. L. Asper (eds) (1989) *U.S. GOFS Planning Report Number 10: Sediment Trap Technology and Sampling*, U.S. JGOFS Planning Office, Woods Hole, 94 pp.

Knauer, G. A., J. H. Martin and K. W. Bruland (1979) "Fluxes of particulate carbon, nitrogen and phosphorus in the upper water column of the northeast Pacific", *Deep-Sea Res.*, **26**, 97–108.

Lampitt, R. S. (1985) "Evidence for the seasonal deposition of detritus to the deep-sea floor and its subsequent resuspension", *Deep-Sea Res.*, **32**, 885–897.

Lee, C., S. G. Wakeham and J. I. Hedges (1988) "The measurement of oceanic particle flux - are "swimmers" a problem?", *Oceanography*, **2**, 34–36.

Lorenzen, C. J., F. R. Shuman and J. T. Bennett (1981) "In-situ" calibration of sediment trap", *Limnol. Oceanogr.*, **26**, 580–585.

Manganini, S. J. and S. Honjo (1985) "In situ" preservation of biogenic material collected by a deep ocean sediment trap", *EOS*, **66**, 1292.

McCave, I. N. (1975) "Vertical flux of particles in the ocean", *Deep-Sea Res.*, **22**, 491–502.

Michaels, A. F., M. W. Silver, M. M. Gowing and G. A. Knauer (1990) "Cryptic zooplankton "swimmers" in the upper ocean sediment traps", *Deep-Sea Res.*, **37**, 1285–1296.

Peterson, M. L., P. J. Hernes, D. S. Thoreson and H. I. Hedges (1993) "Field evaluation of a valved sediment trap", *Limnol. Oceanogr.*, **38**, 1741–1761.

Reynolds, C. S., S. W. Wiseman and W. D. Gardner (1980) *An Annotated Bibliography of Aquatic Sediment Traps and Trapping Methods*, Vol. 11, Fresh-Water Biology Association, 54 pp.

Shanks, A. L. and J. D. Trent (1980) "Marine snow: sinking rates and potential role in vertical flux", *Deep-Sea Res.*, **27**, 137–143.

Siegel, D. A., T. C. Granata, A. F. Michaels and T. D. Dickey (1990) "Mesoscale eddy diffusion, particle sinking, and the interpretation of sediment trap data", *J. Geophys. Res.*, **95**, 5305–5311.

Simoneit, B. R. T., J. O. Grimalt, K. Fischer and J. Dymond (1986) "Upward and downward flux of particulate organic material in abyssal waters of the Pacific Ocean", *Naturwissenschaften*, **73**, 322–325.

Spinrad, R. W. (1986) "A calibration diagram of specific beam attenuation", *J. Geophys. Res.*, **91**, 7761–7764.

Staresinic, N., G. T. Rowe, D. ShaughnesseY and A. J. Williams III (1978) "Measurement of the vertical flux of particulate organic matter with a free-drifting sediment trap", *Limnol. Oceanogr.*, **23**, 559–563.

Staresinic, N., K. Brockel, N. Smodlaka and H. C. Clifford (1982) "A comparison of moored and free-drifting sediment traps of two different designs", *J. Mar. Res.*, **40**, 273–292.

Sternberg, R. W., E. T. Baker, D. A. Mcmanus, S. Smith and D. R. Morrison (1974) "An integrating nephelometer for measuring particle concentrations in the deep sea", *Deep-Sea Res.*, **21**, 887–892.

Suzuki, N. and K. Kato (1953) "Studies on suspended materials marine snow in the sea. Part I. Sources of Marine Snow", *Bulletin of the Faculty of Marine Fisheries of the Hokkaido University*, **4**, 132–137.

Swallow, J. C. (1955) "A neutral-buoyancy float for measuring deep currents", *Deep-Sea Res.*, **3**, 74–81.

Wassmann, P. and A.-S. Heiskanen (eds) (1988) *Sediment Trap Studies in the Nordic Countries*, 1st ed., Tvarminne Zoological Station, Hanko, Finland, 207 pp.

Wefer, G. and G. Fischer (1991) "Annual primary production and export flux in the southern ocean from sediment trap data", *Mar. Chem.*, **35**, 597–613.

6 Evaluation of Sediment Traps with Naturally Occurring Radionuclides

MICHAEL P. BACON

6.1 INTRODUCTION

Because of the flow of water relative to a sediment trap deployed in the ocean, it is possible for bias to occur in the measurement of sinking particle flux (SCOR, 1988; Knauer and Asper, 1989). Several of the members of the natural radioactive decay series have been suggested as tracers to evaluate the hydrodynamic bias and provide for calibration of sediment traps *in situ* (Table 6.1). The daughter nuclides that are listed have two important characteristics: (1) they are supplied to the oceanic water column by decay of their parent nuclides at rates that can be exactly known, and (2) they are chemically reactive in the sense that they are strongly adsorbed by marine particulate matter. All of the parent/daughter pairs show measurable amounts of radioactive disequilibrium in the oceanic water column, the daughter being deficient relative to the parent because of scavenging and removal by the sinking particles. In practice a calibration is based on a determination of the integrated deficiency of the daughter nuclide in the water column above the trap to be calibrated. From this the expected flux of the daughter at the depth of the trap is easily calculated. Comparison of measured flux with expected flux gives a measure of the trapping efficiency.

6.2 MOORED SEDIMENT TRAPS IN THE DEEP OCEAN

Bottom-tethered sediment traps are frequently used to measure the supply of sinking particles to the seafloor. For evaluating the performance of traps moored at great depth in the ocean, the longer-lived daughter nuclides, which show deficiencies throughout the entire water column, are the appropriate tracers to use. They include ^{210}Pb, ^{230}Th, and ^{231}Pa (Table 6.1). Of these the most important is ^{230}Th. It is produced in the oceanic water column at an exactly known rate from decay of ^{234}U, which is uniformly distributed throughout the ocean. The residence time of ^{230}Th is a few decades (Moore and Sackett, 1964; Anderson et al., 1983a),

Particle Flux in the Ocean
Edited by V. Ittekkot, P. Schäfer, S. Honjo and P. J. Depetris

Table 6.1 Naturally occurring parent/daughter radionuclide pairs that have been proposed for *in situ* calibration of sediment traps (Knauer et al., 1979; Brewer et al. 1980; Moore et al., 1981; Bacon et al., 1985). Half-lives are in parentheses.

Parent	Daughter
^{238}U (4.47×10^9 y)	^{234}Th (24.1 d)
^{234}U (2.48×10^5 y)	^{230}Th (7.52×10^4 y)
^{226}Ra (1.62×10^3 y)	^{210}Pb (22.3 y) [a]
^{210}Pb (22.3 y)	^{210}Po (138 d) [a]
^{228}Ra (5.75 y)	^{228}Th (1.91 y) [a]
^{235}U (7.07×10^8 y)	^{231}Pa ($3.25\ 10^4$ y) [a]

a: Produced via one or more intermediates.

and when averaged over that time scale the production of ^{230}Th by decay of ^{234}U and removal by sinking particles are in almost exact balance.

The assumption that there is a balance between production and removal is an important one. Bacon et al., (1985) showed evidence from a PARFLUX sediment trap (Honjo and Doherty, 1988) moored at 3200 m in the Sargasso Sea that there is a seasonal cycle in the flux of radionuclides, including ^{230}Th, similar to that observed for total particle flux (Deuser et al., in press). The measured fluxes of ^{230}Th varied from 25 to 101% of the integrated production in the water column overlying the trap, indicating clearly that on a 2-month time scale the production and removal of ^{230}Th are not in balance, and it was suggested that as a minimum a year-long record is needed to provide an average over the annual cycle. An average of the ^{230}Th flux taken over a one-year period from July 1980 to July 1981 gave an apparent trapping efficiency of 71%. However, there is an additional factor that must be considered for an accurate assessment of the trapping efficiency.

It is also necessary to consider possible convergence or divergence of the ^{230}Th flux due to horizontal transport in the water column overlying the trap. A horizontal flux away from the ocean interior toward the margins could occur as a result of intensified scavenging at the margins, and this effect is known to be especially important for ^{231}Pa, another product of the decay of U in seawater (Anderson et al., 1983b; Bacon 1988). It would cause trapping efficiencies based on a simple vertical flux balance to be underestimated, as illustrated in Figure 6.1. The problem is to determine trapping efficiency E, which is given by

$$E = F/V = F/(P\text{-}H)$$

where F is the ^{230}Th flux measured by the trap (averaged over the annual cycle), P is the production in the water column integrated from the surface down to the depth of the trap, V is the true vertical flux, and H is the net horizontal flux away

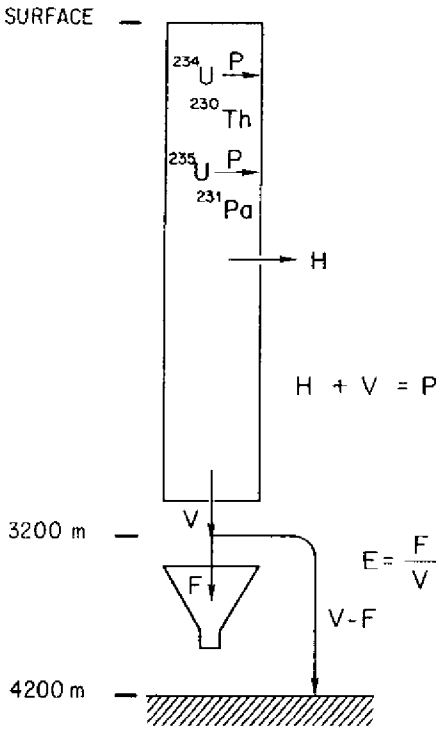

Figure 6.1 Illustration of material balance for ^{230}Th and ^{231}Pa used for *in situ* calibration of the sediment trap used in the Sargasso Sea study (Bacon et al., 1985). P = production rate integrated to the depth of the trap; V = true vertical flux; H = net horizontal transport; F = flux measured by trap; E = trapping efficiency.

from the ocean interior. Neither V nor H is known *a priori*, but Anderson et al. (1983b) suggested a method whereby they could be determined by simultaneously satisfying material balances for both ^{230}Th and ^{231}Pa. When this method was applied to the Sargasso Sea data, E was determined to be 105 ± 17% (Bacon et al., 1985).

In a more recent study employing this method, Yu (1994) determined annual average fluxes of ^{230}Th and ^{231}Pa collected by sediment traps deployed in a variety of locations throughout the oceans. Results for the 10 deployments of PARFLUX traps at depths >1700 m gave trapping efficiencies ranging from 78 to 125%, with an average of 102%, indicating that these traps may be considered to be accurate to within ± 25%. At shallower depths (<1200 m), on the other hand, the results showed a significant tendency toward undertrapping, the results from 4 deployments ranging from 35 to 82%. The undertrapping at the shallower depths most likely results from the higher average flow velocities.

6.3 SEDIMENT TRAPS IN THE UPPER OCEAN

The export of particulate matter from the surface to the deep ocean is important to know for a variety of oceanographic studies. Sediment traps are often used to measure this flux, and for upper ocean studies they are usually deployed in a free-drifting mode. Allowing the traps to drift freely helps to reduce flow relative to the trap but does not eliminate it completely, and it is important to consider the possibility of hydrodynamic bias.

The shorter-lived radionuclides are the most appropriate tracers for validating traps deployed in the upper ocean, and the one used most extensively is ^{234}Th, which is produced by decay of the ^{238}U in seawater (Table 6.1). A deficit of ^{234}Th relative to ^{238}U is usually observed in the euphotic zone, and from this it is a simple matter to determine the export of ^{234}Th on sinking particles at the base of the euphotic zone for comparison with the flux measured in a sediment trap (Figure 6.2). Buesseler (1991) reviewed all of the published data that allowed this comparison to be made and found that measured fluxes of ^{234}Th differed substantially from the expected fluxes, often by more than a factor of 3, suggesting large hydrodynamic biases. Both positive and negative biases (over- and undertrapping) were observed but tended always to be in the same direction for multiple deployments within the same study.

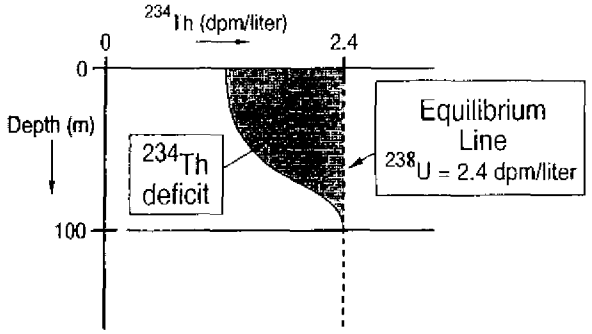

$$\text{Th Export} = \text{Production} - \text{Decay}$$
$$= \lambda\,(\,^{234}\text{Th Deficit}\,)$$
$$= \lambda \int_0^{100} (\,^{238}\text{U} - \,^{234}\text{Th}\,)\,dz$$
$$\lambda = \ell n\, 2 / 24.1\ \text{d} = 0.0288\ \text{d}^{-1}$$

Figure 6.2 Idealized profile of ^{234}Th and material balance used to calibrate sediment traps placed at the base of a 100-m euphotic zone.

Use of ^{234}Th in the surface ocean is subject to the same considerations discussed for the use of ^{230}Th in the deep ocean: temporal and spatial variations in particle flux can cause estimates based on a simple steady-state vertical flux balance to be in error. These factors, which could not be quantified, might explain some of the discrepancies noted by Buesseler (1991). Recognizing this, Buesseler et al. (1994) carried out a three-dimensional time-series study of ^{234}Th distributions and fluxes in the Sargasso Sea off Bermuda. Two independent VERTEX-type trap arrays (Knauer et al., 1979) were used to measure particulate ^{234}Th flux at 95 and 97 m depths over a 4-day period in May 1992. Horizontal transport of ^{234}Th and temporal variation of the ^{234}Th inventory were evaluated explicitly. The results showed consistent overtrapping during the 4-day period of the study. Evidence from long-term measurements at the same site, however, suggested that the traps underestimate the annual flux, and Buesseler et al. (1994) suggest that the traps overestimate flux during low flux periods and underestimate it during high flux periods.

6.4 CONCLUSIONS

Measurements of natural decay-series radionuclides in sediment-trap samples can provide useful limits on the degree of hydrodynamic bias that may have occurred during a deployment. Proper interpretation, however, requires recognition of the effects of horizontal transport and temporal variability on the balance between supply and removal of the reactive daughter nuclide. If good agreement is found between measured and expected fluxes, then it can be taken as evidence that hydrodynamic bias is small. When hydrodynamic biases do occur, it may be possible to apply corrections based on the tracer results, but this would have to be based on the assumption that the nuclide chosen is an unbiased tracer of the whole spectrum of particles that make up the passive settling flux. This assumption needs to be further examined by measurements in samples that have been fractionated according to size, type, or settling velocity. It should also be added that, in addition to hydrodynamic biases, there can also be biases due to poor sample preservation or the presence of swimmers that cannot, in general, be evaluated with the tracers discussed here.

The evidence to date, based on ^{230}Th and ^{231}Pa, suggests that properly designed sediment traps moored in quiescent conditions in the deep ocean (away from boundary currents) can be considered accurate to within ± 25% or better. On the other hand, for traps deployed in the upper ocean, the evidence indicates that significant hydrodynamic bias may occur and that further work is needed to delineate the conditions under which reliable results can be obtained.

6.5 ACKNOWLEDGMENTS

I am indebted to the National Science Foundation for generous financial support of my research, most recently from Grant OCE-9022284.

6.6 REFERENCES

Anderson, R. F., M. P. Bacon and P. G. Brewer (1983a) "Removal of ^{230}Th and ^{231}Pa from the open ocean", *Earth Planet. Sci. Let.*, **62**, 7–23.

Anderson, R. F., M. P. Bacon and P. G. Brewer (1983b) "Removal of ^{230}Th and ^{231}Pa at ocean margins", *Earth Planet. Sci. Let.*, **66**, 73–90.

Bacon, M. P. (1988) "Tracers of chemical scavenging in the ocean: Boundary effects and large-scale chemical fractionation", *Phil. Transac. Roy. Soc. London A*, **320**, 187–200.

Bacon, M. P., C. A. Huh, A. P. Fleer and W. G. Deuser (1985) "Seasonality in the flux of natural radionuclides and plutonium in the deep Sargasso Sea", *Deep-Sea Res.*, **32**, 273–286.

Brewer, P. G., Y. Nozaki, D. W. Spencer and A. P. Fleer (1980) "Sediment trap experiments in the deep North Atlantic: Isotopic and elemental fluxes", *J. Mar. Res.*, **38**, 703–728.

Buesseler, K. O. (1991) "Do upper-ocean sediment traps provide an accurate record of particle flux?", *Nature*, **353**, 420–423.

Buesseler, K. O., A. F. Michaels, D. A. Siegel and A. H. Knap (1994) "A three dimensional time-dependent approach to calibrating sediment trap fluxes", *Glob. Biogeochem. Cycles*, **8**, 179–193.

Deuser, W. G., T. D. Jickells, P. King and J. A. Commeau (in press) "Decadal and annual changes in biogenic opal and carbonate fluxes to the deep Sargasso Sea", *Deep-Sea Res. I.*

Honjo, S. and K. W. Doherty (1988) "Large aperture time-series oceanic sediment traps: Design objectives, construction and application", *Deep-Sea Res.*, **35**, 133–149.

Knauer, G. and V. Asper (1989) *Sediment Trap Technology and Sampling*. U. S. GOFS Planning Report 10, U. S. GOFS Planning and Coordination Office, Woods Hole, Massachusetts, USA.

Knauer, G. A., J. H. Martin and K. W. Bruland (1979) "Fluxes of particulate carbon, nitrogen, and phosphorus in the upper water column of the northeast Pacific", *Deep-Sea Res.*, **26**, 97–108.

Moore, W. S. and W. M. Sackett (1964) "Uranium series inequilibrium in sea water", *J. Geophys. Res.*, **69**, 5401–5405.

Moore, W. S., K. W. Bruland and J. Michel (1981) "Fluxes of uranium and thorium series isotopes in the Santa Barbara Basin", *Earth Planet. Sci. Let.*, **53**, 391–399.

Scientific Committee on Ocean Research (1988) *Particulate Biogeochemical Processes*. SCOR Report Series 1.

Yu, E. F. (1994) *Variations in the Particulate Flux of ^{230}Th and ^{231}Pa and Paleoceanographic Applications of the ^{230}Th / ^{231}Pa ratio*. Ph.D. diss., Massachusetts Institute of Technology/Woods Hole Oceanographic Institution, Woods Hole, Massachusetts, USA.

7 Fluxes of Particles to the Interior of the Open Oceans

SUSUMU HONJO

7.1 INTRODUCTION

It must have been more of a shock than we can now imagine when the Azoic theory was disproved with Charles Wyville Thompson's discovery during his 1868 expedition in the North Atlantic Ocean (re-cited from Mills, 1983) that there are live organisms on the abyssal seafloor of the North Atlantic. However a simple but critical question was, until recently, never answered and remained in speculation: How are energy and nutrients supplied to the animals who live on the deep seafloor where no plants can possibly grow?

About a century later, Osterberg et al. (1963) were among the first researchers who suspected an efficient and direct linkage between euphotic production and bathypelagic ecosystems. They analyzed radionuclides in deep-ocean benthic feeders such as sea urchins collected from the 2800-m seafloor off the coast of Oregon. Among the nuclides they found was ^{95}Zr the half-life of which was only 65 days; therefore the time required for radionuclides to be transferred from atmospheric sources to the ocean bottom would have to be constrained. Thus, these authors concluded that ocean particles which carry radionuclides to the ocean's floor should settle far more quickly (in a few weeks' time) through this water column than individual fine particles whose settling time would be on the order of years - as estimated from Stokes Law. They speculated that radionuclides at this site were delivered to the ocean's floor by rapidly settling particles such as fecal pellets of surface-living zooplankton.

Another example to be reiterated is the so-called "Coccolith Riddle" (Honjo, 1976). This 20-year-old problem involves fundamental aspects of ocean biogeochemical cycles and has provided, for me at least, stimulation for further research regarding ocean particles and their role in the global geochemical cycle. Though the process of attacking this riddle was an impetus to develop modern time-series sediment trap technologies, the results have been findings regarding many crucial aspects of ocean particles and their fluxes, particularly bringing to light the linkage between upper ocean ecology and bottom sediment.

Particle Flux in the Ocean
Edited by V. Ittekkot, P. Schäfer, S. Honjo and P. J. Depetris

The discovery of a transport link between the atmosphere, upper ocean and the ocean's interior with the deep seafloor was not trivial, but promised leaping progress in many other fields of ocean science. All particles and materials that arrive on the ocean's bottom still carry a memory imprint of the air and upper layer environments in which they were produced. Unloading this memory is critically important for understanding the past environment of the ocean and atmosphere. In order to decode environmental information from a microfossil in the sediment sequences, such as ocean temperature, salinity and nutrient concentration, etc., we must know the environmental relationship between the living counterpart of the fossil species and the present-day ocean environments which support them; many of these relationships have been missing from our knowledge. To establish the environmental relationship between a living and fossil assemblage using a trap-collected counterpart (biocoenosis) as the key, the "paleoproximity study" is one of the crucial and exciting ramifications of recent efforts to understand global change. As a token of our progress in this direction, the range of sea surface temperatures interpreted from our global, settling particle collection program using moored sediment traps is illustrated in Figure 7.1.

Beside the contamination of our planet's oceans by a long list of hazardous materials beginning with anthropogenic radionuclides (e.g., Fowler et al., 1983; Kempe et al., 1987), another burning issue has emerged which demands serious attention: the alarming rate of increase of atmospheric carbon dioxide due to the combustion of fossil fuels that upsets the global environment (e.g., Kellogg, 1991), resulting in the rise of earth's atmospheric temperature by the greenhouse effect (e.g., IPCC, 1990; Jones, et al., 1987).

The majority of CO_2 that is fixed by photosynthesis in the euphotic layer returns to the atmosphere within a short period, on the order of days. Some removed organic matter penetrates through the bottom of the euphotic layer with settling particles or in dissolved form. Much of this matter is regenerated throughout the middle or mesopelagic layer by heterotrophs and microbial activity, and a part of the resulting CO_2 also returns to the atmosphere. The deeper the layer where organic carbon is remineralized, the longer it takes to recycle the carbon to the upper ocean layers and the atmosphere. Only a small percent of particulate carbon continues settling to the bathypelagic layer and to the deep ocean floor.

The main role of the deep ocean in maintaining the efficiency of biogeochemical cycles of carbon, the biological pump, is to absorb atmospheric CO_2 and to hold a portion of the excess in the ocean's layers where the depth is too great for regenerated CO_2 to return to the atmosphere within our tangible time scale. A molecule of carbon from CO_2 which reaches the bathypelagic layer would take as long as the period of the ocean's general circulation, several hundreds to a thousand years, until it re-appears in the upper ocean and, ultimately, returns to the atmosphere. Some carbon molecules take hundreds of million years to be re-injected into the atmosphere, going through tectonic processes of the oceanic crust, after being subducted to the mantle and ejected back into atmosphere as

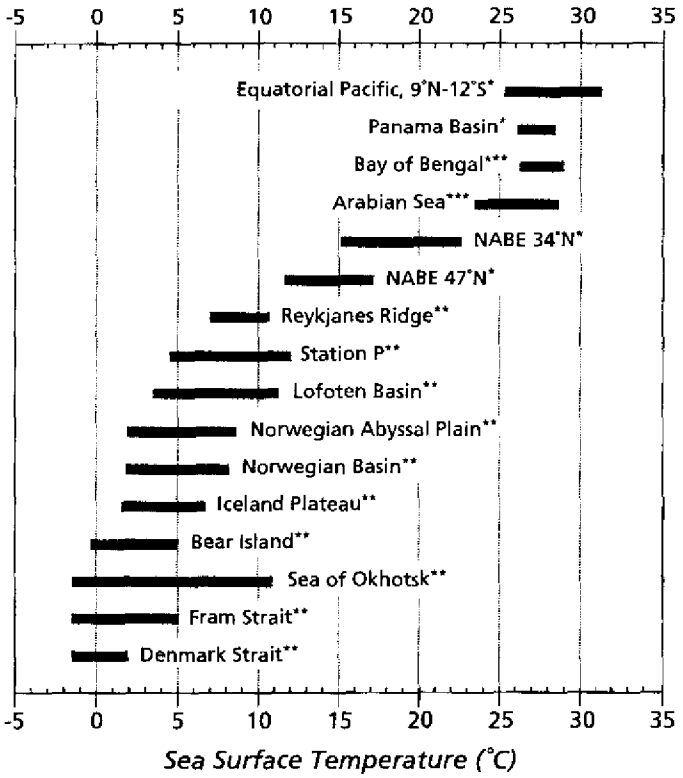

Figure 7.1 A partial list of global planktonic foraminifera sample sets for carbonate isotope measurements collected by time-series sediment trap experiments operated in a wide variety of global open ocean environments with sea surface temperatures ranging from freezing (-1.7°C) to as high as 29°C for ongoing paleoproximity investigations. Each sample set covers a minimum of all seasons of one year and are often of interannual duration. At most sediment trap stations, 2 to 3 traps were deployed in depth series and their open/close timing was synchronized (based on the talk by Dr. W. Curry, SCOPE/ UNEP Symposium, 1993). This work is supported by *the National Science Foundation through the Joint Global Ocean Flux Study (JGOFS), **the High Latitude Ocean Flux Studies of the Office of Naval Research, and ***the University of Hamburg's Biogeochemistry of the Oceans Program.

volcanic CO_2. Therefore the carbon molecule which arrives in the ocean's interior can be treated as a dropout from active recycling. It is critical to understand that this "export carbon" ("transit carbon" of Berger et al., 1989) arrives in the layers of the ocean which are deep enough so that it does not recycle within the time scale of deep-ocean turnover. One of the objectives of particle flux studies is to constrain the quantity and quality of carbon and other materials, as well as anthropogenic pollutants which are exported to this global sink.

This chapter summarizes in a descriptive and narrative manner the results of particle flux experiments using time-series sediment traps during the last 2 decades highlighting questions on the use of sediment traps such as the definitions, units and methods involved, and discussing the performance of sediment traps in various oceanic environments. Hypotheses are proposed on geographic distribution in order to search for the most effective direction of tomorrow's ocean particle flux research.

7.2 OCEAN PARTICLE FLUX: DEFINITION, UNITS AND ATTRIBUTES

The term "flux" ("*flow*" in Latin) is defined as a measure of the rate of transfer of material from one reservoir to another, and one physical or chemical state to another. Another general definition of flux is

Flux = (Proportionality Factor) X (Driving Force).

The dimension of flux is $M\ L^{-2}\ T^{-1}$, where M is a measure of the quantity of material carried by the flux (in our case this is a mass term such as grams), L is a linear dimension (such as meters) and T is time (such as hours).

In the early period of particle flux research, researchers used a variety of practical dimensional units including geological mass units: $g\ cm^{-2}\ ky^{-1}$. The particle flux unit that is now most commonly used is $mg\ m^{-2}\ d^{-1}$; this unit reflects the size of a sediment trap commonly used (between 0.2 and 1 m^2 aperture size), the seasonal variability of particle fluxes (a year or more), resolution of time-series trap openings/closings (minimum of 10–15 days), and the fact that particle fluxes observed in the ocean are normally within the order of $mg\ m^{-2}\ d^{-1}$.

Unless there is either advective or vertical movement of particles, there is no measurable flux. For example, labile organic material is often lighter than seawater and therefore never settles. If we apply Stokes Law, the sinking speed of most of the biomineralized particles produced in the euphotic layer, including coccoliths and diatom frustules, is on the order of $cm\ d^{-1}$ (Honjo, 1977); thus the residence time would be on the order of a hundred years in a deep ocean basin. The theoretical residence time of individual clay particles which are supplied to the open ocean as aerosols is even on an order of magnitude longer than that of these biogenic particles (Lerman, 1979). Such long residence times of ocean particles in water are, in effect, a state of suspension; therefore their vertical flux is negligible. Only particles which are "licensed" to settle can reach the ocean's interior and the deep seafloor (or be caught by a sediment trap). Therefore, the term *particle flux* can only be applied to *settling particles* and not to suspended particles.

7.3 METHODS OF STUDYING OCEAN PARTICLES

Settling particles can be separated from a known volume of bottle-cast or pumped water and, in theory, the flux of particles can be estimated if their mass and settling velocity are known. However estimation of settling velocity involves assumptions, and the estimated flux does not represent a continuous time span (e.g., Bishop et al., 1977). Other noble methods, such as measuring the size and settling speed with time-lapse photography (Asper, 1987) or *in situ* laser holography, for example, have only been used for specific purposes, not world-wide applications (this volume, Chapter 5).

7.3.1 SEDIMENT TRAPS

A sediment trap not only provides a quantity of mass flux but also collects actual material that is settling through the water column. When using a sediment trap, the volume of sample which can be obtained is determined by the size of the trap's aperture and the length of deployment. Depending on the size of trap that can be handled easily onboard, on the order of 100 mg to 1 g of samples can be collected per day from the interior of the oceans (e.g., Honjo and Doherty, 1988). These particles can be examined not only to measure the total mass flux but also their characteristics with chemical and microscopic analyses to establish the mass balance of compounds and find tracers to depict the ocean processes. By applying destructive and non-destructive analyses, research through an extremely wide range of disciplines is possible on a single sediment trap-collected sample. These ramifications include biogeochemistry, radiochemistry, paleoceanography, anthropogenic pollutants and even cosmic dust.

Settling particles which are caught by sediment traps are buffered in time and space; fine-scale events in the upper oceans such as individual diurnal events are averaged in time and space. The optimum time resolution for determining upper ocean events has not been well established but should be related to the residence time of settling particles in the water column. Settling particles are advected by a Lagrangian motion of turbulent flow, and the virtual volume of water from which a sediment trap receives particles can be expressed as an inverted cone relative to a source of particles at the surface (this volume, Chapter 9).

7.3.2 TIME-SERIES ARRAY AND SYNCHRONIZATION

The time-series trap mechanism, which sets the opening and closing of traps according to a pre-programmed schedule, makes it possible to observe the variability of particle flux with time. One deployment of modern sediment traps allows continuous collection of flux and its separation into a set of more than 20 time-series samples (Honjo and Doherty, 1988). An open-close time schedule (a "period") can be set at regular intervals or with a complex schedule of uneven

time spacing, hours to a month, but always allows continuous measurement of particle flux, typically six months to a year. Such intervals provided, for example, measurements of the flux associated with the evolution of blooms in the North Atlantic from their onset to end (e.g., Honjo and Manganini, 1993). If the amplitude of a concurrent oceanographic or meteorological event is known, an ideal minimum sediment trap collection interval is one quarter of that amplitude. The majority of time-series experiments in the deep ocean so far have used uniform 14- to 17-day open/close intervals for deployment of deep ocean traps. In practice, experiments with 17-day intervals have been able to identify tropical instability waves with approximately 3 to 4 weeks of wavelength in the equatorial Pacific (JGOFS - EqPac: Joint Global Ocean Flux Study - Equatorial Pacific; Honjo et al., 1995).

An open-close schedule can be synchronized between two or more sediment traps (sediment-trap "arrays"). Not only can all traps on a bottom-tethered mooring be synchronized, but many traps on many moorings in an area or transect can also be synchronized; an example is shown in Figure 7.2. Synchronization of open-close periods provides an advantage which enables understanding of the vertical and horizontal propagation rate of an oceanographic event. Researchers have found that a synchronized sediment-trap array provides information critical to the understanding, through the variability of particle fluxes, of meso- and large-scale oceanographic variables of ocean and atmospheric cycles of the earth.

7.3.3 CONSTRAINTS IN MEASURING PARTICLE FLUXES WITH SEDIMENT TRAPS

Laboratory plume simulation indicated a significant difference in trapping efficiency due to both the general configuration of the trap and design of the aperture baffle (e.g., Gardner, 1980a, b; Blomqvist and Kofoed, 1981; Butman, 1986; Baker et al., 1988). Complex water movement *within* a sediment trap may enhance the unreliability of particle flux data collected with the sediment trap method (e.g., Gust et al., 1992).

The sediment-trap measurement of particle flux in high-energy environments such as the euphotic layer and upper ocean do not agree with other estimates such as thorium isotope removal rates (e.g., Buesseler, 1991; this volume, Chapter 6). Researchers suspect that there are a number of reasons for this disagreement, including: 1) stable settling particles are not yet well formed in the shallow water; *in situ* marine snow cameras show a great difference in the morphological nature between the aggregates in the upper ocean and the ocean's interior; 2) violent shear usually exists between a sediment trap and the surrounding water; 3) vigorous *in situ* biological activities strongly modify trap-collected samples in warm and sun-lit environments unless strong preservatives are added.

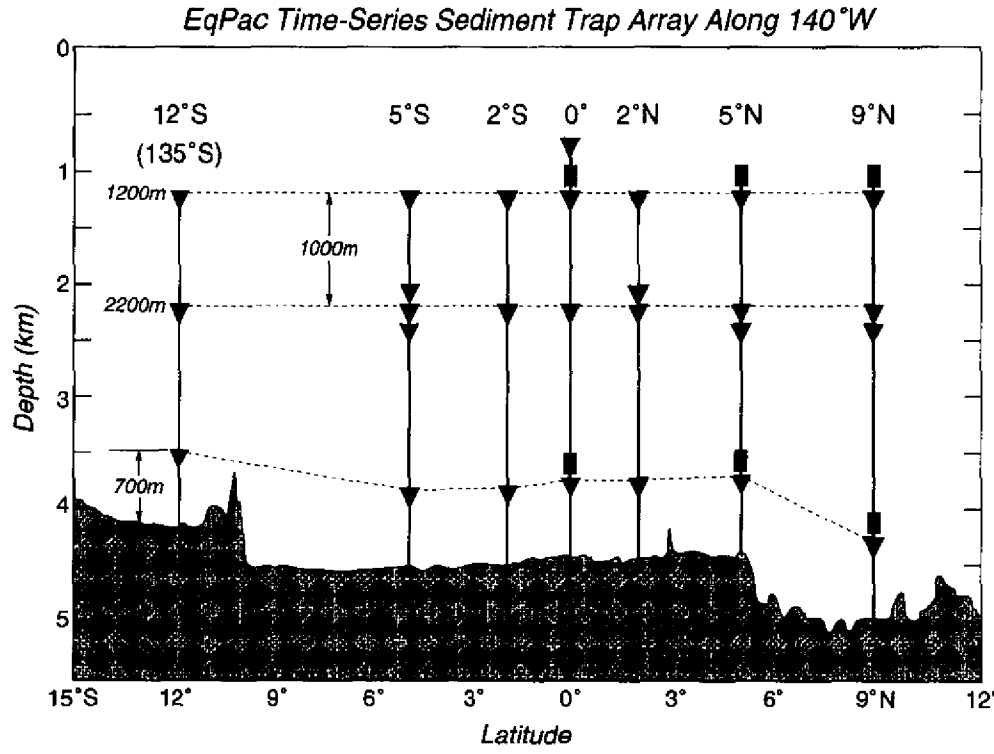

Figure 7.2 An example of a large time-series sediment trap array, deployed along 140°W cross the equator from 9°N to 12°S during JGOFS EqPac Program, for one year starting in early 1992. All sediment traps were synchronized using a single open/close schedule which provided vital information on space-temporal propagation of particles from the upwelling center at 2°N to both sides of the equator (Honjo et al., 1995).

7.3.4 SAMPLE INTEGRITY

7.3.4.1 Swimmers

There are two major biological problems related to maintaining the integrity of samples which are collected by sediment traps: "swimmers" and sample degradation (e.g., Lee et al., 1988; Michaels et al., 1990). "Swimmers" are autotrophs which are attracted by the fresh samples collected and stored in the sampling bottle (cylinder-type traps such as VERTEX traps collect samples on their floor). The presence of swimmers changes the nature of the particles that are already collected, or adds to the apparent flux remaining as part of the sample after they die (often due to the effect of preservatives). In more complex cases, zooplankton or nekton visit the sample bottle, uptake the sample, leave feces and then swim away from the trap, or hatch eggs after they are trapped. The swimmer problem occurs more frequently in the upper ocean simply because of its large and active ecosystem. In the mesopelagic layer a sediment trap attracts metazoans which make scheduled vertical migrations. Researchers often find that the "majority" of the particles collected in traps deployed in the upper oceans are accompanied by swimmers (e.g., Harbison and Gilmer, 1986). They can be manually removed, but the inevitable result would be flux strongly biased for two reasons: uncertainty in identifying genuine settling particles *vs.* swimmers, and the possibility of small swimmer fragments remaining during the picking process, particularly when the sample is not chemically fixed. Many methods to prevent swimmers such as using nets (Karl and Knauer, 1989) or mechanically rotating indented ball valves (Peterson et al., 1993) have been proposed, with successful initial field tests (this volume, Chapter 5).

In the bathypelagic layers, the zones deeper than 1 to 1.5 km, the ocean's interior, this situation changes to the advantage of export production measurement, escaping the serious problems mentioned above; the population of living zooplankton drastically decreases below the mesopelagic layer; the particles are not as fresh as in the upper layers so are probably less attractive to many metazoans. Bathypelagic fish often disturb samples (Honjo and Manganini, 1993). This problem has been solved by placing a thin, 1-cm-mesh nylon net underneath the baffle (Honjo et al., 1995). In some areas, the near-bottom traps (several hundred meters above the seafloor) collect benthopelagic zooplankton as swimmers (Honjo, 1978). In practice, when dealing with deep-ocean trap samples, particles which remain after being sieved through 5-mm mesh need to be examined for freshness. Swimmers are only a small percent of the total flux, and their mis-identification usually falls within analytical error (Honjo and Manganini, 1992; Honjo et al., 1995).

7.3.4.2 Microbial growth and degradation of samples

In situ bacterial degradation of settling particles (e.g., Knauer et al., 1984; Lee et al., 1992; Pfannkuche and Lochte, 1993) could also bias the measurement of

organic matter export. In the upper ocean where temperatures are generally high, the rate of degradation accelerates. For example, in a laboratory incubation when the water temperature was as high as 18°C, the membranes covering a freshly produced copepod fecal pellet were largely degraded within the time it would have taken to settle through the euphotic layer (Honjo and Roman, 1978). In deep layers, fresh organic matter degraded quickly during an experiment due to exposure along a mooring (Gardner et al., 1983). An *in situ* experiment using fresh-cultured phytoplankton at the 4-km ocean bottom showed a rapid degradation rate. However, the same experiment showed particles collected in deep layers were far less susceptible to degradation than fresh organic matter (Cole et al., 1987).

Unless a sediment trap is deployed in low-temperature water such as the polar oceans (Fischer et al., 1988; Honjo, 1990a; Wefer, 1989; 1991), collected samples must be treated with a preservative (e.g., Knauer et al., 1984). Relatively small concentrations of $HgCl_2$ are universally effective in preventing the growth of bacteria and other protists. Compared to other preservatives, $HgCl_2$ remains in the sampling bottle of a trap without diffusing rapidly. However, it does not chemically fix the tissue, as formaldehyde does; thereby labile organic matter often disintegrates before being recovered, and swimmers often become indistinguishable from settling particles. The extreme dominance of Hg molecules in a sample makes many non-destructive chemical analyses, such as X-ray fluorescence analyses, difficult to impossible.

On the other hand, sodium azide offers some advantages. The greatest advantage of using sodium azide is that this preservative does not add any significant alien molecules to the sample (it consists of hydrogen and nitrogen) as Hg does, yet it prevents the growth of a dominant group of bacteria in the seawater. Diffusion can be slowed down by using a diffusion chamber and slightly raising the salinity of water in the sample bottle (Honjo et al., 1979). However, sodium azide does not prevent all microbes and, like $HgCl_2$, does not fix organic tissues. Both $HgCl_2$ and sodium azide are highly hazardous.

Formaldehyde or formalin fixes the tissue and also prevents growth of most protists and microbes. A diffusion of formalin can be retarded by slightly raising salinity in the sampler bottle. The hazard-preventive laboratory protocol for handling a sample containing formaldehyde has been well established. Although re-distilled formalin adds no metals, the addition of alien carbon modules (formalin is a petroleum product) to a sample makes it difficult to measure the amount of dissolved carbon in the supernatant of the sample, and leaves doubt about the reliability of the ^{13}C measurement in organic matter (Manganini et al., 1994).

As is explained more fully in a later section, during a time-series array experiment in the equatorial Pacific, three identical traps were deployed on a mooring approximately 100 m apart at a depth of about 2 km (Figures 7.2 and 7.3). The 21 sampling bottles of each trap were pre-filled with 3 different solu-

tions of preservatives commonly used by researchers: sodium azide, formaldehyde (buffered $NaBO_3$) and $HgCl_2$. All samples were collected during synchronized open periods over the span of about one year in 1992. The total flux of each corresponding period of the 3 traps differed only a few percent. The Na, P, Al, Ti, Fe and Ba content among the 3 traps were within analytical error. However, Mn

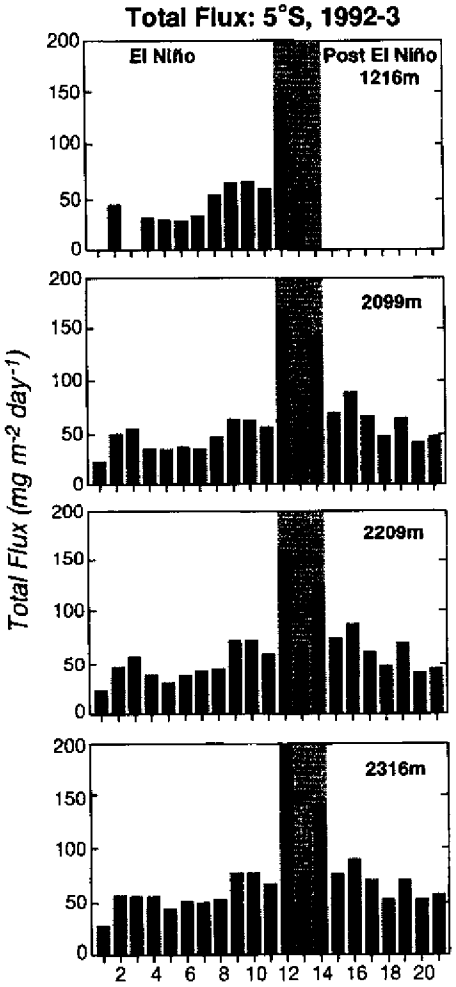

Figure 7.3 For the entire year of 1992, the particle flux collected by 3 sediment traps 100 m apart at 5°S 140°W at a depth of around 2.1 km in 1992 did not change significantly with regard to total fluxes or constituents of particles. A different preservative was added to each trap to test and compare the effect. Also the partially available flux at 1.2 km, showed no difference from the deeper samples (Honjo et al., 1995).

fluxes calculated from samples which were treated by sodium azide were significantly less than fluxes of other elements in all periods; this indicates greater oxygen depletion. The percentage of > 1 mm particle flux in the total flux was largest in the formaldehyde-treated sample, followed by the $HgCl_2$-treated sample, and smallest in the sodium-azide-treated sample, as predicted. DOC measured in the supernatant of the sodium-azide-treated sample indicated that about 10% of the trapped organic carbon was dissolved in the supernatant (Manganini et al., 1994). The pH level in the samples' supernatant which is treated by formaldehyde with an appropriate buffer usually is kept close to the ambient water until recovery in a sealed sample bottle; also no significant elevation of Ca concentration in the supernatant, compared to ambient water, was found, indicating no significant carbonate dissolution. Five to 10% of the biogenic SiO_2 dissolved from formaldehyde-treated samples into the supernatant. The "flux" observed by recent researchers is usually a combination of the solid and dissolved portions which are found in the supernatant. During storage, a sample bottle of any time-series trap must be sealed from the ambient water so that the dissolved phase can be preserved.

7.3.5 *IN SITU* SEDIMENT TRAP INTERCOMPARISON IN THE DEEP WATER COLUMN

A number of sediment trap intercomparison experiments have been performed in deep-ocean layers. For example, an intercomparison experiment in the Santa Barbara Basin indicated that particle flux measured by traps with significant differences in configuration were comparable (e.g., Dymond et al., 1981); in addition the trap-measured flux was generally smaller, not catching the advection near bottom, but matching reasonably well with the general sediment-accumulation rate of the basin.

A large-scale comparison experiment at a Panama Basin location showed that traps with a wide range of opening or aperture size (0.004 m^2 to 1.5 m^2) and with cylinder- or funnel-type configurations collected similar fluxes that included a wide range of particle size and classes during 4 months of deployment along ridged bottom-tethered moorings (supported by strong upward tension to the tautline by applying a large amount of buoyancy to the mooring) (Honjo et al., 1992).

Samples collected from deep traps which were deployed in typical deep-ocean conditions in a deep basin of the Nordic Sea with less than 10 cm s^{-1} advection and indistinct directionality showed no statistical relationship between the flux, size fraction and kind of particles studied (Honjo and Wefer, unpublished data). When water advection was slower than 12 cm s^{-1}, Baker et al. (1988) found no difference in trapping efficiency between a trap which followed the water flow and a trap which was tethered at the bottom. These observations indicated that collection of settling particles by a sediment trap deployed in the deep ocean was not likely to be affected by the physical environment. In contrast, a strong,

unidirectional deep current of about 30 cm s^{-1} influenced the quality and quantity of sediment collected by a bottom-tethered sediment trap which was placed near the slope of the Panama Basin (Honjo, 1982).

7.3.6 SELF CALIBRATION OF PARTCLE FLUXES BY RADIONUCLIDES

The behavior of radionuclides offers an independent estimation of settling particle fluxes. Some radionuclides are chemically reactive, strongly absorbed by ocean particles and are supplied to the water column at rates which are known exactly by the decay of their parent nuclides in decay series (e.g., Bacon et al., 1976; 1988; this volume; Nozaki, 1987). In practice, a calibration is based on a determination of the degree of radioactive disequilibrium (deficiency of a daughter nuclide relative to a parent nuclide) in the water above the trap to be calibrated. Because of its favorable vertical flux balance, a trans-uranium nuclide with a relatively long half-life, ^{230}Th (7.52×10^4 year) has been used for the tracer to calibrate particle fluxes to the ocean's interior (Brewer et al., 1980; Anderson et al., 1983). This method can be better applied to a longer and continuous flux record such as one year (Bacon et al., 1985; this volume). A number of self-calibration efforts using radionuclide tracers on the deep-ocean samples in long-term deployments supports the measured mass flux, matching the disequilibrium model of ^{230}Th within a reasonable error, such as ±15% (e.g., Bacon et al., 1985; this volume). In contrast, radionuclide calibration applied to mass flux measured with floating sediment traps in the euphotic layer and upper ocean differs from the disequilibrium model (Buessler, 1991). Researchers agree a sediment trap tethered to the seafloor produces persistent and explainable results, and particles collected by such a sediment trap represent the vertical flux of settling particles in these deep-ocean layers.

The major alteration of particles including the dissolution of $CaCO_3$ and biogenic SiO_2 occurs within a thin, less than one centimeter thick, boundary layer where seawater and sediment interface (benthic transition layer; Cole et al., 1987). Therefore burial rate can only be estimated on refractory material (such as Al) or by using radioactive tracers (Dymond, 1984; Dymond and Lyle, 1985). At present it is usually not possible to compare a simple accumulation rate to, or calibrate it with, particle flux itself. Sedimentation rates estimated from ^{210}Pb, for example, are often high because they occur at a site where the slope gradient is relatively large, such as trench walls (Nozaki, 1989a) and slopes (e.g., Butman and Folger, 1979), or where there is a source of high energy re-suspension of sediment nearby (Gardner et al., 1985), advectively transported to a layer between the deepest sediment trap and the sea floor. Varved sediments of the Black Sea are thought to provide natural calibration of sediment-trap-measured annual fluxes. However, both studies of particles collected by time-series sediment traps and

analyses of varves on the seafloor in the Gulf of California and the Black Sea shed light on a new hypothesis: that a pair of bands in varves does not necessarily represent a year of particle sedimentation (Hay et al., 1990); on the other hand, the ratio between terrigenous and biogenic matter in the varves of the Gulf of California are well matched with the annual sequence of settling particles measured by time-series sediment traps (Thunnel et al., 1993).

7.4 SAMPLE SHARING AND LABORATORY ANALYSES

A significant advantage of investigating the settling particles collected by a large sediment trap is that this process supports multi-disciplinary studies. A time-series sediment trap with a 0.5 m^2 aperture is capable of collecting 50 mg per period (e.g., an annual per-period average at the Fram Strait) to about 400 mg per period (e.g., Bering Sea) and much more in a neritic environment (Wefer et al., 1988; Thunell et al., 1994a); these amounts are usually sufficient to support several research groups simultaneously working on the sample from one collection period. The inside of a modern sediment trap is coated with or made of analytical-grade polyethylene or its equivalent, and the structural frame is composed of titanium; therefore there is minimal contamination of the collected samples from the trap (Manganini, in preparation).

In order to share a sample among interdisciplinary projects such as listed in Table 7.1, it must be split into a number of aliquots. Samples collected with a VERTEX-type sediment trap (Knauer et al., 1979), which consists of a cluster of several independent collectors, would not require further splitting. All large-aperture, funnel-shaped time-series sediment traps (Honjo and Doherty, 1988) require a controlled sample splitting process. Biocoenosis investigations require the sample not be dehydrated, otherwise foraminifera tests and radiolarian shells would be unidentifiable, so it is mandatory that the sample be split with seawater collected with the sample. A wet-splitter can separate a one-cup sample into 10 equal aliquots with a better than 3.7% precision for typical > 1 mm samples (Honjo et al., 1995).

As explained below in more detail, the basic 5 biogeochemical properties of settling particles, converted to flux terminology (mg m^{-2} d^{-1}), are the total flux, and $CaCO_3$, organic carbon (nitrogen), biogenic opal and the lithogenic constituent fluxes. A typical procedure to analyze these 5 properties is illustrated in Figure 7.4. Although the operation needs improvement, laboratory intercalibration must be practiced frequently and continuously on basic laboratory procedures. Previous comparisons of results show relatively small deviations, less than ±10%, from the norm (Nozaki, 1989; Honjo et al., 1992; 1995). Usually these basic biogeochemical analyses consume 3/10 of the sample, or 3 1/10 aliquots (Figure 7.4).

Table 7.1 A typical sharing plan of a time-series-trap-collected sample using a wet sample splitter which divides the sample and cup water into 10 equal aliquots with known precision for the < 1 mm fractions. The > 1 mm fractions are usually divided by the "wet-cake" method (e.g., Honjo and Manganini, 1993). Basic biogeochemical constituent analyses and biocoenosis investigations usually require further splitting of a 1/10 aliquot.

1.	3 aliquots	Total flux and basic biogeochemical constituents: $CaCO_3$, biogenic SiO_2 (opal); organic elements (carbon, nitrogen and phosphorous); and lithogenic components
2.	2 aliquots	Radiochemistry
3.	1 aliquot	Trace metals and rare earth elements
4.	1 aliquot	Biocoenosis (coccoliths, diatoms, radiolaria and silicoflagellates)
5.	2 aliquots	Organic geochemistry
6.	1 aliquot	Archive (wet samples), to be dehydrated after a few years for dry/cold storage
7.	(1 aliquot)	Emergency supply

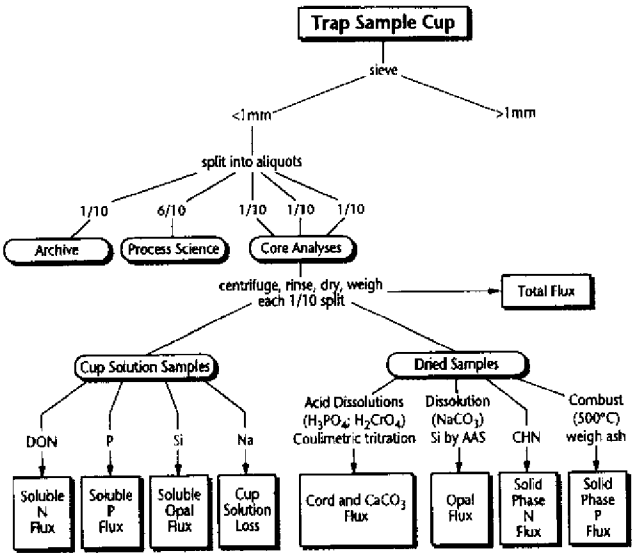

Figure 7.4 A diagram showing an analytical process for basic biogeochemical constituents of settling particle samples collected by a time-series sediment trap practiced by the majority of laboratories.

Since Spencer et al., (1978), many researchers have investigated radionuclides, including ^{234}Th, ^{232}Th, ^{230}Th, ^{228}Th, ^{210}Po and ^{210}Pb, effective tracers to constrain the time scale of the biogeochemical cycle. Typically, 1/5 of the sample is used for these analyses, but counting is a non-destructive process so the left-over samples

may be used for other types of analyses. A 1/10 aliquot is dried, analyzed and digested for trace elements including Ba (Francois et al., 1995), Cd, Ti, Cu, Mn, and many others (e.g., Brewer et al., 1980; Bruland et al., 1981; Tsunogai et al., 1982; Nozaki, 1989b; Jickells et al., 1990 and Thunell et al., 1994b). Organic compound studies usually require 1 or 2 aliquots.

Paleoceanography/paleoproximity research requires 1 aliquot for stable isotope analyses of ^{18}O and ^{13}C. In order to investigate independent taxonomic groups, further splitting of samples is required. For example, diatom or coccolithophorid research requires preparation of a number of 1/100 to 1/1000 aliquots for optical microscopy and SEM investigation. Lithogenic particle flux is usually estimated from the Al (and Ti) content (Dymond and Collier, 1988). Although clay mineral species are excellent tracers of settling particles, (Honjo et al., 1982b; Ramaswamy et al., 1991), X-ray diffraction studies require large amounts of trapped material. One 1/10 aliquot is archived with seawater for a few years then dehydrated for long-term storage. Another 1/10 aliquot is kept refrigerated as an emergency supply (Table 7.1).

7.5 WHAT ARE SETTLING PARTICLES?

7.5.1 ORIGIN OF SETTLING PARTICLES

Later research has indicated that fecal pellets are not the only form of vertical transport to bring ocean particles and organic matter downward (Pilskaln and Honjo, 1987), but that natural aggregates such as amorphous aggregates (often referred to as "marine snow"; Suzuki and Kato, 1953) have been found to be an important and often dominant mode of settling particles (e.g., Silver and Alldredge, 1981). In upper oceans, particularly in more productive areas such as upwelling coastal oceans, amorphous aggregates are abundant and individual aggregates are as large as a centimeter in diameter. Alldredge and Gotschalk (1988) reported a large aggregate with the diameter of about 22.5 mm and 75 mm long from the San Pedro Basin. The agglutinate labile matter suspended in surrounding seawater (Silver and Bruland, 1981), offer microcosms to host microbial activity and are a possibly significant food resource (Gowing and Silver, 1983). Fecal pellets are often attached to large aggregates and settle with them. In any case, the majority of settling particles are biogenic; lithogenic particles which are always heavier than sea water are a minor part - not more than several percent - of open-ocean particles.

As will be explained later, both fecal pellets and marine snow are produced as a reflection of the dominant ecosystems in the upper ocean at a given time. For example, the sediment which settled to deep layers of the northern Weddell Sea right after the retreat of the ice edge was dominated by marine snow which

consisted of flaky aggregates containing diatoms. However, such amorphous particles were later replaced by fecal pellets, and the peak flux consisted of monospecific fecal pellets (Fischer et al., 1988). In lower latitudinal, neritic stations it has been reported that the entire particle flux is made up of fecal pellets (e.g., Dunbar and Berger, 1981; von Bodungen et al., 1987), but this does not necessarily mean the area does not produce amorphous aggregates throughout the year.

The common structure of marine snow is, as Tsujita (1953a, b) originally observed, an agglutination of marine detritus on a "sticky" amorphous matrix. In the upper oceans, the configurations of aggregates are often variable, suggesting different origins. Discarded larvacean (Appendicularians) houses, often abundant in the open ocean (Alldredge, 1976), decaying gelatinous zooplankton such as *Doliolum*, salps, and medosae, and other unknown sources may supply the material to form substance for the late stage of a bloom which offers abundant material to form a matrix. Bacterial growth (Gowing and Silver, 1983) would enhance the matrix's ability to produce a sticky surface by bacterian extracellular biopolymers (e.g., Robb, 1984). The mass settling of living diatoms due to their apparent ecological needs (Smetacek, 1985) or the mass settling of coccolithophores during their "palmeroid" state (Smayda, 1970; Honjo, 1982) are examples of "pseudo-active" settling. The valves and girdles of common open-ocean diatoms such as *Chaetoceros* form into a long chain with protrusions of setae which interlock with each other as well as with other detritus. Also the common diatom *Rhizosolenia* with very fibrous frustules often form lint-ball aggregates by themselves.

Marine snow also occurs in the ocean's interior (Silver and Alldredge, 1981), and the distribution has been quantified, mainly by applying light-scattering photo-optics (Honjo et al., 1984; this volume, Chapter 5). The relationship between abundance of aggregates and particle flux in the deep open oceans has begun to be clarified (Asper et al., 1992; this volume, Chapter 5).

The distribution of aggregates in the ocean's interior is quasi-uniform, suggesting consistent downward settling; if aggregates were supplied constantly from the surface, the steady state of vertical distribution could not be kept. In the deep Panama Basin, however, many zones of higher concentration were found (Figure 7.5). This zoning is explained by marine snow which had accumulated on the near-by shelf, and which was occasionally resuspended by the strong boundary current and advected in an off-shore direction (Asper et al., 1992). A similar re-transportation of marine snow from a shoal to a deep basin by internal wave was observed recently by Tuji using a time-interval scattering camera in Sagami Bay, Japan (Tuji, 1993).

In situ camera observations indicate that individual marine snow particles in the ocean's interior are of lesser volume and more uniform than the aggregates in the upper layers (Honjo et al., 1984). A speculative explanation is that aggregates are shaved into a smaller size as a result of the hydraulic shear of seawater caused by settling through the water column. The resulting size is the product of the balance

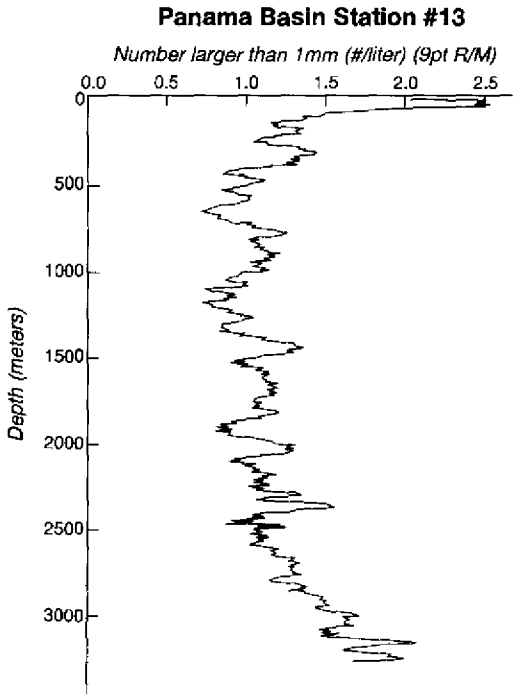

Figure 7.5 The distribution of large amorphous aggregates (> 1 mm diameter) per liter through a water column in Panama Basin using a "marine snow camera" (data collected by Asper and Honjo in 1987, a point flying average).

between the speed and the degree of agglutination which holds fine particles together in one-piece of aggregate. Particles thus sloughed off the hosts become suspended; this is the only process to produce suspended particles in the deep layer, as explained below.

7.5.2 THE CONSTITUENTS OF SETTLING PARTICLES

The process of particle export from the upper ocean to the interior is a complex interplay of the participants in the ocean's ecosystem which involves hundreds of species of animals, plants and microbes as well as land-based material such as pollen and aerosol particles. A flake of marine snow or a piece of pellet is a micro-cosmos that represents the complexity of the ocean. These complicated products of the ecosystem can be divided into four principal particle components: organic matter, $CaCO_3$, biogenic SiO_2 particles and lithogenic particles. The annual constituents of settling particles gained from some locations is presented in Table 7.2. More information is available in Wefer (1989), Tsunogai et al. (1991)

and Milliman (1993). Vertical variability of each of the constituents will be discussed in a later section.

7.5.2.1 The $CaCO_3$ component

$CaCO_3$ particles consist of two major classes. One is phytoplankton-produced exoskeletons, the vast majority of which are coccoliths and coccospheres (Steinmetz, 1991) (here they are referred to as coccoliths). The other is zooplankton-produced shells of planktonic foraminifera. In some areas and seasons, pteropod shells (aragonite) occupy significant portions of the $CaCO_3$ flux, but not consistently (e.g., Betzer et al., 1984; Fabry, 1989). The ratio between phytoplankton-produced and zooplankton-produced calcium carbonates is estimated to be about 6 to 4 (Honjo, 1977; Deuser and Ross, 1989; Fabry, 1989), but this warrants more detailed study. Although aragonitic pteropod ooze is distributed over a relatively large area of the Atlantic, Mediterranean and northern Indian oceans and is important in adjusting the ocean's alkalinity (Milliman, 1974; Berner, 1977; Betzer et al., 1984), the flux of these shells is found to occur sporadically, indicating patchy distribution (Harbison and Gilmer, 1986). However, Meinecke and Wefer (1990) found that the Lofoten Basin may have been an ideal location to grow shell-forming pteropods such as *Limaacina helicina* and *L. retroversa*; they observed a constant flux of shells in the late summer to autumn. Production of Mg-rich $CaCO_3$ is limited to the coral reef phase and produced by plankton (Milliman, 1974). However, Berner and Honjo (1981) reported Mg-rich $CaCO_3$ collected from a deep trap station in the Panama Basin 280 n. miles from the shore line, indicating lateral transport of reef carbonate.

7.5.2.2 The SiO_2 component

Oceanic biogenic SiO_2 mostly consists of poorly crystallized polymorphs of silica classified as *Opal*-AC (Calvert, 1983). In terms of mass, biogenic SiO_2 is largely diatom frustules. Compared to planktonic foraminifera, radiolarian shells arriving at the ocean's interior consist of far more diversified species (e.g., Takahashi, 1991). However, the contribution of radiolarian shells to biogenic SiO_2 fluxes is usually not more than 10%. Despite abundance, silicoflagellates in low-latitudinal, open-sea water are not significant in mass, but are an important paleoproximater (Lisitzin, 1972; Takahashi, 1989).

7.5.2.3 Organic matter

Organic compounds in settling particles are used as valuable environmental tracers. For example, it was found that arabinose sugar is enriched in the particles which settled during a calcareous phytoplankton bloom (coccolithophorids), though more fucose is included in siliceous frustules (Ittekkot et al., 1984a). From a Black Sea sediment-trap experiment, Michaelis et al. (1987) reported that sterol markers can be used to trace the origin of the settling particles. In general, the

ratio of glucose to ribose in the land-derived organic matter is larger than 50 (Mopper and Degens, 1972); the ratio is less than 10 in marine-phytoplankton-derived particles (Tanoué and Handa, 1986). Using this relationship in simple saccharide contents found in settling particles in the Japan Trench, Handa (1989) observed that the glucose/ribose ratio in the settling particles was 5 to 6 in the Japan trench and that a large portion of particles in the deep trap was advectively transported, suggesting that land organic matter does not reach the trench environment despite the relatively short distance between the shore line and the trench axis. On the other hand, using ^{13}C as a tracer, Druffel et al. (1986) observed that a significant portion of land-originating organic carbon was delivered to Ocean Station P, Gulf of Alaska which is located far from a land mass. Hinga et al. (1979) found that a significant portion of organic carbon flux at a deep slope station south of Cape Hatteras consisted of pine and cedar pollen; however, this observation was made during only a part of a year.

Rich information regarding the organic compounds in settling particles has been produced (e.g., Wakeham et al., 1980; Lee et al., 1983; Ittekkot et al., 1984a, b). Beside hard-tissue-producing organisms, there are significant "naked" plankton and microbial masses produced in the upper oceans, but often they are grazed and so are not microscopically isolatable in a sediment-trap sample. In an open-sea trap experiment, organic carbon does not form a flux peak by itself like other particle components. In many cases a large organic carbon flux is more likely to be associated with a biogenic-SiO_2 bloom than with a calcium-carbonate bloom. As an exception, in the Arabian Sea an organic carbon peak during the summer monsoon is associated with a $CaCO_3$ flux maximum (Haake et al., 1993). One reason for this coupling between the fluxes of organic carbon and biogenic SiO_2 is that amorphous opal contains a significant amount of organic carbon as the structural compound, up to 30% (Heath et al., 1976), while, on the other hand, coccoliths consist of pure calcite crystallites and foraminifera shells and contain no significant organic matter compared to diatom frustules.

Organic matter contains water in variable situations which are difficult to constrain by our present analytical methods. Therefore, organic carbon and/or nitrogen are independently analyzed to represent organic matter.

7.5.2.4 The lithogenic component

Lithogenic particles are always being transported from distant land sources to the surface of the ocean, and their distribution pattern reflects the earth's general atmospheric advection. The density of lithogenic particles in the air, which is related to their fallout rate over the sea, differs in several orders of magnitudes depending on the distance from the source (Duce et al., 1991). Three areas supply most of the lithogenic aerosol to the open ocean (this volume, Chapter 3).

Table 7.2 Total fluxes and fluxes of biogeochemically essential constituents measured at globally-distributed deep open-ocean stations, including large marginal seas, neritic environments (10), and the Black Sea (13). These stations were covered by bottom-tethered time-series sediment traps which were deployed at several hundred meters from the bottom yet above the nepheloid layer, for (at least) a full year. The contents of the essential biogeochemical constituents were published or provided by the original investigators. References: (1) Honjo et al. (1995); (2) Honjo et al. (1995) and Honjo and Manganini (unpublished data); (3) Honjo (1984) and C. S. Wong (unpublished data); (4) Nozaki (1989); (5) Honjo et al. (1995); (6) Honjo (1990b); (7) Honjo and Manganini (1993); (8) Pudsey and Honjo (unpublished data); (9) Fischer et al. (1988); (10) Wefer et al. (1988); (11) Nair et al. (1989); (12) Ittekkot et al. (1991); (13) Hay et al. (1991).

Station	Year	Location		Depth	Total	$CaCO_3$	SiO_2	C_o	C_{inc}	$CaCO_3$	SiO_2	C_o	C_a	Si	C_o/C_{inc}	Ca/Si	(Ref.)
					$g\,m^{-2}\,d^{-1}$					Weight %			Mole				
North Pacific																	
C. Okhotsk	90/91	53°N	149°E	1.1	47	4	25	1.7	0.5	9	33	3.6	1.7	11.7	3.4	0.1	1
C. Bering	91/92	58°N	179°E	3.1	52	6	31	1.8	0.7	11	59	3.4	2.7	16.8	2.8	0.1	2
Sta. P	82/83	50°N	145°W	3.8	56	19	30	2.3	2.3	35	54	4.1	7.7	14.1	1.0	0.4	3
Sta. P	83/84	50°N	145°W	3.8	17	9	7	0.9	1.1	52	38	5.2	3.6	3.1	0.8	0.6	3
Sta. P	84/85	50°N	145°W	3.8	22	11	10	0.6	1.3	44	44	2.7	4.3	4.6	0.5	0.7	3
Sta. P-C	85/86	48°N	138°W	3.5	26	12	11	1.2	1.5	42	42	4.7	4.9	5.1	0.8	0.7	3
Kuroshio-JT	88/89	34°N	142°E	4.2	36	12	6	1.1	1.4	33	17	3.1	4.8	2.8	0.8	1.2	4
EqPac	92/93	9°N	140°W	2.3	8	5	2	0.5	0.6	61	25	6.0	2.0	0.8	0.8	1.8	5
EqPac	92/93	5°N	140°W	2.1	27	18	6	1.5	2.2	66	23	5.5	7.2	2.4	0.7	2.1	5
EqPac	92/93	2°N	140°W	2.2	27	18	6	1.3	2.2	67	23	4.9	7.2	2.4	0.6	2.1	5
EqPac	92/93	EQ	140°W	3.6	35	23	7	1.2	2.8	66	21	3.5	9.2	3.4	0.4	1.9	5
EqPac	92/93	2°S	140°W	3.6	31	18	7	1.3	2.1	57	22	4.2	7.1	3.2	0.6	1.6	5
EqPac	92/93	5°S	140°W	2.2	22	15	5	1.0	1.8	66	21	4.5	5.9	2.1	0.6	1.9	5
EqPac	92/93	12°S	135°W	3.6	8	6	1	0.3	0.7	80	10	3.9	2.5	0.4	0.4	4.7	5

North Atlantic																	
Fram Strait	84/85	79°N	1°E	2.4	7	1.4	0.6	0.4	0.2	20	8	5.6	0.6	0.3	2.4	1.4	6
Bear Island	84/85	76°N	11°E	2.8	29	7	2	2.9	0.8	23	7	10.0	2.6	0.9	3.6	2.0	6
Greenland B.	84/85	75°N	7°W	2.8	10	3	3	0.4	0.3	33	26	3.9	1.3	1.2	1.0	0.8	6
Aegir Ridge	85/86	70°N	2°W	2.8	17	9	1	0.5	1.1	53	9	3.1	3.6	0.7	0.5	3.7	6
Lofoten Basin	84/85	69°N	10°E	2.8	24	11	1	1.4	1.4	48	5	5.8	4.6	0.5	1.0	6.5	6
Jan Mayen	85/86	66°N	1°E	2.6	17	9	2	0.6	1.1	53	9	3.4	3.7	0.8	0.5	3.4	6
NABE	89/90	48°N	21°W	3.7	26	15	6	1.0	1.8	59	21	3.8	6.2	2.6	0.6	1.7	7
NABE	89/90	34°N	21°W	4.5	21	13	2	0.9	1.5	61	9	4.3	5.7	0.9	0.6	3.9	7
Southern Ocean																	
S. Georgia Is.	87/88	57°S	37°W	2.7	8	1	7	0.1	0.4	13	88	3.8	0.5	3.3	0.3	0.2	8
Weddell Sea	85/86	62°S	35°W	0.9	0.4	0.01	0.3	0.03	<	2	75	8	<	0.1	25	0.03	9
Bransfield St.	85/86	62°S	58°W	1.6	108	5	39	4.3	0.6	5	36	4.0	2.0	18	7.1	0.08	10
North Indian Ocean																	
Arab. Sea W	86/87	16°N	60°E	2.9	34	19	7	1.8	2.3	56	21	5.3	7.6	3.4	0.8	1.6	11
Arab. Sea C	86/87	14.5°N	65°W	2.8	27	18	3	1.5	2.1	66	12	5.7	7.0	1.5	0.7	3.3	11
Arab. Sea E	86/87	15.5°N	69°E	2.8	24	12	3	1.6	1.4	50	13	6.8	4.6	1.5	1.1	2.2	11
B. Bengal C	87/88	13°N	84°E	2.3	45	17	8	2.6	2.0	38	19	5.8	6.8	7.9	1.3	0.6	12
E. Ind. O	87/88	4.5°N	87°E	3.0	38	19	7	2.0	2.2	49	19	5.3	7.4	8.7	0.9	0.6	12
Black Sea																	
N. of Amasra	82/85	42°N	32°E	1.2	100	28	9	13.1	3.4	28	9	13.0	11.2	4.2	3.8	1.8	13
N. of Sakarya	86/88	42°N	30°E	1.2	28	10	10	5.6	1.2	36	36	20.0	4.0	4.7	4.6	0.6	13

By far the largest airborne transportation of lithogenic matter is Kosa (which means "yellow sand") from Eurasian Drylands, including the Gobi Desert (Tsunogai and Kondo, 1987). Kosa is transported eastward by the high-altitude jet stream and travels to the eastern North Pacific; it covers wide areas of the western and central Pacific seafloor (e.g., Rex and Goldberg, 1958). As a proof of this long-distance transport, mica particles of granitic origin in Kosa, older than Hawaii, have been found in the soil of that mid-ocean basalt island (Dymond et al., 1974).

The second area that supplies lithogenic particles is the central African desert. The trade winds carry dust plumes westward across the North Atlantic. Large plumes in the spring occasionally travel as far as the Florida peninsula, and the dust from Africa is found in the snow fields of the high Andes (this volume, Chapter 3). The third area of open ocean which receives a significant amount of lithogenic aerosol is the Arabian Sea. Desert dust is transported from coastal drylands along the west coast of the Arabian Sea as well as from far-distant interior North Africa. In the Arabian Sea, lithogenic particle fluxes were as large as about 4 to 9 g m^{-2} y^{-1} (Ramaswamy et al., 1991; Haake et al., 1993).

7.6 PARTICLE REMOVAL PROCESSES

7.6.1 REMOVAL PROCESSES OF PRIMARY PRODUCTION BY PARTICLES

At the 48°N 21°W JGOFS station, dissolved inorganic nutrients decreased rapidly during April 1989, as the phytoplankton bloom in the euphotic layer progressed. Between 8 and 18 of May, dissolved SiO_3, NO_3 and PO_4 were virtually depleted from the upper 50 m. After this period, these nutrients slowly recovered in the surface layer. In the same area, during the period from May 29 to June 13, the particle flux, caught in a sediment trap set in the 2-km-deep layer, suddenly increased (Figure 7.6). This scenario is explained as phytoplankton photosynthesis converting all available inorganic nutrients in the euphotic layer to particulate matter, some arriving in the ocean's interior within a short time, supporting the view of rapid transportation to the ocean's interior.

7.6.2 "LEAKY" BELT CONVEYOR

Only a part of the nutrients converted to organic particulate matter actually did arrive in the ocean's interior during the above-mentioned experiment; about 30% of SiO_3 and as little as 1.7% of NO_3 which had been removed from the surface layer was delivered to the 2-km trap; only 1.3% of organic matter was produced

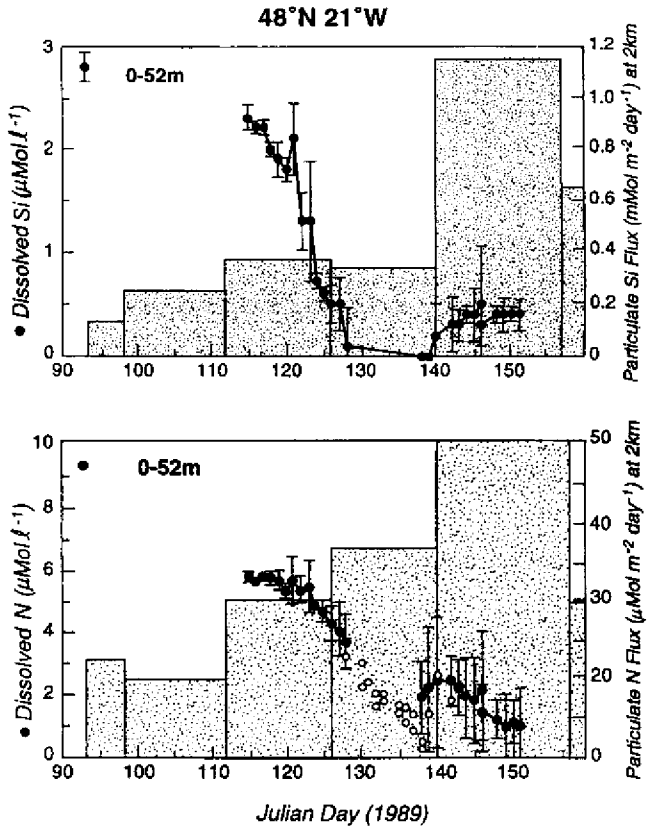

Figure 7.6 Variability of dissolved SiO_3 (upper panel) and NO_3 (lower panel) in the upper surface layer (0–52 m) from April 3 to May 31, 1989 at 48°N 21°W compared with biogenic SiO_2 and particulate N fluxes at the same station (right axis) (Honjo and Manganini, 1993).

by photosynthesis (Honjo and Manganini, 1993). The organic matter in the living cell, in cytoplasm as liquid, can be returned to the DOM pool immediately. The nutrients and organic carbon which did not arrive at 2 km thus were recycled back to the water column before they reached that point. Therefore, a significant portion of nutrients were recycled where the organisms lived. Settling particles, both amorphous aggregates and fecal pellets, attract microbial activity (Turner and Ferrante, 1979; Karl et al., 1984; Alldredge and Hartwig, 1986); thus the mineralization of organic constituents is accelerated, and they also return to the dissolved pool. The protective membranes of fresh fecal pellets of metazoans usually disappear by degradation before they settle through the euphotic layer and allow exchange of interstitial liquids with seawater (Honjo and Roman, 1978).

These observations, as well as the fact that fine particles continue to slough off from the host settling particles, suggest that the transportation mechanism of particles, or the removal process of organic matter from the euphotic layer to the ocean's interior, can be described as a "leaky" belt conveyor.

7.6.3 NEED FOR BALLAST

The physical parameters of aggregates which arrive in the ocean's interior are not well known. As previously explained, an aggregate is highly porous (> 99%; Alldredge and Gotschalk, 1988), encapsulated by a viscose watery layer which further reduces net gravity. The main framework of an amorphous aggregate is made of material of about equal density with water, such as cellulose (dry weight = 1.5 g cm^{-3}) and other biopolymers. The density of living plankton has been reported as 1.025 g cm^{-3} (Smayda, 1970) which is about the same as the density of water. Because of the large water and organic content (Calvert, 1983), the in-water density of biogenic SiO_2 of many diatom frustules and radiolarian shells is not much different from water (Takahashi et al., 1983; Takahashi, 1991). Although shallow-ocean aggregates are different from the ones settling to the deep ocean, Alldredge and Gotschalk (1988) observed that the median absolute density of the aggregates of marine snow collected from the San Pedro Basin (neretic) was 1.02502 g cm^{-3}

It is obvious that an aggregate could not settle vertically through the water column without ballast (e.g., Ittekkot and Haake, 1990). $CaCO_3$ is the densest of marine components (d_{air} = 2.71). Quartz or volcanic glass follow. Coccoliths, juvenile planktonic foraminifera and small pteropod shells (aragonite is slightly denser than calcite) can be used also as efficient ballast to settle aggregates. As previously mentioned, carbonate is usually the most abundant component in settling particles compared to other particle classes in the world's oceans (except for the Antarctic Ocean; Fischer et al., 1988; Wefer et al., 1988). Forty to 60% of the total mass consists of $CaCO_3$ particles. The descending speed of particles is generally faster during the bloom period when coccoliths are abundantly produced in the upper ocean (e.g., Honjo and Manganini, 1993). This can also be observed in the equatorial Pacific where the carbonate content in settling particles is significantly larger (up to 65% of total dry mass) than at other stations (Honjo et al., 1995).

Aerosol particles also serve as ballast to remove settling particles from surface layers. In the Arabian Sea, the variability of particle fluxes in the ocean's interior was more positively correlated with wind speed than with surface temperature, which indicates upwelling (Nair et al., 1989; this volume, Chapter 14). This perhaps can be related to the deposition of airborne clay and framework silicate particles which were incorporated into ordinary settling particles enhancing their settling speeds during productive monsoon periods (Ittekkot and Haake, 1990; Ittekkot, 1991). Ittekkot et al. (1991) also argued that the enhanced particle flux in

the Bay of Bengal was attributed to fresh water which contains denser, suspended lithogenic particles derived during the monsoon from the continent (this volume, Chapter 15). Jickells et al. (1990) found that the organic carbon and Al flux is positively correlated in the samples from the Sargasso Sea.

7.6.4 SETTLING PARTICLES VS. SUSPENDED PARTICLES

Because of large differences in the velocity between settling particles (such as marine snow and fecal pellets) and independently suspended fine particles, the former should continue gathering the latter on their "sticky" surfaces while descending.

Meantime water shear forces tear off detritus from the surface of settling particles, as previously explained. Such particles, resuspended while descending, are recaptured, sooner or later, by other, passing settling particles. This cycle would be repeated throughout the water column. This model implies that particles which are suspended in deep layers are not necessarily older than ones in shallow layers, and vice versa.

A mixture of fresh and more corroded fragments of coccoliths were found suspended in the highly under-saturated layers of the Pacific (Honjo, 1975). This is one piece of evidence which supports the above "bus-rider"-hypothesis explanation of the "Coccolith Riddle" of the 1970's (Honjo, 1976). When a coccolith remains in suspension for relatively long periods, without being re-captured by other settling particles, it progressively loses its volume which further slows the descent speed, or it disappears by disintegration and dissolution. Although their quantity is still unknown, such coccoliths which dissolve *in situ* contribute to increased deep-water alkalinity. In the under-saturated deep layers of the North Pacific, the number of suspended coccoliths rapidly decreases with depth (Okada and Honjo, 1973) (Figure 7.7), supporting the above explanation, but the flux of carbonate is maintained throughout the abyssal layers (Honjo et al., 1995). This implies that the net dissolution of carbonate caused by sloughed-off coccoliths is not significant, but that coccoliths are recaptured by passing-by settling particles, causing the majority to arrive in the deep interior. The rate of exchange between suspended and settling coccoliths can be constrained mainly by: 1) the residence time of suspended coccoliths in the under-saturated water column; 2) the population of suspended coccoliths; and 3) the descending speed of settling particles. The rate of scavenging and departure of fine, independent particles to/from settling particles in the ocean's interior was better constrained by using radionuclei decay factors (Nozaki, 1986; Nozaki et al., 1987) and further developed by Tsunogai (1987) as the "train-passengers model".

Another riddle: Which are the originals, suspended or settling particles? In fact, they are inseparable and their relationship is dynamic. The majority of ocean particles produced in the upper layers are in suspended-particle size. Without settling particles, there will be no suspended particles in the ocean's interior.

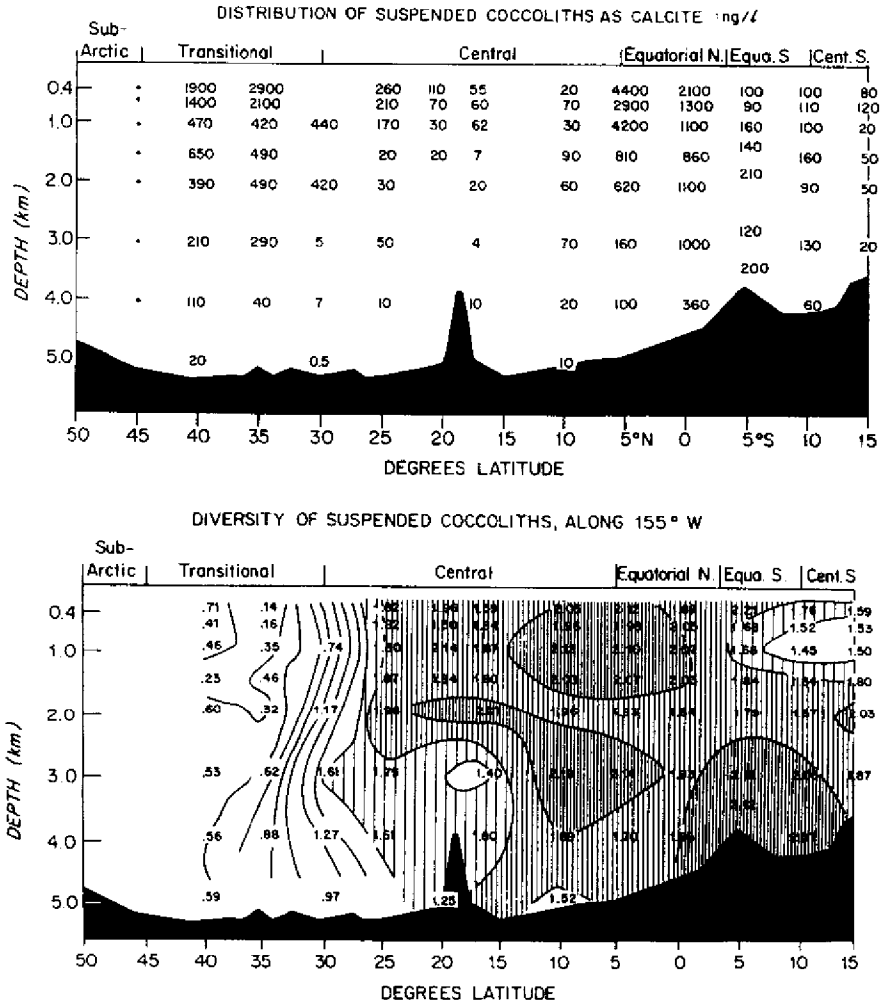

Figure 7.7 The distribution of the estimated total weight of the suspended coccoliths in ng per liter of sea water from 50°N to 15°S along 155°W (upper panel). Note that the weight decreases rapidly with depth at the transitional, central and northern equatorial zone stations. Suspended coccoliths did not decrease as much as at the other stations at the Equator and central zones in the southern hemisphere. On the other hand, the Shannon Weaver's species diversity of suspended coccoliths does not change significantly with depth (lower panel) (Honjo, 1975).

7.7 SETTLING RATES OF PARTICLES

7.7.1 ESTIMATION OF THE RESIDENCE TIME OF PARTICLES FROM OFF-SETTING BENCHMARKS

The "temporal off-set" of "benchmarks" of fluxes have been repeatedly found by a number of open-ocean, synchronized, time-series sediment trap experiments (e.g., Honjo, 1984). "Benchmarks" are defined as traceable time events such as peaks or valleys of total mass or component fluxes, normal and unusual blooms (Honjo and Manganini, 1993), blooms of specific taxonomic units (Takahashi, 1986), and meteorological forcing events such as onset of the monsoon and high-wind events (Ittekkot and Haake, 1990; Nair et al., 1989; Hay et al., 1990; Ramaswamy et al., 1991).

Off-set of benchmarks constrains the residence time of mass or bulk particles between the depths where two or more time-series traps are deployed in a depth series. The open/close timing of all sediment traps involved in an experiment must be synchronized. A flux "peak", one of the most useful benchmarks, is caused by the upper ocean layer producing and supplying a higher density of settling particles such as marine snow and/or settling particles with a higher sinking speed as a pulse. A flux "valley" is generated by a condition in reverse of the peak.

To estimate the average residence time of settling particles (R_{ave}) by offset of arrival of a benchmark, the temporal resolution (and the range of error) is the same as a trap open period. In case benchmarks occur at the same time, the settling particles reside between two traps for a shorter time than one open period (t). When a benchmark arrives at the deeper trap one open period (t) later, R_{ave} equals t. The maximum residence time of individual particles is $2t$, and the minimum is 0. When a benchmark skips one period at the deep trap, R_{ave} is $2t$, the maximum residence time of individual particles is $3t$ and the minimum is t. The shorter the open period (t), the higher the resolution of residence time to be estimated. However, on a practical basis, an open/close schedule cannot be set too short for resolving the finer arrival sequence of benchmarks. Particles collected by a funnel-shaped trap adhere to the interior wall of the cone, then slide down the slope making frequent micro-avalanches before settling in the sample bottles located at the bottom of the trap. This perturbs the chronological relationship between arriving particles. For a commonly used trap with a 0.5 m^2 aperture, this period of perturbation lasts an average of several days (Honjo and Manganini, unpublished data).

7.7.2 SETTLING SPEED OF PARTICLES

The bulk descending speed of settling particles for an open period can be obtained by dividing the depth between a pair of traps (D_p) by R_{ave}. As an example of D_p/R_{ave} estimate, Ocean Station P in the Gulf of Alaska (Honjo, 1984) can be cited. The highest flux peak observed at the 1-km trap appeared one period (t = 15 days) later in the 3.8-km trap moored at the same location (D_p = 2.8 km). The average bulk settling velocity was thus estimated as 200 m d^{-1} with the minimum speed of 93 m d^{-1}. We also found that this average settling velocity was applicable to all three basic particle classes including organic carbon (Figure 7.8) (database by Dr. C. S. Wong, the Institute of Ocean Sciences, Sydney, BC, Canada). The peak maximum of biogenic particle flux observed at this station was as large as 600 mg m^{-2} d^{-1} in late July 1983. The average bulk settling velocity during this high-flux period was faster than during a period of normal flux.

As another example of such estimation, at 48°N 21°W, a JGOFS North Atlantic Bloom Experiment (NABE) station, we deployed 3 traps at approximately 1, 2 and 3.7 km along a mooring (Figure 7.9). The bloom in the spring of 1989 observed at 1 km was repeated at 2 and 3.7 km. The two peaks observed at 2 km (the middle day of the open period: JD 148 = May 29, 1989 and JD 178 = June 27, 1989) were fused into a single broad peak on JD 164 (= June 13, 1989) seemingly retarding the first peak (JD 148). Curiously, the peak on JD 148 at 1 km was smaller than that at 2 km, and the prominent peak on JD 178 was not found at 1 km (Figure 7.9). Eddy movement may be an explanation (Newton, et al., 1994). This "missing flux" has also occurred at a number of other locations (Honjo and Manganini, 1993).

Although the flux at 2 km decreased abruptly after the JD 192 period, the flux at 3.7 km decreased gradually to the end of the post-bloom period, suggesting that the sedimentation ended at 2 km but continued at 3.7 km during this period. The percentage of biogenic SiO_2 increased in the sediment caught at the 3.7-km trap due to the increased content of diatom frustules. We speculate that light frustules with large surface areas took more time to settle through the water column (Honjo and Manganini, 1993). The maximum fluxes of *Bacteriastrum delicatum* at 1 and 2 km, an abundant chain-form diatom, were observed during the periods which occurred on May 13 and June 13, respectively, taking about a month to settle through only one kilometer. The maximum flux of this diatom species at 3 km occurred during the period on June 27, only two weeks later, even though covering more distance, 1.7 km. Such apparent acceleration of sedimentation at deep layers at this station was observed in a number of other diatom species and silicoflagellate species.

The sequential pattern of the total flux during the 1990 bloom period at 34°N 21°W at the 1248-m trap was generally repeated at deeper traps, particularly in the first month, indicating that the onset of surface bloom rapidly propagated to the ocean's interior within one open/close time period (Figure 7.9). At the middle

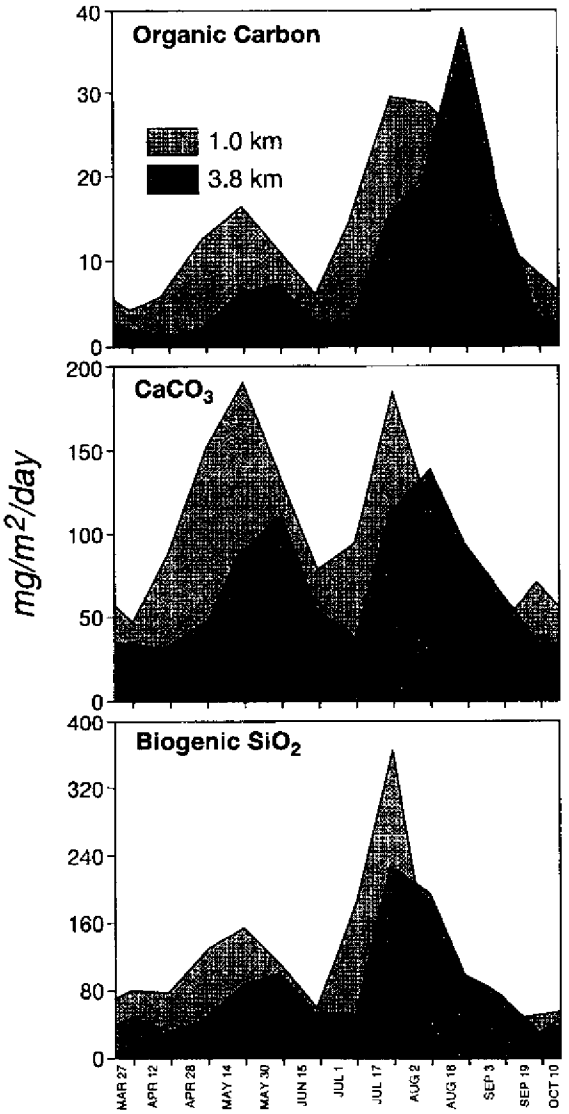

Figure 7.8 Organic carbon, $CaCO_3$ and biogenic SiO_2 flux at Ocean Station P, 50°N 145°W from March to October, 1983. The bench marks of flux delays for one open period (15 days). A significant peak of organic carbon during the period August 15 to September 3 at 3.8 km which was dominated by gelatinous zooplankton remains, was not observed at 1.0 km depth. This may indicate an eddy effect (Honjo, 1985).

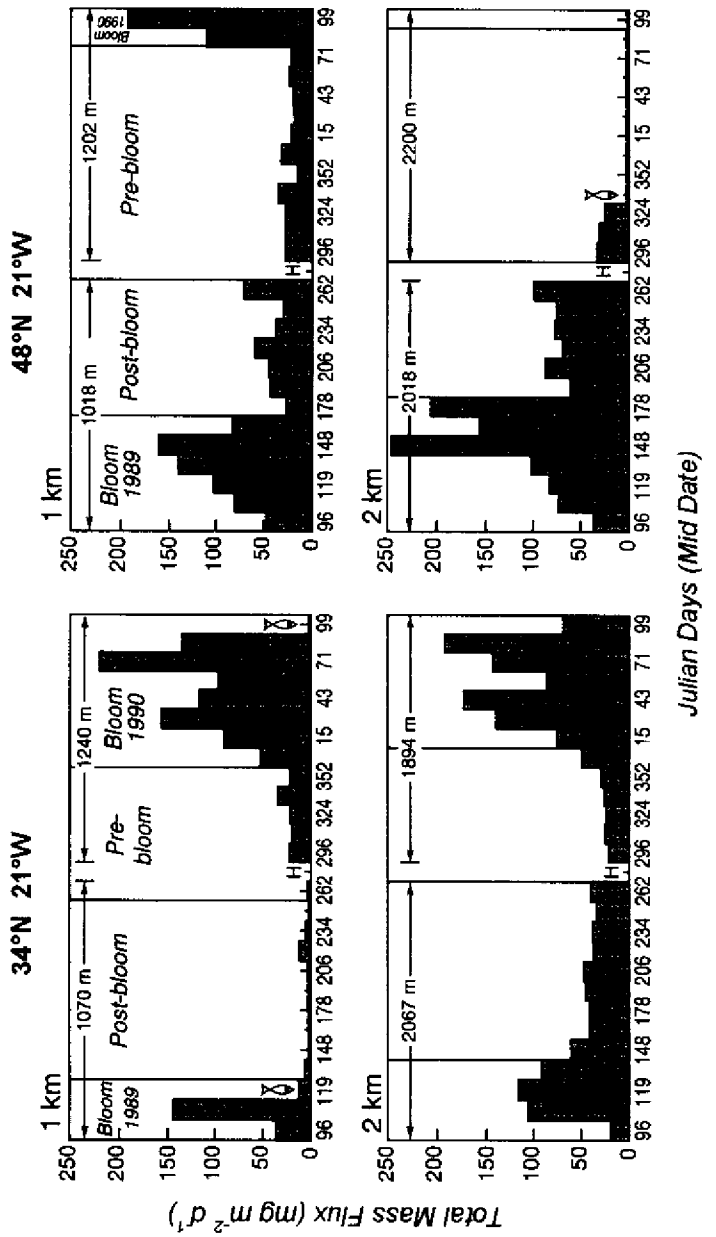
34°N 21°W
48°N 21°W
1 km
2 km
Bloom 1989
Post-bloom
Pre-bloom
Bloom 1990
1070 m
1240 m
2067 m
1894 m
1018 m
1202 m
2018 m
2200 m
Total Mass Flux (mg m-2 d-1)
Julian Days (Mid Date)

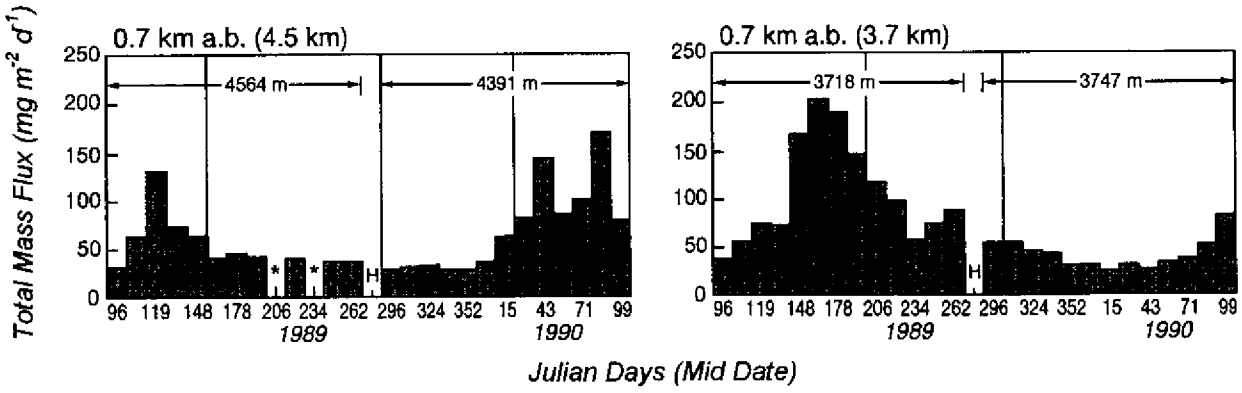

Figure 7.9 Annual variability of mass flux at 34°N and 48°N 21°W at three depths with distinction between bloom, pre- and post-bloom episodes with 14-day resolution. Note that the majority of the annual particle flux is provided by a spring bloom at these North Atlantic Stations. The periods indicated by a fish symbol indicate when an argentine fish was accidentally caught, spoiling the flux data thereafter. Note the peak of flux during the 1989 spring bloom at 48°N was delayed toward the deeper layers. This delay has been observed in many other areas of the ocean. On the other hand, the spring bloom of 1990 at 34°N did not show a clear delay in particle arrival at the greater depths (Honjo and Manganini, 1993).

trap, only 628 m deeper than the shallowest, at 1248 m, two peaks fused into one peak. Although the amplitude of flux variability during each period was reduced in the deepest (4371-m) trap, the benchmarks of the middle trap, which was 2.5 km above, arrived during the same period. This observation suggests that, at this station, the settling speed of bulk particles during the bloom episode was more rapid in the deeper than in the shallower part of the water column.

The observations explained above indicate that the descending speed of particles appears to fall in a relatively narrow range; the average ranges from 80 m d^{-1} to 200 m d^{-1}. This is in the range of the descending speed of fecal pellets produced by common grazing mesozoans as determined under laboratory conditions (Smayda, 1966; Small et al., 1979). However, some classes of ocean particles are de-coupled from this normal settling particle sedimentation scheme and show much faster settling velocities. For example, although not yet confirmed in the field, Fowler and Small (1972) reported, from a laboratory experiment, a much faster (several thousand meters a day) sinking speed of euphausid's fecal pellets. At 48°N 21°W, adult-stage planktonic foraminifera tests (> 150 μm) were caught in the same period at all depths from 1 km to 3.4 km, indicating that they settle independently at their own Stokesian sinking speed (Berger and Piper, 1972; Takahashi and Bé, 1984) penetrating the layer of more slowly settling marine snow (Figure 7.10). This suggests near instant copying of the environment where the foraminifera are grown on the deep ocean floor. If this mode of plankton growth is common in the other oceans, this fact would strengthen the proximity of

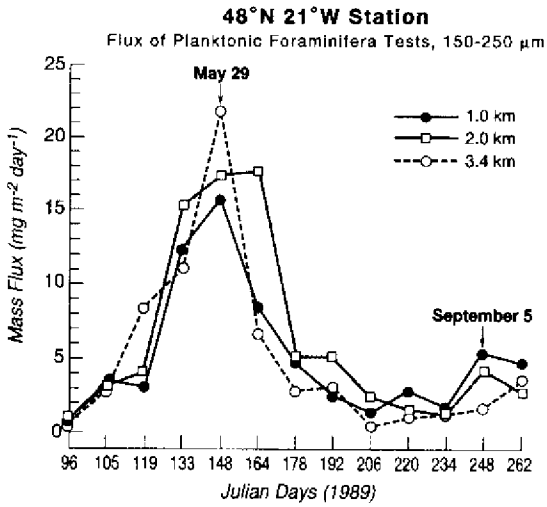

Figure 7.10 Flux of adult planktonic foraminifera tests (150–250 μm) at 48°N 21°W at three depths during the earlier half of 1989, showing no off-set of arrival time at deeper traps, indicating a rapid settling speed (Honjo and Manganini, 1993).

planktonic foraminifera tests with SST and hydrology (Curry et al., 1982; Deuser, 1986; Thunell and Honjo, 1989) such as pinpointing the timing of upwelling in the Arabian Sea (Curry et al., 1992).

Shanks and Trent (1990) and Alldredge and Gotschalk (1988) reported that the median *in situ* sinking rate of aggregates in the upper ocean (SCUBA depth) is about 50 to 100 m d^{-1}. The rates measured by *in situ* settling cylinders also suggested the rate is not as high as the ones estimated from the off-set of benchmarks (Asper, 1978; this volume). No explanation has been offered concerning why these two independent estimates give significantly different results. The excess density of upper ocean aggregates may be smaller than that of the deep ocean aggregates because of the former's fresher organic matter and less ballast.

A number of researchers have attempted to measure the descending speed of settling particles using several methods other than the off-set of benchmarks. For example, Lampitt (1985) observed the rate of arrival of plant detritus on the deep seafloor using a time-lapse camera, also collected very fresh detritus by tube corer, and compared its timing with the surface bloom. Asper (1987) measured the rate of arrival of settling particles at the bottom of a cylindrical sediment trap as well as from the side of a transparent *in situ* settling chamber using sequential photography. These experiments have resulted in settling speeds equivalent to the slow range of settling rates estimated by the off-set method mentioned above.

7.7.3 REVERSE ESTIMATE OF THE SUCCESSION OF AN UPPER OCEAN EVENT

Assuming that each settling particle carries "memory" of its production in the upper ocean by ecological and biogeochemical processes, and that it settles with relatively high speed at a known rate, the succession of events in the upper ocean can be estimated semiquantitatively by examining a set of time-series trap samples.

As an example, a scenario of an ecosystem sequence from the onset of the spring bloom (end of April) to the virtual cessation of surface productivity in late summer was estimated semiquantitatively at a North Atlantic station 48°N 21°W (Figure 7.11). The majority of sediment collected before May 29 (1989), consisted of fine particles which are apparently disintegrated amorphous aggregates and contained fewer fecal pellets of a size smaller than the annual norm. As previously mentioned, the sample collected from May 20 to June 6 contained a large number of adult foraminifera tests, resulting in a significant increase of carbonate flux during this period. A planktonic foraminifera bloom occurred rather early in the zooplankton bloom stage (Figures 7.10 and 7.11), but it is not clear whether, because of their fast settling speed, foraminifera tests arrived earlier than the fecal pellet flux maximum or plankton foraminifera are indeed the early birds when the bloom begins. Also diatom frustule flux reached maximum at the 2- and 3.7-km traps during the same period. The number and also the individual size of fecal

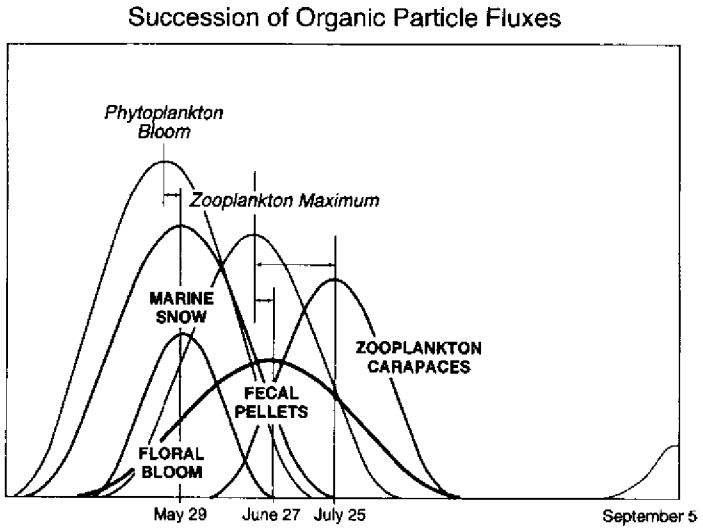

Figure 7.11 An example of qualitative reconstruction of ecosystem succession from flux samples collected in time series at a depth of 2 km during the bloom episode (48°N 21°W).

pellets in the sample increased, and this was maintained to late June, the end of the 1989 bloom episode. The two samples collected during the post-bloom episodes, August and September, contained a large number of zooplankton carapaces in the > 1 mm fraction. Samples from the latter period included chunks of gelatinous zooplankton; many were larger than 1 mm, but these were limited to the 1.2-km trap (Honjo and Manganini, 1992).

This observed sequence represents a text-book case of ecosystem succession in the open sea, showing the interaction between primary productivity, grazing, and removal from the upper layers (e.g., Peinert et al., 1987; Peinert et al., 1989; Heiskanen, 1990; Wassmann and Slagstad, 1990). First, an earlier spring phytoplankton bloom takes place in the thickened mixed layer when solar radiation is enhanced and water temperature elevated. The mass of phytoplankton is quickly removed from the surface layer to the ocean's interior as soon as the bloom starts. About the time of the maximum bloom at this station, grazing zooplankton become more dominant and advance their growth stages, becoming larger in size, as estimated from the increasing size and production of fecal pellets.

When nutrients are exhausted from the euphotic layer by phytoplankton and are totally removed from the euphotic layer, the zooplankton population is removed as large carapaces. As the final stage, in summer, the gelatinous zooplankton die and their carapaces arrive in the ocean's interior, but this large amount of fresh organic matter is more labile, is remineralized much more rapidly than normal

settling particles, and does not arrive at deeper layers. Gardner et al. (1983) observed that fresh labile ocean products degraded at rapid rates in the deep layers while they were exposed along moorings.

7.8 MESOSCALE EDDIES AND VERTICAL VARIABILITY OF FLUXES

Both the movement of eddies and the Lagrangian movement of settling particles are crucial for understanding the mass flux of particles in the deep ocean (Deuser et al., 1988; Siegel et al., 1990; Newell et al., 1994), particularly to explain the vertical variability of consecutive particle components such as $CaCO_3$ (Figures 7.8 and 7.9). In particular, mesoscale eddies of coccolithophorids such as reported by Holligan et al. (1983) from the North Atlantic, and Honjo (1982) from the Panama Basin, can be used to test the model in detail.

This model explains that if a depth-series sediment trap array is located right below the localized surface bloom, vertical flux would decrease with depth and increase with increased distance from the bloom. In the equatorial Pacific, a set of traps which were set 100 m apart at 2 km collected, for one year, almost identical mass fluxes in all particulate classes (Figure 7.3). This experience confines the term of Lagrangian diffusion, indicating that the source of particles is consistent. On the other hand, the deep ocean fluxes at two trap arrays in the mid Atlantic separated by about 100 km were almost indistinguishable during their main blooms. However, a peak of particle flux in the autumn of 1990 was far smaller at trap locations about 100 km away than at another location. This was interpreted as being caused by the shifting of a mesoscale eddy in this area at that time (Newton et al., 1994).

However, not all of the changes can be attributed to mesoscale eddy diffusion. Near the continent where a large quantity of fine bottom sediment is re-suspended by the boundary current, the flux increases significantly with depth (Honjo et al., 1983; Asper et al., 1992). It is conceivable that more quickly descending particles could catch up with the slowly descending particles below, resulting in an increase of flux by integrating produced particles which previously left the upper layers. In such a case, a benchmark of settling particles does not represent the productive event. A deep-ocean marine snow camera has captured many zones where settling particles are far more concentrated in a water column (Asper et al., 1992). Alternating dense and thin clouds of marine snow are often visible from the portholes of descending deep-sea submersibles. Beside a pulsing supply of settling particles from the source (Asper et al., 1988), such zonal or vertically uneven distribution of settling particle density can also be produced by a difference in settling speed.

7.9 ALTERATION OF SETTLING PARTICLES

Some biogeochemical components of the settling material to the ocean's interior are altered greatly; other components are not significantly altered. In general, $CaCO_3$ and lithogenic particles are well preserved even in calcite-under-saturated water, but organic matter is altered far more while settling through a water column. Biogenic SiO_2 is more susceptible to dissolution, but usually the mass does not decrease significantly within the bathypelagic water column.

At most of the deep ocean stations where sediment trap experiments were conducted, only a few percent of the labile matter or the labile portion of particles arrived in the ocean's interior; other portions were mineralized into solutions and returned to the water before reaching the abyssal layer. However, the majority of $CaCO_3$ (which occupies up to 60% of the settling particles in many deep oceans), all lithogenic particles, and about a third of the biogenic SiO_2 particles should arrive in the ocean's interior. In other words, about 75% of the particles which are produced in the upper oceans will arrive in the deep layers and on the ocean bottom.

7.9.1 INORGANIC CARBON: $CaCO_3$

At all stations in the North Atlantic, including a Nordic Sea station, $CaCO_3$ particle flux showed no evidence of decreasing with depth (Honjo, 1990a; Honjo and Manganini, 1993). In the North Pacific where the calcite compensation depth is as shallow as several hundred meters, the flux of $CaCO_3$ particles can decrease with depth; however, a limited number of depth-series measurement of $CaCO_3$ fluxes in the Pacific were not conclusive, differing by season, location and perhaps eddy effects. In the Gulf of Alaska, annual $CaCO_3$ flux at Ocean Station P decreased significantly with depth throughout a long-term time-series observation (Honjo, 1984) (Figure 7.8). On the other hand, at equatorial Pacific stations along 140°W, the calcite compensation depth is as low as approximately 400 m for example at 10°N 140°W (Takahashi, 1975). However, annual $CaCO_3$ fluxes did not decrease significantly with depth (Honjo et al., 1995). At a subtropical Pacific Gyre station, 15°N 151°W, the $CaCO_3$ flux at 2.8 and 4.3 km was virtually the same, but decreased to 57% at 5.6 km although this non-time-series experiment lasted only 2 months in the autumn (Honjo, 1980). At a station at the great depth of 8.8 km in a Pacific trench, $CaCO_3$ flux decreased to a larger degree than at 4.3 km (Nozaki, 1986a); this subject will be elaborated later in this chapter.

If particulate inorganic carbon is produced proportionally to particulate organic carbon, primary production can be estimated from the flux of $CaCO_3$ which is not essentially influenced by depth in a $CaCO_3$-saturated basin such as the North Atlantic. The ratio of primary production of organic carbon to inorganic carbon was estimated to be about 10 at the 48°N 21°W station (Goyet et al., 1990); the

inorganic carbon flux in the ocean's interior at this station was about 10 mole C; the estimated primary production during this time was about 100 mole C. This estimate coincides with the maximum estimation of primary production by other methods, including ^{14}C fixation method.

7.9.2 ORGANIC MATTER AND ORGANIC CARBON

Investigation of the processes of alteration and depletion of organic matter from settling particles, fresh to old, is critical in further understanding carbon cycles in the oceans. Various studies on many compound classes of organic matter including amino acids, amino sugar, protein, fatty acids, sterols and sugar compounds have begun to clarify their complex pathway and the rate of alteration of these materials while carbon compounds are transported through a water column (Wakeham et al., 1980; Lee and Cronin, 1984; Lee et al., 1983; Ittekkot et al., 1984a, b; Wakeham and Canuel, 1988; Handa, 1989).

Organic matter decreases at much higher rates than other particle classes because of the degradation process, particularly in the upper and mesopelagic layers. The export production of organic carbon and the nitrogen fluxes in the ocean's interior is theoretically the same as their new production; i.e., additional flux produced by resources other than recycled carbon and nitrogen (Eppley and Peterson, 1979). In general, fluxes of organic matter in the mesopelagic layer decrease in succession of two numerical modes: 1) exponential decrease in the upper-ocean layers; and 2) slow, linear-appearing decrease in the bathypelagic layers. This indicates that the rate of recycling is exponentially faster in the mesopelagic layers than in the deeper ones. Thus mineralized organic carbon in the upper ocean is allowed to return to the atmosphere within a relatively short time (on the order of minutes, hours or months). On the other hand, organic matter reaching the ocean's interior is unaltered while settling through the bathypelagic water column (deeper than 1 to 1.5 km) where the rate of remineralization is far smaller compared to the upper ocean. Organic carbon which arrives in the ocean's interior takes hundreds of years to recycle with atmospheric CO_2.

One of the most desired capabilities for ocean science at present is the ability to estimate the flux of organic matter at any ocean depth relative to production in the euphotic layer (Suess, 1980; Broecker and Peng, 1982); many empirical models have since been proposed (e.g., Berger et al., 1987; Martin et al., 1987; Pace et al., 1987; Berger et al., 1989). Although such empirical equations are useful for the first order approximation of export production, because of seasonal complexity, none of these equations is sufficiently realistic to be applied universally (e.g., Honjo et al., 1982a; Haake et al., 1993).

The *E*-ratio, the percentage of flux in the ocean's interior of the total production at the upper surface, reflects the complex seasonal sequence of production, changing mode of the removal process, and water column biogeochemistry as

explained in this chapter. An *E*-ratio of organic carbon and nitrogen reflects the characteristics of settling organic matter, metabolism in the water column, particularly in the upper and mid layers, and the physical condition of the packaging of settling particles. Meantime, it is essential to further understand the spatio-temporal variability of global primary production.

To access the *E*-ratio of carbon (and other nutrients) is not an easy task, requiring the value of photosynthesized carbon as well as measurement of particulate organic carbon in the ocean's interior in the same area, both measurements in time-series, covering all seasons. A year-round variability of the *E*-ratio of organic carbon has been obtained along the 140°W transect of the equatorial Pacific; it varied from 0.2 to 0.6 during the El Niño season of 1990. When El Niño conditions temporarily disappeared in the latter part of that year, the ratio varied from almost zero to 1.4 (Figure 7.12) (Honjo et al., 1995). The *E*-ratio estimated from the time-series carbon fixation value taken from sediment-trap-collected organic carbon flux during the 1989 spring bloom at a North Atlantic station, 48°N 21°W, was 1.7 (Honjo and Manganini, 1993).

During the post-bloom period, zooplankton carapaces and their fragments are often removed from the upper layers to the deep layer. The sedimentation of gelatinous zooplankton carapaces which occurred in the summer and autumn of 1983 at Ocean Station P in the Gulf of Alaska provided a several-fold greater quantity of organic carbon flux than in a normal year (joint study with C.S. Wong, the Institute of Ocean Sciences, Sydney, BC, Canada; Honjo, 1990b). The large quantity of post-bloom zooplankton carapaces was exported to a depth of 1 km in the North Atlantic but apparently was rapidly regenerated before reaching the deep interior (Honjo and Manganini, 1993) (Figure 7.13); however this can also be attributed to the moving of the upper ocean source of supply.

In exceptional cases, for example, fluxes of organic matter increase at deeper layers. In the Panama Basin, the mass of combustible matter (organic matter plus indigenous water) increased in the layer below 2 km (Honjo et al., 1982a; Honjo et al., 1992). Combustible flux increased approximately 50% at 4 km compared to that at 2 km, although it decreased in the shallower layers. This was interpreted as an additional flux of organic matter which was supplied advectively from the near-by continental slope by re-suspended marine snow caused by the strong boundary current (Asper et al., 1992).

Less than 2% of dissolved nitrogen (NO_3) arrived at the 2-km trap at 48°N 21°W during the 1989 bloom. On an annual basis, the ratio of nitrogen and phosphorus in organic matter decreases with depth. However, such ratios also differ with locations and seasons. At the North Atlantic Stations, the C/N ratio at 1 km was often close to the plankton value (6.6) but increased to 8 at about 2 km and 8.5 and more at deeper layers. The C/N value remained low during the Atlantic bloom and significantly high during post-bloom episodes (Honjo and Manganini, 1993). The flux of phosphorus in organic matter is understudied and

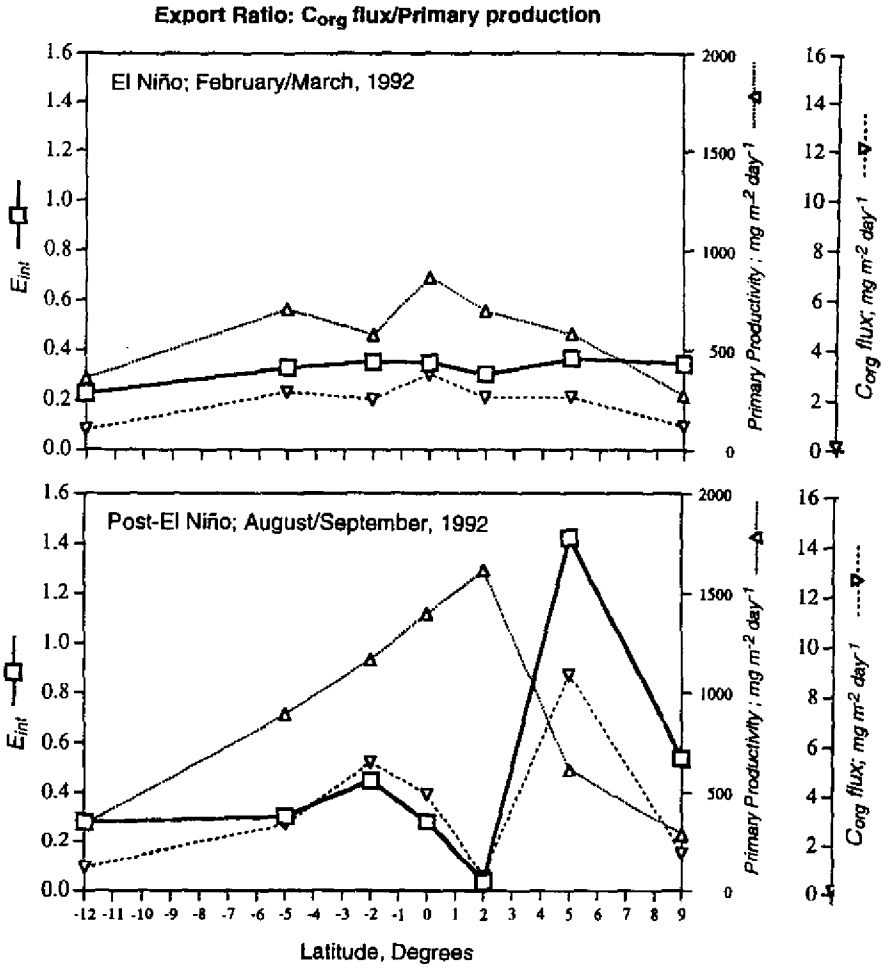

Figure 7.12 The export ratio of carbon to the ocean's interior (open squares; E_{int}) along 140°W, from 9°N to 12°S during February/March (upper panel: El Niño) and August/September (lower panel: post El Niño). Triangles represent primary productivity (mg m^{-2} d^{-1}) measured during the EqPac survey cruises (Murray et al., 1994), and inverted triangles depict organic carbon fluxes during the periods when primary productivity measurements were made.

not well understood. Phosphorus is strongly recycled in shallow water. Seasonal C/N/P values obtained from 34°N 21°W and 48°N 21°W are presented in Table 7.3, showing that, at these two stations, phosphorus among the three elements in settling particles decreases at the fastest rate.

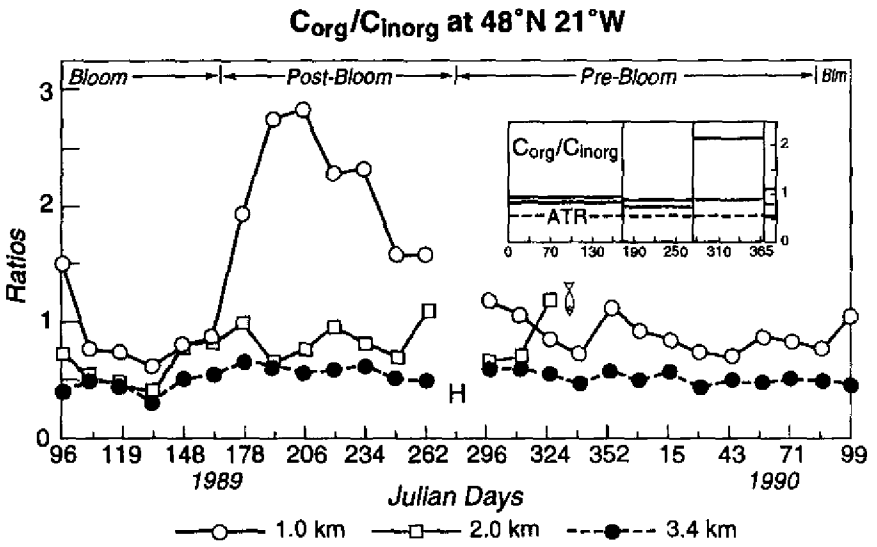

Figure 7.13 Vertical and temporal variability of the ratio of organic carbon to inorganic carbon at 48°N 21°W (NABE, Table 7.2) throughout a year, spring of 1989 to 1990. The ratio decreased with the depth and was consistently 0.5 (Attainable Terminal Ratio: ATR) at 3.4 km depth (insert) (Honjo and Manganini, 1993).

7.9.3 BIOGENIC SiO_2

The vertical flux of biogenic SiO_2 is complicated because of the irregular nature of mineralized tissue, which differs by taxa, compared to $CaCO_3$ tissue. Biogenic opal dissolves in the upper ocean (Nelson and Goering, 1977) as a function of water temperature (Hurd, 1983). For example, at 48°N 21°W about 27% of the dissolved SiO_2 which was converted to diatom frustules and radiolarian shells in the euphotic layer (0 – 52 m) arrived in the ocean's interior during the bloom. This amount was compared with the peak biogenic SiO_2 flux at 2 km which took place a few weeks later. The *E*-ratio of biogenic SiO_2, the ratio of production in the euphotic layer *vs.* flux in the ocean's interior, was thus estimated as 28% during the spring bloom (Honjo and Manganini, 1993) (Figure 7.8). This export ratio of biogenic SiO_2 partially supports previous ocean-chemical models which indicated about 30% of biogenic SiO_2 reaches the ocean's interior by escaping remineralization (Spencer, 1983).

The annual opal flux at 2 km during 1989 at this station was about 6 g m^{-2} y^{-1} (Honjo and Manganini, 1993), and is comparable to the lower end of the estimated flux derived from models, 7 to 12 g m^{-2} d^{-1} (Heath et al., 1976). Two thirds of the silicic acid is returned in solution to the surface and intermediate layers. The majority of stored SiO_2 generated by the bloom ought to be recycled to

Table 7.3 Ratios of biogenic carbon, nitrogen and phosphorus in settling particles at 3 depths relative to annual flux and fluxes during the bloom episode at 2 stations in the North Atlantic; 34°N 21°W and 48°N 21°W in 1989/90 (NABE, Table 7.2, Ref. 7). The total annual fluxes at these stations are given in Table 7.2 (Ref. 7). Details of bloom, pre- and post-bloom at these stations are explained in Honjo and Manganini (1993).

	34°N 21°W			48°N 21°W		
	C	N	P	C	N	P
Pre-Bloom						
1 km	53	8	1	49	6	1
2 km	99	12	1	63	8	1
D	153	17	1	89	10	1
Bloom						
1 km	40	6	1	101	15	1
2 km	148	19	1	136	19	1
D	154	18	1	177	23	1
Post-Bloom						
1 km	—	—	—	150	16	1
2 km	102	11	1	121	14	1
D	151	16	1	209	23	1
Annual						
1 km	47	7	1	96	12	1
2 km	128	16	1	120	16	1
D	154	18	1	148	18	1

the surface layer before the next annual bloom in order to keep the SiO_2 concentration at steady state. The rest is delivered to the ocean's interior and to the seafloor in the form of opal particles.

It seems that biogenic SiO_2 dissolves in two ocean zones. One is in the upper layers where dissolution is controlled by temperature and occurs quickly, on the scale of days to weeks. The diatom frustule flux and the species assemblage did not change significantly while settling from the 2-km to 3.7-km depth at this station (Honjo and Manganini, 1993), indicating that once biogenic opal reaches the ocean's interior, it does not further dissolve but arrives at the deep seafloor intact. Part of the reason would be that the majority of frustules are protected within fecal pellets (Schrader, 1971), though frustules, particularly centric frustules, are more pulverized in metazoan fecal pellets. However, sediment in the north-central Atlantic, including at the 48°N 21°W station, is carbonate-rich and low in opal, usually only a few percent (Lisitzin, 1972). It is reported that species diversity of radiolaria drastically decreased in bottom sediment at a tropical Atlantic site, from over 400 species in the trap to merely a dozen in the sediment below (Takahashi, 1991). Some suspect that the diatom frustules in the North Atlantic are generally less silicified, and that settling frustules are dissolved in the

upper and intermediate layers at a higher rate than in other ocean settings (Berger, 1976). Nevertheless, major dissolution should occur at the ocean bottom which is not constrained by water temperature.

7.9.4 VERTICAL INCREASE OF LITHOGENIC PARTICLE FLUXES

Studies of lithogenic matter in settling particles have found that the export of lithogenic particles to the ocean's interior is not simply constrained by the rate of fallout at the ocean's surface, as was envisioned by researchers. The main claim regarding lithogenic particle flux is its increase with depth (e.g., Honjo et al., 1982b; Masuzawa et al., 1989; Tsunogai et al., 1990). For example, a sediment trap deployed in the deep layers at 34°N 21°W collected approximately 2.2 g m^{-2} of lithogenic particles per year in 1989 to 1990. This station was located at the edge of the trade winds where lithogenic particles are effectively transported. At 48°N 21°W, where no significant supply of airborne lithogenic particles is feasible, a relatively large lithogenic flux, 1.3 g m^{-2} y^{-1}, was observed in the deep ocean layers. At both stations the Al flux (which usually represents the lithogenic component) increased linearly with depth through the meso- and bathypelagic layers (Figure 7.14). The increase of lithogenic flux is independent from the total flux which also often increases with depth. Therefore the meso-scale eddy diffusion model (Siegel et al., 1990) does not explain vertical increase of lithogenic particles which requires sources which supply refractory particles advectively.

7.9.5 PARTICLE FLUX IN THE INTERIOR OF THE VERY DEEP OCEAN TRENCHES IN THE PACIFIC

The deep trench system provides a natural laboratory for studying settling particles through a very long water column - as long as 9 km and even more. A set of samples collected by sediment traps set throughout such a very deep water column provides amplified information compared to a "normal" deep water column of 3 to 4 km - demonstrating chemical modification of particles, particularly by *in situ* dissolution and remineralization of $CaCO_3$, SiO_2 and organic matter, as well as scavenging of radionuclides and surface reactive elements. For example, the degree of under-saturation of $CaCO_3$ in the deep trenches in the North Pacific is the greatest in the world ocean (CFS level of 0.5; Takahashi, 1975).

Settling particles were first successfully collected from the interior of the Japan Trench (Sagami Trough) at a trap depth of 8.8 km (400 m above the bottom). They were compared with samples from a 4.3-km trap which was moored at a location equivalent to the depth of the rest of the basin. Even at such a great depth, near the deepest part of the world's ocean, hazardous anthropogenic radionuclides such as ^{239}Pu, ^{240}Pu and ^{137}Cs were found in settling particles (Nozaki, 1986). From the 8.8-km trap, a suite of palynomorph, including fungal, fern

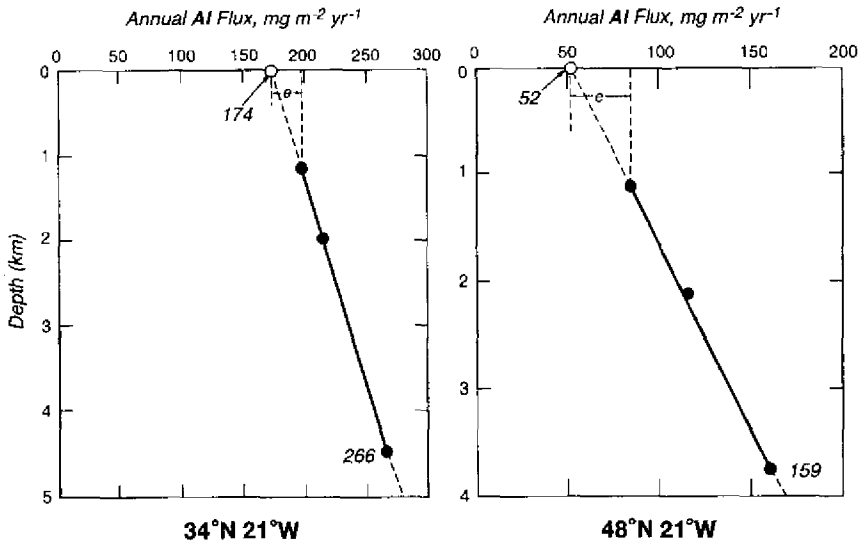

Figure 7.14 Plots showing the increase of lithogenic flux with depth at the 34°N 21°W and 48°N 21°W stations. Extrapolation to the surface allows an estimation of aeolian input (white circles). Dashed lines in the Figures indicate maximum and minimum estimates of aeolian input. The difference between these estimates, denoted as *e*, suggests an uncertainty of roughly 20% in the estimate of aeolian input.

spores, dinoflagellates, et cetera, were found; also found were pollens from pine and cedar (Matsuoka, 1989). The sedimentational route of pollen from the atmosphere to a depth of 8.8 km warrants further study since some pollen is virtually unsinkable in water (Traverse, 1988).

The flux of $CaCO_3$ in the 8.8-km trap was, compared to the 4.3-km trap, significantly less, and the surfaces of foraminifera tests were more extensively corroded. Biogenic SiO_2 was also less, but not to the same degree as $CaCO_3$. Seventy percent of the 8.8-km samples consisted of lithogenic particles; their flux surged sporadically, indicating that they were supplied by turbidite activity in the trench (Nozaki, 1989a). This technically challenging program has been continued from 1982 to the present (Dr. Y. Nozaki, pers. comm., 1994).

7.10 SEASONAL AND GEOGRAPHIC VARIABILITY

7.10.1 PARTICLE FLUXES IN THE MARGIN

Particle flux to the deeper layers, specifically the production, regeneration and burial of organic matter in a margin environment, plays a major role in the global

carbon cycle (e.g., Walsh, 1988; Berger et al., 1989; Milliman, 1993). Light has begun to be shed on the transportation of particles from shelves and slopes to the ocean's interior, but this warrants further study (e.g., Thunell et al., 1994a; Biscaye et al., 1994a, b). Particle behavior in the margin environment seems to be, undeservedly, understudied. However, as the title of this chapter indicates, I am not well qualified to elaborate on this large area of ocean studies and will not do so in this review. Shelf and upper slope areas are far more active with regard to primary production, high velocity water movement, and are, in general, unstable, high energy environments compared to the ocean's interior.

Primary productivity in the margins is 250 gC m^{-2} y^{-1}, in a rough average, which is about 10 times greater than in the open seas (Berger et al., 1989). Organic matter which is vigorously recycled by the large ecosystem continues to the bottom boundary and into the sediment. However, because of the high burial rate, the role of the margin environment as a carbon sink is still very high (e.g., Walsh et al., 1981; Romankevich, 1984). Carbon fluxes measured by long-term sediment trap experiments in the San Pedro Basin were about 12 gC m^{-2} y^{-1} (Thunnel et al., 1994) and the fluxes on the Middle Atlantic Bight near the bottom of the shelf were 28 gC m^{-2} y^{-1}, and 32 g m^{-2} y^{-1} along the slope (Andersen et al., 1994). Wassmann and Slagstad (1990) estimated particle flux in the central Barents Sea as 24.6 gC m^{-2} y^{-1}. These values are one or two orders of magnitudes larger than the rate of carbon export to the ocean's interior (Table 7.2).

The Middle Atlantic Bight study (SEEP-II Project) found no evidence to support the hypothesis that biogenic particles settling to the interior of the margin environment are re-exported to the deep ocean environment; but it appears that they are consumed *in situ* (Biscaye and Anderson, 1994). This is contrary to an established view of material being exported from the margin to the basin (e.g., Walsh, 1988, and some field results such as at Cape Hatteras, Walsh, 1994). Such contradiction may indicate the complex individualization of a margin environment in general. For example, export of re-suspended marine snow particles from the shelf edge to the deep basin has been observed by a marine snow camera off Cape Hatteras where the Gulf Stream hits the shelf edge (Asper et al., 1992), and a large intermittent slide of the bottom brine layer containing a large amount of fresh organic carbon ("winter burst") was caught by time-series sediment traps in the northern Barents Sea during mid winter using natural radionuclides as tracers (Honjo et al., 1988) (Figure 7.15). Narita et al. (1990) estimated the amount of time necessary for particles settled in shallow areas of the East China Sea to be transferred to the interior of the Okinawa Trough (1.9 km deep) to be approximately 16 years.

7.10.2 CONTRAST BETWEEN AND IN THE GLOBAL BASINS

Processes for removal and transport of particles and their biogeochemically essential constituents have been clarified by detailed studies at a number of

stations. The main sources of errors in measuring particle fluxes, the amplitude of inter-annual difference as well as the eddy effect to the vertical fluxes, have begun to be understood. However, before we reach generalizations regarding the mode of particle fluxes in the world ocean and to further understand the role of settling flux in a global context, more geographic coverage by long-term trap deployment is warranted to represent not only the latitudinal ocean zones but also the major marginal seas.

Nevertheless, global efforts to deploy many time-series sediment trap moorings at strategic locations in the ocean's interior covering all seasons as well as inter-annual periods have begun to reveal some fundamental contrasts in biogeochemical functions between major oceanic regions (Honjo, in preparation). For example, organic carbon fluxes in the interior of the North Pacific (>1 g m^{-2} y^{-1}) are generally larger than in the interior of the North Atlantic (<1 g m^{-2} y^{-1}). The flux of inorganic carbon reverses this trend; more $CaCO_3$ is transported to the interior of the North Atlantic than the North Pacific. Biogenic SiO_2 fluxes in the North Pacific are several times larger than in the North Atlantic; the Ca/Si_{bio} ratio is >1 in the North Atlantic and <1 in the North Pacific. The former can be called a "carbonate ocean" and the latter a "silica ocean". An extreme representation of a silica ocean is the Weddell Sea where only a trace of $CaCO_3$ was exported, but where the flux was overwhelmed by diatom frustules (Fischer et al., 1988). The equatorial Pacific Ocean seems to be independent from the rest of the Pacific; it is a strongly carbonate ocean with a high Ca/Si_{bio} ratio; C_{org}/C_{inorg} is within the same range as in the North Atlantic; and the flux of organic carbon in the interior is about a half that of the North Pacific (Honjo et al., 1995). Another difference between the North Atlantic and North Pacific is that the majority of annual particle export in the former is done during a bloom while in the boreal Northern Pacific no seasonally defined bloom similar to that of the North Atlantic has been observed (Table 7.2).

7.10.3 SEASONAL AND INTERANNUAL VARIABILITY OF PARTICLE FLUXES

It is understood that particle fluxes in the interior of any ocean change by season. The contrast in flux between the bloom- and slack-time observed in the ocean's interior is strong; in many oceans, the ratio between the highest and lowest yearly fluxes is as large as more than 100. It seems that the equatorial Pacific is the only exception so far known where fluxes change relatively little throughout a year (Figure 7.16) (Honjo et al., 1995). The constituents of settling particles also change, reflecting the ecological sequence in the surface ocean. Specifically, the content of $CaCO_3$ and biogenic SiO_2 changes with time and location. The oceanic forcing which causes such variability is beginning to be understood, but this subject warrants further study. For example, the strong annual variability of the

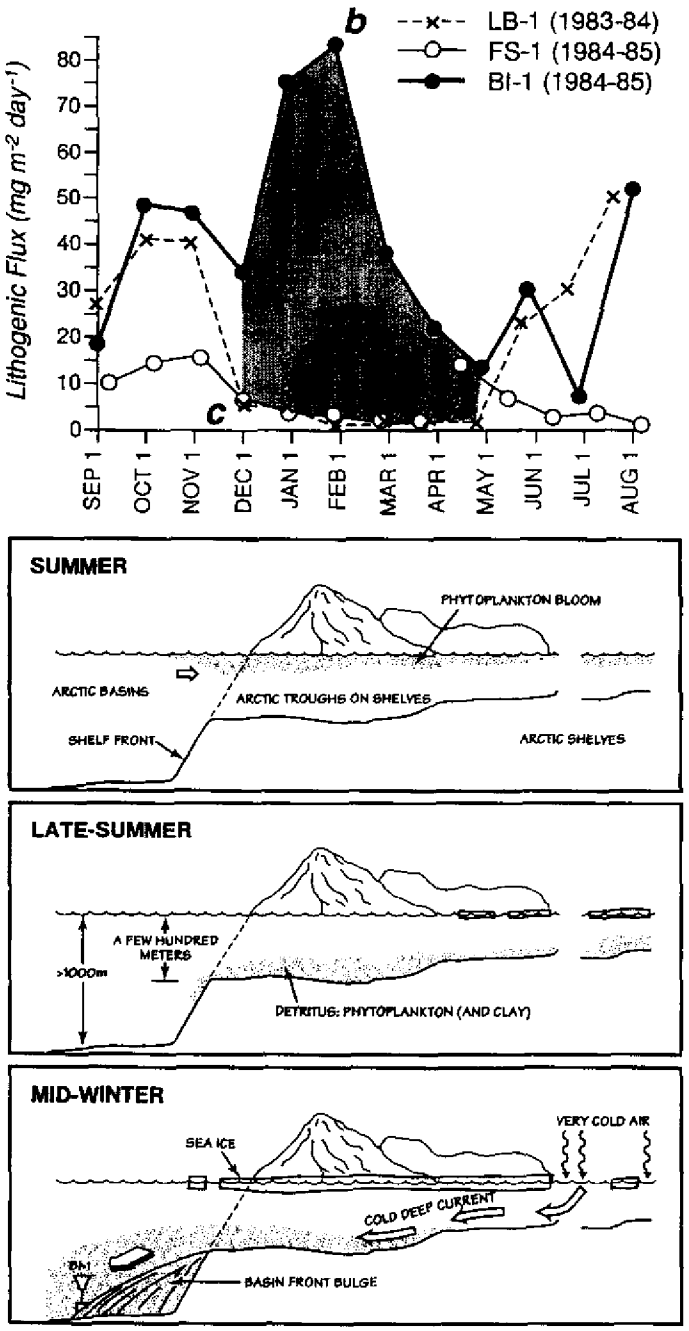
b
LB-1 (1983-84)
FS-1 (1984-85)
BI-1 (1984-85)
Lithogenic Flux (mg m-2 day-1)
80
70
60
50
40
30
20
10
0
c
SEP 1
OCT 1
NOV 1
DEC 1
JAN 1
FEB 1
MAR 1
APR 1
MAY 1
JUN 1
JUL 1
AUG 1
SUMMER
PHYTOPLANKTON BLOOM
ARCTIC BASINS
ARCTIC TROUGHS ON SHELVES
SHELF FRONT
ARCTIC SHELVES
LATE-SUMMER
A FEW HUNDRED METERS
>1000m
DETRITUS: PHYTOPLANKTON (AND CLAY)
MID-WINTER
SEA ICE
VERY COLD AIR
COLD DEEP CURRENT
BI
BASIN FRONT BULGE

flux in the Arabian Sea has been explained by the evolution of the NE and SW monsoons, the processes of upwelling and the removal of carbon accelerated by mineral aerosol fallout with intensified wind (Nair et al., 1989; Ittekkot, 1991; Curry et al., 1992; Haake, et al., 1993; this volume).

Our understanding of interannual variability of particle export in the ocean's interior is limited to several stations. At a Bermuda time-series station (this volume, Chapter 9) and at a station in the Gulf of Alaska (C.S. Wong, pers. comm.) decadal information has been gathered. Also at 6 stations across the Arabian Sea and the Bay of Bengal, sediment trap moorings have been maintained for almost 10 years (Ittekkot, 1991; Haake et al., 1993; this volume, Chapters 14 and 15). To the north and east of Iceland, two long-term sediment trap stations have been maintained for several years (J. Olafsson and D. Ostermann, pers. comm.). Three new long-term time-series sediment trap stations/transects have been recently initiated near Hawaii (D. Karl, pers. comm.), in the Okinawa Trough (M. Honda, pers. comm.) and the South China Sea (this volume, Chapter 16). The results so far suggest that the total fluxes and the fluxes of the main constituents of settling particles change on the order of a factor which corresponds to the interannual changes of forcing events such as monsoons, El Niño and intertropical convergence.

7.10.4 NORTH ATLANTIC AND NORTH PACIFIC

The bloom-type sequence export of particles from the euphotic layer to the interior appears to be commonly found in the temperate and subarctic North Atlantic. At the 34° 21°W and 48°N 21°W stations, more than half of the particle export depends on a single bloom. The onset of this bloom is delayed with increase in latitude; the bloom peak at 34°N was in late February to early March, while at the 48°N station it was delayed to May (Honjo and Manganini, 1993). When the bloom reaches as far north as the Lofoten Basin, about 69°N, the main peak appears as late as September/October (Honjo, 1990). In the Norwegian Current area of the Nordic Seas the bloom is much broadened, but essentially follows the same sequence; however, the length of bloom is longer than in southern zones (Honjo, 1990a; G. Wefer, pers. comm.).

Figure 7.15 Upper panel: A large flux, particularly of lithogenic particles during mid-winter, was observed at a 2-km-deep slope station near a large shallow fjord along the west cost of Spitsbergen (Bear Island, Table 7.2). The "winter burst" contains a high percentage of organic carbon. The comparison of two offshore basin stations located nearby did not show such mid-winter increase of fluxes (Honjo et al., 1989). Lower panel: a schematic explanation of winter burst. The phytoplankton bloom during summer was not all grazed and consumed because of the early arrival of winter. There is a large supply of glacial lithogenic matter and organic matter deposits at the bottom of the fjord. The cold brine is generated during winter and flows along the bottom of the fjord (the continental slope is as deep as 2 km), it carries with it fresh organic-rich sediment (Honjo, 1990).

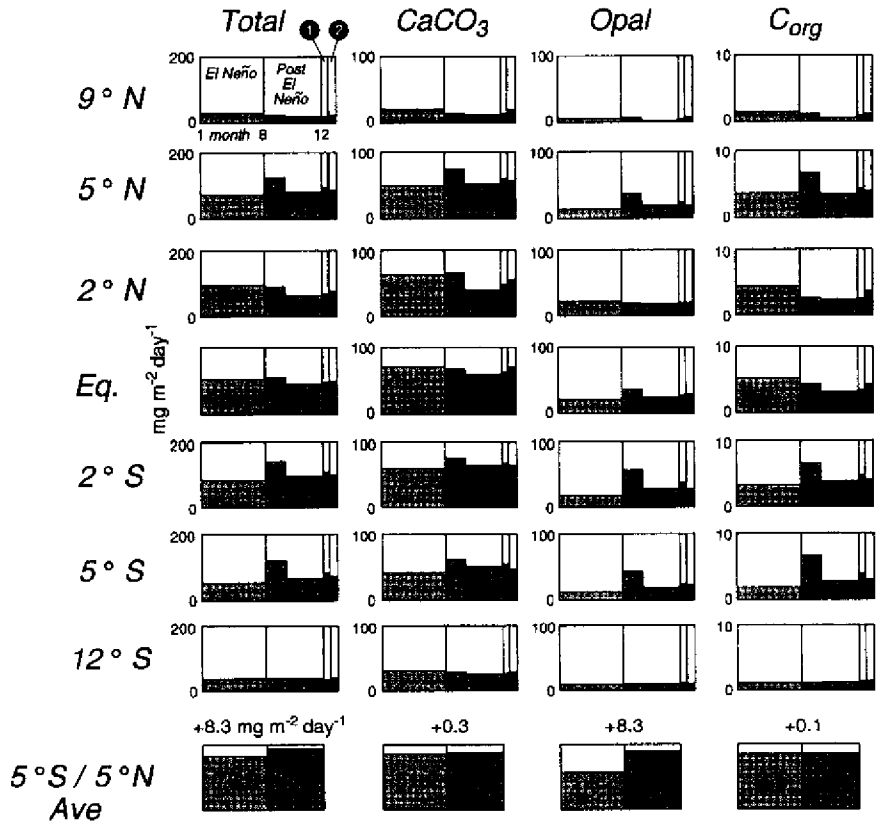

Figure 7.16 Total $CaCO_3$, biogenic SiO_2 and organic carbon flux (mg m^{-2} d^{-1}) at each EqPac station. (Table 7.2). Each box is divided into El Niño and post El Niño, 1992. Post El Niño is separated into instability wave periods (middle of the box) and the later periods. The two narrow dark columns on the right indicate: 1) post El Niño average and 2) annual average. At the bottom line, the grand average of fluxes (mg m^{-2} d^{-1}) from the 5°N to 5°S stations during El Niño and post El Niño are compared (Honjo et al., 1995).

The export of particles to the interior of the northwestern Pacific consists of a significantly larger annual biogenic SiO_2 flux than the northeastern Pacific/Gulf of Alaska (Tsunogai and Noriki, 1991). These authors explained this difference by the former being bloom-type production, and the latter upwelling-type production. Time-series trap experiments in the Gulf of Alaska, Bering Sea and the Sea of Okhotsk all show that the succession of exports begins with a massive flux of biogenic SiO_2 with diatom frustules in the spring. $CaCO_3$ (inorganic-carbon) particle blooms appeared in the autumn and sometimes continued to late November, often separated by a summer flux slack. The Sea of Okhotsk is an extreme exam-

ple where large fluxes of biogenic SiO_2 in the spring and $CaCO_3$ flux in the autumn are clearly separated by a brief cessation of flux in mid to late summer (Figure 7.17). In contrast, as previously described, the biogenic SiO_2 and $CaCO_3$ export events are not separable in the North Atlantic bloom (e.g., Figure 7.8).

In general, the ratio between $CaCO_3$ and biogenic SiO_2 in the higher-latitude North Pacific is far smaller than in the North Atlantic, north of 34°N. This is attributed to the lack of spring diatom bloom in the North Atlantic. The annual organic carbon flux is generally larger in the North Pacific compared to the North Atlantic (Table 7.2). This also can be explained as the organic carbon flux in the North Pacific being associated with the high export event of biogenic SiO_2 in the spring. However, in the North Atlantic, organic carbon appears to be associated with calcium carbonate which is dominate in this basin.

7.10.5 PACIFIC AND ATLANTIC SOUTHERN OCEAN

In the southern Pacific Ocean at 61.5°S 150°E, south of the Antarctic Convergence Zone, at a station about 3.8 km deep, Tsunogai et al. (1986) measured biogenic particle flux as large as 2.5 g m^{-2} d^{-1} from January 4 to 14, 1984. Fluxes during the other periods of the austral summer were approximately 1 g m^{-2} d^{-1}. Although the trap was deployed only about 2 months during the maximum austral summer, the estimated minimum of the annual flux was 69 g m^{-2} d^{-1} - comparable to the annual flux in the interior of the Bering Sea. Similar to the Weddell Sea, the majority of collected particles were biogenic SiO_2, as high as 78%, with only 2% of $CaCO_3$. However, the total annual flux in the Weddell Sea was only 0.4 g m^{-2} y^{-1} during 1985 (Fischer et al., 1988).

The highest seasonal contrast in particle flux was found in the Bransfield Strait, Antarctic Peninsula, at 1.6 km deep, during a multi-year, time-series trap experiment (Wefer, 1989), where an enormous flux of biogenic particles, as large as about 1 g m^{-2} d^{-1}, was observed for a few weeks during the maximum austral summer; the flux virtually died off during the rest of the year. The total particle flux in this year was 109 g m^{-2} y^{-1} (about 50% was lithogenic particle flux) which is larger than any other ocean flux so far recorded. Like the fluxes from the other southern stations, the majority of the biogenic flux was biogenic SiO_2 with a small $CaCO_3$ flux (Wefer et al., 1988), showing a strong contrast from the biogeochemical characteristics of settling particles in the Nordic Sea which is dominated by $CaCO_3$ (Honjo, 1990), but similar to areas of the northwestern Pacific such as the Bering Sea (Table 7.2).

In the northern Weddell Sea, the variability of particle fluxes was controlled by the regression of the ice edge. The flux was concentrated within the few months of the austral summer, and there was virtually no flux during the ice-fast period. The annual flux was extremely small compared to any other time-series stations discussed in this chapter (0.4 m^{-2} y^{-1} in 1986) and, noticeably, $CaCO_3$ flux was only a trace amount, as at all other Southern Ocean stations (Fischer et al., 1988).

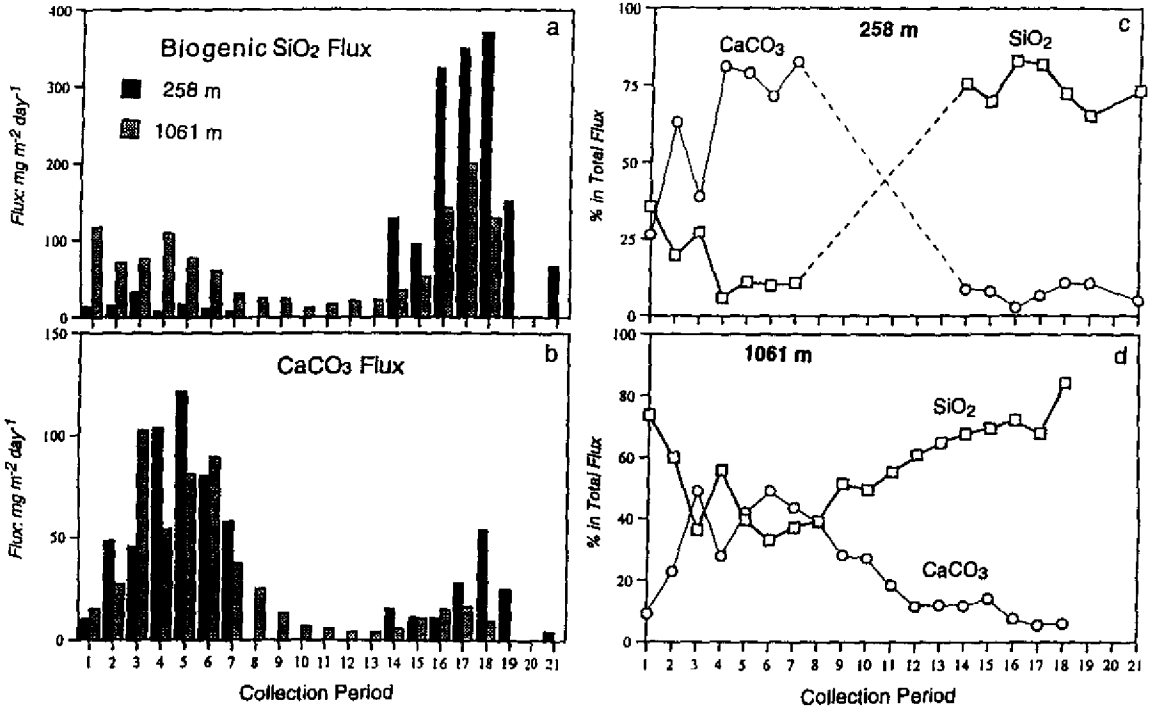

Figure 7.17 Flux of (a) biogenic SiO_2, and (b) $CaCO_3$ at 258 m (dark shadowed) and 1061 m (light-hatched) in the Sea of Okhotsk from August 1990 to August 1991. Comparison of the percentage of $CaCO_3$ and SiO_2 in the total flux at (c) 258 m and at (d) 1061 m (Honjo et al., in review). Collection started on August 12, 1990, with sampling intervals of 17 days. The first $CaCO_3$-rich bloom is an autumn bloom (end of August, period 2, to beginning of December, period 7). The large SiO_2 spring bloom began in late March (period 14) and continued to the last period (21), July 26 to August 12, 1991.

7.10.6 EQUATORIAL PACIFIC

The annual succession of particle export in the equatorial Pacific (EqPac) differs significantly from the other regions studied so far. The equatorial Pacific is a zone on both sides of the equator, about 10° both to the north and south, characterized by latitudinal boundary conditions set by the equatorial current and counter current systems which interlace with equatorial meridianal instability waves. Vigorous upwelling along the equator induced by the trade winds results in a high rate of production. When the trade winds stall and upwelling stops, the open ocean ecosystem becomes less productive and El Niño conditions prevail. From the results of an extensive sediment trap array experiment conducted between 9°N and 12°S, along 140°W (Figure 7.2), in 1991, which began as a mild El Niño year and then resumed post El Niño conditions (Murray et al., 1994), the evolution of particle sedimentation was observed with reference to the succession of the strength of trade winds and other conditions. In the Panama Basin in the eastern-most equatorial Pacific environment, particle fluxes are strongly influenced by the behavior of the Intertropical Convergence Zone, differing significantly between windy, wet periods and dry, relatively calm periods (Honjo, 1982).

When upwelling along the equator resumed in the summer of 1991 and the ocean was then in a post El Niño condition, more biogenic material was produced, the productive zone spreading to both sides of the equator by equatorial instability waves. During post El Niño, more biogenic SiO_2 and organic carbon is exported than during the earlier half of the year (Figure 7.16). During a non El Niño year, compared to an El Niño year, more vigorous upwelling as well as more active tropical instability waves occur along the equator. This enhances export of biogenic SiO_2 to the interior of the equatorial zone (Dymond and Collier, 1988). However, $CaCO_3$ was consistently exported, regardless of the El Niño conditions, and the ratio of $CaCO_3$ to biogenic SiO_2 was always large. Thus the ratio of organic carbon to inorganic carbon became smaller; this discourages the notion that this large productive ocean is an effective sink of atmospheric CO_2.

7.11 SUMMARY AND CONCLUSIONS

In order to understand the biogeochemical cycle of matter in the sea, it is crucial to investigate ocean particle flux in order to find the missing link which connects material flowing from the surface to the ocean's bottom. Settling particles are critical in the transfer of energy, nutrients from the sun-light filled surface, to the abyssal ocean floor several thousand meters below. The biological pump catches atmospheric CO_2 and sends it down through the ocean's layers in the form of organic carbon. Only a small percent of organic matter produced in the upper ocean arrives in the ocean's interior, and the amount of carbon contained in settling particles exported to the ocean's interior is equivalent to the quantity of

carbon which is removed from atmospheric CO_2. Therefore, assessing organic carbon flux in the ocean's interior and clarifying the process of this organic-carbon export is crucial to understanding the fate of fossil-fuel CO_2.

In order to use microfossil assemblages in the seafloor sediment to reconstruct the glacial and interglacial environment of the earth, information must be ascertained regarding how present-day counterpart organisms arrive on the ocean floor, are collected by a sediment trap (biocoenosis), and adjust to ocean conditions. In order to establish a proximity link, it is necessary to gather atmospheric, air-sea interface and upper-ocean hydrographic information.

At this time, in order to meet the above objectives of understanding biogeochemical cycles, time-series sediment traps deployed with bottom-tethered moorings are one of the best approaches to collecting settling particles in the ocean's interior. Time-series, synchronized sediment trap arrays which are deployed over a long period have proven to be an efficient tool to attack a wide range of particle flux problems. Recent introduction of large, basin-scale arrays has assisted understanding of the impact of atmospheric forcing on biogeochemical cycles in the ocean by, for example, such events as seasonal monsoons and El Niño. Importantly, sediment trap experiments continued for more than one year in all ocean depths have begun to provide us with "total annual flux", covering all seasons, and, for the first time, have permitted us to match particle flux information with the paleoceanographic time scale and information on the temporal variability of the ocean particle fluxes. Uncertainties regarding the efficiency of a sediment trap still need to be constrained. However, traps deployed in the deep ocean perform better because the deep ocean is less energetic and the levels of biological activities are low. Perhaps the most important problem to be solved is the effect of mesoscale eddy diffusion which results in the apparent variability of vertical fluxes at the same mooring site.

Time-series collection of particle fluxes from many mooring locations, distributed throughout all major basins and marginal seas, has revealed a surprisingly large degree of seasonality. In the North Atlantic stations, particle fluxes in the ocean's interior responded to the rapid increase of surface productivity during the spring bloom with a short delay in the export of the major portion of annual flux. On the other hand, total particle fluxes in the quatorial Pacific changed little throughout the year; only biogenic SiO_2 and organic carbon fluxes were controlled by upwelling along the equator. In the northern Pacific a very large variability of biogenic SiO_2 flux was observed. In the Arabian Sea two monsoon phases, SW and NE wind-forcing, essentially controlled the flux to the interior. Knowledge of time-series variability of fluxes in the ocean's interior allows us to reconstruct the ecological sequences which have evolved in the upper layers. In areas where we have deployed year-round sediment traps (except for the deep polar regions) organic carbon flux in the ocean's interior ranges from 0.3 to 1.8 g m^{-2} y^{-1} (Table 7.2).

We have begun to understand the processes of removal of biogenic matter from the upper ocean to the interior. An important contribution of the last two decades with regard to the ocean's biogeochemical cycle is the re-confirmation of the hypothesis that the upper ocean and the ocean's interior are linked by "settling particles" which are biologically mediated aggregations of upper-ocean-generated particles which settle at speeds that are orders of magnitude faster than the descending rate of individual fine and light particles. Arrays of traps, distributed at vertical distances, with their open/close timing synchronized, have provided data on the bulk residence time of settling particles in water columns; this was estimated as 100 to 200 m d^{-1}.

Taking advantage of this rapid transportation, nearly all $CaCO_3$ particles arrive in the deep ocean, even when it is under-saturated with calcite in the very deep layers below 6 km. An experiment in the Atlantic showed that about two-thirds of biogenic SiO_2 is dissolved in the upper layers, the remainder entering the ocean's interior. The flux of lithogenic matter, a minor constituent but important as a ballast of settling particles, often increases with depth. About three quarters of the particles which are produced in or enter at the upper layers arrive in the ocean's interior.

Only a small percentage of organic matter successfully descends with settling particles as far as the ocean's interior. If the downward removal of particulate organic matter from the euphotic layer ceases, the oceanic biological pump will stop. But organic particles are often lighter than sea water. Therefore, a critical mechanism for maintaining the carbon cycle in the open ocean is the ballasting of settling particles, enabling them to sink through ocean layers. The majority of settling organic matter is remineralized or dissolved while settling through the upper and middle layers. To maintain a steady-state DOM level, dissolved organic matter which is supplied to the upper oceans must be recycled to the euphotic layer within one year - or the time between the spring bloom of one year and the spring bloom of the next.

7.12 OUTLOOK

Deep-ocean time-series sediment trap and associated deployment technology is functioning well. To constrain the instability of vertical particle fluxes caused by mesoscale eddy diffusion is the immediate problem to attack at individual sites. The data we have so far gained fall short of constraining the variability of export fluxes and their relationship to surface productivity and other ocean data. In order to assess the variability of export flux of organic carbon and other biogeochemically critical particles in time and space, particularly in the ocean's interior, regional and basin-wide deep-sea sediment-trap experiments should be further conducted with international cooperation.

The geographical scale of sediment trap arrays must be expanded to a global scale. Larger-scale synchronization of trap opening/closing such as is presently conducted (or planned to be conducted) from the Bering Sea to the Arabian Sea (in order to cover the propagation of seasonal monsoons) should also cover the world's oceans. Particle fluxes in the high-latitude oceans and marginal seas and their relationship to the deep basins must also be attacked.

Detailed process studies of ocean particles must be continued at as many stations as possible, to represent each ocean setting, in order to constrain the information link between the air, upper ocean, ocean's interior and the deep-sea floor. Biocoenosis studies must be further developed on all major taxa to better establish paleoproximity functions. Other atmospheric and oceanographic criteria including long-term meteorology, air-sea interface, continuous ocean color sensing, satellite observation of sea surface temperatures, ship-board measurement of productivity, plankton ecology, salinity, thickness of mixed layers and nutrient concentration should be measured to establish proximity. Deployment of meteorological buoys with relevant sensors and long-term time-series trap arrays is recommended.

7.13 ACKNOWLEDGMENTS

This paper is based on my overview talk entitled "Perspectives in Ocean Biochemical Flux Studies" which was read at the SCOPE/UNEP workshop on Particle Flux in the Ocean, sponsored by the United Nation's Environmental Programme, at the University of Hamburg, on September 20, 1993. I very much appreciate the encouragement from Prof. Venugopalan Ittekkot, the convenor of the workshop and valuable discussions and suggestions from the participants. I thank all my international colleagues who have worked with JGOFS and the High Latitude Ocean Flux Program. Steven J. Manganini and I have collaborated since the inception of our global particle flux program, the PARFLUX Program, at Woods Hole Oceanographic Institution. Many of the findings and interpretations in this article are the result of constant field collaborations and discussions with him. I am also grateful to Ken Doherty who has developed many advanced tools to investigate ocean particle fluxes. I am grateful for their insights and generosity in allowing their presentation here. Also I thank Katherine Brown for her great effort in editing this manuscript.

This research was supported by the National Science Foundation, Arlington, Virginia, under grant # OCE 9311199 and the High-Latitude Ocean Flux study was supported by the Office of Naval Research, Arlington, Virginia, under grant N00014-89-J-1288. I sincerely thank them for their persistent encouragement and sponsorship of global particle flux research. This is Contribution No. 168 of JGOFS and No. 9006 from Woods Hole Oceanographic Institution.

7.14 REFERENCES

Alldredge, A. L. (1976) "Discarded appendicularian houses as sources of food, surface habitats, and particulate organic matter in planktonic environments", *Limnol. Oceanogr.*, **21**, 14–23.

Alldredge, A. L. and Gotschalk, C. (1988) "In situ settling behavior of marine snow", *Limnol. Oceanogr.*, **33**, 339–351.

Alldredge, A. L. and E. O. Hartwig (eds) (1986) *Aggregate Dynamics in the Sea.* Workshop report, Office of Naval Research, American Institute of Biological Sciences.

Alldredge, A. L. and M. W. Silver (1988) "Characteristics, dynamics and significance of marine snow", *Prog. Oceanogr.*, **20**, 41–82.

Altabet, M. A., W. G. Deuser, S. Honjo and C. Stienen (1991) "Seasonal and depth-related changes in the source of sinking particles in the North Atlantic", *Nature*, **345**, 136–130.

Anderson, R. F., M. P. Bacon, P. G. Brewer (1983) "Removal of Th-230 and Pa-231 from the open ocean", *Earth Planet. Sci. Let.*, **62**, 7–12.

Anderson, F. A., G. T. Rowe, P. F. Kemp, S. Trumbore and P. E. Biscaye (1994) "Carbon budget for mid-slope depocenter of the Middle Atlantic Bight", *Deep-Sea Res.*, **4**, 669–703.

Asper, V. L (1987) "Measuring the flux and sinking speed of marine snow aggregates", *Deep-Sea Res.*, **34**, 1–17.

Asper, V. L., S. Honjo and T. H. Orsi (1992) "Distribution and transport of marine snow aggregates in the Panama Basin", *Deep-Sea Res.*, **39**, 939–952.

Bacon, M. P. (1988) "Tracers of chemical *scavenging* in the ocean: Boundary effects and large scale chemical fractionation", *Philosoph. Trans. Roy. Soc. London*, A, **320**, 187–200.

Bacon, M. P., D. W. Spencer and P. G. Brewer (1976) "$^{210}Pb/^{226}Ra$ and $^{210}Po/^{210}Pb$ disequilibria in seawater and suspended particulate matter", *Earth Planet. Sci. Lett.*, **32**, 227–296.

Bacon, M. P., C.-A. Huh, A. P. Fleer and W. G. Deuser (1985) "Seasonality in the flux of natural radionuclides and plutonium in the deep Sargasso Sea", *Deep-Sea Res.*, **32**, 273–286.

Baker, E. T., H. B. Milburn and D. A. Tennant (1988) "Field assessment of sediment trap efficiency under varying flow conditions", *J. Mar. Res.*, **46**, 573–592.

Berger, W. H. (1976) "Biogenous deep sea sediments: Production, preservation and interpretation", in J. P. Riley and R. Chester (eds) *Chemical Oceanography*, 2nd Ed., Vol. 5, Academic Press, London and New York, 265–388.

Berger, W. H. and D. Piper (1972) "Planktonic foraminifera: differential settling dissolution and redeposition", *Limnol. Oceanogr.*, **17**, 275–287.

Berger, W. H., K. Fisher, C. Lai and G. Wu (1987) "Ocean carbon flux: Global maps of primary production and export production", in C. Agegian (ed) *Biogeochemical Cycling and Fluxes between the Deep Euphotic Zone and Other oceanic Realms*, NOAA Symp. Ser. for Undersea Research, NOAA Undersea Research Program, vol. 3(2). Preprint in SIO ref. 87–30.

Berger, W. H., V. S. Smetacek and G. Wefer (1989) "Ocean productivity and paleoproductivity - an overview", in W. H. Berger, V. S. Smetacek and G. Wefer (eds), *Productivity of the Ocean: Present and Past*, John Wiley & Sons, Chichester, 1–34.

Berner, R. A. and S. Honjo (1981) "Pelagic sedimentation of aragonite: Its geochemical significance", *Science*, **211**, 940–942.

Betzer, P. R., W. J. Showers, E. A. Laws, D. C. Winn, G. R. DiTullio and P. M. Kroopnick (1984) "Primary productivity and particle fluxes on a transect of the equator at 153°W in the Pacific Ocean", *Deep-Sea Res.*, **31** ,1–11.

Biscaye, P. E. and R. F. Anderson (1994) "Fluxes of particulate matter on the slope of the southern Middle Atlantic Bight, SEEP-II", *Deep-Sea Res.*, **41**, 459–509.

Biscaye, P. E., C. N. Flagg and P. G. Falkowsky (1994a) "The shelf edge exchange processes experiment, SEEP-II: An introduction to hypotheses, results and conclusions", *Deep-Sea Res.*, **41**, 231–252.

Biscaye, P. E., G. T. Csanady, P. G. Falkowsky and J. J. Walsh (1994b) "Shelf edge exchange processes in the southern middle Atlantic bight: SEEP-II, tropical studies in Oceanography", *Deep-Sea Res. II*, **41**, 229–703.

Bishop, J. K. B., J. M. Edmond, D. R. Ketten, M. P. Bacon and W. B. Silker (1977) "The chemistry, biology and vertical flux of particulate matter from the upper 400 m of the equatorial Atlantic Ocean", *Deep-Sea Res.*, **24**, 511–548.

Blomqvist, S. and C. Kofoed (1981) "Sediment trapping - a subaquatic in-situ experiment", *Limnol. Oceanogr.*, **26**, 585–590.

Brewer, P. G., Y. Nozaki, D. W. Spencer and A. P. Fleer (1980) "Sediment trap experiments in the deep North Atlantic: isotopic and elemental fluxes", *J. Mar. Res.*, **38**, 703–728.

Broecker, W. S. and T. H. Peng (1982) *Tracers in the Sea*, Eldigio Press, Palisades, NY, 690 pp.

Bruland, K. W., R. P. Franks, W. M. Landing and A. P. Fleer (1981) "Southern California inner basin sediment trap calibration", *Earth Planet. Sci. Let.*, **53**: 400–408.

Buesseler, K. (1991) "Do upper-ocean sediment traps provide an accurate record of particle flux?", *Nature*, **353**, 420–423.

Butman, C. A. (1986) "Sediment trap biases in turbulent flows: Results from a laboratory flume study", *J. Mar. Res.*, **44**, 645–693.

Butman, B. and D. W. Floger (1979) "Long-term observations of bottom current and bottom sediment movement of Mid-Atlantic Continental Shelf", *J. Geophys. Res.*, **84**, 1187–1205.

Butman, C. A., W. D. Grant and K. D. Stolzenbach (1986) "Predictions of sediment trap biases in turbulent flows: a theoretical analysis based on observations from the literature", *J. Mar. Res.*, **44**, 601–644.

Calvert, S. (1983) "Sedimentary geochemistry of silicon", in S. R. Aston (ed), *Silicon Geochemistry and Biochemistry*, Academic Press, London, 143–186.

Cole, J. J., S. Honjo and E. Erez (1987) "Benthic decomposition of organic matter at a deep-water site in the Panama Basin", *Nature*, **327**, 703–704.

Curry, W. B., R. C. Thunell and S. Honjo (1983) "Seasonal changes in the isotopic composition of planktonic foraminifera collected in Panama Basin sediment traps", *Earth Planet. Sci. Let.*, **64**, 33–43.

Curry, W. B., D. R. Ostermann, M. V. S. Guptha and V. Ittekkot (1992) "Foraminiferal production and monsoonal upwelling in the Arabian Sea: evidence from sediment traps", in C. P. Summerhayes, W. L. Prell and K. C. Emeis (eds) *Upwelling Systems: Evolution Since the Early Miocene*, Geological Society Special Publication No. 64, 93–106.

Deuser, W. G. (1986) "Seasonal and interannual variations in deep-water particle fluxes in the Sargasso Sea and their relationship to surface hydrography", *Deep-Sea Res.*, **33**, 225–246.

Deuser, W. G. and E. H. Ross (1989) "Seasonally abundant planktonic foraminifera of the Sargasso Sea: succession, deep-water fluxes, isotopic compositions, and paleoceanographic implications", *J. Foraminiferal Res.*, **19**, 268–293.

Deuser, W. G., F. E. Muller-Karger and C. Hemleben (1988) "Temporal variations of particle fluxes in the deep subtropical and tropical North Atlantic: Eulerian versus Lagrangian effects", *J. Geophys. Res.*, **93**, 6857–6862.

Druffel, E. R. M., S. Honjo, S. Griffin and C. S. Wong (1986) "Radiocarbon in particulate matter from the eastern Sub-Arctic Pacific Ocean: Evidence of a source of terrestrial carbon to the deep sea", *Radiocarbon*, **28**, 397–407.

Duce, R. A., P. S. Liss, J. T. Merrill, E. L. Atlas, P. Buat-Menard, B. B. Hicks, J. M. Miller, J. M. Prospero, R. Arimoto, T. M. Church, W. Ellis, J. N. Galloway, L. Hansen, T. D. Jickells, A. H. Knap, K. H. Reinhardt, B. Schneider, A. Soudine, J. J. Tokos, S. Tsunogai, R. Wollast and M. Zhou (1991) "The atmospheric input of trace species to the world ocean", *Glob. Biogeochem. Cycles*, **5**, 193–259.

Dunbar, R. B. and W. N. Berger (1981) "Fecal pellet flux to modern bottom sediments of Santa Barbara Basin (California) based on sediment trapping", *Bull. Geol. Soc. Am.*, **92**, 212–218.

Dymond, J. (1984) "Sediment traps, particle fluxes, and benthic boundary layer processes", in *Global Ocean Flux Study, Proceedings of a Workshop*, National Academy Press, Washington, D.C., 260–284.

Dymond, J. and R. Collier (1988) "Biogenic particle fluxes in the equatorial Pacific: Evidence for both high and low productivity during the 1982–1983 El Niño", *Glob. Biogeochem. Cycles*, **2**, 129–137.

Dymond, J. and M. Lyle (1985) "Flux comparisons between sediments and sediment traps in the eastern tropical Pacific: Implications for atmospheric CO_2 variations during the Pleistocene", *Limnol. Oceanogr.*, **30**, 699–712.

Dymond, D., P. E. Biscaye and R. W. Rex (1974) "Eolian origin of mica in Hawaiian soils", *Bull. Geol. Soc. Am.*, **85**, 37–40.

Dymond, J., K. Fisher, M. Clauson, R. Cobler, W. Richardson, M. R. Gardner, W. Berger, A. Soutar and R. Dunbar (1981) "A sediment trap intercomparison study in the Santa Barbara Basin", *Earth Planet. Sci. Let.*, **53**, 409–481.

Eppley, R. W. and B. J. Peterson (1979) "Particulate organic matter flux and planktonic new production in the deep ocean", *Nature*, **289**, 677–680.

Erez, J. and S. Honjo (1981) "Comparison of isotopic composition of planktonic foraminifera in plankton tows, sediment traps and sediments", in W. H. Berger and A. W. H. Bé (eds) *Stable Isotopes and Calcareous Remains in the Ocean, Palaeogeogr., Palaeoclim., Palaeoecol.*, **33**, 129–156.

Fabry, V. J. (1989) "Aragonite production by pteropod mollusks in the subarctic Pacific", *Deep-Sea Res.*, **36**, 1735–1751.

Fischer, G., D. Fuetterer, R. Gersonde, S. Honjo, D. R. Ostermann and G. Wefer (1988) "Seasonal variability of particle flux in the Weddell Sea and its relation to ice cover", *Nature*, **335**, 426–428.

Fowler, S. W., S. Barlestra, J. LaRosa and R. Fukai (1983) "Vertical transport of particulate-associated plutonium and americum in the upper water column of the northeast Pacific", *Deep-Sea Res.*, **30**, 1221–1233.

Francois, R., S. Honjo, S. J. Manganini and G. Ravizza (1995) "Biogenic barium fluxes to the deep-sea: Implications for paleoproductivity reconstruction", *Glob. Biogeochem. Cycles*, **9**, 289–303.

Gardner, W. D. (1980a) "Sediment trap dynamics and calibration: A laboratory evaluation", *J. Mar. Res.*, **38**, 17–39.

Gardner, W. D. (1980b) "Field assessment of sediment traps", *J. Mar. Res.*, **38**, 41–52.

Gardner, W. D., K. R. Hinga and J. Marra (1983) "Observations on the degradation of biogenic material in the deep ocean with implications on accuracy of sediment trap fluxes", *J. Mar. Res.*, **41**, 195–214.

Gardner, W. D., J. B. Southard and C. D. Hollister (1985) "Sedimentation, resuspension and chemistry of particles in the northwest Atlantic", *Mar. Geol.*, **65**, 199–242.

Gowing, M. M. and M. W. Silver (1983) "Origins and microenvironments of bacteria mediating fecal pellet decomposition in the sea", *Mar. Biol.*, **73** ,7–16.

Gust, G., R. H. Byrne, R. E. Bernstein, P. R. Betzer and W. Bowles (1992) "Particle fluxes and moving fluids: Experience from synchronous trap collections in the Sargasso Sea", *Deep-Sea Res.*, **39**, 1071–1083.

Haake, B. and V. Ittekkot (1990) "Die Wind-getriebene 'biologische Pumpe' und der Kohlenstoffentzug im Ozean", *Naturwissenschaften*, 77, 75–79.

Haake, B., V. Ittekkot, T. Rixen, V. Ramaswamy, R. R. Nair and W. B. Curry (1993) "Seasonality and interannual variability of particle fluxes to the deep Arabian Sea", *Deep-Sea Res. I*, **40**, 1323–1344.

Handa, N. (1989) "Flux of organic matter at Japan Trench Sites (JT-01 and 02)", *Kaiyo Monthly*, **21**, 197–202.

Harbison, G. R. and R. Gilmer, R. (1986) "Effects of animal behavior on sediment trap collections: implications for the calculation of aragonite fluxes", *Deep-Sea Res.*, **33**, 1017–1024.

Hay, B. J., S. Honjo, S. Kempe, V. Ittekkot, E. T. Degens, T. Konuk and E. Izdar (1990) "Interannual variability in particle flux in the southwestern Black Sea", *Deep-Sea Res.*, **37**, 911–928.

Heath, G. R., T. C. Moore and J. P. Dauphin (1976) "Late Quaternary accumulation rates of opal, quartz, organic carbon, and calcium carbonate in the Cascadia Basin area, northeast Pacific", *Geol. Soc. Am. Memoir*, **145**, 393–409.

Heiskanen, A.-S. (1990) "Spring bloom dynamics and sedimentation in the coastal northern Baltic Sea", in P. Wassmann, A.-S. Heiskanen and O. Lindahl (eds) *Sediment Trap Studies in the Nordic Countries*, Symposium Proceedings, Kristineberg Marine Biological Station, Sweden, 157–175.

Hinga, K. R., J. M. Sieburth and G. R. Heath (1979) "The supply and use of organic material by the deep-sea benthos", *J. Mar. Res.*, **37**, 557–579.

Holligan, P. M., M. Viollier, D. S. Harbour, P. Camus and Campagne-Phillips (1983) "Satellite and ship studies of coccolithophore production along a continental shelf edge" *Nature*, **304**, 339–342.

Honjo, S. (1975) "Dissolution of suspended coccoliths in the deep-sea water column and sedimentation of coccolith ooze", in W. Sliter, A. W. H. Bé and W. H. Berger (eds) *Cushman Found. Foram. Res. Sp. Publ.*, **13**, 114–128.

Honjo, S. (1976) "Coccoliths: production, transportation and sedimentation", *Mar. Micropaleont.*, **1**, 65–79.

Honjo, S. (1977) "Biogenic carbonate particles in the ocean; do they dissolve in the water column", in N. R. Andersen and A. Malahoff (eds) *The Fate of Fossil Fuel CO_2*, Plenum Press, New York, 269–294.

Honjo, S. (1978) "Sedimentation of materials in the Sargasso Sea at a 5,367 m deep station", *J. Mar. Res.*, **36**, 469–492.

Honjo, S. (1980) "Material fluxes and modes of sedimentation in the mesopelagic and bathypelagic zones", *J. Mar. Res.*, **38**, 53–97.

Honjo, S. (1982) "Seasonality of biogenic and lithogenic fluxes in the Panama Basin", *Science*, **218**, 883–884.

Honjo, S. (1984) "Study of ocean fluxes in time and space by bottom-tethered sediment trap arrays: a recommendation", in *Global Ocean Flux Study, Proceedings of a Workshop*, National Academy Press, Washington, D.C., 305–324.

Honjo, S. (1990a) "Particle fluxes and modern sedimentation in the polar oceans", in W. O. Smith, Jr. (ed) *Polar Oceanography*, Academic Press, New York, Vol. II, Chapter 13, 322–353.

Honjo, S. (1990b) "Ocean particle and fluxes of material to the interior of the deep ocean; the azoic theory 120 years later", in V. Ittekkot, S. Kempe, W. Michaelis and A. Spitzy (eds) *Facets of Modern Biogeochemistry*, Springer, Berlin, 62–73.

Honjo, S. and K. W. Doherty (1988) "Large aperture time-series sediment traps: design objectives, construction and application", *Deep-Sea Res.*, **35**, 133–149.

Honjo, S. and Manganini, S. J. (1992) "*Biogenic Particle Fluxes at the 34°N 21°W and 48°N 21°W Stations, 1989–1990: Methods and Analytical Data Compilation*", Technical Report of the Woods Hole Oceanographic Institution, WHOI–92–15.

Honjo, S. and S. J. Manganini (1993) "Annual biogenic particle fluxes to the interior of the North Atlantic Ocean; studied at 34°N 21°W and 48°N 21°W", *Deep-Sea Res. II*, **40**, 587–607.

Honjo, S. and M. R. Roman (1978) "Marine copepod fecal pellets: Production, transportation and sedimentation", *J. Mar. Res.*, **36**, 45–57.

Honjo, S., J. F. Connell and P. Sachs (1979) "*Construction of PARFLUX Mark II Sediment Trap; Engineering Report*", Technical Report of Woods Hole Oceanographic Institution, WHOI–79–80, 51 pp.

Honjo, S., S. J. Manganini and J. J. Cole (1982a) "Sedimentation of biogenic matter in the deep ocean", *Deep-Sea Res.*, **29**, 609–625.

Honjo, S., S. J. Manganini and L. J. Poppe (1982b) "Sedimentation of lithogenic particles in the open sea" *Mar. Geol.*, **50**, 199–220.

Honjo, S., S. J. Manganini and G. Wefer (1988) "Annual particle flux and a winter outburst of sedimentation in the northern Norwegian Sea", *Deep-Sea Res.*, **35**, 1223–1234.

Honjo, S., D. W. Spencer and J. W. Farrington (1982c) "Deep advective transport of lithogenic particles in Panama Basin" *Science*, **216**, 516–518.

Honjo, S., D. W. Spencer and W. D. Gardner (1992) "A sediment trap intercomparison experiment in the Panama Basin 1979", *Deep-Sea Res.*, **39**, 333–358.

Honjo, S., K. W. Doherty, Y. C. Agrawal and V. L. Asper (1984) "Direct optical assessment of macroscopic aggregates in the deep ocean", *Deep-Sea Res.*, **31**, 67–76.

Honjo, S., J. Dymond, R. Collier and S. J. Manganini (1995) "Export production of particles to the interior of equatorial Pacific Ocean during 1992 EqPac experiment", *Deep-Sea Res. II*, **42**, 831–870.

Hurd, D. C. (1983) "Physical and chemical properties of siliceous skeletons", in S. R. Aston (ed) *Silicon Geochemistry and Biogeochemistry*, Academic Press, London, 187–244.

IPCC (1990) "*Climate Change: The IPCC Scientific Assessment Report*", prepared for IPCC by Working Group 1, J. T. Houghton, G. J. Jenkins and J. J. Ephramus, Cambridge University Press.

Ittekkot, V. (1991) "Particle flux studies in the Indian Ocean", *EOS*, **72**, 527–530.

Ittekkot, V. and B. Haake (1990) "The terrestrial link in the removal of organic carbon", in V. Ittekkot, S. Kempe, W. Michaelis and A. Spitzy (eds) *Facets of Modern Biogeochemistry*, Springer, Berlin, 319–325.

Ittekkot, V., E. T. Degens and S. Honjo (1984a) "Seasonality in the fluxes of sugars, amino acids, and amino sugars to the deep ocean: Panama Basin", *Deep-Sea Res.*, **31**, 1071–1083.

Ittekkot V., W. G. Deuser and E. T. Degens (1984b) "Seasonality in the fluxes of sugars, amino acids, and amino sugars to the deep ocean: Sargasso Sea", *Deep-Sea Res.*, **31**, 1057–1069.

Ittekkot, V., B. Haake, M. Bartsch, R. R. Nair and V. Ramaswamy (1992) "Organic carbon removal in the sea: The continental connection", in C. P. Summerhayes, W. L. Prell and K. C. Emeis (eds) *Upwelling Systems: Evolution Since the Early Miocene*, Geological Society Special Publication No. 64, 167–176.

Ittekkot, V., R. R. Nair, S. Honjo, V. Ramaswamy, M. Bartsch, S. J. Manganini and B. N. Desai (1991) "Enhanced particle fluxes in Bay of Bengal induced by injection of water", *Nature*, **351**, 385–387.

Jickells, T. D., W. G. Deuser, A. Fleer and C. Hemleben (1990) "Variability of some elemental fluxes in the western tropical Atlantic", *Oceanologica Acta*, **13**, 291–298.

Jones, P. D., T. M. L. Wigley and S. C. B. Raper (1987) "The rapidity of CO_2-induced climatic change: observations, model results and paleoclimatic implications", in W. H. Berger and L. D. Labeyrie (eds) *Abrupt Climatic Change*, Reidel, Dordrecht, 47–55.

Karl, D. M. and G. A. Knauer (1989) "Swimmers: A recapitulation of the problem and a potential solution", *Oceanography*, **2**, 25–32.

Karl, D. M., G. A. Knauer, J. H. Martin and B. B. Ward (1984) "Bacterial chemolithotrophy in the ocean is associated with sinking particles", *Nature*, **309**, 54–56.

Kellogg, W. W. (1991) "Response to skeptics of global warming", *Bull. Am. Meteorol. Soc.*, **72**, 499–511.

Kempe, S., H. Nies, V. Ittekkot, E. T. Degens, K. O. Buesseler, H. D. Livingston, S. Honjo, B. J. Hay and S. J. Manganini (1987) "Comparison of Chernobyl nuclide deposition in the Black Sea and in the North Sea", in E. T. Degens, E. Izdar and S. Honjo (eds) *Particle Flux in the Ocean*, Mitt. Geol.-Paläont. Inst. Univ. Hamburg No. 62, 165–178.

Kitani, K. (1973) "An oceanographic study of the Okhotsk Sea - Particularly in regard to cold waters", *Bull. Far Seas Fish. Res. Lab.*, **9**, 45–76.

Knauer, G. A., J. H. Martin and K. W. Bruland (1979) "Fluxes of particulate carbon, nitrogen, and phosphorus in the upper water column of the northeast Pacific", *Deep-Sea Res.*, **26**, 97–108.

Knauer, G. A., D. M. Karl, J. H. Martin and C. N. Hunter (1984) "*In-situ* effects of selected preservatives on total carbon, nitrogen and metals collected in sediment traps", *J. Mar. Res.*, **42**, 445–462.

Lampitt, R. S. (1985) "Evidence for the seasonal deposition of detritus to the deep-seafloor and its subsequent resuspension", *Deep-Sea Res.*, **32**, 885–897.

Lee, C. and C. Cronin (1984) "Particulate amino acids in the sea: Effects of primary production and biological decomposition", *J. Mar. Res.*, **42**, 1075–1097.

Lee, C., S. G. Wakeham and J. W. Farrington (1983) "Variations in the composition of particulate organic matter in a time-series sediment trap", *Mar. Chem.*, **13**, 181–194.

Lee, C., S. G. Wakeham and J. I. Hedges (1988) "The measurement of oceanic particle flux - are "swimmers" a problem?", *Oceanography*, **1**, 34–36.

Lee, C., J. I. Hedges, S. G. Wakeham and N. Shu (1992) "Effectiveness of various treatments in retarding microbial activity in sediment trap material and their effects on the collection of swimmers", *Limnol. Oceanogr.*, **37**, 117–130.

Lerman, A. (1979) *Geochemical Processes, Water and Sediment Environments*, John Wiley & Sons, New York, 48 pp.

Lisitzin, A. P. (1972) *Sedimentation in the World Ocean*, Society of Economic Paleontologists and Mineralogists, Special Publication No. 17, 218 pp.

Manganini, S. J., S. Honjo, M. Altabet and M. Honda (1994) "The effects of preservatives on settling particles as collected by sediment traps during the EqPac experiment", *Am. Geophys. Union, Am. Soc. Limnol. Oceanogr.*, **75** (3), 84 (Abstract).

Martin, J. H., G. A. Knauer, D. M. Karl and W. W. Broenkow (1987) "VERTEX: Carbon cycling in the northeast Pacific", *Deep-Sea Res.*, **34**, 267–285.

Masuzawa, T., S. Noriki, T. Kurosaki, S. Tsunogai and M. Koyama (1989) "Compositional change of settling particles with water depth in the Japan Sea", *Mar. Chem.*, **27**, 61–78.

Matsuoka, K. (1989) "Palynomorphy in the sediment trap materials collected from Japan Trench (JT-01 and 02) ", *Kaiyo Monthly*, **21**, 232–268.

Meinecke, G. and G. Wefer (1990) "Seasonal pteropod sedimentation in the Norwegian Sea", *Palaeogeogr., Palaeoclim., Palaeoecol.*, **79**, 127–147.

Michaelis, W., P. Schümann, V. Ittekkot and T. Konuk (1987) "Sterol markers for organic matter fluxes in the Black Sea", in E. T. Degens, E. Izdar and S. Honjo (eds) *Particle Flux in the Ocean*, Mitt. Geol.-Paläont. Inst. Univ. Hamburg No. 62, 89–98.

Michaels, A. F., M. W. Silver, M. M. Gowing and G. A. Knauer (1990) "Cryptic zooplankton "swimmers" in upper ocean sediment traps", *Deep-Sea Res.*, **37**, 1285–1296.

Milliman, J. D. (1974) *Marine Carbonates*, Springer-Verlag, New York, 375 pp.

Milliman, J. D. (1993) "Production and accumulation of calcium carbonate in the ocean: budget of a long-term steady state? ", *Glob. Biogeochem. Cycles*, 7, 927–957.

Mills, E. L. (1983) "Problems of deep-sea biology: An historical perspective", in T. T. Row (ed) *Deep-Sea Biology, 8. The Sea*, John Wiley & Sons, New York, 1–76.

Mopper, K. and E. T. Degens (1972) "*Aspects of the biogeochemistry of carbohydrates and proteins in aquatic environments*", Woods Hole Oceanographic Institution Technical Report, WHOI–72–68, 188 pp.

Murray, J. W., R. T. Barber, M. R. Roman, M. P. Bacon and R. A. Feely (1994) "Physical and biological controls on carbon cycling in the equatorial Pacific", *Science*, **226**, 58–65.

Nair, R. R., V. Ittekkot, S. J. Manganini, V. Ramaswamy, B. Haake, E. T. Degens, B. N. Desai and S. Honjo (1989) "Increased particle flux to the deep ocean related to monsoons", *Nature*, **338**, 749–751.

Nelson, D. M. and J. J. Goering (1977) "Near-surface silica dissolution in the upwelling region off northwest Africa", *Deep-Sea Res.*, **24**, 31–36.

Newton, P. P., R. S. Lampitt, T. D. Jickells, P. King and C. Boutle (1994) "Temporal and spatial variability of biogenic particle fluxes during the JGOFS northeast Atlantic process studies at 47°N, 20°W", *Deep-Sea Res.*, **41**, 1617–1642.

Narita, H., K. Harada and S. Tsunogai (1990) "Lateral transport of sediment particles in Okinawa Trough determined by natural radionuclides", *Geochem. J.*, **24**, 207–216.

Noriki, S. and S. Tsunogai (1986) "Particle fluxes and major components of settling particles from sediment trap experiments in the Pacific Ocean", *Deep-Sea Res.*, **33**, 903–912.

Nozaki, Y. (1986) "Ocean-scavenging model", *Geochemistry* (in Japanese), **20**, 69–77.

Nozaki, Y. (1989a) "On the environmental study of trench", *Kaiyo Monthly*, **21**, 187–191.

Nozaki, Y. (1989b) "Radionuclide fluxes obtained by a super-deep sediment trap experiment", *Kaiyo Monthly*, **21**, 192–196.

Nozaki, Y., H. S. Yang and M. Yamada (1987) "Scavenging of thorium in the ocean", *J. Geophys. Res.*, **92**, 772–778.

Okada, H. and S. Honjo (1973) "The distribution of oceanic coccolithophorids in the Pacific", *Deep-Sea Res.* **20**, 355–374.

Osterberg, C., A. G. Carey, and H. Curl (1963) "Acceleration of sinking rates of radionuclides in the sea", *Nature*, **200**, 1276–1277.

Pace, M. L., G. A. Knauer, D. M. Karl and J. M. Martin (1987) "Primary production, new production and vertical flux in the eastern Pacific ocean", *Nature*, **325**, 803–804.

Paffehofer, G. A. and S. C. Knowles (1979) "Ecological implications of fecal pellet size, production and consumption by copepods", *J. Mar. Res.*, **37**, 35–49.

Peinert, R., B. von Bodungen and V. S. Smetacek (1989) "Food web structure and loss rate" in W. H. Berger, V. S. Smetacek and G. Wefer (eds) *Productivity of the Ocean: Present and Past*, John Wiley & Sons, Chichester, 35–48.

Peinert, R., U. Bathmann, B. von Bodungen and T. Noji (1987) "The impact of grazing on spring phytoplankton growth and sedimentation in the Norwegian Current", in E. T. Degens, E. Izdar and S. Honjo (eds) *Particle Flux in the Ocean*, Mitt. Geol.-Paläont. Inst. Univ. Hamburg No. 62, 149–164.

Peterson, M. L., P. J. Hernes, D. S. Thoreson, J. I. Hedges, C. Lee and S. G. Wakeham (1993) "Field evaluation of a valved sediment trap", *Limnol. Oceanogr.*, **38**, 1741–1761.

Pfannkuche, O. and K. Lochte (1993) "Open ocean pelago-benthic coupling: Cyanobacteria as tracers of sedimenting salp faeces", *Deep-Sea Res.*, **40**, 727–737.

Pilskaln, C. H. and S. Honjo (1987) "The fecal pellet fraction of biogeochemical particle fluxes to the deep sea", *Glob. Biogeochem. Cycles*, **1**, 31–48.

Ramaswamy, V., R. R. Nair, S. J. Manganini, B. Haake and V. Ittekkot (1991) "Lithogenic fluxes to the deep Arabian Sea measured by sediment traps", *Deep-Sea Res.*, **38**, 169–184.

Rex, R. W. and E. D. Goldberg (1958) "Quartz contents of pelagic sediments of the Pacific Ocean", *Tellus*, **10**, 153–159.

Robb, D. (1984) "Stereo-biochemistry and function of polymers in microbial adhesion and aggregation", in K. C. Marshall (ed) *Microbial Adhesion and Aggregation*, Springer-Verlag, Berlin, 39–49.

Romankevich, E. A. (1984) *Geochemistry of Organic Matter in the Ocean*, Springer-Verlag, Berlin. 334 pp.

Schrader, H. J. (1971) "Fecal pellets in sedimentation of pelagic diatoms", *Science*, **174**, 55–57.

Shanks, A. L. and J. D. Trent (1980) "Marine snow: Sinking rates and potential role in vertical flux", *Deep-Sea Res.*, **27**, 137–144.

Siegel, D. A., T. C. Granata, A. F. Michaels and T. D. Dickey (1990) "Mesoscale eddy diffusion, particle sinking, and the interpretation of sediment trap data", *J. Geophys. Res.*, **95**, 5305–5311.

Silver, M. W. and A. L. Alldredge (1981) "Bathypelagic marine snow: Deep-sea algal and detrital community", *J. Mar. Res.*, **39**, 501–530.

Silver, M. W. and K. W. Bruland (1981) "Differential feeding and fecal pellet composition of slaps and pteropods, and the possible origin of deep water flora and olive green "cells"", *Mar. Biol.*, **62**, 263–273.

Small, L. F., S. W. Fowler and M. Y. Ünlü, M. Y. (1979) "Sink rates of natural copepod fecal pellets", *Mar. Biol.*, **51**, 233–241.

Smayda, T. J. (1970) "Normal and accelerated sinking of phytoplankton in the sea", *Oceanogr. Mar. Biol.*, **8**, 353–414.

Smetacek, V. S. (1985) "The role of sinking in diatom life-history cycles: ecological, evolutionary and geological significance", *Mar. Biol.*, **84**, 239–251.

Spencer, C. P. (1983) "Marine biogeochemistry of silicon", in S. R. Aston (ed), *Silicon Geochemistry and Biochemistry*, Academic Press, London, 101–141.

Spencer, D. W., P. G. Brewer, A. Fleer, S. Honjo, S. Krishnaswami and Y. Nozaki (1978) "Chemical fluxes from a sediment trap experiment in the deep Sargasso Sea", *J. Mar. Res.*, **36**, 493–523.

Steinmetz (1991) "Calcareous nannoplankton biocoenosis: sediment trap studies in the equatorial Atlantic, central pacific, and Panama Basin", in S. Honjo (ed) *Ocean Biocoenosis*, Series No. 1, Woods Hole Oceanographic Institution Press, Woods Hole, Mass., I–85.

Suess, E. (1980) "Particulate organic carbon flux in the ocean-surface productivity and oxygen utilization", *Nature*, **288**, 260–263.

Suzuki, N. and K. Kato (1953) "Studies on suspended materials. Marine snow in the sea, part 1, Source of marine snow", *Bulletin of the Faculty of Fisheries, Hokkaido University*, **4**, 132–135.

Takahashi, K. (1983) "Radiolaria: sinking population, standing stock and production rate", *Marine Micropaleontology*, **7**, 441–447.

Takahashi, K. (1986) "Seasonal fluxes of pelagic diatoms in the subarctic pacific 1982–1983", *Deep-Sea Res.*, **33**, 1225–1251.

Takahashi, K. (1989) "Silicoflagellates as productive indicators: evidence from long temporal and spatial flux variability responding to hydrography in the northeastern Pacific", *Glob. Biogeochem. Cycles*, **3**, 43–61.

Takahashi, K. (1991) "Radiolaria: Flux, Ecology, and Taxonomy in the Pacific and Atlantic", in S. Honjo (ed) *Ocean Biocoenosis*, Series No. 3, Woods Hole Oceanographic Institution, Woods Hole, MA 02543, USA, 303 pp.

Takahashi, K. (1994) "Coccolithophorid biocoenosis production and flux in the deep sea", in J. C. Green and B. S. C. Leadbeater (eds) *Systematics Association Special Volume 51*, Clarendon Press, Oxford, 335–350.

Takahashi, K. and A. W. H. Bé (1984) "Planktonic foraminifera: factors controlling sinking speeds", *Deep-Sea Res.*, **31**, 1477–1500.

Takahashi, K. and S. Honjo (1981) "Vertical flux of Radiolaria: A taxon-quantitative sediment trap study from the western Tropical Atlantic", *Micropaleontology*, **27**, 140–190.

Takahashi, K. and S. Honjo (1983) "Radiolarian skeletons: size, weight, sinking speed, and residence time in tropical pelagic oceans", *Deep-Sea Res.*, **30**, 543–568.

Takahashi, K., D. C. Hurd and S. Honjo (1983) "Phaeodarian skeletons: their role in silica transport to the deep sea", *Science*, **222**, 616–618.

Takahashi, T. (1975) "Carbonate chemistry of sea water and the calcite compensation depth in the oceans", in W. V. Sliter, A. H. Bé and W. H. Berger (eds) *Dissolution of Deep-Sea Carbonates*, Cushman Foundation Foraminiferal Res. Sp. Pub. 13, 11–26.

Takahashi, T., C. Goyet, D. Chipman, E. Peltzer, J. Godard and P. G. Brewer (1990) "Ratio of the organic carbon and calcium carbonate productions observed at JGOFS 47°N 20°W site", (abstract). JGOFS North Atlantic Bloom Study Symposium, 1990, Washington, D. C.

Tanoué, E. and N. Handa (1986) "Origin of sugars and amino-sugars in marine sediments", *Oceanogr. Acta*, **10**, 91–99.

Thunell, R. C. and S. Honjo (1987) "Foraminiferal fluxes as an indicator of productivity variability at Ocean Station P, Gulf of Alaska", *Nature*, **326**, 216–218.

Thunnel, R., C. Pride, E. Tappa and F. Muller-Karger (1993) "Varve formation in the Gulf of California: insights from time series sediment trap sampling and remote sensing", *Quaternary Science Review*, **12**, 451–464.

Thunell, R. C., C. H. Pilskaln, E. Tappa and L. Reynolds-Sauter (1994a) "Temporal variability in sediment fluxes in the San Pedro Basin, Southern California Bight", *Continent. Shelf Res.*, **14**, 333–352.

Thunell, R. C., W. S. Moore, J. Dymond and C. H. Pilskaln (1994b) "Elemental and isotopic fluxes in the Southern California Bight: A time-series sediment trap study in the San Pedro Basin", *J. Geophys. Res.*, **99**, 875–889.

Traverse, A. (1988) *Paleopalynology*, Unwin Hyman, Boston, xxiii + 600 pp.

Tsujita, T. (1953a) "A preliminary study on naturally occurring suspended organic matter", *Records of Oceanographic Works in Japan*, **2**, 94–100.

Tsujita, T. (1953b) "Studies on naturally occurring suspended organic matter in waters adjacent to Japan. On an application of the suspended organic matter for the analysis of water masses", *Records of Oceanographic Works in Japan*, **2**, 113–126.

Tsunogai, S. (1987) "'Train-passenger model' as an oceanic removal mechanism of chemical elements in seawater", *Geochemistry*, **21**, 75–82 (in Japanese).

Tsunogai, S. and T. Kondo (1987) "Sporadic transport and deposition of continental aerosols to the Pacific Ocean", *J. Geophys. Res.*, **87**, 8870–8874.

Tsunogai, S. and S. Noriki (1991) "Particulate fluxes of carbonate and organic carbon in the ocean. Is the marine biological activity working as a sink of the atmospheric carbon?", *Tellus*, **43B**, 256–266.

Tsunogai, S., S. Noriki, K. Harada and K. Tate (1990) "Vertical change index for the particulate transport of chemical and isotopic components in the ocean", *Geochem. J.*, **24**, 229–244.

Tsunogai, S., S. Noriki, K. Harada, T. Kurosaki, Y. Watanabe and M. Maeda (1986) "Large but variable particulate flux in the Antarctic Ocean and its significance for chemistry of Antarctic water", *Journal of the Oceanographical Society of Japan*, **42**, 83–90.

Tuji, S. (1993) "Time-lapse observation of marine snow in Sagami Bay using new optics", (abstract). Biogeochemical Cycles in the Ocean. JAMSTEC workshop, Yokosuka, Dec. 1993.

Turner, J. T. and J. A. Ferrante (1979) "Zooplankton fecal pellets in aquatic ecosystems", *BioScience*, **29**, 670–677.

von Bodungen, B., G. Fischer, E.-M. Nöthig and G. Wefer (1987) "Sedimentation of krill faeces during spring development of phytoplankton in Bransfield Strait, Antarctica", in E. T. Degens, E. Izdar and S. Honjo (eds) *Particle Flux in the Ocean*, Mitt. Geol.-Paläont. Inst. Univ. Hamburg No. 62, 243–257.

Wakeham, S. G. and E. A. Canuel (1986) "Lipid composition of the pelagic crab *Pleuroncodes planipes*, its feces, and sinking particulate organic matter in the equatorial North Pacific Ocean", *Org. Geochem.*, **9**, 331–343.

Wakeham, S. G., J. W. Farrington, R. B. Gagosian, C. Lee, H. de Baar, G. E. Nigrelli, W. Tripp, S. O. Smith and N. M. Frew (1980) "Organic matter fluxes from sediment traps in the equatorial Atlantic Ocean", *Nature*, **286**, 798–799.

Walsh, J. J. (1988) *On the Nature of Continental Shelves*, Academic Press, San Diego, 520 pp.

Walsh, J. J. (1994) "Particle export at Cape Hatteras", *Deep-Sea Res.*, **41**, 603–628.

Walsh, J. J., G. T. Rowe, R. L. Iverson and C. P. McRoy (1981) "Biological export of shelf carbon: a neglected sink of the global CO_2 cycle", *Nature*, **291**, 196–201.

Wassmann, P. and D. Slagstad (1990) "Mathematical modeling, an important tool to explore the dynamics of vertical flux of organic matter", in P. Wassmann, A.-S. Heiskanen and O. Lindahl (eds) *Sediment Trap Studies in the Nordic Countries*, Symposium Proceedings, 2, Kristineberg Marine Biological Station, Sweden, 255–279.

Wefer, G. (1989) "Particle flux in the ocean: effects of episodic production", in W. H. Berger, V. S. Smetacek and G. Wefer (eds), *Productivity of the Ocean, Present and Past*, John Wiley & Sons, Chichester, 139–153.

Wefer , G. (1991) "Stoffransport zun Meeresboden: Eine Übersicht", *Naturwissenschaften*, **78**, 1–6.

Wefer, G., G. Fischer, D. Fütterer and R. Gersonde (1988) "Seasonal particle flux in the Bransfield Strait (Antarctica)", *Deep-Sea Res.*, **35**, 891–898.

8 Nitrogen and Carbon Isotopic Tracers of the Source and Transformation of Particles in the Deep Sea

MARK A. ALTABET

8.1 INTRODUCTION

The formation of particulate organic matter (POM) in surface waters and its subsequent removal to depth is a principal control on the distribution of inorganic carbon and other biogeochemically-significant species in the ocean (see Fowler and Knauer, 1986, and this volume for reviews). Though it is generally accepted that large, fast sinking particles are the principal form in which organic matter is transported into the ocean's interior, major issues remain regarding the processes controlling their production and transformation.

In an ever growing body of literature, natural variations in $^{15}N/^{14}N$ and $^{13}C/^{12}C$ ratios have been employed as useful natural tracers for testing hypotheses regarding the biogeochemical cycles of nitrogen and carbon in the marine environment. Isotopic signals are produced when transformation processes cause isotopic discrimination between substrate and product. Their use is particularly important on the time and space scales of the deep sea in which important transformations are both difficult to directly probe and observe. Use of isotopic data involves either recognition of ratios characteristic of specific organic matter sources or transformations or exploitation of temporal or spatial variations as 'natural' tracer experiments in which an isotopic signal propagates from one organic pool to another and from the surface into the ocean's interior.

Since in theory any transformation process can alter isotopic ratios (e.g., photosynthesis, trophic transfer, decomposition), it is possible that interpretations of data could be hopelessly ambiguous. Fortunately, a few isolatable processes dominate isotopic signatures in the marine environment and these will be discussed below. The first section is a brief overview of the principles of isotopic fractionation. The following sections discuss changes in isotopic ratio brought about during primary production and during subsequent transformation of organic matter, respectively. The last section summarizes the findings from a recent case study.

Particle Flux in the Ocean
Edited by V. Ittekkot, P. Schäfer, S. Honjo and P. J. Depetris

8.2 ISOTOPIC FRACTIONATION DURING BIOGEOCHEMICAL REACTIONS

Because natural variations in isotopic ratio are rather small, the 'δ' notation is used in the literature and is defined as:

$$1)\ \delta = \frac{R_{sample} - R_{standard}}{R_{standard}} - 1 \times 1000 \quad (‰)$$

R refers to the isotopic ratio. For $\delta^{15}N$, atmospheric N_2 is the standard used for literature values. For $\delta^{13}C$, values are referenced against the PDB standard. The range in $\delta^{15}N$ and $\delta^{13}C$ is on the order of tens of per mill (‰). By comparison, analytical reproducibility is on the order of ± 0.1 to 0.4‰. Natural variations in isotopic ratio occur when the specific reaction rates vary for chemical species containing the different isotopes of an element (e.g., $^{12}CO_2$ vs. $^{13}CO_2$). The fractionation factor is defined as the ratio of these rates:

2) $\alpha = k/k^*$ where * denotes the heavier isotope.

For ease of comparison fractionation factors are often transformed to the same units as the 'δ' notation:

3) $\varepsilon = (\alpha - 1) \times 1000$

Since reaction rates are usually faster for chemical species containing the lighter isotope, ε is usually positive and product pools have lower δ values than sources:

4) $\delta_{product} = \delta_{source} - \varepsilon$

(see Goericke et al., 1994, for an example of an expanded mathematical treatment). As will be seen below actual observed differences in isotopic ratios depend on a number of other factors.

For inorganic reactions, ε is a function of reaction conditions, particularly temperature. However, for biogeochemical processes, ε is often not only a function of enzyme biochemistry but also organism physiology, and in the literature it usually refers to the net observed fractionation associated with a process that may in reality be the sum of several others. For example, isotopic fractionation during primary production reflects effects occurring during both CO_2 diffusion across the cell membrane and its subsequent enzymatic fixation into organic matter (e.g., Goericke et al., 1994; O'Leary et al., 1992). On the cellular level, fractionation factors associated with enzymatic reactions where covalent bonds are either broken or formed are usually large compared with those associated with diffusion or active transport of substrates (O'Leary, 1989). For example, RuBP carboxylase has a value of ε ranging from 20 to 30‰ (Guy et al., 1986; Roeske and O'Leary,

1984) where diffusion is only on the order of 1‰ (O'Leary, 1984). Consider the simple system:

$$CO_{2\,(ext.)} \underset{r_{-1}}{\overset{r_1}{\leftrightarrow}} CO_{2\,(int.)} \overset{r_2}{\rightarrow} C_{org}$$

where r_1 is the rate of diffusion into the cell, r_{-1} is the rate of diffusion out of the cell, and r_2 is the fixation rate of carbon into organic carbon with only this second step producing isotopic fractionation (ε_2). Observed fractionation is given by:

$$5)\ \varepsilon_{obs} = \frac{\varepsilon_2 + r_{-1}/r_2}{1 + r_{-1}/r_2}$$

When r_{-1} is large compared to r_2 (enzyme catalysis limits the overall rate of carbon fixation), ε_{obs} approaches ε_2. At the other extreme, when $r_1 = r_2$ and $r_{-1} = 0$ (diffusion limits the overall rate), ε_{obs} approaches 0.

This logic can be applied at larger scales. The microbial remineralization of organic nitrogen and its transformation to NO_3^- by nitrification involves several steps, some carried out by different bacterial groups, which in oxic, subsurface waters are, for the most part, irreversible:

$$N_{org} \rightarrow NH_4^+ \rightarrow NO_2^- \rightarrow NO_3^-$$

The last two steps are known to have moderate to large values for ε of 15 to 40‰ (Cifuentes et al., 1989; Horrigan et al., 1990; Miyake and Wada, 1971; Velinsky et al., 1989). However, the first step does not appear to be substantially fractionating (Sweeney and Kaplan, 1980; Velinsky et al., 1991) and since it limits the overall rate, $\delta^{15}N$ for newly formed NO_3^- should be similar to the $\delta^{15}N$ for the organic source under steady state in the deep sea. In fact, little variation has been observed in the $\delta^{15}N$ of NO_3^- outside of denitrification regions, generally ranging from 5 to 6‰ (Liu and Kaplan, 1989), despite large changes in concentration.

In the case of a phytoplankton bloom, in contrast, there are large temporal changes in $\delta^{15}N$ of both NO_3^- and particulate nitrogen (PN) due to progressive depletion of nutrients and moderate values of ε associated with NO_3^- utilization. Mass balance dictates that the isotopic ratio of substrate increases as a function of depletion as governed by Rayleigh fractionation (Figure 8.1):

$$6)\ \delta^{15}NO_{3\,(f)}^- = \delta^{15}NO_{3\,(f=1)}^- - \varepsilon \times \ln(f)$$

where f is the fraction of unutilized substrate ($[NO_3^-]_{obs.}/[NO_3^-]_{initial}$). The $\delta^{15}N$ of the PN produced at any instant is given by eq. 4. However, if the system is closed

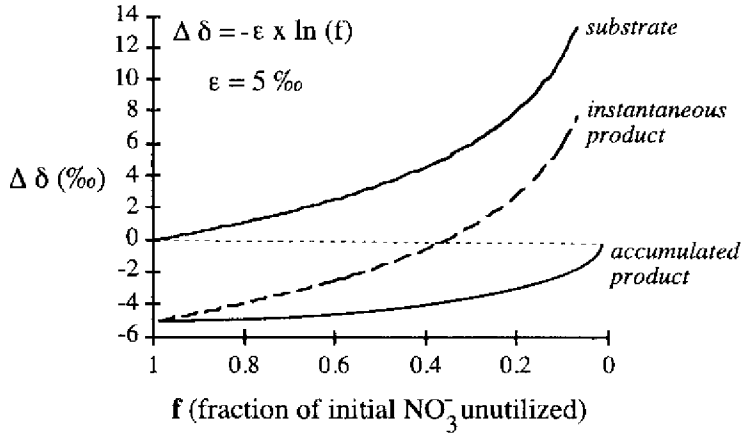

Figure 8.1 Expected variation in 'δ' value as a function of substrate depletion as predicted by Rayleigh fractionation kinetics. f is the fraction of unutilized substrate. The change in δ for the substrate is given by eq. 6. The change in δ for the instantaneous product is given by the combination of eqs. 4 and 6. The change in δ for the accumulating product is given by eq. 7.

with respect to the product its observed δ as it accumulates is given by the integral of the combination of eqs. 4 and 6 with respect to f (Figure 8.1):

7) $\delta^{15}N - PN_{(f)} = \delta^{15}NO_3^-{}_{(f=1)} + f/(1-f) \times \varepsilon_u \times \ln(f)$

In this case, mass balance requires that the $\delta^{15}N$ of substrate at f = 1 equals the $\delta^{15}N$ of product at f = 0 (Figure 8.1).

8.3 SOURCE EFFECTS - ^{15}N

Much of the temporal and regional variation in isotopic variation in POM observed in the marine environment is imparted during primary production, the initial formation of organic matter from inorganic precursors. For nitrogen, utilization of new nitrogen (in contrast to recycled forms) appears to be a critical step. In some settings such as polluted estuaries and anoxic basins (e.g., Black Sea), NH_4^+ may be the principal new nitrogen source. Rarely, nitrogen fixation from dissolved N_2 by cyanobacteria makes a major contribution to the fixed N budget. N-fixation occurs with little fractionation so $\delta^{15}N$ values for this source are near 0‰ (e.g., Minagawa and Wada, 1986). In the open ocean, NO_3^- transported to the surface from below is the predominant form of 'new' nitrogen for phytoplankton production. On average, the downward flux of PN from the surface ocean balances the utilization of NO_3^- (Eppley and Peterson, 1979). As

there is balance in N fluxes, there must be balance in isotopic composition. In the oligotrophic Sargasso Sea, where NO_3^- utilization is complete, the $\delta^{15}N$ of sinking PN was shown to be the same as for subsurface NO_3^- (Altabet, 1988). As a result, any variations in $\delta^{15}NO_3^-$ should be reflected in particulate $\delta^{15}N$.

$\delta^{15}NO_3^-$ in subsurface waters varies mainly in response to partial removal of NO_3^- by denitrification ($NO_3^- \rightarrow N_2$) which occurs only under suboxic conditions. Denitrification is strongly fractionating having values for ε of 20 to 40‰ (Cline and Kaplan, 1975; Liu and Kaplan, 1988; Miyake and Wada, 1971), whereas marine $\delta^{15}NO_3^-$ averages 6‰. Values can reach 18‰ in regions such as the Eastern Tropical N. Pacific (ETNP). Subsurface waters from the ETNP flow northward to the S. California Bight where values for $\delta^{15}NO_3^-$ are found to be 8 to 9‰ and $\delta^{15}N$ for sinking PN is correspondingly about 8‰ (Nelson et al., 1987). As expected in other regions with significant volumes of suboxic water such as the Eastern Tropical S. Pacific and the Arabian Sea, elevated $\delta^{15}N$ is also found (Schäfer and Ittekkot, 1993). Substantial decreases in $\delta^{15}N$ for sediments in the Arabian Sea during glacial stages has been cited as evidence of climatically driven variations in denitrification in this region (Altabet et al., 1995).

Partial utilization of NO_3^- transported to surface waters occurs in large segments of the global ocean either seasonally of perennially. Under these conditions, isotopic fractionation during NO_3^- uptake by phytoplankton results in significant ^{15}N depletion of PN relative NO_3^-. In laboratory cultures (Wada and Hattori, 1978; Montoya and McCarthy, 1995) ε for NO_3^- can be as high as 19‰. The earlier study indicated that there was an inverse relationship between ε and algal growth rate while the latter one showed no change with growth rate but varied instead with species. Diatoms had higher values (9 to 12‰) whereas other forms studied had average ε values between 1 and 3‰. Field estimates for ε from the Southern Ocean, Subarctic Pacific, and temperate N. Atlantic fall within the narrow range of 8 to 9‰ (Altabet and Francois, 1994b). However, in the tropical equatorial Pacific, ε appears to be substantially lower, about 3 to 5‰ (Altabet and Francois, 1994a; Altabet and Francois, manuscript in prep.). This difference may be the result of regional variations in the phytoplankton species responsible for NO_3^- depletion. Clearly, more study is required into the factors influencing ε for NO_3^- uptake.

When NO_3^- depletion is small, the $\delta^{15}N$ of PN should be predicted by eq. 4. In reality, use of recycled N also influences the $\delta^{15}N$ of suspended PN and is discussed in the next section. Nevertheless, the lowest values for marine POM (ca. -4 to -5 ‰; Altabet et al., 1991; Altabet and Francois, 1994a) are found where and when there is little depletion of surface ocean NO_3^-. As NO_3^- is depleted, its $\delta^{15}N$ rises as dictated by first-order Rayleigh fractionation kinetics (eq. 6). In near-surface, vertical profiles from the Subarctic Pacific and Southern Ocean, $\delta^{15}NO_3^-$ increased with decreasing $[NO_3^-]$ toward surface (Altabet and Francois, 1994b; Figure 8.2). The linear relationship between $\delta^{15}NO_3^-$ and ln $[NO_3^-]$ predicted by

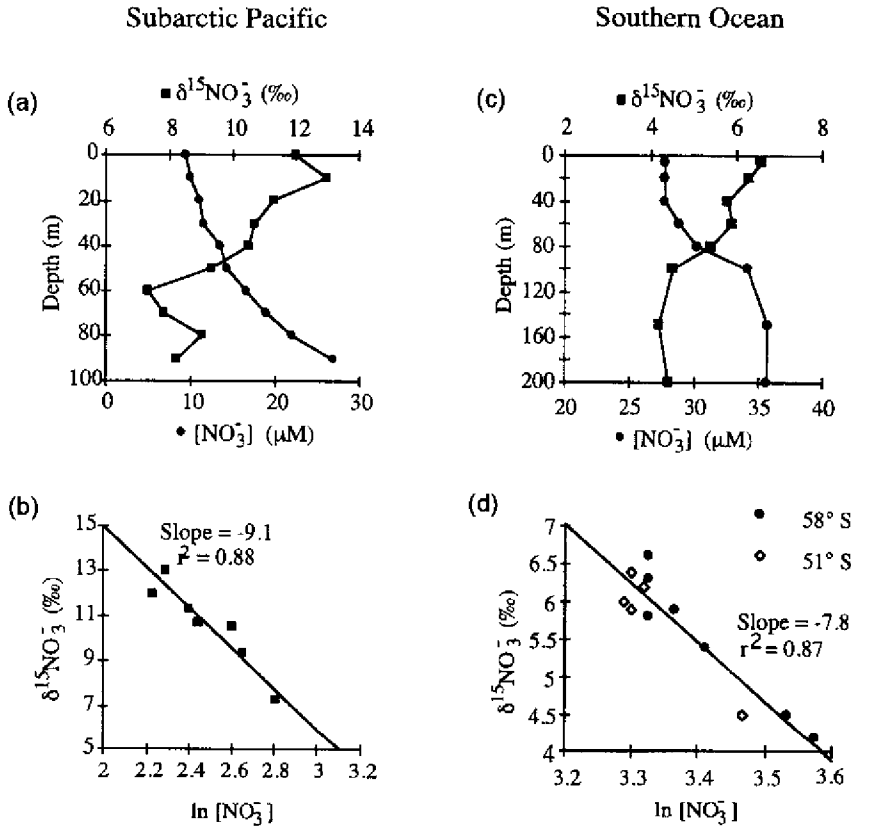

Figure 8.2 (a) Vertical variations in $[NO_3^-]$ and $\delta^{15}NO_3^-$ for a site in the central Subarctic Pacific demonstrating isotopic fractionation as function of NO_3^- utilization. (b) ln ($[NO_3^-]$) vs. $\delta^{15}NO_3^-$ for this data set. According to eq. 6, the slope of the linear regression equals -1 x ε_u (9.1‰). (c) Vertical variations in $[NO_3^-]$ and $\delta^{15}NO_3^-$ for a site in the S.W. Indian Ocean sector of the Southern Ocean showing similar behavior. (d) ln ($[NO_3^-]$) vs. $\delta^{15}NO_3^-$ for this data set and another station from the same transect. Calculated ε_n = 7.8‰.

eq. 5 is observed with the inverse of the slope estimating ε, in this case showing consistency between the two regions.

Isotopic enrichment in NO_3^- by phytoplankton utilization causes the subsequent increase in the $\delta^{15}N$ of newly produced PN. Analogous to the vertical variations in $\delta^{15}NO_3^-$ with concentration, $\delta^{15}N$ values for euphotic zone suspended PN are often lowest at the base of this layer where $[NO_3^-]$ is the highest, rising toward surface with decreasing $[NO_3^-]$ (Altabet and McCarthy, 1986). Where there are large horizontal gradients in surface $[NO_3^-]$, such as across the northern edge of the Southern Ocean (Figure 8.3a) and the equatorial Pacific (Figure 8.4), there are

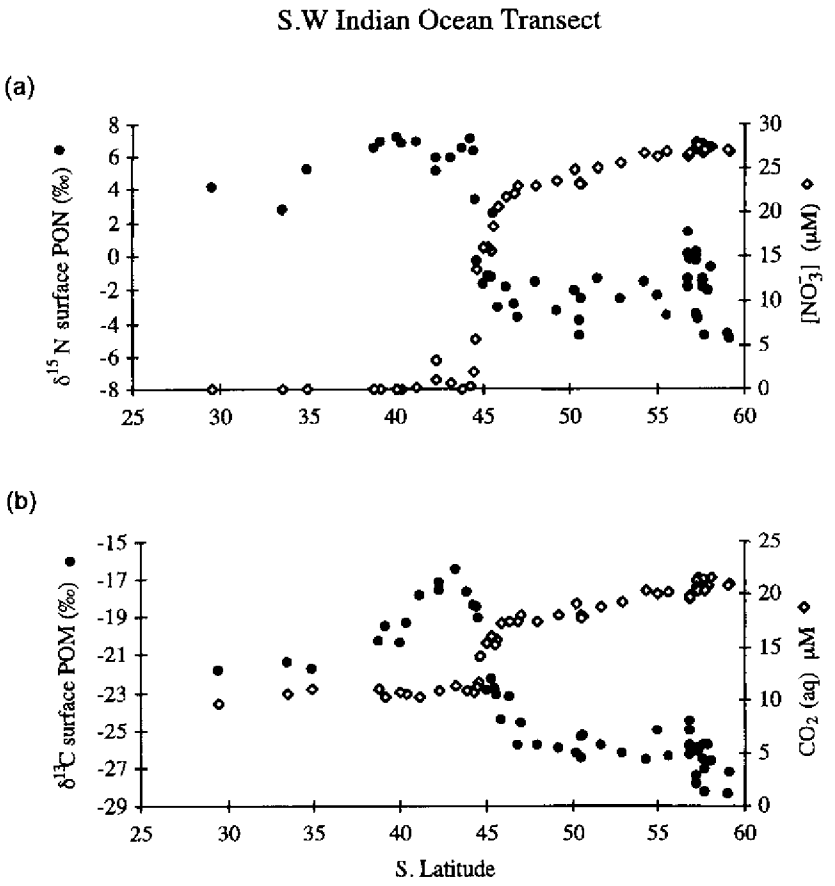

Figure 8.3 (a) Surface [NO_3^-] and $\delta^{15}N$ for suspended PN along a transect of the Southern Ocean frontal system (S.W. Indian Ocean sector). The sharp nutrient front at 45° S marks the boundary between subtropical and subpolar water. (b) Surface [CO_2 (aq)] and $\delta^{13}C_{org}$ for suspended PN along the same transect.

large variations in $\delta^{15}N$ of suspended PN inversely correlated with [NO_3^-] (Altabet and Francois, 1994b). It is important to note that the $\delta^{15}N$ of PN in these regions vary as a function of f not [NO_3^-]. How changes in [NO_3^-] reflect f is highly dependent on the physics of these systems. In the case of the equatorial Pacific, the $\delta^{15}N$ of surface NO_3^- clearly shows increases with decreasing concentration confirming that latitudinal variations in the $\delta^{15}N$ of particles result from partial nutrient utilization (Figure 8.4).

Phytoplankton blooms in which there is substantial drawdown of NO_3^- over time result in large temporal/seasonal excursions in particulate $\delta^{15}N$. If the residence

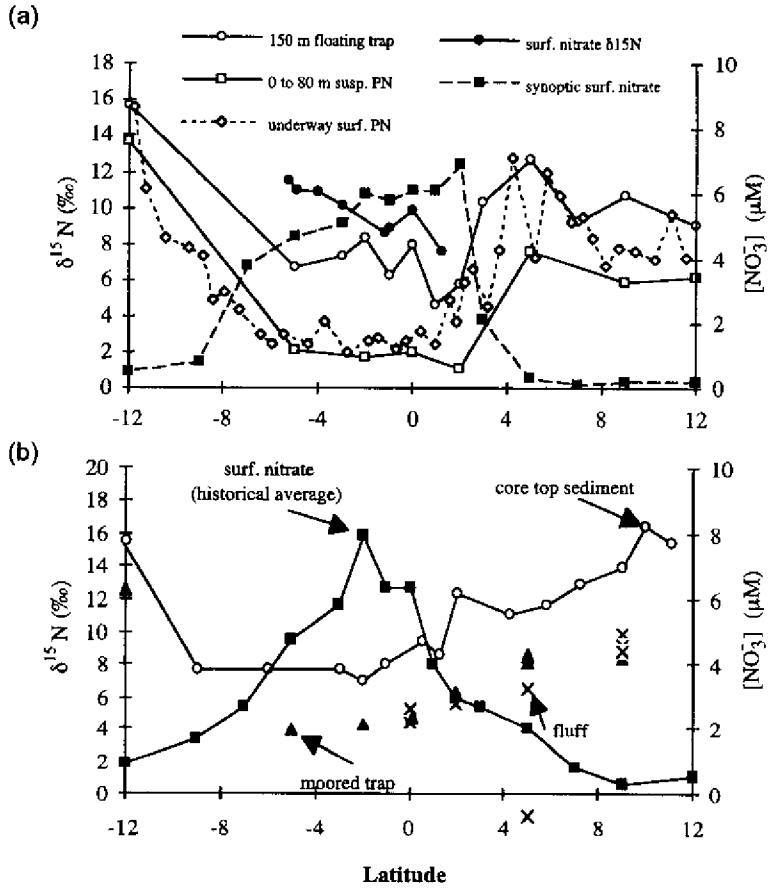

Figure 8.4 Results for north-south transects of the equatorial Pacific between 135 and 140° W. (a) Comparison of latitudinal variations for synoptic samples collected during the U.S. JGOFS EqPac Fall Survey cruise. Surface concentration and $\delta^{15}N$ values for NO_3^-, sinking particles collected at 150 m by floating sediment trap, surface suspended particles, and suspended particles averaged over the upper 80 m are shown. (b) Comparison of latitudinal variations in surface $[NO_3^-]$ and $\delta^{15}N$ values for sediment surface fluff layer, annual average of moored sediment trap collections (880 to 3800 m), and $\delta^{15}N$ for core-top sediments. NO_3^- data are the historically averaged data of Barber and Chavez (1991).

time of PN in the euphotic zone is short compared to the depletion time of NO_3^-, the rise in $\delta^{15}N$ with f will follow more closely eq. 6, otherwise, if PN accumulates in the euphotic zone without any removal, the rise will be more modest and follow eq. 7. The occurrence of this phenomenon is widespread. It has been observed in Gulf Stream warm-core rings (Altabet and McCarthy, 1985), the Sargasso Sea

(Altabet, 1989; Altabet and Deuser, 1985), a coastal Alaska embayment (Goering et al., 1990), mesocosm studies (Nakatsuka et al., 1992), the Arabian Sea (Schäfer and Ittekkot, 1993), the Bay of Bengal (Schäfer and Ittekkot, 1995), the Greenland and Norwegian Seas (Voss et al., 1990) and the temperate N. Atlantic (Altabet et al., 1991). This latter case in which $\delta^{15}N$ increased by 13‰ over the course of the bloom will be discussed in greater detail below.

8.4 SOURCE EFFECTS - ^{13}C

In contrast to nitrogen isotopes, most of the variation in the $\delta^{13}C$ of POM in the ocean results principally from variations in ε for carbon fixation and not through changes in the isotopic composition of the inorganic source. Dissolved inorganic carbon (DIC) is fairly abundant in the ocean and while it is slightly depleted near-surface due to biological utilization, the corresponding rise in $\delta^{13}C$ is only 2 to 3‰ (Kroopnick, 1985). In contrast, marine $\delta^{13}C$ values vary by up to 12‰ (-30 vs. -18‰) with lowest values in cold, Antarctic waters and highest values in warm subtropical and tropical waters (Francois et al., 1993; Rau et al., 1982; Rau et al., 1989; Rau et al., 1991; Figure 8.3b). About 3‰ of this change is attributable to temperature dependence of the equilibrium fractionation effect (the difference in ε for forward and reverse reactions) between HCO_3^- and $CO_2(aq)$ (Deuser et al., 1968; Mook et al., 1974). While it is CO_2 that it is used by the principal carbon fixing enzyme (RuBP carboxylase), at the typical oceanic pH of 8.2, the bulk of DIC is in the form of HCO_3^- which is 8.5 to 11.5‰ enriched in ^{13}C (as a function of temperature) relative to total DIC. Since $\delta^{13}C$ DIC is about 1.5‰, $\delta^{13}CO_2$ ranges from -7 to -10‰.

There are alternate carbon fixation pathways employing enzymes such as PEP carboxylase (PEPC) and PEP carboxykinase (PEPCK). While PEPCK has ε similar for RuBP carboxylase (Arnelle and O'Leary, 1992), the value for PEPC is much less at 2‰ (O'Leary, 1981). Though, at times, measured activities for these enzymes in natural phytoplankton populations can be high (Descolas-Gros and Fontugne, 1988; Descolas-Gros and Fontugne, 1990; Fontugne et al., 1991) and have been cited as the mechanism for variations in marine $\delta^{13}C$, from biochemical considerations they are likely to account for only a very small proportion of total C fixation (Goericke et al., 1994).

Terrestrial carbon (C3 source) has an average $\delta^{13}C$ (-27‰) substantially less than what has been considered 'typical' marine $\delta^{13}C$ (-22‰) probably as a result of lessened diffusion control of carbon fixation in gas phase ($\delta^{13}C$ for atmospheric CO_2 is higher than for dissolved CO_2). This difference between terrestrial and marine endmembers has been the basis for studies quantifying the importance of terrestrial carbon to marine sediments (Peters et al., 1978). However, most

previous work along these lines ignored the possibility that marine organic carbon could also have low $\delta^{13}C$ values.

Given the range in $\delta^{13}C$ for marine $CO_2(aq)$ and ε for RuBP carboxylase (ε_p), $\delta^{13}C$ for POM would thus be expected to vary from -26 to -39‰, substantially lower than observed. In has been pointed out, more recently, that ε_p is inversely correlated with $CO_2(aq)$ which ranges from 9 to 26 μM in surface ocean waters (Popp et al., 1989; Rau et al., 1989). $CO_2(aq)$ is a function of total DIC concentration, pH, and temperature, but most of the observed range is the result of changes in the latter (at lower temperatures, the equilibrium between HCO_3^- and CO_2 is pushed toward CO_2). The simplest explanation for the correlation between $CO_2(aq)$ and ε_p is that, at the CO_2 concentrations found in the ocean, diffusion into phytoplankton cells (which is partially controlled by the CO_2 concentration gradient across the cell membrane) controls or partially controls the overall rate of C fixation and reduces ε_p toward the relatively low value for diffusion (about 1‰). For terrestrial plants, Farquhar et al. (1982) developed a model in which ε_p was a specific function of the external/internal difference in $[CO_2]$. In this model, increasing C fixation rate (equivalent to growth rate) resulted in an increased CO_2 gradient and lowered ε_p. Rau et al. (1992) observed during the JGOFS NABE (Joint Global Ocean Flux Study - North Atlantic Bloom Experiment) increasing $\delta^{13}C$ with decreasing CO_2 (due to biological drawdown of DIC). Since the overall correlation showed increased sensitivity in comparison to studies of regional variations, the Farquhar model was used to explain these observations as also resulting from changes during the bloom in 'biological demand' (more precisely growth rate or specific C fixation rate). Other cases of temporal variations in $\delta^{13}C$ associated with bloom events have been observed (Goering et al., 1990; Nakatsuka et al., 1992).

A number of physiological parameters influence the degree to which CO_2 diffusion controls C fixation rate and ε_p. Francois et al. (1993) modeled the effects of cell surface to volume ratios and found variations in ε_p just as large as for growth rate. It is therefore likely that there are also substantial variations in ε_p with species. Fry and Wainright (1991) give evidence that large diatoms (low surface to volume) are relatively enriched in $\delta^{13}C$. Hinga et al.(1994) provide further evidence for the influence of species and pH. The excursion of $\delta^{13}C$ to values as high as -16‰ independent of $[CO_2(aq)]$ in the region just north of the Subantarctic front in the Southern Ocean is further evidence of the importance of these other factors (Figure 8.3b). Laws et al. (1995) have shown in culture studies that growth rate can be as important as $[CO_2(aq)]$ in determining ε_p.

Much of the recent interest in the relationship between $\delta^{13}C_{org}$ and $CO_2(aq)$ is driven by the potential for using sedimentary $\delta^{13}C_{org}$ as a paleobarometer of surface ocean pCO_2 ($[CO_2(aq)]$ is related to pCO_2 by temperature using Henry's Law). Paleo-reconstruction of pCO_2 would permit mapping of ocean regions in disequilibrium with the atmosphere and extending the current Vostock ice record for atmospheric pCO_2 back in time. This information would be critical in under-

standing the links between atmospheric pCO_2 and climate. However, the validity of such reconstructions depends on the observed correlation between $\delta^{13}C_{org}$ (ε_p) and $CO_2(aq)$ representing a causal relationship. More investigation into its physiological basis is required and the degree to which other factors such as growth rate and species composition influence $\delta^{13}C$ must be better understood to avoid biasing the paleo-records. Diagenetic effects during organic carbon preservation have also not been ruled out, but their possibility has motivated isotopic analyses of purified biomarker compounds retrieved from ancient sediments (Hayes et al., 1989; Jasper and Hayes, 1990; Popp et al., 1989).

8.5 TRANSFORMATION EFFECTS - SURFACE OCEAN

Trophic transfer of N results in about a 3.5‰ upward shift in $\delta^{15}N$ between the food source and the consuming organism (DeNiro and Epstein, 1981; Fry, 1988; Minagawa and Wada, 1984). $\delta^{13}C$ appears to rise a more modest 1‰ amongst heterotrophic organisms but changes between primary producers and herbivores are less clear (DeNiro and Epstein, 1978; Rau et al., 1983). As a result, in any given ecosystem primary producers have the lowest $\delta^{15}N$ and $\delta^{13}C$ values followed by herbivores, etc. The 3.5‰ shift in $\delta^{15}N$ evidently reflects the balance in fractionation effects for assimilation and excretion. While zooplankton fecal pellets are consistently enriched in ^{15}N relative to food source (Altabet and Small, 1990; implying isotopically depleted N is assimilated), ε associated with the cleavage of amino groups and excretion of NH_4^+ is evidently large (Checkley and Miller, 1989) resulting in the net retention of ^{15}N and higher $\delta^{15}N$ values. Excreted NH_4^+ has been shown to be depleted in ^{15}N by 3‰ relative to zooplankton (Checkley and Miller, 1989).

Trophic effects result in several important patterns of variation in $\delta^{15}N$ for the surface ocean. First, $\delta^{15}N$ increases with particle size since phytoplankton, particularly in oligotrophic regions, tend to be among the smallest of the plankton (as small as about 0.5 μm) with larger organisms being at higher trophic levels. Second, larger, fast sinking particles are often aggregates of macrozooplankton fecal matter. Makrozooplankton is often omnivorous so that $\delta^{15}N$ of its food sources is higher than $\delta^{15}N$ of phytoplankton. Also given that fecal pellets are higher in $\delta^{15}N$ than the material consumed, it is not surprising that sinking POM is often enriched by up to 5‰ as compared to suspended POM in the euphotic zone. The difference in $\delta^{15}N$ ($\Delta\delta^{15}N$) between suspended and sinking PN has been proposed as a measure of the number of trophic steps linking primary production to the export of POM from the euphotic zone as sinking particles (Altabet, 1988). In fact, a $\Delta\delta^{15}N$ of 0 has been observed during a bloom event, when phytoplankton may be expected to aggregate and sink directly out of the euphotic zone without any trophic transfer (Altabet et al., 1991). In contrast, in the equatorial Pacific,

where extensive recycling of N is thought to inhibit nitrate uptake, $\Delta\delta^{15}N$ is as high as 6‰ (Figure 8.4a). $\Delta\delta^{15}N$ may thus be related to the efficiency of nutrient recycling in the euphotic zone (f-ratio). The larger the number of trophic steps the greater the proportion of nitrogen supplied to phytoplankton in the form of NH_4^+ (or urea) recycled by consumers.

Though at first counter-intuitive, the need for balance between new nitrogen (NO_3^-) utilized by phytoplankton and the export of sinking PN from the euphotic zone requires that the $\delta^{15}N$ of utilized NO_3^- equals on average the $\delta^{15}N$ of sinking PN (Figure 8.5). This is important in that it is the isotopic composition of sinking PN, not euphotic zone suspended PN, which records the isotopic imprint of denitrification and partial utilization of NO_3^- on $\delta^{15}NO_3^-$. This observation is an important prerequisite for the use of sedimentary PN (which is derived from the sinking PN reaching the seafloor) as a record of past changes in either denitrification or surface ocean nutrient utilization. It follows that when there is substantial recycling of nitrogen in the euphotic zone, the $\delta^{15}N$ of suspended PN decreases as a result of increasing utilization by phytoplankton of NH_4^+ depleted

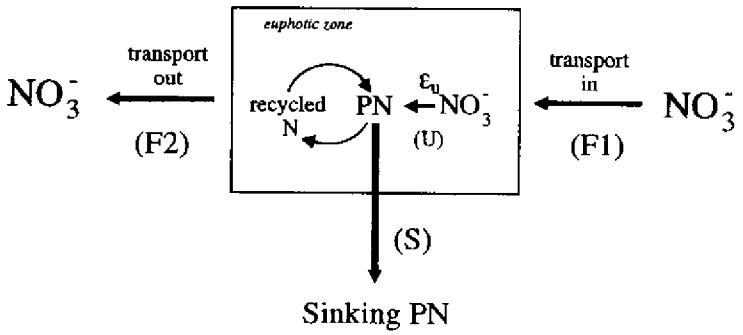

$$F1 = F2 + S$$

$$F1 \times \delta^{15}N_{F1} = (F2 \times \delta^{15}N_{F2}) + (S \times \delta^{15}N_S)$$

$$\delta^{15}N_{F2} - \delta^{15}N_{F1} = -\varepsilon_U \times \ln(F2/F1)$$

Figure 8.5 Schematic of major nitrogen fluxes in the surface ocean pertinent for determining N isotopic ratios. The most important terms are the input of new NO_3^- and any subsequent export of the unutilized fraction, fractionation during uptake into suspended PN, and the removal of sinking PN. Recycling does not influence the overall nitrogen balance. Corresponding equations for nitrogen and nitrogen isotopic balance are shown.

in ^{15}N. This makes sense when it is realized that the production of ^{15}N depleted NH_4^+ and its subsequent imprint on the phytoplankton (in open ocean waters NH_4^+ rarely accumulates but instead is immediately taken up) balances the ^{15}N enrichment of higher trophic levels. As a result, values for suspended PN in oligotrophic waters (f for $NO_3^- = 0$) approaching 0‰ or less should not necessarily be interpreted as reflecting large inputs from nitrogen fixation (which has an isotopic composition similar to atmospheric N_2; Minagawa and Wada, 1986), but are likely to be caused by N-recycling. The low values for suspended PN in the equatorial Pacific (Figure 8.4a) are another example of this phenomenon.

8.6 TRANSFORMATION EFFECTS - WATER COLUMN AND SEDIMENT SURFACE

Below the euphotic zone and in the ocean's interior there is a net heterotrophic destruction of organic matter and remineralization to inorganic constituents (DIC and NO_3^-). In principle, isotopic fractionation can accompany this process resulting in modification of the isotopic composition of the residual POM. The ubiquitous increase in the $\delta^{15}N$ of small, suspended particles with depth below the euphotic zone correlated with decreasing concentration has often been cited as evidence for isotopic fractionation during the destruction of PN (Altabet and McCarthy, 1986; Saino and Hattori, 1980; Saino and Hattori, 1985). Alternatively, it has been suggested that the increase in $\delta^{15}N$ reflects contributions to the suspended PN pool from the fragmentation of large, fast sinking particles (Altabet, 1988). Large, fast sinking particles show, in contrast, no increase in $\delta^{15}N$ with depth and below 1000 m often decrease in $\delta^{15}N$ when overall fluxes are low (Altabet et al., 1991). Sedimentary $\delta^{15}N$ does appear to be enriched by several ‰ compared to $\delta^{15}N$ of sinking particles (Altabet and Francois, 1994a; Figure 8.4b). $\delta^{13}C_{org}$ for sinking particles also shows little vertical variation, but suspended $\delta^{13}C$ appears to decrease with depth (Eadie and Jeffrey, 1973; Jeffrey et al., 1983). Sedimentary $\delta^{13}C$, in contrast, is higher by up to 4‰ as compared to sinking particles in the few studies made (Fischer, 1991). Together these observations appear to present a confusing picture of diagenetic effects on $\delta^{15}N$ and $\delta^{13}C$.

If there are diagenetic effects on isotopic composition there are two types of mechanisms that could be responsible. In the first, there is isotopic fractionation during organic N and C remineralization on a molecular scale; released N or C has a lower isotopic ratio than their precursors thereby isotopically enriching the residual. Significant isotopic fractionation has been shown to occur during acid hydrolysis (abiotic) of simple peptides (Silfer et al., 1992), with preferential releases of amino acids containing the lighter isotope. During biological remineralization, though, fractionation effects appear to be rather small. NH_4^+ extracted from organic-rich nearshore sediments (still containing a large fraction of labile

PON) with KCl was $1 \pm 0.4‰$ ($n = 5$) heavier than bulk sediment $\delta^{15}N$ (Altabet and Christensen, unpublished), suggesting a small fractionation effect during bacterial decay of organic matter. A similar relationship between sedimentary PN and NH_4^+ has been found in the S. California Bight (Sweeney and Kaplan, 1980), Framvaren Fjord, and Great Marsh Delaware (Velinsky et al., 1991). Similarly, respired CO_2 has $\delta^{13}C$ values only slightly lower than the source organic matter (DeNiro and Epstein, 1978). Another piece of evidence against a significant molecular isotope fractionation during diagenesis is the lack of increases in the $\delta^{15}N$ and $\delta^{13}C$ of sinking particles with depth despite large decreases in N flux (Altabet, 1989; Altabet et al., 1991). In this case, though, these observations could be explained if the decrease in flux with depth was brought about by ingestion of large particles by metazoans instead of microbial remineralization.

Alternatively, there may be selective removal/preservation of different organic components that vary in $\delta^{15}N$ and $\delta^{13}C$. In this case, mass balance dictates the residual POM changes accordingly. Due to fractionation along biosynthetic pathways, major biochemical classes vary substantially in isotopic ratio (e.g., Degens et al., 1968; Macko et al., 1987). The best example of this is the observation that lipids are depleted in ^{13}C relative to proteins and carbohydrates. The decrease in $\delta^{13}C$ for POC with depth has been attributed to the selective preservation of lipids. Organic nitrogen in living biomass is found chiefly in the form of amino acids and proteins, but Macko (1987) has found in bacteria that $\delta^{15}N$ and $\delta^{13}C$ for individual amino acids can vary by up to $12‰$ and $26‰$, respectively, mostly as a result of fractionation during transamination. In the water column, though, amino acid distribution pattern does not change markedly with depth (e.g., Haake et al., 1992).

Regarding the sediments, a consensus has developed that almost all labile material is removed shortly after deposition in the deep sea (Martin et al., 1991). Since $\delta^{15}N$ values for seafloor 'fluff' material are similar to sediment trap values but lower than the top layers of consolidated sediment (Altabet et al., in prep.; Figure 8.4b), the shift in $\delta^{15}N$ observed appears to happen during this process. Protection of surviving material could occur via the formation of high molecular weight refractory organic matter during humification. In the case of nitrogen, amino acids in proteins and peptides are the dominant forms of N in living organisms, but they account for less than 50% in sinking PN (Ittekkot et al., 1984; Haake et al., 1992; Haake et al., 1993) and less than 10% in surficial deep-sea sediments (Mopper and Degens, 1972; Whelan, 1977). A similar trend is found for organic carbon identifiable as proteins, carbohydrates or lipids. The survival of refractory biomass components with distinct isotopic composition may indeed account for the apparent diagenetic shifts in the isotopic composition of deep-sea sediments.

Selective preservation could also occur as a result of the close association of specific organic pools with mineral phases which protect them from bacterial degradation (Altabet and Curry, 1989; Shemesh et al., 1993). In fact, all the amino

acids present in deep-sea sediments may be in association with minerals (Müller and Suess, 1977). In general, all organic matter in deep-sea sediments may have been preserved by adsorption to surfaces (Keil et al., 1994). Also significant are the organic templates of calcareous and siliceous skeletons produced during biomineralization (King, 1975; King, 1977) which may account for a significant fraction of total organic matter in some deep-sea sediments (e.g., Froelich, 1980).

The view that emerges is that diagenetic shifts in $\delta^{15}N$ and $\delta^{13}C$ are likely to be caused by selective removal of particulate components which vary in isotopic ratio. However, explicit evidence is needed for the mechanisms accounting for the upward shifts in $\delta^{15}N$ with apparent diagenesis of suspended particles in the water column and between sinking particles and the sediments.

8.7 THE JGOFS NORTH ATLANTIC BLOOM EXPERIMENT - A CASE STUDY

In 1989, the JGOFS NABE program studied a spring phytoplankton bloom in the N.E. Atlantic Ocean. Intense biological activity produced large changes in surface water biogeochemical properties. NO_3^- decreased in concentration from 6 μM to near 0 (Figure 8.6a) over the course of the bloom and DIC (ΣCO_2) concentrations correspondingly decreased from 2093 to 2040 μM (Chipman et al., 1993). CO_2(aq) decreased from 13 to 10 μM in response to the drop in DIC since there was little change in surface temperature during the bloom (Figure 8.6c). Consistent with previous observations discussed above there were substantial increases in $\delta^{15}N$ and $\delta^{13}C$ for near-surface suspended and sinking POM (Figures 8.6b and d).

8.7.1 NEAR-SURFACE TIME-SERIES SIGNALS IN $\delta^{15}N$ AND $\delta^{13}C$

Hypothetically, seasonal variations in $\delta^{15}N$ may be roughly divided into three phases; pre-bloom, bloom, and post-bloom. During the pre-bloom period, euphotic zone NO_3^- is not yet significantly depleted and $\delta^{15}N$ for POM produced at this time would be expected to be a function of the $\delta^{15}N$ value for NO_3^- and the fractionation factor (ε_u, if there is little recycling of ^{15}N nitrogen during the early stage of the bloom). NO_3^- prior to depletion should have $\delta^{15}N$ values between 5 and 6‰ since deepwater NO_3^- (in regions uninfluenced by water column denitrification) has been found to be fairly homogenous in $\delta^{15}N$ within this range (Liu and Kaplan, 1989). With $\delta^{15}NO_3^- = 5$ to 6‰ and $\delta^{15}N_{POM} = -3$, ε_u is 8 to 9‰ (also see Altabet et al., 1991). Similar values for ε_u have been found for the Subarctic Pacific and the Southern Ocean (Figure 8.2) and are consistent with recent laboratory determinations of ε_u for diatoms which dominated the early portion of the bloom.

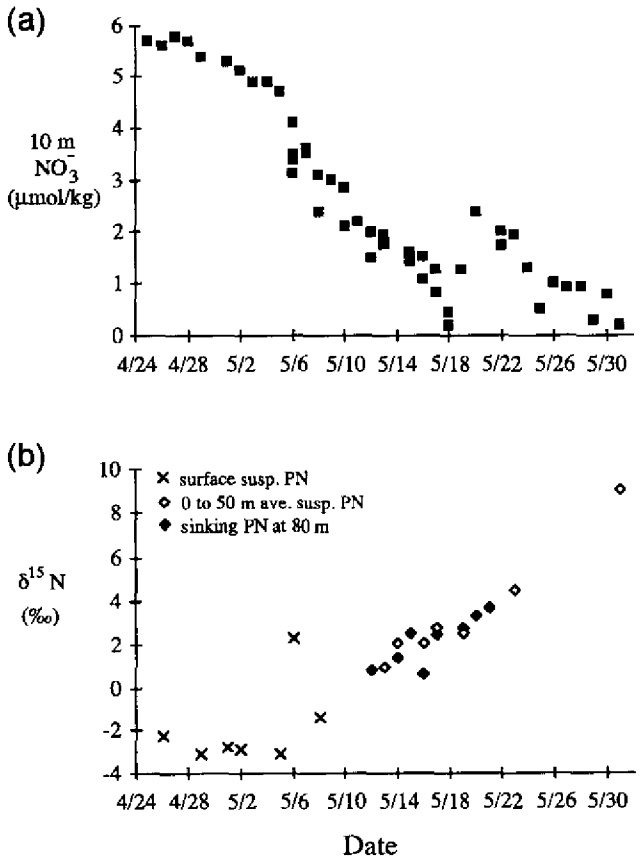

Figure 8.6 Time-series variations in near-surface properties during the JGOFS N. Atlantic Bloom Experiment (NABE). (a) NO_3^- concentration at 10 m. (b) $\delta^{15}N$ of suspended and sinking PN. Values for suspended PN averaged over the upper 50 m (nominal depth of euphotic zone) are weighted by PN concentration. (c) Surface ΣCO_2 (Chipman et al., 1993) and $CO_2(aq)$ concentrations. (d) $\delta^{13}C$ of suspended and sinking POC. Values for suspended POC averaged over the upper 50 m (nominal depth of euphotic zone) are weighted by POC concentration. Where indicated, surface suspended POC $\delta^{13}C$ data are from Rau et al. (1992).

During the bloom phase, significant biological depletion of euphotic zone NO_3^- occurs and $\delta^{15}NO_3^-$ increases according to eq. 6. The actual temporal response in bulk $\delta^{15}N_{POM}$ depends strongly on its residence time in the euphotic zone. Plotting predicted $\delta^{15}N$ shows that observations lie in between those predicted by the instantaneous (zero residence time) and accumulated (infinite residence time) product equations; eqs. 6 and 7 (Figure 8.7). Predictions for $\delta^{15}N_{POM}$ and PN

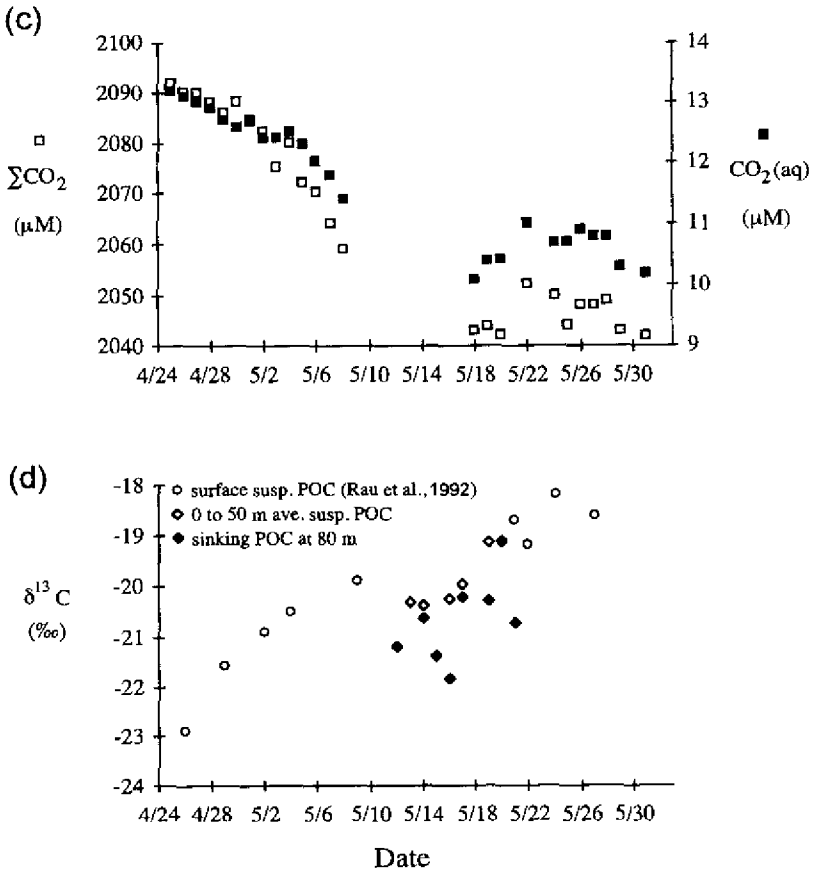

Figure 8.6 *(continued)*

concentration based on a time-dependent numerical model (Altabet, in prep.) suggest a residence time for suspended PN in the euphotic zone of 2 weeks, a significant fraction of the depletion time for NO_3^-.

In the post-bloom period, the NO_3^- originally present in the euphotic zone has been depleted and any new transport into the euphotic zone from below is completely consumed. $\delta^{15}N$ for near-surface ocean POM will decrease to the value for $\delta^{15}NO_3^-$ or lower depending on recycling effects. Our near-surface data cover well the first two phases of the bloom (Figure 8.6) but not this third phase. More recently, a complete $\delta^{15}N$ time series was obtained for the subtropical Gulf of Eilat showing the 3 expected phases (Figure 8.8). In the winter there is deep convective mixing homogenizing NO_3^- concentrations throughout the water column. In early

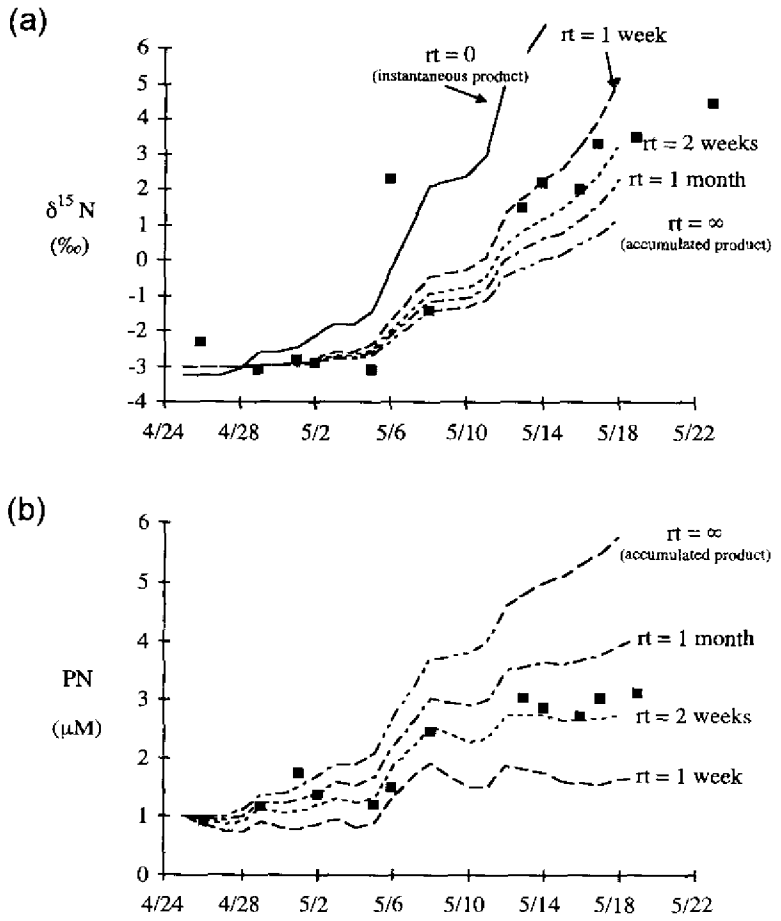

Figure 8.7 Comparison of observations (points) from the JGOFS NABE with simulated results (lines) for different particle residence times (rt). For rt = 0 and rt = ∞, simulations correspond to the instantaneous and accumulated product eqs. respectively (eqs. 6 and 7). For intermediate values of rt, a numerical model was used (Altabet, in prep.) (a) $\delta^{15}N$ for suspended PN. (b) Suspended PN concentration. Observed data points are for mixed layer averages.

spring, stratification promotes a phytoplankton bloom, drawing down NO_3^- and raising $\delta^{15}N$ values. After complete NO_3^- removal, $\delta^{15}N$ relaxes to lower values probably due to both complete utilization of NO_3^- subsequently transported upward by vertical eddy diffusion and increased N-recycling.

As discussed above, the increasing $\delta^{13}C$ of near-surface POM during the bloom cannot be attributed to isotopic enrichment of the substrate (Figure 8.6c and d).

Assuming a net photosynthetic fractionation factor of 22‰ (ε_p), the observed 2.4% decrease in dissolved inorganic carbon (DIC) during the bloom period would produce only a 0.5‰ increase in $\delta^{13}C$ consistent with the 0.3‰ increase in $\delta^{13}C$ for carbonate in sinking particles observed by Rau et al. (1992). Moreover, the 1° temperature increase observed would have had a minor influence on the equilibrium fractionation effect between HCO_3^- and CO_2(aq). Instead, as observed previously, the photosynthetic fractionation factor appears to vary directly with [CO_2(aq)]. Since there is an apparent greater sensitivity of $\delta^{13}C$ to CO_2(aq) than previously observed, Rau et al. (1992) also suggest a role for increasing 'biological demand' for CO_2 (on a cellular not community level) with the progression of the bloom. Other factors such as changes in phytoplankton species composition with progression of the bloom (from diatoms to flagellates) may have also influenced $\delta^{13}C$ values. Increases in $\delta^{13}C$ during the bloom substantially lead increases in $\delta^{15}N$ (Figure 8.6) underscoring the independence of their forcing functions.

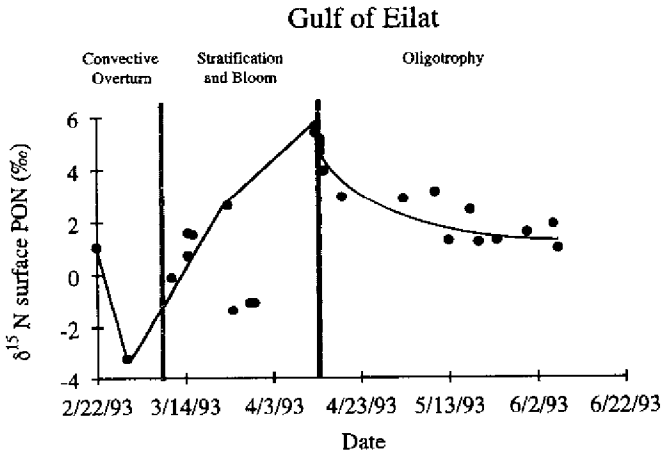

Figure 8.8 Time series of $\delta^{15}N$ values for near-surface POM collected in the Gulf of Eilat. Progression as a function of nutrient input to surface water and subsequent depletion is similar to observations made during the JGOFS NABE. However, this time series is sufficiently long to record the expected relaxation of $\delta^{15}N$ after the peak of the bloom.

8.7.2 NEAR-SURFACE FORMATION OF SINKING PARTICLES

Floating sediment trap $\delta^{15}N$ (80 m) closely follows the temporal increase in near-surface suspended particle $\delta^{15}N$ (Figure 8.6). Examination of vertical profiles show sediment trap values to be most similar to $\delta^{15}N$ for suspended PN in the upper 30 m suggesting this depth region which also has the highest PN

concentration (Figure 8.10a) is the principal source for sinking particles (Figure 8.9). The reason $\delta^{15}N$ values for suspended PN increase toward the surface in the upper 50 m is because of the corresponding vertical depletion of nitrate. C/N ratios also show no difference, on average, between sinking particles exiting the euphotic zone (upper 40 to 50 m) and suspended particles within it (Figure 8.10a). The relationship in $\delta^{13}C_{org}$, however, is variable with sinking particles being modestly depleted in ^{13}C relative to suspended ones (Figure 8.10b). On average, though, our $\delta^{13}C$ results agree with those of Rau et al. (1992).

As discussed above, trophic transfers increase $\delta^{15}N$ on the average of 3.5‰ per step (Minagawa and Wada, 1984; Fry, 1988) and fecal pellets are enriched by 2.2‰ compared to food sources (Altabet and Small, 1990). Either of these processes contributing to the transformation of suspended into sinking particles would raise $\delta^{15}N$ values. Overall, the data imply that during the bloom the packaging of small, suspended particles into large, sinking ones consisted of relatively short and direct pathways which produced little alteration of organic matter.

These results further indicate that export of organic matter from the euphotic zone occurred relatively efficiently, consistent with the high f ratios estimated for this period (Martin et al., 1993). Our floating sediment trap observations occurred just after depletion of silicate in the euphotic zone coincident with a sharp reduction in diatom numbers (Sieracki et al., 1993). We suspect sinking particles were formed primarily by the mass flocculation of diatoms which would account

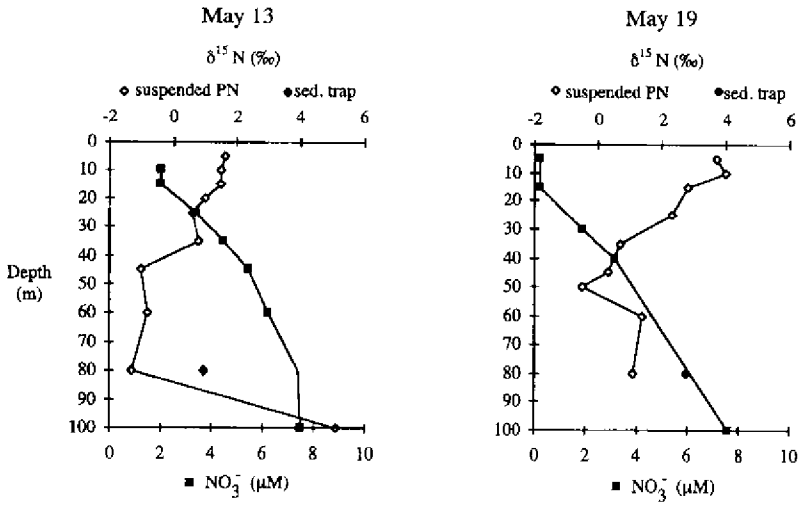

Figure 8.9 Near-surface profiles of NO_3^- concentration and $\delta^{15}N$ for suspended PN taken on two separate dates during the middle third of the bloom period at the NABE site. $\delta^{15}N$ values for sinking PN are also shown.

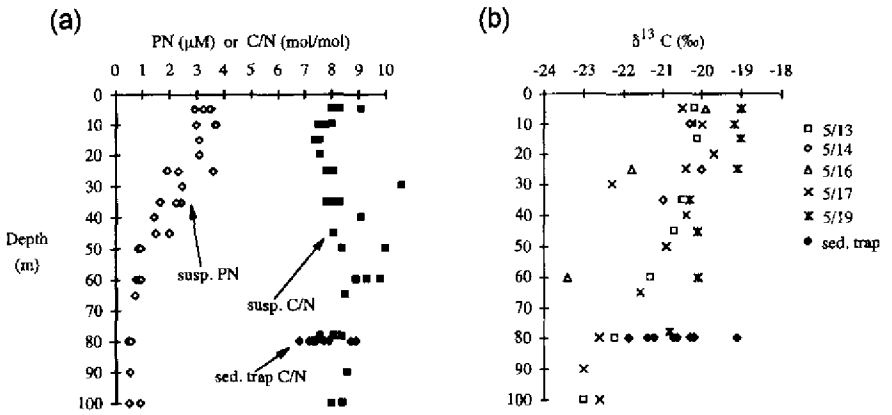

Figure 8.10 (a) Comparison of C/N (mol/mol) for near-surface suspended and sinking POM at the NABE site during the bloom period. These data are from suspended particle profiles and floating sediment trap deployments (24 hr at 80 m) carried out daily to bi-daily from May 12 to May 21, 1989. Suspended PN concentrations are also shown. (b) Comparison of $\delta^{13}C$ data for floating sediment traps and suspended POC profiles.

for the $d^{15}N$ and C/N results. Such a phenomenon has been directly observed in coastal waters (Alldredge and Gotschalk, 1989). The $d^{13}C$ results could be accounted for if the flocculating diatoms and associated extracellular material were enriched in lipid material (which is low in $d^{13}C$ relative to proteins and carbohydrates). However, higher C/N ratios for sinking particles would then be expected.

8.7.3 COMPARISON OF NEAR-SURFACE AND 1000 M ISOTOPIC SIGNALS

It is clear that the strong near-surface bloom signals in $\delta^{15}N$ and $\delta^{13}C$ are rapidly carried into the deep ocean by large, fast-sinking particles. Even the near-surface difference in phase between the ^{15}N and ^{13}C isotopic signals is manifest at depth (Figure 8.11). However, significant modification of the $\delta^{15}N$ and $\delta^{13}C$ signals appears to have occurred between the euphotic zone and the shallowest moored trap (see Figure 8.12 for a close comparison). The near-surface $\delta^{15}N$ time series has nearly twice the amplitude as observed for deeply sinking particles at 1000 m (12 vs. 6‰) and both a lower minimum and higher maximum (further modifications below 1000 m will be discussed below). A similar comparison is apparent for the $\delta^{13}C$ time series.

Important clues for explaining these differences are the persistently high $\delta^{15}N$ and $\delta^{13}C$ values at 1000 m during fall and winter and the extended period of decreasing $\delta^{15}N$ at 1000 m during the early bloom period (April to May). Deep

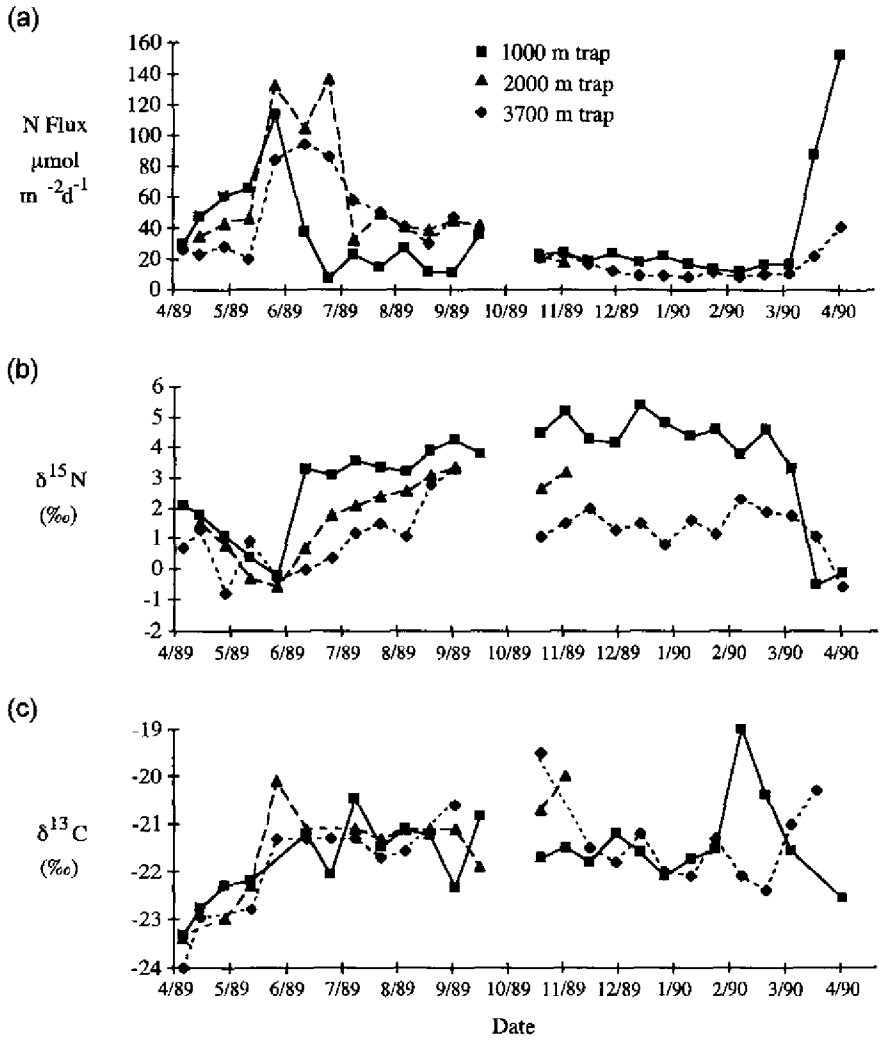

Figure 8.11 Deep-moored sediment trap time series taken during JGOFS NABE between April 1989 and April 1990 with 2-week sampling intervals. (a) PN flux at 1000, 2000 and 3700 m. (b) Corresponding $\delta^{15}N$ values. (c) Corresponding $\delta^{13}C$ values for the organic carbon fraction.

convective mixing in late fall and winter would have elevated surface NO_3^- and $CO_2(aq)$ concentrations (lowered temperature would also raise $[CO_2(aq)]$) resulting in lowered $\delta^{15}N$ and $\delta^{13}C$ for any newly produced POM to values at least as low as the minima observed. In contrast, deeply sinking particles reaching

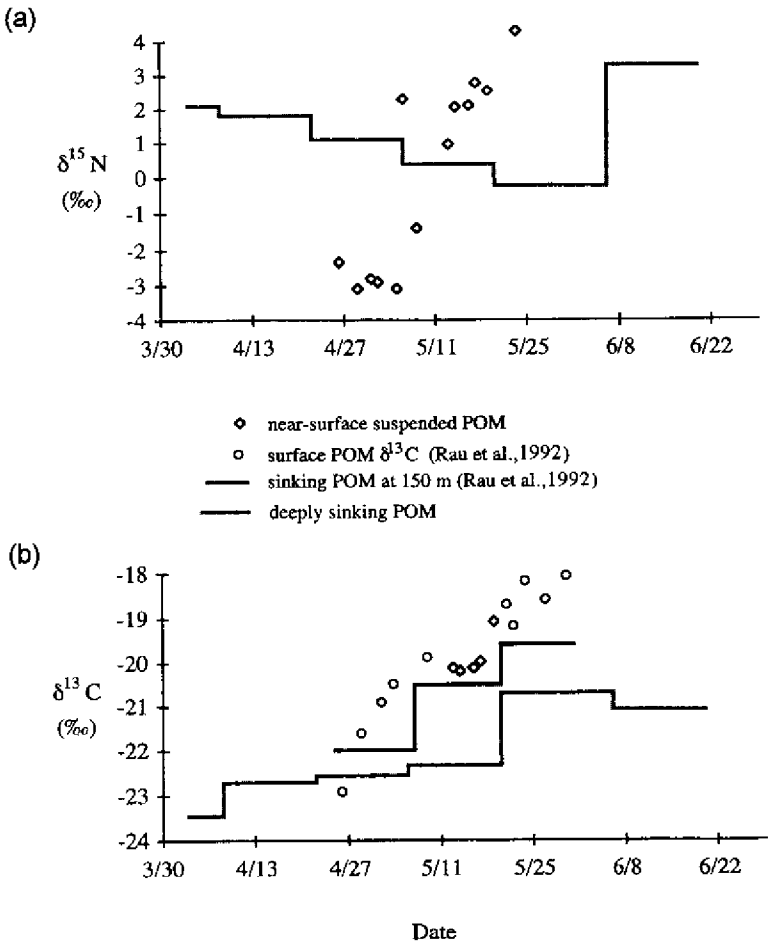

Figure 8.12 Comparison of near-surface and deep time series for the JGOFS NABE (1000 m). (a) δ^{15}N data. (b) δ^{13}C data. The data are plotted to make apparent the instantaneous nature of suspended POM collections (points) relative to the moored sediment traps which collected material in 2-week intervals (lines).

1000 m during these seasons instead appear to be derived from a source that is more enriched in ^{15}N and ^{13}C as compared to presumed late fall/wintertime production. This source could be from the aggregation of suspended particles in the region above 1000 m, but clearly not contemporaneous surface production transported directly by the uninterrupted sinking of large particles. It follows that, during initiation of the bloom (April to early May), there is a transition in dominance from this 'background' source to the near-surface bloom-production

source causing the decreasing trend in $\delta^{15}N$ at 1000 m observed in April and May. Similar observations would be likely to have been made for $\delta^{13}C$ if the time series began earlier since, on average, wintertime values in 1989/90 were elevated as compared to the beginning of the time series.

Damping at depth of the surface-generated isotopic time-series signal during the bloom peak in particle flux is evidence for a steady influence from a background, water column source of moderate isotopic composition even during this time of the year (Figure 8.12). Wintertime $\delta^{15}N$ and $\delta^{13}C$ values at 1000 m are consistent with this perspective; 4 to 5‰ as compared to near-surface range of -3 to 9‰ and -22 to -20‰ vs. -23 to -18‰, respectively. If suspended particles at depth are a water column source for sinking particles, they should have an isotopic composition similar to the wintertime particle flux. Unfortunately samples of this type were not collected and $\delta^{15}N$ and $\delta^{13}C$ for suspended particles were too regionally variable (Saino and Hattori, 1987) to rely on the results of studies distant from the NABE site.

Both the $\delta^{15}N$ and $\delta^{13}C$ time series exhibit a 2–3 week time lag between near-surface and the 1000 m time series during the bloom period (Figure 8.12). In the case of $\delta^{15}N$, this time lag is identified based on the difference in date of the rapid rise in values found for both times series. For $\delta^{13}C$, the lag was given by the temporal offset between the time series for the 150 m sediment trap data of Rau et al. (1992) and our moored sediment trap results. A 2 to 3 week time-lag translates into an average sinking rate of 50 to 70 m/day, similar to the estimate of 30 to 70 m/day based on lags between peaks in flux components for these same samples (Honjo and Manganini, 1992).

8.7.4 MODIFICATIONS OF THE LARGE PARTICLE FLUX BELOW 1000 M

Between 1000 and 3700 m the isotopic time series exhibit several distinct features (Figure 8.11). $\delta^{13}C$ variations are generally temporally in phase with depth except for a few spikes during the fall and winter. $\delta^{15}N$ variations are in phase with depth only prior to the peak in flux. The apparent phase lags afterward are mirrored in the N flux time series. In fall and winter, there is a substantial drop in $\delta^{15}N$ with depth which Altabet et al. (1991) have discussed in detail. Focusing first on the post-bloom period (June to September), the increasing time delay with depth in the particle flux and $\delta^{15}N$ signals is consistent with estimated sinking speeds. Observed time broadening is consistent with the progressive influence of a background flux with depth. $\delta^{13}C$ shows no coherent phase lag during this period because its signal had already become relatively time invariant. The background flux between 1000 m and 3700 m evidently has relatively low $\delta^{15}N$ values. There is a progressive decrease in the $\delta^{15}N$ of the total flux with depth following the bloom and continuing into winter. It would be unusual if suspended particle $\delta^{15}N$

decreased with depth below 1000 m at this site since all previous observations have shown consistently enriched values in the deep ocean (Saino and Hattori, 1980; Altabet and McCarthy, 1986; Saino and Hattori, 1987; Altabet, 1988). Altabet et al. (1991) speculated that bacterial utilization of NO_3^- or DON could be the source. $\delta^{13}C$ in contrast shows no clear depth-dependent variation indicating no change in carbon isotopic composition of the background source with depth.

8.8 SUMMARY AND RECOMMENDATIONS FOR FURTHER RESEARCH

The JGOFS NABE study illustrates both many of the processes influencing $\delta^{15}N$ and $\delta^{13}C$ values for POM and how they can be used as natural tracers of particle dynamics. Large temporal variations in $\delta^{15}N$ and $\delta^{13}C$ of primarily produced organic matter occured during the course of the bloom as the result of the drawdown of inorganic N and C substrates. These temporal signatures rapidly propagate into sinking particles leaving the euphotic zone and then being transported deep into the ocean's interior. However, there is substantial modification of the near-surface temporal signal. As discussed above, the isotopic evidence confirms the importance of surface productivity in directly supporting particle fluxes in the deep ocean but is also proof for other important sources which are only indirectly linked to surface processes. This approach making use of a 'natural' tracer experiment has several advantages: nitrogen and carbon isotopic composition characterizes the bulk properties of POM in contrast to the trace metal or trace organic compositions. Processes occurring on difficult to examine time and space scales (10's to 1000's m and weeks to months) can be effectively probed. Results are not dependent on experimental manipulations which may introduce artifacts.

Future studies need to better characterize the processes creating the primary isotopic signatures. Does ε for NO_3^- uptake vary principally as a function of species or is the range in growth conditions found in the ocean a contributor? These results should be compared with additional field estimates of ε_u. More detail is needed in understanding how N recycling influences $\delta^{15}N$ values for suspended POM: what are $\delta^{15}N$ values for recycled forms of NH_4^+? Similarly, the physiological basis for the relationship between $CO_2(aq)$ and $\delta^{13}C$ needs to better detailed: does the expression of HCO_3^--uptake at low $CO_2(aq)$ play a role?

While the shifts in isotopic composition with trophic level are fairly well characterized (though not their physiological basis), microbially-based diagenetic effects in the water column have not been identified, let alone mechanistically understood. Does the ubiquitous increase in $\delta^{15}N$ of suspended POM with depth in the ocean's interior reflect diagenetic processes or contributions of the fragmentation of sinking particles? Sediments appear to be typically several ‰ enriched in

$\delta^{15}N$ relative sinking particles. Does this shift reflect isotopic fractionation at the molecular level or selective preservation of resistant components of sinking particles enriched in ^{15}N? For $\delta^{13}C$, it is not clear if there are significant diagenetic effects on $\delta^{13}C$. In both instances, what are the implications of diagenetic effects on the use of these isotopes for paleoceanographic reconstruction?

For the present, the NABE study provides a good model for how isotopic studies of particle dynamics in the open ocean should be carried out. Settings need to be chosen in which there are likely to be large isotopic transients (either in time or in space as in the JGOFS EqPac study). Sampling resolution needs to be sufficient to resolve the isotopic signals. Furthermore, all the compartments of interest need to be sampled. In this respect, the NABE study lacked time-series sampling for NO_3^- and suspended POM in the region below the euphotic zone.

8.9 REFERENCES

Alldredge, A. L. and C. C. Gotschalk (1989) "Direct observations of the mass flocculation of diatom blooms: characteristics, settling velocities, an formation of diatom aggregates", *Deep-Sea Res.*, **36**, 159–171.

Altabet, M. A. (1988) "Variations in nitrogen isotopic composition between sinking and suspended particles: implications for nitrogen cycling and particle transformation in the open ocean", *Deep-Sea Res.*, **35**, 535–554.

Altabet, M. A. (1989) "A time-series study of the vertical structure of nitrogen and particle dynamics in the Sargasso Sea", *Limnol. Oceanogr.*, **34**, 1185–1201.

Altabet, M. A., and W. B. Curry (1989) "Testing models of past ocean chemistry using foraminiferal $^{15}N/^{14}N$", *Glob. Biogeochem. Cycles*, **3**, 107–119.

Altabet, M. A. and W. G. Deuser (1985) "Seasonal variations in natural abundance of ^{15}N in particles sinking to the deep Sargasso Sea", *Nature*, **315**, 218–219.

Altabet, M. A. and R. Francois (1994a) "Sedimentary nitrogen isotopic ratio as a recorder for surface ocean nitrate utilization", *Glob. Biogeochem. Cycles*, **8**, 103–116.

Altabet, M. A. and R. Francois (1994b) "The use of nitrogen isotopic ratio for reconstruction of past changes in surface ocean nutrient utilization", in R. Zahn, M. Kaminski, L. Labeyrie and T. F. Pederson (eds) *Carbon Cycling in the Glacial Ocean: Constraints on the Ocean's Role in Global Change*, Springer Verlag, Berlin, 281–306.

Altabet, M. A. and J. J. McCarthy (1985) "Temporal and spatial variations in the natural abundance of ^{15}N in PON from a warm-core ring.", *Deep-Sea Res.*, **32**, 755–772.

Altabet, M. A. and J. J. McCarthy (1986) "Vertical patterns in ^{15}N natural abundance in PON from the surface waters of warm-core rings", *J. Mar. Res.*, **44**, 185–201.

Altabet, M. A. and L. F. Small (1990) "Nitrogen isotopic ratios in fecal pellets produced by marine zooplankton", *Geochim. Cosmochim. Acta*, **54**, 155–163.

Altabet, M. A., W. G. Deuser, S. Honjo and C. Stienen (1991) "Seasonal and depth-related changes in the source of sinking particles in the N. Atlantic", *Nature*, **354**, 136–139.

Altabet, M. A., R. Francois, D. W. Murray and W. L. Prell (1995) "Climate-related variations in denitrification in the Arabian Sea from sediment $^{15}N/^{14}N$ ratios", *Nature*, **373**, 506–509.

Arnelle, D. R. and M. H. O'Leary (1992) "Binding of carbon dioxide to phosphoenolpyruvate carboxykinase deduced from carbon kinetic isotope effects". *Biochem.*, **31**, 4363–4367.

Barber, R. T. and F. P. Chavez (1991) "Regulation of primary productivity rate in the equatorial Pacific Ocean.", *Limnol. Oceanogr.*, **36**, 1803–1815.

Checkley, D. M., Jr. and C. A. Miller (1989) "Nitrogen isotope fractionation by oceanic zooplankton", *Deep-Sea Res.*, **36**, 1449–1456.

Chipman, D. W., J. Marra and T. Takahashi (1993) "Primary production at 47°N and 20°W in the North Atlantic Ocean - A comparison between the ^{14}C incubation method and the mixed layer carbon budget", *Deep-Sea Res.*, **40**, 151–169.

Cifuentes, L. A., M. L. Fogel, J. R. Pennock and J. H. Sharp (1989) "Biogeochemical factors that influence the stable nitrogen isotope ratio of dissolved ammonium in the Delaware Estuary", *Geochim. Cosmochim. Acta*, **53**, 2713–2721.

Cline, J. D. and I. R. Kaplan (1975) "Isotopic fractionation of dissolved nitrate during denitrification in the Eastern Tropical North Pacific Ocean", *Mar. Chem.*, **3**, 271–299.

Degens, E. T., R. R. L. Guillard, W. M. Sackett and J. A. Hellebust (1968) "Metabolic fractionation of carbon isotopes in marine plankton - I. Temperature and respiration experiments", *Deep-Sea Res.*, **15**, 1–9.

DeNiro, M. J. and S. Epstein (1978) "Influence of diet on the distribution of carbon isotopes in animals", *Geochim. Cosmochim. Acta*, **42**, 495–506.

DeNiro, M. J. and S. Epstein (1981) "Influence of diet on the distribution of nitrogen isotopes in animals", *Geochim. Cosmochim. Acta*, **45**, 341–351.

Descolas-Gros, C. and M. Fontugne (1988) "Carboxylase activities and carbon isotope ratios of Mediterranean phytoplankton", *Oceanol. Acta*, **11**, 245–250.

Descolas-Gros, C. and M. Fontugne (1990) "Stable carbon isotope fractionation by marine phytoplankton during photosynthesis", *Plant Cell Env.*, **13**, 207–218.

Deuser, W. G., E. T. Degens and R. R. L. Guillard (1968) "Carbon isotope relationships between plankton and sea water", *Geochim. Cosmochim. Acta*, **32**, 657–660.

Eadie, B. J. and L. M. Jeffrey (1973) "$\delta^{13}C$ analyses of oceanic particulate organic matter", *Mar. Chem.*, **1**, 199–209.

Eppley, R. W. and B. J. Peterson (1979) "Particulate organic matter flux and planktonic new production in the deep ocean", *Nature*, **282**, 677–680.

Farquhar, G. D., M. H. O'Leary and J. A. Berry (1982) "On the relationship between carbon isotope discrimination and the intercellular carbon dioxide concentration in leaves", *Aust. J. Plant Physiol.*, **9**, 121–137.

Fischer, G. (1991) "Stable carbon isotope ratios of plankton carbon and sinking organic matter from the Atlantic sector of the Southern Ocean", *Mar. Chem.*, **35**, 581–596.

Fontugne, M., C. Descolas-Gros and G. Debilly (1991) "The dynamics of CO_2 fixation in the Southern Ocean as indicated by carboxylase activities and organic carbon isotopic ratios", *Mar. Chem.*, **35**, 371–380.

Fowler, S. W. and G. A. Knauer (1986) "Role of large particles in the transport of elements and organic compounds through the oceanic water column", *Prog. Oceanogr.*, **16**, 147–194.

Francois, R., M. A. Altabet, R. Goericke, D. C. McCorkle, C. Brunet and A. Poisson (1993) "Changes in $\delta^{13}C$ of surface water particulate organic matter across the subtropical convergence in the S. W. Indian Ocean", *Glob. Biogeochem. Cycles*, 7, 627–643.

Froelich, P. N. (1980) "Analysis of organic carbon in marine sediments". *Limnol. Oceanogr.*, **25**, 564–572.

Fry, B. (1988) "Food web structure on Georges Bank from stable C, N, and S isotopic compositions", *Limnol. Oceanogr.*, **33**, 1182–1190.

Fry, B. and S. C. Wainright (1991) "Diatom sources of ^{13}C-rich carbon in marine food webs", *Mar. Ecol. Prog. Ser.*, **76**, 149–157.

Goericke, R., J. P. Montoya, and B. Fry (1994) "Physiology of isotopic fractionation in algae and cyanobacteria", in K. Lajtha and R. H. Mitchener (eds) *Stable Isotopes in Ecology and Environmental Science*, Blackwell, Oxford, 187–221.

Goering, J., V. Alexander and N. Haubenstock (1990) "Seasonal variability of stable carbon and nitrogen isotopic ratios of organisms in a North Pacific bay", *Estuar. Coast. Shelf Sci.*, **30**, 239–260.

Guy, R. D., M. L. Fogel, J. A. Berry and T. C. Hoering (1986) "Isotope fractionation during oxygen production and consumption by plants", in J. Biggens (ed) *Progress in Photosynthesis Research*, Kluwer Acad. Publ., Dordrecht, 597–600.

Haake, B., V. Ittekkot, S. Honjo and S. Manganini (1993) "Amino acid, hexosamine, and carbohydrate fluxes to the deep Subarctic Pacific (Station P)", *Deep-Sea Res.*, **40**, 547–560.

Haake, B., V. Ittekkot, V. Ramaswamy, R. R. Nair and S. Honjo (1992) "Fluxes of amino acids and hexosamines to the deep Arabian Sea", *Mar. Chem.*, **40**, 291–314.

Hayes, J. M., B. N. Popp, R. Takigiku and M. W. Johnson (1989) "An isotopic study of biogeochemical relationships between carbonates and organic carbon in the Greenhorn Formation", *Geochim. Cosmochim. Acta*, **53**, 2961–2972.

Hinga, K. R., M. A. Arthur, M. E. Q. Pilson and D. Whitaker (1994) "Carbon isotope fractionation by marine phytoplankton in culture: The effects of CO_2 concentration, pH, temperature, and species", *Glob. Biogeochem. Cycles*, **8**, 91–102.

Honjo, S. and S. J. Manganini (1992) "Annual biogenic particle fluxes to the interior of the North Atlantic Ocean; studied at 34°N 21°W and 48°N 21°W", *Deep-Sea Res.*, **40**, 587–607.

Horrigan, S. G., J. P. Montoya, J. L. Nevins and J. J. McCarthy (1990) "Natural isotopic composition of dissolved inorganic nitrogen in the Chesapeake Bay", *Estuar. Coast. Shelf Sci.*, **30**, 393–410.

Ittekkot, V., W. G. Deuser and E. T. Degens (1984) "Seasonality in the fluxes of sugars, amino acids, and amino sugars to the deep ocean: Sargasso Sea", *Deep-Sea Res.*, **31**, 1057–1069.

Jasper, J. P. and J. M. Hayes (1990) "A carbon-isotopic record of CO_2 levels during the late Quaternary", *Nature*, **347**, 462–464.

Jeffrey, A. W. A., R. C. Pflaum, J. M. Brooks and W. M. Sackett (1983) "Vertical trends in particulate organic carbon ^{13}C:^{12}C ratios in the upper water column", *Deep-Sea Res.*, **30**, 971–983.

Keil, R. G., E. Tsamakis, C. B. Fuh, J. C. Giddings and J. I. Hedges (1994) "Mineralogical and textual controls on the organic composition of coastal sediments: Hydrodynamic separation using SPLITT-fractionation", *Geochim. Cosmochim. Acta*, **58**, 879–893.

King, K., Jr. (1975) "Amino acid composition of the silicified organic matrix in fossil polycystine Radiolaria", *Micropaleontol.*, **21**, 215–226.

King, K., Jr. (1977) "Amino acid survey of Recent calcareous and siliceous deep-sea microfossils", *Micropaleontol.*, **23**, 180–193.

Kroopnick, P. (1985) "The distribution of ^{13}C of ΣCO_2 in the world oceans.", *Deep-Sea Res.*, **32**, 57–84.

Laws, E. A., B. N. Popp, R. R. Bidigare, M. C. Kennicutt and S. A. Macko (1995) "Dependence of phytoplankton carbon isotopic composition on growth rate and $[CO_2]_{aq}$: Theoretical considerations and experimental results". *Geochim. Cosmochim. Acta*, **59**, 1131–1138.

Liu, K.-K. and I. R. Kaplan (1989) "The eastern tropical Pacific as a source of ^{15}N-enriched nitrate in seawater off southern California", *Limnol. Oceanogr.*, **34**, 820–830.

Macko, S. A., M. L. Fogel, P. E. Hare and T. C. Hoering (1987) "Isotope fractionation of nitrogen and carbon in the synthesis of amino acids by microorganisms", *Chem. Geol.*, **65**, 79–92.

Martin, J. H., S. E. Fitzwater, R. M. Gordon, C. N. Hunter and S. J. Tanner (1993) "Iron, primary production and carbon nitrogen flux studies during the JGOFS North Atlantic Bloom Experiment", *Deep-Sea Res.*, **40**, 115–134.

Martin, W. R., M. Bender, M. Leinen and J. Orchard (1991) "Benthic organic carbon degradation and biogenic silica dissolution in the central equatorial Pacific", *Deep-Sea Res.*, **38**, 1481–1516.

Minagawa, M. and E. Wada (1984) "Stepwise enrichment of ^{15}N along food chains: Further evidence and the relation between $\delta^{15}N$ and animal age", *Geochim. Cosmochim. Acta*, **48**, 1135–1140.

Minagawa, M. and E. Wada, E (1986) "Nitrogen isotope ratios of red tide organisms in the East China Sea: A characterization of biological nitrogen fixation", *Mar. Chem.*, **19**, 245–249.

Miyake, Y. and E. Wada (1971) "The isotope effect on the nitrogen in biochemical, oxidation-reduction reactions", *Rec. Oceanogr. Works Japan*, **11**, 1–6.

Montoya, J. P. and J. J. McCarthy (1995) "Isotopic fractionation during nitrate uptake by phytoplankton grown in continuous culture", *J. Plankton Res.*, **17**, 439–464.

Mook, W. G., J. C. Bommerson and W. H. Staverman (1974) "Carbon isotope fractionation between dissolved bicarbonate and gaseous carbon dioxide", *Earth Planet. Sci. Let.*, **22**, 169–176.

Mopper, K. and E. T. Degens (1972) *Aspects of the Biogeochemistry of Carbohydrates and Proteins in Aquatic Environments*, (Technical Report No. WHOI–72–68). Woods Hole Oceanographic Inst., 118 pp.

Müller, P. J. and E. Suess (1977) "Interaction of organic compounds with calcium carbonate - III. Amino acid composition of sorbed layers", *Geochim. Cosmochim. Acta*, **42**, 941–949.

Nakatsuka, T., N. Handa and C. S. Wong (1992) "The dynamic changes of stable isotopic ratios of carbon and nitrogen in suspended and sedimented particulate organic matter during a phytoplankton bloom", *J. Mar. Res.*, **50**, 267–296.

Nelson, J. R., J. R. Beers, R. W. Eppley, G. A. Jackson, J. J. McCarthy and A. Soutar (1987) "A particle flux study in the Santa Monica-San Pedro Basin off Los Angeles: Particle flux, primary production, and transmissometer survey", *Cont. Shelf Res.*, 7, 307–328.

O'Leary, M. H. (1981) "Carbon isotope fractionations in plants", *Phytochem.*, **20**, 553–567.

O'Leary, M. H. (1984) "Measurement of the isotope fractionation associated with diffusion of carbon dioxide in aqueous solution", *J. Phys. Chem.*, **88**, 823–825.

O'Leary, M. H. (1989) "Multiple isotope effects on enzyme-catalyzed reactions", *Ann. Rev. Biochem.*, **58**, 377–401.

O'Leary, M. H., S. Madhavan and P. Paneth (1992) "Physical and chemical basis of carbon isotope fractionation in plants", *Plant Cell. Environ.*, **15**, 1099–1104.

Peters, K. E., R. E. Sweeney and I. R. Kaplan (1978) "Correlation of carbon and nitrogen stable isotope ratios in sedimentary organic matter", *Limnol. Oceanogr.*, **23**, 598–604.

Popp, B. N., R. Takigiku, J. M. Hayes, J. W. Louda and E. W. Baker (1989) "The post-paleozoic chronology and mechanism of ^{13}C depletion in primary marine organic matter", *Am. J. Sci.*, **289**, 436–454.

Rau, G. H., R. E. Sweeney and I. R. Kaplan (1982) "Plankton ^{13}C:^{12}C ratio changes with latitude: Differences between northern and southern oceans", *Deep-Sea Res.*, **8**, 1035–1039.

Rau, G. H., T. Takahashi and D. J. Des Marais (1989) "Latitudinal variations in plankton $\delta^{13}C$: Implications for CO_2 and productivity of past oceans", *Nature*, **341**, 516–518.

Rau, G. H., T. Takahashi, D. J. Des Marais and C. W. Sullivan (1991) "Particulate organic matter $\delta^{13}C$ variations across the Drake Passage", *J. Geophys. Res.*, **96**, 15,131–15,135.

Rau, G. H., T. Takahashi, D. J. D. Marais, D. J. Repeta and J. H. Martin (1992) "The relationship between the $\delta^{13}C$ of organic matter and $[CO_{2(aq)}]$ in ocean surface water: Data from a JGOFS site in the northeast Atlantic ocean and a model", *Geochim. Cosmochim. Acta*, **56**, 1413–1419.

Rau, G. H., A. J. Mearns, D. R. Young, R. J. Olson, H. A. Schafer and I. R. Kaplan (1983) "Animal $^{13}C/^{12}C$ correlates with trophic level in pelagic food webs", *Ecology*, **64**, 1314–1318.

Roeske, C. A. and M. H. O'Leary (1984) "Carbon isotope effects on the enzyme catalyzed carboxylation of ribulose biphosphate", *Biochem.*, **23**, 6275–6285.

Saino, T. and A. Hattori (1980) "^{15}N natural abundance in oceanic suspended particulate matter", *Nature*, **283**, 752–754.

Saino, T. and A. Hattori (1985) "Variation of ^{15}N natural abundance of suspended organic matter in shallow oceanic waters", in A. C. Sigleo and A. Hattori (eds) *Marine and Estuarine Geochemistry*, Lewis Publishers, Chelsea, MI, 697–709.

Saino, T. and A. Hattori (1987) "Geographical variation in the water column distribution of suspended particulate organic nitrogen and its ^{15}N natural abundance in the Pacific and its marginal seas", *Deep-Sea Res.*, **34**, 807–827.

Schäfer, P. and V. Ittekkot (1993) "Seasonal variability in $\delta^{15}N$ in settling particles in the Arabian Sea and its palaeogeochemical significance", *Naturwissenschaften*, **80**, 511–513.

Schäfer P. and V. Ittekkot (1995) "Isotopic biogeochemistry of nitrogen in the northern Indian Ocean", *Mitt. Geol.-Paläont. Inst. Univ. Hamburg*, **78**, 67–93.

Shemesh, A., S. A. Macko, C. D. Charles and G. H. Rau (1993) "Isotopic evidence for reduced productivity in the glacial southern ocean", *Science*, **262**, 407–410.

Sieracki, M. E., P. G. Verity and D. K. Stoecker (1993) "Plankton community response to sequential silicate and nitrate depletion during the 1989 North Atlantic spring bloom", *Deep-Sea Res.*, **40**, 213–226.

Silfer, J. A., M. H. Engel and S. A. Macko (1992) "Kinetic fractionation of stable carbon and nitrogen isotopes during peptide bond hydrolysis - experimental evidence and geochemical implications", *Chem. Geol.*, **101**, 211–221.

Sweeney, R. E. and I. R. Kaplan (1980) "Natural abundances of ^{15}N as a source indicator for near-shore marine sedimentary and dissolved nitrogen", *Mar. Chem.*, **9**, 81–94.

Velinsky, D. J., D. J. Burdige and M. L. Fogel (1991) "Nitrogen diagenesis in anoxic marine sediments: Isotope effects" (Annual Report No.) Carnegie Inst., 154–162.

Velinsky, D. J., J. R. Pennock, J. H. Sharp, L. A. Cifuentes and M. L. Fogel (1989) "Determination of the isotopic composition of ammonium-nitrogen at the natural abundance level from estuarine waters", *Mar. Chem.*, **26**, 351–361.

Voss, M., M. Altabet and H. Erlenkeuser (1990) Stable isotopes in suspended and sedimented organic matter in the Nordic Seas. In *International Scientific Symposium, Joint Global Ocean Flux Study North Atlantic Bloom Experiment*, National Academy of Science, Washington, D.C.

Wada, E. and A. Hattori (1978) "Nitrogen isotope effects in the assimilation of inorganic nitrogenous compounds by marine diatoms", *Geomicrobio. J.*, **1**, 85–101.

Whelan, J. K. (1977) "Amino acids in a surface sediment core of the Atlantic abyssal plain", *Geochim. Cosmochim. Acta*, **41**, 803–810.

9 Temporal Variability of Particle Flux in the Deep Sargasso Sea

WERNER G. DEUSER

9.1 INTRODUCTION

This chapter gives an outline of some of the features of the longest series of deep-ocean particle flux measurements by sediment traps. The mooring is located in the Sargasso Sea, near 31°50'N, 64°10'W. Water depth is 4400 m. At the present time we have over 16 years of data from traps at a depth of 3200 m, ten years of data from 1500 m, and about seven years from 500 m (Figure 9.1). There is good coherence between the flux variabilities recorded by the two deeper traps, but for a number of reasons, not all of which are understood, coherence between the shallowest and deep traps is not as good. However, in this paper I will confine my remarks to the 3200-m series only. Its flux data represent 86% of the time elapsed since April of 1978. We employed a bimonthly sampling scheme for the first eleven years and quadrupled the sampling frequency to biweekly in 1989. Since then our temporal coverage has been 94%.

9.2 THE ANNUAL CYCLE

The deep series was the first to document seasonal flux changes, related to the annual cycle of primary production near the surface (Deuser and Ross, 1980) and the rapidity of the particulate transport to great depth (Deuser et al., 1981). This feature has since been observed in many parts of the ocean as well as in enclosed seas; e.g., in the Pacific (Honjo, 1982; Smith and Baldwin, 1984), the Indian Ocean (Nair et al., 1989), the Southern Ocean (Wefer et al., 1988), the Black Sea (Izdar et al., 1984), the polar North Atlantic (Bathmann et al., 1990; Wassmann et al., 1991), and the eastern North Atlantic (Honjo and Manganini, 1993). As can be seen in Figure 9.1, the annual cycle persists throughout the 16-year record from 3200 m. The shape of the average cycle over those years, and the band width of its variance are shown in Figure 9.2. The basic shape of this cycle has not changed in many years, although the variance is still influenced by two unusually high flux

Particle Flux in the Ocean
Edited by V. Ittekkot, P. Schäfer, S. Honjo and P. J. Depetris

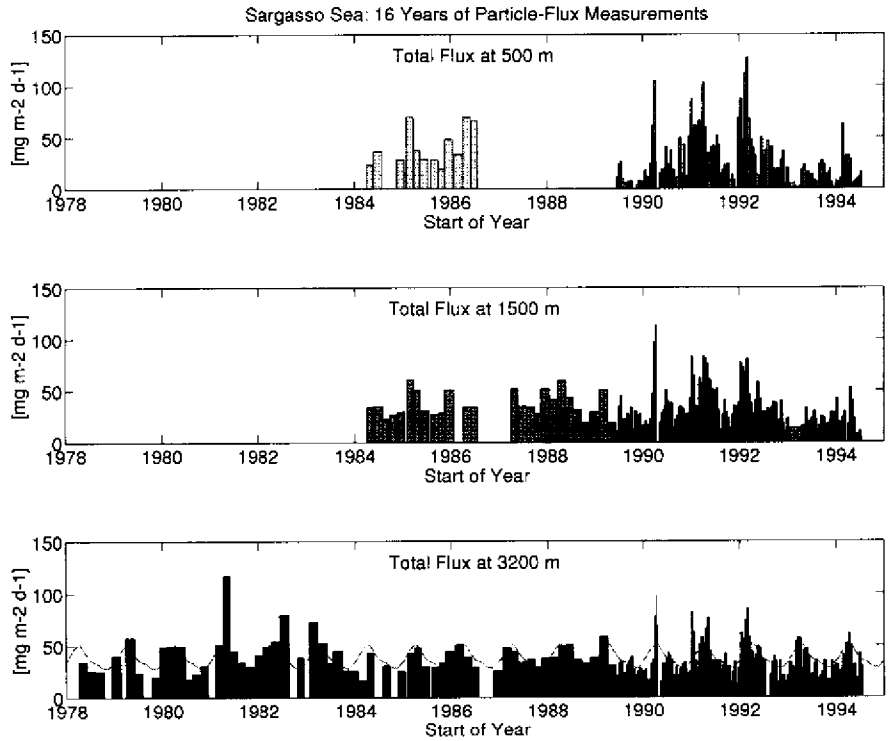

Figure 9.1 Sixteen-year record of particle flux measurements in the Sargasso Sea. Sampling intervals were shortened from bimonthly to biweekly in mid-1989. The dotted line in the bottom panel represents repetitions of the average annual flux cycle at 3200 m, as shown in Figure 9.2.

periods in 1981 and 1982 (Figure 9.1). Is it worth continuing the series? I believe there are several good reasons for doing so.

We know that the seasonal changes are ultimately driven by insolation changes, but we do not know what the forcing functions of the remaining variability are. One of the objectives of this continued work is to identify those functions through spectral coherence tests between deep-ocean particle flux and meteorologic and surface-ocean variables. Potential candidates are, for example, mixed-layer depth, wind stress and heat loss. All of these have annual cycles, as shown by the example of wind speed (Figure 9.3). But so do many other natural phenomena and human activities, as, for example, unemployment (Figure 9.4) or mammalian brain weight (Weiler, 1992)! The implication is clear: annual cycles are not diagnostic of causal relationships between variables. It is the anomalies (Figure 9.5) and other-than-annual periods which are more useful.

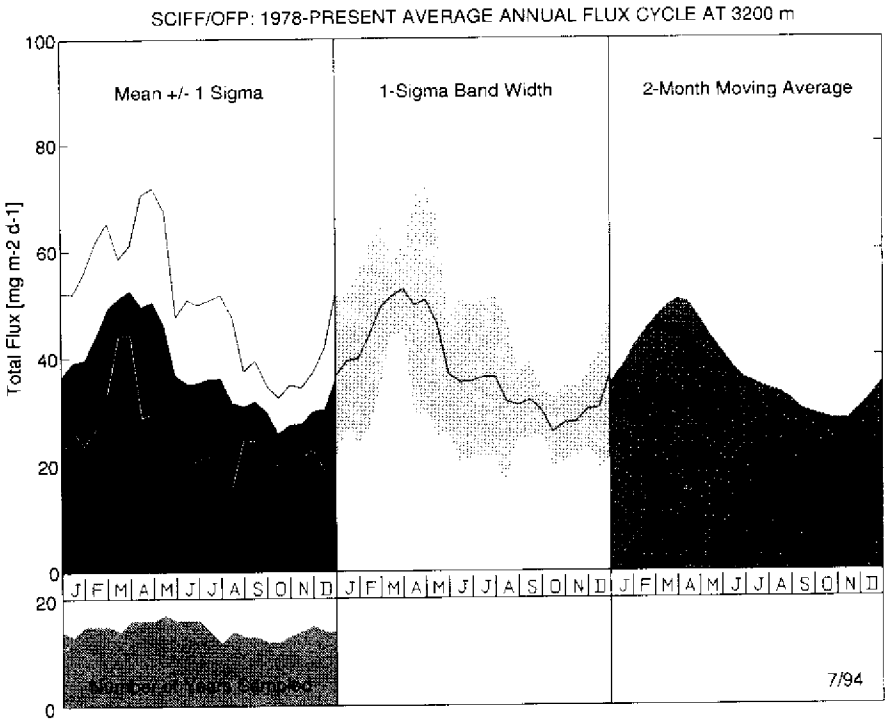

Figure 9.2 The average annual cycle of particle flux at a depth of 3200 m in the Sargasso Sea. The 1-standard-deviation band is shown in the middle panel; the two-month moving average of the mean (left panel) is shown in the right panel. The small panel at the bottom left indicates the number of years for which flux data were available for averaging at the different times of year.

9.3 OTHER PERIODS

While the annual period contains much of the spectral energy, it is becoming increasingly apparent that deep-ocean particle flux exhibits a continuous variability spectrum as, indeed, do all other oceanic variables which have been the subject of time-series measurements (Wunsch, 1981). The bimonthly sampling scheme of the first 11 years limited us to studying periods longer than about six months. But we now have over five years of biweekly flux data and can begin to look at periods as short as monthly.

Sixteen years of bimonthly variability are shown in Figure 9.6. For the purposes of this Figure the biweekly data of the last five years were averaged over 2-month periods. The average annual cycle is shown repeatedly as a frame of reference. The spectral power distribution of this series is shown in Figure 9.7 against the

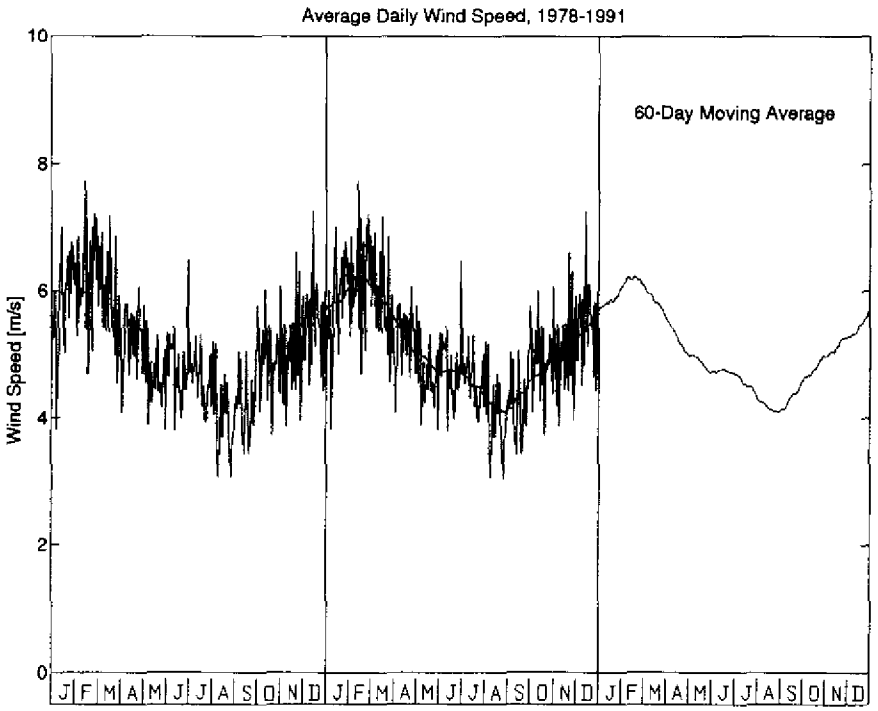

Figure 9.3 Average annual cycle of wind speed on the island of Bermuda for the period 1978–1991.

backdrop of the power spectrum of the average annual cycle. There is a strong peak near the annual period, but other periods, both longer and shorter, also can be seen, though their significance is quite minor compared to that of the annual period. El Niño periodicity and the sunspot cycle are possible candidates for the longer periods, but we cannot yet identify any of them with confidence. An example of a multi-year trend in our data is shown in Figure 9.8. There was an eight-year period of increasing flux from 1984 through 1991 which paralleled an increase in surface wind speed in the area. Possibly, this is related to longer-term climatic changes in the area, as suggested by the wind speed data shown in Figure 9.9. But we can't be sure of this until we have a few more years of data. The weakness of any longer-than-annual periodicities in the existing data is underscored by the lack of peaks in the power spectrum of the bimonthly flux anomalies, except for a minor 4-year peak (Figure 9.10). That is not surprising because a "rule of thumb" in time-series measurement is that, in order to assess trends on a given time scale with any confidence, one needs measurement series extending over at least three times that time scale. Thus, to check for periodicity

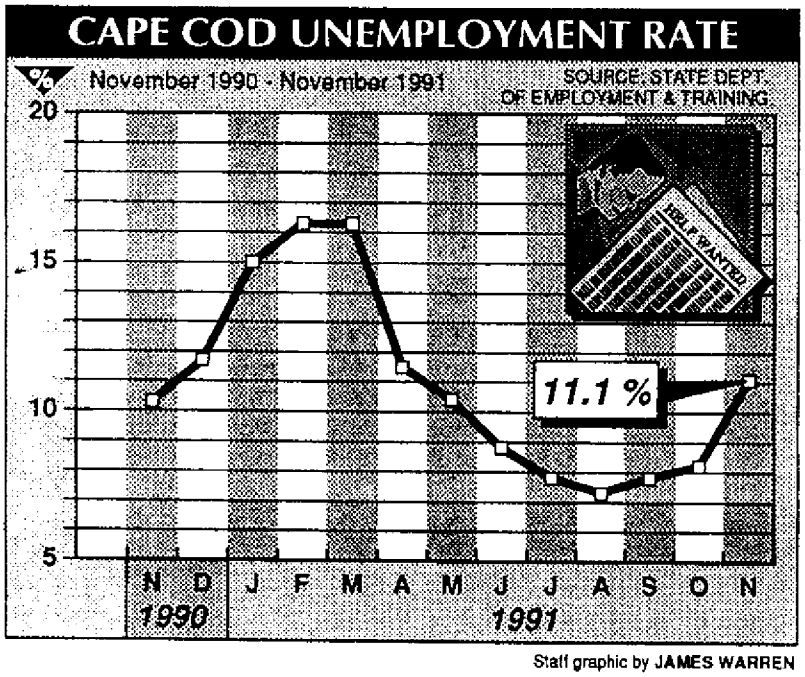

Figure 9.4 Example of an annual cycle in human activity (from the Cape Cod Times).

on the scale of the sunspot cycle, we need about 35 years of data. More below on the question of whether or not that is reasonable or even desirable.

Five years of biweekly flux variability are shown in Figure 9.11. Again, the 16-year average annual cycle is shown repeatedly for reference. As one might suspect from inspection of this plot, the power spectrum shows a peak near the annual period, but there are also marginally significant peaks at shorter periods (Figure 9.12). Those same periods, 2.0, 3.3 and 4.2 months, stand out, however, in the power spectrum of the biweekly flux anomalies (Figure 9.13); i.e., after removal of the annual cycle from the data. Their identity and significance ought to become clearer with more data, but two remarks are in order: (1) It appears likely that the 2-month period is an artifact introduced by surface characteristics of the trap cones. In almost all instances (24 out of 25) the second 2-week sample collected after deployment of cleaned traps was larger than the first. The magnitude of the effect is dependent on the time of year; i.e., on the magnitude of the particle flux. We are presently investigating its cause, but tentatively conclude that the inner surface of the trap cones, newly exposed to seawater and sinking material, impedes the material's descent toward the collection cup at the bottom of the funnel. The impedance might be effective for a given period of time or until the

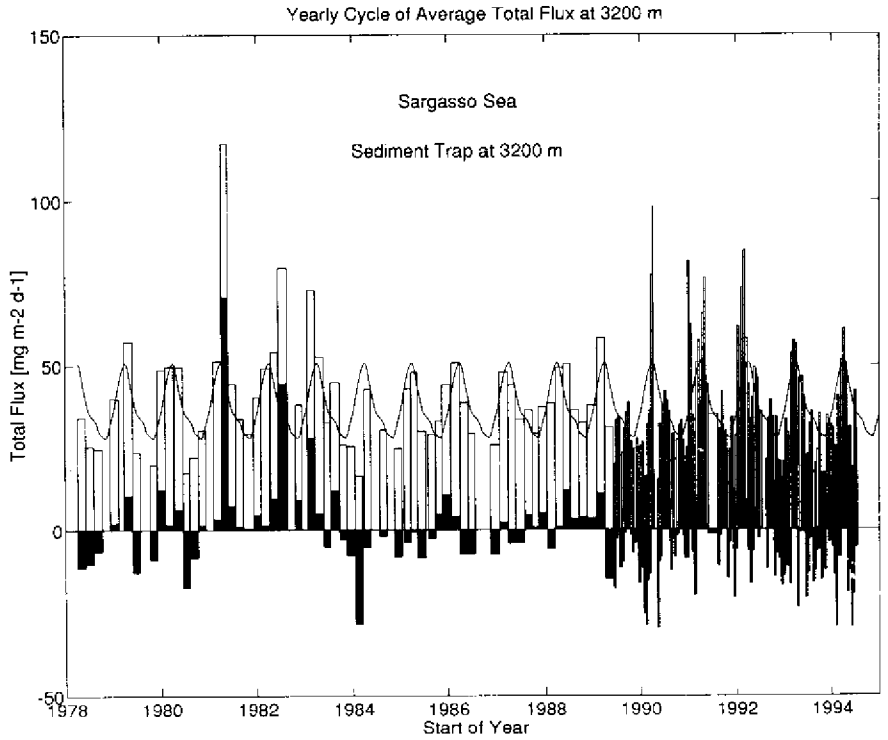

Figure 9.5 Total flux at 3200 m (open bars) and anomalies relative to the 16-year average annual cycle (filled bars).

surface has acquired a state of dynamic equilibrium with the sinking material. (2) There might well be a lunar period in the data. Some marine organisms, such as foraminifera, have lunar reproduction cycles (Spindler et al., 1979; Bijma et al., 1990 and 1994), but a biweekly sampling scheme cannot detect it because of aliasing (Figure 9.14). The average sampling period was too close to half the lunar period. Higher sampling frequency might seem desirable to get around this problem but, unless larger traps are used, the sample yields quickly become too small to be of much use. Also, sample numbers become too large to be handled by the typical laboratory.

The important point is that the other-than-annual periods are the most promising means by which we might identify forcing functions of deep particle flux, especially carbon flux. In addition, they might help identify more-easily-measured proxies for deep carbon flux. I maintain that we need such proxies for assessing the efficacy of, and secular trends in, the biological pump. Flux measurements by sediment traps alone are far too expensive and limited in their geographic

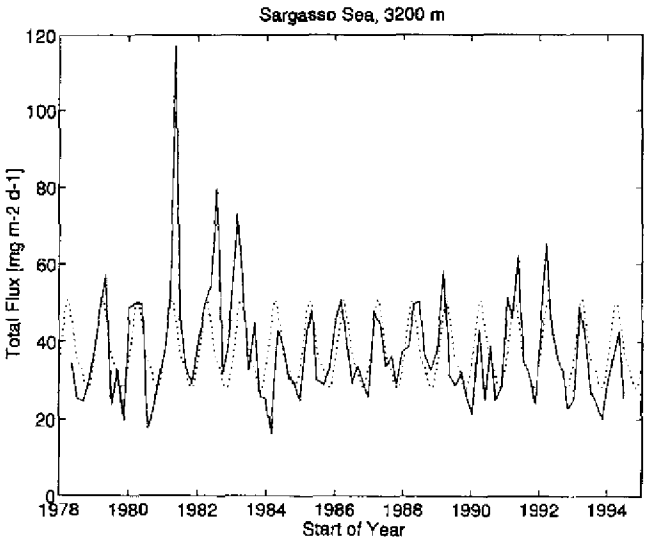

Figure 9.6 Variability of 16 years of bimonthly particle-flux measurements in the deep Sargasso Sea. Each 2-month collection period is represented by its midpoint only. The dotted line repeats the average annual cycle shown in the right panel of Figure 9.2.

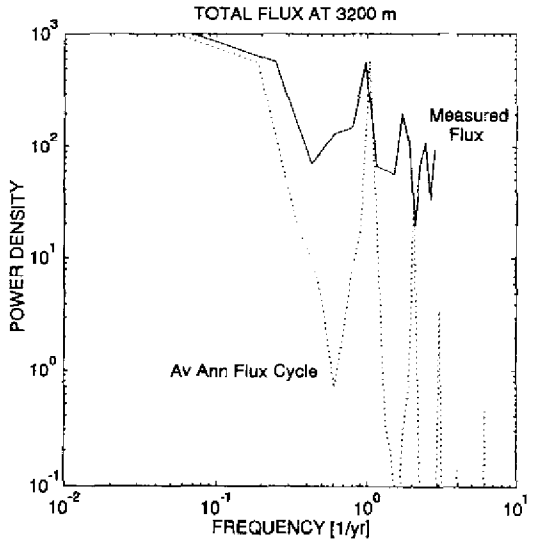

Figure 9.7 Power spectra of 16 years of bimonthly measured flux variability (solid line) and of the 16-year average annual cycle (dotted line) as shown in Figure 9.6.

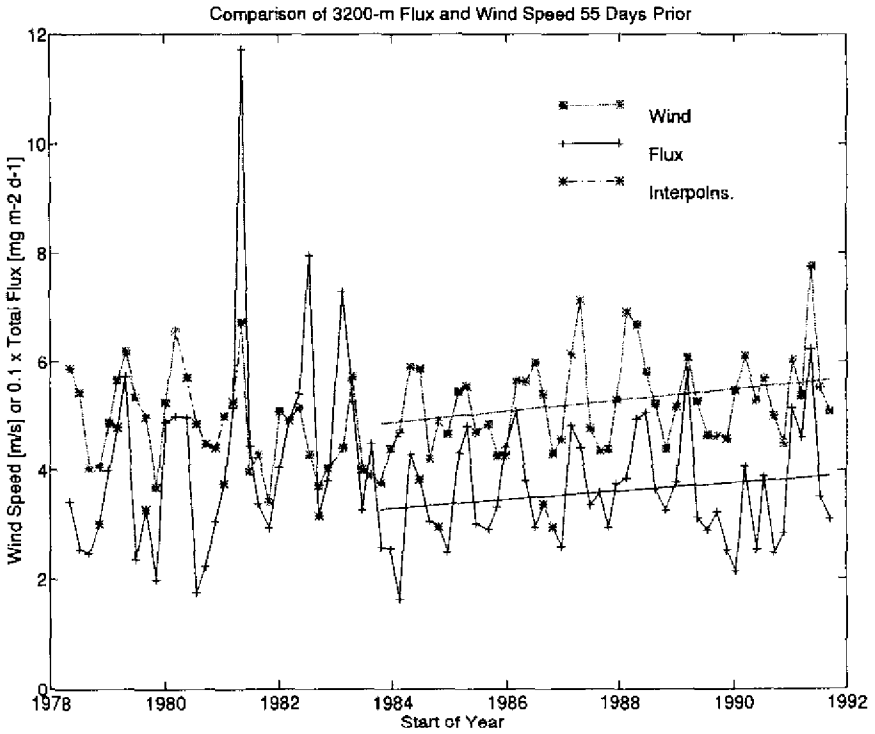

Figure 9.8 Similar eight-year trends of increasing wind speed and deep-ocean particle flux in the Sargasso Sea. Wind speed is offset by 55 days and averaged over periods identical to the collection times of the sediment trap. The offset was determined by spectral analysis and represents the response time of the particle-producing biota to physical forcing plus the time required for particles to sink to a depth of 3200 m.

coverage to assess the pump on a global scale, let alone in a synoptic fashion. It is to be expected, however, that different proxies are needed for different oceanic regimes. What might work for the Sargasso Sea will not necessarily work for the subarctic Pacific or the Southern Ocean.

9.4 EPISODIC EVENTS

Finally, there are the episodic or "unusual" events. By definition, these are unpredictable. Yet, they could have the highest diagnostic value *if* they and their forcing conditions are properly recorded. Their statistics are quite odd (Weatherhead, 1986) and they have a vanishingly small chance of being recorded by means of periodic snapshot measurements. It is increasingly appreciated that they can

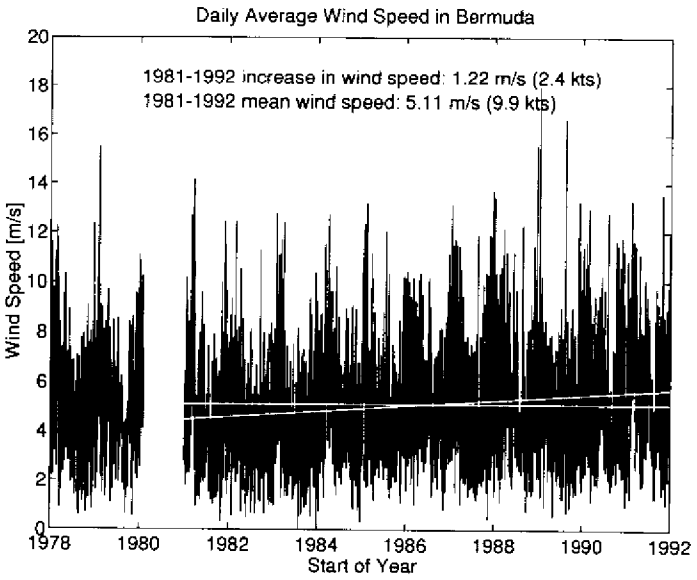

Figure 9.9 A steady change in daily average wind speed on the island of Bermuda. The best fit indicates a 24% increase over 11 years. The trend is significant well above the 99% confidence level.

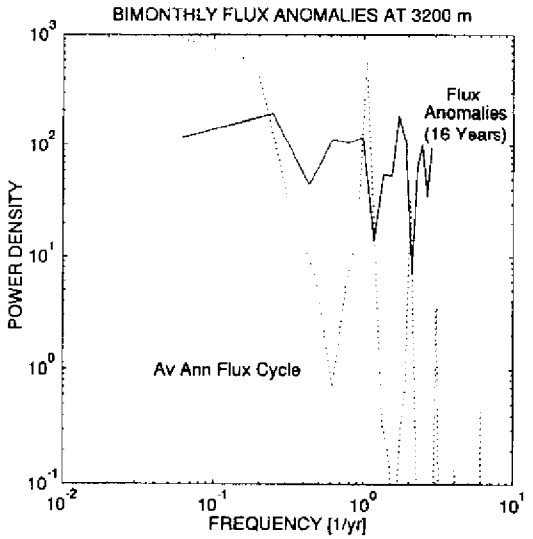

Figure 9.10 Power spectrum of 16 years of bimonthly flux anomalies (solid line), compared to that of the average annual cycle (dotted line).

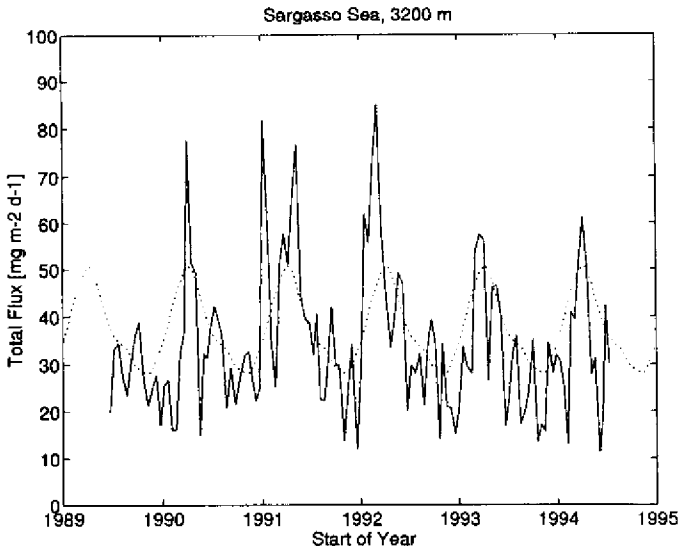

Figure 9.11 Variability of 5 years of biweekly particle-flux measurements in the deep Sargasso Sea. Each 2-week collection period is represented by its midpoint only. The dotted line repeats the average annual cycle shown in the right panel of Figure 9.2.

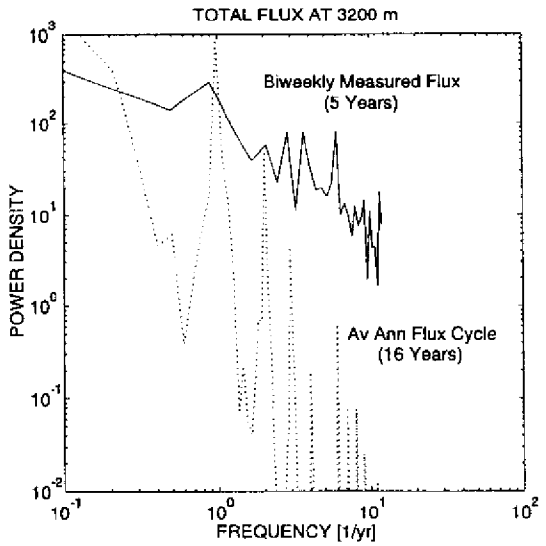

Figure 9.12 Power spectra of five years of biweekly flux variability (solid line) and of the 16-year average annual cycle (dotted line) as shown in Figure 9.11.

have major impact on ecosystems, far beyond their duration (e.g., Scranton et al., 1993). There are several examples of high-flux periods in our long-term record which cannot be attributed to unusual hydrographic conditions because the intermittent hydrographic measurements at Station "S" and, more recently, at the JGOFS BATS site, missed recording those conditions. Another good example was reported by Honjo (1982) who measured a carbonate flux (almost all consisting of coccoliths of *Umbellicosphaera sibogae*) of 1.6 g m^{-2} d^{-1}, orders of magnitude higher than what is normally measured! And that was the average flux over two months. There can be little doubt that, in fact, the true flux was much higher for a much briefer period. Similarly high fluxes were recorded for the same time interval at three different depths. What were the conditions which triggered that event? What effect would such a massive (and geologically instantaneous!) sedimentation pulse have on the sedimentary record? How often do such events occur locally, or in the entire ocean? We cannot answer any of these questions.

9.5 WHAT IS NEEDED?

Time-series measurements in the ocean, while not widely appreciated just a few years ago, have proven their value. Their establishment and maintenance, however, are still entirely dependent on the rules and priorities of short-term funding schemes. This is not a healthy situation because the set of issues referred to as "Global Change" requires long measurement series. Their lack induces some people to make unreasonable claims based on short measurement series. It is quite impossible, for example, to attribute interannual differences in a two-year measurement series to the presence or absence of an El Niño event unless the interannual variability over a much longer period is known. Yet, this has been attempted. Sampling duration and frequency have to be planned with clear objectives in mind. For example, the lunar period cannot be assessed with monthly or biweekly sampling schemes.

Not even a large number of series of just one or a few years' duration can replace the value of a single series of a few decades' length. Similarly, once a series is stopped, a restart is unlikely and of questionable value (for example, the demise of the Ocean Weather Ships: while widely lamented, it is now irreversible). More series ought to be started and they ought to be maintained in a variety of oceanographic settings. And the measurements ought to be *continuous* in order that those rare but important unusual events can be recorded. Particle-flux measurements by sediment traps, in particular, are presently the best tools at our disposal for recording the link between climate-dependent events at the sea surface and their, by chemical and biological agents greatly "edited", record on the seafloor. While traps certainly do have their limitations and shortcomings,

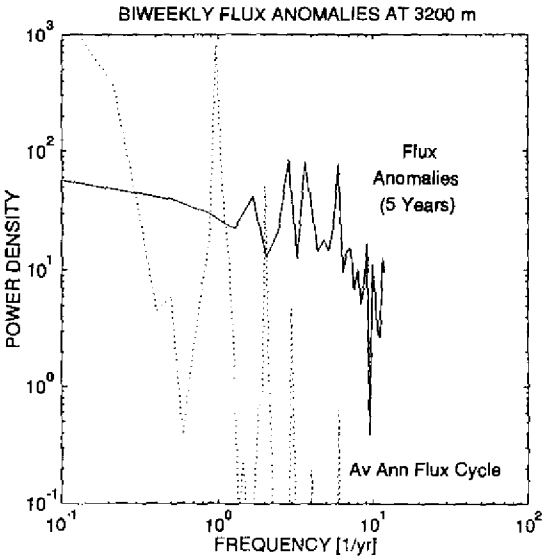

Figure 9.13 Power spectrum of the biweekly flux anomalies (five years of data), compared to that of the average annual cycle. Compare to Figure 9.12 and note the dominant peaks after removal of the annual cycle.

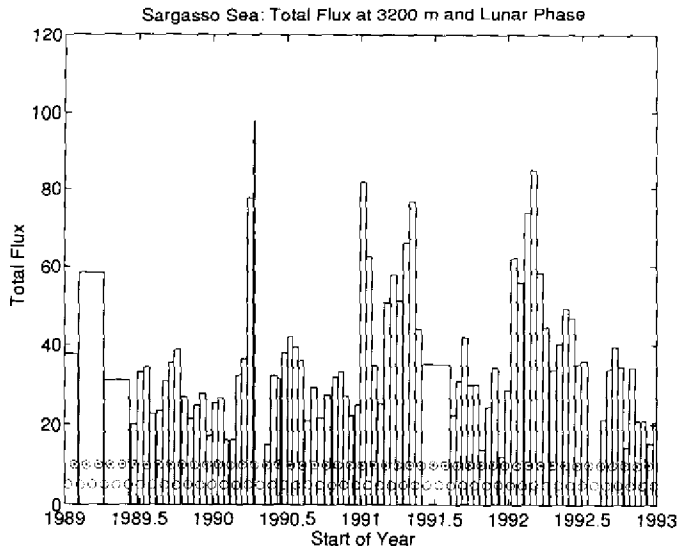

Figure 9.14 Superposition of total-flux measurements and lunar phase. The biweekly sampling scheme was too close to half the lunar period to allow a distinction between the two.

they do sample continuously and record the signatures of *all* upper ocean conditions and processes and not just those accessible to shipboard sampling at low and moderate sea states. They are also amenable to sampling on hourly to yearly schedules, depending on a study's objectives.

Clearly, simultaneous long-term sediment trapping in a variety of oceanic domains is not an easy order. Nobody appreciates that more than I do, as can be seen in Figure 9.15, which presents a juxtaposition of the rhythms of flux measurements and of my "oscillations" between Woods Hole and Bermuda for the purpose of regular recoveries of the mooring.

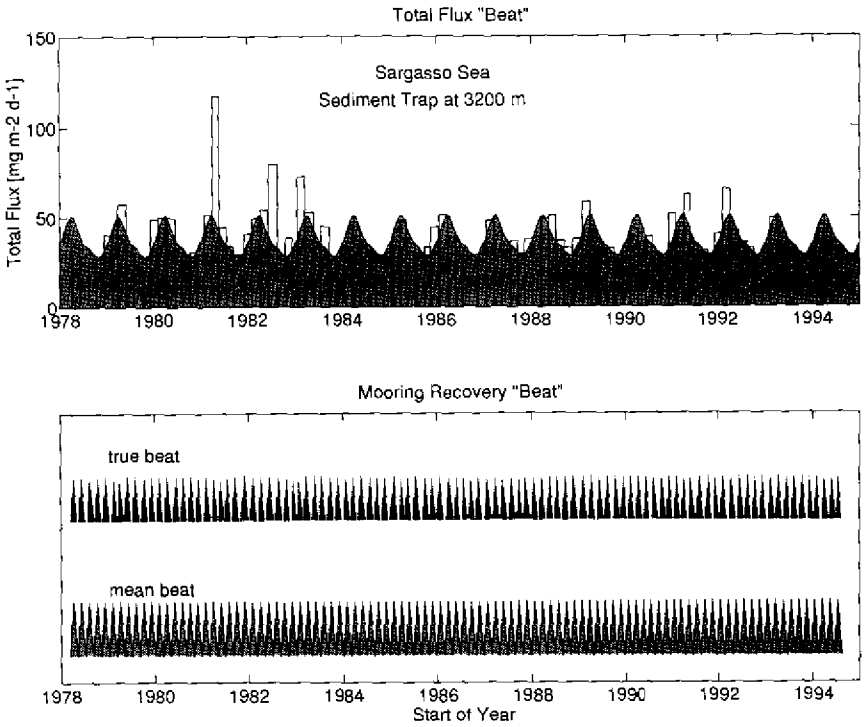

Figure 9.15 Juxtaposition of the rhythms of particle flux (upper panel) and mooring recoveries over the duration of the Sargasso Sea project (lower panel).

9.6 ACKNOWLEDGMENTS

This work was supported by the Ocean Sciences Section of the U.S. National Science Foundation. Contribution No. 8498 from the Woods Hole Oceanographic Institution and No. 1352 from the Bermuda Biological Station.

9.7 REFERENCES

Bathmann, U. V., R. Peinert, T. T. Noji and B. v. Bodungen (1990) "Pelagic origin and fate of sedimenting particles in the Norwegian Sea", *Progr. Oceanogr.*, **24**, 117–125.

Bijma, J., J. Erez and C. Hemleben (1990) "Lunar and semi-lunar reproductive cycles in some spinose planktonic foraminifers", *J. Foraminif. Res.*, **20**, 117–127.

Bijma, J., C. Hemleben and K. Wellnitz (1994) "Lunar-influenced carbonate flux of the planktic foraminifer Globigerinoides sacculifer (Brady)", *Deep-Sea Res.*, **41**, 511–530.

Deuser, W. G. and E. H. Ross (1980) "Seasonal change in the flux of organic carbon to the deep Sargasso Sea", *Nature*, **283**, 364–365.

Deuser, W. G., E. H. Ross and R. F. Anderson (1981) "Seasonality in the supply of sediment to the deep Sargasso Sea and implications for the rapid transfer of matter to the deep ocean", *Deep-Sea Res.*, **28A**, 495–505.

Honjo, S. (1982) "Seasonality and interaction of biogenic and lithogenic particulate flux at the Panama Basin", *Science*, **218**, 883–884.

Honjo, S. and S. J. Manganini (1993) "Annual biogenic particle fluxes to the interior of the North Atlantic Ocean; studied at 34°N 21'W and 48°N, 21'W", *Deep-Sea Res.*, **40**, 587–607.

Izdar, E., T. Konuk, S. Honjo, V. Asper, S. Manganini, E. T. Degens, V. Ittekkot and S. Kempe (1984) "First data on sediment trap experiment in Black Sea deep water", *Naturwissenschaften*, **71**, 478–479.

Nair, R. R., V. Ittekkot, S. J. Manganini, V. Ramaswamy, B. Haake, E. T. Degens, B. N. Desai and S. Honjo (1989) "Increased particle flux to the deep ocean related to monsoons", *Nature*, **338**, 749–751.

Scranton, M. I., P. Crill, M. A. de Angelis, P. L. Donaghay and J. M. Sieburth (1993) "The importance of episodic events in controlling the flux of methane from an anoxic basin." *Glob. Biogeochem. Cycles*, **7**, 491–507.

Smith, K. L., Jr. and R. J. Baldwin (1984) "Seasonal fluctuations in deep-sea sediment community oxygen consumption: Central and eastern North Pacific", *Nature*, **307**, 624–626.

Spindler, M., C. Hemleben, U. Bayer, A. W. H. Bé and O. R. Anderson (1979) "Lunar periodicity of reproduction in the planktonic foraminifer Hastigerina pelagica", *Mar. Ecol. Progr. Ser.*, **1**, 61–64.

Wassmann P., R. Peinert and V. Smetacek (1991) "Patterns of production and sedimentation in the boreal and polar Northeast Atlantic", *Polar Res.*, **10**, 209–228.

Weatherhead, P. J. (1986) "How unusual are unusual events?", *Am. Naturalist*, **128**, 150–154.

Wefer, G., G. Fisher, D. Fuetterer and R. Gersonde (1988) "Seasonal particle flux in the Bransfield Strait, Antarctica", *Deep-Sea Res.*, **35**, 891–898.

Weiler, E. (1992) "Seasonal changes in adult mammalian brain weight", *Naturwissenschaften*, **79**, 474–476.

Wunsch, C. (1981) "Low-frequency variability of the sea", in B. A. Warren and C. Wunsch (eds) *Evolution of Physical Oceanography*, MIT Press, Cambridge, 342–374.

10 Seasonal and Interannual Particle Fluxes in the Eastern Equatorial Atlantic from 1989 to 1991: ITCZ Migrations and Upwelling

GERHARD FISCHER AND GEROLD WEFER

10.1 INTRODUCTION

The NE and SE trade winds are a dominant feature in the eastern Atlantic Ocean and largely determine biological production and sedimentation in the coastal and equatorial upwelling regimes off Africa. The trade winds are separated by a calm zone, the Intertropical Convergence Zone (ITCZ) which is characterized by high atmospheric and oceanic temperatures. In the eastern equatorial Atlantic (Guinea Basin), this zone migrates seasonally from about 2–4°N in March to 8–12°N in August (Figure 10.1) in response to larger-scale climatic variations and the intensity of the trade winds (Servain and Legler, 1986). The wind regime is strongly coupled with oceanic and biological processes operating in this area. The equatorial "upwelling" zone is believed to be a production regime with elevated biomasses and biological production especially during the boreal summer when the southeasterlies are commonly strong and sea surface temperatures (SST) are relatively low (Voituriez and Herbland, 1982). Consequently, during the boreal summer, high export fluxes of organic carbon and other biogenic components were expected. Due to a distinct interannual variability in wind forcing and ocean response (Houghton and Colin, 1986; Peterson and Stramma, 1991), year-to-year flux variations may also be anticipated. The intensity of upwelling may decrease in certain years (Voituriez and Herbland, 1977) and is occasionally accompanied by large anomalies in sea surface temperatures linked to anomalous southerly positions of the ITCZ (Merle, 1980).

With this long-term flux study conducted at 10°W in the Guinea Basin, we monitored the seasonal and year-to-year variations in sedimentation comparing a northern (GBN) and a southern site (GBS) (Figure 10.1). Both sites were located close to the equatorial upwelling area. The northern site (GBN) was located in the vicinity of the mean southernmost boundary of the ITCZ in boreal winter and is

Particle Flux in the Ocean
Edited by V. Ittekkot, P. Schäfer, S. Honjo and P. J. Depetris

expected to be substantially affected by precipitation and influx of land-derived materials. The southern site was located close to a thermal ridge at 2–3°S which is a permanent feature of the equatorial circulation in the Gulf of Guinea during the warm spring season (Voituriez and Herbland, 1977). We attributed the seasonal peaks of total matter, organic carbon, carbonate and biogenic opal to corresponding summer upwelling influenced by the zonal winds or to thermal ridging in spring representing the "typical tropical situation" (TTS; Voituriez and Herbland, 1977, 1981, 1982) and tried to monitor these variations on a longer time scale.

10.2 MATERIAL AND METHODS

Time-series sediment traps were used to measure export fluxes well below the mixed layer and at least 500 m above the seafloor to minimize a strong dominance of "swimmers" in the trap samples and, on the other hand, reduce the influx of resuspended material from the seafloor (Gardner and Richardson, 1992). For our studies, we deployed cone-shaped multisample sediment traps (Aquatec, Kiel, Germany) with 20 cups and 0.5 m^2 collection area. All traps were fitted with a grid at the top. The sampling cups were filled with filtered seawater to which Suprapur NaCl was added to increase the density (increase of the salinity to around 40‰). The solution was poisoned with $HgCl_2$ prior to and after deployments. Samples were carefully wet-sieved through a 1 mm screen and "swimmers" were removed by hand. The < 1 mm fraction was split into aliquots and the freeze-dried material was analyzed as described by Fischer and Wefer (1991). Lithogenic matter (Lith.) was estimated according to: Lith. flux = total flux - (opal flux + carbonate flux + 2 x C_{org} flux). Biogenic opal was determined by automated wet leaching (Müller and Schneider, 1993). Fluxes were not corrected for dissolution in the sampling cups. From measurements of the cup solutions, we conclude that dissolution in the cups was rapid and not related to the deployment time, and thus affects all samples to a similar extent. We therefore regard all fluxes as minimal values.

10.3 OCEANOGRAPHIC AND BIOLOGICAL SETTING

The large variability of the surface currents in the Gulf of Guinea is due to a combination both of local and remote wind forcing (Richardson and Walsh, 1986; Servain et al., 1985; Servain and Legler, 1986; Houghton and Colin, 1986, Houghton, 1989). The oceanographic situation is characterized by the westward flowing South Equatorial Current (SEC) (Figure 10.1), which is underlain by the eastward flowing Equatorial Current or Lomonossov Current at more than 50 m depth (EUC) (Peterson and Stramma, 1991; Voituriez and Herbland, 1982;

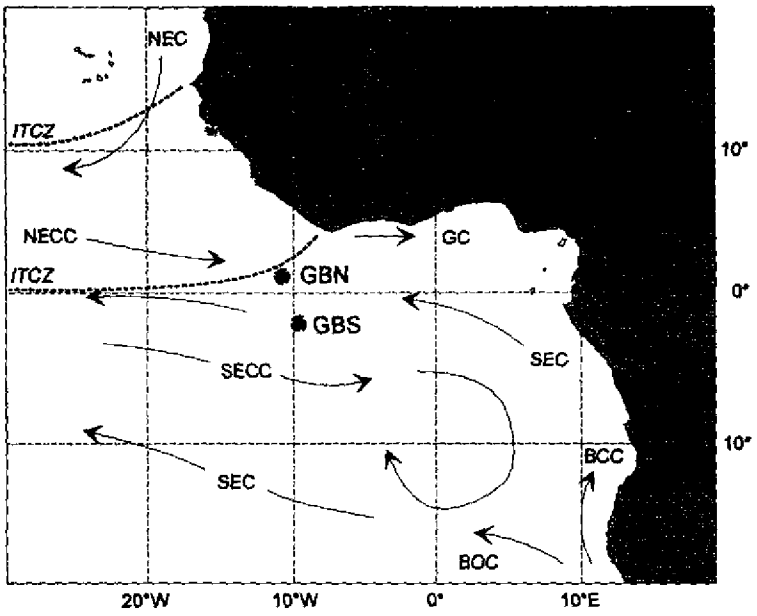

Figure 10.1 Simplified map of surface currents in the eastern Atlantic (NEC = North Equatorial Current; NECC = North Equatorial Counter Current; GC = Guinea Current; SEC = South Equatorial Current; SECC = South Equatorial Counter Current; BCC = Benguela Coastal Current; BOC = Benguela Oceanic Current). The seasonal boundaries of the ITCZ are shown by stippled lines. The trap sites were named GBN and GBS.

Hastenrath and Merle, 1987). The high production upwelling area in the tropical Atlantic where both sites (GBN and GBS) (Figure 10.1) were located is at least partly controlled by the superficial equatorial countercurrent systems which supply nutrients through the South Atlantic Central Water (SACW) (Voituriez and Herbland, 1982). The northern Guinea Basin is also partly influenced by the eastward flowing coastal-near Guinea Current (GC) which is the prolongation of the North Equatorial Counter Current (NECC). The SEC, the NECC and the GC are strongest in the boreal summer when the ITCZ is farthest north (Figure 10.1).

The interannual variability in SST in the eastern Atlantic is stronger than previously thought (Servain and Legler, 1986). A zonal band of maximal SST follows the ITCZ shifting from 8–12°N during the boreal summer to its southernmost position in winter at 2–4°N, close to the position of the northern study site (GBN) (Figure 10.1). The NE and the SE trades differ seasonally (Servain and Legler 1986): the magnitude of the SE trades is strongest in June-July whereas the NE trades are strongest in February. Although the monthly SE trade wind values are smaller than the northeasterlies, they have, due to their longer duration, a mean magnitude of the same order.

Nitrate is the limiting nutrient in the entire tropical Atlantic throughout the year except along the equatorial divergence zone during the cold summer season (Voituriez and Herbland, 1981). The SE trades result in a strong westward advection of the SEC, a shallowing of the thermocline (Voituriez and Herbland, 1981; 1982; Düing et al., 1980) and the presence of maximal nutrients notably around 10°W (Voituriez and Herbland 1981, 1982). Primary production reaches 500 mgC m^{-2} d^{-1} at this point (Voituriez and Herbland, 1981). This zone of higher biomass and production ("active upwelling") occurs between 0°30'N and 1°30'S in the eastern Atlantic and is characterized by SST between 22° and 25°C (Voituriez and Herbland, 1977).

In the boreal winter, the ITCZ is at its southernmost position and is then located nearby the northern trapping site GBN (Figure 10.1). Westward advection of the SEC is weakened, turbulent mixing ("upwelling") is strongly reduced and SST are between 26° and 28°C (Düing et al., 1980; Voituriez and Herbland, 1981). During this season, the southern site (GBS) (Figure 10.1) was located close to a thermal ridge centered at between 2° and 3°S characterized by a deep chlorophyll maximum and elevated biological production (Voituriez and Herbland, 1977). According to Voituriez and Herbland (1981, 1982), this production system is characterized by nutrient depletion in the surface layer ("typical tropical situation", TTS). Primary production is then largely determined by the nitracline depth in relation to optimal light conditions.

10.4 OCEAN CURRENTS

In combination with the traps, Aanderaa current meters were deployed. At the northern Guinea Basin sites, current velocities in the AAIW (Antarctic Intermediate Water) layer during 1989 (GBN6 upper trap) were generally lower than 20 cm s^{-1}. However, some spikes of up to 45 cm s^{-1} were recorded which were, however, not related to the measured fluxes. Directions revealed two maxima with roughly east-west and west-east directions. Fluxes increased during changes to the west-east direction, e.g., in August. In the deeper waters (NADW, North Artlantic Deep Water, GBN6 lower trap) current speeds were still relatively high, mostly between 10–20 cm s^{-1}. Again, some peak velocities of short duration were measured with values of up to 50 cm s^{-1}. Current directions were generally south to southeastwards. At the southern sites, currents in 726 m water depth were measured during the GBZ5 deployment. They oscillate around 10 cm s^{-1} with some peaks of 30 cm s^{-1} in June and July. No correlation to fluxes was observed. Current directions in this water mass (AAIW) were commonly to the east, mostly ESE, and rarely NE.

10.5 RESULTS AND DISCUSSION

10.5.1 SEASONALITY AND INTERANNUAL VARIABILITY OF FLUXES AND COMPOSITION

10.5.1.1 Northern Guinea Basin sites (GBN)

In the upper trap level total flux peaks were observed in spring (115.3 to 197.5 mg m^{-2} d^{-1}) and summer (212 to 240.5 mg m^{-2} d^{-1}) which generally recurred with similar timing (Figure 10.2a). The deeper trap fluxes revealed a similar but somewhat smoothed pattern (Figure 10.2b) with higher average values due to a larger contribution of terrigenous material (see Richardson and Gardner 1991). However, peak fluxes in spring and summer were still present. By comparing the timing of the upper and lower trap flux peaks, we estimated average sinking velocities for the total particulate matter in the order of 150 m d^{-1}. This appears to be a typical range for settling velocities of larger particles; i.e., fecal material (Honjo and Roman, 1978). A study performed by Bishop et al. (1977) close to our site indicated that 99% of the vertical mass flux through 388 m water depth was probably transported via fecal matter. Terrigenous fluxes constituted between 15 and 20% of the total particulate mass at this site and peaked generally in spring. An exception was 1991, when consistently higher background fluxes were observed throughout the year (Figure 10.2). Biogenic fluxes were clearly dominated by carbonate (e.g., foraminifers and nannofossils) reaching from 19.7 to 80.7% of the total mass. The most prominent carbonate signals were measured during the boreal summer, particularly during 1989 (131.7 mg m^{-2} d^{-1}) (Figure 10.3).

Biogenic opal, mostly composed of diatoms and radiolariansm, showed maximal fluxes in spring and summer on the seasonal cycle (Figure 10.3) and constituted only between 1.9 and 19.7% of the total mass. Spring fluxes were highest in 1989; the summer sedimentation peaks were almost identical in 1989 and 1991 (Figure 10.3). Detailed studies on the seasonal diatom distribution conducted by Lange et al. (1994) revealed highest valve fluxes in spring (March-April) and another maximum in summer 1989 (August-September). The summer signal in 1989 was almost exclusively manifested by small bicapitate *Nitzschia* species representing 68–83% of the total diatom fluxes. This group is known to be typical for tropical oceanic waters (Sancetta, 1992). Radiolarian fluxes showed a rather similar pattern with prominent peaks in spring and summer to fall (Boltovskoy et al., 1993). Organic carbon which contributed 4.1 to 28.2% to the total material showed a bimodal flux pattern with maxima in spring and particularly in summer, displaying only small interannual variation (Figure 10.3). The spring organic carbon flux signal in 1989 is characterized by relatively high C/N ratios (10–11.6) and low $\delta^{13}C_{org}$ ratios (-22.4 to -22.8‰) which indicates a significant contribution of terrestrial organic matter supplied by the NE trades. In addition, the spring opal

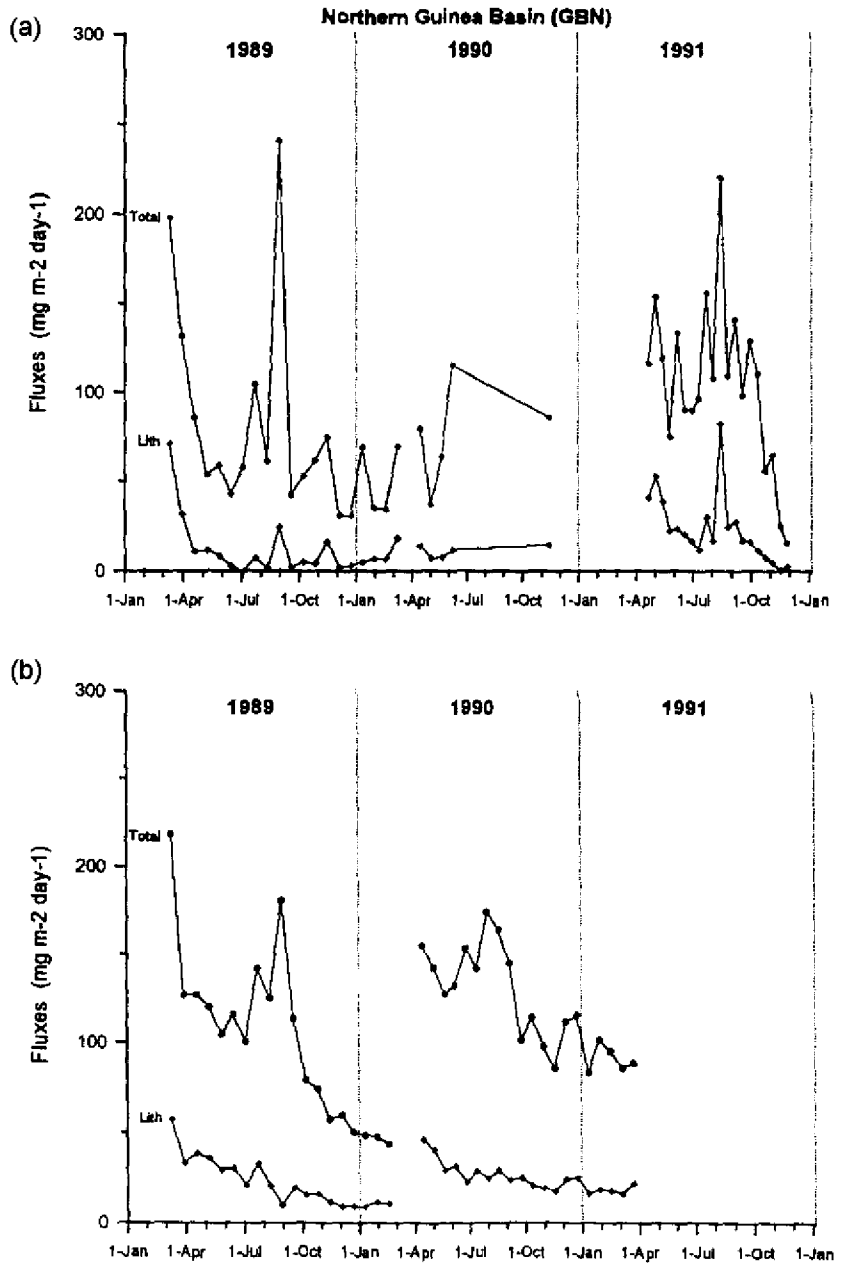

Figure 10.2 Seasonal total and lithogenic fluxes in the northern Guinea Basin (GBN). (a) upper traps (853–953 m). (b) lower traps (3921 and 3965 m; see Table 10.1).

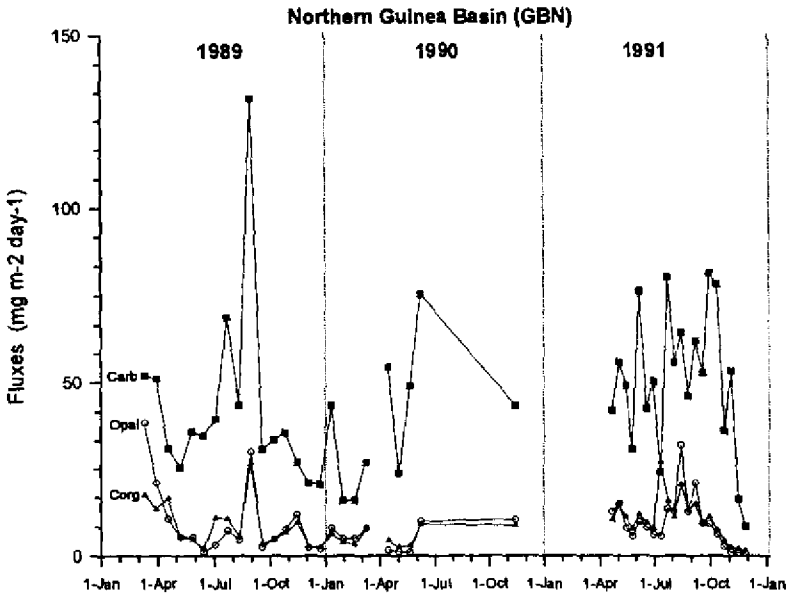

Figure 10.3 Seasonal carbonate, opal and organic carbon fluxes at GBN (upper traps: 853–953 m).

Table 10.1 Description of the sampling sites.

Site name	Long	Lat	Water depth (m)	Trap depth (m)	Sampling duration	Samples x days
a) Northern Equatorial Upwelling Area (GBN)						
GBN3	01°48.N	11°08.W	4481	853 3921	03/01/89– 03/16/90	20 x 19 19 x 19
GBN6	01°47.N	11°08.W	4522	859 3965	04/04/90– 04/07/91	4 x 18, 1 x 297 20 x 18
EA2	01°47.N	11°15.W	4399	953	04/13/91– 11/29/91	20 x 11.5
b) Southern Equatorial Upwelling Area (GBS)						
GBZ4	02°11.S	09°54.W	3912	696	03/01/89– 03/16/90	20 x 19
GBZ5	02°12.S	09°56.W	3920	597 3382	04/01/90– 03/30/91	2 x 4.75, 12 x 29.6 20 x 18
EA4	02°11.S	10°06.W	3906	1068	04/13/91– 11/29/91	20 x 11.5

peak in 1989 (38.9 mg m^{-2} d^{-1}) was characterized by a significant contribution of freshwater diatoms and phytoliths (Lange et al., 1994) obviously transported by the NE trades and precipitated within the ITCZ which is normally located at its southernmost position during this period (Servain and Legler, 1986). In contrast, the spring signal in 1991 appeared to be much less influenced by terrestrial input as deduced from a low C/N ratio of 8.9 and a relatively high $\delta^{13}C_{org}$ value of -21.7‰. The summer upwelling events were generally characterized by lower C/N and higher $\delta^{13}C_{org}$ ratios; 8.9 and -21.1‰ in August 1989 and even 6.1 and -19.6‰ in August 1991. These isotope values are typical for a marine endmember at low latitudes (Hedges and Mann, 1979) and document a high contribution of phytoplankton, particularly in 1991.

10.5.1.2 Southern Guinea Basin sites (GBS)

This flux pattern, in contrast to the site further north is characterized by (1) a less clear bimodal distribution, (2) lower total, biogenic and lithogenic fluxes and (3) higher spring relative to the summer fluxes (Figure 10.4). Peak fluxes at both depth levels occurred in spring (89.5 to 165.5 mg m^{-2} d^{-1}) and summer to fall (32.6–167.3 mg m^{-2} d^{-1}). However, no distinct summer peak representing the cold upwelling season was observed in 1989. Lithogenic fluxes were significantly smaller compared to the GBN site and revealed slightly higher values in spring. Biogenic carbonate constituted the main proportion of the total fluxes (14.3–85%). Spring sedimentation increased from 1989 to 1991 and a summer upwelling peak was only present in 1991 (Figure 10.5). However, in 1990, a second prominent maximum occurred in fall, probably documenting equatorial upwelling.

Opal flux peaks were recorded in spring and obviously increased from 1989 to 1991; fluxes in summer-fall were highest in 1990 and lowest in 1989 (Figure 10.5). Similar to the GBN site, we found relatively low contributions of biogenic opal (0.5–14.1%). Mean diatom fluxes were about three times lower in 1989 compared to the site further north (Lange et al., 1994) and the spring flux peak was characterized by lower abundances of freshwater diatoms. The opal peak during the equatorial upwelling season was rather weakly expressed in the summer of 1989 (July). However, the summer diatom assemblages were similar to GBN, also dominated by oceanic *Nitzschia bicapitata* (Lange et al., 1994).

Organic carbon, which constituted 3.6 to 23.8% of the total flux, also peaked in spring, except in 1990 when a distinct fall maximum was present (Figure 10.5). Similar to the GBN site, the spring organic carbon flux in 1989 was marked by a high C/N ratio (13.5) and a low $\delta^{13}C_{org}$ value of -23‰ suggesting a contribution of terrestrial organic carbon delivered by the NE trades and precipitated at the southernmost boundary of the ITCZ. In contrast, spring peaks in 1990 were characterized by C/N and $\delta^{13}C_{org}$ ratios of 9.9 and -22.8‰; in 1991 these values were 10.9 and -22‰ during the sampling period. These data appear to document

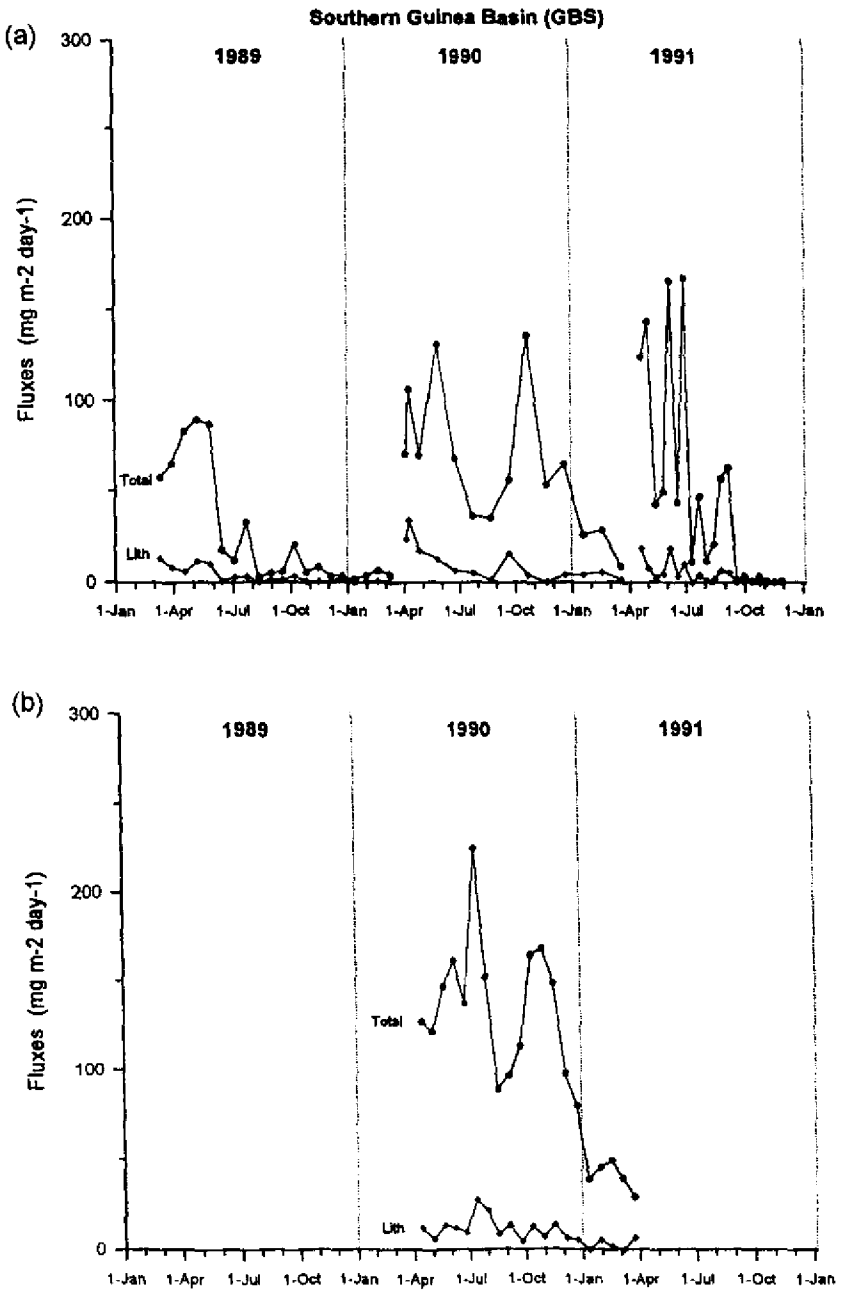

Figure 10.4 Seasonal total and lithogenic fluxes in the southern Guinea Basin (GBS). (a) upper traps (597–1068 m). (b) lower traps (3382 m).

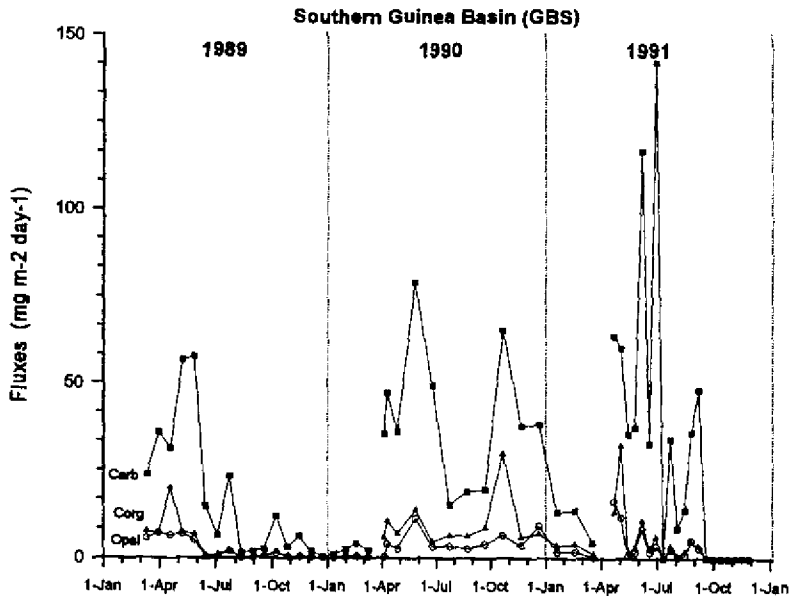

Figure 10.5 Seasonal carbonate, opal and organic carbon fluxes at GBS (upper traps: 597–1068 m).

a decreasing influence of the ITCZ in spring. The relatively low summer carbon fluxes revealed C/N ratios between 8.0 and 9.1 and $\delta^{13}C_{org}$ ratios of -21.4 to -21.8‰ suggesting a predominantly marine planktonic origin.

Spring sedimentation and primary production at the GBS site was also influenced by a thermal ridge at 2–3°S which is a permanent feature of the equatorial warm season (Voituriez and Herbland, 1977). This season is characterized by nutrient depletion in the surface layer (TTS) and primary production which is primarily controlled by the nitracline depth in relation to optimal light conditions. The occurence of a deep chlorophyll maximum and the intensive biological production result in carbon export as measured with the traps.

10.5.1.3 Annual fluxes and year-to-variations

Annual fluxes, their composition and some ratios as well as the interannual variability given in percent of the annual average are listed in Table 10.2. The composition of the fluxes during the three year sampling period did not differ significantly. On an annual basis, the northern and southern sites were relatively similar with respect to composition and ratios except biogenic opal and lithogenic materials which constituted higher proportions (10.8 and 17.8% on average) at GBN. However, the absolute fluxes showed significant year-to-year variation,

Table 10.2 Annual fluxes, percentages of total fluxes and ratios in the northern (GBN) and southern Guinea Basin (GBS). Annual averages and interannual variability is also shown.

Site	Year	Trap depth (m)	FLUXES in g m^{-2} Total	Opal	C_{org}	N_{gen}	$CaCO_3$	Lith.	PERCENTAGES Opal	C_{org}	N_{gen}	$CaCO_3$	Lith.	RATIOS C/N atom	C_{org}/ Opal*	C_{org}/ $C(CaCO_3)$	$\delta^{13}C$ ‰ PDB
NORTHERN GUINEA BASIN																	
GBN *upper level*																	
GBN3	1989	853	25.3	3.1	2.8	0.34	13.1	3.8	12.1	10.9	1.34	51.6	15.2	9.5	0.9	1.8	-21.9
GBN6	1990	859	20.9	2.2	1.9	0.27	13.1	3.4	10.5	9.1	1.29	62.7	16.3	8.4	0.9	1.4	-21.6
EA2	1991	953	27.0	2.6	2.8	0.39	13.0	5.9	9.6	10.4	1.45	48.2	21.9	8.2	1.1	1.8	-21.3
Ann. aver.			*24.4*	*2.6*	*2.5*	*0.33*	*13.1*	*4.4*	*10.8*	*10.1*	*1.36*	*54.2*	*17.8*	*8.7*	*1.0*	*1.7*	*-21.6*
Interann. var. (%)			*24.9*	*32.8*	*36.2*	*36.0*	*0.8*	*57.1*									
GBN *lower level*																	
GBN3	1989	3921	34.2	4.3	2.0	0.25	18.5	7.5	12.5	5.8	0.73	54.1	21.8	9.4	0.5	0.9	-21.3
GBN6	1990	3965	38.0	5.1	1.9	0.24	21.2	8.0	13.5	5.0	0.63	55.6	21.0	9.3	0.4	0.7	-21.7
EA2	1991	no data	—	—	—	—	—	—	—	—	—	—	—	—	—	—	—
Ann. aver.			*36.1*	*4.7*	*2.0*	*0.25*	*19.8*	*7.7*	*13.0*	*5.4*	*0.68*	*54.8*	*21.4*	*9.4*	*0.5*	*0.8*	*-21.5*
Interann. var. (%)			*10.5*	*17.9*	*5.1*	*4.1*	*13.7*	*7.0*									
SOUTHERN GUINEA BASIN																	
GBS *upper level*																	
GBZ4	1989	696	9.5	0.7	1.1	0.13	5.3	1.2	7.7	11.6	1.37	56.0	13.1	10.1	1.5	1.7	-22.1
GBZ5	1990	597	20.4	1.4	2.7	0.30	11.3	2.3	6.9	13.3	1.47	55.0	11.3	10.7	1.9	2.0	-22.8
EA4	1991	1068	12.9	0.8	1.2	0.17	8.1	1.3	6.2	9.3	1.32	62.8	10.1	8.6	1.6	1.3	-21.8
Ann. aver.			*14.3*	*1.0*	*1.7*	*0.20*	*8.2*	*1.6*	*6.9*	*11.4*	*1.39*	*57.9*	*11.5*	*9.8*	*1.7*	*1.7*	*-22.2*
Interann. var. (%)			*76.2*	*68.6*	*96.0*	*85.0*	*71.6*	*65.7*									
GBS *lower level*																	
GBZ4	1989	no data	—	—	—	—	—	—	—	—	—	—	—	—	—	—	—
GBZ5	1990	3382	36.4	5.4	2.1	0.28	23.6	3.2	14.9	5.8	0.77	64.8	8.6	8.8	0.4	0.8	-22.0
EA4	1991	no data	—	—	—	—	—	—	—	—	—	—	—	—	—	—	—

* weight/weight

particularly in the upper traps. The recorded variation for the total fluxes was 25% at the GBN site and as much as 76% at the GBS site. These values are comparable to the interannual variability given by Lyle et al. (1992) for the northeastern Pacific. The annual values at GBN were largely determined by the magnitude of the summer sedimentation event occurring during equatorial upwelling. In contrast, annual fluxes at GBS were much more influenced by spring sedimentation representing the TTS.

Bishop et al. (1977) determined flux values through the 388 m water depth for a site nearby to GBN and found 11.3 g C m^{-2} y^{-1}, 11 g $CaCO_3$ m^{-2} y^{-1} and 3.4 g biogenic opal m^{-2} y^{-1}. Our annual averages were 2.5 g C m^{-2} y^{-1}, 13.1 g $CaCO_3$ m^{-2} y^{-1} and 2.6 g biogenic opal m^{-2} y^{-1}. This comparison may suggest significant regeneration of organic carbon between 400 m and 853–953 m water depth. Considering some interannual variability, the carbonate and biogenic opal fluxes show similar values. However, one has to keep in mind that different sampling techniques (traps versus pumps) were used to estimate annual flux values.

10.5.1.4 Comparison between the northern (GBN) and southern sites(GBS)

We will compare the longer records of biogenic fluxes from the upper traps with respect to the timing and magnitude of the spring and summer sedimentation events which correspond to the TTS and equatorial upwelling, respectively. For this comparison, we used the 3-point average fluxes of carbonate, biogenic opal and organic carbon depicted in Figure 10.6. Spring sedimentation events were found both north and south of the equator. However, the spring sedimentation event appeared to be more pronounced further south where thermal ridging during the TTS occurs (Voituriez and Herbland, 1981). During the three-year sampling period, the magnitude of the spring carbonate, opal and C_{org} peak increased at GBS (Figure 10.6b). This may indicate a shallowing of the south equatorial thermal ridge centered at 2–3°S in spring in conjunction with nutrient injection into the photic layer and increased biological production. Organic carbon and biogenic opal flux maxima seem to precede the carbonate maxima by approximately one to two months.

Spring sedimentation at GBN is at least partly influenced by land-derived material supplied by the NE trades (Wefer and Fischer, 1993). Dust plumes which also contain lithogenic materials and pollen grains may be washed out within the southern boundary of the ITCZ and supply equatorial surface waters with micro- and macronutrients (Schütz, 1980; this volume, Chapter 3). We presume that these processes influence biological production north of the equator (GBN) during the nutrient-limited TTS in spring. The $\delta^{13}C_{org}$ and C/N data indicate that the highest land-derived contribution occurred in 1989, associated with highest organic carbon and biogenic opal fluxes. The ITCZ was farthest south almost approaching the GBS position.

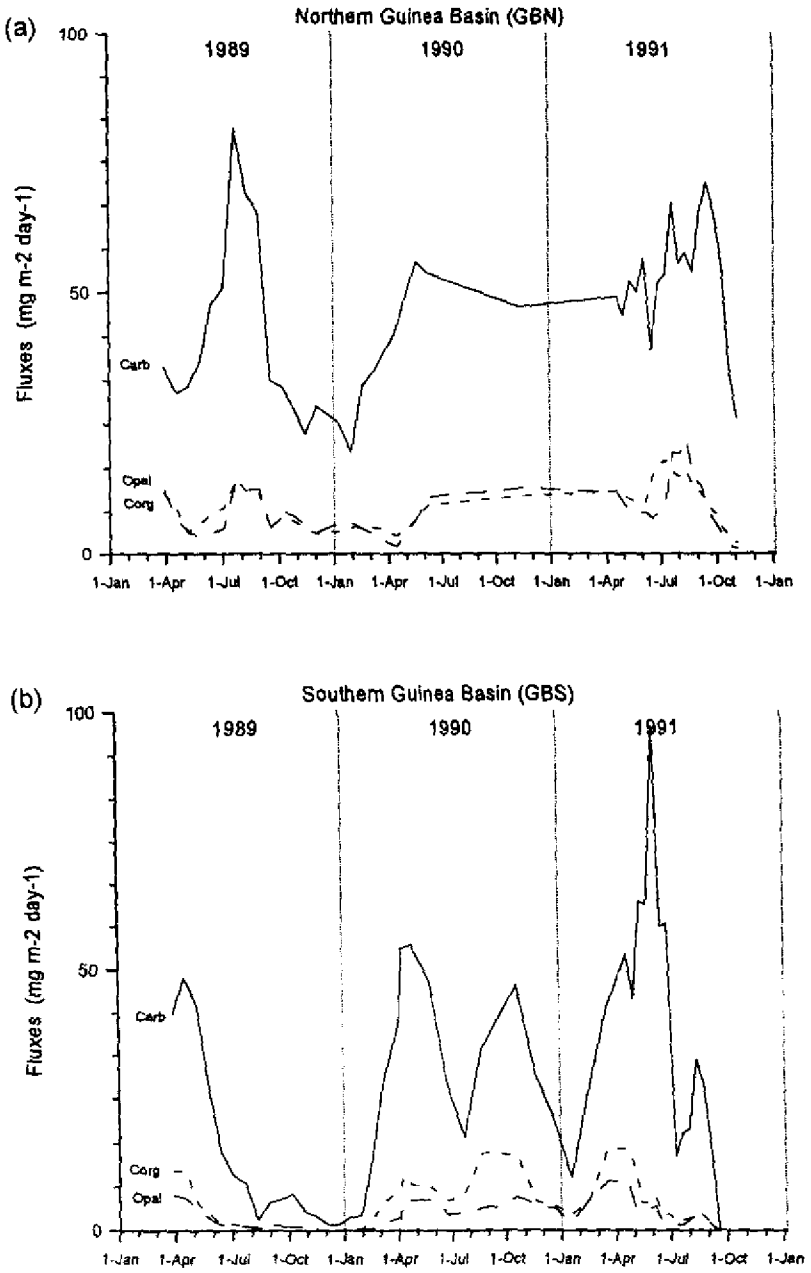

Figure 10.6 Three-point average carbonate, opal and C_{org} fluxes to the upper traps in the (a) northern (GBN) and (b) southern Guinea Basin (GBS).

Equatorial divergence generally occurring in summer in response to the intensification of the zonal winds in the western Atlantic (Houghton, 1989) was clearly documented by high fluxes of organic carbon, carbonate and biogenic opal at the northern site, particularly during 1989 (Figure 10.6a). Organic carbon flux peaks slightly preceded biogenic opal fluxes. Further south, at the GBS station, equatorial upwelling during summer was not evident in 1989 (Wefer and Fischer, 1993) but was probably reflected in the fall of 1990 by a considerable peak in the fluxes of carbonate and organic carbon. In summer of 1991, a carbonate sedimentation peak was present which was also observed further north. These findings provide evidence of a regionally variable extension of the equatorial upwelling band which affected sedimentation at both investigation sites in 1991, and probably also in 1990.

10.6 SUMMARY AND CONCLUSIONS

In this study we compared two three-year lithogenic and biogenic flux records from the eastern equatorial upwelling area. One site (GBN) was located at 1°48.N which is roughly the southernmost penetration of the ITCZ during spring; the other site was located at about 2°S (GBS) in the vicinity of a thermal ridge at 2–3°S occurring during the warm season. We inferred from this comparison:

1. Equatorial upwelling during the boreal summer was clearly documented by high fluxes at the northern site (GBN) and weakly at GBS, particularly in 1989. However, in 1991, and probably also in 1990, sedimentation due to equatorial upwelling was recorded at both sites suggesting a regionally variable extension of the equatorial upwelling band.
2. The ITCZ appears to have reached the southernmost position in spring 1989. Dust fallout at the southernmost boundary of the ITCZ then obviously contributed to sedimentation both north and south of the equator. The southern boundary of the ITCZ, however, generally did not reach the GBS site.
3. Production and sedimentation during the warm spring season due to thermal doming at 2–3°S was preferably expressed at the site south of the equator (GBS); increasing spring sedimentation was observed from 1989 to 1991.
4. Annual fluxes at GBN were largely determined by the summer flux magnitude; at GBS, annual fluxes were dominated by spring sedimentation during the TTS. Interannual flux variations were substantial, reaching 25% at GBN and as much as 76% at GBS.

The flux patterns indicated substantial seasonal and interannual variation in the eastern equatorial upwelling area. We also found important differences between both trap sites although they were located close to each other. The study area appeared to be highly variable, both spatially and temporally, with respect to surface water properties, atmospheric circulation (e.g., ITCZ movements), and the

resulting downward fluxes. Detailed studies covering the eastern (10°W) and western equatorial Atlantic (30°W) with N-S transects are currently underway and will increase our knowledge of sedimentation in the equatorial upwelling area. Long-term records and reconstructions of sea surface temperatures using stable isotopes of calcareous planktonic shells will provide information on the intensity of upwelling, year-to-year variations and occasionally occurring anomalies: e.g., El Niño-like responses (Hisard, 1980) in the eastern tropical Atlantic.

10.7 ACKNOWLEDGMENTS

We are grateful to the officers and crew of the research vessel *Meteor* for competent assistance in the deployments and recoveries of the moorings. We also thank G. Krause (AWI, Bremerhaven) and S. Catewicz for processing the current meter data. This research was funded by the Deutsche Forschungsgemeinschaft (Sonderforschungsbereich 261 at Bremen University, Contribution 88).

10.8 REFERENCES

Bishop, J. K. B., J. M. Edmond, D. R. Ketten, M. P. Bacon and W. B. Silkers (1977) "The chemistry, biology, and vertical flux of particulate matter from the upper 400 m of the equatorial ocean", *Deep-Sea Res.*, **24**, 511–548.

Boltovskoy, D., V. A. Alder and A. Abelmann (1993) "Radiolarian sedimentary imprint in Atlantic equatorial sediments: Comparison with the yearly flux at 853 m", *Mar. Micropaleontol.*, **23**, 1–12.

Düing W., F. Ostaapoff and J. Merle (1980) "Physical Oceanography of the tropical Atlantic Ocean during GATE", Global Atmospheric Research Program (GARP) *Atlantic Tropical Experiment*, Miami.

Fischer, G. and G. Wefer (1991) "Sampling, preparation and analysis of marine particulate matter", in D. C. Hurd and D. W. Spencer (eds) *The Analysis and Characterization of Marine Particles*, Geophysical Monograph, **63**, 391–397.

Gardner, W. and M. J. Richardson (1992) "Particle export and resuspension fluxes in the western North Atlantic", in G. T. Rowe and V. Pariente (eds) *Deep-Sea Food Chains and the Global Carbon Cycle*, Kluwer Acad. Publ., Dordrecht, 339–364.

Hastenrath, S. and J. Merle (1987) "Annual cycle of subsurface thermal structure in the Tropical Atlantic Ocean", *J. Phys. Oceanogr.*, **17**, 1518–1538.

Hedges, J. I. and D. C. Mann (1979) "The characterization of plant tissue by their lignin oxidation products", *Geochim. Cosmochim. Acta*, **43**, 1803–1807.

Hisard, P. (1980) "Observation de réponses de type "'El Niño' dans l'Atlantique tropical orientale Golfe de Guinée", *Oceanologica Acta*, **3**, 69–87.

Honjo, S. and M. R. Roman (1978) "Marine copepod fecal pellets: production, preservation and sedimentation", *J. Mar. Res.*, **36**, 45–57.

Houghton R. W. and C. Colin (1986) "Thermal structure along 4°W in the Gulf of Guinea during 1983–1984", *J. Geophys. Res.*, **91**, 11,727–11,739.

Houghton, R. W. (1989) "Influence of local and remote wind forcing in the Gulf of Guinea", *J. Geophy. Res.*, **94**, 4816–4828.

Lange, C. B., U. Treppke and G. Fischer (1994) "Seasonal diatom fluxes in the Guinea Basin and their relationships to trade winds, hydrography and upwelling events", *Deep-Sea Res.*, **41**, 859–878.

Lyle, M., R. Zahn, F. Prahl, J. Dymond, R. Collier, N. Pisias and E. Suess (1992) "Paleoproductivity and carbon burial across the California Current: The multitracers transect, 42°N", *Paleoceanography*, 7, 251–272.

Merle, J. (1980) "Variabilité thermique annuelle et interannuelle de l'océan Atlantique équatorial Est. L'hypothèse d'un 'El Niño' Atlantique", *Oceanologica Acta*, **3**, 209–220.

Müller, P. J. and R. Schneider (1993) "An automated leaching method for the determination of opal in sediments and particulate matter", *Deep-Sea Res.*, **40**, 425–444.

Peterson, R. G. and L. Stramma (1991) "Upper-level circulation in the south Atlantic Ocean", *Progr. Oceanogr.*, **26**, 1–73.

Richardson, P. L. and D. Walsh (1986) "Mapping climatological seasonal variations of surface current in the Tropical Atlantic using ship drifts", *J. Geophys. Res.*, **91**, 10,537–10,550.

Sancetta, C. (1992) "Comparison of phytoplankton in sediment traps time series and surface sediments along a productivity gradient", *Paleoceanography*, 7, 183–194.

Schütz, L. (1980) "Long range transport of desert dust with special emphasis on the Sahara", in T. J. Kneip and P. J. Lioy (eds) *Aerosols: Anthropogenic and Natural, Sources and Transport*, Annals of the New York Academy of Sciences, Vol. 338, New York, 515–532.

Servain, J., J. Picaut and A. J. Busalacchi (1985) "Interannual and seasonal variability of the tropical Atlantic Ocean depicted by sixteen years of sea-surface temperature and wind stress", in J. C. J. Nihoul (ed) *Coupled Ocean-Atmosphere Models*, Elsevier Oceano-graphy Series 40, Amsterdam, 211–237.

Servain, J. and D. M. Legler (1986) "Empirical orthogonal function analysis of tropical Atlantic sea surface temperature and wind stress", *J. Geophys. Res.*, **91**, 181–191.

Voituriez, B. and A. Herbland (1977) "Etude de la production pélagique de la zone équatoriale de l'Atlantique à 4°W. I. Relations entre la structure hydrologique de la production primaire", *Cah. O.R.S.T.O.M. sér Océanogr.*, **XV**, 313–330.

Voituriez, B. and A. Herbland (1981) "Primary production in the tropical Atlantic ocean mapped from the oxygen values of Equalant 1 and 2 (1963)", *Bull. Mar. Sci.*, **31**, 853–863.

Voituriez, B. and A. Herbland (1982) "Comparaison des systèmes productifs de l'Atlantique tropical est: Dômes thermiques, upwellings côtiers et upwelling équatorial", *Rapp. P.-v. Reun. Cons. int. Explor. Mer.*, **180**, 114–130.

Wefer, G. and G. Fischer (1993) "Seasonal patterns of vertical particle flux in equatorial and coastal upwelling areas of the eastern Atlantic", *Deep-Sea Res.*, **40**, 1613–1645.

11 Preliminary Data on Particle Flux off the São Francisco River, Eastern Brazil

T. C. JENNERJAHN, V. ITTEKKOT AND C. E. V. CARVALHO

11.1 INTRODUCTION

Fresh water and nutrient inputs from the rivers influence the biogeochemical processes in the coastal seas and affect the quality and quantity of material accumulating in marine sediments. The latter results both from the direct inputs of river-derived terrigenous material and from the changes in marine biogenic inputs. Changes in salinity brought about by fresh water, and the introduction of river-derived nutrients have been found to promote the growth of siliceous plankton which increased the fluxes of biogenic opal and organic matter (Ittekkot et al., 1991).

Here we present preliminary data on particle flux in a marine region off the São Francisco River in eastern Brazil (Figure 11.1). The São Francisco drains an area of 631133 km^2 (Paredes et al., 1983). It has an annual mean water discharge of 99 km^3 (Bessa and Paredes, 1990). The annual sediment discharge of 6×10^6 t is influenced by the construction of dams and the related retention of sediments in reservoir lakes (Milliman, 1975).

11.2 MATERIALS AND METHODS

A mooring system consisting of two PARFLUX Mark 7G-21 sediment traps was deployed from January 1995 to May 1995 at a location 50 km off the São Francisco River in eastern Brazil (10°56'S, 36°13'W; water depth 2100 m; Figure 11.1). The period of deployment coincided with the period of high water discharge of the river (Figure 11.2). The traps were positioned at water depths of 500 m and 1550 m. Prior to deployment the sampling cups were filled with seawater from 500 m water depth. To avoid organic matter decomposition cup waters were

Particle Flux in the Ocean
Edited by V. Ittekkot, P. Schäfer, S. Honjo and P. J. Depetris

poisoned with $HgCl_2$ (3.3 g l^{-1}). The traps were programmed to collect settling particles at intervals of 6 days (Table 11.1).

The samples were wet sieved and the fraction < 1 mm was split with a precision rotary splitter. The splits were filtered and the filters dried at 40°C. Material from one split was used for calculation of the total flux and for the analyses of total carbon, total nitrogen, carbonate and biogenic opal. Total carbon and nitrogen were analyzed by high temperature combustion with a Carlo Erba (Milan, Italy) Elemental Analyzer NA-1500. Inorganic carbon was measured conductometrically with a Wösthoff (Bochum, Germany) Carmhograph 6. Biogenic opal was determined photometrically as silicomolybdate complex using a modification of Mortlock and Froelich's (1989) method.

Organic carbon (C_{org}) was calculated as the difference between total carbon and carbonate carbon (C_{carb}) and the organic matter by multiplying organic carbon

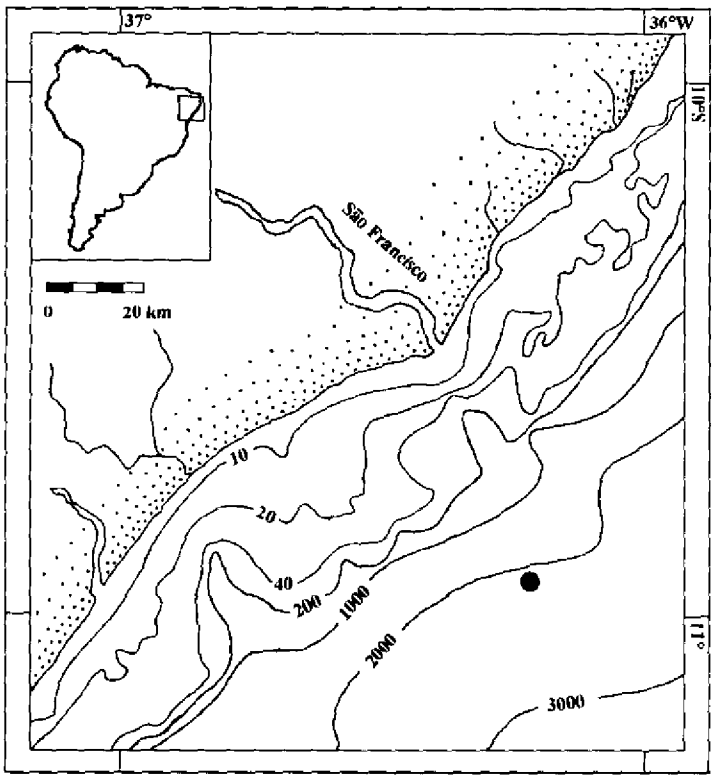

Figure 11.1 Location of the sediment trap system off the São Francisco River, eastern Brazil.

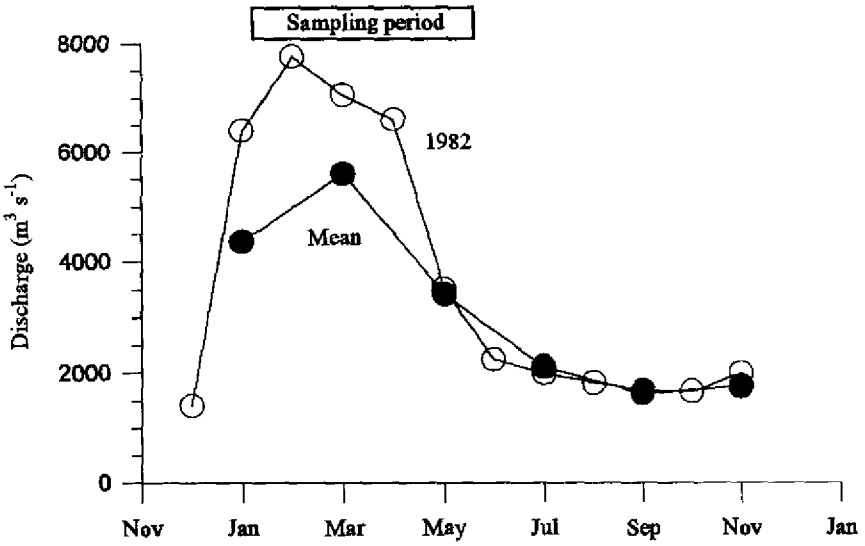

Figure 11.2 Discharge of the São Francisco River, eastern Brazil. Monthly discharge data from 1982 (open circles) from Paredes et al. (1983), bimonthly means (solid circles) from Coleman and Wright (1971). Bar on top of the graph denotes sampling period of the sediment trap system.

content with a factor of 1.8 (Müller et al., 1986). Lithogenic matter flux was estimated by subtracting the sum of carbonate, biogenic opal, total nitrogen and organic matter fluxes from the total flux. C/N, carbonate/opal and C_{org}/C_{carb} ratios were calculated by weight percent.

11.3 RESULTS AND DISCUSSION

The measured total flux for the 4 months of deployment period was 16.5 g m^{-2} in 1550 m water depth. The respective fluxes for carbonate, biogenic opal, lithogenics and organic matter for the same period were 5.5 g m^{-2}, 0.97 g m^{-2}, 8.8 g m^{-2} and 1.2 g m^{-2}, respectively. The observed flux variations were in the range of 42.2 to 292.2 mg m^{-2} d^{-1} for total material and of 18.3 to 95.5 mg m^{-2} d^{-1}, 2.3 to 16.3 mg m^{-2} d^{-1}, 18 to 160.5 mg m^{-2} d^{-1} and 3.3 to 18.8 mg m^{-2} d^{-1} for carbonate, biogenic opal, lithogenics and organic matter, respectively. The respective averages for the period of deployment were 130.9 mg m^{-2} d^{-1}, 43.3 mg m^{-2} d^{-1}, 7.7 mg m^{-2} d^{-1}, 69.7 mg m^{-2} d^{-1}, 9.5 mg m^{-2} d^{-1}. Carbonate, opal and lithogenics and organic matter contributed respectively 34.7%, 5.8%, 51.5% and 7.5% to the total flux.

Table 11.1 Total and component fluxes off the São Francisco River and their ratios.

Cup No.	Interval	Fluxes in mg m^{-2} d^{-1}						Ratios		
		Total flux	Carbonate	Opal	Litho-genics	C_{org}	N	C/N	Carb./ Opal	C_{org}/ C_{carb}
1	01/04 - 01/10/95	160.0	37.5	9.6	100.6	6.5	0.7	9.8	3.9	1.4
2	01/10 - 01/16/95	114.5	33.3	7.0	65.4	4.5	0.5	8.6	4.7	1.1
3	01/16 - 01/22/95	53.7	21.8	3.0	22.7	3.2	0.4	8.9	7.1	1.2
4	01/22 - 01/28/95	84.5	34.9	4.4	35.4	5.2	0.6	8.9	8.0	1.3
5	01/28 - 02/03/95	163.8	55.1	9.0	88.6	5.7	0.7	8.1	6.2	0.9
6	02/03 - 02/09/95	144.0	48.0	8.3	77.7	5.2	0.6	9.0	5.8	0.9
7	02/09 - 02/15/95	158.8	55.7	8.9	82.7	6.0	0.8	7.8	6.3	0.9
8	02/15 - 02/21/95	109.7	39.5	7.0	54.9	4.4	0.5	8.2	5.7	0.9
9	02/21 - 02/27/95	156.4	44.2	9.6	84.2	9.6	1.1	8.7	4.6	1.8
10	02/27 - 03/05/95	176.5	55.1	11.9	91.2	9.6	1.1	9.1	4.6	1.5
11	03/05 - 03/11/95	188.1	48.9	12.5	109.1	9.2	1.0	8.8	3.9	1.6
12	03/11 - 03/17/95	292.2	95.5	16.3	160.5	10.5	1.2	8.9	5.9	0.9
13	03/17 - 03/23/95	239.2	67.7	13.6	145.5	6.5	0.8	7.8	5.0	0.8
14	03/23 - 03/29/95	89.3	32.0	4.6	47.2	2.9	0.4	7.8	6.9	0.7
15	03/29 - 04/04/95	70.9	26.0	3.7	36.0	2.7	0.3	7.9	7.0	0.9
16	04/04 - 04/10/95	42.2	18.3	2.3	18.0	1.8	0.3	7.1	8.0	0.8
17	04/10 - 04/16/95	50.7	21.8	2.7	22.3	2.0	0.3	8.2	8.0	0.8
18	04/16 - 04/22/95	75.6	26.0	4.4	38.3	3.6	0.4	8.3	5.9	1.2
19	04/22 - 04/28/95	157.2	63.1	9.1	74.7	5.2	0.8	6.3	6.9	0.7
20	04/28 - 05/04/95	105.2	41.7	6.6	50.5	3.3	0.5	7.2	6.3	0.7
21	05/04 - 05/10/95	115.7	42.9	6.3	59.0	3.9	0.5	7.8	6.8	0.8

Maximum fluxes of biogenic and lithogenic components coincided with maximum discharge of the São Francisco during February and March (Figure 11.3). Despite the relatively low primary productivity in the coastal region (60–90 g C m^{-2} y^{-1}; Berger, 1989; Summerhayes et al., 1976) and the fairly low sediment input from the São Francisco River, the measured total flux of 16 g m^{-2} during the four month of deployment lies at the higher end of the annual fluxes measured in other marine regions of the world.

The carbonate/opal ratios of settling particles varied between 3.9 and 8, and the C_{org}/C_{carb} between 0.66 and 1.81. The average C_{org}/C_{carb} value of 1.0 is lower than that measured in the Bay of Bengal, a marine region affected by some of the largest rivers of the world (Ittekkot et al., 1991; this volume, Chapter 15) and are similar to or slightly higher than those measured at deeper traps (3000 m) in offshore regions (e.g., this volume, Chapter 7). Peak C_{org}/C_{carb} ratios of up to 1.8 between February and the middle of March coincided with the minimum carbonate/opal ratios (Figure 11.4). In general, peak total fluxes and the fluxes of individual biogenic and abiogenic components occured in the middle of March. However, for organic matter, nitrogen and biogenic opal the increase in fluxes occured three weeks earlier with increasing fresh water discharge from the São Francisco River. As has been observed in several other regions the fresh water input appears to promote the growth of siliceous plankton and enhance the sedimentation of both biogenic opal and organic matter (e.g., this volume, Chapter 15). Similar plankton bloom and particle flux patterns have been observed in the northern North Sea (Kempe and Jennerjahn, 1988) and the Black Sea (Hay et al., 1990).

Inner shelf sediments adjacent to the rivers of eastern Brazil between 8° and 24°S have a mean C_{org} content of 1.4% (Jennerjahn, 1994). Assuming that the lithogenic material collected in the trap originates from the São Francisco or its delta, the fluxes of organic matter from this source can be calculated by multiplying the fluxes of lithogenic matter with the average C_{org} content of the deltaic and shelf sediments. This will further allow estimation of the organic matter derived from autochthonous production. The results of this exercise are presented in Figure 11.5. In general, the contribution of allochthonous organic matter to total organic matter was about 19% with the maximum value in association with the peak total flux. However, its contribution to total C_{org} was comparatively smaller at the end of February and at the beginning of March, when C_{org} fluxes and the ratios of C_{org}/C_{carb} as well as carbonate/opal were higher.

These preliminary results suggest that despite the low sediment discharge, the São Francisco is of importance in the production and sedimentation of organic matter along the Brazilian continental margin.

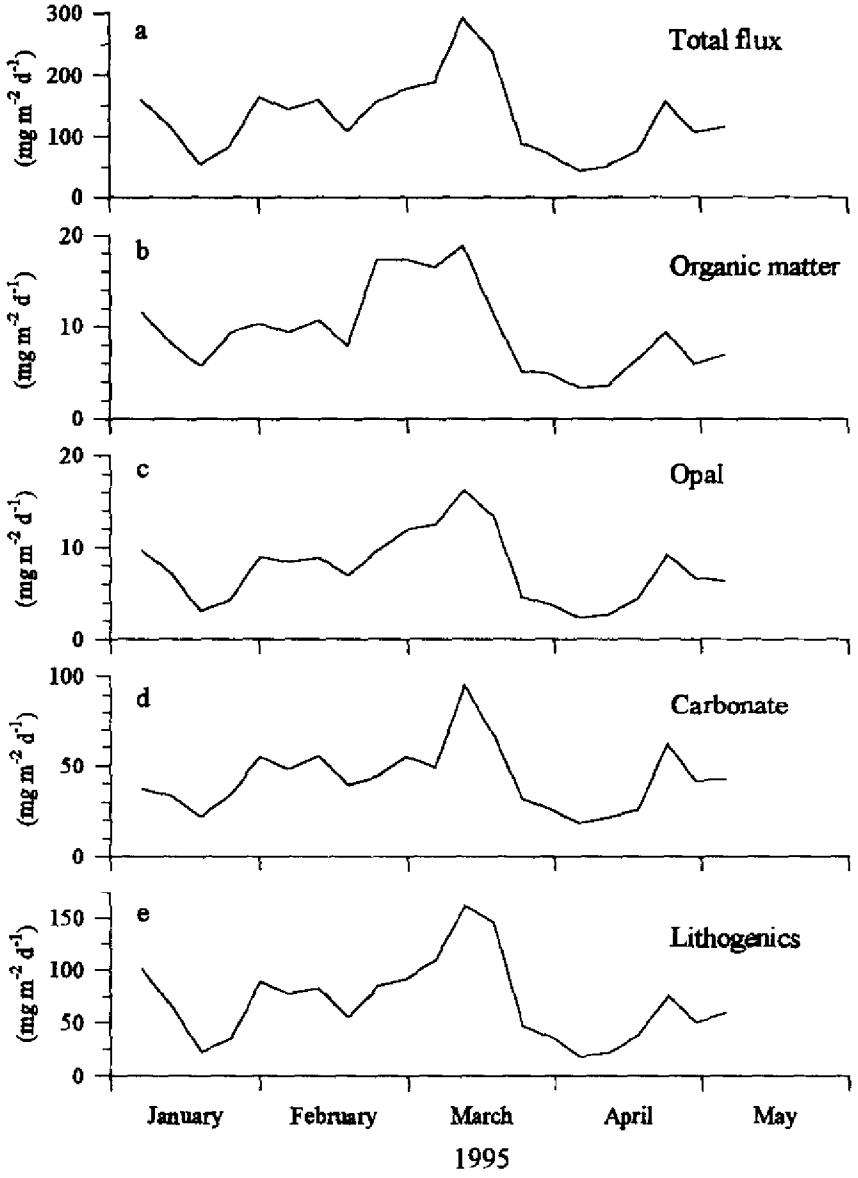

Figure 11.3 (a) Total, (b) organic matter, (c) opal, (d) carbonate, and (e) lithogenic fluxes off the São Francisco River.

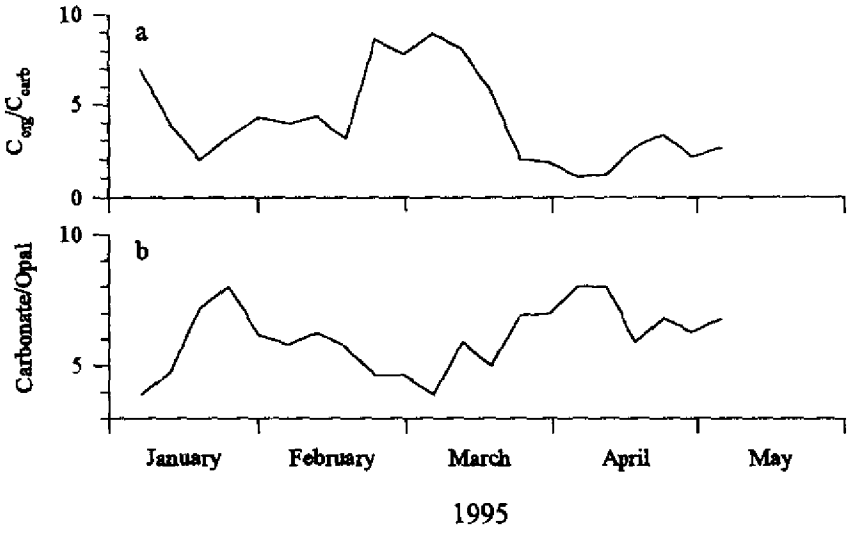

Figure 11.4 (a) C_{org}/C_{carb} and (b) carbonate/opal ratios off the São Francisco.

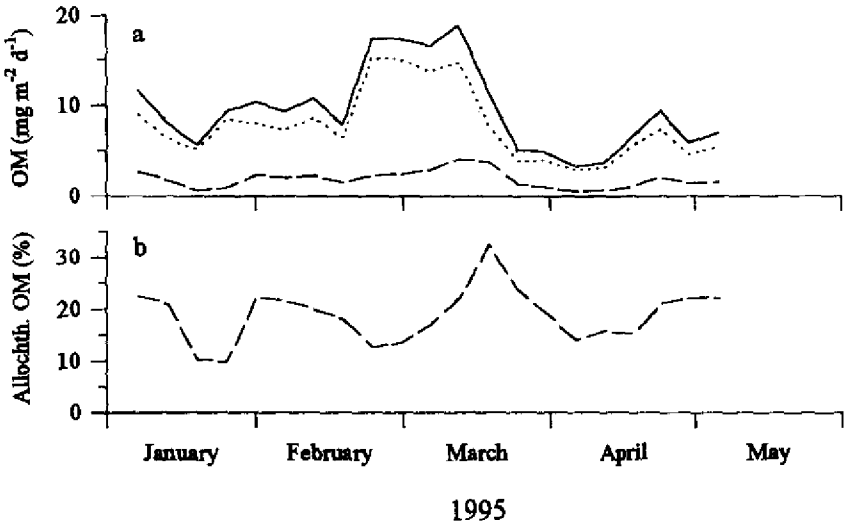

Figure 11.5 (a) Total organic matter flux (solid line), subdivided in autochthonous (dotted line) and allochthonous (dashed line) organic matter fluxes and (b) contribution of allochthonous organic matter to total organic matter off the São Francisco River.

11.4 ACKNOWLEDGMENTS

The project was carried out within the framework of science and technology cooperation between Germany and Brazil in the field of ocean sciences. We thank the officers and crew of R/V *Victor Hensen* for their assitance in the deployment and recovery of the mooring. Financial support for the project was provided by the Federal German Ministry for Education, Science, Research and Technology (BMBF, Bonn).

11.5 REFERENCES

Berger, W. H. (1989) "Global maps of ocean productivity" in W. H. Berger, V. S. Smetacek and G. Wefer (eds) *Productivity of the Ocean: Present and Past*, Dahlem Workshop Reports, John Wiley & Sons, Chichester, 429–455.

Bessa, M. F. and J. F. Paredes (1990) "Transporte do carbono e do nitrogênio orgânico e inorgânico dissolvidos pelo rio São Francisco, Brasil, durante um ano hidrológico (1984–1985)", *Geochim. Brasil*, **4**, 17–31.

Coleman, J. M. and L. D. Wright (1971) *Analysis of major river systems and their deltas: Procedure and rationale, with two examples*, Louisiana State University Press, Coastal Studies Series 28, 94 pp.

Hay, B. J., S. Honjo, S. Kempe, V. A. Ittekkot, E. T. Degens, T. Konuk and E. Izdar (1990) "Interannual variability in particle flux in the southwestern Black Sea", *Deep-Sea Res.*, **37**, 911–928.

Ittekkot, V., R. R. Nair, S. Honjo, V. Ramaswamy, M. Bartsch, S. Manganini and B. N. Desai (1991) "Enhanced particle fluxes in Bay of Bengal induced by injection of fresh water", *Nature*, **351**, 385–387.

Jennerjahn, T. C. (1994) "Biogeochemie der Sedimente des brasilianischen Kontinentalrandes und angrenzender Mangrovengebiete zwischen 8° und 24°S", Unpublished Dissertation, Fachbereich Geowissenschaften, Universität Hamburg, 152 pp.

Kempe, S. and T. C. Jennerjahn (1988) "The vertical particle flux in the northern North Sea, its seasonality and composition", in S. Kempe, G. Liebezeit, V. Dethlefsen and U. Harms (eds) *Biogeochemistry and Distribution of Suspended Matter in the North Sea and Implications to Fisheries Biology*, Mitt. Geol.-Paläontol. Inst. Univ. Hamburg, **65**, 229–268.

Milliman, J. D. (1975) "Upper continental margins sedimentation off Brazil: Part VI: A synthesis", *Contr. Sedimentol.*, **4**, 151–176.

Mortlock, R. A. and P. N. Froelich (1989) "A simple method for the rapid determination of biogenic opal in pelagic marine sediments", *Deep-Sea Res.*, **36**, 1415–1426.

Müller, P. J., E. Suess and C. A. Ungerer (1986) "Amino acids and amino sugars of surface particulate and sediment trap material from waters of the Scotia Sea", *Deep-Sea Res.*, **33**, 819–838.

Paredes, J. F., A. J. Paim, E. M. Costa Doria and W. L. C. Rocha (1983) "São Francisco River: Hydrobiological studies in the dammed lake of Sobradinho", in E. T. Degens, S. Kempe and H. Soliman (eds) *Transport of Carbon and Minerals in Major World Rivers, Part 2*, Mitt. Geol.-Paläont. Inst. Univ. Hamburg, No. **55**, 193–202.

Summerhayes, C. P., U. Melo and H. T. Barretto (1976) "The influence of upwelling on suspended matter and shelf sediments off southeastern Brazil", *J. Sed. Petrol.*, **46**, 819–828.

12 Organic Carbon Fluxes and Sediment Biogeochemistry on the French Mediterranean and Atlantic Margins

H. ETCHEBER, S. HEUSSNER, O. WEBER, A. DINET, X. DURRIEU de MADRON, A. MONACO, R. BUSCAIL AND J. C. MIQUEL

12.1 INTRODUCTION

It is now widely accepted that to obtain a better understanding of the oceanic organic carbon cycle special attention must be paid to continental margins. These areas represent some of the highest primary production zones of the ocean and receive important organic inputs from the continents (Jorgensen, 1983; Wollast and MacKenzie, 1989; Wollast, 1990). Organic fluxes to shelf and slope sediments are therefore generally higher than in the open ocean and the subsequent preservation of organic matter confer to margins the role of a preferential sink area for C_{org}.

ECOMARGE (Ecosystèmes de MARGE continentale), part of JGOFS-France, is a multidisciplinary program designed to study the transfer of matter and energy across margins, as well as the response of the benthic ecosystem to such transfers. This paper summarizes results obtained by this program over the last few years on continental margins of the northwestern Mediterranean and northeastern Atlantic. Carbon fluxes through the slope water column and data on the biogeochemistry of surficial sediments are presented and compared with the aim of giving new insights into the overall functioning of these areas and of elucidating the major factors controlling particle transfer processes in these highly contrasted environments.

12.2 SAMPLING SITES AND STRATEGY

In order to define the respective roles of physical, chemical and biological factors in controlling mass and carbon fluxes on continental margins, identical strategies

Particle Flux in the Ocean
Edited by V. Ittekkot, P. Schäfer, S. Honjo and P. J. Depetris

and methods were used during the ECOMARGE program to investigate two contrasting regions: the northwestern Mediterranean (Gulf of Lions) - a non tidal sea characterized by a fine-grained shelf sedimentation, and the northeastern Atlantic (Bay of Biscay) - a tidal sea with sandy-silty shelf sedimentation. Both regions, however, present the common feature of being subject to large riverine inputs (respectively the Rhône and the Gironde) and to a pronounced alongslope circulation of water masses. Results obtained by DYFAMED, another JGOFS-France program, on two northwestern Mediterranean sites representative of open ocean areas are also given for comparison (Figure 12.1 and Table 12.1).

12.2.1 MEDITERRANEAN SITES

In the Mediterranean experiment, the investigations focused on two sites within the Gulf of Lions: one located at the eastern entrance, off the Rhône River, and the other located at the southwestern end, off the Pyrenean coastline. At this latter site, four time series traps (cylindroconical model PPS3 from Technicap, 0.125 m^2 collection area, 6 receiving cups; Heussner et al., 1990) were moored in the Lacaze-Duthiers Canyon (site LD), in a 645 m deep water column, at depths of 50, 100, 300 and 600m (Monaco et al., 1990b). Three consecutive deployments of five sampling periods were obtained (ECO I, ECO II, ECO III), leading to a total of 15 samples; the sampling interval was 16 days. At the entrance of the Gulf of Lions, the moorings were located in the Grand-Rhône Canyon (site GR) and on the open slope (site IF) between the Grand-Rhône and Petit-Rhône canyons (Monaco et al., in preparation). Four traps were moored in a 965 m water column, at 80, 200, 600 and 900 m depth in the axis of the canyon. A single trap was moored at 900 m, near the bottom of the interfluve site. The sampling interval was set at 15 days.

The two DYFAMED moorings were located in the Ligurian Sea, at 12.8 miles off Corsica (DYFAMED 1) and 28 miles off continental France (DYFAMED 2), in a water column of respectively 2100 and 2300 m (Miquel et al., 1993; 1994). These sites were equipped with PPS3 traps at 80–100 m, 200 m, 500 m and 1000 m. Sampling intervals varied between 9 and 15 days.

12.2.2 ATLANTIC SITES

Traps were deployed on two experimental sites within the Cap-Ferret Canyon, in the southern part of the continental slope of the Bay of Biscay (Heussner et al., 1996). The first mooring site (MS1), equipped with 4 PPS3 traps and associated Aanderaa current meters, was located at the confluence of the northern and southern axes of the upper canyon, in a 2300 m water column. Traps were deployed at nominal depths of 380, 1350, 1900 and 2250 m. The second site (MS2), located at the foot of the slope, in a 3000 m water column, was equipped with two

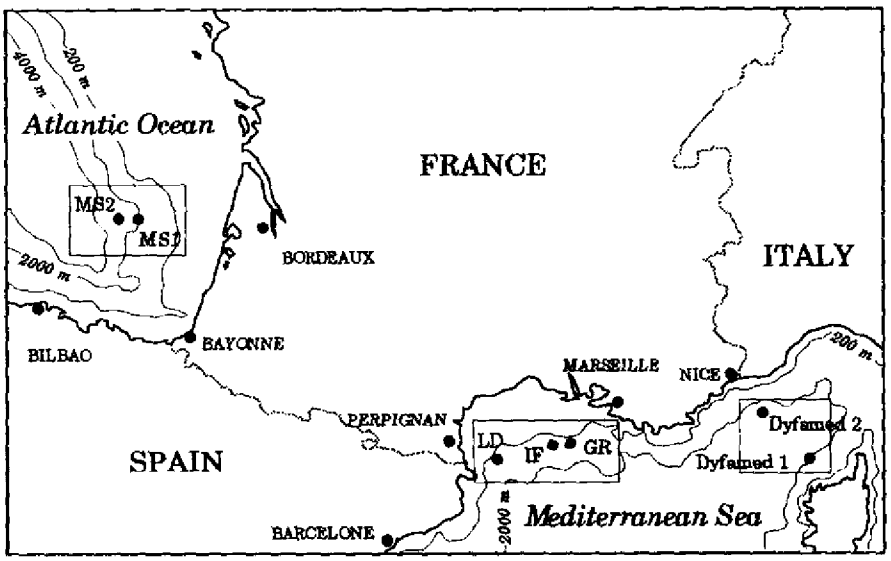

Figure 12.1 Location of the sediment trap mooring sites from the various ECOMARGE experiments on the northwestern Mediterranean (Gulf of Lions) and northeastern Atlantic (Bay of Biscay) continental margins. GR: Grand-Rhône Canyon; IF: Grand-Rhône open slope; LD: Lacaze-Duthiers Canyon; MS1 and MS2: mooring sites of the Cap-Ferret canyon. DYFAMED 1 and 2 are open ocean moorings from the French DYFAMED program in the Ligurian Sea.

Table 12.1 Location and sampling periods of the various moorings deployed during the ECOMARGE and DYFAMED experiments.

	Latitude N	Longitude E	Water depth m	Sampling period
MEDITERRANEAN SITES				
GR: Grand Rhône Canyon	42°50'	04°49'	965	Jan. 1988 - Jan. 1989
IF: Grand Rhône Open Slope	42°45'	04°46'	960	Jan. 1988 - Jan. 1989
LD: Lacaze-Duthier Canyon	42°29'	03°29'	645	Jul. 1985 - Apr. 1986
DYFAMED site 1	42°44'	08°32'	2100	Jan. 1987 - Oct. 1988
DYFAMED site 2	43°25'	07°52'	2300	Dec. 1988 - Nov. 1990
ATLANTIC SITES				
Cap-Ferret Canyon MS 1	44°43'	02°17'	2290	Jun. 1990 - Aug. 1991
Cap-Ferret Canyon MS 2	44°47'	02°38'	3010	Jun. 1990 - Aug. 1991

traps, at 1900 and 2950 m depth. Samples were collected over a period of 14 months, during 3 consecutive deployments. Sampling intervals were respectively 20 (ECOFER II), 27 (ECOFER III) and 16 days (ECOFER IV).

12.3 RESULTS

12.3.1 SPATIAL VARIATIONS IN TOTAL MASS AND ORGANIC CARBON FLUXES

All results from the different sites are reported in Table 12.2.

12.3.1.1 Mediterranean sites

At the GR and LD locations, in the Gulf of Lions, time-weighted mean mass and C_{org} fluxes were quite high. They increased with depth from the surface to the bottom. The comparison of fluxes at the GR and LD sites shows that, at all depths, fluxes increased from the northeast to the southwest (i.e., downstream the general circulation of water masses): 148 to 639 mg m^{-2} d^{-1} in surface traps and 268 to 6025 mg m^{-2} d^{-1} in near-bottom traps for mass fluxes; 27 to 121 mg m^{-2} d^{-1} and 9 to 83 mg m^{-2} d^{-1} for C_{org} fluxes. At the LD station, the most striking feature was the strong reduction in C_{org} fluxes between the two shallowest traps (50 m and 100 m), and the strong increase in total mass fluxes and, to a lesser extent, in C_{org} fluxes at 300 and 600 m. At both stations, the C_{org} content of settling particles strongly decreased from surface to deeper traps: from 182 to 34 mg C_{org} g^{-1} (dry weight) at the GR site and from 189 to 14 mg C_{org} g^{-1} at the LD site. Fluxes obtained at the IF station, on the open slope, were lower than those observed nearby within the GR canyon: 72 and 6 mg m^{-2} d^{-1}, respectively for total mass and C_{org} fluxes. The amount of particulate C_{org} in the trapped material remains, however, important (83 mg C_{org} g^{-1}).

Fluxes recorded at the open ocean stations from the DYFAMED experiment were quite different. Mean mass fluxes were low and decreased drastically with depth from 93 mg m^{-2} d^{-1} in surface waters (100m) down to 33 mg m^{-2} d^{-1} at 1000 m (mid-water). Organic carbon fluxes varied in the same way, from 17 mg m^{-2} d^{-1} in the shallow trap down to 3.3 mg m^{-2} d^{-1} at 1000 m. At all depths, C_{org} concentrations in trapped particulates were high: 183 mg C_{org} g^{-1} at 100 m and still 100 mg C_{org} g^{-1} at 1000 m.

12.3.1.2 Atlantic sites

At MS1, time-weighted mean total mass fluxes for the whole experiment (15 months) increased continuously from 500 mg m^{-2} d^{-1} in the surface trap, down to the near-bottom trap, where a mean flux of 1470 mg m^{-2} d^{-1} was found. The same downward flux increase was observed for MS2 traps, where the values increased from 326 to 457 mg m^{-2} d^{-1}. Fluxes registered by the 1900 m trap of MS2 were always lower than those measured at the same depth on MS1. This general trend of flux increase with depth and seaward decrease was also observed for C_{org}

Table 12.2 Time-weighted annual mean mass fluxes (mg m^{-2} d^{-1}) and organic carbon fluxes (mg m^{-2} d^{-1}) and content (%) on French continental margins. GR: Grand-Rhône Canyon; IF: Grand-Rhône open slope; LD: Lacaze-Duthiers Canyon; MS1 and MS2: mooring sites of the Cap-Ferret Canyon. DYFAMED 1 and 2 are open ocean moorings from the French DYFAMED program in the Ligurian Sea.

Mooring Site		Surface Water		Intermediate Water		Deep Water
MEDITERRANEAN SEA						
	Trap depth	85	200	500		900
GR	*Mass Flux*	148	253	387		268
(1000 m)	C_{org} *Flux*	27	15	18		9
	C_{org} %	18.2	5.9	4.7		3.4
	Trap depth					900
IF	*Mass Flux*					72
(1000 m)	C_{org} *Flux*					6
	C_{org} %					8.3
	Trap depth	50	100	300		600
LD	*Mass Flux*	639	379	3108		6025
(650 m)	C_{org} *Flux*	121	21	57		83
	C_{org} %	18.9	5.5	1.8		1.4
	Trap depth	100	200	500		1000
DYFAMED	*Mass Flux*	93	82	36		33
Site 1 & 2	C_{org} *Flux*	17	11	3.6		3.3
	C_{org} %	18.3	13.4	10.0		10.0
ATLANTIC OCEAN						
	Trap depth		380	1350	1900	2250
MS1	*Mass Flux*		498	768	1197	1470
(2300 m)	C_{org} *Flux*		23	28	32	41
	C_{org} %		4.6	3.6	2.7	2.8
	Trap depth				1900	2950
MS2	*Mass Flux*				326	457
(3000 m)	C_{org} *Flux*				14	15
	C_{org} %				4.3	3.3

fluxes: two-fold increase between the MS1 surface and near-bottom traps (23 to 41 mg m^{-2} d^{-1}) and two-fold decrease between the two at the same depth. Organic carbon content of the trapped particles slightly decreased with depth at both sites. At MS1 for example the flux-weighted mean content decreased from 46 mg C_{org} g^{-1} in the surface trap to 28 mg C_{org} g^{-1} in the near-bottom trap.

12.3.2 SEASONAL VARIATIONS IN TOTAL MASS AND ORGANIC CARBON FLUXES

12.3.2.1 Mediterranean sites

Variations of total mass and C_{org} fluxes with time and depth are given in Figure 12.2. At both mooring sites located at the entrance of the Gulf of Lions (IF and GR), no clear seasonal trend in total mass and C_{org} fluxes were observed: fluxes were quite constant for most part of the experiment, except for a very important flux increase recorded by all traps and which lasted roughly two months (around day 100 of the experiment). On the contrary, at the exit of the Gulf of Lions, within the LD Canyon, total mass and C_{org} fluxes were characterized by a high seasonal variability (Monaco et al., 1990a, b). At 50 m, fluxes varied by one order of magnitude depending on the season (114 to 1500 mg m^{-2} d^{-1}), with the highest values observed during summer. The strong reduction in fluxes between the 50 m and the 100 m traps suggests important recycling processes (degradation and/or consumption) of the organic-rich particles settling through the upper water column. Mass fluxes at 300 and 600 m depth showed a general trend to increase from summer to winter with respective peaks at around 10000 and 20000 mg m^{-2} d^{-1}, which coincided roughly with storm and rainfall events (Monaco et al., 1990b). Secondary peaks were observed in July (both depths) and in mid-September (300 m). It was clear that the highest mass fluxes were characterized by low C_{org} content, suggesting a terrigenous and/or resuspended origin of the trapped particles.

At the DYFAMED sites, fluxes were characterized by a high seasonal variability: they were highest in winter and spring (330-350 mg m^{-2} d^{-1}) and lowest in late summer (5.5 to 8.4 mg m^{-2} d^{-1}). The C_{org} fluxes followed approximately the same pattern as total mass fluxes (Peinert et al., 1992; Miquel et al., 1993; 1994).

12.3.2.2 Atlantic sites

The strongest temporal variations were observed in the surface traps, where mass fluxes varied from a few tens of mg to almost 1.5 g m^{-2} d^{-1} (Figure 12.3). At any depth, there was an important similarity between mass and C_{org} flux variations. The most striking feature is that no clear seasonal trend was detected in the variations of the total mass and organic fluxes (Heussner et al., 1996). Flux changes were rapid and the variation from one sample to the next one was sometimes equivalent to the overall flux range observed at any given depth. C_{org} content of settling particles varied between 30 and 50 mg C_{org} g^{-1} and was quite homogenous over the entire experiment. Only a few peaks were observed on both mooring lines. Based on the study of coccolithophorid fluxes, Beaufort and Heussner (1996) interpreted these peaks, which were also registered by the deepest traps, as primary production signals directly derived from the overlying waters.

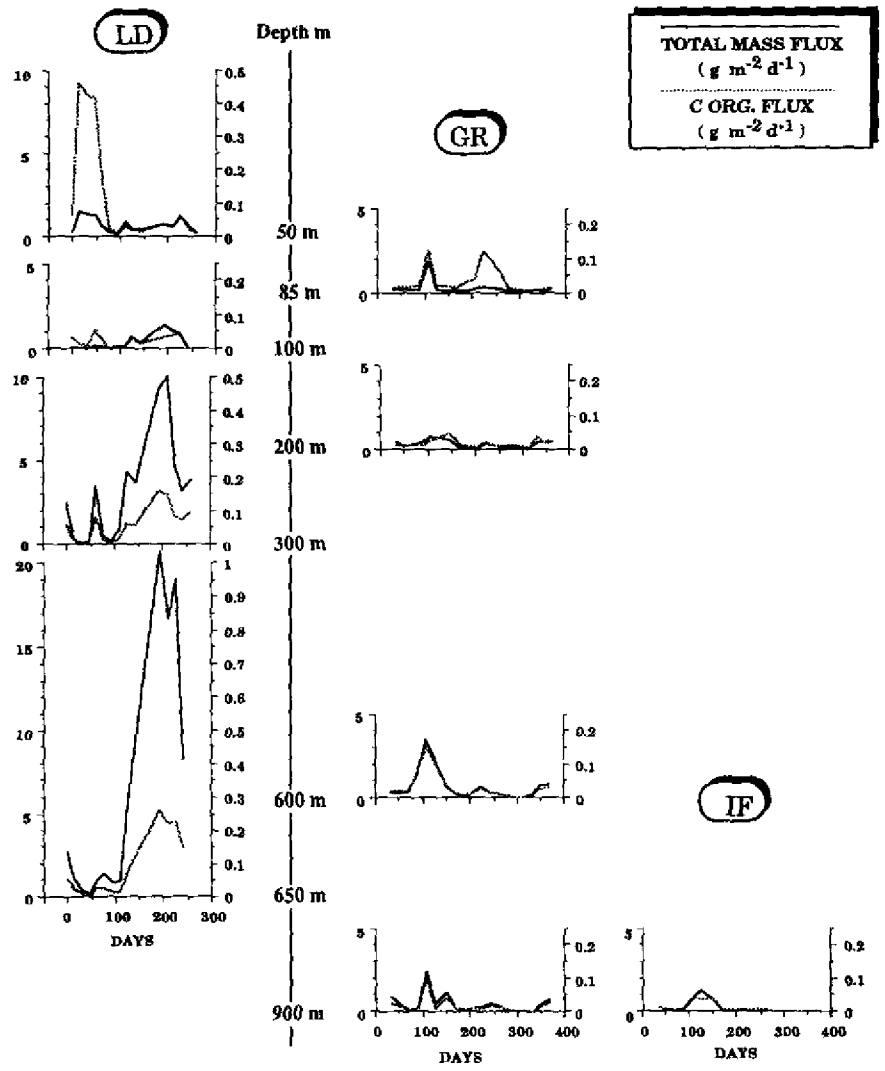

Figure 12.2 Time series plots of total mass (plain lines) and organic carbon (C_{org}) fluxes (dotted lines) at various locations and depths on the Mediterranean margin. LD: Lacaze-Duthiers Canyon; GR: Grand-Rhône Canyon; IF: open slope. See Table 12.1 for more details on mooring position and date of deployment.

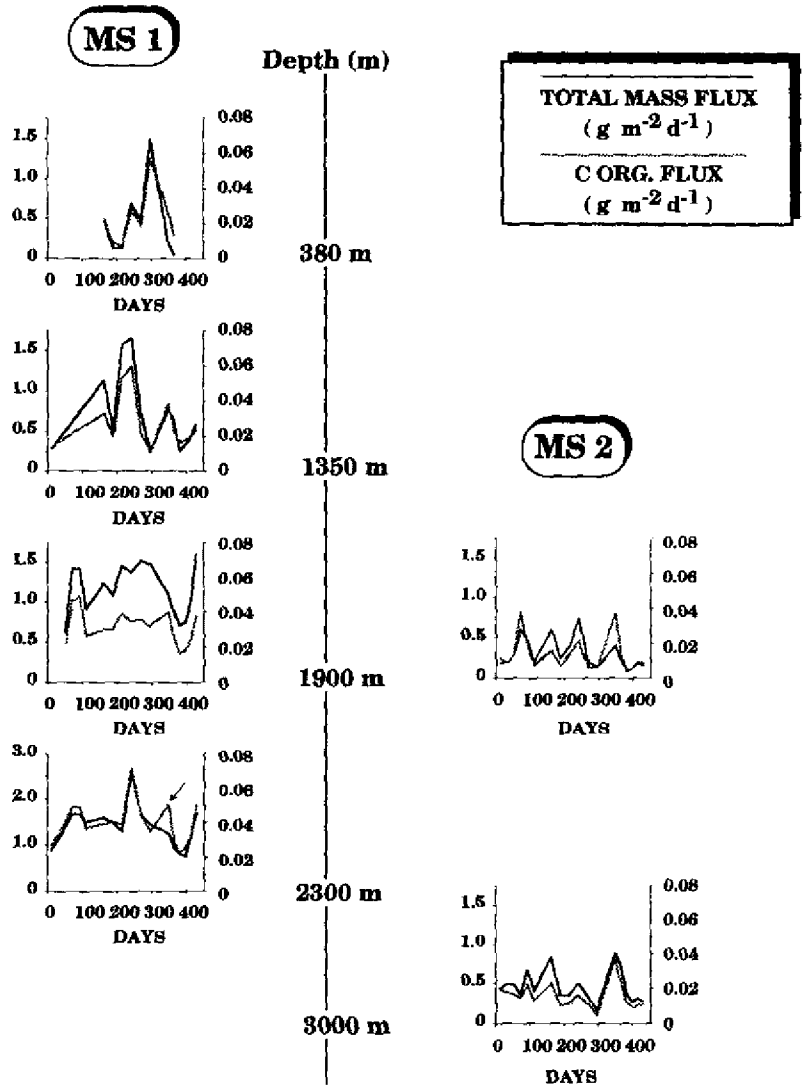

Figure 12.3 Time series plots of total mass (plain lines) and organic carbon (C_{org}) fluxes (dotted lines) at the two mooring sites on the Atlantic margin. MS1: Cap-Ferret Canyon, 2300 m; MS2: Cap-Ferret Canyon, 3000 m. See Table 12.1 for more details on mooring position and date of deployment.

12.3.3 BIOGEOCHEMISTRY OF SURFICIAL SLOPE SEDIMENTS

Both the northwestern Mediterranean and northeastern Atlantic margins are characterized by similar C_{org} distributions within the sediments and by high sedimentation rates, which underline the role of margins as preferential accumulation areas for organic matter. Organic content in the slope sediments are, in fact, high in comparison to those observed on the shelf, or in deep-sea fans and deep ocean sediments: on the Mediterranean side, 6–9 mg g^{-1} in the muddy deposits of the canyon, and 2–5 mg g^{-1} in circalittoral muds and silts or deep-sea fan sediments (Buscail et al., 1995); on the Atlantic side, 13–18 mg g^{-1} for muddy material from the Cap-Ferret Canyon, and 1–5 mg g^{-1} for sandy and silty sediments from the continental shelf (Etcheber et al., 1996). On a finer scale, in both margins, the highest C_{org} contents were found within an intermediate zone at the mid-slope depth (600–1300 m in the Mediterranean; 1500–2000 m in the Atlantic). The complex bathymorphology of the slope and the general circulation of water masses can induce the observed gradients in the distribution of high contents in sedimentary C_{org} (Buscail and Germain, 1995; Etcheber et al., 1996): for example, the canyon axes are enriched in comparison to the adjacent open slopes in the Mediterranean Sea.

Another feature common to both margins is the high sedimentation rates calculated from ^{210}Pb activities: 0.19 cm y^{-1} in the NE side of the Lacaze-Duthiers Canyon (Buscail et al., 1996); 0.37 cm y^{-1} at the head of the Cap-Ferret Canyon and 0.20 cm y^{-1} at 2300 m (Radakovitch and Heussner, 1996). These values are probably overestimated, due to bioturbation processes, but they yield, as a first approximation, the same high C_{org} accumulation rate, on the order of 10 g C m^{-2} y^{-1} at 2300 m in Atlantic, and at 650 m in the Mediterranean.

Besides these similarities between the two margins, there are also a some marked differences. On the northwestern Mediterranean margin, a seasonal response of the surface sediment to the near-bottom organic fluxes was observed (Figure 12.4). The amount of C_{org} increased progressively in the first centimeter of sediment during autumn and winter. During spring, one extra milligram of C_{org} was found to be stored per gram of sediment (Buscail et al., 1990). During this period, organic matter became increasingly more labile. The increase of amino acids was five-fold and sugars increased by a factor of 1.2. These values were well correlated with near-bottom C_{org} fluxes, which increased by a factor of 10 during this period (from 21 to 217 mg C_{org} m^{-2} d^{-1}). Between summer and the following winter to early spring period, amino acid and sugar fluxes increased respectively from 5 to 170 mg m^{-2} d^{-1} and from 3 to 28 mg m^{-2} d^{-1}. These inputs of labile material explain the increasing biodegradability of organic matter observed within the surficial sediments. Seasonal variations were also observed at DYFAMED station 2, located much deeper, at 2300 m: an increase of the C_{org} content was found between winter and early spring (from 5.3 to 6.8 mg g^{-1}). During the following periods, a gradual increase of C_{org} content was observed from spring

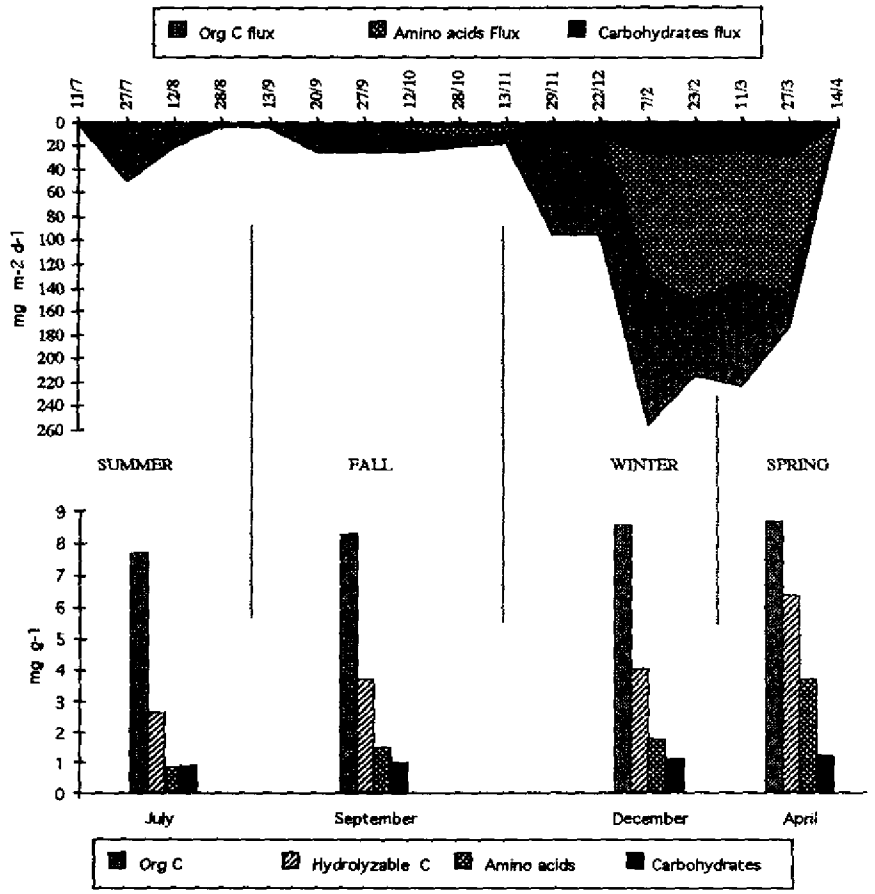

Figure 12.4 Time series plots of organic constituents fluxes in the near-bottom trap (600 m) of the Lacaze-Duthiers site (NW Mediterranean) (upper Figure) and contents of the same in the underlying surficial sediments (lower Figure).

(6.0 mg g^{-1}) to summer (6.6 mg g^{-1}) and autumn (7.3 mg g^{-1}) (Buscail, unpublished data).

On the contrary, the Atlantic margin, presents no marked seasonal variations in the organic fraction of surficial sediments. The biochemical characteristics of surficial sediments in the Cap-Ferret Canyon remained relatively constant over the year: surficial C_{org} contents and even protein concentrations in the first millimeter sediment did not reveal any significant seasonal trend (Etcheber et al., 1996).

Another important difference between both margins concerns the remineralization activity within the surficial sediments, which was less important on the Atlantic side. This is seen in the ratio between C_{org} content in particles of the

near-bottom sediment traps (30 mg g^{-1} on average on the Atlantic margin and 18 mg g^{-1} on the Mediterranean margin) and surficial sediments (18 mg g^{-1} in the first millimeter at the Atlantic site and 8 mg g^{-1} at the Mediterranean site) is 1.7 in the Cap-Ferret Canyon (Etcheber et al., 1996) and reaches 2.2 on the Mediterranean margin (Buscail et al., 1990; Buscail, 1991).

The input of natural organic matter at the sediment-water interface was simulated by injection of ^{14}C-labelled diatoms (*Navicula incerta*) in the overlying water of sediment cores. When comparing incubation experiments on the Atlantic and Mediterranean margins, the main differences are the lower quantity of CO_2 and the lower proportion of metabolites released in overlying waters of cores from the Cap-Ferret Canyon compared to those sampled within the Rhône Canyon (Figure 12.5) (Buscail, 1992; Buscail and Guidi-Guilvard, 1993). Metabolic processes responsible for the release of dissolved organic matter are clearly less pronounced on the Atlantic side, while the proportion of ^{14}C incorporated into sediments from the Cap-Ferret Canyon is higher than for the Rhône Canyon. This lower degradation activity at the Atlantic sediment-water interface can be related

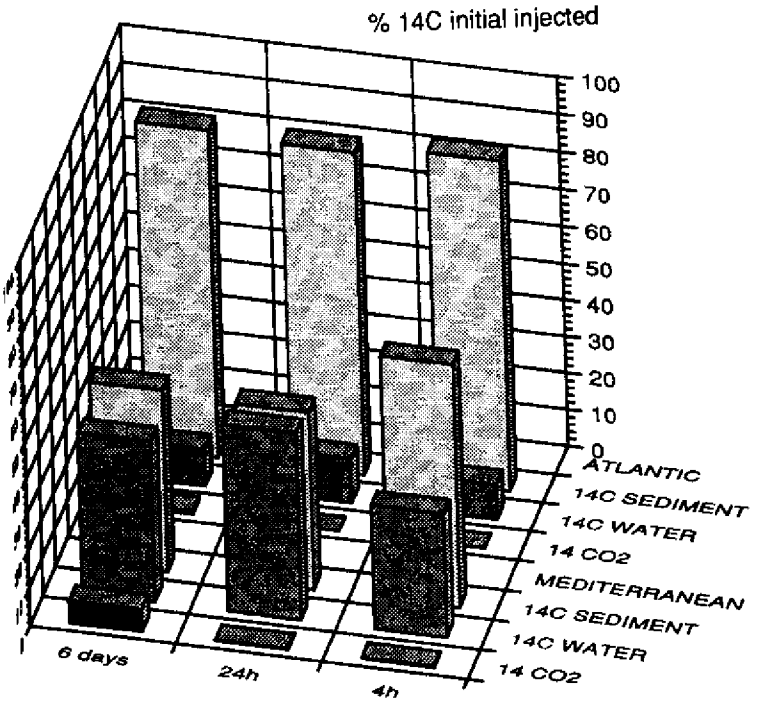

Figure 12.5 Distribution, after various periods of incubation, of ^{14}C-labelled diatoms (*Navicula incerta*), as per cent of the amount of ^{14}C initially injected in the water overlying surficial sediment cores.

to the low temperature of bottom waters (3°C) compared to 13°C in the deep Mediterranean waters and also to a less abundant benthic biomass in the Atlantic compared to the Mediterranean sea (De Bovée et al., 1990; Dinet et al., 1993).

12.4 DISCUSSION

Several features of the overall functioning of these two French margins can be drawn from the data on total mass, organic fluxes and quality of sedimentary organic matter, summarized in Table 12.3.

Table 12.3 Major characteristics of the French northwestern Mediterranean and northeastern Atlantic continental slopes with respect to mesoscale water dynamics, particle flux pattern and sediment response.

Environmental characteristics	Mediterranean Site	Atlantic Site
Alongslope water circulation	persistent unidirectional	fluctuant bidirectional
Flux pattern on the slope	depth increase seaward decrease advection-dominated	
Sources	direct seasonal pulses terrigenous >> marine	delayed periodic, non seasonal pulses terrigenous >> marine
Sedimentary record	strong seasonality stronger biodegradation of organic matter	no seasonality weaker biodegradation of organic matter

12.4.1 IMPORTANCE OF DYNAMICAL FACTORS ON THE TRANSFER OF PARTICLES

The general circulation of water masses is a predominant factor, if not the most important one, controlling the distribution of suspended and settling particles in the margin environments studied during ECOMARGE. Indeed, in the northwestern Mediterranean, some important features observed during our experiments could be linked to the cyclonic Liguro-Provençal Current (L-PC), which follows the continental slope from the coast of Provence to the Catalonian Sea (Millot, 1990). The seaward extension of turbid layers was directly controlled by the position of the L-PC. This current closely follows the shelf break in the northeast (entrance), but moves progressively further offshore in the southwestern part (exit)

of the Gulf of Lions. This shift induced an increase of suspended particles (by a factor of 7) between the entrance and the exit of the Gulf of Lions (Durrieu de Madron et al., 1990). Total mass fluxes increased by roughly the same factor between the GR and LD canyons (Monaco et al., 1990b).

The general circulation is quite more complex on the Atlantic side, but several physical processes with different temporal variabilities were recognized as playing a role in particle distribution and fluxes (Castaing et al., 1996a, b; Durrieu de Madron et al., 1996; Heussner et al., 1996). Seasonal thermohaline fronts, located either on mid-shelf during winter or at the shelf break during summer, definitely represent a dynamical barrier reducing seaward transfer of shelf particles, as demonstrated by shelf nepheloid structures (Durrieu de Madron et al., 1996); on the contrary, particle transport towards the slope could be enhanced during the transitional periods of front formation (late spring) and disappearance (fall). Hydrodynamic processes, associated with these fronts (i.e., internal waves, eddies, upwelling), participate in the transfer of particulate matter. On the continental slope, inside the canyon, recorded speeds were linked to cycles of semi-diurnal and lunar tides, and they varied accordingly. Residual speeds were low (< 2 cm s^{-1}) and always directed upslope, a feature which tends to confine particles in the upper canyon, where the quiet environment favors deposition. Above 600 m, the alongslope residual flow was preferentially to the north, but sudden, occasional changes resulted in southward currents. Most of the particle sources are therefore to be sought in areas south of the experimental sites (see below). Below 600 m, residual flow of the different water masses were generally directed northward and residual speeds were low (around 2 cm s^{-1}).

12.4.2 IMPORTANCE OF ADVECTION

Particle flux increase with depth is one of the most characteristic features of continental margins (e.g., Biscaye et al., 1988; Monaco et al., 1990a; Biscaye and Anderson, 1994; Heussner et al., 1996). The phenomenon is more or less marked at the different sites. The intensity of the flux increase with depth depends on the location on the slope; i.e., with the intensity and position of the general alongslope circulation and the position of particle sources. On the Mediterranean margin, the depth effect increases from the GR to LD sites: at similar depths, advection becomes more important in the downstream direction. This effect could not be studied on the Atlantic margin as only one transect was used. On both margins also, the importance of advective inputs decreased seaward (Monaco et al., 1990b; Heussner et al., 1996); such a decrease can be considered as a quite common feature of particle fluxes on continental margins, as it was also observed in other experiments such as SEEP-I and SEEP-II in the Middle Atlantic Bight (Biscaye et al., 1988; Biscaye and Anderson, 1994). According to the intensity of advective processes, margins can be classified into two categories (Heussner et al., 1993): "oceanic" margins, which are characterized by a C_{org} flux decreasing with depth

(e.g., the GR site) similar to open ocean systems (e.g., the DYFAMED sites), and "continental" margins, which are characterized by an important C_{org} flux increase at depth (e.g., the LD, MS 1 and MS 2 sites)

By examining the spatial and temporal characteristics of mass and major constituent fluxes in the light of prevailing hydrodynamical conditions, Heussner (1995) and Heussner et al. (1996) proposed a scenario of particle transfer in the Cap-Ferret Canyon, which helps to understand how advection operates. The model takes into account recent considerations about particle transfer and trap measured fluxes (e.g., Heussner and Fowler, 1987; Siegel et al., 1990), the general circulation of slope water masses (Durrieu de Madron et al., 1996), and the main features of the flux pattern, namely a flux increase with depth at each mooring and seaward decrease between the two mooring sites. Particle trajectories are oblique, since they are mainly controlled by the motion of alongslope flowing water masses. All particles arriving at depth on the slope are therefore advected from an "upstream" source. The two mooring sites are working in parallel, which means that there is no direct transfer between MS1 and MS2. Fluxes are higher at MS1 because of a seaward decreasing gradient in the particle concentration within the source. The fact that fluxes increase with depth at each mooring results from a limited horizontal extension of the source and/or from a downstream decreasing gradient in the particle concentration of the source. Progressive discharges of the settling particles through the water column, as the water masses move downstream, leads to more particles reaching the deep traps compared to the shallow ones. This scenario was further improved by Radakovitch and Heussner (1996), who recognized two major sources, on the basis of a mass balance budget for ^{210}Pb, in this region. One is located in shallow waters from the outer shelf and upper slope (<380 m; i.e., the depth of the shallowest trap of MS1) and supplies the entire slope region (i.e.; MS1 and MS2). The second, probably located deeper (at depths between 380 and 1350 m), feeds only the upper and intermediate slope region (i.e.; MS1, but not MS2). The fact that the major constituents (i.e.; organic and inorganic carbon, biogenic silica, lithogenic fraction) of the trapped particles at depth exhibit a relative temporal constancy indicates that both sources represent quite homogenous particle stocks which could be dominated by resuspended material.

12.4.3 SEASONAL VARIABILITY

Seasonal variability of mass fluxes can be linked to climatic and biological factors (Monaco et al., 1990b): at the exit of the Gulf of Lions (LD site), two winter peaks at 300 m and 600 m depth coincided with storms and continental rainfall events registered at the shelf site. Secondary peaks, observed in July (both depths) or in Mid-September (300 m), enriched in C_{org}, were mainly composed of biogenic constituents and related to surface phytoplankton blooms.

On the Atlantic site, at any depth, particle fluxes did not reveal any clear seasonal trend. Direct signals from phytoplanktonic blooms were nevertheless recognized, even in the deep traps, but were not large enough to significantly affect the overall variability of the bulk material (Beaufort and Heussner, 1996). Advection of large amounts of particles, with a strong resuspension and/or continental origin, from the above-mentioned shelf and upper slope sources diluted the primary biogenic signal. Thus, it is less easy to determine the lack of seasonal trend in the lithogenic contribution. One possible explanation lies in the dimensions of the margin: the distance from the main continental sources (the Gironde estuary essentially and other southern sources), which exhibit strong seasonal variations, could prevent direct inputs of material to the slope (Ruch et al., 1993). Continental inputs do not arrive at the slope as directly as in the Gulf of Lions. Sedimentation of particles onto the shelf and upper slope sediments followed by subsequent resuspension and transport by the general alongslope circulation of water masses could level out the original seasonal variations of the continental sources.

12.4.4 BENTHIC RESPONSE TO ORGANIC PARTICLE FLUXES ON MARGINS

Some interesting points can also be derived from the comparison of the distribution of sedimentary organic matter between the two margins, and from the biogeochemical processes observed within the surficial sediments.

First, the combination of high sedimentation rates and high C_{org} contents leads to the conclusion that such environments are preferential C_{org} accumulation areas (Buscail et al., 1990; Etcheber et al., 1996).

Second, the Lacaze-Duthiers Canyon presents some important erosion zones on the flanks, characterized by low C_{org} content, and areas of high sedimentation rates and high C_{org} concentrations within the canyon axis (Buscail and Germain, 1995). Such local differences within the canyon do not exist in the Cap-Ferret Canyon (Etcheber et al., 1996). This feature seems to be related to the general morphology of these canyons: the smaller the size, the greater the spatial and temporal distribution heterogeneities of sedimentary organic matter. Complex interactions of bottom topography with the general circulation could be responsible of these size effects.

Third, the bottom water temperature seems to have a direct influence on the intensity of organic matter degradation processes at the sediment-water interface: the higher benthic activity on the Mediterranean margin, compared to the Atlantic, could be related to the warmer bottom water temperature (13°C vs. 3°C) (Buscail, 1992; Etcheber et al., 1996). C_{org} budgets drawn for both margins nevertheless reveal that important amounts of C_{org} are buried in these areas (Buscail et

al., 1990; Etcheber et al , 1996), which can be therefore considered as preferential sinks for organic carbon.

Finally, benthic populations from canyons (especially meiofauna) of both margins are more abundant than on open slope areas. This fact proves the fertile nature of the canyons, where direct response of benthic fauna to changes in particle supply was observed (Monaco et al., 1990a; Dinet et al., 1993).

12.4 CONCLUSIONS

From the comparison of Atlantic and Mediterranean margins presented here, several conclusions can be drawn on particle flux on continental margins and on the organic carbon cycle, in particular. Some of the following conclusions are still quite tentative, or strictly applicable to our study sites and would need to be further refined for general use.

1. The general circulation of water masses (physical factor) represents a major forcing function of the spatial and temporal variability of particle transfer in these two environments. Its effect is modulated by seasonal changes of continental inputs (climatic factor) and marine productivity (biological factor).
2. Particle fluxes through the slope water column exhibit a pattern typical of continental margins, namely a seaward flux decrease and a downward flux increase.
3. Seasonal variability is less pronounced in the case of the Atlantic margin. On the contrary, the Mediterranean margin presents important seasonal changes in fluxes, with minimum values during summer and highest values during winter.
4. Advection plays a prominent role in the transfer of matter and energy on these margins; on the basis of organic carbon flux profiles through the water column a functional distinction can be made between "continental" (strong flux increase with depth) and "oceanic" (constant flux or even decrease with depth) margins.
5. There is an enrichment of sedimentary organic carbon in these margins, which are further characterized by high sedimentation rates and enhanced biological activity.
6. Distance from the continental sources (i.e., rivers) and morphology have a direct influence on spatial and temporal heterogeneity of the biochemical characteristics of sedimentary organic matter; futhermore, water temperature seems to play a direct role on its degradation at the sediment/water interface.

12.5 REFERENCES

Beaufort, L. and S. Heussner (1996) "Coccolithophorids on the continental slope of the Bay of Biscay. 1. Production, transport and contribution to mass fluxes", submitted to *Deep-Sea Res. II.*

Biscaye, P. E. and R. F. Anderson (1994) "Fluxes of particulate matter on the slope of the southern Middle Atlantic Bight: SEEP-II", *Deep-Sea Res. II*, **41**, 459–509.

Biscaye, P. E., R. F. Anderson and B. L. Deck (1988) "Fluxes of particles and constituents to the eastern United States continental slope and rise: SEEP-I", *Cont. Shelf Res.*, **8**, 855–904.

Buscail, R. (1991) "Benthic fluxes of organic matter and geochemical response of sediment-water interface in the northwestern Mediterranean slope (Gulf of Lions-France)", in D. A. C. Manning (ed) *Org. Geochem. Advances and Application in the Natural Environment*, 501–504.

Buscail, R. (1992) "Dégradation de la matière organique dissoute et particulaire à l'interface eau-sédiment sur les marges du Golfe du Lion et du Golfe de Gascogne." XXXIIIe Congrès Assemblée Plénière de la CIESM-Trieste 12–16 Octobre 1992. Rapport Comm. int. Mer Medit., 33, 379.

Buscail, R. and C. Germain (1995) "Present-day organic matter sedimentation in surface deposits of the northwestern Mediterranean margin: A result of export from shelf and shelf-break to continental slope", submitted to *Limnol. Oceanogr.*

Buscail, R. and L. Guidi-Guilvard (1993) "Organic inputs and transformations at the sediment-water interface of the NW Mediterranean slope (Gulf of Lions-France)", *Ann. Inst. Océanog.*, **69**, 147–153.

Buscail, R., R. Pocklington and C. Germain (1995) "Seasonal variability of the organic matter in a sedimentary coastal environment: Sources, degradation and accumulation (continental shelf of the Gulf of Lions - NW Mediterranean Sea)", *Cont. Shelf Res.*, **15**, 843–869.

Buscail, R., P. Ambastsian, A. Monaco and M. Bernat (1996) "^{210}Pb, manganese and carbon: Indicators of focusing processes on the continental margins", submitted to *Mar. Geol.*

Buscail, R., R. Pocklington, R. Daumas, and L. Guidi (1990) "Fluxes and budget of organic matter in the benthic boundary layer over the northwestern Mediterranean margin", *Cont. Shelf Res.*, **10**, 1089–1122.

Castaing, P., J. M. Froidefond, O. Weber, R. Prud'homme (1996a) "Modes of supply of suspended sediments to the Bay of Biscay", submitted to *Deep-Sea Res. II.*

Castaing, P., J. Carbonne, M. Cremer, J. M. Froidefond, S. Heussner, J. M. Jouanneau, O. Möller, V. Valencia and O. Weber (1996b) "General hydrodynamic conditions in the Bay of Biscay. Result from the ECOFER experiment", submitted to *Deep-Sea Res. II.*

De Bovée, F., L. Guidi and J. Soyer (1990) "Quantitative distribution of deep-sea meiobenthos in the Northwestern Mediterranean (Gulf of Lions)", *Cont. Shelf Res.*, **10**, 1123–1145.

Dinet, A., L. Guidi-Guilvard, P. Albert and R. Buscail (1993) "Répartition quantitative du méiobenthos et de la matière organique sédimentaire dans le canyon du Cap Ferret (Golfe de Gascogne, nord-ouest Atlantique)", Actes du IIIe Colloque International "Océanographie du Golfe de Gascogne", 253–256.

Durrieu de Madron, X., T. Courp and F. Nyffeler (1996) "Hydrographical and nephelometric structures in the Cap Ferret Canyon: Spatial and temporal variations", submitted to *Deep-Sea Res. II.*

Durrieu de Madron, X., F. Nyffeler and C. H. Godet (1990) "Hydrographic structure and nepheloid spatial distribution in the Gulf of Lions continental margin", *Cont. Shelf Res.*, **10**, 915–929.

Etcheber, H., J. C. Relexans, O. Weber, R. Buscail and S. Heussner (1996) "Distribution and quality of sedimentary matter on the Aquitanian Margin (Bay of Biscay)", submitted to *Deep-Sea Res. II.*

Heussner, S. (1995) "Sources and fate of settling particles on a northeastern Atlantic margin: Recent issues from the ECOMARGE program (France-JGOFS)", Proceedings of the International Symposium on Global Fluxes of Carbon and its related substances in the Coastal Sea-Ocean-Atmosphere System (1994 Sapporo IGBP Symposium), Sapporo (Japan), 183–188.

Heussner, S. and S. W. Fowler (1987) "La sédimentation des pelotes fécales, particules biogènes, et la notion de flux vertical", Coll. Intern. Océanol., Perpignan, C.I.E.S.M., 49.

Heussner, S., A. Monaco and J. Carbonne (1993) "Biogenic particle transfer on the NW Mediterranean continental margin: A summary of ECOMARGE results", *Ann. Inst. Océanogr.*, **69**, 141–145.

Heussner, S., C. Ratti and J. Carbonne (1990) "The PPS 3 time-series sediment trap and the trap sample processing techniques used during the ECOMARGE experiment", *Cont. Shelf Res.*, **10**, 943–958.

Heussner, S., A. Monaco, P. E. Biscaye, J. Carbonne, H. Etcheber, X. Durrieu de Madron, O. Radakovitch, N. Delsaut and L. Beaufort (1996) "Composition, temporal patterns and controling factors of particulate fluxes on the continental slope of the Bay of Biscay (Northeastern Atlantic)", submitted to *Deep-Sea Res. II.*

Jorgensen, B. B. (1983) "Processes at the sediment water interface", in B. Bolin and R. B. Cook (ed), *The Major Biogeochemical Cycles and Their Interactions*, SCOPE 21, Wiley & Sons, Chichester, 477–509.

Miquel, J. C., S. W. Fowler and J. La Rosa (1993) "Vertical particle fluxes in the Ligurian Sea", *Ann. Inst. Oceanogr.*, **69**, 107–110.

Miquel, J. C., S. W. Fowler, J. La Rosa and P. Buat-Menard (1994) "Dynamics of the downward flux of particles and carbon in the open northwestern Mediterranean Sea", *Deep-Sea Res.*, **41**, 243–261.

Millot, C. (1990) "The Gulf of Lions' hydrodynamics", *Cont. Shelf Res.*, **10**, 885–894.

Monaco, A., P. Biscaye, J. Soyer, R. Pocklington and S. Heussner (1990a) "Particle fluxes and ecosystem response on a continental margin: The 1985–1988 Mediterranean ECOMARGE experiment", *Cont. Shelf Res.*, **10**, 809–839.

Monaco, A., T. Courp, S. Heussner, J. Carbonne, S. W. Fowler and B. Deniaux (1990b) "Seasonality and composition of particulate fluxes during ECOMARGE-I, western Gulf of Lions", *Cont. Shelf Res.*, **10**, 959–987.

Peinert, R. D., S. W. Fowler, J. La Rosa and J. L. Teyssie (1992) "Vertical flux and microplancton assemblages in the Gulf of Lions during spring 1990", Water Poll. Res. Report (CEE), 28, Eros 2000, 4132–424.

Radakovitch, O. and S. Heussner (1996) "Fluxes and budget of ^{210}Pb on the continental margin of the Bay of Biscay (Northeastern Atlantic)", submitted to *Deep-Sea Res. II.*

Ruch, P., M. Mirmand, J. M. Jouanneau and C. Latouche (1993) "Sediment budget and transfer of suspended sediment from the Gironde Estuary to Cap-Ferret canyon", *Mar. Geol.*, **111**, 109–119.

Siegel, D. A., T. C. Granata, A. F. Michaels and T. D. Dickey (1990) "Mesoscale eddy diffusion, particle sinking, and the interpretation of sediment trap data", *J. Geophys. Res.*, **95**, 5305–5311.

Wollast, R. (1990) "The coastal organic carbon cycle: Fluxes, sources and sinks", in R. F. C. Mantoura, J. M. Martin and R. Wollast (eds) *Ocean Margin Processes in Global Change*, J. Wiley & Sons, Chichester, 365–381.

Wollast, R. and F. T. MacKenzie (1989) "Global biogeochemical cycles and climates", in A. Berger, S. Schneider and J. C. Duplessy (eds) *Climates and Geoscience*, NATO-ASI Series, 285, Kluwer Acad. Publ., Dordrecht, 453–473.

13 Abiotic and Biotic Forcing on Vertical Particle Flux in the Southern Ocean

ULRICH V. BATHMANN

13.1 THE SCENARIOS

The objective of this paper is to show the importance of physical, chemical and biological constraints for structuring the pelagic ecosystems (Priddle et al., 1992) and determining the eventual fate of the organic matter (Bathmann, 1991) and the role of zooplankton thereby (Bathmann, 1992). For this, data collected by the author on pelagic system structure, on mechanisms and fluxes within the pelagic realm are, reviewed for various scenarios from different sites in the Weddell Sea in the course of a year. I will start with the description of copepod biology in winter along a transect across the ice covered Weddell Sea and continue by presenting three scenarios for pelagic system structure during austral spring and summer (November to January). An autumn situation completes the course through the annual succession within pelagic Antarctic ecosystems of the Weddell Sea.

13.2 WINTER

Seasonal cycles of the biota in the Southern Ocean are strongly influenced by the dynamics of the 20 x 10^6 km^{-2} of sea ice, as 16 x 10^6 km^{-2} reform and melt each year. In the Weddell Sea these figures are 10 and 8 x 10^6 km^{-2}, respectively (Viehoff et al., 1994). Thus, nearly the entire Weddell Gyre is covered by sea ice in winter. Life under sea ice especially when it is covered by snow is limited by light which should result in low or no primary production (Nöthig et al., 1991). However, observations reveal the importance of phytoplankton production in the sea ice which is thought to be 200–2800 mg C m^{-2} d^{-1} and therefore as much as or even double, the amount which is produced in the open water during this time (Gleitz et al., 1994). New results on zooplankton distribution in winter demonstrate that a great percentage of the copepod population of the central Weddell Sea

Particle Flux in the Ocean
Edited by V. Ittekkot, P. Schäfer, S. Honjo and P. J. Depetris

is actively feeding in the winter water directly under the sea ice with grazing rates similar to those of the summer population (Bathmann et al., 1991). Vertical particle fluxes under such conditions in the central Weddell Sea are reported to be the lowest in the world oceans (Wefer and Fischer, 1991). Protozoan grazing and, thus, the production of minipellets in this situation may also be responsible for effective recycling of organic material in the water column (Nöthig and Gowing, 1991). Thus, winter active copepods (*Calanus propinquus*) appear to be an important component to structure the pelagic food web by effectively recycling algae, protozooplankton and other organic material in the upper water column under the sea ice during winter. This might result in a reduced vertical particle flux (Figure 13.1).

13.3 SPRING

During the austral spring, varied circumstances pertaining in different portions of the Weddell Sea basin result in varied ecosystem responses. Three such systems of response have been identified and are described below.

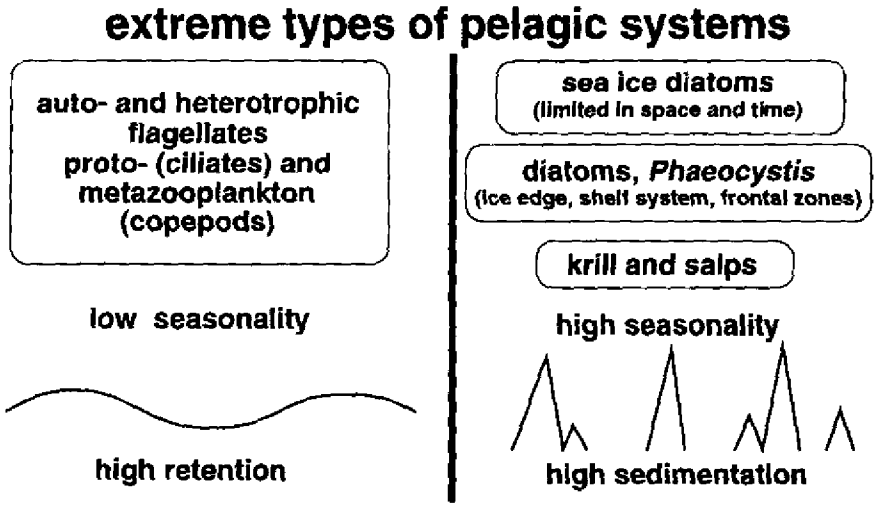

Figure 13.1 Conceptual models of two extreme organizational structures of pelagic ecosystems. Left hand side: recycling system with low annual variability in total biomass and low sedimentation output. Right hand side: export system with large sized organisms creating high biomass blooms which results in high vertical flux.

Under "normal" conditions sea ice cover decreases in the Coastal Current (CC) on the north-eastern Weddell Sea shelves by breaking up and gradual melting. Bathmann et al. (1991) have described five stages in pelagic system succession associated with these conditions of ice retreat and biological production.

1. The first stage (shortly before ice melting) was similar to that described above for the ice covered Weddell Sea with copepods dominating and with little vertical flux mainly consisting of sinking copepod fecal pellets.
2. Shortly after the start of sea ice melting in beginning of January 1989, in the second stage, ice algae sank to at least 500 m water depth (which was the depth of a sediment trap recording sinking material in 2.5 days intervals).
3. Five to 8 days later, during the third stage, euphausiid pellets occurred in the sinking material indicating feeding of krill on released ice algae.
4. The next peak in vertical flux, the fourth stage, was attributed to phytoplankton. The $\delta^{13}C_{org}$ values of -32‰ indicated the pelagic origin of this material as opposed to the less negative $\delta^{13}C$ values (-23‰) of organic material released by the ice.

These latter three stages of enhanced vertical flux resulted in a sedimentation rate of about 100 mg C m^{-2} d^{-1} (Bathmann et al., 1991).

5. The three stages of high sedimentation were followed by low sedimentation of material dominated mainly by minipellets (detected by microscopical observations) and probably produced by protozooplankter (e.g., heterotrophic dinoflagellates, radiolaria, foraminifera; Nöthig and v. Bodungen, 1989) which comprises the fifth stage of pelagic succession.

Thus, ice melting in spring on a continental shelf in the eastern Weddell Sea may induce several stages in the pelagic system succession, with periods of regeneration and export (Figure 13.1) *sensu* Smetacek et al. (1991).

A completely different situation of spring plankton development under sea ice is reported for the south-eastern Weddell Sea in austral spring 1990/91. During the spring, melting of sea ice was very much reduced in the Weddell Sea (Viehoff et al., 1994) and strong northeasterly winds forced the remaining ice into the interior of the Weddell Sea. In the midst of this sea ice (strongly compressed and deformed) the research ice breaker *Polarstern* stuck for about 14 days, being incapable of moving out (Bathmann et al., 1992). Primary production was very low in the ice and in the surface waters of this area (< 100 mgC m^{-2}; Gleitz et al., 1994). Microbial activity was nearly as high as primary production but only in the sea ice and in melt water pools on top of, and in-between, the ice (Grossmann et al., 1994). The vertical particle flux measured with sediment traps attached at 4 and 50 m below the sea ice showed a decrease in the vertical flux of carbon and nitrogen as well as in chlorophyll with depth. The composition of the material changed from ice algae (at 4 m) to krill fecal strings at 50 m indicating heavy krill grazing in the upper 50 m water column directly under the ice (Gonzalez et al.,

1994). These authors confirm their conclusions by presenting data demonstrating that the maximum concentrations of krill fecal string were dispersed in the upper 100 m of the water column. Cyclopoid copepods (of the genus *Oncaea*) probably were feeding heavily on these pellets, and reduced pellet sedimentation significantly, especilly where the numbers of cyclopoid copepods exceeded some 30 ind. m^{-3} (Gonzalez et al., 1994). In this scenario of low primary production but heavy sea ice coverage in spring in the Southern Ocean, vertical particle flux was strongly controlled by zooplankton grazing activity either on ice algae, sinking algal material or fecal matter.

A third situation of spring bloom impacts on sinking matter was recorded from the ice free areas at the Polar Frontal zone (PFz) at about 48°S 6°W (Smetacek et al., 1994). The investigations were carried out within the framework of the JGOFS Southern Ocean Process Study and one of its main conclusions is briefly summarized below. The full details of the results will be presented elsewhere. The sedimentation within the three domains in the Marginal Sea Ice Zone (MIZ) at 60°S (i. at the northern border of the Weddell Gyre, ii. in the southern branch of the Antarctic Circumpolar Current (ACC) and, iii. in the PFz) was controlled by three different factors.

In the MIZ, deep water mixing overrode the small potential effect of water column stabilization induced by melt water from the sea ice (Bathmann et al., 1994) with the result that phytoplankton biomass accumulation (spring bloom at the ice edge) did not occur. This situation probably was prolonged until at least mid December (Lancelot and Veth, 1995). In the southern ACC, huge swarms of the aggregating form of *Salpa thompsonii* exploited the phytoplankton with grazing rates well above areal primary production (Dubischar and Bathmann, 1996). Phytoplankton biomass was dominated by small auto- and heterotrophic nanoplankters (Detmer and Bathmann, 1996); export of material from this system due to sedimentation was very limited (Rutgers van der Loeff et al., 1996). So we postulate that salp grazing in the southern ACC in spring was effectively structuring the pelagial toward a highly retentive system (Figure 13.1).

Zooplankton grazing in the area of the PFz was, in contrast, less than 5% of primary production. In the PFz three distinct phytoplankton blooms developed (Bathmann et al., 1996) which were at least partially favored by the naturally high concentrations of suspended iron (de Baar et al., 1995). The dissolved iron possibly was transported into the waters of the PFz by a jet stream (Veth et al., 1995). These blooms finally sank out of the surface ocean layers as intact senescent cells (Rutgers van der Loeff et al., 1996). The blooms were composed of different algae species of which the sinking of one (*Fragellariopsis kerguelensis*)

not only transported organic matter but also silicate (opal) in its thick frustules during sinking (Bathmann et al., 1996).

In conclusion, the spring situation of pelagic system structure and the pathways and magnitude of the flux of organic matter in the pelagic systems in the Weddell Sea, Antarctica very much depend on physical conditions (sea ice distribution; surface water mixing; light regime), chemical constraints (micronutrient concentrations), algal species composition (silicified versus non-silicified species), and the composition and impact of various zooplankton grazers. Superimposed and probably even more important is the gearing of those factors in space as well as in time for structuring of the pelagic ecosystems and determination of the eventual fate of the organic matter (recycled *versus* exported; Figure 13.1).

13.4 AUTUMN

Here I concentrate only on one of the various scenarios from the literature for biomass pathways at the end of the growing season in the Weddell Sea. Bathmann et al. (1992) reported a high phytoplankton accumulation (> 4 mg chl a m^{-3}) in the Coastal Current (CC) over the shelves of the Lazarev Sea (eastern Weddell Sea). This high phytoplankton biomass could accumulate in the absence of strong zooplankton grazing and under stable hydrographical conditions. One of the numerous autumn storms eventually compressed the surface waters of the CC containing this biomass near the shelf ice coast and subsequently dispersed the surface water and its plankton biomass to greater water depths (shelf depth is between 250 and 500 m in this area). One consequence was a homogenous distribution of phytoplankton biomass throughout the entire water column with the subsequent input of most of this phytoplankton biomass to the benthos (13 gC m^{-2} $week^{-1}$; Bathmann et al., in prep.). There, plankton biomass was buried and partially utilized by the infauna. In part, the plankton material also was transported further down slope on the continental rise (F. Riemann pers. communication).

In the upper water column phytoplankton growth potential was still as high as during summer (Gleitz et al., 1994) but ice formation cleared the surface water of algae which were incorporated and concentrated in freshly forming sea ice (Grossmann et al., 1994). The growth rates of the new ice community were equally high compared to the rates measured from the planktonic algae (Gleitz and Thomas, 1993).

13.5 CONCLUSION

This short article compares some scenarios describing the variability of plankton succession and of the vertical particle flux observed in the Weddell Sea. These scenarios result from the interaction of various biological and physico-chemical factors which match or mismatch in space and time. It has to be stressed that the examples given are selected from the Weddell Sea, one of the many areas of the Southern Ocean. Similar conclusions were reported from nearby areas such as the Weddell-Scotia Sea (Bianchi et al., 1992). Very littele information is available on the production and fluxes during winter and about biological patterns and processes from some regions of the Southern Ocean; one area of interest in this context is the south-western and permanently ice covered Weddell Sea. On the other hand, the biological processes we recently discovered at the Polar Front changed our paradigm of pelagic system organization in Antarctic waters that the melting sea ice positively influences biological production. We now have evidence to believe that superimposed on hydrographical and chemical constraints on phytoplankton blooming and sedimentation, the biological impact of grazers (micro- and macrozooplankter) plays a major role in pelagic system structuring in Antarctic waters.

13.6 ACKNOWLEDGMENTS

This contribution has AWI publication number 952. Many thanks to E.-M. Nöthig for comments on the manuscript.

13.7 REFERENCES

Bathmann, U. V. (1991) "Carbon fluxes in the Southern Ocean", *Global Change Prisma*, **2**, 7–10.

Bathmann, U. V. (1992) "*Partikelfluss im Ozean: Modifikation durch Zooplankter*", Habilitationsschrift, Univ. Bremen, 53 pp.

Bathmann, U. V., R. Scharek and C. Dubischar (1996) "Chlorophyll and phytoplankton species distribution in the Atlantic sector of the Circumpolar Current", *Deep-Sea Res. Part II* (in press).

Bathmann, U. V., G. Fischer, P. Müller and D. Gerdes (1991) "Short-term variations in particulate matter sedimentation off Kapp Norvegia, Weddell Sea, Antarctica: relation to water mass advection, ice cover, plankton biomass and feeding activity", *Pol. Biol.*, **11**, 185–195.

Bathmann, U. V., R. R. Makarov, V. A. Spiridonov and G. Rohard (1993) "Winter distribution and overwintering strategies of the Antarctic copepod species Calanoides

acutus, Rhincalanus gigas and Calanus propinquus (Crustacea, Calanoida) in the Weddell Sea", *Pol. Biol.*, **13**, 333–346.

Bathmann, U. V., M. Schulz-Baldes, E. Fahrbach, V. Smetacek and H.-W. Hubberten (eds) (1992) "Die Expeditionen ANTARKTIS IX/1–4 des Forschungsschiffes 'Polarstern' 1990/91. The expeditions ANTARKTIS IX/1–4 of the research vessel 'Polarstern' 1990/91", *Ber. Polarforsch.*, **100**, 403 pp.

Bathmann, U. V., V. Smetacek, H. de Baar, E. Fahrbach and G. Krause (eds) (1994) "Die Expeditionen ANTARKTIS X/6–8 des Forschungsschiffes 'Polarstern' 1992/3. The expeditions ANTARKTIS X/6–8 of the research vessel 'Polarstern' 1992/93", *Ber. Polarforsch.*, **135**, 236 pp.

Bianchi, F., A. Boldrin, F. Cioce, G. Dieckmann, H. Kuosa, A.-M. Larsson, E.-M. Nöthig, P.-J. Sehlstedt, G. Socal and E. E. Syvertsen (1992) "Phytoplankton distribution in relation to sea ice, hydrography and nutrients in the northwestern Weddell Sea in early spring 1988 during EPOS", *Pol. Biol.*, **12**, 225–235.

de Baar, H. J. W., J. T. M. de Jong, D. C. E. Bakker, B. M. Löscher, C. Veth, U. Bathmann and V. Smetacek (1995) "Importance of iron for plankton blooms and carbon dioxide drawdown in the Southern Ocean", *Nature*, **373**, 412–415.

Deter, A. and U. V. Bathmann (1996) "Distribution patterns of autotrophic pico- and nanoplankton and their relative contribution to algal biomass during spring in the Atlantic sector of the Southern Ocean", *Deep-Sea Res. Part II* (in press).

Dubischar, C. and U. V. Bathmann (1996) "Metazooplankton grazing across frontal systems in the Southern Ocean", *Deep-Sea Res. Part II* (in press).

Gleitz, M., U. Bathmann and K. Lochte (1994) "Build-up and decline of summer phytoplankton biomass in the eastern Weddell Sea, Antarctica", *Pol. Biol.*, **14**, 413–422.

Gleitz, M. and D. N. Thomas (1993) "Variation in phytoplankton standing stock, chemical composition and physiology during sea-ice formation in the southeastern Weddell Sea, Antarctica", *J. Exp. Mar. Biol. Ecol.*, **173**, 211–230.

Gonzalez, H. E., F. Kurbjeweit and U. V. Bathmann (1994) "Occurrence of cyclopoid copepods and faecal material in the Halley Bay region, Antarctica, during January-February 1991", *Pol. Biol.*, **14**, 331–342.

Grossmann, S. and M. Gleitz (1993) "Microbial responses to experimental sea-ice formation: implications for the establishment of Antarctic sea-ice communities", *J. Exp. Mar. Biol. Ecol.*, **173**, 273–289.

Nöthig, E.-M. and B. v. Bodungen (1989) "Occurrence and vertical flux of faecal pellets of probably protozoan origin in the southeastern Weddell Sea (Antarctica)", *Mar. Ecol. Prog. Ser.*, **56**, 281–289.

Nöthig, E.-M. and M. M. Gowing (1991) "Late winter abundance and distribution of phaeodarian radiolarians, other large protozooplankton and copepod nauplii in the Weddell Sea, Antarctica", *Mar. Biol.*, **111**, 473–484.

Nöthig, E.-M., U. Bathmann, J. Jennings, E. Fahrbach, R. Gradinger, L. Gordon and R. Makarov (1991) "Regional relationships between biological and hydrographical properties in the Weddell Gyre in late austral winter 1989", *Mar. Chem.*, **35**, 325–336.

Priddle, J., V. Smetacek and U. Bathmann (1992) "Antarctic marine primary production, biogeochemical carbon cycle and climate change", *Phil. Trans. R. Soc. Lond.*, **B 338**, 289–297.

Rutgers van der Loeff, M., J. Friedrichs and U. V. Bathmann (1996) "Carbon export during the spring bloom quantified with the natural tracer ^{234}Th", *Deep-Sea Res. Part II* (in press).

Smetacek, V., U. Bathmann, J. A. van Franeker and C. Veth (1994) "Spring at the ice-edge: Southern Ocean JGOFS cruise of RV 'Polarstern'", *EOS*, **75**, 158.

Veth, C., I. Peeken and R Schareck (1995) "Physical anatomy of fronts and surface waters in the ACC near the 6° W meridian during austral spring 1992", *Deep-Sea Res. Part II* (in press).

Viehoff, T., A. Li, C. Oelke and H. Rebhan (1994) "Characteristics of winter sea ice conditions in the southwestern Weddell Sea in 1992 as derived from multi-sensor observations", *IEEE*, **2/94**, 150–152.

Wefer, G. and G. Fischer (1991) "Annual primary production and export flux in the Southern Ocean from sediment trap data", *Mar. Chem.*, **35**, 597–613.

14 Processes Determining Seasonality and Interannual Variability of Settling Particle Fluxes to the Deep Arabian Sea

B. HAAKE, T. RIXEN, T. REEMTSMA, V. RAMASWAMY AND V. ITTEKKOT

14.1 INTRODUCTION

Sediment traps are a tool for sampling particulate matter in the water column (see this volume, Chapters 5 through 7). The development of time-series traps has, moreover, enabled us to determine the temporal variations in particle fluxes at intervals from hours to weeks. Such data collected at various oceanic stations have improved our knowledge about oceanic processes such as the mechanisms leading to settling of fine grained particulate matter in the ocean (Honjo, 1978), the coupling between surface processes and sedimentation in the deep sea (Deuser, 1986; Deuser et al., 1990) and degradation of organic matter in the water column (Lee and Cronin, 1984; Wakeham et al., 1984). Long-term sediment trap studies such as the Sargasso Sea experiment (Deuser, 1986; this volume, Chapter 9) or the trap investigations in the northern Indian Ocean (Nair et al., 1989; Haake et al., 1993) can be utilized to study the relationship between climatic variations and sedimentation in the deep sea.

Sediment trap investigations have been carried out in the Arabian Sea since 1986 (Nair et al., 1989; Haake et al., 1993). Here we will give an overview on the influence of climatic processes on sedimentation in the Arabian Sea basin and summarize the information obtained about the sources of organic matter and its decomposition pathways in the water column.

14.2 STUDY AREA

The monsoons are strong atmospheric circulations which have evolved since the Miocene in southern Asia due to the uplift of the Himalayas and which determine

Particle Flux in the Ocean
Edited by V. Ittekkot, P. Schäfer, S. Honjo and P. J. Depetris

the climate of the region (e.g., Molnar et al., 1993). During the northern hemisphere summer, the Tibetian Plateau is heated so that a low pressure cell forms, which reverses the normally occurring Hadley circulation cell and leads to strong SW winds at the surface (SW monsoon: June-September). These winds blow from the sea to the continent and thus bring seasonal rains to a large part of southern Asia. Over the western part of the Indian Ocean a low-level jet stream evolves which flows from south of the equator, touches coastal Kenya and turns SW to the Arabian Sea where it forms the area of maximum wind speed parallel to the Arabian Peninsula (Findlater, 1969). Its second branch turns to the east and blows south of India and into the Bay of Bengal. During the dry NE monsoon (November-March) the winds blow roughly in opposite direction. The overall wind pattern leads to a semiannual reversal of surface water circulation in the northern Indian Ocean from clockwise during the SW monsoon to anti-clockwise during the NE monsoon. During the SW monsoon upwelling occurs along the coasts of Somalia and the Arabian Peninsula as well as spatially along the west coast of India (Wyrtki, 1973). An area of open ocean upwelling has its maximum upward Ekman transport below the Findlater Jet in the western Arabian Sea (Brock et al., 1992). Upwelling and wind-induced mixing result in a cooling of surface waters during both monsoons.

14.3 METHODS

Mark VI time-series sediment traps have been deployed since 1986 in the western (16°20'N, 60°30'E), central (14°30'N, 64°45'E) and eastern (15°30'N, 68°45'E) Arabian Sea (Figure 14.1). During most of the sampling period mooring systems consisted of 2 traps each with a shallow trap at depths between 750 m and 1000 m and a deep trap at 3000 m water depth. During some of the years an additional intermediate trap has been deployed at 2000 m depth. During the first one and a half years sampling intervals were about 2 weeks, during the following years they were extended to 3 to 4 weeks. Some of the sampling periods had to be excluded due to malfunctioning traps or disturbance by fish or other swimming organisms.

Sampling cups were filled with seawater from the trap depths with 35 g l^{-1} NaCl and 3.3 g l^{-1} $HgCl_2$ added for preservation and poisoning. Samples were stored at 4°C and processed within 3 days after recovery. Processing consisted of a visual sample description, sieving into > 1 mm and < 1 mm fractions, hand-picking of copepods from the < 1 mm fraction, splitting the fractions into aliquots of 1/4 to 1/64 of the total sample volume, filtering the samples onto preweighed Nuclepore filters (0.4 μm) and drying at 45°C.

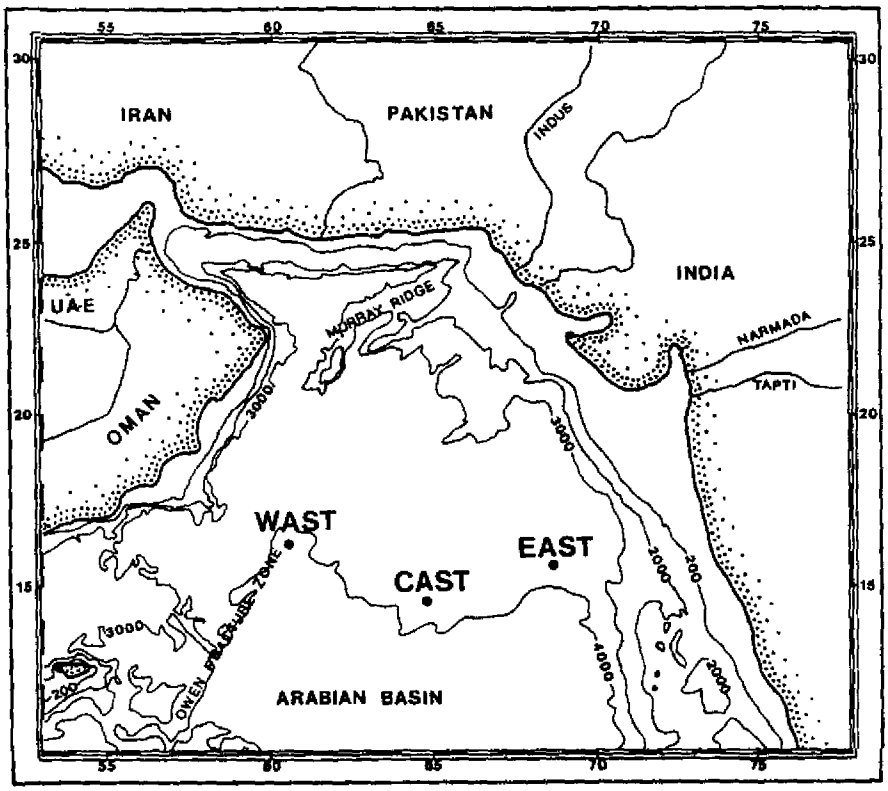

Figure 14.1 Sites of sediment trap moorings in the western (WAST), central (CAST) and eastern (EAST) Arabian Sea.

14.4 SAMPLE ANALYSES

Aliquots of the samples were analyzed for carbonate, organic carbon, total nitrogen, biogenic opal and lithogenic matter (methods in Haake et al., 1993), amino acids and hexosamines (methods in Haake et al., 1992; Rixen and Haake, 1993), carbohydrates (methods in Ittekkot et al., 1984b), fatty acids (methods in Reemtsma et al., 1990), and mineral constituents (methods in Ramaswamy et al., 1991).

14.5 RESULTS AND DISCUSSION

14.5.1 PROCESSES DETERMINING SEASONALITIES OF BIOGENIC AND LITHOGENIC FLUXES

Particle fluxes measured by traps in intermediate and deep waters of the Arabian Sea basically reveal a semiannual periodicity with maxima during the SW and NE monsoon seasons. These flux maxima coincide with maxima of wind speeds and minima of sea surface temperatures (Figure 14.2). Sea surface temperature charts (Multi Channel Sea Surface Temperature = MCSST, Advanced Very High

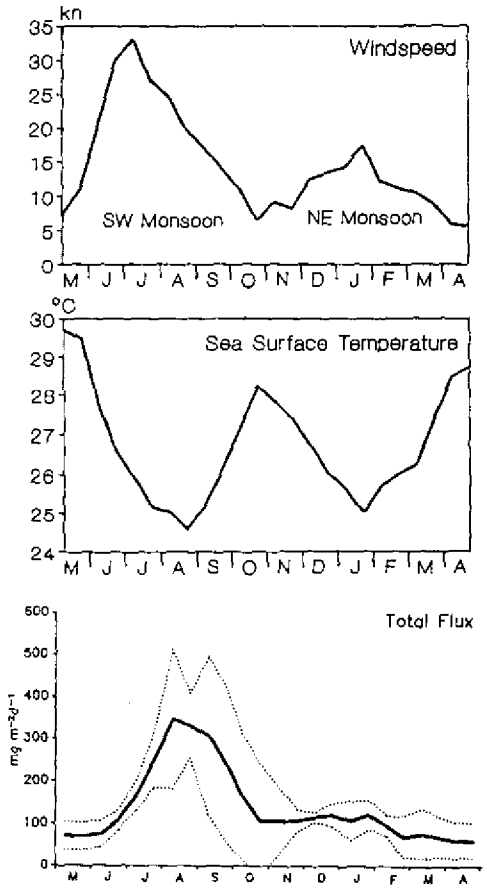

Figure 14.2 Monthly averages of wind speeds (kn), sea surface temperatures (MCSST data) and total fluxes at the western trap location. The standard deviation of ± 1 sigma is indicated by the dotted line.

Resolution Radiometer = AVHRR data) of the Arabian Sea show that intermonsoons are warm with temperatures between 28° and 30°C whereas the temperatures of the SW and NE monsoons are several degrees lower (Figure 14.3). Maximum cooling occurs during the SW monsoon in the western, and during the NE monsoon in the north-western, Arabian Sea. Centers of coastal upwelling in the SW monsoon are indicated by temperatures below 22°C. A broad area of open ocean upwelling is marked roughly by the 25°C isotherm (Figure 14.3). The cooling of surface waters is accompanied by nutrient entrainment into the mixed layer and increased primary productivity and particle fluxes due to: (i) monsoonal upwelling during the SW monsoon in the western part of the basin, (ii) wind-mixing of cold nutrient-rich subsurface waters into the euphotic zone during both

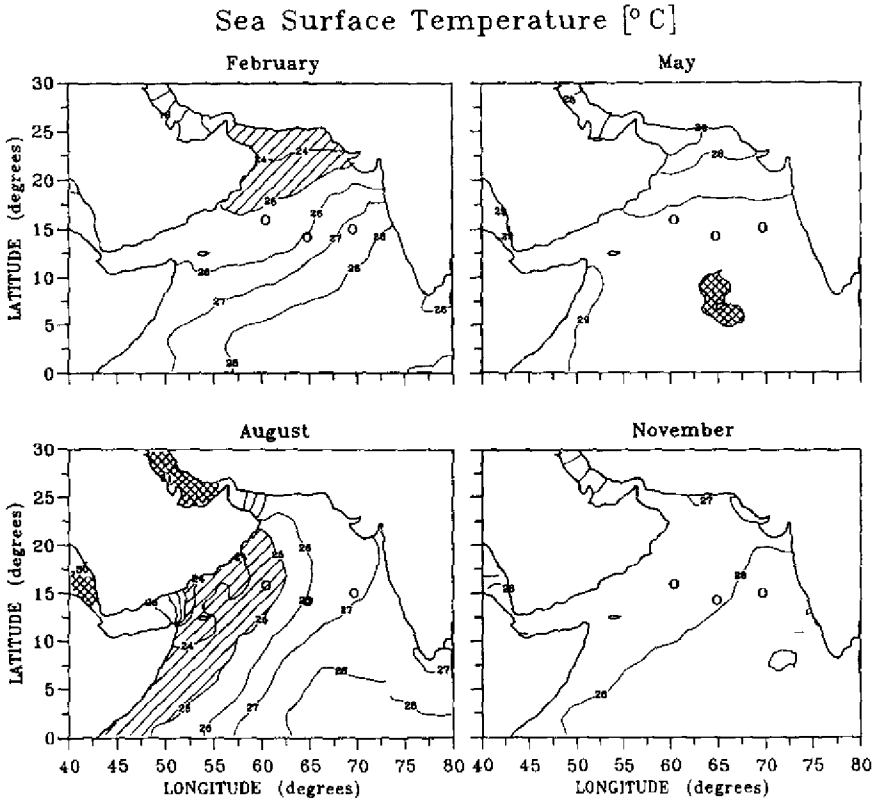

Figure 14.3 Satellite derived sea surface temperature (MCSST) distributions in the Arabian Sea averaged for four different months from 1986 to 1992. The selected months represent the height of the four different seasons in the region: NE monsoon (February), intermonsoon 1 (May), SW monsoon (August) and intermonsoon 2 (November). Circles represent the three sediment trap locations.

monsoons and, (iii) northern hemisphere winter cooling adding to the wind induced mixing of the NE monsoon (Nair et al., 1989; Haake et al., 1993).

Biogenic material dominates over lithogenic material in sinking particles in the Arabian Sea and makes up more than 80% of the total fluxes in almost all samples. Carbonate is the major biogenic component and contributes more than 50% of the total flux. Despite the similar general flux patterns with monsoonal maxima and intermonsoonal minima the magnitude of biogenic fluxes differed significantly among the three locations. In the western Arabian Sea biogenic fluxes are more than three times higher than at the other two locations in most years (Figure 14.4). The major biogenic constituents are calcareous frustules made up mainly of coccolithophorids and foraminifers (Curry et al., 1992). The only exceptions are the SW monsoon peak fluxes in the western Arabian Sea (Figure 14.4). Associated with these peaks, biogenic opal can reach maxima of more than 40% of the total material and was made up mainly of *Rhizosolenia* sp. - a diatom typical of upwelling conditions (Takahashi et al., in prep.). This upwelling induced opal peak occurrred once every year with a temporal shift of about one to one and a half months from year to year. It was usually preceded by a carbonate peak indicating a coccolithophorid bloom (Haake et al., 1993). The coccolithophorid bloom developed with the beginning of the monsoons when nutrient entrainment at the base of the mixed layer brought phosphate and nitrate but relatively little silicate into the euphotic zone. Nutrient profiles with detailed sampling of the upper 200 m show that phosphate and nitrate concentrations increased immediately below the mixed layer whereas silicate concentrations remained low to a depth of approximately 150 m (Haake et al., 1993). Thus, only the upwelling of waters from greater depths can lead to sufficient entrainment of silicate for a diatom bloom. A dominance of calcareous primary producers almost throughout the year has been also observed in other tropical and subtropical regions (e.g., Honjo et al., 1982; Deuser et al., 1981).

Biogenic and lithogenic matter was transported into the deep ocean in the form of biologically formed large particles such as macroaggregates or fecal pellets (e.g., Alldredge and Silver, 1988). Biological productivity is, thus, a prerequisite for the transport of fine lithogenic matter into the deep ocean as the sinking speeds of individual mineral grains are too low to overcome turbulence (Degens and Ittekkot, 1984). Lithogenic matter in addition to organism frustules can, on the other hand, enhance particle densities and, hence, the sinking speeds of aggregates (Ittekkot, 1993).

In the Arabian Sea productivity and lithogenic matter supply are enhanced at about the same time as the monsoons not only increase primary productivity but also the supply of lithogenic material from land. Lithogenic matter is being transported via rivers into the northern and eastern parts of the Arabian Sea. These rivers have their maximum discharges during the SW monsoon in August/ September. The major contributing rivers are Indus, Narmada and Tapti (Borole et al., 1982; Ittekkot and Arain, 1986). A more important source for lithogenic

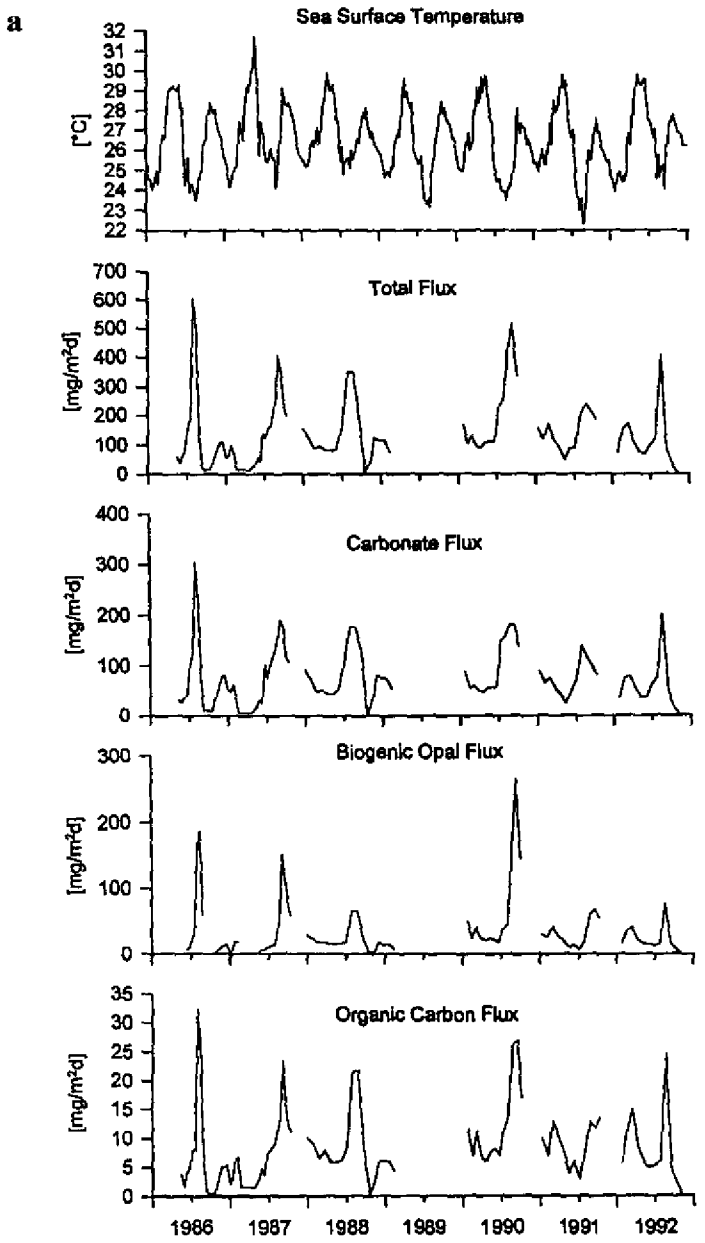

Figure 14.4a Sea surface temperatures (MCSST), total flux, and carbonate, biogenic opal and organic carbon fluxes measured at the western trap location.

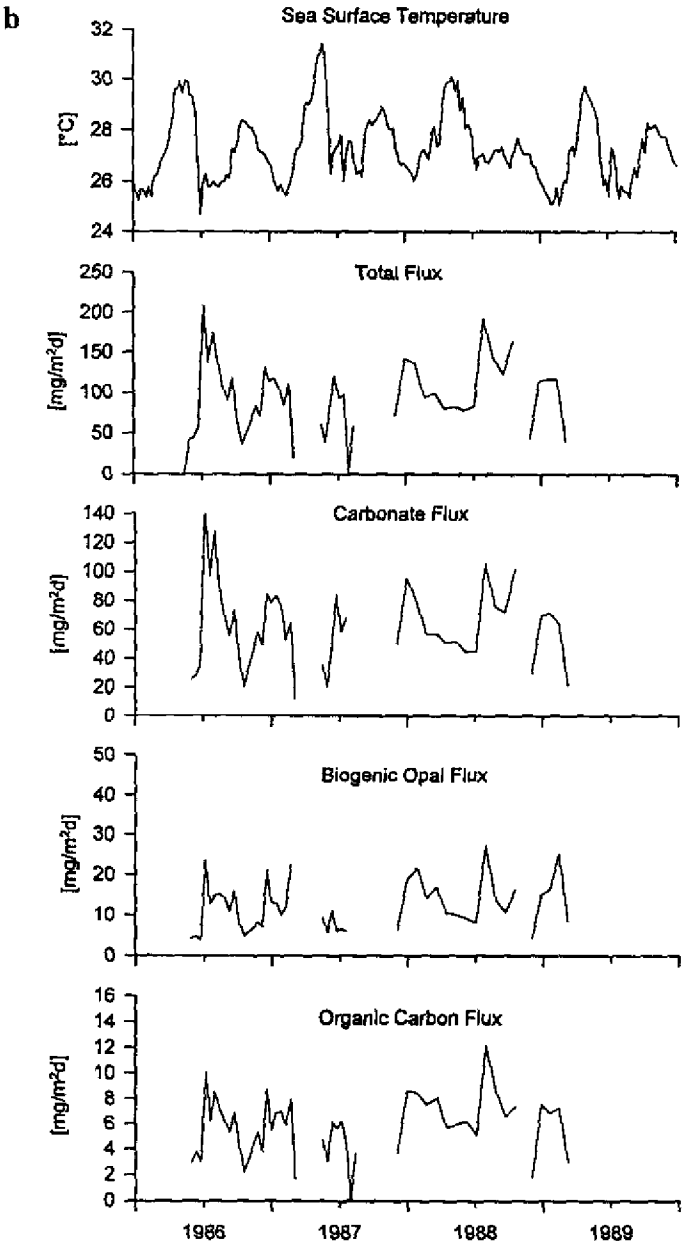

Figure 14.4b Sea surface temperatures (MCSST), total flux, and carbonate, biogenic opal and organic carbon fluxes measured at the central trap location.

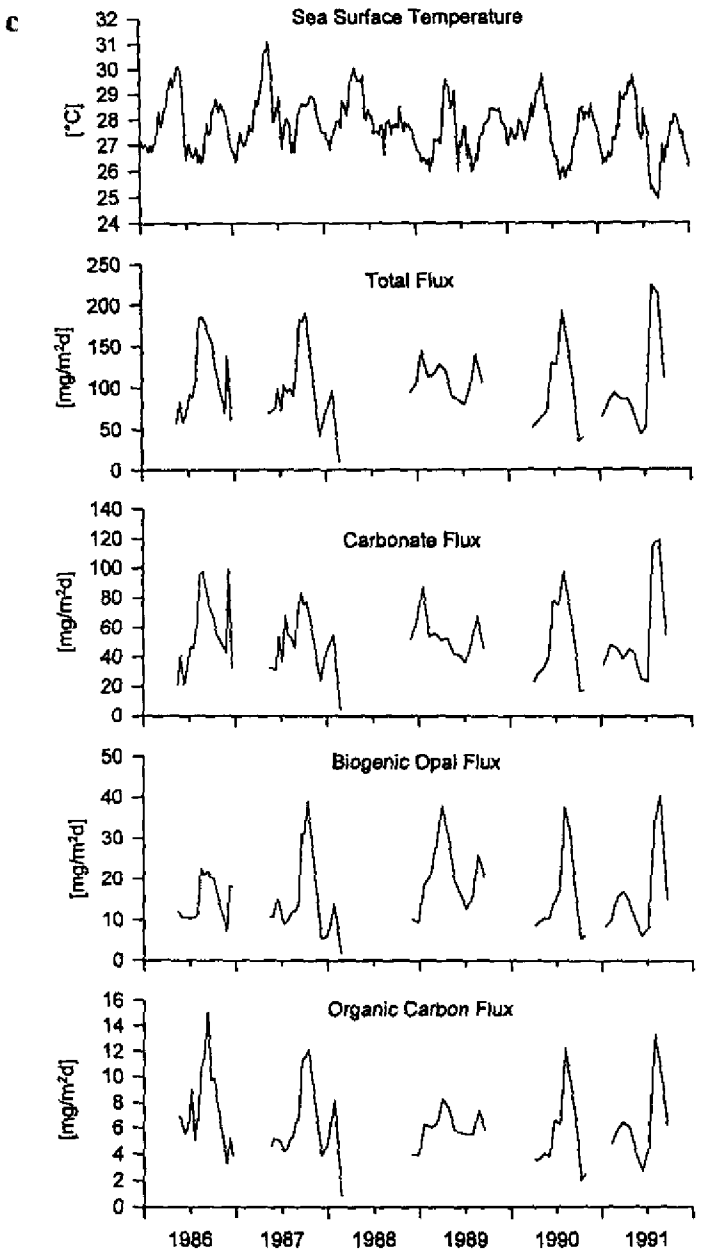

Figure 14.4c Sea surface temperatures (MCSST), total flux, and carbonate, biogenic opal and organic carbon fluxes measur+ed at the eastern trap location.

matter is the aeolian transport from the deserts of the Arabian peninsula and Somalia during the SW monsoon (Sirocko and Sarnthein, 1989; this volume, Chapter 3). During the NE monsoon aeolian transport also occurs from the Thar Desert. During this season, however, the amount delivered to the Arabian Sea is much less compared to that delivered during the SW monsoon (Chester et al., 1984).

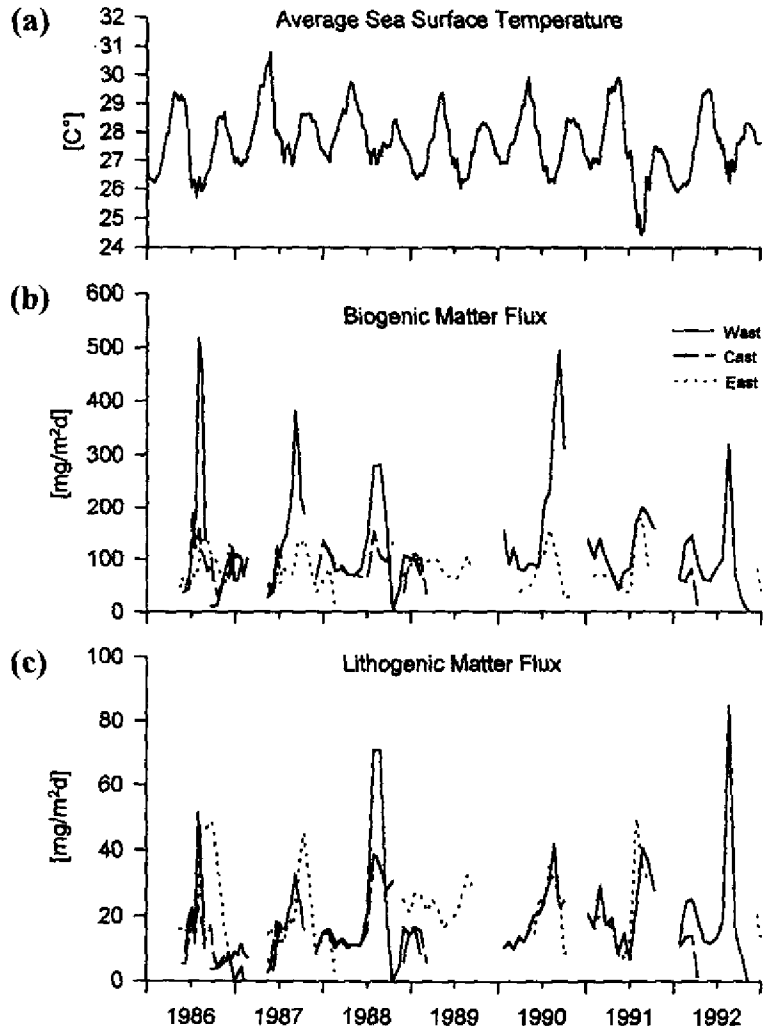

Figure 14.5 (a) Seasonality of average sea surface temperatures in the Arabian Sea from MCSST charts, (b) biogenic matter fluxes and (c) lithogenic matter fluxes at the three trap locations measured at 3000 m water depth from 1986 to 1992.

In contrast to flux patterns of biogenic matter those of lithogenic matter are similar at all three trap locations (Figure 14.5) suggesting a common source. The western trap collected higher lithogenic fluxes than the central, a feature, which may be explained by a reduction of lithogenic fluxes with increasing distance from the source areas of aeolian material, west of the Arabian Sea. However, the eastern trap which is farther away from the source of the aeolian material, collected more material in 1986 and 1987 and very similar amounts as the western trap in 1990 and 1991. The source area of this lithogenic matter can often be deduced from the clay mineral assemblage. Both, aeolian material and fluvial particles from the Indus are basically illite dominated (Kolla et al., 1981). However, aeolian material has a higher content of palygorskite originating from local sources on the Arabian Peninsula (Kolla et al., 1981). The fluvial material derived from the Narmada and Tapti has a higher smectite content related to weathering on the Deccan Plateau. Based on smectite content Ramaswamy et al. (1991) have estimated that less than 5% of riverine material from the Narmada and Tapti can escape the shelf areas and is transported to the deep sea. Similarly, lithogenic matter transported by the Indus is mainly being deposited on the wide continental shelf and does not influence the deep sea (Sirocko and Sarnthein, 1989). The clay mineral assemblages in sediment trap samples do not show any distinct differences between the three stations. Palygorskite and smectites are almost equally high in the eastern, central and western Arabian Sea (Ramaswamy et al., 1991). The high palygorskite and low smectite contents support the suggestion that the major amount of mineral matter is aeolian in origin and that fluvial contributions are relatively small even in the eastern Arabian Sea (Ramaswamy et al., 1991). The amount of aeolian material reaching the western and eastern Arabian Sea is evidently similar, despite the different distances from the source areas. The reason for this may be the rains. Monsoon rainfalls are extremely low in the western and central Arabian Sea but are almost as high as in the coastal areas in the eastern Arabian Sea (Rixen, in prep.). As rains effectively remove mineral matter, similar amounts of aeolian material can reach the eastern and western part of the basin, though the latter is much closer to the source areas of aeolian material.

Peak lithogenic fluxes in 1986 and 1987 occurred at the eastern site in October/November after the end of SW monsoon. Therefore these peaks are not related to SW monsoon aeolian transport but could be due to resuspension on the Indian continental margin and to riverine transport. Such peaks, decoupled from the flux patterns in the central and western Arabian Sea, could be typical of very weak monsoons.

14.5.2 SOURCES AND DECOMPOSITION OF ORGANIC MATTER

The distribution of individual organic compounds can provide information about the sources of organic matter as well as pathways and intensities of organic matter

decomposition. Ratios of individual compounds and statistical analyses of compound distributions have been used to decipher the sources of organic matter (Cowie and Hedges, 1994; Moers and Larter, 1993; Reemtsma et al., 1993). The identification of sources is, however, difficult as only a small portion of the multitude of organic constituents can be identified and quantified. Amino acids, hexosamines, carbohydrates and fatty acids are the major constituents of marine and terrigenous organic matter (Rashid, 1985). In particles caught by sediment traps in deep water, amino acids and carbohydrates can contribute up to 50% to total organic carbon (Ittekkot et al., 1984a, b) whereas the fatty acid contribution is around 1% (Reemtsma et al., 1990). Most of the individual amino acids and carbohydrates and many of the fatty acids are ubiquitous as they are essential for animal and plant life. However, since they are easily degradable organic constituents, their contents and spectral distributions may in many cases reflect degradation rather than the source of the organic matter.

Fatty acids determined in the central Arabian Sea during the SW monsoon are predominantly marine. Minor contributions from long chain fatty acids indicate terrestrial input most probably of aeolian origin (Reemtsma et al., 1990). A relative increase of terrigenous markers from shallow to deep sediment trap is due to their higher stability compared to short chain fatty acids which are largely marine in origin.

Spectral distributions of carbohydrates (Figure 14.6) are very similar to those observed in other trap experiments from the deep marine environment (Ittekkot et al., 1984a, b). They do not suggest any significant contribution of terrigenous material which would be indicated for example by high arabinose or glucose contents

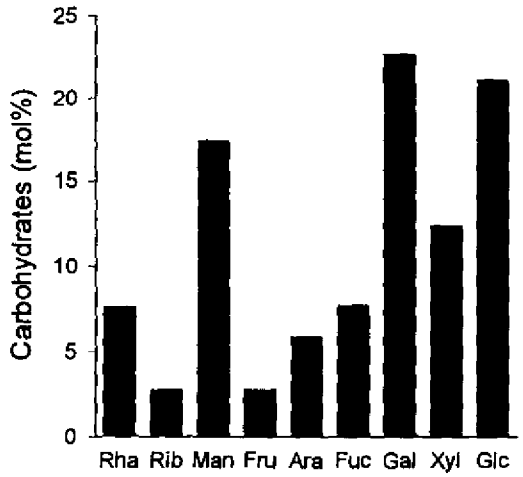

Figure 14.6 Average spectral distribution of carbohydrates (in mol %) of all trap samples collected between May 1986 and November 1987 in the Arabian Sea.

(Hedges et al., 1994, Ochiai et al. 1988). A predominance of marine over terrigenous organic matter is generally observed in sinking particulate matter from the open marine environment. This is even true in the northern Bay of Bengal (Reemtsma et al., 1993) where fluvial material can make up more than 60% of total fluxes (Ittekkot et al., 1991; this volume, Chapter 15). Due to its higher stability terrigenous organic matter may become quantitatively more important in the sediments (Ittekkot, 1988).

Organic carbon, amino acid, fatty acid and hexosamine contents are low during high flux periods (Figure 14.7). This could be due (i) to the lower organic matter content of primary produced material, (ii) to dilution with inorganic matter or (iii) to the stronger decomposition of organic matter in the water column. Reemtsma et al. (1990) found stronger decomposition of fatty acids when fluxes where higher during the SW monsoon period of 1986. Comparing SW, NE and intermonsoons for the whole period between 1986 and 1990 their findings could be confirmed for amino acids and hexosamines (Rixen et al., in prep.). Similarly, biogenic indicators such as the ratio of aspartic acid to ß-alanine (Asp/ß-Ala) revealed that organic matter was more labile when total material fluxes were higher, such as during bloom periods (Haake et al., 1992). It is thus likely that organic matter decomposition in the water column is more intense during blooms since the settling material is more labile. Carbohydrate contents did not decrease during high flux periods (Figure 14.7) and may be less affected by decomposition in the water column.

Total organic carbon, fatty acids, amino acids, hexosamines and carbohydrates are being decomposed between the shallow and deep traps (Table 14.1). The loss rates were greatest for fatty acids and smallest for carbohydrates and hexosamines. Whereas the contributions of fatty acids and amino acids to total organic carbon (FA-C%, AA-C%) decreased considerably with water depth, those of carbohydrates and hexosamines (CHO-C %, HA-C %) remained almost constant or increased slightly. Preferential loss of nitrogenous compounds was regularly observed with increasing depth in the water column and in the sediments. This was reflected in the increasing C/N ratios and decreasing contents of AA-C % from fresh plankton to the sediments (Rixen and Haake, 1993). AA-C % can be used in combination with C/N to compare intensities of alteration and diagenetic stage of organic matter of mixed origin and from different environments (Figure 14.8) (Cowie and Hedges, 1994).

The preferential loss of amino acids might be induced by higher activity of the enzyme protease compared to other digestive enzymes such as chitinase or glucosidase so that amino acids are solubilized and made available for bacterial uptake much faster than hexosamines and carbohydrates (Smith et al., 1992). Contents of branched chain fatty acids (Reemtsma et al., 1990) and the hexosamine galactoseamine (Haake et al., 1992) relatively increase in particulate matter samples between the shallow and deep traps. Both are indicators of the

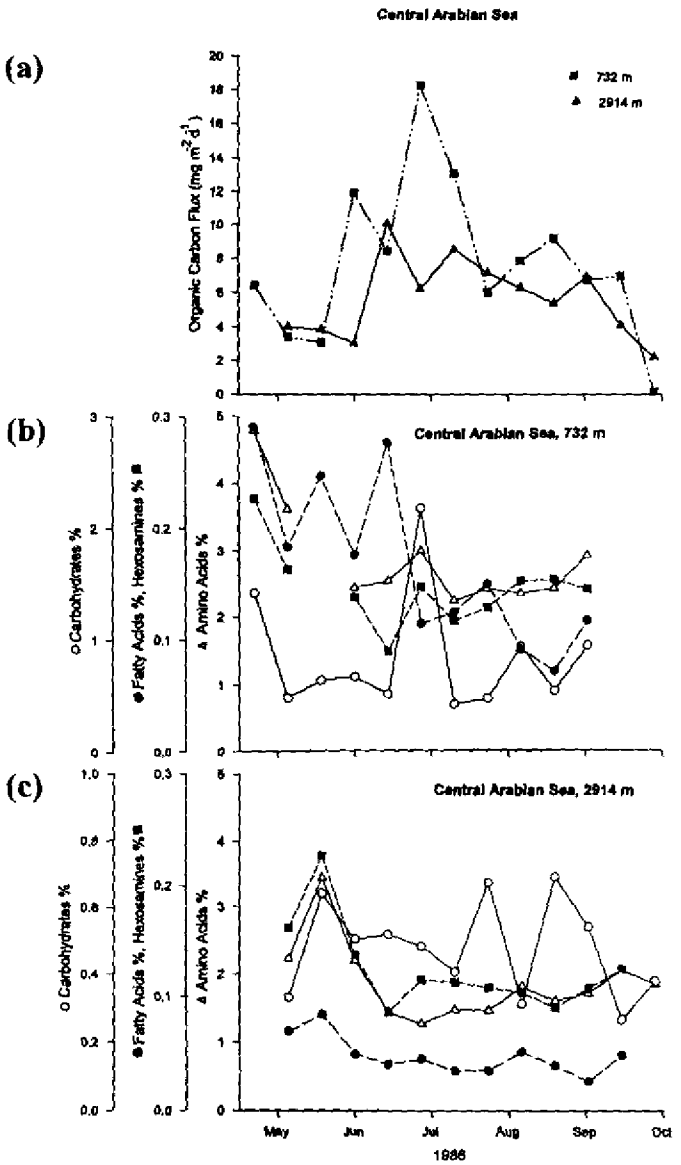

Figure 14.7 (a) Organic carbon fluxes at 732 m and 2914 m water depth between May and October 1986, and percentages of carbohydrates, hexosamines, fatty acids and amino acids in the trap (b) at 732 m and (c) at 2914 m in the central Arabian Sea.

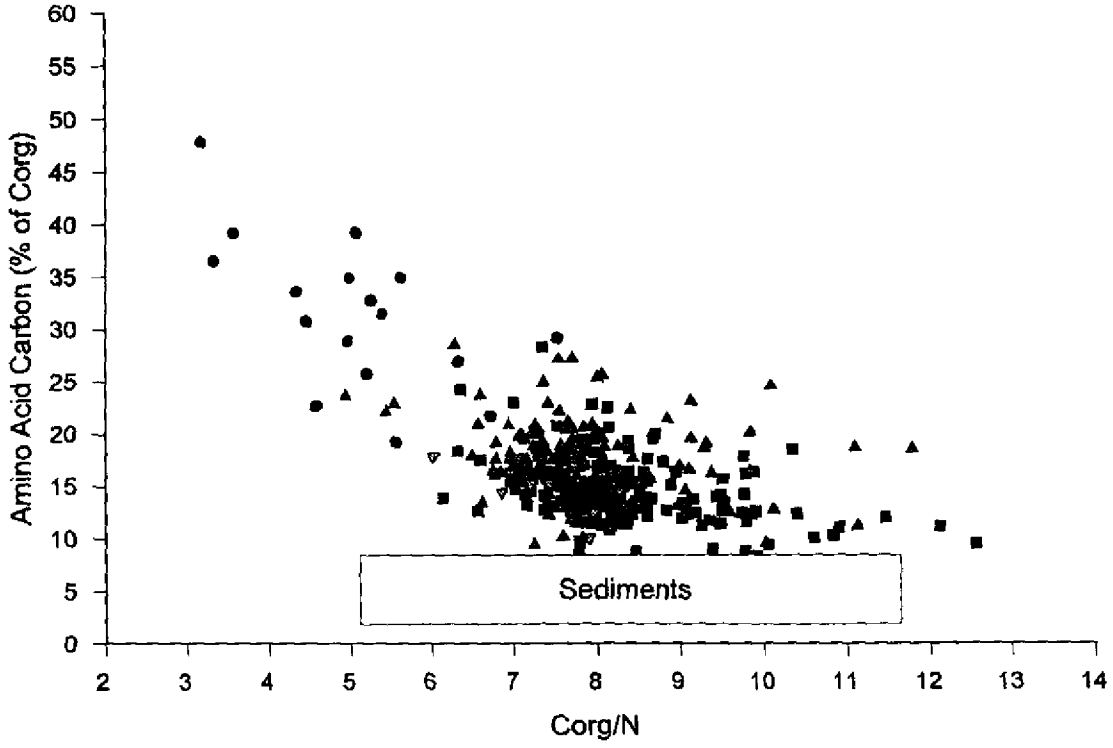

Figure 14.8 Amino acid carbon as per cent of organic carbon (C_{org}) versus C/N ratio in plankton (dots), shallow (triangles) and deep traps (squares) from the Arabian Sea, and in sediments from the Arabian Sea (box).

Table 14.1 Total amino acid (AA), hexosamine (HA), carbohydrate (CHO) fluxes measured between May 1986 and October 1987 at the western (WAST), central (CAST) and eastern (EAST) trap locations in the shallow and deep traps. Contents of AA, HA, CHO and fatty acids (FA) are given in mg g^{-1} for the whole period, AA-C %, HA-C %, CHO-C % and FA-C % represent the contributions of the organic constituents to total organic carbon.

	WAST		CAST		EAST	
	1040 m	3020 m	850 m	2900 m	1455 m	2770 m
AA-Flux (mg m^{-2} y^{-1})	1277	852	908	399	417	388
HA-Flux (mg m^{-2} y^{-1})	107	66	76	43	30	29
CHO-Flux (mg m^{-2} y^{-1})	286	180	201	104	124	114
AA (mg g^{-1})	30.3	22.0	36.4	22.5	20.9	17.8
HA (mg g^{-1})	2.6	1.7	3.1	2.4	1.5	1.4
CHO (mg g^{-1})	6.8	4.7	8.1	5.9	6.2	5.2
AA-C %	18.6	16.7	19.9	15.6	14.1	12.9
HA-C %	1.2	1.0	1.3	1.3	0.8	0.8
CHO-C %	3.9	3.3	4.1	3.8	3.9	3.7
FA (mg g^{-1}) *			1.4	0.4		
FA-C % *			1.3	0.5		

* Fatty acid data are for samples collected between May and October 1986.

accumulation of bacterial biomass on sinking particles suggesting that bacteria play a key role in organic matter decomposition.

14.5.3 INTERANNUAL VARIATIONS

The monsoons vary interannually in their intensities; i.e., in their wind speeds, precipitation and timing of arrival and retreat (e.g., Singh, 1994; Khandekar, 1991). Very little research has been done on the NE monsoon as it is much weaker and in most parts not associated with rains. In contrast, the SW monsoon precipitation over India, its duration, amount and seasonal distribution has been studied in detail for a long time. It has been stated that a stronger monsoon on land (i.e., a monsoon with higher amounts of precipitation) must be associated with a stronger Findlater Jet (Findlater, 1969). Systematic investigations of this phenomenon are, however, scarce (Dube et al., 1990).

The precipitation over India is measured at hundreds of rain gauges every year and averaged for the whole country (e.g., Singh, 1994). The deviation of this average from the long term mean precipitation can give an idea of the relative intensity of a monsoon (given as the Monsoon Index, MI). The Monsoon Indices for 1986 to 1992 (from Singh, 1994) revealed a significantly positive correlation with annual average lithogenic fluxes at the western and central trap sites (Figure

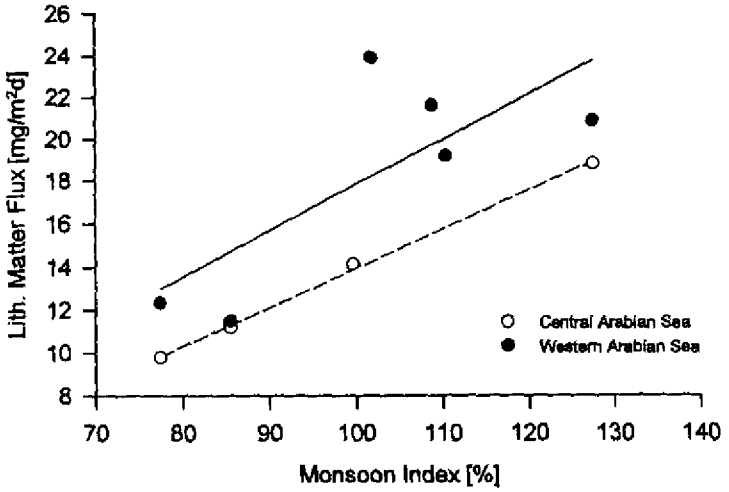

Figure 14.9 Monsoon Index (%) versus annual averages of lithogenic fluxes (mg m^{-2} d^{-1}) for six years in the western (1986–88, 1990–92) and four years in the central (1986–88, 1992) deep traps.

14.9). Stronger winds during SW monsoons and higher precipitation led to the transport of more dust from the continents to the ocean. In the eastern Arabian Sea there was no relationship between MI and lithogenic fluxes, most probably due to the interference of lithogenic matter of resuspended or fluvial origin which was observed in some of the years of investigation after the retreat of the SW monsoon in October/November (see above). These findings suggest that the total amount of lithogenic matter could be a proxy-indicator of monsoon intensity at locations not affected by near-bottom lateral transport.

14.5 CONCLUSIONS

Monsoon related processes are responsible for the particle flux patterns found in the deep Arabian Sea. The difference between the three stations is large for biogenic fluxes as one of them is influenced by upwelling and, therefore, receives higher amounts of biogenic matter than the other two. Lithogenic fluxes are quite uniform over the basin and consist mainly of aeolian material from desert areas west of the Arabian Sea.

Organic matter in sinking material is of predominantly marine origin throughout the year. During bloom periods the material reaching the deep ocean is more labile and its decomposition in the deep ocean is, therefore, enhanced compared to the periods of lower fluxes. As amino acids are preferentially degraded, C/N ratios

in combination with amino acid carbon percentages can be used to define intensity of alteration and diagenetic stage of organic matter. Tracers of bacterial biomass as well as the difference in stability of amino acids, carbohydrates and hexosamines indicate that bacteria play a key role in organic matter decomposition.

Total annual lithogenic fluxes are positively related to monsoon strength. Its use as a proxy-indicator for SW monsoon intensity in short term studies has to be checked carefully as the lateral transport in the nepheloid layer may alter the accumulation of lithogenic matter in sediments. For long-term studies changes in land vegetation have to be taken into account.

14.6 ACKNOWLEDGMENTS

MCSST data were obtained from the NASA Physical Oceanography Distributed Active Archive Center at the Jet Propulsion Laboratory/California Institute of Technology. Help from Dr. P. Schlüssel and S. Ewald in processing MCSST data is gratefully acknowledged. We thank the mechanical and electronic engineers of the National Institute of Oceanography, Goa, and the University of Hamburg for technical assistance, the officers and crew of the research vessels R/V *Sagar Kanya* and R/V *Sonne* for their help in the deployments and recoveries of the mooring systems. Financial support for the ongoing Indo-German sediment trap program was provided by the Federal Ministry for Education, Science, Research and Technology (BMBF, Bonn), the German Research Council (DFG, Bonn, Grant It 6/1–1, 2, 3), the Council of Scientific and Industrial Research (CSIR, New Delhi) and the Department of Ocean Development (DOD, New Delhi).

14.7 REFERENCES

Alldredge, A. L. and M. W. Silver (1988) "Characteristics, dynamics and significance of marine snow", *Prog. Oceanogr.*, **20**, 41–82.

Borole, D. V., M. M. Sarin and B. L. K. Somayajulu (1982) "Composition of Narmada and Tapti estuarine particles and adjacent Arabian Sea sediments", *Indian J. Mar. Sci.*, **11**, 51–62.

Brock, J. C., C. R. McClain and W. W. Hay (1992) "A southwest monsoon hydrographic climatology for the northwestern Arabian Sea", *J. Geophys. Res.*, **97**, 9455–9465.

Chester, R., E. J. Sharples and G. S. Sanders (1984) "The concentration of particulate aluminum and clay minerals in aerosols from the northern Arabian Sea", *Journ. Sed. Petrol.*, **55**, 37–41.

Cowie, G. L. and J. I. Hedges (1994) "Biochemical indicators of diagenetic alteration in natural organic matter mixtures", *Nature*, **369**, 304–307.

Curry, W. B., D. R. Ostermann, M. V. S. Guptha and V. Ittekkot (1992) "Foraminiferal production and monsoonal upwelling in the Arabian Sea: Evidence from sediment traps", in C. P. Summerhayes, W. L. Prell and K. C. Emeis (eds) *Upwelling Systems: Evolution Since the Early Miocene*, Geological Society Special Publication No. 64, 93–106.

Degens, E. T. and V. Ittekkot (1984) "A new look at clay-organic interactions", in E. T. Degens, W. A. Krumbein and A. A. Prashnowsky (eds) *Festband Georg Knetsch*, Mitt. Geol.-Paläont. Inst. Univ. Hamburg No. 56, 229–248.

Deuser, W. G. (1986) "Seasonal and interannual variations in deep-water particle fluxes in the Sargasso Sea and their relation to surface hydrography", *Deep-Sea Res.*, **33**, 225–246.

Deuser, W. G., F. E. Müller-Karger, R. H. Evans, O. B. Brown, W. E. Esaias and G. C. Feldman (1990) "Surface-ocean color and deep-ocean carbon flux: how close a connection?", *Deep-Sea Res.*, **37**, 1331–1344.

Deuser, W. G., E. H. Ross and R. F. Anderson (1981) "Seasonality in the supply of sediment to the deep Sargasso Sea and implications for the rapid transfer of matter to the deep ocean", *Deep-Sea Res.*, **28**, 495–505.

Dube, S. K., M. E. Luther and J. J. O'Brien (1990) "Relationship between interannual variability in the Arabian Sea and Indian Summer monsoon rainfall", *Meteorol. Atmos. Phys.*, **44**, 153–165.

Findlater, J. (1969) "A major low-level air current near the Indian Ocean during the northern summer", *Quart. J.R. Met. Soc.*, **95**, 362–380.

Haake, B., V. Ittekkot, V. Ramaswamy, R. R. Nair and S. Honjo (1992) "Fluxes of amino acids and hexosamines to the deep Arabian Sea", *Mar. Chem.*, **40**, 291–314.

Haake, B., V. Ittekkot, T. Rixen, V. Ramaswamy, R. R. Nair and W. B. Curry (1993) "Seasonality and interannual variability of particle fluxes to the deep Arabian Sea", *Deep-Sea Res.*, **40**, 1323–1344.

Hedges, J. I., G. L. Cowie, J. E. Richey, P. D. Quay, R. Benner, M. Strom and B. R. Forsberg (1994) "Origins and processing of organic matter in the Amazon River as indicated by carbohydrates and amino acids", *Limnol. Oceanogr.*, **39**, 743–761.

Honjo, S. (1978) "Sedimentation of materials in the Sargasso Sea at a 5,347 m deep station", *J. Mar. Res.*, **36**, 459–492.

Honjo, S., S. J. Manganini and J. J. Cole (1982) "Sedimentation of biogenic matter in the deep ocean", *Deep-Sea Res.*, **29**, 609–625.

Ittekkot, V. (1988) "Global trends in the nature of organic matter in river suspensions", *Nature*, **332**, 436–438.

Ittekkot, V. (1993) "The abiotically driven biological pump in the ocean and short-term fluctuations in atmospheric CO_2 contents", *Global Planet. Change*, **8**, 17–25.

Ittekkot, V. and R. Arain (1986) "Nature of particulate organic matter in the river Indus, Pakistan", *Geochim. Cosmochim. Acta*, **50**, 1643–1653.

Ittekkot, V., E. T. Degens and S. Honjo (1984a) "Seasonality in the fluxes of sugars, amino acids and amino sugars to the deep ocean: Panama Basin", *Deep-Sea Res.*, **31**, 1071–1083.

Ittekot, V., W. G. Deuser and E. T. Degens (1984b) "Seasonality in the fluxes of sugars, amino acids and amino sugars to the deep ocean: Sargasso Sea", *Deep-Sea Res.*, **31**, 1057–1069.

Ittekkot, V., R. R. Nair, S. Honjo, V. Ramaswamy, M. Bartsch, S. Manganini and B. N. Desai (1991) "Enhanced particle fluxes in Bay of Bengal induced by injection of freshwater", *Nature*, **351**, 385–387.

Khandekar, M. L. (1991) "Eurasian snow cover, Indian monsoon and El Niño/Southern oscillation - a synthesis", *Atmosphere-Ocean*, **29**, 636–647.

Kolla, V., J. A. Kostecki, F. Robinson, P. E. Biscaye and P. K. Kray (1981) "Distribution and origin of clay minerals and quartz in surface sediments of the Arabian Sea", *J. Sed. Petrol.*, **51**, 563–569.

Lee, C. and C. Cronin (1984) "Particulate amino acids in the sea: Effects of primary productivity and biological decomposition", *J. Mar. Res.*, **42**, 1075–1097.

Moers, M. E. C. and S. R. Larter (1993) "Neutral monosacchacarides from a hypersaline tropical environment: Applications to the characterization of modern and ancient ecosystems", *Geochim. Cosmochim. Acta*, **57**, 3063–3071.

Molnar, P., P. England and J. Martinod (1993) "Mantle dynamics, uplift of the Tibetian Plateau, and the Indian Monsoon", *Rev. Geophys.*, **31**, 357–396.

Nair, R. R., V. Ittekkot, S. J. Manganini, V. Ramaswamy, B. Haake, E. T. Degens, B. N. Desai and S. Honjo (1989) "Increased particle fluxes to the deep ocean related to monsoons", *Nature*, **338**, 749–751.

Ochiai, M., M. Ogino, K. Sasaki and T. Okazawa (1988) "Behaviour of particulate carbohydrates and amino acids in the estuary of the Tama river", *Mar. Chem.*, **25**, 265–278.

Ramaswamy, V., R. R. Nair, S. J. Manganini, B. Haake and V. Ittekkot (1991) "Lithogenic fluxes to the deep Arabian Sea measured by sediment traps", *Deep-Sea Res.*, **38**, 169–184.

Rashid, M. A. (1985) *Geochemistry of Marine Humic Compounds*, Springer, Berlin, 300 pp.

Reemtsma, T., B. Haake, V. Ittekkot, R. R. Nair and U. H. Brockmann (1990) "Downward flux of particulate fatty acids in the Central Arabian Sea", *Mar. Chem.*, **29**, 183–202.

Reemtsma, T., V. Ittekkot, M. Bartsch and R. R. Nair (1993) "River inputs and organic matter fluxes in the northern Bay of Bengal: Fatty acids", *Chem. Geol.*, **103**, 55–71.

Rixen, T. and B. Haake (1993) "Fluxes and decomposition of organic matter in the western Arabian Sea: Amino acids and hexosamines", in V. Ittekkot and R. R. Nair (eds) *Monsoon Biogeochemistry*, Mitt. Geol.-Paläont. Inst. Univ. Hamburg 76, 113–130.

Sirocko, F. and M. Sarnthein (1989) "Wind-borne deposits in the Northwestern Indian Ocean: Record of Holocene sediments versus modern satellite data", in M. Leinen and M. Sarnthein (eds) *Paleoclimatology and Paleometeorology: Modern and Past Patterns of Global Atmospheric Transport*, NATO ASI Series C., 282, Kluwer Acad. Publ., Dordrecht, 401–433.

Singh, N. (1994) "Optimizing a network of rain-gauges over India to monitor summer monsoon rainfall variations", *Internat. J. Climatol.*, **14**, 61–70.

Smith, D. C., M. Simon, A. L. Alldredge and F. Azam (1992) "Intense hydrolytic enzyme activity on marine aggregates and implications for rapid particle dissolution", *Nature*, **359**, 139–141.

Wakeham, S. G., C. Lee, J. W. Farrington and R. B. Gagosian (1984) "Biogeochemistry of particulate organic matter in the oceans: Results from sediment trap experiments", *Deep-Sea Res.*, **31**, 509–528.

Wyrtki, K. (1973) "Physical oceanography of the Indian Ocean", in B. Zeitzschel (ed) *The Biology of the Indian Ocean*, Springer, Berlin, 18–36.

15 Fresh Water Influx and Particle Flux Variability in the Bay of Bengal

P. SCHÄFER, V. ITTEKKOT, M. BARTSCH,
R. R. NAIR AND J. TIEMANN

15.1 INTRODUCTION

In this chapter we review the results from an ongoing continuous sediment trap experiment at three locations in the Bay of Bengal, a marine region which comes under the influence of some of the largest rivers in the world - the Ganges/ Brahmaputra river system. The results from the study are expected to provide information on the response of marine biogeochemical cycles to this fresh water influx. Such information is critical to understanding the past, and possibly also future, changes in the marine carbon cycle and those induced by the injection of fresh water into the oceans from melting ice sheets, in particular.

In the following we discuss the major processes controlling particle fluxes to the deep Bay of Bengal based on information obtained from deep-moored traps (1727 m – 3010 m, compare Table 15.1) covering four years of study from October 1987 to November 1991. For detailed illustration of these processes, especially the influence of fresh water and sediment inputs, we have included a description of the fluxes and of the geochemical ratios measured at shallow and deep traps in the northern, central and southern areas of the Bay of Bengal during the period of 1987–88.

15.2 STUDY AREA

The Bay of Bengal is the catch basin for fresh water and sediment input from some of the world's largest rivers (Figure 15.1). It is estimated that annually about 2×10^9 tons of sediments enters the Bay of Bengal with the major input coming from the rivers such as Ganges and Brahmaputra draining the Himalayas (Milliman and Meade, 1983). The inputs from these rivers exhibit high seasonal variabilities with the bulk occurring during the SW monsoon (Figure 15.2a). The other major contributors of terrigenous material to the Bay of Bengal are the

Particle Flux in the Ocean
Edited by V. Ittekkot, P. Schäfer, S. Honjo and P. J. Depetris

Table 15.1 Sampling data of the sediment trap experiment in the Bay of Bengal

	Position N	Position E	Trap depth (m)	Trap depth (m)	Water depth (m)	Sampling start	Sampling end	Sampling interval (d)
$NBBT_N$ - Northern Bay of Bengal Trap - North								
01	17°27'	89°36'	809	1727	2263	10/28/87	02/28/88	13 x 9.5
02	17°27'	89°36'	754	1790	2267	04/01/88	10/06/88	13 x 14.5
03	17°27'	89°36'	967	2029	2265	11/02/88	10/19/89	13 x 27
$NBBT_S$ - Northern Bay of Bengal Trap - South								
04	15°14'	89°10'	1131	1717	2738	01/02/90	10/28/90	13 x 23
05	15°31'	89°13'	1131	2120	2706	12/05/90	10/26/91	13 x 25
CBBT - Central Bay of Bengal Trap								
01	13°09'	84°22'	906	2282	3259	10/28/87	02/28/88	13 x 9.5
02	13°09'	84°22'	950	2227	3263	04/01/88	10/06/88	13 x 14.5
03	13°09'	84°21'	950	2286	3263	11/02/88	10/19/89	13 x 27
04	13°08'	84°17'	988	2327	3312	04/06/90	11/21/90	1x21, 8x23, 4x6
05	13°09'	84°20'	893	2282	3267	12/05/90	10/26/91	13 x 25
SBBT - Southern Bay of Bengal Trap								
01	04°28'	87°19'	1040	3006	4017	10/28/87	02/28/88	13 x 9.5
02	04°28'	87°18'	1017	2983	4045	04/01/88	10/06/88	13 x 14.5
05	05°01'	87°09'	1071	3010	3996	12/05/90	10/26/91	13 x 25

Errors in rotation:
CBBT-01, 2282 m = deep: 11/06/87 to 03/22/88, 12 x 9.5, 1 x 23
CBBT-03, 2286 m = deep: Cup 11 sampled 2 intervals (07/30/89 to 09/22/89)
CBBT-03, 2286 m = deep: Cup 12 = interval 13

peninsular Indian rivers such as the Mahanadi, Godavari, Krishna and Cauvery which have their peak discharges during the later phase of the SW monsoon. The enormous fresh water discharges cause changes in the surface salinity of the Bay of Bengal over a wide range of values both seasonally and geographically (LaViolette, 1967). The greatest change (by more than 7‰) occurs towards the end of the SW monsoon when the water discharge from the Ganges and Brahmaputra and from the peninsular Indian rivers is at a maximum.

The drainage basins of the rivers are drastically affected by human activities such as deforestation which has an effect also on nutrient transport of the rivers. It has been found that nitrogen transport in these rivers has, in addition to the dissolved nitrogen load, a major component associated with the particulate fraction and which is derived from eroding soils (Ittekkot and Zhang, 1989). This nutrient loading is enhanced by the use of nitrogen fertilizers for agriculture and by the direct introduction of nutrients from highly populated areas.

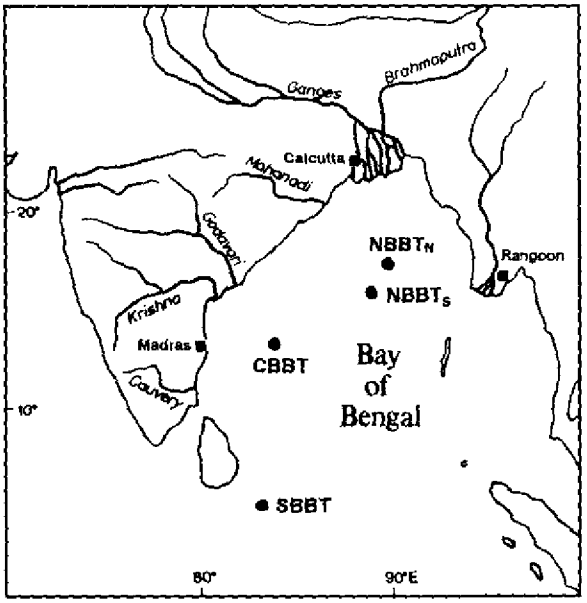

Figure 15.1 Locations of the sediment trap moorings in the northern ($NBBT_N$, $NBBT_S$), central (CBBT) and southern (SBBT) Bay of Bengal (for details see Table 15.1).

15.3 METHODS

15.3.1 SAMPLING

Samples were collected during an ongoing sediment trap experiment in the Bay of Bengal since October 1987. Briefly, three moorings, each consisting of two time-series sediment traps (Mark VI, Honjo and Doherty, 1988) were deployed at three locations in the northern, central and southern Bay of Bengal (Figure 15.1). The traps are programmed to collect settling particles at intervals of approximately one to four weeks (Table 15.1).

Prior to deployment the collection cups were filled with deep-sea water to which 35 g NaCl l^{-1} and 3.33 g $HgCl_2$ l^{-1} were added in order to minimize loss by diffusion and biological alteration during underwater storage (Knauer et al., 1984; Lee et al., 1992). On recovery of the traps the samples were wet-sieved and split using a precision rotary splitter. The < 1 mm fraction was filtered through preweighed polycarbonate filters (0.45 μm, Nuclepore) and dried at 40°C for 24 hours. This fraction was used for flux calculations.

15.3.2 ANALYSES

Carbonate was determined by heating the sample with phosphoric acid and subsequent quantification of the evolved CO_2 in a NaOH solution by conductivity (WÖSTHOFF Carmhograph). Biogenic opal was determined photometrically after extraction of silica into a Na_2CO_3 solution (modified after Mortlock and Froelich, 1989). Nitrogen and total carbon content were determined using a CN analyzer (NA-1500 Nitrogen Analyzer, Carlo Erba). Organic carbon was calculated as the difference between total carbon and carbonate carbon. The content of lithogenic material was calculated as the difference between 100 and the sum of carbonate, opal and organic matter (organic matter = C_{org} x 1.8, Müller et al., 1986) content. For further details see Haake et al., (1993). C/N, Carbonate/opal and C_{org}/ $C_{Carbonate}$ ratios were calculated by weight percent.

15.3.3 WIND SPEED AND SEA SURFACE TEMPERATURE

Wind speed data are from ship observations within a radius of 2° around the study sites (Indian Daily Weather Report).

The sea surface temperature (SST) data used in this study were provided by the Distributed Active Archive Center (DAAC) of the Jet Propulsion Laboratory (JPL). The data base is a weekly composite, Multichannel Sea Surface Temperature (MCSST) estimate based on the AVHRR (Advanced Very High Resolution Radiometer) measurements. The MCSST data are interpolated for 18 km resolution. We present time series of MCSST for the pixel location closest to the three sediment trap locations.

15.4 TOTAL AND COMPONENT FLUXES

Total fluxes in the Bay of Bengal vary between 52–340 mg m^{-2} d^{-1} during the period of investigation. The associated component fluxes are in the range of 11–140 mg m^{-2} d^{-1} for carbonate, 6–137 mg m^{-2} d^{-1} for opal, 9–199 mg m^{-2} d^{-1} for lithogenic matter, and 2.4–14.6 mg m^{-2} d^{-1} for organic carbon. The variability of these fluxes at the individual stations is discussed below.

15.4.1 NORTHERN BAY OF BENGAL

The highest fluxes were recorded in 1988 during the SW monsoon (Figures 15.2b and 15.3). The Indian summer monsoon was the strongest in the year 1988. The year also saw severe floods in Bangladesh which caused large scale losses in property and human lives (Das et al., 1989b). Enormous amounts of fresh water and sediments were discharged into the Bay of Bengal during that year. These inputs and the associated nutrients led to high primary productivity in coastal

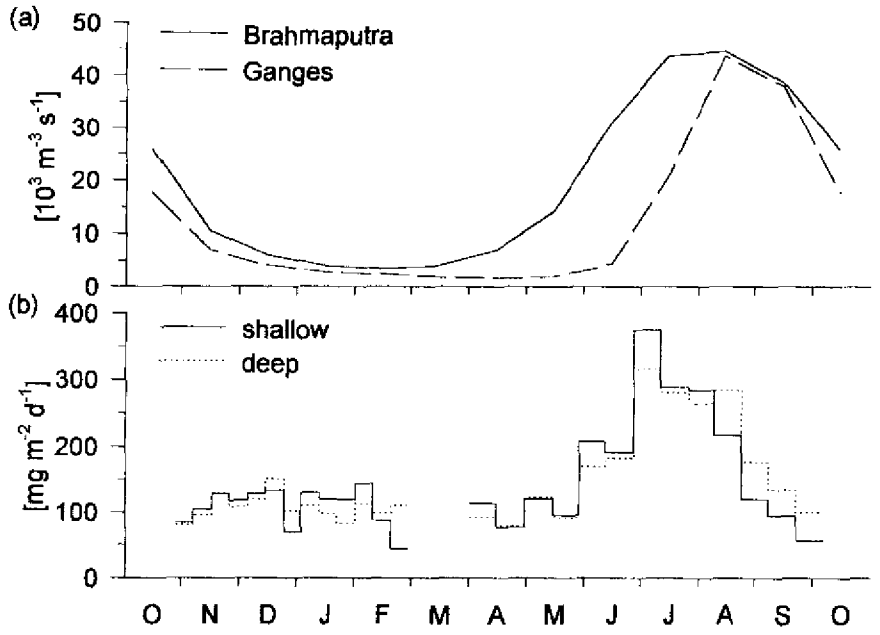

Figure 15.2 (a) Water discharge (from Unesco, 1979) and (b) total fluxes in the northern Bay of Bengal from October 1987 to October 1988.

areas and river plumes with the effect of enhancing the particle flux to the deep ocean. In the Bay of Bengal, the effects of these processes were felt at the northern station ($NBBT_N$) which is located approximately 480 km off the mouth of the Ganges/Brahmaputra river system (Figure 15.1).

The seasonal pattern of particle flux in 1989 at the same station differs from 1988 (Figure 15.3). The particle flux maximum which was observed in 1988 was absent. The 1989 SW monsoon was also weaker than 1988 (Parthasarathy et al., 1992) and this had the effect of reducing river inputs to the Bay of Bengal. On the other hand wind speeds were much stronger in 1989 which resulted in a rapid cooling of the surface layers in March. This also indicated nutrient input from deeper water layers and subsequently elevated biological production of particles. Therefore particle fluxes at this station in 1989 showed a prolonged period of high fluxes between March and October instead of recording peak fluxes for a short time period as in 1988 (Figure 15.3). Thus, although there was a difference in the seasonal flux pattern, the total annual fluxes recorded for the two years were almost identical (52 g m^{-2}, Table 15.2a).

An interesting feature of particle flux in the northern parts of the Bay of Bengal was the spatial variability observed. The fluxes measured at a station about 200

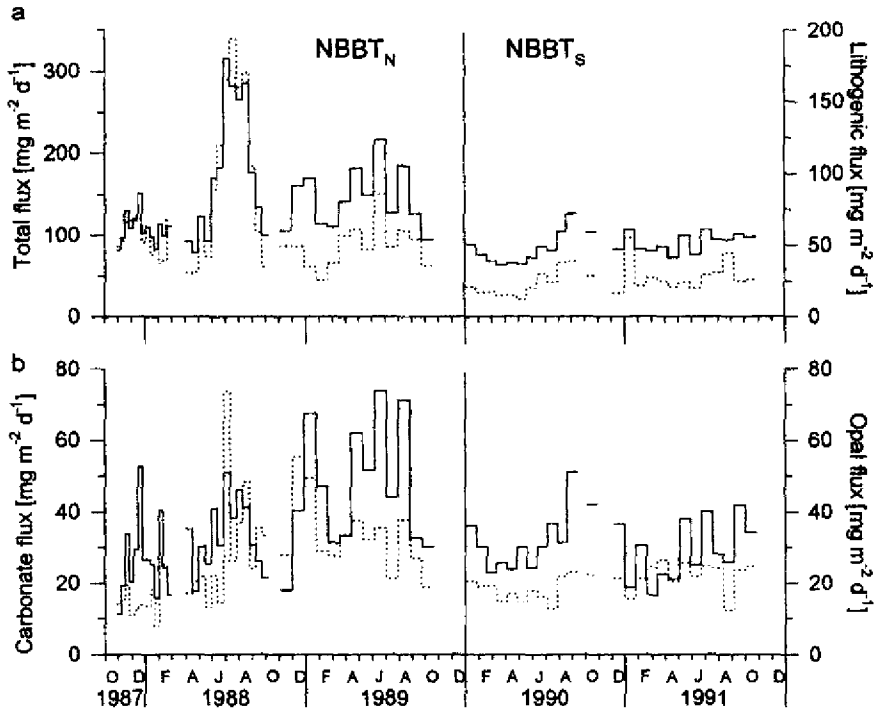

Figure 15.3 (a) Total fluxes (—) and lithogenic fluxes (·····), and (b) carbonate fluxes (—) and opal fluxes (·····) in the northern Bay of Bengal.

km south of the northern station (NBBT$_S$, Figure 15.1) in 1990 and 1991 were characterized by low fluxes and an absence of any pronounced seasonal signals (Figure 15.3). This may be due, on the one hand, to the weaker SW monsoon in the years 1990 and 1991 in comparison to the two previous years (Parthasarathy et al., 1992) and, on the other, to the diversion of the river plume away from the trap location by the prevailing surface circulation pattern in the northern Bay of Bengal (Madhusudana Rao, 1985). The difference in flux patterns observed at these two stations located about 200 km away from each other may result from the varying influence of the inputs from the Ganges/Brahmaputra river system. If river-derived mineral particles are incorporated into large organic aggregates derived from primary production within river plumes, then this also may accelerate particle sedimentation in the sea (Ittekkot, 1991; 1993; Figure 15.4). Primary production in river plumes effectively acts as a biological barrier preventing the dispersal of river-derived suspended material towards the open ocean.

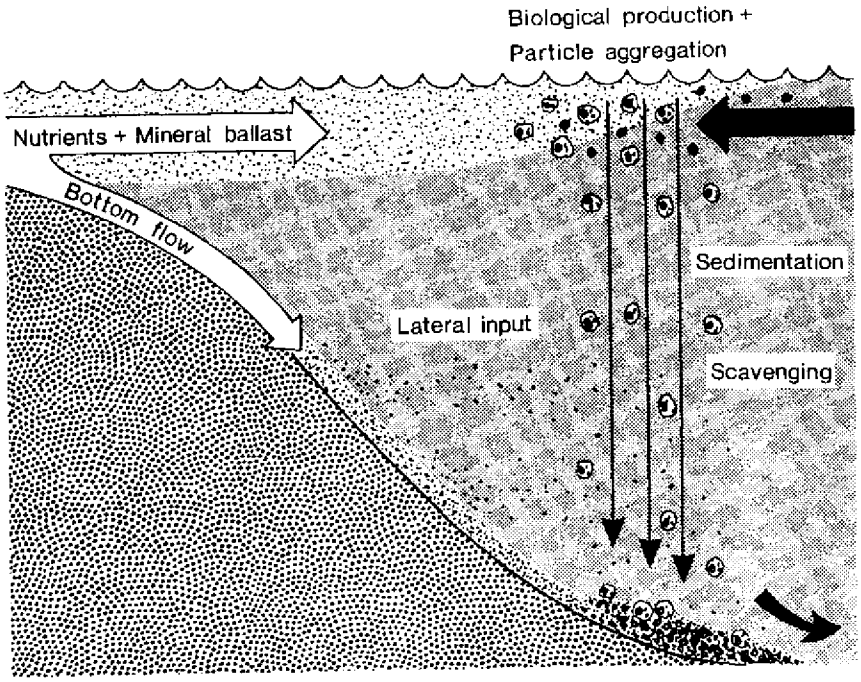

Figure 15.4 The supply of nutrients by the rivers leads to high primary productivity in river plumes advected far into the open ocean. The biogenic particles incorporate suspended lithogenic particles which are also supplied by the river and can thus be transported faster into the deep sea where they scavenge fine lithogenic particles advected from the continental slope (from Ittekkot, 1991).

During the monsoons, carbonate fluxes in the northern Bay of Bengal were more than twice those recorded during the intermonsoon periods. The flux pattern correlated well with the wind speed pattern which suggests that biological carbonate production was mainly controlled by nutrient input to the surface layers by wind-induced mixed layer deepening. Foraminiferal populations less tolerant to salinity changes (e.g., *Globigerinoides sacculifer*) had lower flux rates in the northern Bay of Bengal than in the central Bay of Bengal (Guptha et al., 1996). The temporal and spatial pattern of their appearance and abundance was indicative of strong surface salinity fluctuations even within the SW monsoon periods. Such changes were consistent with particle fluxes associated with an advancing and retreating river plume postulated by Reemtsma et al. (1993) and are reminiscent of particle flux changes to the deep sea encountered in polar regions in association with seasonal changes in ice cover (this volume, Chapters 7 and 13).

The fluxes of opal and lithogenic material at the northern station (Figure 15.3) appeared to be directly related to discharge from the rivers and there was no clear-cut correlation between wind speeds and fluxes as was observed for carbonate fluxes (Bartsch, 1993). Biogenic opal and lithogenic fluxes were highest during the 1988 SW monsoon, which was also characterized by high rainfall and high river inputs. Lithogenic matter made up to 59% and opal up to 32% of the total flux in 1987/88 at the northern station (Bartsch, 1993) and both were much higher than those measured in most of the other oceanic regions (this volume, Chapter 7). The river inputs contributed directly to the fluxes by introducing lithogenic material, and indirectly by bringing in nutrients including large quantities of dissolved silicate to the surface layers stimulating biological productivity, especially of diatoms. This increase in diatom production in the upper ocean due to fresh water influx was reflected in the flux pattern at this station. Similar to the pattern observed in total fluxes, biogenic opal and lithogenic fluxes were less variable in 1990 and 1991 at $NBBT_S$, where the traps were located 200 km south of $NBBT_N$ (Figure 15.3). Also the fluxes of both components were lower than those measured at the northern station indicating the absence of fluvial influence.

15.4.2 CENTRAL BAY OF BENGAL

At the central Bay of Bengal station (CBBT) marked seasonality was observed in each of the investigated years with high fluxes during both SW and NE monsoon periods (Figure 15.5, Table 15.2b).

Carbonate fluxes in the central Bay of Bengal were higher than those measured at the northern stations. Higher fluxes (more than twice) occurred during the monsoons than during the intermonsoon periods. The opal fluxes were generally higher during both monsoons whereas high lithogenic fluxes occurred mainly during the SW monsoon. The particle flux maximum observed between October 1990 and January 1991 represents an exception to this general trend. During this period of four months, opal fluxes of 8.2 g m^{-2} and fluxes of lithogenic material of 19.4 g m^{-2} were recorded. Lithogenic material contributed 54% of the total flux indicating a strong influence of land-derived material introduced from the rivers during this period. The terrigenous nature of the settling particles was further confirmed by their comparatively low $\delta^{15}N$ values (Schäfer and Ittekkot, 1995). The central trap location was about 480 km off the mouths of the Indian peninsular rivers, Godavari and Krishna (Figure 15.1), the drainage basins of which received more than double the annual average rainfall during August 1990 (Gupta et al., 1991b). Also, the recorded rainfall between October and December 1990 was more than thrice that of the average, resulting in high water levels in the rivers and floods in the drainage area (Gupta et al., 1991c).

The Bay of Bengal is also affected by storms and the track of one such storm crossed the location on November 1, 1990 (Gupta et al., 1991a). The resulting

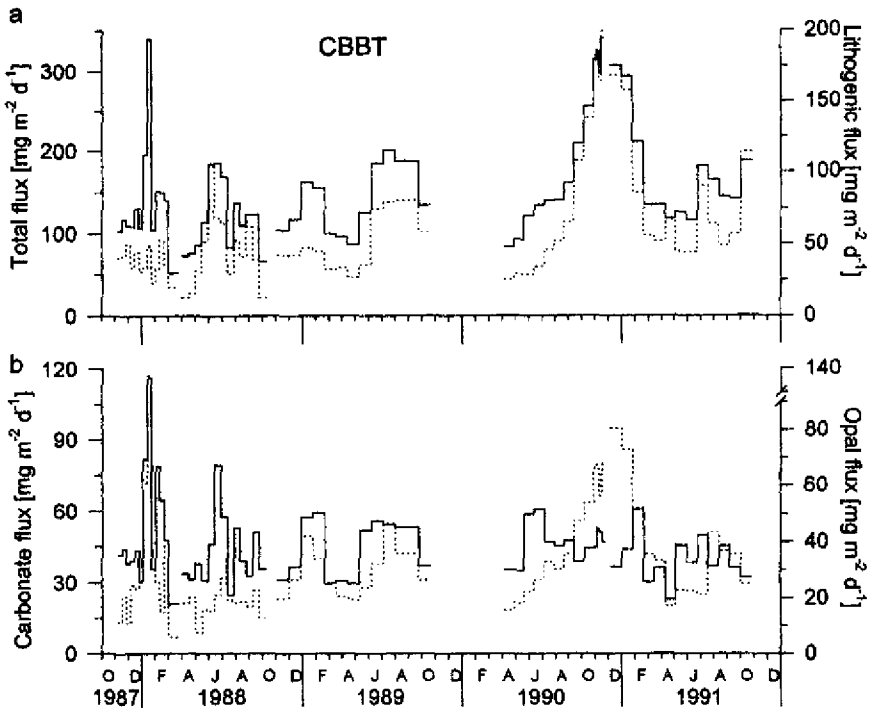

Figure 15.5 (a) Total fluxes (—) and lithogenic fluxes (·····), and (b) carbonate fluxes (—) and opal fluxes (·····) in the central Bay of Bengal.

turbulent mixing of the upper ocean entraining nutrients from the deeper layers to the euphotic zone enhances biological productivity in the surface layers. This, and the increased terrigenous influx from rivers and from shelf sediments, could have contributed to the high fluxes and to the pattern of component fluxes observed during this period. A peak flux in January 1988 consisting mainly of opal in the central Bay of Bengal also appeared to be related to enhanced cyclonic activity in the region between November and December 1987 (Das et al., 1989a; Figure 15.5).

15.4.3 SOUTHERN BAY OF BENGAL

In contrast to the northern and central stations, seasonality in wind speeds was much stronger in the southern Bay of Bengal (Figure 15.6). The increase in wind speeds caused a decrease in sea surface temperature of about 3°C during the SW monsoon, and of 1–2°C during the NE monsoon (Figure 15.6). High particle fluxes were recorded in the deep sea within about 3 to 4 weeks after the decrease

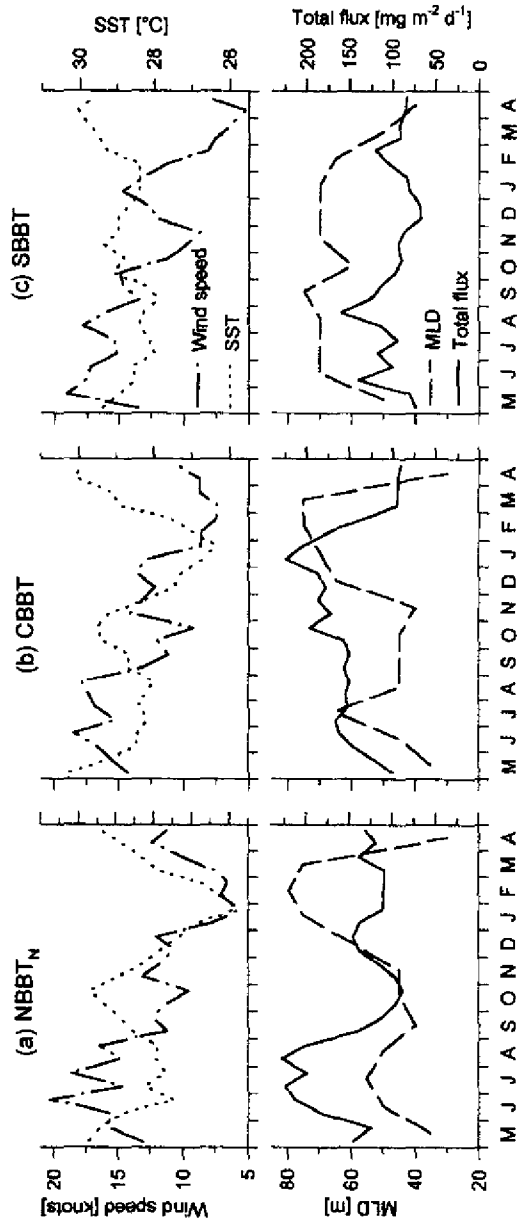

Figure 15.6 Biweekly means of wind speed, sea surface temperature (SST), mixed layer depth (MLD, from Rao et al., 1989) and total flux in the (a) northern, (b) central and (c) southern Bay of Bengal.

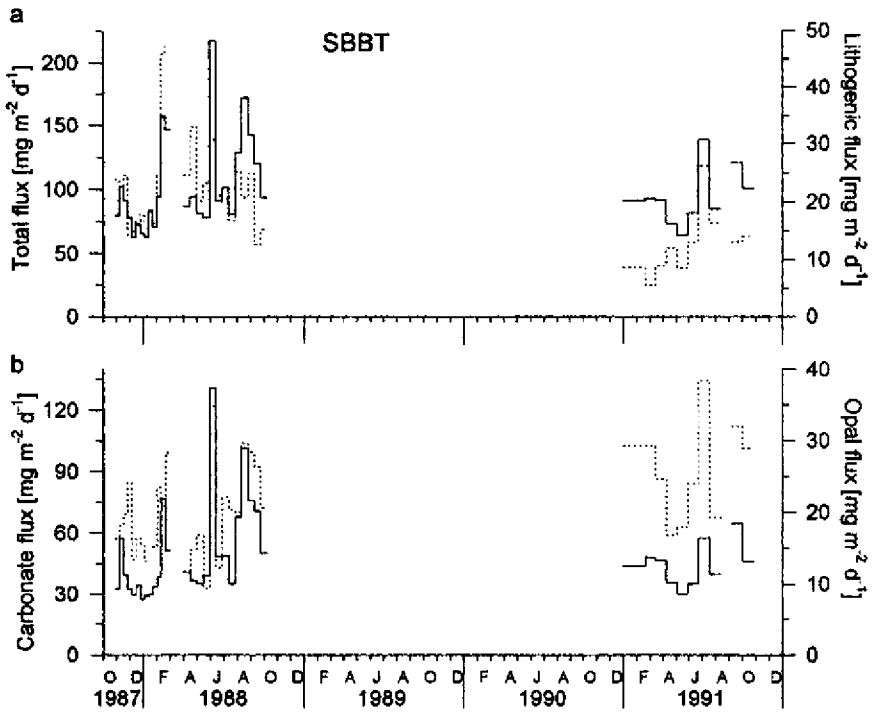

Figure 15.7 (a) Total fluxes (—) and lithogenic fluxes (·····), and (b) carbonate fluxes (—) and opal fluxes (·····) in the southern Bay of Bengal.

in surface temperature (Figure 15.6). Wind-induced mixed layer deepening brings nutrient-rich subsurface waters to the euphotic zone and enhances primary productivity and as a consequence particle flux to the deep ocean (Nair et al., 1989). Because of technical problems data for only two years are presented here (i.e., 1987–88 and 1991) during which period the particle flux patterns were similar (Figure 15.7).

The southern Bay of Bengal is characterized by higher carbonate fluxes and lower opal and lithogenic fluxes in comparison with the northernmost and the central stations. The total flux pattern was mainly determined by carbonate fluxes. Here again, the close association of total fluxes and wind speeds suggests that wind-induced mixed layer deepening had the general effect of increasing carbonate production in the Bay of Bengal.

Table 15.2a Fluxes of components to the deep northern Bay of Bengal and their ratios.

Period	Total flux ($g\,m^{-2}$)	Carb. flux ($g\,m^{-2}$)	Carb. (%)	Opal flux ($g\,m^{-2}$)	Opal (%)	Lith. flux ($g\,m^{-2}$)	Lith. (%)	C_{org} flux ($g\,m^{-2}$)	C_{org} (%)	N flux ($g\,m^{-2}$)	N (%)	C/N	C_{org} / $C_{Carb.}$	Carb./ Opal
$NBBT_N$														
SW-NE 1987	6.00	1.19	19.8	1.23	20.5	3.04	50.7	0.30	5.00	0.037	0.62	8.11	2.10	0.97
NE 1987/88	9.96	2.56	25.7	1.38	13.9	5.09	51.1	0.54	5.42	0.066	0.66	8.18	1.76	1.86
NE-SW 1988	9.17	2.49	27.2	1.62	17.7	4.18	45.6	0.56	6.11	0.065	0.71	8.62	1.87	1.54
SW 1988	26.68	4.51	16.9	4.30	16.1	15.53	58.2	1.30	4.87	0.150	0.56	8.67	2.40	1.05
1987/88	**51.81**	**10.75**	**20.7**	**8.53**	**16.5**	**27.84**	**53.7**	**2.70**	**5.21**	**0.318**	**0.61**	**8.49**	**2.09**	**1.26**
SW-NE 1988	6.42	1.21	18.8	1.87	29.1	2.74	42.7	0.33	5.14	0.039	0.61	8.46	2.27	0.65
NE 1988/89	12.83	4.45	34.7	3.53	27.5	3.26	25.4	0.73	5.69	0.101	0.79	7.23	1.37	1.26
NE-SW 1989	13.74	4.22	30.7	3.08	22.4	4.80	34.9	0.91	6.62	0.121	0.88	7.52	1.80	1.37
SW 1989	19.23	6.52	33.9	3.62	18.8	7.26	37.8	1.02	5.30	0.139	0.72	7.34	1.30	1.80
1988/89	**52.22**	**16.40**	**31.4**	**12.10**	**23.2**	**18.06**	**34.6**	**2.99**	**5.73**	**0.400**	**0.77**	**7.48**	**1.52**	**1.36**
SW-NE 1989	5.44	2.02	37.1	1.10	20.2	1.79	32.9	0.30	5.51	0.036	0.66	8.33	1.24	1.84
$NBBT_S$														
NE 1989/90	7.30	2.73	37.4	1.72	23.6	1.94	26.6	0.51	6.99	0.061	0.84	8.36	1.56	1.59
NE-SW 1990	6.06	2.38	39.3	1.49	24.6	1.38	22.8	0.45	7.43	0.056	0.92	8.04	1.58	1.60
SW 1990	12.06	4.57	37.9	2.32	19.2	3.84	31.8	0.74	6.14	0.089	0.74	8.31	1.35	1.97
SW-NE 1990	6.32	2.30	40.8	1.36	21.5	1.76	27.8	0.34	5.38	0.043	0.68	7.91	1.10	1.90
1989/90	**31.74**	**12.26**	**38.6**	**6.89**	**21.7**	**8.92**	**28.1**	**2.04**	**6.43**	**0.249**	**0.78**	**8.19**	**1.39**	**1.78**
NE 1990/91	7.84	2.41	30.7	1.75	22.3	2.66	33.9	0.56	7.14	0.062	0.79	9.03	1.94	1.38
NE-SW 1991	7.78	2.35	30.2	2.23	28.7	2.20	28.3	0.56	7.20	0.065	0.84	8.62	1.99	1.05
SW 1991	11.51	3.93	34.1	2.61	22.7	3.67	31.9	0.72	6.26	0.082	0.71	8.78	1.53	1.51
SW-NE 1991	5.06	1.79	35.4	1.28	25.3	1.38	27.3	0.34	6.72	0.042	0.83	8.10	1.58	1.40
1990/91	**32.19**	**10.48**	**32.6**	**7.87**	**24.4**	**9.91**	**30.8**	**2.18**	**6.77**	**0.251**	**0.78**	**8.69**	**1.73**	**1.33**

Table 15.2b Fluxes of components to the deep central Bay of Bengal and their ratios.

Period	Total flux ($g\,m^{-2}$)	Carb. flux ($g\,m^{-2}$)	Carb. (%)	Opal flux ($g\,m^{-2}$)	Opal (%)	Lith. flux ($g\,m^{-2}$)	Lith. (%)	C_{org} flux ($g\,m^{-2}$)	C_{org} (%)	N flux ($g\,m^{-2}$)	N (%)	C/N	C_{org} / $C_{Carb.}$	Carb./ Opal
CBBT														
SW-NE 1987	5.62	2.41	42.9	0.80	14.2	1.91	34.0	0.27	4.80	0.033	0.59	8.18	0.93	3.01
NE 1987/88	14.07	5.29	37.6	3.79	26.9	3.42	24.3	0.88	6.25	0.110	0.78	8.00	1.39	1.40
NE-SW 1988	7.16	2.77	38.7	1.17	16.3	2.41	33.7	0.45	6.28	0.051	0.71	8.82	1.35	2.37
SW 1988	16.31	5.75	35.3	2.38	14.6	6.54	40.1	0.91	5.58	0.104	0.64	8.75	1.32	2.42
1987/88	**43.16**	**16.22**	**37.6**	**8.14**	**18.9**	**14.28**	**33.1**	**2.51**	**5.82**	**0.298**	**0.69**	**8.42**	**1.29**	**1.99**
SW-NE 1988	5.59	2.00	35.8	1.09	19.5	1.98	35.4	0.29	5.19	0.035	0.63	8.29	1.21	1.83
NE 1988/89	12.58	4.38	34.8	2.99	23.8	3.90	31.0	0.72	5.72	0.092	0.73	7.83	1.37	1.46
NE-SW 1989	9.28	3.24	34.9	2.00	21.6	2.91	31.4	0.63	6.79	0.080	0.86	7.88	1.62	1.62
SW 1989	22.32	6.42	28.8	4.40	19.7	9.15	41.0	1.30	5.82	0.176	0.79	7.39	1.69	1.46
1988/89	**49.77**	**16.04**	**32.2**	**10.48**	**21.1**	**17.94**	**36.0**	**2.94**	**5.91**	**0.383**	**0.77**	**7.68**	**1.53**	**1.53**
SW-NE 1989	8.18	2.25	27.5	1.61	19.7	3.54	43.3	0.43	5.26	0.056	0.68	7.68	1.59	1.40
NE 1989/90 *	16.63	4.97	29.9	4.21	25.3	5.87	35.3	0.88	5.27	0.110	0.66	7.98	1.47	1.18
NE-SW 1990	8.29	3.49	42.1	1.56	18.8	2.43	29.3	0.45	5.43	0.055	0.66	8.18	1.07	2.24
SW 1990	18.46	6.01	32.6	4.00	21.7	6.80	36.8	0.92	4.98	0.110	0.60	8.36	1.28	1.50
SW-NE 1990	17.48	2.76	15.8	3.69	21.1	9.69	55.4	0.75	4.29	0.091	0.52	8.24	2.26	0.75
1989/90 *	**60.86**	**17.23**	**28.3**	**13.46**	**22.1**	**24.79**	**40.7**	**3.00**	**4.92**	**0.366**	**0.60**	**8.19**	**1.45**	**1.28**
NE 1990/91	23.24	4.04	17.4	5.86	25.2	11.75	50.6	0.89	3.83	0.111	0.48	8.02	1.84	0.69
NE-SW 1991	11.68	3.14	26.9	2.41	20.6	4.98	42.6	0.64	5.48	0.074	0.63	8.65	1.70	1.30
SW 1991	18.33	5.04	27.5	3.91	21.3	7.43	40.5	1.09	5.95	0.125	0.68	8.72	1.80	1.29
SW-NE 1991	10.27	2.19	21.3	1.59	15.5	5.55	54.0	0.52	5.06	0.064	0.62	8.13	1.98	1.38
1990/91	**63.52**	**14.41**	**22.7**	**13.77**	**21.7**	**29.71**	**46.8**	**3.14**	**4.94**	**0.374**	**0.59**	**8.40**	**1.82**	**1.05**

* = Data from the period NE 1989/90 are missing. The values for this period have been interpolated.

Table 15.2c Fluxes of components to the deep southern Bay of Bengal and their ratios.

Period	Total flux ($g\,m^{-2}$)	Carb. flux ($g\,m^{-2}$)	Carb. (%)	Opal flux ($g\,m^{-2}$)	Opal (%)	Lith. flux ($g\,m^{-2}$)	Lith. (%)	C_{org} flux ($g\,m^{-2}$)	C_{org} (%)	N flux ($g\,m^{-2}$)	N (%)	C/N	$C_{org}/C_{carb.}$	Carb./ Opal
SBBT														
SW-NE 1987	5.43	2.59	47.7	1.16	21.4	1.24	22.8	0.25	4.60	0.031	0.57	8.06	0.80	2.23
NE 1987/88	8.25	3.52	42.7	1.66	20.1	2.17	26.3	0.40	4.85	0.050	0.61	8.00	0.95	2.12
NE-SW 1988	9.11	3.94	43.2	1.48	16.2	2.68	29.4	0.56	6.15	0.067	0.74	8.36	1.18	2.66
SW 1988	15.58	8.53	54.7	2.91	18.7	2.56	16.4	0.88	5.65	0.108	0.69	8.15	0.86	2.93
1987/88	**38.37**	**18.58**	**48.4**	**7.21**	**18.8**	**8.65**	**22.5**	**2.09**	**5.45**	**0.256**	**0.67**	**8.16**	**0.94**	**2.58**
NE 1990/91	5.47	2.67	48.8	1.76	32.2	0.48	8.8	0.31	5.67	0.042	0.77	7.38	0.97	1.52
NE-SW 1991	7.26	3.61	49.7	1.97	27.1	0.84	11.6	0.46	6.34	0.059	0.81	7.80	1.06	1.83
SW 1991	12.88	6.09	47.3	3.40	26.4	2.04	15.8	0.75	5.82	0.088	0.68	8.52	1.03	1.79
SW-NE 1991	5.36	2.68	50.0	1.43	26.7	0.66	12.3	0.33	6.16	0.041	0.76	8.05	1.03	1.87
1990/91	**30.97**	**15.05**	**48.6**	**8.56**	**27.6**	**4.02**	**13.0**	**1.85**	**5.97**	**0.230**	**0.74**	**8.04**	**1.02**	**1.76**

15.5 INTERANNUAL VARIABILITY

15.5.1 SEASONAL SIGNALS

In the northern Bay of Bengal ($NBBT_N$) the seasonal pattern of particle fluxes was highly variable from year to year (Figure 15.3, Table 15.2a). The particle flux maximum between June and September 1988 correlated with periods of high river inputs and was a result of a strong monsoon during that year. The recorded rainfall was one of the highest in this century (Parthasarathy et al., 1992). A weak SW monsoon in 1989 resulted in less marked flux peaks during that year. Particle flux was influenced more by wind speeds than by river inputs in 1989 (Bartsch, 1993). At $NBBT_S$ the fluxes were lower in both years, with slightly elevated SW monsoon fluxes (Table 15.2a).

In the central Bay of Bengal the investigated years were marked by a distinct seasonality in the flux pattern with maxima during both the monsoons (Figure 15.5, Table 15.2b). The exceptional particle flux maximum of 36 g m^{-2} measured between October 1990 and January 1991 was due to an extreme flood event which led to a lateral injection of particulate matter to the deep sea. This event contributed about 60% to the total annual flux at this station.

Seasonality of particle fluxes with slightly higher fluxes during the SW monsoon was seen in both the investigated years in the southern Bay of Bengal (Figure 15.7, Table 15.2c).

15.5.2 TOTAL AND COMPONENT FLUXES

The total annual particle fluxes in the Bay of Bengal did not show any significant interannual variability except for the central station where it resulted mainly from the effect of extreme events such as floods and cyclonic activities in 1989/90 and 1990/91 (Table 15.2b). The observed higher fluxes during these extreme events were caused by higher lithogenic matter and opal fluxes.

In the northern Bay of Bengal ($NBBT_N$), the total annual fluxes were very similar in both the investigated years. The component fluxes varied however considerably from year to year as a result of the varying intensities of fluvial influence. The fluxes of lithogenic matter decreased from 1987/88 to 1988/89 whereas the carbonate and opal fluxes increased (Table 15.2a). At $NBBT_S$ the component fluxes were comparatively similar within the two years studied. No significant interannual variability was observed in carbonate fluxes. The data of two years sampling at the southern Bay of Bengal station suggested very low interannual variabilities in the total and the component fluxes (Table 15.2c).

15.6 COMPARISON WITH OTHER MARINE REGIONS

The total annual flux rates in the Bay of Bengal varied between 31 and 64 g m^{-2}, a range which is found in other marine regions such as the Arabian Sea (Haake et al., 1993; this volume, Chapter 14), eastern Atlantic (Wefer and Fischer, 1993; thsi volume, Chapter 10), polar regions and in the Gulf of Alaska (Honjo, 1990). Higher fluxes have been reported from the Bransfield and Fram Straits, where laterally derived lithogenic material influences the flux pattern (Wefer et al., 1988; Hebbeln and Wefer, 1991) and in the Panama Basin where an unusual coccolithophorid bloom contributed to the observed high flux in 1980 (Honjo, 1982). The total annual fluxes determined in the Bay of Bengal are higher than those recorded in the western tropical Pacific (this volume, Chapter 17), the northeast Pacific (Dymond and Roth, 1988), the South China Sea (this volume, Chapter 16) and within the subtropical and north Atlantic (Deuser, 1986; this volume, Chapter 9; Honjo and Manganini, 1993; this volume Chapter 6; Von Bodungen et al., 1991).

Another important feature of the Bay of Bengal flux pattern is the low carbonate flux in the northern and central Bay of Bengal compared to other marine regions. The average lithogenic matter content in the Bay of Bengal (25–54%) is higher than in other tropical marine regions (1–25%; Dymond and Collier, 1988; Haake et al., 1993). Similar lithogenic matter contributions to total fluxes (up to 60%) are seen however in polar regions, where particle flux pattern is influenced by the extent of the seasonal ice cover and/or by processes occurring at the ice edge (Wefer et al., 1990; Von Bodungen et al., 1991).

Fluxes of nitrogen and organic carbon in the northern Bay of Bengal (Table 15.2a) are among the highest values ever reported for marine regions and are similar to those from regions influenced by upwelling processes such as the western Arabian Sea (Haake et al., 1993; this volume, Chapter 14) and along the coast of West Africa (Wefer and Fischer, 1993; this volume, Chapter 10).

15.7 GENERAL DISCUSSION

Marine ecosystems under the influence of fresh water discharges have been found to have specific characteristics with respect to the prevailing upper ocean biology and sedimentary geochemistry. For example, the fresh water plume of the Amazon has a decisive influence on the chemistry and sediment distribution in the tropical Atlantic (Milliman et al., 1975; Gibbs, 1976). The inputs from the Amazon also increase the biological production in shelf areas. The major components of suspended matter in brackish water lenses along the Amazon river mouth are frustules of diatoms (Kidd and Sander, 1979). The high diatom production resulting from high silicate content of river water is, however, not

reflected in the sediments because of the lateral transport of the freshly produced material and/or a result of high dissolution rates within the water column. The influence of the Amazon River is also observed in the hydrochemistry and the biological productivity of the western tropical Atlantic and of the eastern Caribbean Sea during spring and summer, which is the period of high rainfall in South America. During these periods fresh water lenses of up to 600 km in diameter have been observed several hundred kilometers north and east of the Amazon estuary. Data on particle flux to the deep western tropical Atlantic show a variability which appeared to be related to the northwestern movement of the plumes of the rivers Amazon and Orinoco (Deuser et al., 1988).

In order to illustrate the importance of river discharge for such processes we present the detailed information collected during the first year of the experiment in the Bay of Bengal. These data were chosen since they most strikingly demonstrate the effect of fresh water inputs on marine sedimentation, and the effects of other factors are less significant. Periods immediately following high river discharge are characterized by high total fluxes caused by enhanced inputs of lithogenic material from the rivers in the northern Bay of Bengal (Figure 15.2).

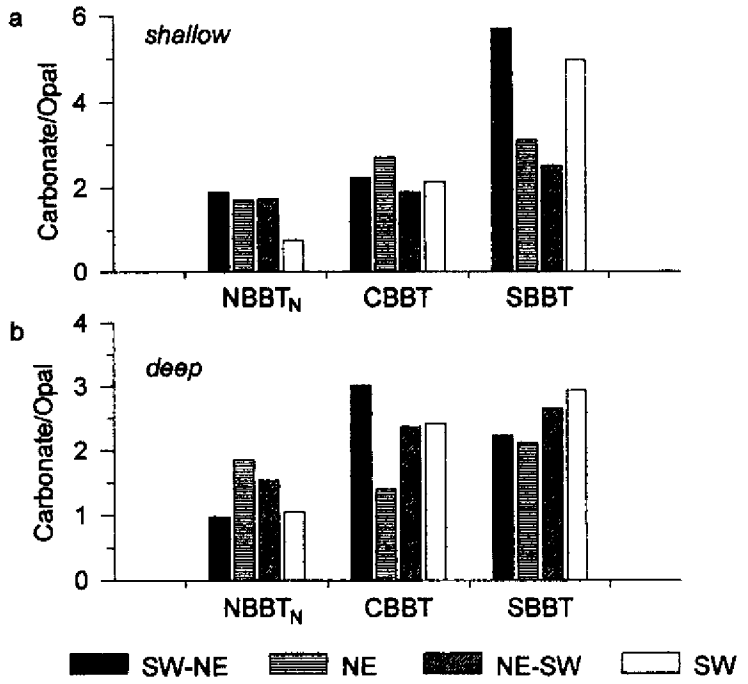

Figure 15.8 Carbonate/opal ratios of settling particles in the Bay of Bengal 1987/88.

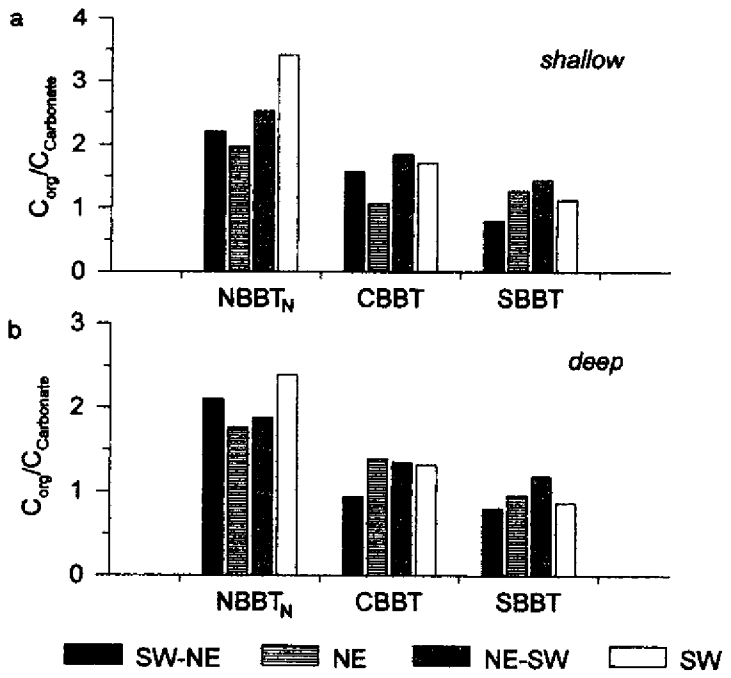

Figure 15.9 $C_{org}/C_{Carbonate}$ ratios of settling particles in the Bay of Bengal 1987/88.

Furthermore, biogenic matter associated with these high fluxes exhibit low carbonate to opal ratios which in turn increase the rain ratios of $C_{org}/C_{Carbonate}$ especially during the SW monsoon period (Figures 15.8 and 15.9). Carbonate/opal ratios increase and the $C_{org}/C_{Carbonate}$ ratios decrease towards the central and southern stations.

The changes in the ratios of individual communities contributing to biological productivity in marine regions are of significance within the context of the marine carbon cycling and, in particular, the uptake of CO_2 by the oceans. Carbon cycling in the ocean is determined in part by the composition of primary producers. It determines the rain ratio of $C_{org}/C_{Carbonate}$ with higher ratios resulting in a more efficient biological carbon dioxide pump (Heinze et al., 1991). The settling of particulate organic carbon decreases the total carbon and partial pressure of CO_2 in the surface layers, whereas the removal of carbonate from surface waters aids in increasing atmospheric CO_2 by shifting the carbonate equilibria (Berger and Keir, 1984; Dymond and Lyle, 1985). Thus the differences in initial production ratio of calcium carbonate to organic carbon can effect significant short term variations in atmospheric CO_2. The changes in upper ocean plankton community structure favoring, for example, diatoms over coccolithophorids will increase the rain ratio

of $C_{org}/C_{Carbonate}$ and hence the efficiency of the marine organic carbon pump (Ittekkot et al., 1991).

The results from the Bay of Bengal thus have implications for research on the recent history of the earth's climate, specifically that relating to short-term CO_2 fluctuations in the atmosphere during glacial-interglacial transitions. For example, the retreat of the ice sheets during the last deglaciation proceeded stepwise, with at least two large influxes of fresh water into the oceans accompanied by changes in the pattern of ocean circulation (Fairbanks, 1989). In analogy to our above-mentioned results for a marine region, such recorded inputs might have caused short-term changes in marine removal processes of climatic significance.

Yet another aspect of the results from the Bay of Bengal is the effect of extreme events such as floods and cyclonic activity in the region. Two major sedimentation events were recorded at the central Bay of Bengal station during January 1988 in the aftermath of a cyclone and from October to December 1990 during floods affecting the peninsular Indian rivers. The impact of these events in marine carbon cycling is yet to be ascertained. The projected climate changes due to an increase in CO_2 concentrations in the atmosphere are expected to have an impact on the frequency and intensity of extreme events of the type encountered in the Bay of Bengal. One of the messages from our results is that these changes could have significant feedbacks to global carbon cycle and to the global climate system.

15.8 CONCLUSIONS

Particle flux patterns in the Bay of Bengal are influenced to a large extent by fresh water and sediment inputs from the rivers and from wind-induced mixed layer deepening. The effect of river inputs decreases in an offshore direction. The quantity of fluxes is largely determined by lithogenic matter. Interannual variability of total fluxes is a result of variations in the lithogenic matter fluxes at the northern and central locations. Fresh water and nutrient inputs associated with the river discharges also induce seasonal changes in the relative contributions of opal and carbonate to the biogenic components which are characterized by low carbonate/opal ratios and, as a result, high organic carbon/carbonate-carbon ratios. These results are reminiscent of particle sedimentation in the polar regions where the extent of ice cover and ice edge production are major controlling factors. At locations away from the influence of rivers wind-driven biological processes determine the nature and quantity of fluxes. In general, these processes lead to a dominance of carbonate sedimentation in the Bay of Bengal especially in its southern parts. Superimposed on these processes are those of sedimentation induced by extreme events such as floods and cyclonic activity.

15.9 ACKNOWLEDGMENTS

Financial support for the project is being given by the Federal German Ministry for Education, Science, Research and Technology (BMBF, Bonn), the Council of Scientific and Industrial Research (CSIR, New Delhi) and the Department of Ocean Development (DOD, New Delhi).

15.10 REFERENCES

Bartsch, M. R. (1993) "Biogeochemische Untersuchungen an Sinkstoffen aus dem Golf von Bengalen" Dissertation, Fachbereich Geowissenschaften, Universität Hamburg, 115 pp.

Berger, W. H. and R. S. Keir (1984) "Glacial-Holocene changes in atmospheric CO_2 and the deep-sea record", in J. E. Hansen and T. Takahashi (eds) *Climate processes and climate sensitivity*, Geophys. Monogr., 29, Am. Geophys. Union, Washington, 337–351.

Das, N., D. S. Desai and N. C. Biswas (1989a) "Cyclones and depressions over the Indian seas and the Indian sub-continent during 1987", *Mausam*, **40**, 1–12.

Das, N., D. S. Desai and N. C. Biswas (1989b) "Weather - Monsoon season (June-September 1988)", *Mausam*, **40**, 351–364.

Deuser, W. G. (1986) "Seasonal and interannual variations in deep-water particle fluxes in the Sargasso Sea and their relation to surface hydrography", *Deep-Sea Res.*, **33**, 225–246.

Deuser, W. G., F. E. Muller-Karger and C. Hemleben (1988) "Temporal variations of particle fluxes in the deep subtropical and tropical North Atlantic: Eulerian versus Lagrangian effects", *J. Geophys. Res.*, **93**, 6857–6862.

Dymond, J. and R. Collier (1988) "Biogenic particle fluxes in the equatorial Pacific: Evidence for both high and low productivity during the 1982-1983 El Niño", *Global Biogeochem. Cycles*, **2**, 129–137.

Dymond, J. and M. Lyle (1985) "Flux comparisons between sediments and sediment traps in the eastern tropical Pacific: Implications for atmospheric CO_2 variations during the Pleistocene", *Limnol. Oceanogr.*, **30**, 699–712.

Dymond, J. and S. Roth (1988) "Plume dispersed hydrothermal particles: A time-series record of settling flux from the Endeavour Ridge using moored sensors", *Geochim. Cosmochim. Acta*, **52**, 2525–2536.

Fairbanks, R. G. (1989) "A 17,000-year glacio-eustatic sea level record: Influence of glacial melting rates on the Younger Dryas event and deep-ocean circulation", *Nature*, **342**, 637–642.

Gibbs, R. J. (1976) "Amazon River sediment transport in the Atlantic Ocean", *Geology*, **4**, 45–48.

Gupta, G. R., D. S. Desai and N. C. Biswas (1991a) "Cyclones and depressions over the Indian seas and neighbourhood during 1990", *Mausam*, **42**, 227–240.

Gupta, G. R., D. S. Desai and N. C. Biswas (1991b) "Weather - Summer monsoon season (June-September 1990) ", *Mausam*, **42**, 309–328.

Gupta, G. R., D. S. Desai and N. C. Biswas (1991c) "Weather - Post monsoon season (October-December 1990) ", *Mausam*, **42**, 419–428.

Guptha, M. V. S., W. B. Curry, V. Ittekkot and A. S. Muralinath (1996) "Seasonal variation in the flux of planktonic foraminifera: Sediment trap results from the Bay of Bengal (Northern Indian Ocean) ", in prep.

Haake, B., V. Ittekkot, T. Rixen, V. Ramaswamy, R. R. Nair and W. B. Curry (1993) "Seasonality and interannual variability of particle fluxes to the deep Arabian Sea", *Deep-Sea Res.*, **40**, 1323–1344.

Hebbeln, D. and G. Wefer (1991) "Effects of ice coverage and ice-rafted material on sedimentation in the Fram Strait", *Nature*, **350**, 409–411.

Heinze, C., E. Maier-Reimer and K. Winn (1991) "Glacial pCO_2 reduction by the world ocean: Experiments with the Hamburg Carbon Cycle model", *Paleoceanography*, **6**, 395–430.

Honjo, S. (1982) "Seasonality and interaction of biogenic and lithogenic particulate flux at the Panama Basin", *Science*, **218**, 883–884.

Honjo, S. (1990) "Particle fluxes and modern sedimentation in the polar oceans", in W. O. Smith, Jr. (ed) *Polar Oceanography*, Academic Press, New York, Vol. II, Chapter 13, 322–353.

Honjo, S. and K. W. Doherty (1988) "Large aperture time-series oceanic sediment traps: design objectives, construction and application", *Deep-Sea Res. I*, **35**, 133–149.

Honjo, S. and S. J. Manganini (1993) "Annual biogenic particle fluxes to the interior of the North Atlantic ocean; studied at 34°N 21°W and 48°N 21°W", *Deep-Sea Res. I*, **40**, 587–607.

Ittekkot, V. (1991) "Particle flux studies in the Indian Ocean", *EOS*, **72**, 527 + 530.

Ittekkot, V. (1993) "The abiotically driven biological pump in the ocean and short-term fluctuations in atmospheric CO_2 contents", *Global and Planetary Change*, **8**, 17–25.

Ittekkot, V. and S. Zhang (1989) "Pattern of particulate nitrogen transport in world rivers", *Global Biogeochem. Cycles*, **3**, 383–391.

Ittekkot, V., R. R. Nair, S. Honjo, V. Ramaswamy, M. Bartsch, S. Manganini and B. N. Desai (1991) "Enhanced particle fluxes in Bay of Bengal induced by injection of fresh water", *Nature*, **351**, 385–387.

Kidd, R. and F. Sander (1979) "Influence of Amazon River discharge on the marine production system off Barbados, West Indies", *J. Mar. Res.*, **37**, 669–681.

Knauer, G. A., D. M. Karl, J. H. Martin and C. N. Hunter (1984) "*In situ* effects of selected preservatives on total carbon, nitrogen and metals collected in sediment traps", *J. Mar. Res.*, **42**, 445–462.

LaViolette, P. E. (1967) *Temperature, Salinity, and Density of the World's Seas: Bay of Bengal and Andaman Sea*, Informal Report WO 67–57, Naval Oceanographic Office, Washington D.C., 81 pp.

Lee, C., J. I. Hedges, S. G. Wakeham and N. Zhu (1992) "Effectiveness of various treatments in retarding microbial activity in sediment trap material and their effects on the collection of swimmers", *Limnol. Oceanogr.*, **37**, 117–130.

Madhusudana Rao, Ch. (1985) "Distribution of suspended particulate matter in the waters of eastern continental margin of India", *Indian J. Mar. Sci.*, **14**, 15–19.

Milliman, J. D. and R. H. Meade (1983) "World-wide delivery of river sediment to the oceans", *J. Geol.*, **9**, 1–19.

Milliman, J. D., C. P. Summerhayes and H. T. Barretto (1975) "Oceanography and suspended matter off the Amazon River February-March 1973", *J. Sed. Petrol.*, **45**, 189–206.

Mortlock, R. A. and P. N. Froelich (1989) "A simple method for the rapid determination of biogenic opal in pelagic marine sediments", *Deep-Sea Res.*, **36**, 1415–1426.

Müller, P. J., E. Suess and C. A. Ungerer (1986) "Amino acids and amino sugars of surface particulate and sediment trap material from waters of the Scotia Sea", *Deep-Sea Res.*, **33**, 819–838.

Nair, R. R., V. Ittekkot, S. J. Manganini, V. Ramaswamy, B. Haake, E. T. Degens, B. N. Desai and S. Honjo (1989) "Increased particle fluxes to the deep ocean related to monsoons", *Nature*, **338**, 749–751.

Parthasarathy, B., K. Rupa Kumar and D. R. Kothawale (1992) "Indian summer monsoon rainfall indices: 1871–1990", *Meteorological Magazine*, **121**, 174–186.

Rao, R. R., R. L. Molinari and J. F. Festa (1989) "Evolution of the climatological near-surface thermal structure of the tropical Indian Ocean. 1. Description of mean monthly mixed layer depth, and sea surface temperature, surface current, and surface meteorological fields", *J. Geophys. Res.*, **94**, 10801–10815.

Reemtsma, T., V. Ittekkot, M. Bartsch and R. R. Nair (1993) "River inputs and organic matter fluxes in the northern Bay of Bengal: Fatty acids", *Chem. Geol.*, **103**, 55–71.

Schäfer, P. and V. Ittekkot (1995) "Isotopic biogeochemistry of nitrogen in the northen Indian Ocean", *Mitt. Geol.-Paläont. Inst. Univ. Hamburg*, **78**, 67–93.

UNESCO (1979) *Discharge of Selected Rivers of the World, Vol. III, Mean Monthly and Extreme Discharges (1972–1975)*, UNESCO, Paris, 104 pp.

Von Bodungen, B., U. Bathmann, M. Voß and M. Wunsch (1991) "Vertical particle flux in the Norwegian Sea - resuspension and interannual variability", in P. Wassmann, A.-S. Heiskanen and O. Lindahl (eds) *Sediment Trap Studies in the Nordic Countries*, Symposium proceedings, NurmiPrint Oy, Nurmijärvi, 116–136.

Wefer, G. and G. Fischer (1993) "Seasonal patterns of vertical particle flux in equatorial and coastal upwelling areas of the eastern Atlantic", *Deep-Sea Res.*, **40**, 1613–1645.

Wefer, G., G. Fischer, D. Fütterer and R. Gersonde (1988) "Seasonal particle flux in the Bransfield Strait, Antarctica", *Deep-Sea Res.*, **35**, 891–898.

Wefer, G., G. Fischer, D. K. Fütterer, R. Gersonde, S. Honjo and D. Ostermann (1990) "Particle sedimentation and productivity in Antarctic waters of the Atlantic sector", in U. Bleil and J. Thiede (eds) *Geological History of the Polar Oceans: Arctic Versus Antarctic*, Kluwer Acad. Publ., Dordrecht, 363–379.

16 Fluxes of Particulate Matter in the South China Sea

MARTIN G. WIESNER, LIANFU ZHENG, HOW KIN WONG, YUBO WANG AND WENBIN CHEN

16.1 INTRODUCTION

Time-series sediment trap experiments in various oceanic regions have revealed a close coupling between biological activity in the surface waters and the fluxes of particulate matter to the deep sea (Deuser et al., 1983; Wefer, 1989; Honjo, 1990). In tropical oceans the fertility of the surface waters may be susceptible to variations in the lower tropospheric wind regime which exerts a strong control on the position and strength of upwelling and mixed layer deepening (Tchernia, 1980; Klein and Coste, 1984; Bauer et al., 1991). As a consequence the injection of nutrients stimulating biological productivity in the euphotic zone is a seasonal phenomenon yielding pulses in the downward flux of particles (Honjo, 1982; Nair et al., 1989; Haake and Ittekkot, 1990; Wefer and Fischer, 1993). The atmospheric circulation may also govern the areal extension of aeolian dust plumes and fallout enhancing sedimentation by particle loading (Deuser, 1986; Nair et al., 1989; Wefer and Fischer, 1993; this volume, Chapter 3). Where large rivers drain into these areas, the forcing function of the winds is modulated or overwhelmed by the rates of fluviatile sediment discharge (Ramaswamy et al., 1991; Ittekkot et al., 1991; this volume, Chapter 15). In analogy, the supply of high loads of riverine nutrients and mineral particles leads to an increase in primary production and ensures rapid sedimentation in coastal regions. This process may even be operative in offshore areas as part of the material is laterally advected in river plumes (Deuser et al. 1988, Ittekkot et al., 1991). The interaction between marine-biogenic particles and mineral matter derived from aeolian or fluvial sources has been implied to be one of the major mechanisms triggering oceanic sedimentation and the removal of biologically-fixed atmospheric carbon dioxide into the deep sea (Ittekkot et al., 1992).

In the South China Sea significant variations in the fluxes of particulate matter may be expected not only because this area is subject to a strongly monsoonal climate and enormous riverine supply but in particular because it is affected by

Particle Flux in the Ocean
Edited by V. Ittekkot, P. Schäfer, S. Honjo and P. J. Depetris

UNEP

island-arc volcanism (Simkin et al., 1982; Wolfe and Self, 1983). Though local in nature, this type of volcanic activity may significantly influence oceanic sedimentation on a regional scale. Due to the high explosivity of the associated eruptions massive quantities of volcanic dust are ejected to upper tropospheric and stratospheric elevations (Hirschboeck, 1980). The high-velocity upper level winds, in turn, induce a strong longitudinal dispersal of the particles yielding extensive ash falls, which may provide both mineral ballast and nutrients to vast areas of the oceans (Lisitzin, 1972; Kennett, 1981).

In this communication time-series data of the northern and central South China Sea are compared and their link to the prevailing meteorological and hydrographical conditions is assessed. In addition we report here a submarine fallout of volcanic ash recorded by the traps in the central part of the basin and describe its effect on the water column processes. The study aims to extend our present understanding of the factors that may control particle sedimentation in tropical seas.

16.2 CLIMATE AND HYDROGRAPHY

Almost every feature of the oceanographic environment of the South China Sea is conditioned by the monsoons. Unobstructed by the Himalayas and channeled by the mountain ranges of Myanmar, the northeast monsoon (November to April) blows out vigorously from the intense polar anticyclone located over central Asia; the southwest monsoon (June to September) is a comparatively gentle phenomenon reflecting the small pressure gradient between the South China Sea and the Asian land mass (Ramage, 1971). This wind regime causes a strong seasonal reversal of the surface water circulation from nearly counterclockwise in winter to a predominantly northeasterly directed flow pattern in summer (LaViolette and Frontenac, 1967).

With the onset of the northeast monsoon cold and saline water is forced from the open Pacific into the South China Sea through the Bashi Channel and Taiwan Strait. These waters spread over the northernmost part of the basin and, being constantly modified, extend down the Vietnam coast (Wyrtki, 1961; LaViolette and Frontenac, 1967). Off the coastal areas, the winter sea surface temperatures generally increase from north (23°C) to south (28°C), reflecting the latitudinal differences in the effectiveness of solar insolation (e.g., Pohlmann, 1987). Upwelling has been suggested from numerical models to take place off the west coast of the Philippines (Pohlmann, 1987; Shaw and Chao, 1994), but verification by *in situ* data is still lacking. In summer, the sea surface temperatures are around 29°C in most of the region, and the salinity is lower because of the admixture of riverine waters from the Mekong, Hunghe and Zhujiang (LaViolette and Frontenac, 1967); the Mekong triples its annual average runoff (115 $m^3 s^{-1}$) and the relative change is even greater for the Hunghe (17 $m^3 s^{-1}$) (LaFond, 1966). At the height

of the SW monsoon intense upwelling occurs off southeastern Vietnam (Wyrtki, 1961; LaFond, 1963).

The deeper water characteristics of the South China Sea are less variable. At around 500 m a low-salinity zone equivalent to the Pacific Subarctic Intermediate Water is recognized in the northern and central parts of the sea (Wyrtki, 1961). The zone closely corresponds to the oxygen minimum layer, concentrations ranging from 1.7 to 2.1 mg O_2 l^{-1} (LaFond, 1966). Below 2000 m the water masses are similar in temperature and salinity to the Pacific Deep Water at sill depth in the Strait of Luzon (Shaw, 1991).

The intensity of the monsoons also determines the input of allochthonous material to the South China Sea. The major supply of this material occurs as dust from eastern China (McDonald, 1938; Liu, 1985) and through the rivers Mekong, Zhujiang and Hunghe (360 x 10^6 t y^{-1} sediment discharge; Milliman and Meade, 1983). Further contributions are provided by the volcanoes on the Philippine and Indonesian archipelagoes which have a relatively high eruption frequency of 4–10 eruptions per decade (Simkin et al, 1982). Their activities are evidenced by the abundance of pumice and glass shards throughout the bottom sediments of the basin (Niino and Emery, 1961; Chen, 1978; Wang et al., 1992). Aeolian particles may be also supplied from the Philippines during the high season of typhoons (August-September; Ramage, 1971) but little information exists on the significance of this source.

16.3 MATERIALS AND METHODS

The mooring stations were located in the northern (SCS-N) and central (SCS-C) South China Sea at 18.47°N, 116.02°E and 14.60°N, 115.10°E, respectively (Figure 16.1). Two sediment traps (Mark-VI) were placed along each mooring at depths of 1000 and 3350 m (SCS-N) and 1190 and 3730 m (SCS-C) below sea level. Total water depth was 3766 and 4270 m, respectively. Collection intervals were 15 and 28–31 days covering the time span from September 1987 to October 1988 (SCS-N) and from December 1990 to May 1993 (SCS-C).

The collecting cups were filled with water taken from the respective areas and water depths. 3.33 g NaCl and 0.33 g $HgCl_2$ were added per 100 ml cupwater to retard diffusion and bacterial activity. After retrieval, the trap material was stored at 4°C and processed within 7 days. The samples were wet-sieved through a 1-mm screen and split into aliquots by a precision rotary splitter; copepods were removed from the < 1 mm fraction with forceps. The aliquots were filtered on Nuclepore filters (0.4 μm) and dried at 40°C. As the fraction > 1 mm contained mostly "swimmers" (pteropods and copepods), the fine fraction was used for total flux calculations and component analyses. Data on the fluxes and weight

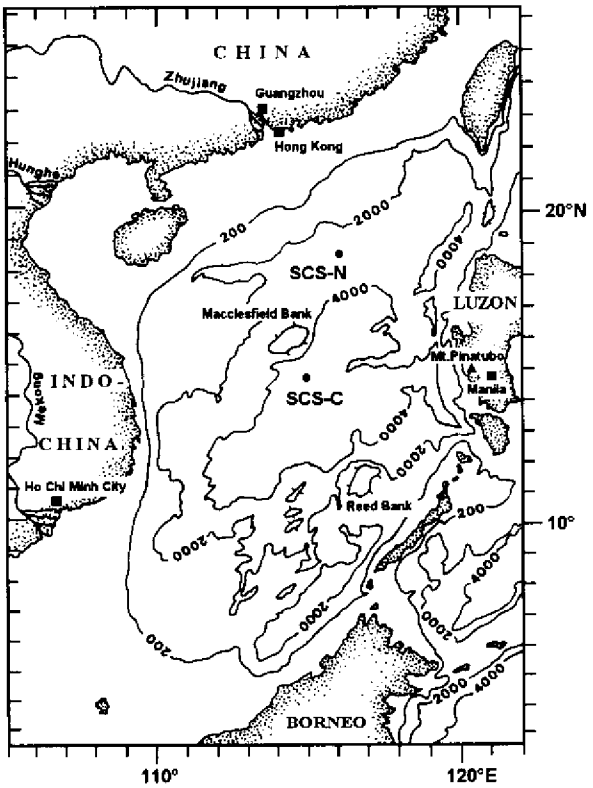

Figure 16.1 Sediment trap locations in the northern (SCS-N) and central (SCS-C) South China Sea (isobaths in m).

percentages of carbonate, biogenic opal, organic carbon and lithogenics at the northern station were initially published by Jennerjahn et al. (1992).

Total carbon and nitrogen were measured with a Carlo Erba NA 1500 Elemental Analyzer. The standard deviation of the duplicate analyses was 0.05% for carbon and 0.02% for nitrogen. Carbonate carbon analyses were performed on a Wösthoff Carmhograph 6 (standard deviation < 1%). Organic carbon was taken as the difference between total carbon and carbonate carbon. An empirical factor of 1.8 was used to convert organic carbon into total organic matter concentrations (e.g., Müller et al., 1986).

Biogenic opal was determined by applying a modified version of the method described by Koroleff (1983) and Mortlock and Froelich (1989). Briefly, the samples were treated sequentially with 2 N HCl and H_2O_2 (2%) to remove carbonate and organic matter. After drying at 40–60°C, the residual material was extracted with a solution of 7% Na_2CO_3 at 85°C for 5 hours. Subsequently, the

concentration of dissolved silica in the supernatant was measured photometrically. Assuming an average water content of 10% for biogenic opal (SiO_2 x 0.4 H_2O) (Mortlock and Froelich, 1989), Si concentrations were multiplied by 2.4 to calculate biogenic opal contents. The standard deviation of the method was 1%.

The amounts of lithogenic matter were obtained by subtracting the contents of carbonate, organic matter and biogenic opal from the total weight of the sample. It has to be mentioned that small quantities of volcanic glass were recognized to contribute to the mineral matter intercepted at the central trap site during the first four sampling intervals between March 20 and July 25, 1992. This material is likely to affect the determination of biogenic opal as it may release appreciable concentrations of silicon at high temperatures (Stefansson, 1966). Extensive laboratory experiments (Reschke, 1994) and microscopic particle countings (Chen, oral communication, 1994) have shown, however, that in case of the above samples the error introduced is minimal, making up less than 5% of the fluxes calculated for biogenic opal (and lithogenic matter).

Splits of the aliquots < 1 mm were also used to calculate the fluxes of the major plankton groups present. Counting was performed on microslides of the total fraction or dry-sieved subfractions (<63, 63–125, 125–250, 250–500 and 500–1000 μm). Results are expressed in units of number of individuals < 1 mm per square meter per day. Details of the preparation and counting methods and a comprehensive presentation of the data including the fluxes of individual plankton species are given in Chen (1994).

Monthly averaged surface wind speeds within a radius of 2° around the trap locations were calculated from the data files of D. M. Legler, Florida State University, Tallahassee, according to the method described in Legler et al. (1989). Sea surface temperature (SST) data were provided by the NASA Physical Oceanography Distributed Active Archive Center at the Jet Propulsion Laboratory, California Institute of Technology. The data base is a weekly composite, multichannel SST estimate based on the NOAA Advanced Very High Resolution Radiometer (AVHRR) measurements, interpolated for 18 km resolution. Here monthly SST means for the pixel location closest to each of the mooring stations are presented.

16.4 RESULTS

16.4.1 NORTHERN SOUTH CHINA SEA

Total particle fluxes at 1000 m water depth in the northern South China Sea varied between 11 and 180 mg m^{-2} d^{-1} (Figure 16.2). A maximum was recorded from November 1987 through February 1988, with peak fluxes occurring in November and January (170–180 mg m^{-2} d^{-1}). Carbonate and lithogenic matter

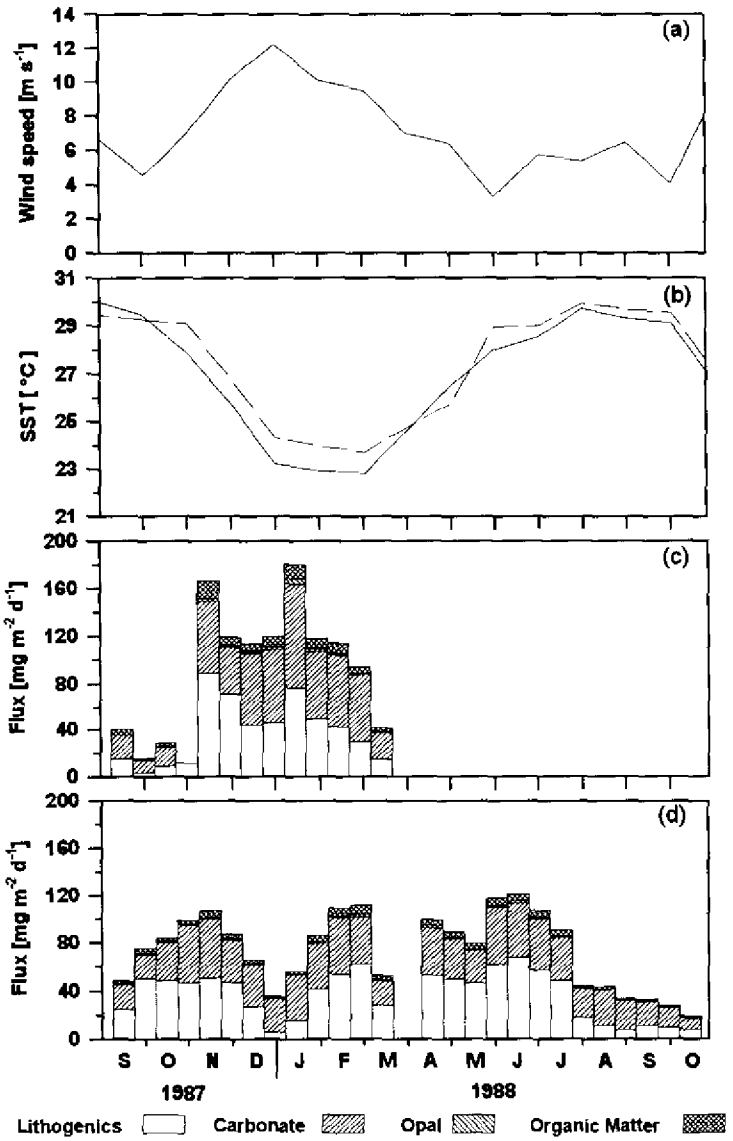

Figure 16.2 (a) Wind speeds, (b) sea surface temperatures and component fluxes at (c) 1000 m (deployed only until March) and (d) 3350 m water depth in the northern South China Sea for 1987–1988. In (b) solid line represents satellite measurements and broken line *in situ* measurements by a data telemetring buoy moored close to the trap station. Note: due to the small amount of material collected for the interval October 25 to November 9, 1987, only the total particle flux is recorded in (c).

were the major constituents of the particulate matter and accounted for 33–67% and 22–60%, respectively, of the total fluxes.

Carbonate percentages were highest in September-October 1987 and February-March 1988; i.e., during the SW-NE intermonsoon period and the late phase of the NE monsoon. At the height of the winter monsoon carbonate flux rates increased to 40–90 mg m^{-2} d^{-1}. Foraminifers had their peak flux in November (150 x 10^3 ind. m^{-2} d^{-1}) being largely composed of *Globigerinoides sacculifer* and *G. ruber*. Secondary maxima of around 110 x 10^3 ind. m^{-2} d^{-1} were counted for January and February-March. Coccolithophorid abundances maximized in November (350 x 10^3 ind. m^{-2} d^{-1}) and January (650 x 10^3 ind. m^{-2} d^{-1}). Simultaneously with the peak flux of the calcareous plankton, the contributions of lithogenic matter reached a maximum (40–60% of the total flux) (Figure 16.2).

Biogenic opal contents usually ranged from 0.4 to 1.2% with slight increases up to about 2.5% during the high flux period and at the end of the NE monsoon in March. Diatoms and silicoflagellates dominated the siliceous plankton. The diatom fluxes peaked in November (1600 x 10^3 ind. m^{-2} d^{-1}) and January (2650 x 10^3 ind. m^{-2} d^{-1}), with *Thalassionema* sp. and *Rhizosolenia* sp. being the major species (50% and 25%, respectively). The percentages of organic matter and total nitrogen were 6–11% and 0.4–1.1%, respectively, both having higher values in September-October 1987. C/N ratios ranged between 4 and 8 and tended to be higher during the NE monsoon.

At 3350 m water depth total fluxes showed a bimodal distribution during the NE monsoon, maximizing in November 1987 (107 mg m^{-2} d^{-1}) and February-March 1988 (112 mg m^{-2} d^{-1}). A third maximum occurred in June 1988 (121 mg m^{-2} d^{-1}) which cannot be compared with the upper trap because of the lack of data (Figure 16.2). Average flux rates in the deep trap were lower for all components but lithogenic matter (Figure 16.2). Losses were 19% for carbonate, 33% for biogenic opal and 48% for organic matter. A 10% gain was calculated for the lithogenics.

16.4.2 CENTRAL SOUTH CHINA SEA

Total fluxes at 1190 m water depth in the central South China Sea were between 23 and 29841 mg m^{-2} d^{-1}. Relative maxima were measured during the NE monsoon in December 1990-January 1991 (91 mg m^{-2} d^{-1}), in May 1991 through March 1992 (29841 mg m^{-2} d^{-1}), and during the SW monsoon in June-July 1992 (170 mg m^{-2} d^{-1}) (Figure 16.3). The major components of the particulate matter were carbonate (31–61%) and biogenic opal (20–45%) except for the sampling period May 1991 to March 1992 (see below).

Similar to the northern station, the highest contributions of carbonate were measured during the changeover of the monsoons (April-May 1991, May-June 1992, September-October 1992 and April 1993). Average carbonate fluxes during the SW monsoon were higher than those of the NE monsoon periods which provided quite comparable amounts of around 27 mg m^{-2} d^{-1} (Table 16.1).

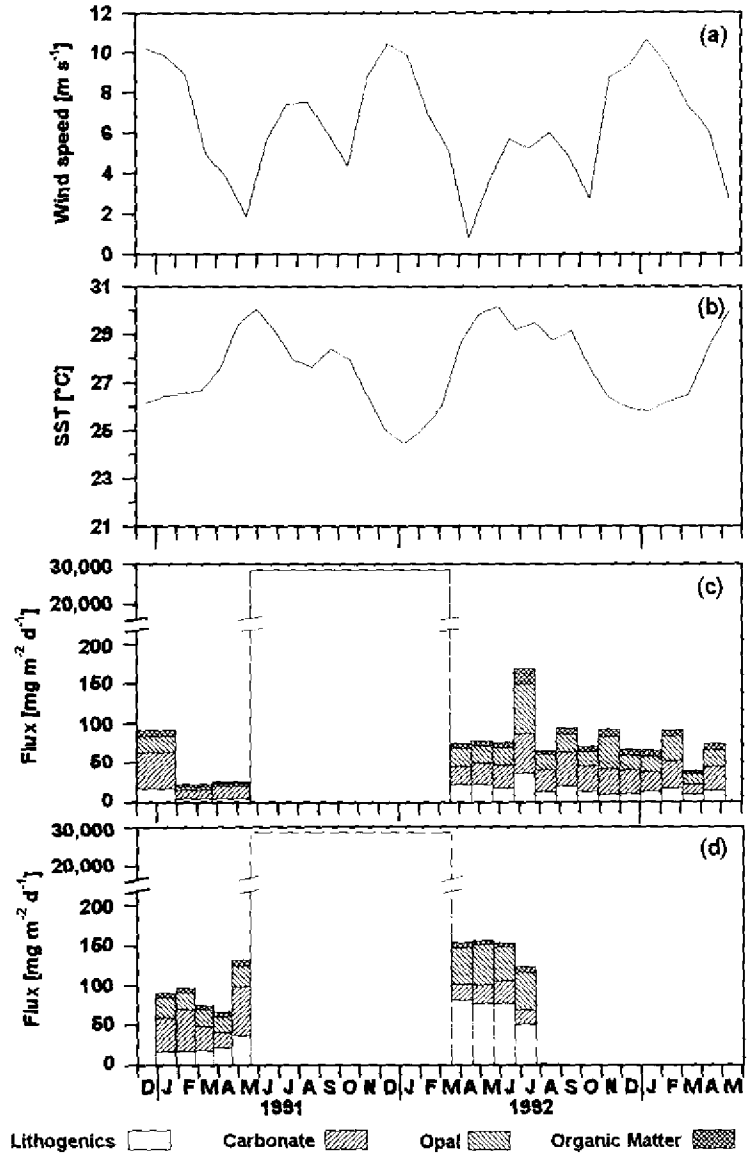

Figure 16.3 (a) Wind speeds, (b) sea surface temperatures and component fluxes at (c) 1190 m and (d) 3730 m water depth in the central South China Sea for 1990–1993 (for explanation of the long high flux period see text).

Foraminiferal flux was enhanced in December 1990-January 1991, June-July 1992, August-September 1992 and April-May 1993. Maximum flux was during the late summer 1992 (270 x 10^3 ind. m^{-2} d^{-1}); again *Globigerinoides sacculifer* and *G. ruber* were the most prominent species. Coccolithophorids had their highest abundances in April-May, June-July and August-September 1992 (around 2700 x 10^3 ind. m^{-2} d^{-1}). Biogenic opal peaked in June-July 1992 (63 mg m^{-2} d^{-1}) and November 1992 (41 mg m^{-2} d^{-1}). Diatoms and silicoflagellates had their flux maxima at the height of the 1992 SW monsoon. At this time the flux of diatoms was approximately 34000 x 10^3 ind. m^{-2} d^{-1} and the major species encountered were *Thalassionema* sp. (21%), *Rhizosolenia* sp. (12%) and *Nitzschia* sp. (9%). Organic matter varied between 7% and 12%, and total nitrogen between 0.5% and 0.8%. C/N ratios were generally higher than in the north (7–10) but similarly maximized at the height of the monsoons.

Lithogenic matter comprised 10–35% of the total fluxes but from May 21, 1991 to March 18, 1992, the contributions increased to more than 99% (Figure 16.3). All the cups were found to be completely filled with pale-gray sediment (in total 1689 g). Another 2817 g of the same material covered with a thin veneer of olive-green pelagic sediment was recovered from the cone. This was due to a choking of the rotation unit at the end of the first sampling period in December 1991, whereby the trap continued to collect material on the last cup until recovery in March 1992. Thus the total amount of particulate matter intercepted during the whole period was 9012 g m^{-2}. Microscopic inspection revealed that the sediment

Table 16.1 Fluxes (in mg m^{-2} d^{-1}) and weight percentages of particulate matter measured by the shallow sediment traps in the northern (SCS-N) and central (SCS-C) South China Sea. Data are averaged for the northeast (November to April) and southwest (June to September) monsoons and for the periods between the monsoons (NE-SW and SW-NE).

	SCS - N		SCS - C					
	SW-NE 87	NE 87/88	NE 90/91	NE-SW 92	SW 92	SW-NE 92	NE 92/93	NE-SW 93
Total flux	27.8	109.5	57.1	74.8	99.9	68.0	69.3	72.4
Carbonate flux	15.3	52.8	28.7	25.3	37.3	31.4	26.2	28.9
Biogenic opal flux	0.3	1.7	13.7	21.3	31.6	17.3	24.4	21.9
Organic matter flux	2.9	7.9	4.7	6.6	9.6	5.6	6.7	7.4
Lithogenic flux	9.3	47.1	11.1	21.7	21.4	13.7	12.0	14.6
Organic carbon (%)	5.6	4.2	5.1	4.9	5.0	4.6	5.3	5.7
Nitrogen (%)	1.1	0.7	0.6	0.6	0.6	0.7	0.7	0.8
C/N ratio	5.1	6.6	7.7	7.7	7.7	6.9	7.8	7.0
$CaCO_3$ / Opal ratio	73.7	44.6	2.3	1.2	1.4	1.8	1.1	1.4
C_{org}/C_{carb} ratio	0.8	0.7	0.9	1.2	1.1	0.8	1.2	1.2

consisted of volcanic ash with a mean modal composition of 74% volcanic glass (pumice and glass shards), 15% plagioclase and 9% hornblende. Minor constituents were biotite, quartz, cummingtonite, zircon, apatite and magnetite (2% by volume). This mineralogical composition and the chemical characteristics of the volcanogenic matter (Wang, 1994) are compatible with those reported for the airfall ash ejected by the June 15, 1991 eruption of Mount Pinatubo on Luzon Island (15.14°N, 120.35°E) (Bernard et al., 1991; Pallister et al., 1992) (see also Figure 16.1). Considering that the May-June 1991 cup closed on June 18 at 00:05 hours, the total transit time of the initial dust signal from the volcano to the trap was less than three days. A detailed investigation of the lithogenic matter intercepted by the central traps during the post-fallout period March 1992 to May 1993 revealed that small amounts of very fine-grained Pinatubo products were still present until July 1992 (Gerbich, 1995).

At 3730 m water depth total flux rates usually varied from 23 to 156 mg m^{-2} d^{-1} and did not correlate with the upper water column data (Figure 16.3). The influx of volcanic ash was observed simultaneously (Figure 16.3). Likewise, all the collecting cups were completely filled and the system was found to be positioned on the last cup. Upon recovery, however, the trap turned upside down and a large plume of whitish sediment was observed in the surface waters. This suggested that the cone contained volcanic ash in quantities comparable to the upper trap (Figure 16.3). The size spectra of the pyroclasts per cup were identical to those in the upper trap (Figure 16.4a) which documents a rapid down-column transfer and

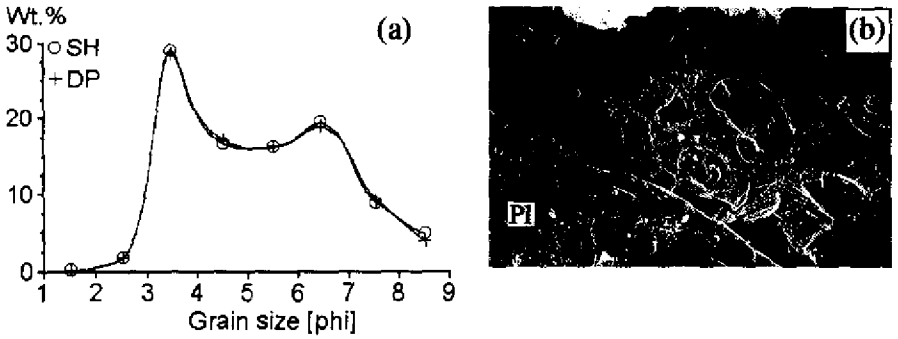

Figure 16.4 (a) Comparison of the bulk particle-size frequency curves (in phi units) of the ash front collected by cup # 6 during the interval May 21 to June 18, 1991, at 1190 m (SH) and 3730 m (DP) water depth in the central South China Sea (note the almost perfect congruence of the distributions). The bimodality is related to co-aggregation of larger pyroclasts with fine ash as illustrated by the scanning electron micrograph in (b) for sample DP. (b) Pumice fragment with vesicle fillings consisting of interlocked glass shards; the surface of the plagioclase phenocryst (Pl) is covered with fine, adhering dust (width of field of view: 63 μm).

rules out horizontal advection or buoyancy-forced up-column migration of the particles. Wiesner et al. (1995) carried out a numerical simulation of the fallout at the trap site based on eruption column heights, stratospheric ash plume movement, wind velocity profiles and the size and subaerial settling velocities of the pyroclasts. Their results indicated that the bulk of the ash arrived at the deep trap prior to June 18 at subaqueous settling speeds > 1670 m d^{-1}. These high velocities are attributed to a co-aggregation of larger pyroclasts with fine ash (Figure 16.4b) yielding bimodal grain size distribution patterns at both trap depths (Figure 16.4a). Thus the ash accumulated in the cones of the traps and as successive cups rotated into position under the cones they became filled with this material.

For the non-volcanic flux periods monitored by both traps, carbonate and organic matter fluxes were reduced by 35% and 38%, respectively, in deeper water. In contrast, biogenic opal increased by 46% and lithogenic matter by 170% (Figure 16.3).

16.5 DISCUSSION

The onset of the monsoons in the South China Sea is characterized by a pronounced increase of wind speeds from low values of 1–4 m s^{-1} during the short intermonsoon periods to more than 12 m s^{-1} during the NE monsoon and 4–8 m s^{-1} during the SW monsoon (Figures 16.2 and 16.3). Concomitantly with the onset of the NE monsoon the sea surface temperature drops by 4–7 °C in all the years observed; during the SW monsoon sea surface temperatures remain nearly constant in the north and decrease by 1–3 °C in the central South China Sea (Figures 16.2 and 16.3).

Within less than 2 weeks after the drop in sea surface temperature particle fluxes in the northern South China Sea increase considerably. At this time, the calcareous and siliceous plankton have their first flux maximum but the peak flux occurs almost simultaneously with the NE monsoon sea surface temperature minimum. In the central South China Sea such a correlation is less evident. First, the 1992–1993 NE monsoon fluxes do not show a clear increase although the wind speeds and sea surface temperature changes are not significantly different from the 1990–1991 record (Figure 16.3). Secondly, multiple productivity peaks exist per semi-annual cycle but the maximum plankton productivity is associated with the sea surface temperature low of the 1992 SW monsoon. Considering that the peak fluxes of the siliceous and calcareous plankton are more than one order of magnitude higher than at the northern station, nutrient replenishment in the euphotic zone cannot be straightforwardly related to a regulation of the mixed layer by wind stirring. Establishing cause-and-effect relationships, however, is greatly complicated by the fact that the fluxes of particulate matter in the northern and central South China Sea were not recorded synchronously. In addition, a

positive sea surface temperature anomaly was observed at both trap locations during the 1987-1988 NE monsoon (K. Arpe, written communication, 1995). This anomaly is probably related to the El Niño/Southern Oscillation episode of these years (Climate Diagnostics Bulletin, 1996) and may have affected biogenic production. We therefore refer to the following general scenario derived from previous studies, which provides a tentative explanation for many of the observations made.

During the NE monsoon period peak winds usually occur over the Strait of Luzon, curving and gradually diminishing across the central part of the South China Sea towards the Sunda Shelf (see Figure 16.5). Under this region and to the southeast, the mixed layer is at shallow depths (25–50 m); off eastern Vietnam and in the northern South China Sea west of 118°E, the top of the thermocline is strongly deflected to depths of 75–100 m (LaFond, 1963; State Oceanic Administration, 1988; Wang and Kester, 1993). The deep mixed layers do not coincide with increases in near-surface plankton productivity as indicated by the distribution of chlorophyll *a*: concentrations are generally > 0.20 mg m^{-3} in the central waters but < 0.05 mg m^{-3} off the northern continental slope (South China Sea Institute of Oceanography 1982, 1985; State Oceanic Administration, 1988). A numerical model (Figure 16.5) suggests that this situation is tied to Ekman flow. Ekman-induced vertical velocities show a broad downwelling area covering the northwestern and northern South China Sea (Figure 16.5). Upward Ekman-pumping occurs in the central and southeastern parts of the basin (Figure 16.5), where cold and saline water rises from intermediate depths (150–200 m) to the subsurface (State Oceanic Administration, 1988). As the transition between the NE and SW monsoon takes place, the top of the thermocline shoals to less than 25 m throughout the sea (State Oceanic Administration, 1988; Wang and Kester, 1993). With the onset of the SW monsoon, deep water is upwelled off southeastern Vietnam and displaced northeastward at shallow depths (< 100 m) into the central basin (Figure 16.5; Pohlmann, 1987). Maximum penetration of these cold water masses is in midsummer (Shaw and Chao, 1994). At this time, the SW monsoon wind-stress maximum builds up over the central South China Sea (Figure 16.5) where the mixed layer deepens to about 50 m, coincident with a significant increase in chlorophyll *a* (> 0.17 mg m^{-3}) (South China Sea Institute of Oceanography 1982, 1985; State Oceanic Administration, 1988). Downwelling prevails off Palawan and Borneo but in the northern South China Sea, the mixed layer depth remains fairly uniform at the intermonsoon level, probably because of the weak SW monsoon wind velocities north of 16°N (see Figure 16.5). Here the concentrations of chlorophyll *a* are generally as low as during the NE monsoon period (South China Sea Institute of Oceanography 1982, 1985; State Oceanic Administration, 1988). These data suggest that during both monsoon seasons, cold and nutrient-rich subsurface waters may be more easily incorporated into the euphotic zone at the central trap site. This, in turn, could have counterbalanced the latitudinal gradient in winter sea surface temperatures between the two trap

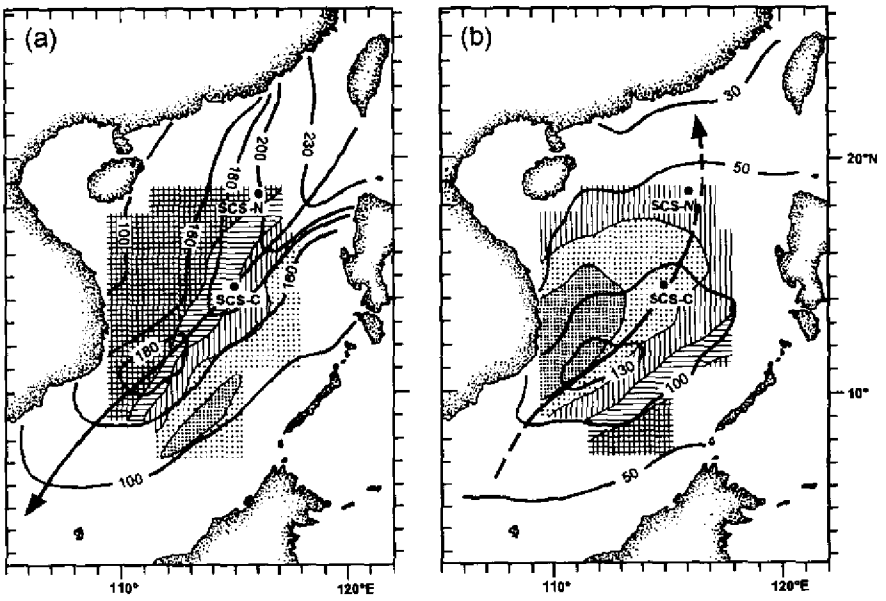

Figure 16.5 Monthly averaged wind-stress field and divergence of Ekman transport in (a) January and (b) July calculated from the 1870-1976 climatology (Hellerman and Rosenstein, 1983). Wind stress (solid contour-lines) is given in mPa; arrow indicates the position and direction of the major wind axis for each season. Ekman-induced vertical velocities are indicated as follows: dense stippling, > 60 cm d^{-1}; light stippling, 30 to 60 cm d^{-1}; vertical hatching, 0 to 30 cm d^{-1}; horizontal hatching, -30 to 0 cm d^{-1}; cross hatching, < -30 cm d^{-1}.

sites, and may explain why the temperature drop is of similar magnitude. Notably, a pronounced seasonal bimodality in the fluxes of particulate matter was registered at the central station for the period June 1993 to May 1994 (Wiesner et al., manuscript in preparation). Interannual variations in the above scenario such as shifts in the wind-stress maximum and associated variations in the intensity and timing of Ekman transport are therefore likely to occur. Moreover, the South China Sea is frequently affected by meso- to large-scale, cyclonic, cold-core eddies (South China Sea Institute of Oceanography, 1982; 1985; Soong et al., 1995), and the spatial and temporal variability of these short-term phenomena may spike the flux patterns thus introducing further irregularities.

Question arises, whether the 1991 eruption of Mount Pinatubo exercised any influence on the production of plankton. The major nutrient vehicle delivered by subaerial volcanic eruptions to the sea surface is volcanic glass (Lisitzin, 1972). Upon hydration, these particles may preferentially stimulate siliceous plankton blooms because the main component that dissolves is silicate (albeit being a very slow process at normal sea surface temperatures); only minor concentrations of

phosphate and no nitrates are released to the surrounding seawater (Stefansson, 1966). Nutrient leaching from volcanic glass has also been put forward to explain the close correspondence between volcanic maxima and shifts from planktonic carbonate to silicate producers (relatively and absolutely) recorded in deep-sea cores from the South China Sea (Wang et al., 1992) and other oceanic regions (Huang et al., 1974). A similar correspondence emerges at the trap site when the time-series data June 1993 to May 1994 are included, and when biogenic opal (carbonate) is used as a proxy for siliceous (calcareous) plankton (a strong positive correlation exits between these components at the central station; Chen, 1994). From March 1992 to May 1993, the ratios of carbonate to biogenic opal were consistently low (1.1–1.8), with the opal fluxes averaging 25 mg m^{-2} d^{-1} (Table 16.1). During the 1993 SW and the 1993–1994 NE monsoon carbonate/opal ratios averaged 2.6 and 2.3, respectively, and remained high during the periods between the monsoons (2.2–2.8); the mean opal flux was 16 mg m^{-2} d^{-1} (Wiesner et al., manuscript in preparation). Note that these values are comparable to those obtained for the pre-fallout phase December 1990 to May 1991 (see Table 16.1 and Figure 16.3).

To speculate, we consider the simplifying assumption that among the many variables influencing siliceous plankton growth, silicate is the major limiting factor (Huang et al., 1974). We extrapolate from theoretical considerations (Friedman and Long, 1976; Zielinski, 1980) that it would take about 1 year to dissolve a 0.005 μm-thick surface layer from rhyolitic glass at temperatures of between 25–30°C. The Pinatubo glass shards collected by the traps averaged 11 μm in size, with 77% SiO_2 and a mean grain density of 2.37 g cm^{-3} (Wiesner et al., 1993). Assuming sphericity, such a particle would then annually release SiO_2-concentrations of about 0.0035 ng. The annual biogenic opal flux totals 8906 mg m^{-2} for the period June 1992 to May 1993, and 6077 mg m^{-2} for the period June 1993 to May 1994. The difference in opal flux is 2829 mg m^{-2} y^{-1}, which calculates to a SiO_2-flux of 2526 mg m^{-2} y^{-1}. Now to supply this surplus from the glass shards, a total glass quantity of 1203 g m^{-2} y^{-1} (3296 mg m^{-2} d^{-1}) has to be discharged to the mixed layer (of which about 3.28 g m^{-2} y^{-1} are lost through hydration). This is about 10^3 times higher than the lithogenic fluxes measured by the shallow trap (Table 16.1). Even though the actual concentrations of suspended lithogenics are not known, enhanced nutrient availability via *in situ* leaching seems unrealistic, because the Pinatubo glass shards were already out of the water column by July 1992 (Gerbich, 1995). Thus, if any volcanic stimulation did occur, nutrients should have been supplied from outside the trap position. Possible sources would be those areas where high loads of glass have been deposited, and where the general surface water circulation and Ekman dynamics are likely to advect the plumes enriched in silicate into the central South China Sea. The distribution and composition of the ash layer on the seafloor (Wiesner and Wang, 1995) and the above oceanographic scenario suggest that the continental slope off southeastern Vietnam and open-ocean shoals such as the Macclesfield Bank are the most

favourable areas (see Figure 16.1). Recall, however, that due to the short flux record obtained so far, the "normal" background level in opal flux is not known, and the above differences may simply reflect its natural (interannual) variability. On the seafloor, the massive sedimentation of pyroclasts caused a mass mortality of benthic biota in the eastern central South China Sea, followed by a step-wise recolonization of the ash-substrate; even three years after the eruption, the benthic community structure was still far from its background levels (Hess and Kuhnt, 1995).

Another striking difference between the northern and central South China Sea is that the average fluxes and relative abundances of lithogenic matter are almost two times higher in the north (Table 16.1). This does not appear to be function of fluvial inputs from the Zhujiang (or Hunghe). Riverine runoff is lowest during the NE monsoon period (LaFond, 1966) and the sediment load is largely transported along the inner shelf to the west (Li et al., 1991). During the SW monsoon most of the riverine material is deposited in the estuaries because of the northerly directed surface currents (State Oceanic Administration, 1988). Moreover, the mineral assemblage discharged by the Zhujiang into the South China Sea (illite and quartz; Ren, 1986) is different from that collected by the traps (see below). We suggest that a large part of the lithogenic material delivered to the northern station is aeolian in origin. Estimates on the annual fluxes of atmospheric dust to the South China Sea indicate that this area is one of the major global sinks for mineral aerosols; flux rates are as high as in the eastern equatorial Atlantic and the northwestern Pacific (> 10000 mg m^{-2} y^{-1}; Duce et al., 1991). Satellite images show that during the NE monsoon period mineral dust is uplifted from the loess plateaus of eastern China and rapidly transported southward to latitudes of at least 20°N (Liu, 1985). Dust analyses have revealed that more than 90% of the mineral matter is composed of quartz, feldspar and calcite (Liu, 1985). The exact loadings for these minerals are not known but may be similar to their proportions in the loess deposits, quartz and feldspar being the major phases (Liu, 1985; Zhang et al., 1989). In fact, Rieger (1995) has shown that at the height of the winter monsoon the lithogenic material delivered to the northern traps drastically changes in composition from a clay-mineral (illite/chlorite) to a quartz and feldspar-dominated assemblage. Such a change was not recorded at the central station (Gerbich, 1995). The likely explanation is that the fallout of dust particles is largely confined to the northern parts of the basin because of the decrease in the NE monsoon wind strength from the Strait of Luzon towards the central South China (Figure 16.5; Shaw and Chao, 1994). Considering that the summer winds largely cross open-ocean regions, the lithogenic contributions at the central station remain at low levels throughout the year (SW monsoon dust loads average 0.21 μg m^{-3}; Aston et al., 1973). Notably, the total flux of carbonate during the NE monsoon period is about 2 times higher in the north (Table 16.1) although the fluxes of the calcareous plankton (foraminifers plus coccolithophorids) are lower by a factor of 10. Since significant differences in the size distribution (and hence

total weight) of the plankton tests between the stations were not obvious (Chen, unpublished results), this discrepancy may indicate the existence of an aeolian carbonate source.

Despite the lower export production of both calcareous and siliceous plankton in the northern South China Sea, the fluxes of organic matter are quite comparable to those at the central station, at least at the height of the monsoons (Table 16.1). This may have been brought about by the greater availability of mineral ballast whereby the organic matter is more rapidly transferred to deeper waters, thus significantly reducing the effects of downcolumn degradation (Haake and Ittekkot, 1990). Another factor that might have "balanced" the fluxes between the stations could be a greater input of terrigenous organic matter in the north. Based on the C/N ratios, however, a similar (and dominantly marine) type of the organic matter is suggested (Table 16.1).

In deeper water, the fluxes of particulate matter did not vary in phase with the fluxes measured by the shallow traps. The most distinct change was an increase in lithogenics with depth at both stations, which may be attributed to lateral advection. In the northern South China Sea, advected material may originate from the continental slope, where sediment mass wasting such as slumping and sliding has been documented to be a common process (Gaedicke et al., 1992). For the central station, the likely source are the steep flanks of the Macclesfield Bank, rising up to less than 200 m below sea level (Figure 16.1).

16.6 CONCLUSIONS

Particle fluxes in the South China Sea appear to be basically controlled by monsoon-related processes. Upwelling phenomena and wind-induced nutrient entrainment into the euphotic zone may account for the overall enhanced production of biogenic components in the central part of the basin. In the northern South China Sea, bioproductivity is at comparatively low levels probably because of an Ekman-induced downward deflection of the thermocline in winter and reduced wind strengths in summer. Here the seasonal flux signal seems to be related to the latitudinal extension of the monsoonal dust veils, yielding significantly higher lithogenic contributions. In response to the greater availability of mineral ballast, the fluxes of organic matter in the northern South China Sea are as high as at the central station. Increased carbonate fluxes during the NE monsoon may be misinterpreted to reflect calcareous plankton production as they could be due to a fallout of calcite from the dust plumes.

A fallout of volcanic ash (9012 g m^{-2}) from the 1991 paroxysmal explosion of Mount Pinatubo (Philippines) was recorded simultaneously in mid- and deep water in the central South China Sea. The bulk of the ash arrived in the deep sea within less than 3 days after the release of the major eruption plume (subaqueous

settling velocities > 1670 m d^{-1}). The recovery of the surface water ecosystem from this massive injection was very rapid as compared to the deep sea but not stimulated by nutrients derived from *in situ* leaching of the ash in the mixed layer. The dissolution of glass is too slow, and the amounts of pyroclasts that did remain suspended were too low to have produced the enhanced biosiliceous flux observed during the post-eruption year. If any volcanic stimulation did occur, the likely process is lateral advection of nutrients from the mid- or shallow-water locales of massive glass deposition.

16.7 ACKNOWLEDGMENTS

We are indebted to the officers and crews of the research vessels R/V *Sonne*, R/V *Xiangyanghong-5* and RV *Xiangyanghong-14* for their assistance in the deployment and recovery of the traps. Thanks are also due to V. Ittekkot for his ongoing support of the project. Financial support by the Federal German Ministry for Education, Science, Research and Technology (BMBF, Bonn) and the State Oceanic Administation (Beijing) is gratefully acknowledged.

16.8 REFERENCES

Aston, S. R., R. Chester, L. R. Johnson and R. C. Padgham (1973) "Eolian dust from the lower atmosphere of the eastern Atlantic and Indian Oceans, China Sea and Sea of Japan", *Mar. Geol.*, **14**, 15–28.

Bauer, S., G. L. Hitchcock and D. B. Olson (1991) "Influence of monsoonally-forced Ekman dynamics upon surface layer depth and plankton biomass distribution in the Arabian Sea", *Deep-Sea Res.*, **38**, 531–553.

Bernard, A., D. Demaiffe, N. Mattielli and R. S. Punongbayan (1991) "Anhydrite-bearing pumices from Mount Pinatubo: Further evidence for the existence of sulphur-rich silicic magmas", *Nature*, **354**, 139–140.

Chen, P. Y. (1978) "Minerals in bottom sediments of the South China Sea", *Geol. Soc. Amer. Bull.*, **89**, 211–222.

Chen, W. (1994) *Vertical Flux of Radiolaria and Other Microplankton at the Sediment Trap Site SCS-C, Central South China Sea, Report to the German Ministry of Research and Technology, 03G0513A*, Institute of Biogeochemistry and Marine Chemistry, University of Hamburg.

Climate Diagnostics Bulletin (1996), Volumes **96/2**, U.S. Department of Commerce, NOAA National Weather Service, Washington, D.C.

Deuser, W. G., P. G. Brewer, T. D. Jickels and R. F. Commeau (1983) "Biological control on the removal of abiogenic particles from the surface ocean", *Science*, **219**, 388–391.

Deuser, W. G. (1986) "Seasonal and interannual variations in the deep-water particle fluxes in the Sargasso Sea and their relation to surface hydrography", *Deep-Sea Res.*, **33**, 225–246.

Deuser, W. G., F. E. Müller-Karger and C. Hemleben (1988) "Temporal variations of particle fluxes in the deep subtropical and tropical North Atlantic: Eulerian versus Lagrangian effects", *J. Geophys. Res.*, **93**, 6857–6862.

Duce, R. A., P. S. Liss, J. T. Merrill, E. L. Atlas, P. Buat-Menard, B. B. Hicks, J. M. Miller, J. M. Prospero, R. Arimoto, T. M. Church, W. Ellis, J. N. Galloway, L. Hansen, T. D. Jickells, A. H. Knap, K. H. Reinhardt, B. Schneider, A. Soudine, J. J. Tokos, S. Tsunogai, R. Wollast, and M. Zhou (1991) "The atmospheric input of trace species to the world ocean", *Global Biogeochem. Cycles*, **5**, 193–259.

Friedman, I. and W. Long (1976) "Hydration rate of obsidian", *Science*, **191**, 347–352.

Gaedicke, C., H. K. Wong and Y. Liang (1992) "Seismic stratigraphy and Holocene sedimentation at the northern margin of the South China Sea", in X. Jin, H. R. Kudrass and G. Pautot (eds) *Marine Geology and Geophysics of the South China Sea*, China Ocean Press, Qingdao, 228–235.

Gerbich, C. (1995) *Lithogener Partikelfluß im zentralen Südchinesischen Meer: Quellen, Transport und Sedimentation*, Unpublished M.Sc. Thesis, University of Hamburg.

Haake, B. and V. Ittekkot (1990) "Die Wind-getriebene biologische Pumpe und der Kohlenstoffentzug im Ozean", *Naturwissenschaften*, 77, 75–79.

Haake, B., T. Rixen and V. Ittekkot (1993) "Variability of monsoonal upwelling signals in the deep western Arabian Sea", in V. Ittekkot and R. R. Nair (eds) *Monsoon Biogeochemistry*, Mitt. Geol.-Paläont. Inst. Univ. Hamburg, No. 76, 85–95.

Hellerman, S. and M. Rosenstein (1983) "Normal monthly wind stress over the world ocean with error estimates", *J. Phys. Oceanogr.*, **13**, 1093–1104.

Hess, S. and W. Kuhnt (1995) "Deep sea benthic foraminiferal recolonization of the 1991 Pinatubo ash layer in the South China Sea", *Mar. Micropaleontol.*, in press.

Hirschboeck, K. K. (1980) "A new worldwide chronology of volcanic eruptions", *Palaeogeogr., Palaeoclimat., Palaeoecol.*, **29**, 223–241.

Honjo, S. (1982) "Seasonality and interaction of biogenic and lithogenic particulate flux at the Panama Basin", *Science*, **218**, 883–884.

Honjo, S. (1990) "Particle fluxes and modern sedimentation in the polar oceans", in W. O. Smith (ed) *Polar Oceanography*, Academic Press, New York, 687–739.

Huang, T. C., R. H. Fillon, N. D. Watkins and D. M. Shaw (1974) "Volcanism and siliceous microfaunal 'diversity' in the southwest Pacific during the Pleistocene period", *Deep-Sea Res.*, **21**, 337–383.

Ittekkot, V., R. R. Nair, S. Honjo, V. Ramaswamy, M. Bartsch, S. Manganini and B. N. Desai (1991) "Enhanced particle fluxes in the Bay of Bengal induced by injection of fresh water", *Nature*, **351**, 385–387.

Ittekkot, V., Haake, B., Bartsch, M., Nair, R. R. and Ramaswamy, V. (1992) "Organic carbon removal in the sea: The continental connection", in C. P. Summerhayes, W. L. Prell and K. C. Emeis (eds) *Upwelling Systems: Evolution Since the Early Miocene*, Geological Society Special Publication No. 64, 167–176.

Jennerjahn, T. C., G. Liebezeit, S. Kempe, L. Xu, W. Chen and H. K. Wong (1992) "Particle flux in the northern South China Sea", in X. Jin, H. R. Kudrass and G. Pautot (eds) *Marine Geology and Geophysics of the South China Sea*, China Ocean Press, Qingdao, 228–235.

Kennett, J. P. (1981) "Marine tephrochronology", in C. Emiliani (ed) *The Sea, Vol. 7, The Oceanic Lithosphere*, Wiley Interscience, New York, 1373–1436.

Klein, P. and B. Coste (1984) "Effects of wind-stress variability on nutrient transport into the mixed layer", *Deep-Sea Res.*, **31**, 21–37.

Koroleff, F. (1983) "Determination of silicon", in K. Grasshoff, M. Ehrhardt and K. Kremling (eds) *Methods of Seawater Analysis*, 2. ed., Verlag Chemie, Weinheim, 174–187.

LaFond, E. C. (1963) "Physical oceanography and its relation to the marine organic production in the South China Sea", *Scripps Inst. Oceanogr. Ref.*, **63–6**, 5–33.

LaFond, E. C. (1966) "South China Sea", in *The Encyclopedia of Oceanography*, Reinhold Publ., New York, 829–836.

LaViolette, P. E. and T. R. Frontenac (1967) *Temperature, Salinity and Density of the World's Seas: South China Sea and Adjacent Gulfs, Informal Manuscript*, 67–5, U.S. Naval Oceanographic Office, Washington, D.C.

Legler, D. M., I. M. Navon and J. J. O'Brien (1989) "Objective analysis of pseudo-stress over the Indian Ocean using a direct minimization approach", *Monthly Weather Rev.*, **117**, 709–720.

Li, C., G. Chen, M. Yao and P. Wang P. (1991) "The influences of suspended load on the sedimentation in the coastal zones and continental shelves of China", *Mar. Geol.*, **96**, 341–352.

Lisitzin, A. P. (1972) "Sedimentation in the world ocean", *Soc. Econ. Paleont. Mineralog. Spec. Pub.*, **17**, 1–218.

Liu, D. (1985) *Loess and Environment*, Science Press, Beijing.

McDonald, W. F. (1938) *Atlas of Climatic Charts of the Oceans*, U. S. Government Printing Office, Washington, D.C.

Milliman, J. D. and R. H. Meade (1983) "World-wide delivery of river sediment to the oceans", *J. Geol.*, **91**, 1–21.

Mortlock, R. A. and P. N. Froelich (1989) "A simple method for rapid determination of biogenic opal in pelagic sediments", *Deep-Sea Res.*, **36**, 1415–1426.

Müller, P. J., E. Suess and A. C. Ungerer (1986) "Amino acids and amino sugars of surface particulate and sediment trap material from waters of the Scotia Sea", *Deep-Sea Res.*, **33**, 819–839

Nair, R. R., V. Ittekkot, S. Manganini, V. Ramaswamy, B. Haake, E. T. Degens, B. N. Desai and S. Honjo (1989) "Increased particle fluxes to the oceans related to monsoons", *Nature*, **338**, 749–751.

Niino, H. and K. O. Emery (1961) "Sediments of shallow portions of East China Sea and South China Sea", *Geol. Soc. Amer. Bull.*, **72**, 731–762.

Pallister, J. S., R. P. Hoblitt and A. G. Reyes (1992) "A basalt trigger for the 1991 eruptions of Pinatubo volcano?", *Nature*, **356**, 426–428.

Pohlmann, T. (1987) "Three-dimensional circulation model of the South China Sea", in J. C. J. Nihoul and B. M. Jamert (eds) *Three-Dimensional Models of Marine and Estuarine Dynamics*, Elsevier Science Publ., Amsterdam, 245–268.

Ramage, C. S. (1971) *Monsoon Meteorology*, Academic Press, New York.

Ramaswamy, V., R. R. Nair, S. Manganini, B. Haake and V. Ittekkot (1991) "Lithogenic fluxes to the deep Arabian Sea measured by sediment traps", *Deep-Sea Res.*, **38**, 169–184.

Ren, M. (1986) *Modern Sedimentation in the Coastal and Nearshore Zones of China*, China Ocean Press, Beijing.

Reschke, S. (1994) *Biogeochemische Untersuchungen an Sinkstoffen aus dem Südchinesischen Meer*, Unpublished M.Sc. Thesis, University of Hamburg.

Rieger, M. (1995) *Quellen, Transport und Sedimentation lithogener Partikel im nördlichen Südchinesischen Meer*, Unpublished M.Sc. Thesis, University of Hamburg.

Shaw, P. T. and S. Y. Chao (1994) "Surface water circulation in the South China Sea", *Deep-Sea Res.*, **41**, 1663–1683.

Simkin, T., L. Siebert, L. McClelland, D. Bridge, C. Newhall and J. H. Latter (1982) *Volcanoes of the World*, Huchinson and Ross, Stroudsburg.

Soong, Y. S., J.-H. Hu, C.-R. Ho and P. P. Niiler (1995) "Cold-core eddy detected in the South China Sea", *Eos*, **76**, 345 and 347.

South China Sea Institute of Oceanography (1982) *Research Report on a Comprehensive Survey of Parts of the South China Sea - Vol. 1*, Science Press, Beijing.

South China Sea Institute of Oceanography (1985) *Research Report on a Comprehensive Survey of Parts of the South China Sea - Vol. 2*, Science Press, Beijing.

State Oceanic Administration (1988) *Report on a Comprehensive Survey of the Environmental Resources in the Central South China Sea*, Ocean Press, Beijing.

Stefansson, U. (1966) "Influence of the Surtsey eruption on the nutrient content of the surrounding seawater", *J. Mar. Res.*, **24**, 241–268.

Tchernia, P. (1980) *Descriptive Regional Oceanography*, Pergamon Press, Oxford.

Wang, H., F. Zhou and Z. Lin (1992) "Volcanic clasts in the periplatform carbonate ooze near Zhongsha Islands and their bearing on paleoenvironment", in Z. Ye and P. Wang (eds) *Contributions to Late Quaternary Paleoceanography of the South China Sea*, Qingdao Ocean Press, Qingdao, 42–55.

Wang, Y. (1994) *Petrographie und Korngrößencharakteristika vulkanischer Aschen des Mount Pinatubo (Luzon, Philippinen)*, Unpublished M.Sc. Thesis, University of Hamburg.

Wang, Z. and D. R. Kester (1993) "Seasonal variation in the South China Sea continental shelf water", *Proceedings of the First Conference on the Biology of the South China Sea*, South China Sea Institute of Oceanography, Academia Sinica, Guangzhou, 81–93.

Wefer, G. (1989) "Particle flux in the ocean: Effects of episodic production", in W. H. Berger, V. S. Smetacek and G. Wefer (eds) *Productivity of the Ocean: Present and Past*, Wiley and Sons, Berlin, 139–153.

Wefer, G. and G. Fischer (1993) "Seasonal patterns of vertical particle flux in equatorial and coastal upwelling areas of the eastern Atlantic", *Deep-Sea Res.*, **40**, 1613–1645.

Wiesner, M. G. and Y. Wang (1995) "Dispersal of the 1991 Pinatubo tephra in the South China Sea", in C. G. Newhall and R. S. Punongbayan (eds) *The 1991–1992 Eruptions of Mount Pinatubo, Philippines*, U.S. Geol. Surv. Prof. Paper, in press.

Wiesner, M. G., Y. Wang and L. Zheng (1995) "Fallout of volcanic ash to the deep South China Sea induced by the 1991 eruption of Mount Pinatubo (Philippines)", *Geology*, **23**, 885–888.

Wiesner, M. G., Y. Wang, K. Arikas, H. K. Wong and L. Zheng (1993) "Volcanic particles from the 1991 eruption of Mount Pinatubo intercepted in the deep South China Sea", *Beih. z. Eur. J. Mineral.*, **5**, 302.

Wolfe, J. and S. Self (1983) "Structural lineaments and Neogene volcanism in southwestern Luzon", in D. E. Hayes (ed) *The Tectonic and Geologic Evolution of Southeast Asian Seas and Islands*, Amer. Geophys. Un. Monogr., No. 27, 157–172.

Wyrtki, K. (1961) *Physical Oceanography of the Southeast Asian Waters, NAGA Report*, 2, Scripps Institution of Oceanography, La Jolla, California.

Zhang, Z., Z. Zhang and Y. Wang (1989). *Loess in China*, Geology Press, Beijing.

Zielinski, R. A. (1980) "Stability of glass in the geologic environment: Some evidence from studies of natural silicate glasses", *Nucl. Techn.*, **51**, 197–200.

17 Vertical Particle Flux in the Western Pacific Below the North Equatorial Current and the Equatorial Counter Current

STEPHAN KEMPE AND HEIKO KNAACK

17.1 INTRODUCTION

In the open ocean, the vertical particle flux is largely determined by the primary productivity of the euphotic zone. Primary productivity in turn is a function of nutrient concentration. Areas low in nutrients should therefore coincide with areas of low vertical particle flux and low sedimentation rates.

In order to test this hypothesis, we deployed two sediment trap moorings in an area where the surface waters are known to have extremely low nutrient concentration; i.e., the western Pacific (e.g., King, 1954).

17.2 MATERIALS AND METHODS

Both systems consisted of two Mark VI time-series sediment traps (13 cups) (Honjo and Doherty, 1988), Benthos buoyancy balls and a Benthos acoustic release. One of the systems was deployed in the West Caroline Basin where the Equatorial Counter Current originates (ECC-System, Table 17.1; Figure 17.1). The second system was deployed in the Philippine Basin in a region where the North Equatorial Current terminates (NEC-System). This location is situated west of the near-by Palau-Kyushu Ridge. The sampling cups were filled with a NaCl-saturated solution to keep the cup fluid from convecting out during the collection phase. Furthermore, the cups were poisoned with $HgCl_2$ to avoid bacterial respirative consumption of the collected material.

The samples were wet-sieved through a 1 mm sieve and the fraction < 1 mm was filtered through pre-weighted 0.4 μm pore-size Nuclepore filters. Filters and sediment were dried at 40°C and their weight was determined. All data refer to

Particle Flux in the Ocean
Edited by V. Ittekkot, P. Schäfer, S. Honjo and P. J. Depetris

Table 17.1 General information on deployments

System	ECC	NEC
Location		
Latitude	5°00.60'N	12°01.00'N
Longitude	138°49.81'E	134°17.16'E
Water depth	4130 m	5300 m
Upper trap	1130 m / ECC-T	1200 m / NEC-T
Lower trap	3130 m / ECC-B	4300 m / NEC-B
Deployment date	November 1988	
Cruise	R/V *Sonne* 59B	
Recovery date	July 1990	
Cruise	R/V *Sonne* 69B	
Collection interval	11/21/88–12/16/89	
Interval per cup	30 days	
Preservation	$NaCl/HgCl_2$	$NaCl/HgCl_2$

the < 1 mm fraction. Due to the very small size of all samples, the material could only be analyzed for major components. In order to determine how much of the collected material had gone into lysis, cup waters were analyzed for dissolved constituents as well. The amounts recovered from the dissolved phase were added to the particulate phase retained on the filters in order to calculate the total vertical flux. The samples were analyzed for total carbon and total nitrogen content by high temperature combustion (Carlo Erba CHN Analyzer) and for SiO_2 and phosphorus content by photometry. Carbonate was measured with a Carmhograph and the resulting inorganic carbon concentration was subtracted from the total carbon content to obtain organic carbon concentrations. In case of samples ECC-T12, ECC-B1, ECC-B12, ECC-B13, NEC-T6, NEC-T11, NEC-T12 not enough material for carbonate determination was available and carbonate was measured by acidifying samples and measuring organic carbon in the CHN analyzer. Carbonate was then calculated as the difference between total and organic carbon. Recalculating these data allows determination of the composition of the samples with regard to $CaCO_3$, organic matter (1.8 x C_{org}), opal (SiO_2 x 0.4 H_2O; Mortlock and Froelich, 1989) and lithogenics.

17.3 DISCUSSION OF RESULTS

All measured concentrations are listed in Tables 17.2–17.5. The recorded flux rates were very low at both stations. The averages amounted to 4.75 and 7.52 mg m^{-2} d^{-1} in case of the NEC-T and NEC-B traps and to 18.04 and 11.18 mg m^{-2} d^{-1} in case of the ECC-T and ECC-B traps, respectively. Fluxes between 45 and 20 mg m^{-2} d^{-1} were encountered in November/December 1988 and April/

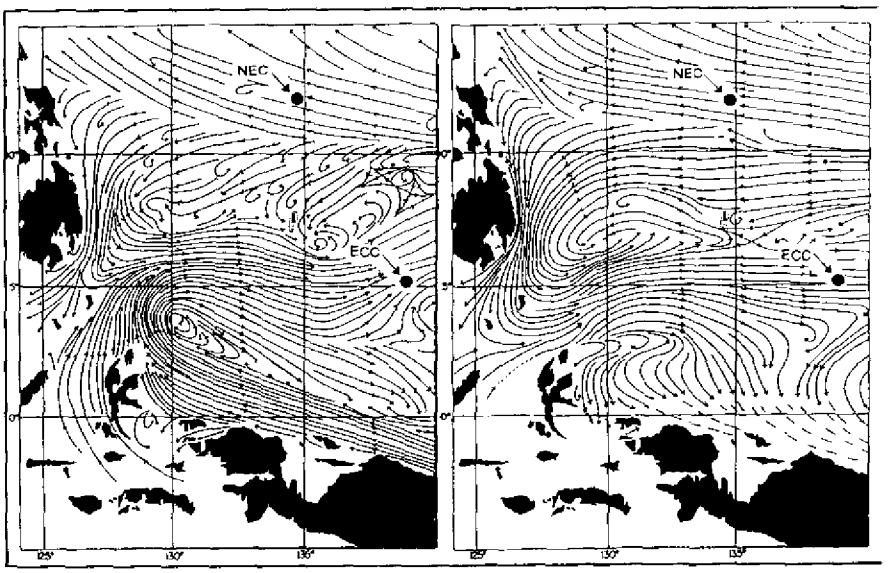

Figure 17.1 The equatorial currents of the western Pacific Ocean (left northern summer, right northern winter) and the positions of sediment traps (NEC = North Equatorial Current; ECC = Equatorial Counter Current) (Kendall, 1970; after Schott, 1939).

May to June/July 1989 in the ECC-T trap and only once (May/June) 1989 in the ECC-B trap (Figure 17.2). In the NEC traps individual fluxes rarely exceeded 10 mg m^{-2} d^{-1} (Figure 17.3).

Total fluxes showed a pronounced seasonality at the ECC location in the West Caroline Basin. Fluxes showed the highest values in late spring and early summer (mid-April to mid-July) with a maximum of 43.3 mg m^{-2} d^{-1} (mid-April to mid-June, ECC-T). Intermediate fluxes occurred in winter and early spring (mid-November to mid-April) in the upper trap and in late winter to late spring in the lower trap (mid-February to mid-April).Low fluxes occurred in late summer to early winter (mid-July to mid-December).

In contrast to this, the NEC traps from the Philippine Basin did not record any pronounced seasonality in vertical particle flux except for a period of lower than average flux in late autumn and early winter (mid-September to mid-December). The absolute minimum flux, 0.72 mg m^{-2} d^{-1}, was recorded in mid-October to mid-November.

The seasonal differences in vertical particle flux in the West Caroline Basin most probably arise from seasonal changes in wind and current direction. During the northern summer with a normal trade wind, part of the ECC arises from a current flowing NW along the northern coast of New Guinea probably advecting higher loads of nutrients than during NW-monsoon winter conditions when the

Table 17.2 Particle flux < 1 mm at station ECC (5°00.60'N/138°49.81'E) 1130 m

Opened	Closed		Total flux mg/m²/d	C_{org} %	C_{org} mg/m²/d	N_{tot} %	N_{tot} mg/m²/d	P_{tot} %	P_{tot} µg/m²/d	Carbonate %	Carbonate mg/m²/d	Opal %	Opal mg/m²/d	Organic %	Organic mg/m²/d	Lithogenic %	Lithogenic mg/m²/d
11/21/88	12/21/88	(N/D)	23.80	9.82	2.34	1.14	0.27	0.09	21	56.2	13.37	16.0	3.81	17.7	4.20	10.1	2.41
12/21/88	01/20/89	(D/J)	15.60	6.51	1.02	0.92	0.14	0.05	7	75.1	11.72	9.1	1.41	11.7	1.83	4.1	0.64
01/20/89	02/19/89	(J/F)	18.61	6.49	1.21	0.85	0.16	0.19	35	76.4	14.22	6.7	1.25	11.7	2.17	5.2	0.97
02/19/89	03/21/89	(F/M)	14.93	8.03	1.20	1.00	0.15	0.08	11	72.4	10.81	6.7	1.00	14.5	2.16	6.4	0.96
03/21/89	04/20/89	(M/A)	11.91	9.87	1.18	1.37	0.16	0.15	18	65.4	7.79	9.6	1.14	17.8	2.12	7.3	0.87
04/20/89	05/20/89	(A/M)	43.25	9.57	4.14	1.19	0.52	0.10	45	52.2	22.58	22.6	9.77	17.2	7.45	8.0	3.45
05/20/89	06/19/89	(M/J)	43.32	11.30	4.90	2.54	1.10			55.6	24.09	11.7	5.05	20.3	8.81	12.4	5.37
06/19/89	07/19/89	(J/J)	37.81	9.54	3.61	1.31	0.50	0.16	62	53.3	20.15	19.4	7.34	17.2	6.49	10.1	3.82
07/19/89	08/18/89	(J/A)	11.43	12.83	1.47	1.76	0.20	0.15	17	54.7	6.25	13.8	1.58	23.1	2.64	8.4	0.96
08/18/89	09/17/89	(A/S)	4.84	12.81	0.62	1.54	0.07	0.14	7	56.1	2.71	13.7	0.66	23.1	1.12	7.1	0.35
09/17/89	10/17/89	(S/O)	3.62	14.39	0.52	1.79	0.06	0.17	6	56.2	2.03	9.3	0.34	25.9	0.94	8.6	0.31
10/17/89	11/16/89	(O/N)	1.48	12.77*	0.19*	1.96	0.03			81.0*	1.20*	7.1	0.10	23.0*	0.34*		
11/16/89	12/16/89	(N/D)	3.91	18.30	0.72	1.99	0.08	0.21	8	49.7	1.94	8.5	0.33	32.9	1.29	8.9	0.35
Average			18.04	9.85	1.78	1.47	0.26	0.13	23	59.2	10.68	14.4	2.60	17.7	3.20	8.7	1.56

* Note that the organic carbon and calcium carbonate content were determined with a less precise method in cup ECC-T12 due to the small amounts recovered in this cup. In this sample calcium carbonate contents could therefore be overestimated and the organic carbon content underestimated (see text).

Table 17.3 Particle flux < 1 mm at station ECC (5°00.60'N/138°49.81'E) 3130 m

Opened	Closed		Total flux	C_{org}		N_{tot}		P_{tot}		Carbonate		Opal		Organic		Lithogenic	
			mg/m²/d	%	mg/m²/d	%	mg/m²/d	%	µg/m²/d	%	mg/m²/d	%	mg/m²/d	%	mg/m²/d	%	mg/m²/d
11/21/88	12/21/88	(N/D)	0.91	9.93*	0.09*	1.35	0.01			58.7*	0.53*	25.1	0.23	17.9*	0.16*		
12/21/88	01/20/89	(D/J)	2.80	8.58	0.24	1.10	0.03	0.09	2	46.4	1.30	22.3	0.62	15.4	0.43	15.9	0.45
01/20/89	02/19/89	(J/F)	18.67	3.83	0.72	0.59	0.11	0.05	9	73.5	13.72	14.0	2.61	6.9	1.29	5.6	1.05
02/19/89	03/21/89	(F/M)	17.98	8.60	1.55	0.99	0.18	0.09	17	56.4	10.14	17.2	3.10	15.5	2.78	10.9	1.96
03/21/89	04/20/89	(M/A)	15.58	5.76	0.90	0.75	0.12	0.07	11	62.7	9.77	15.7	2.44	10.4	1.62	11.3	1.76
04/20/89	05/20/89	(A/M)	14.58	4.43	0.65	0.57	0.08	0.14	21	71.4	10.41	13.6	1.98	8.0	1.16	7.0	1.02
05/20/89	06/19/89	(M/J)	28.52	5.40	1.54	0.70	0.20	0.10	30	66.8	19.05	19.1	5.46	9.7	2.77	4.4	1.24
06/19/89	07/19/89	(J/J)	15.82	5.21	0.82	0.64	0.10	0.06	9	65.6	10.38	16.1	2.55	9.4	1.48	8.9	1.41
07/19/89	08/18/89	(J/A)	13.35	5.78	0.77	0.82	0.11	0.07	9	60.1	8.02	20.4	2.72	10.4	1.39	9.1	1.21
08/18/89	09/17/89	(A/S)	8.65	7.23	0.62	0.95	0.08	0.10	8	60.0	5.19	20.9	1.81	13.0	1.12	6.1	0.53
09/17/89	10/17/89	(S/O)	6.37	10.48	0.67	1.33	0.08	0.11	7	61.1	3.89	15.5	0.99	18.9	1.20	4.6	0.29
10/17/89	11/16/89	(O/N)	1.34	6.51*	0.09*	0.96	0.01	0.06	1	76.5*	1.03*	13.4	0.18	11.7*	0.16*		
11/16/89	12/16/89	(N/D)	0.83	9.57*	0.08*	1.48	0.01			77.0*	0.64*			17.2*	0.14*		
Average			11.18	6.00	0.67	0.78	0.09	0.09	10	64.7	7.24	17.1	1.91	10.8	1.21	7.4	0.84

* Note that the organic carbon and calcium carbonate content were determined with a less precise method in cups ECC-B1, ECC-B12 and ECC-B13 due to the small amounts recovered in these cups. In these samples calcium carbonate contents could therefore be overestimated and the organic carbon content underestimated (see text).

Table 17.4 Particle flux < 1 mm at station NEC (12°01.00'N/134°17.16'E) 1200 m

Opened	Closed		Total flux	C_{org}		N_{tot}		P_{tot}		Carbonate		Opal		Organic		Lithogenic	
			mg/m²/d	%	mg/m²/d	%	mg/m²/d	%	µg/m²/d	%	mg/m²/d	%	mg/m²/d	%	mg/m²/d	%	mg/m²/d
11/21/88	12/21/88	(N/D)	3.76	7.57	0.28	1.05	0.04	0.24	9	69.0	2.59	7.8	0.29	13.6	0.51	9.6	0.36
12/21/88	01/20/89	(D/J)	11.87	7.09	0.84	1.01	0.12	0.08	10	70.0	8.31	10.1	1.20	12.8	1.51	7.1	0.85
01/20/89	02/19/89	(J/F)	8.60	7.09	0.61	0.93	0.08	0.10	9	73.7	6.34	8.8	0.75	12.8	1.10	4.8	0.41
02/19/89	03/21/89	(F/M)	5.84	8.40	0.49	1.02	0.06	0.09	5	67.5	3.95	9.8	0.57	15.1	0.88	7.6	0.45
03/21/89	04/20/89	(M/A)	2.21	8.46	0.19	1.02	0.02	0.07	2	68.0	1.50	9.2	0.20	15.2	0.34	7.6	0.17
04/20/89	05/20/89	(A/M)	4.74														
05/20/89	06/19/89	(M/J)	3.74	10.48	0.39	1.40	0.05	0.07	3	67.4	2.52	9.5	0.36	18.9	0.71	4.2	0.16
06/19/89	07/19/89	(J/J)	4.83	8.11	0.39	1.01	0.05	0.29	14	67.9	3.28	10.3	0.50	14.6	0.70	7.2	0.35
07/19/89	08/18/89	(J/A)	5.37	9.25	0.50	0.96	0.05	0.16	8	69.9	3.75	7.3	0.39	16.7	0.89	6.2	0.33
08/18/89	09/17/89	(A/S)	5.57	7.44	0.41	1.10	0.06	0.07	4	70.3	3.91	8.8	0.49	13.4	0.75	7.6	0.42
09/17/89	10/17/89	(S/O)	1.31	10.22*	0.13*	1.60	0.02	0.15	2	79.8*	1.05*	8.3	0.11	18.4*	0.24*		
10/17/89	11/16/89	(O/N)	0.72	11.46*	0.08*	1.19	0.01			42.3*	0.31*			20.6*	0.15*		
11/16/89	12/16/89	(N/D)	3.20	8.83	0.28	1.12	0.04	0.10	3	66.3	2.12	9.1	0.29	15.9	0.51	8.7	0.28
Average			4.75	8.08	0.38	1.05	0.05	0.12	6	69.5	3.30	9.2	0.43	14.5	0.69	6.4	0.31

* Note that the organic carbon and calcium carbonate content were determined with a less precise method in cups NEC-T11 and NEC-T12 due to the small amounts recovered in these cups. In these samples calcium carbonate contents could therefore be overestimated and the organic carbon content underestimated (see text).

Table 17.5 Particle flux < 1 mm at station NEC (12°01.00'N/134°17.16'E) 4300 m

Opened	Closed		Total flux	C_{org}		N_{tot}		P_{tot}		Carbonate		Opal		Organic		Lithogenic	
			mg/m²/d	%	mg/m²/d	%	mg/m²/d	%	µg/m²/d	%	mg/m²/d	%	mg/m²/d	%	mg/m²/d	%	mg/m²/d
11/21/88	12/21/88	(N/D)	6.83	6.82	0.47	0.87	0.06	0.07	5	48.9	3.34	21.1	1.44	12.3	0.84	17.7	1.21
12/21/88	01/20/89	(D/J)	11.63	5.07	0.59	0.63	0.07	0.05	6	56.9	6.62	15.6	1.81	9.1	1.06	18.4	2.14
01/20/89	02/19/89	(J/F)	7.49	5.88	0.44	0.76	0.06	0.07	5	53.0	3.97	17.2	1.29	10.6	0.79	19.2	1.44
02/19/89	03/21/89	(F/M)	8.18	5.67	0.46	0.75	0.06	0.06	5	52.8	4.32	19.0	1.55	10.2	0.83	18.0	1.47
03/21/89	04/20/89	(M/A)	9.48	5.97	0.57	0.77	0.07	0.05	5	48.9	4.64	18.5	1.76	10.7	1.02	21.8	2.07
04/20/89	05/20/89	(A/M)	10.30	5.61	0.58	0.76	0.08	0.05	6	51.3	5.29	17.0	1.75	10.1	1.04	21.6	2.23
05/20/89	06/19/89	(M/J)	8.73	4.77	0.42	0.65	0.06	0.04	4	59.0	5.15	14.9	1.30	8.6	0.75	17.5	1.53
06/19/89	07/19/89	(J/J)	6.77	6.74	0.46	0.80	0.05	0.10	7	47.8	3.23	18.5	1.25	12.1	0.82	21.6	1.46
07/19/89	08/18/89	(J/A)	7.74	5.97	0.46	0.84	0.07	0.06	4	50.6	3.92	19.3	1.49	10.8	0.83	19.4	1.50
08/18/89	09/17/89	(A/S)	7.74	5.97	0.46	0.84	0.07	0.06	4	50.6	3.92	19.3	1.49	10.8	0.83	19.4	1.50
09/17/89	10/17/89	(S/O)	3.36	5.58	0.19	0.66	0.02	0.05	2	56.9	1.91	16.6	0.56	10.0	0.34	16.5	0.55
10/17/89	11/16/89	(O/N)	3.68	6.40	0.24	0.82	0.03	0.10	4	58.4	2.15	16.0	0.59	11.5	0.42	14.1	0.52
11/16/89	12/16/89	(N/D)	5.80	4.97	0.29	0.72	0.04	0.04	2	66.0	3.83	13.0	0.75	8.9	0.52	12.1	0.70
Average			7.52	5.74	0.43	0.75	0.06	0.06	4	53.5	4.02	17.4	1.31	10.3	0.78	18.7	1.41

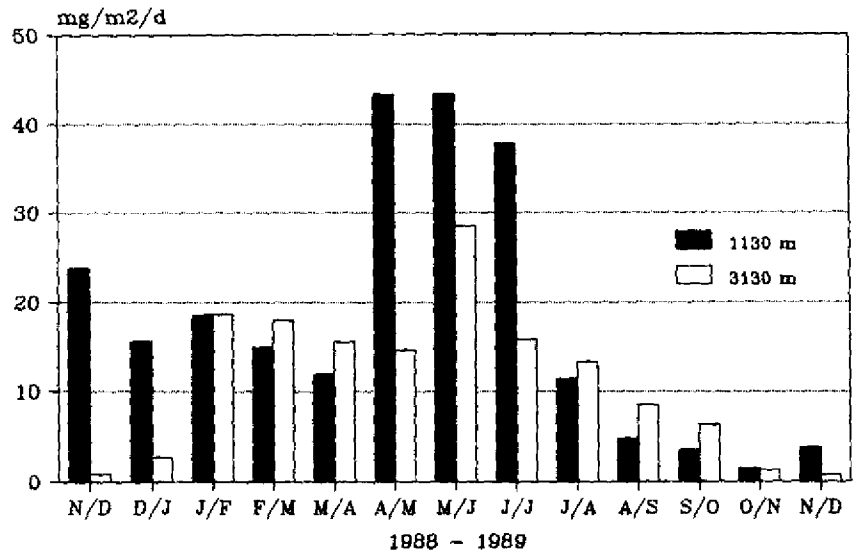

Figure 17.2 Total particle flux (< 1 mm) at station ECC (Western Caroline Basin) November-December 1988 / November-December 1989.

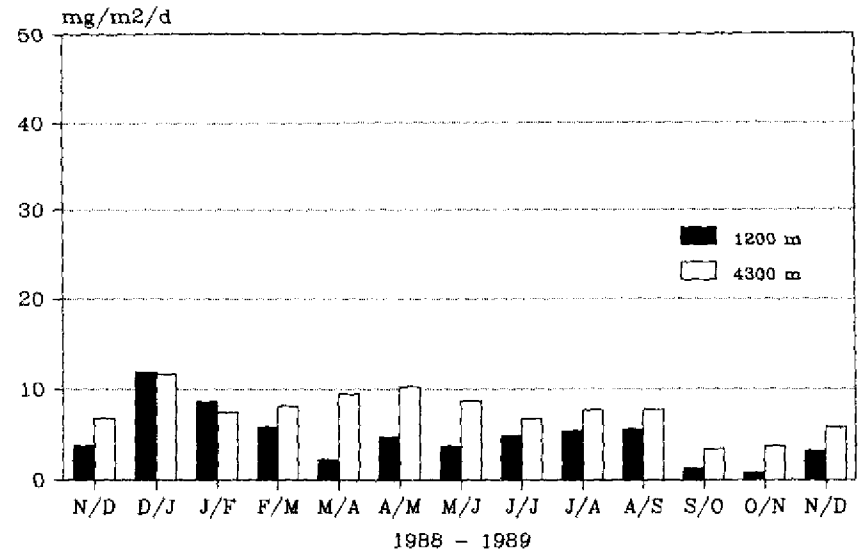

Figure 17.3 Total particle flux (< 1 mm) at station NEC (Philippine Basin) November-December 1988 / November-December 1989.

ECC is almost entirely composed of rerouted NEC water (Figure 17.1). Such a seasonality is not observed in the Philippine Basin. The NEC is stable throughout the year. It does, however, intensify in winter, thereby advecting nutrient impoverished water faster across the Pacific than in summer and giving less opportunity for nutrients to mix into the euphotic zone. Overall, the western terminus of the NEC apparently is one of the least productive regions of the entire ocean.

Because the 13-cup sediment trap was programmed to collect settling particles once every month, the November/December flux interval was sampled twice. In the case of the NEC trap, the recorded fluxes in the repeated interval were similar. This was also true for the deeper ECC trap, but not for the shallower ECC trap. There, a six times larger flux was recorded in 1988 than in 1989, suggesting that the change to more nutrient-rich conditions in surface waters occurred much earlier in 1988 than in 1989. Interannual variations such as these are rather common in particle flux records (e.g., Deuser et al., 1981; Izdar et al., 1987; this volume, Chapters 9, 14, 15).

Due to the large distance the water masses above the trap positions have traveled since last encountering coastal waters, lithogenic material comprises less than 10% of the vertical particle flux (Figure 17.4). The overwhelming mass of the material intercepted is biogenic. Only the lower NEC trap had a higher lithogenic component of ca. 20%. This may be attributed to the vicinity of the Palau-Kyushu Ridge. There, deep-sea currents could remobilize sediments rich in lithogenics and material inert to dissolution. This admixture of resuspended sediment may also explain why the total flux rate in the lower trap was significantly higher than the flux rate in the upper trap at this position.

Calcium carbonate was the single most important constituent of particles recovered at both stations. It reached annual means of 50–70% of the total flux. Investigation by SEM showed that coccolithophorids, foraminifers, pteropods and cysts of dinoflagellates (in decreasing order of significance) were the principle source of $CaCO_3$.

Biogenic opal is derived from diatoms, radiolaria and silicoflagellates (in decreasing order of importance) and contributed 14% (ECC-T) and 9% (NEC-T) to the material intercepted by the upper traps and 17% to the material of the lower traps. Variation in composition between cups was more pronounced in the ECC material than in the NEC samples, but clear correlations among concentration changes of parameters were missing.

The recorded dominance of $CaCO_3$ versus opal fits into the picture of global oceanic particle flux composition. In general, arctic regions have sinking particles composed of less than 5% $CaCO_3$ but 80–90% opal (this volume, Chapter 7). Towards the tropics $CaCO_3$ increases to more than 50% of the sinking material and opal decreases to less than 20% (e.g., Wefer et al., 1982; Honjo et al., 1982; Noriki and Tsunogai, 1986; Ittekkot et al., 1991; this volume, Chapters 7, 14, 15). Flux rates (4.5–7 mg m^{-2} d^{-1}) and composition (ca. 70% $CaCO_3$, 9% opal, 8%

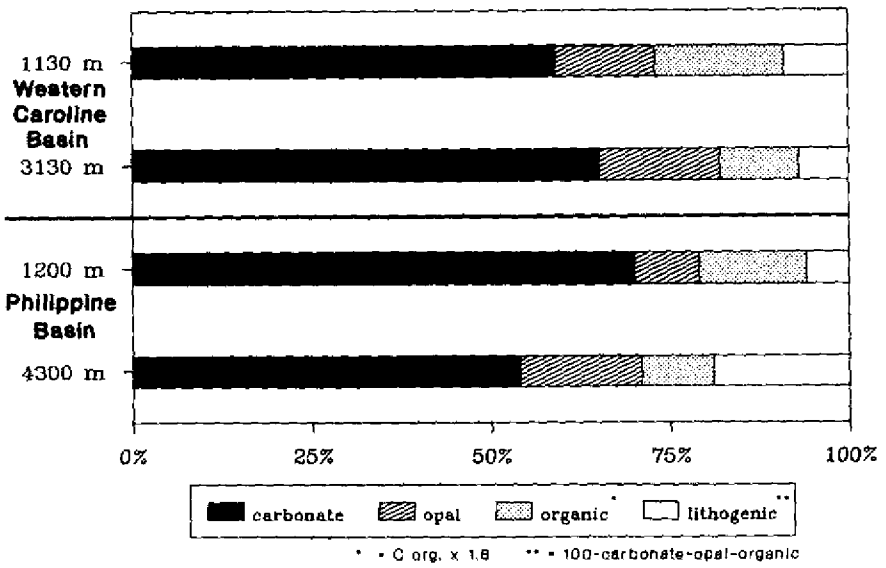

Figure 17.4 Comparison of average percentage composition of top and bottom traps from station ECC (upper two bars) and NEC (lower two bars).

C_{org}) of the NEC-T trap material were almost identical to measurements reported by Honjo (1980) from a position 15°N, 151°W. Even though this position is 7000 km away from our NEC-position, both traps sampled the North Equatorial Current and therefore have similar conditions of primary productivity and for the formation of sinking particles.

The contribution of organic carbon to the total flux varied from 4% to 18% (organic matter 7% to 33%) but was below 10% for most of the samples. At both stations the lower traps collected significantly less (ca. 3%) organic carbon than the upper traps (Figure 17.4). This is in accordance with progressive bacterial respiration of fresh organic matter settling slowly to the seafloor. The C/N (weight) ratio amounted to 8.9 in the NEC and to 9.0 in the ECC; i.e., the organic material at both stations is probably of similar composition. C/N/P ratios did not show considerable difference between the upper and the lower traps. This indicates that most of the easily remineralized phosphate-bearing organic compounds had been consumed before the settling particles reach the upper traps at a depth of 1000 m. Further degradation of organic matter during settling towards the deep traps must therefore have resulted in rather constant releases of C, N and P to maintain the observed constancy in the C/N/P ratios.

Both opal and phosphorus bearing organic matter proved to be highly soluble in the cup waters. 20–35% of the total opal was found to have dissolved and 50% to 70% of the phosphorus. These measurements illustrate that total fluxes are

minimal values at best if only the particulate matter present in the cups is analyzed. Even if the dissolved phase is analyzed in addition, flux values are likely to be significantly lower compared to the composition of the material which originally sank into the cup. Partial exchange of the cup waters with ambient seawater during the collection period might extract an appreciable amount of opal and phosphorus.

17.4 ACKNOWLEDGMENTS

The project was funded by two grants from the Federal German Ministry for Education, Science, Research and Technology (BMBF, Bonn).

17.5 REFERENCES

Deuser, W. G., E. H. Ross and R. F. Anderson (1981) "Seasonality in the supply of sediment to the deep Sargasso Sea and implications for the rapid transfer of matter to the deep ocean", *Deep-Sea Res.*, **28**, 495–505.

Honjo, S. (1980) "Material fluxes and modes of sedimentation in the mesopelagic and bathypelagic zones", *J. Mar. Res.*, **38**, 53–97.

Honjo, S. and K. W. Doherty (1988) "Large aperture time-series oceanic sediment traps: design objectives, construction and application", *Deep-Sea Res.*, **35**, 133–149.

Honjo, S., S. J. Manganini and J. J. Cole (1982) "Sedimentation of biogenic matter in the deep ocean", *Deep-Sea Res.*, **29**, 609–625.

Ittekkot, V., R. R. Nair, S. Honjo, V. Ramaswamy, M. Bartsch, S. Manganini and B. N. Desai (1991) "Enhanced particle fluxes in Bay of Bengal induced by injection of fresh water", *Nature*, **351**, 385–387.

Izdar, E., T. Konuk, V. Ittekkot, S. Kempe and E. T. Degens (1987) "Particle flux in the Black Sea: Nature of the organic matter", in E. T. Degens, E. Izdar and S. Honjo (eds) *Particle Flux in the Ocean*, Mitt. Geol.-Paläont. Inst. Univ. Hamburg No. 62, 1–18.

Kendall, T. R. (1970) *The Pacific Equatorial Counter Current*, International Center for Environmental Research, Nova University Press, Laguna Beach, California.

King, J. E. (1954) "Variations in zooplankton abundance in the central Equatorial Pacific 1950–1952", in *Symposium on Marine and Fresh Water Plankton in the Indo-Pacific*, Bangkok 1954, FAO, UNESCO, 10–17.

Mortlock, R. A. and P. N. Froelich (1989) "A simple method for the rapid determination of biogenic opal in pelagic marine sediments", *Deep-Sea Res.*, **36**, 1415–1426.

Noriki, S. and S. Tsunogai (1986) "Particulate fluxes and major components of settling particles from sediment trap experiments in the Pacific Ocean", *Deep-Sea Res.*, **33**, 903–912.

Schott, G. (1939) "Die äquatorialen Strömungen des westlichen Stillen Ozeans", *Ann. Hydrogr. mar. Met.*, **67**, 247–257.

Wefer, G., E. Suess, W. Balzer, G. Liebezeit, P. J. Müller, C. A. Ungerer and W. Zenk (1982) "Fluxes of biogenic components from sediment trap deployment in circumpolar waters of the Drake Passage", *Nature*, **299**, 145–147.

18 Vertical Particle Flux in Lake Baikal

STEPHAN KEMPE AND MARTINA SCHAUMBURG

18.1 INTRODUCTION

Since the invention of the time-series sediment trap twenty years ago, much has been learned about the vertical particle flux in the oceans (this volume, Chapter 7). One of the major results is that the particle flux is accomplished mainly by large flocs (e.g., "marine snow", Honjo, 1980; Shanks and Trent, 1979; Alldredge and Silver, 1988; Urrere and Knauer, 1981), with sinking speeds of about 100 m d^{-1} (Asper, 1987). Therefore seasonal changes in the particle flux and its chemical composition are transmitted to the sea bed, providing "seasons" to abyssal life.

Little, if nothing, is, however, known about the vertical particle flux in deep fresh water bodies. Not many fresh water bodies exist, which have depths comparable to marine conditions. Only three lakes are deeper than 1000 m: Lake Baikal (1710 m), Lake Tanganyika (1450 m) and the Caspian Sea (1025 m). Of these only Lake Baikal and Tanganyika contain fresh water. In the recent geological past, at least one other, ca. 2000 m deep fresh water body existed: the Black Sea. During Glacial low-sea-level-times it became a fresh water lake with a volume equal to all modern fresh water bodies (53×10^4 km^3 versus ca. 51×10^4 km^3). The study of the vertical particle flux in fresh water lakes has therefore implications for our understanding of lake sediments in the geological past as well as for the genesis of modern lacustrine sediments.

Several principal differences exist between Lake Baikal and Lake Tanganyika: The latter is stratified, lacking oxygen in bottom waters and it has a temperature of ca. 28°C. Lake Baikal is oxygenated and has a temperature close to 3°C at depth. Lake Baikal therefore offers the only opportunity to investigate a deep oxygenated fresh water body and its biogeochemical fluxes.

In contrast to the long tradition of biological research, which was initiated by the exiled Polish scientist B. J. Dybowskii (1835–1930), detailed hydrological and biogeochemical investigations of the deep Lake Baikal have begun only recently. International cooperation with joint expeditions employing modern scientific gear suitable for deep water research, were conducted only after Lake Baikal scientists were allowed to handle their own scientific affairs under "glasnost". A milestone

Particle Flux in the Ocean
Edited by V. Ittekkot, P. Schäfer, S. Honjo and P. J. Depetris

was the SCOPE/UNEP conference on Interactions of Biogeochemical Cycles in Aqueous Ecosystems at the Institute of Limnology at Lysvianka/Baikal, in 1988 (Degens et al., 1992). The contacts established during the meeting led to two joint expeditions with the participation of the Institute of Biogeochemistry and Marine Chemistry of the Hamburg University in 1989 and 1990 during which a sediment trap mooring was deployed and recovered from Lake Baikal (Wong et al., 1991).

18.2 LAKE BAIKAL

Lake Baikal (Figure 18.1, Table 18.1) occupies an elongated, NNE-SSW striking trough, caused by tectonic rifting at the border of the Siberian craton and several microplates of south-central Asia (Zonenshain and Savostin, 1981). The trough is divided into three separate basins, each representing a tectonically separate halfgraben structure. The southernmost basin (7828 km^2) is 1414 m deep. It is separated from the central basin by the sublacustrine section of the Selenga Delta where the depth decreases to less than 400 m. The central basin (9634 km^2) is the deepest. It is interesting to note that its depth has not been finally determined: National Geographic (1981), cites 1620 m; Weiss et al. (1991) and Scholz et al. (1993) quote 1632 m; Wong et al. (1991) give 1637 m; and Edington et al. (1991) suggest 1710 m for the depth of the central basin. The northern basin (13500 km^2) is the shallowest with 989 m depth and is separated from the central basin by the Academician Ridge (Figure 18.1a). All basins are asymmetric in structure: the eastern walls have gradients of 6–15° while the western slopes can be as steep as 45° (Figure 18.1b). They represent the faults along which the basin floor is downfaulted. The largest island is Ol'khon, which is 72 km long and 14 km wide and borders the central basin to the west.

Geological development of the basin started in the Eocene/Lower Oligocene. Shallow depressions developed in the area of the southern basin, accumulating up to 1500 m of fine-grained, fossiliferous sediments (Nikolaev et al., 1985). In the Lower Miocene the first deep water lake developed and the rising Khamar-Dapan

Table 18.1 Lake Baikal, morphometric data (Wong et al., 1991).

Lake surface above sealevel	456.6	m
N-S length of lake	636.0	km
Maximal width	79.4	km
Minimal width	25.0	km
Area of lake surface	31500	km^2
Maximal depth	1620–1710	m
Water volume	23000	km^3
Shore line length	1760	km

Range south of the lake delivered coarse sediments to the southern basin (Belova et al., 1983). In the north, fine-grained sediments with peat and lignite formed a sediment suite, 4000 m thick (Logatchev and Zorin, 1987). In the Upper Pliocene

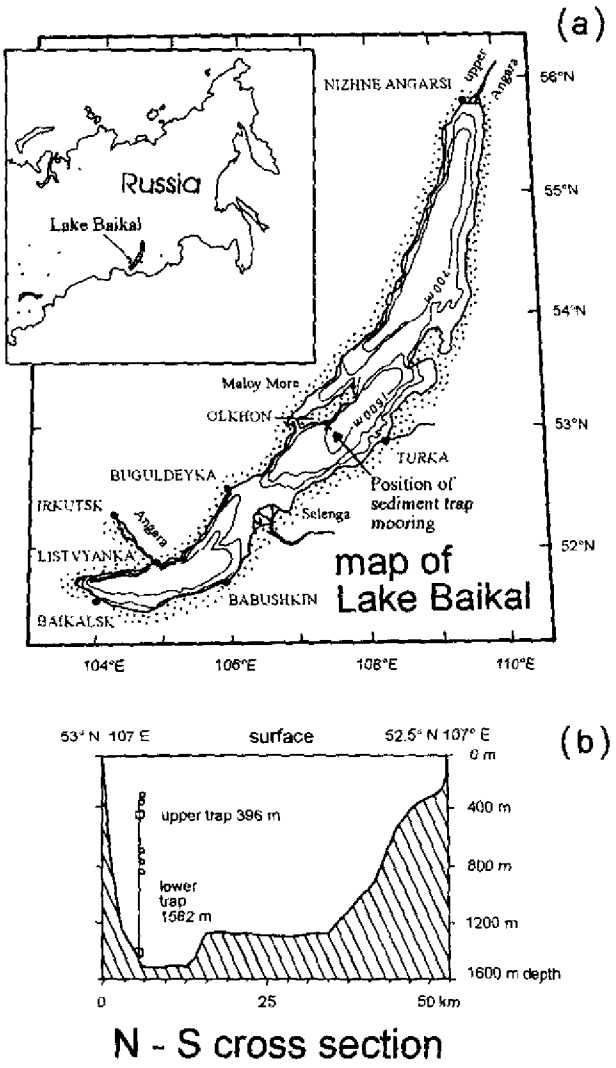

Figure 18.1 (a) Map of Lake Baikal and the position of the sediment trap mooring in the central basin east of the Island of Ol'khon and (b) N-S cross-section across the central basin slightly east of sediment trap position. Note that the sediment trap mooring is projected into the profile and that the lower trap was moored in reality at a lower position than suggested in the graph.

the modern development of the lake basin started, which led to higher relief gradients and to the development of the present deep water basins. Increased erosion led to the deposition of lacustrine conglomerates and gravel with an overall average sedimentation rate of 0.3 mm y^{-1}. Even though this rate is a factor of magnitude larger than during the first phase of basin development (0.03 mm y^{-1}; Artyushkov et al., 1990), downfaulting proceeded faster than the accumulation of sediments resulting in the formation of the deep basins of Lake Baikal.

Lake Baikal is fed by ca. 300 rivers, very diverse in size, discharge and physiography of their catchment areas. Total input to the lake amounts to 60 km^3 y^{-1}. Most rivers are low in mineralization (between 25 and 250 mg total dissolved solids (TDS) per liter), and have a HCO_3-SiO_2-Ca or HCO_3-Ca-SiO_2 character (Votintsev, 1985). The Selenga is the largest tributary to the lake, accounting for 50% of its input and having a TDS of 100–200 mg l^{-1}. It drains the mountainous steppe landscapes of Northern Mongolia and the forest-steppe and taiga areas of Western Transbaikalika. The Upper Angara (15% of discharge tributary to the lake and 50–100 mg TDS l^{-1}) and the Barguzin rivers (9% of water input, 139 mg TDS l^{-1}) are next in size.

The composition of Lake Baikal with regard to major ions is - within the error margins of such mass balance calculations - apparently well explained by the added average input from tributaries and direct precipitation (total 9 km^3 y^{-1}) (Table 18.2). This data set suggests the conservative behavior of all major elements in their passage through Lake Baikal. We will later see that this cannot be entirely true for Ca and HCO_3.

The waters of Lake Baikal are oligotrophic (Table 18.3). In surface waters the highest concentrations of NO_3 and PO_4 are reached in winter (ca. 6 and 0.32–0.48 µmol l^{-1}, respectively) and lowest in summer (2.1–3.6 and 0.06–0.16, µmol l^{-1}, respectively). For silica, two maxima occur, one in winter and one in summer. Water column sampling showed that nutrient concentrations increased significantly downward with oxygen decreasing at the same time (Table 18.3).

Exact concentrations of nutrients depend largely on methods employed. Therefore detailed measurements of depth profiles conducted by Liebezeit (1992) and Weiss et al. (1991) report somewhat different concentrations for nitrate,

Table 18.2 Lake Baikal and tributaries, major ion composition in mg l^{-1} (after Votintsev, 1985).

	HCO_3	SO_4	Cl	Ca	Mg	Na+K	TDS
Baikal tributaries	79.3	6.7	0.7	20.0	4.3	5.1	116.1
Precipitation	5.8	0.9	0.3	1.0	0.1	0.1	9.1
Average input	66.2	5.6	0.7	16.7	3.6	4.2	97.0
Lake Baikal	66.6	5.2	0.6	15.2	3.1	3.8	96.4
Lake Baikal*			0.44	16.1	3.06	3.6+0.94	

* for comparison, Falkner et al., 1991

Table 18.3 Differences in oxygen and nutrient concentrations observed in Lake Baikal between the surface and ca. 1500 m depth.

Parameter	Surface water	Deep water
pH	7.3 – 8.7	7.0 – 7.1
C_{org} mg l^{-1}	1.5 – 1.6	up to 1.0
Si µmol l^{-1}	38	up to 90
NO_3 µmol l^{-1}	2.9 – 4.3	5.7 – 6.4
PO_4 µmol l^{-1}	0.2 – 0.3	0.38 – 0.48
O_2 saturation %	ca. 100	75 – 80

phosphate, and silica compared to the values in Table 18.4. Weiss et al. showed that NO_3 increased to 9 µmol l^{-1}, PO_4 to 0.6 µmol l^{-1} and SiO_2 to 70 µmol l^{-1} at 1500 m depth in the central basin. Below, values decrease somewhat. Liebezeit (1992) also found increases in reactive PO_4 to 0.6 µmol l^{-1} at 1500 m but for SiO_2 only increases of up to 50 µmol l^{-1}. Liebezeit (1992) also published ammonia values which varied between 0.3 and 0.7 µmol l^{-1} without a distinct depth-dependent trend.

Oxygen decreases with depth, caused by the remineralization of the sinking organic matter. Weiss et al. found a decrease down to 300 µmol l^{-1} and Liebezeit down to 325 µmol l^{-1} at 1500 m. The maximum occurs near the surface with about 390 µmol l^{-1}. In Table 18.3 the differences in oxygen and nutrients are listed in order to estimate later the amount of sinking particulate carbon consumed and to compare it with the carbon fluxes intercepted with the sediment trap.

The fact that oxygen does decrease significantly with depth but is not exhausted suggests that the deeper water column is not mixed completely annually, rather, complete mixing seems to take several years.

This question was addressed by the study of Weiss et al. (1992) who sampled the water column of Lake Baikal for CFC-12. Results showed that the mixing time

Table 18.4 Annual average composition of surface and deep waters of Lake Baikal (after Votintsev, 1985).

Parameter	Votintsev	Liebezeit	Weiss et al.
Oxygen µmol l^{-1}	-	- 65	- 90
NO_3 µmol l^{-1}	ca. + 3	-	ca. + 3
PO_4 µmol l^{-1}	ca. + 0.2	+ 0.5	+ 0.3
SiO_2 µmol l^{-1}	ca. + 50	ca + 20	ca. + 45
N/P	15	-	10
O/P	-	130	300

increased from ca. 1 year in the well mixed surface layer (down to 250 m) to 16 years in the layer between 1200 and 1400 m. Below that depth, mixing time decreased to 9–8 years.

The mechanism which governs deep water mixing in Lake Baikal is - because of its enormous depth - singular among fresh water lakes. In temperate, shallow fresh water lakes mixing occurs normally twice annually, once in early winter and once in spring, when the surface water temperature reaches 4°C, the temperature of highest density ($T_{\rho max}$) of fresh water. Then the surface layer becomes more dense than the bottom waters and convection starts, mixing the entire lake and filling the deeper basin with water at $T_{\rho max}$. In this respect fresh water lakes differ from oceans, where bottom waters (even though much colder than 4°C) do not attain the temperature of highest density, which is - because of the higher salt content of seawater - at several degrees below 0°C.

The problem of mixing deep fresh water lakes arises from the fact that $T_{\rho max}$ decreases with increasing pressure with ca. -0.021 °C bar^{-1} (Eklund, 1965; Chen and Millero, 1986). Therefore, water cooled to 4°C at the surface, cannot convect down because it is less dense at depth than the colder water already filling the hypolimnion. Weiss et al. (1991) suggest that mixing of deep fresh water lakes is occurring only if deep wind mixing of surface waters colder than 4°C (and colder than the already existing bottom waters) occurs (see scheme in Figure 18.2). Only then is the lower part of the mixed surface layer dense enough to start deep convection. Such a convection would be initiated locally and episodically, therefore limiting deep convection to certain periods of the year when both fast cooling occurs and strong winds mix the surface layer deeply. This mechanism explains why the bottom temperatures of deep fresh water lakes are significantly lower than 4°C. In fact, the potential temperature of Lake Baikal decreases to almost 3.1°C at the bottom of the central basin. Certainly deep mixing in Lake Baikal cannot occur during times of ice cover. Temperature profiles recorded by Weiss et al. (1991) show that temperature follows the $T_{\rho max}$ line down to about 250 m; i.e., down to that depth mixing occurs when the surface layer has temperatures lower than 4°C but higher than bottom temperatures. Below 250 m mixing is only episodically, apparently restricted to times of strong external forcing and when temperatures in the surface layer are cooled to below 3.5°C. Newly forming bottom waters originate therefore at a depth of at least 200 m and not necessarily at the air-water interface. Water mixed down may therefore not be fully equilibrated with atmospheric gases.

Deep convection in lakes is an essential process needed to replenish nutrients to the surface waters. Considering that the volume of Lake Baikal is 23000 km^3 and that the annual water input is 60 km^3 (neglecting the balance between precipitation and evaporation), then water has an average residence time of close to 400 years in Lake Baikal. Considering the decadal time scale of vertical mixing, it is

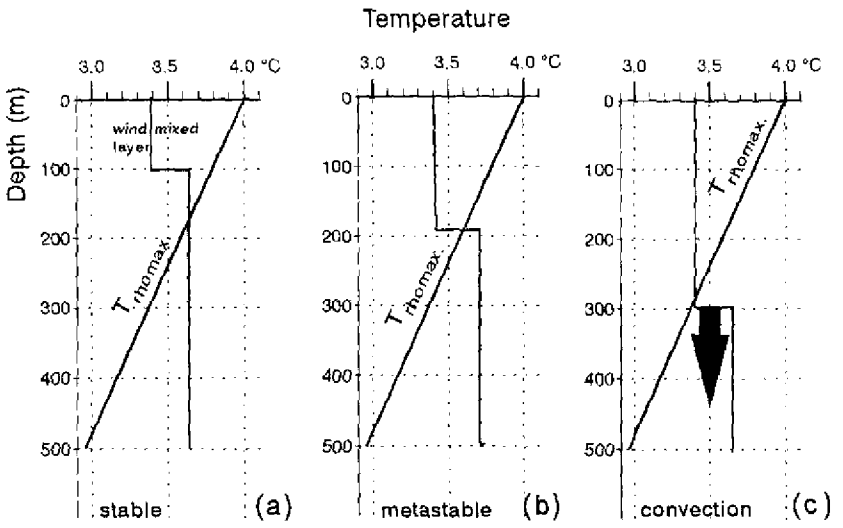

Figure 18.2 Relationship between vertical temperature structure and $T_{\rho max}$ (T_{rhomax}, temperature of highest density). Mixing in deep fresh water lakes can only proceed when wind mixing of surface water - cooled to below 4°C - to a depth where $T_{\rho max}$ is surpassed occurs. (a) stable stratification with less dense, colder water topping warmer bottom water; (b) metastable situation where the interface of the cold wind-mixed layer intersects the $T_{\rho max}$ curve; (c) unstable situation where the lower part of the colder wind-mixed surface layer is depressed below the $T_{\rho max}$ curve, starting convection towards the depth. Exchange of water originates at a depth of several hundred meters and not necessary at the air-water interface. Therefore water mixed down may not be fully equilibrated with atmospheric gases (after Weiss et al., 1991).

apparent that water and therefore also nutrients are recycled several times between bottom and surface waters before leaving the lake.

This conclusion is of course very general, because the individual river input exchange times differ due to their varying distances from the Angara River, the "output" of Lake Baikal. Selenga water, for example, has a good chance of leaving the lake within a year because of its proximity to the Angara and of the general pattern of surface circulation (Figure 18.3). In the lake N-S transport occurs along the western shore and S-N transport along the eastern shore. Five major gyres turning anticlockwise accomplish water transport across the lake basin. Water entering with the Upper Angara should therefore take a much longer time to reach the Baikal outlet than that of the Selenga and has a better chance of being incorporated into the deep bottom waters than Selenga water.

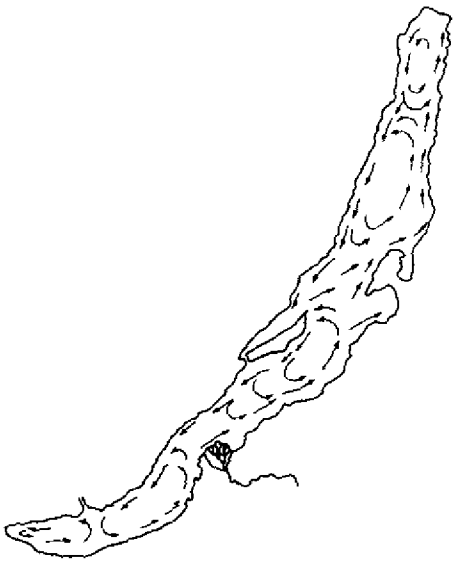

Figure 18.3 Surface currents of Lake Baikal (after Kozhov, 1963).

18.3 MATERIALS AND METHODS

18.3.1 SEDIMENT TRAP MOORING

The double sediment trap mooring was deployed in the central basin of Lake Baikal at 53°00.0 N, 107°35.5 E at a water depth of 1610 m (Table 18.5); i.e., close to the deepest point of the lake. The upper trap was at a depth of 396 m (i.e., already deeper than most fresh water lakes world-wide), and the lower trap at a depth of 1582 m; i.e., 28 m above the lake bottom. The two traps were programmed to sample at the same time. The sampling cups were filled with a NaCl solution of 200 mS cm^{-1} conductivity and preserved with saturated $HgCl_2$ solution.

The trap was programmed to close on September 1, 1990 but the mooring had to be recovered on August 4, 1990 because of a change in expedition timing. Therefore cup 13 was open upon recovery and cannot be evaluated. The rotation dates are given in Table 18.6.

18.3.2 ANALYTICAL METHODS

After recovery of the traps, the pH and the conductivity of the cupwaters were measured. The cups of the upper trap had a strong putrefactive smell and the very low conductivities of cupwaters showed that almost all of the preservative had

Table 18.5 Sediment trap mooring, technical data.

Position	53°00.0 N / 107°35.5 E	
Water depth	1610 m	
Length of mooring	ca. 1230 m	
Buoyancy spheres	20	
Release	acoustic Benthos release 895	
Anchor	1000 kg	
Deployed	09/07/89	
Recovered	08/04/90	
Trap designation	Lake Baikal LB-T	Lake Baikal LB-B
Trap depth	396 m	1,582 m
Trap opening	0.509 m^2	0.509 m^2
Trap type	Honjo Mark VI	Honjo Mark VI
Number of cups	13	13
Collection time	09/10/89–08/04/90	09/10/89–08/04/90
Sampling intervals	13: 28 or 27 days	13: 28 or 27 days
Preservation	NaCl - $HgCl_2$	NaCl - $HgCl_2$
Problems	cup 13 open	cup 13 open

Table 18.6 Rotation dates of LB-T and LB-B (cups closed at midnight).

Cup No.	Opened	Closed	Days	Interval
1	09/10/1989	10/07/1989	28	September/October
2	10/08/1989	11/03/1989	27	October/November
3	11/04/1989	12/01/1989	28	November/December
4	12/02/1989	12/29/1989	28	December
5	12/30/1989	01/26/1990	28	December/January
6	01/27/1990	02/22/1990	27	January/February
7	02/23/1990	03/21/1990	27	February/March
8	03/22/1990	04/17/1990	27	March/April
9	04/18/1990	05/14/1990	27	April/May
10	05/15/1990	06/10/1990	27	May/June
11	06/11/1990	07/07/1990	27	June/July
12	07/08/1990	08/03/1990	27	July/August
13	08/04/1990	-	-	

disappeared from the cups. The cups were then sealed and taken to the laboratory at Hamburg. There cupwaters were decanted and the still wet samples were sieved through a 1 mm sieve. The fraction of > 1 mm contained only macroorganisms and was therefore not included in the chemical flux determinations. Due to the

presence of decaying organics, it was impossible to filter the samples with the < 1 mm fraction through the nucleopore filters. Therefore the samples where desalted with bidistilled water and freeze-dried in small portions. Most of the particulate sample was ground in an agate mortar but a small aliquot was kept for SEM investigation.

On the dissolved fraction the following investigations were conducted:

- pH and conductivity, aboard the research vessel (using battery powered hand-held instruments, pH 91 meter, LF 91 meter, both by WTW);
- dissolved silica (photometry at 880 nm, Koroleff, 1983a);
- dissolved reactive phosphate (photometry at 880 nm, Koroleff, 1983b);
- dissolved nitrite (photometry at 545 nm, Grasshoff, 1983);
- dissolved ammonia (photometry at 630 nm, Koroleff, 1983c).

The particulate fraction was analyzed for the following parameters:

- total weight;
- total carbon and nitrogen (using Carlo Erba NA 1500 Nitrogen Analyzer);
- organic carbon (same as total carbon, carbonate removed by 2 N H_3PO_4; to obtain total organic matter, C_{org} values were multiplied by the factor 1.8 in accordance with Ittekkot et al. (1991), and Müller et al. (1986));
- carbonate (as difference between C_{tot} and C_{org});
- biogenic opal (after Mortlock and Froelich (1989); samples were decarbonated and organic carbon was removed with 2% H_2O_2, opal was dissolved by boiling for 5 h in 5% Na_2CO_3 solution and the resulting solution was then photometrically determined as in the cupwaters; according to Mortlock and Froelich (1989) biogenic opal is assumed to have a water content of 10%, opal (SiO_2 x 0.4 H_2O) weight was therefore determined from Si concentrations by multiplying with a factor of 2.4);
- total phosphorus (after Williams et al. (1976); samples were incinerated at 550°C and dissolved in 1 N HCl, and the solution was then photometrically determined as in the cupwaters);
- lithogenic fraction (because of the low sample amounts available, the lithogenic fraction could only be determined by difference between the biogenic components and total weight; because all analytical mistakes add in this determination and because of the factors used to calculate total organic carbon and silica the sum may not represent the conditions of the material in the samples accurately, since the values for lithogenic fraction are relatively inaccurate; evidence for this is the resulting negative values in the upper trap which is very low in lithogenics);
- SEM and EDAX (aliquots of the unground samples were glued to aluminum studs and sputtered with gold and then investigated by scanning electron microscopy and energy dispersive analysis with X-rays).

The results of all determinations are listed in the appendix. Results are more fully discussed by Schaumburg (1994).

18.4 DISCUSSION OF RESULTS

18.4.1 DISSOLVED FRACTION AND REMINERALIZATION

When the cups were taken off the rotor after recovery of the traps, a strong smell was noticed, putrefactive in the cups of the upper trap and fishy in the cups of the lower trap. The measurement of the conductivity (Tables 18.A1 and 18.A2 of the appendix) showed that in fact most of the salt solution had been lost from the cups. Ambient lake water has a conductivity of 130 to 137 $\mu S\ cm^{-1}$ while the salt solution had originally a conductivity of 200 $mS\ cm^{-1}$. We can therefore calculate that between 94.7% and 99.9% and between 98.9% and 100% of the original solution had been lost from the cups in the upper and lower traps, respectively. This loss was more thorough and regular in the lower trap than in the upper trap where losses in winter were smaller than during the warm season. Remains of small fish (upper trap) and crustaceans (lower trap) recovered in the > 1 mm fraction shows that apparently these swimmers entered the cups and displaced most of the original solution. A few of these intruders were caught in the cups when the rotor moved on to the next position and were killed. The problem of swimmers entering cups is common with sediment trap research (Gardner et al., 1983; this volume, Chapters 5 and 7) but so far we never encountered such a massive cupwater loss in any of the traps deployed in oceanic environments. It remains unclear if the swimmers could carry any of the collected particulate material out of the cup or even out of the trap cone. The strong chemical gradient across the cup opening should have in fact prevented fresh water biota from entering highly concentrated salt solutions. Nevertheless a loss of particulates may have occurred and all values should be considered to represent minimum flux values.

Due to the overall low concentrations of carbonates in the sinking material and in the water of Lake Baikal, the pH is not well buffered against changes when additional CO_2 is generated by bacterial remineralization. pH measurements in the cupwaters therefore tell something about the lability of the trapped material, even more so since the preservative apparently had been diluted in the cups to the point to became ineffective. In the upper trap, pH values of between 5.85 and 7.3 (which is representative of ambient lake water at the depth of the upper trap) were measured and a linear trend was evident, illustrating the progress of remineralization with passing time. In the lower trap values were higher (between 6.9 and 8.0), suggesting that the organic material caught above the floor of Lake Baikal is more inert and is not rapidly degraded by microorganisms.

The analysis of dissolved nutrients recovered small amounts of silica and nitrite and large amounts of reactive phosphate and of ammonia (Tables 18.A1 and 18.A2, appendix).

The concentration of silica in the cup waters was, on average, three times higher in the bottom than in the top trap. However, the recovered amounts (up to 2.5 μmol l^{-1} at most) were much lower than in the ambient water (see Table 18.3). Because the cup solution was exchanged almost completely with ambient lake water, much higher silica concentrations should have been present. Consequently, opal was precipitated in the cups due to their acidic condition. The lower concentrations in the top trap were therefore in accordance with the lower pH values encountered in the cups of the top trap in comparison to the cups of the bottom trap. The conclusion that opal was precipitated in cupwaters is also substantiated by the missing time trend in the data. Precipitation would occur fast and would not show a similar time dependency as for example observed in bacterial remineralization.

In contrast to silica, the phosphorus concentration of the cupwaters (in the upper trap 50–150 μmol l^{-1} and in the lower trap 1.2 to 10 μmol l^{-1}) exceeded by far those in the ambient lake water. Phosphorus must have been released from the collected organic matter. The upper trap has much higher values than the lower trap, again (as in case of pH) a clear indication that the upper trap intercepted much more labile matter than the lower trap. When one compares the P amounts remineralized with the total intercepted P (particulate plus dissolved), one finds remineralization proportions of between 1.2% and 17% (upper trap) and between << 1% and 6% (lower trap). Concentrations and remineralization rates are plotted in Figure 18.4 (for values see Tables 18.A3 and 18.A4 in the appendix). Apparently in both traps lowest remineralization values occurred in winter. In the top trap the most labile material apparently arrived in November, May and July, while in the lower trap the May peak arrived one cup later and the July peak seemed to be mirrored by a peak in cup 1. It is also interesting to note that no trend with time was apparent. This suggests that remineralization of phosphorus is fast, degrading the available, easily remineralizable phosphorus-bearing compounds and then stopping. The overall remineralization ratio (calculated from the total flux; i.e., weighted for time and concentrations) amounted to 3.9% and 1.0% suggesting that phosphorus in the lower trap is present mostly as inorganic forms (Table 18.7). The total measured phosphorus fluxes during the observation period amounted to 420 mg (13.5 mmol) m^{-2} in the upper trap and 118 mg (3.8 mmol) m^{-2} in the lower trap; i.e., it intercepted 3.56 times less P than the upper trap. It has to be noted that some remineralized phosphorus may be locked in dissolved organic compounds. Therefore remineralization ratios and total fluxes may be underestimated.

The cupwaters contained high concentrations of ammonia and nitrite, much higher than their occurrence in ambient waters (Figures 18.5a, b). In all cups more ammonia than nitrite was found, but the ratio of nitrite to ammonia and the overall nitrite concentration was significantly higher in the lower trap (0.1–14 μmol l^{-1}) than in the top trap (0.04–0.9 μmol l^{-1}), indicating that the cupwaters of the lower trap were less reducing than in the top trap. In fact, ammonia concentrations in the upper trap reached values of between 0.5 and 11 mmol l^{-1}, while in

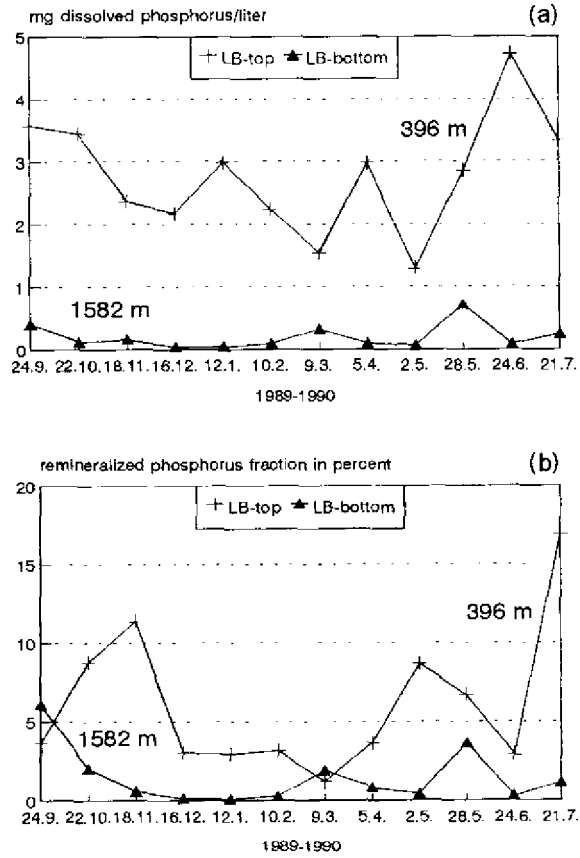

Figure 18.4 (a) Comparison of the concentrations of dissolved phosphorus in the cupwaters of both traps and (b) of the fraction of phosphorus remineralized from the total flux.

the lower trap concentrations range only between 3 and 800 μmol l^{-1}. Because of the high ammonia concentration, nitrate, which was not measured, could not occur in significant concentrations. Even nitrite hardly playes a significant role in the nitrogen budget. In Tables 18.A3 and 18.A4, appendix, the dissolved fraction is added to the particulate nitrogen (Figure 18.6a) and the remineralization fraction was calculated (Figure 18.6b). It ranged between 8 and 85% in the upper trap and between < 1 and 7% in the lower trap. Remineralization was one order of magnitude higher in the top trap than in the bottom trap (averages 43.3 and 3.8%, respectively) (Table 18.7). Nevertheless, it is astonishing how well the relative changes of the remineralization ratio matched between the two traps (Figure

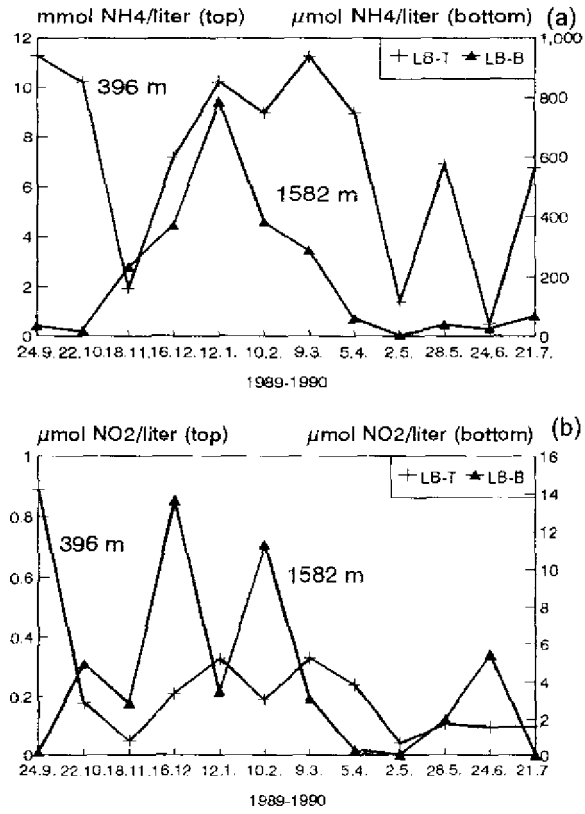

Figure 18.5 (a) Concentrations of ammonia and (b) nitrite in the upper (LB-T) and lower (LB-B) Lake Baikal traps.

18.6b; r=0.56, p=95%), indicating that material of higher lability reached both traps during winter and of lower lability during summer. The differences between total P and N fluxes between the top and bottom traps was similar (factors 3.6 and 3.2, respectively). Therefore remineralization was - averaged over the water column - similar for N and P compounds, slightly more than one third of the material passing the upper trap was intercepted by the lower trap.

When comparing the total phosphorus with the total nitrogen fluxes, an interesting pattern emerged (Table 18.7): In the remineralized fraction nitrogen was clearly present in higher proportions than normally present in organic matter (represented by the so called Redfield C/N/P ratio of 106/16/1). This was true for both traps, but especially for the top trap. The fraction was also much larger than the N/P ratio of the water column (see Table 18.3) which was close to Redfield ratio. In the particulate fraction and overall, however, the ratios were clearly

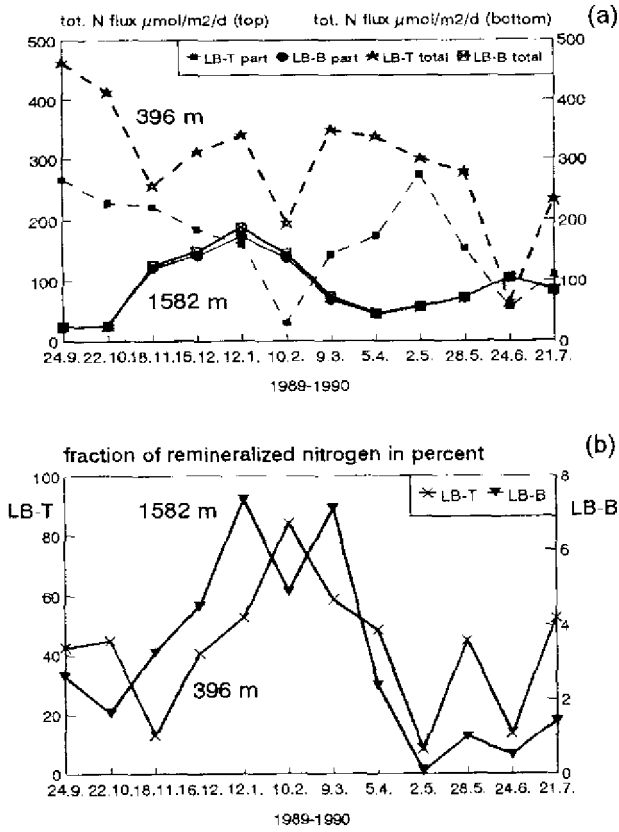

Figure 18.6 (a) Comparison of total nitrogen fluxes in mg m^{-2} d^{-1} (residual particulate phase and dissolved remineralized phase) for both traps (dashed lines = LB-T, solid lines = LB-B), and (b) the fraction of remineralized nitrogen in the upper and lower Lake Baikal trap.

phosphorus dominated (compared to Redfield). Apparently two different sorts of material were involved in contributing to the intercepted material, one with a mineral phosphate component (such as fish bones or sedimentary apatite) and one with a component containing easily remineralizable nitrogen (such as proteins).

18.4.2 PARTICULATE FRACTION

The total vertical flux (preserved in particulate form in the cups) showed strong seasonal changes and a large difference between the top and the bottom trap (Figure 18.7; Tables 18.A5 and 18.A6 in the appendix). Both traps showed distinct flux maxima in winter and summer. In winter fluxes peaked at 55.7 mg m^{-2} d^{-1} (in

Table 18.7 Phosphorus and nitrogen fluxes (per m^2) for the time period 09/10/89–04/08/90 (328 days, cups 1–12), and various elemental ratios.

Traps	LB-T, 396 m		LB-B, 1582 m	
	mmol m^{-2}	mg m^{-2}	mmol m^{-2}	mg m^{-2}
Dissolved inorganic P	0.53	16.4	0.037	1.16
Total particulate P	13.00	403.2	3.765	116.70
Sum of P fluxes	13.53	419.6	3.802	117.86
Remineralization ratio %	3.9		1.0	
Ratio of flux top/bottom	3.56			
Total dissolved N (NH_4+NO_2)	42.0	588	1.15	16.1
Total particulate N	55.0	770	28.94	405.2
Sum of nitrogen fluxes	97.0	1358	30.09	421.3
Remineralization ratio %	43.3		3.8	
Ratio of flux top/bottom	3.22			
N/P ratio dissolved	79/1		31/1	
N/P ratio particulate	4.2/1		7.7/1	
N(sum)/P(sum) ratio	7.2/1		7.9/1	

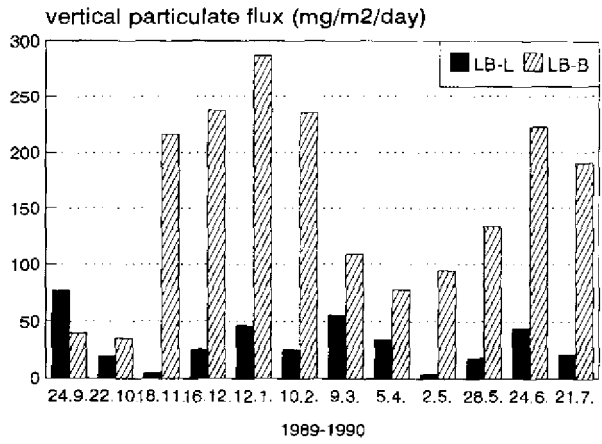

Figure 18.7 Comparison of total fluxes of the intercepted particulate matter in the upper (LB-T) and lower (LB-B) Lake Baikal traps.

February) and at 77.5 mg m^{-2} d^{-1} (in September). In the lower trap the maxima occurred in January (287 mg m^{-2} d^{-1}) and in June (222 mg m^{-2} d^{-1}). During times of low vertical particle flux, the upper trap received 19 times, and the lower trap 8 times, less material than during peak flux. In total the upper trap received 5 times less matter than the lower trap. These results indicate that much of the vertical particle flux was generated along the slopes of the lake at greater depth and that this material should be less labile than the matter generated in the photic zone.

This conclusion is substantiated by comparing the general composition of the two traps (Figures 18.8a, b) which are fundamentally different. When discussing composition, one has to keep in mind that organic matter is calculated by multiplying the difference between the total carbon measurement and the inorganic carbon measurement with a factor of 1.8. Not all the organic matter may be represented by this factor. Therefore, in samples with large C_{org} concentrations, the lithogenic fraction, which is also calculated by difference, may have negative values (see Table 18.A5 in the appendix). These negative values are omitted in Figure 18.7a and are not used in calculating fluxes in Table 18.8. Lithogenic

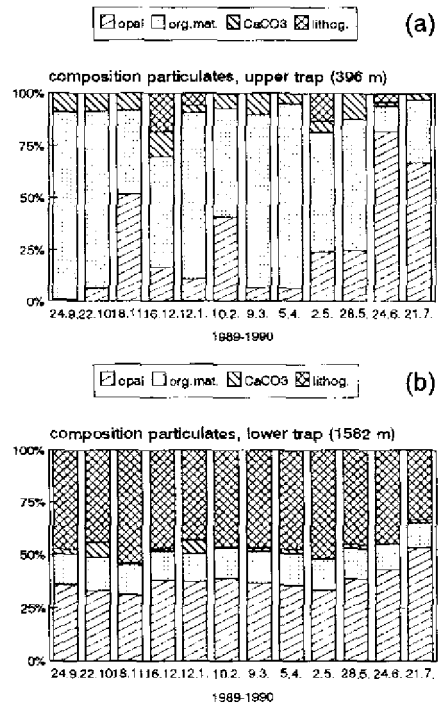

Figure 18.8 Relative composition of the intercepted particulate matter in the (a) upper and (b) lower Lake Baikal traps.

Table 18.8 Totals (calculated for actual trap area) and fluxes (calculated per m^2 and day) of total particulate matter intercepted and of principal components for the time period 09/10/89–08/04/90 (328 days, cups 1–12).

Traps (0.509 m^2)	LB-T, 396 m	LB-B, 1582 m
Total intercepted weight	5.256 g	26.26 g
Average flux	31.48 mg m^{-2} d^{-1}	157.30 mg m^{-2} d^{-1}
Ratio of flux bottom/top	5.0	
Total intercepted opal	1.33 g	10.15 g
Average opal flux	7.96 mg m^{-2} d^{-1}	60.82 mg m^{-2} d^{-1}
Ratio of flux bottom/top	7.6	
Total interc. organic matter	3.90 g	3.57 g
Average organic matter flux	23.35 mg m^{-2} d^{-1}	21.40 mg m^{-2} d^{-1}
Ratio of flux bottom/top	0.9	
Total intercepted $CaCO_3$	0.41 g	0.54 g
Average $CaCO_3$ flux	2.47 mg m^{-2} d^{-1}	3.24 mg m^{-2} d^{-1}
Ratio of flux bottom/top	1.3	
Total interc. lithogenics	0.135 g	12.00 g
Average lithogenics flux	0.8 mg m^{-2} d^{-1}	71.86 mg m^{-2} d^{-1}
Ratio of flux bottom/top	90	

fluxes can therefore be higher than calculated (or lower where present) depending on the factor by which C_{org} concentration is converted to total organic matter.

From Figure 18.8 it is noted that the composition of the material intercepted by the lower trap was rather stable, while that of the upper trap varies with seasons substantially. The upper trap contained hardly any lithogenic material. Its material was dominated by organic matter (maxima in autumn and spring) and by opal (maxima in November, February and June/July). Lithogenics were noticeable only in December and May. In the lower trap lithogenics dominated the composition followed by opal, organic matter and $CaCO_3$ in very stable proportions throughout the year (except for $CaCO_3$ which had a distinct maximum in January). Thus we must conclude that the material of the lower trap had a different source with a very stable composition. Resuspension of slope sediments seems to be the most likely process to account for this observation.

When we compared total intercepted particulate fluxes in the two traps (Table 18.8) it becomes clear that not only lithogenics but also opal must derive from this resuspension source. In fact, if one compares their flux data in Table 18.6A (appendix), it is clear that they co-vary significantly. In contrast, the average fluxes of organic matter and $CaCO_3$ were comparable in size in the top and bottom trap. However, their seasonal patterns (Figure 18.9) were not identical in the two traps.

In the case of organic matter, the winter maximum in the top trap was present in the lower trap in similar magnitude. This seems to indicate that during winter much of the organic matter from the surface reaches the bottom and is instrumental in extracting the resuspended lithogenics and opal. This conclusion is also corroborated by the marked ammonia and nitrite (Figure 18.5) and nitrogen remineralization maxima (Figure 18.6b) in the winter cups of the lower trap. In summer, however, the organic matter flux in the bottom trap exceeded that of the upper trap, and must therefore be associated with resuspended matter.

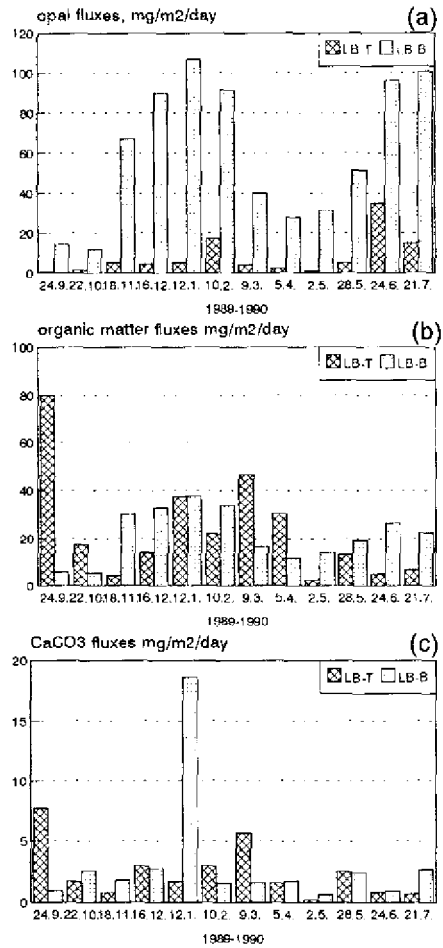

Figure 18.9 Comparison of the fluxes of (a) opal, (b) organic matter, and (c) $CaCO_3$ between the upper trap (LB-T) and lower trap (LB-B) in Lake Baikal.

This material is inert and not as easily remineralized as the organic matter reaching the lake bottom in winter.

18.4.3 ORGANIC MATTER

The total flux of organic matter is, on average (Table 18.7), very similar in the top and bottom traps. However, lability is different. In Table 18.A9 of the appendix, the CO_2-partial pressure (pCO_2) for the cups at recovery was calculated (Kempe, 1975) using the average composition of Lake Baikal water given in Table 18.2 and the measured pH values. In the upper trap, CO_2 pressures reached 70000 ppmv (T1), compared to an atmospheric pressure of 350 ppmv. While in the lower trap values were one order of magnitude lower and reached only 6700 (B9) ppmv. Recalculating the pressures for the amount of dissolved CO_2 (Table 18.A9, appendix), concentrations of up to 4.5 mmol $l^{-1}$and up to 0.4 mmol l^{-1} in the upper and lower trap are found. If one compares the amounts of CO_2 with the carbon flux preserved as particulate matter in the traps (Figure 18.10a; Tables 18.A7, 18.A8 and 18.A9 in the appendix), then it is apparent that in some of the cups with small C_{org} fluxes up to ten percent of the carbon was present as dissolved free CO_2. However, in the cups with large C_{org} fluxes, the free CO_2 amounted to only a few percent. Because of diffusion of CO_2 out of the cup and degassing after recovery a sizable loss of carbon from the samples is possible, the size of which cannot be reconstructed. Because of this insecurity, the organic matter flux has not been corrected for dissolved CO_2. When comparing CO_2 with organic matter flux, it is apparent that - apart from a CO_2 increase with time - the large fluxes in September and January to April caused high free CO_2 values (Figure 18.10a). In the lower trap higher CO_2 values were associated with the high winter fluxes but also with the sample of May which has a relatively low C_{org} flux.

Calculating the Redfield ratio for the cup samples (Figure 18.10b; Tables 18.A8, 18.A9, appendix) it becomes clear that the lower trap had very constant values. Its C/N values were close to the Redfield C/N ratio of 7. The N/P ratio was, however, only half as large as the Redfield ratio (7.6 on average compared to 15 for Redfield), illustrating that the remineralization of nitrogen was twice as effective as that of phosphorus and that lake sediments become a trap for phosphorus in excess of the biogenic N/P ratio. In the upper trap much larger changes of the atomic ratios occurred, including a couple of puzzling C/N values with ratios below 1. It can only be assumed that large amounts of ammonium were adsorbed to the freeze-dried samples, therefore causing an offset of the C/N ratios. Similarly the N/P ratios showed large changes: high relative nitrogen concentrations occurred in October and November and May and low relative nitrogen concentrations in winter. We face the problem that we do not know which samples contained more fish than others. Therefore the upper trap results have to be treated with caution.

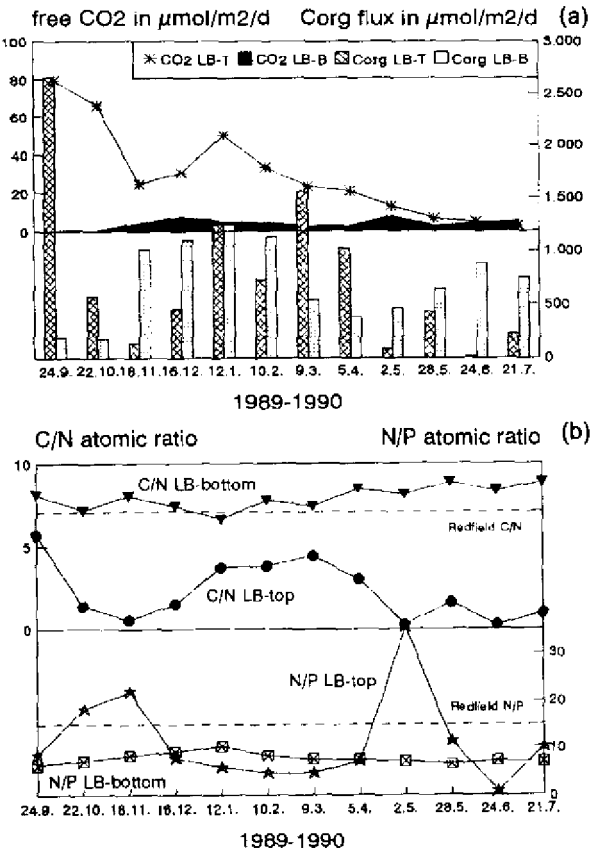

Figure 18.10 (a) Comparison of the free CO_2 with the particulate organic carbon and (b) comparison of the C/N and N/P ratios in both Lake Baikal traps. The C/N and N/P ratio is calculated using the sum of the analyzed dissolved and particulate nitrogen and phosphorus species. For carbon no correction for remineralization loss was made.

18.4.4 SEM INVESTIGATIONS

In addition to the geochemical analyses, the larger particulate samples were inspected visually under a scanning electron microscope (SEM). In the upper trap significant seasonal changes were found. The prominent flux peak in September consisted of unstructured organic matter, while the flux maxima in winter were dominated by *Stephanodiscus* sp. (Figure 18.11a) and that in summer by *Melosira baikalensis* frustrules (Figure 18.11b). In the samples of the bottom trap, frustules of *Stephanodiscus* sp. and *Melosira baikalensis* were found throughout the year, underscoring the conclusion that this material was largely supplied by resuspension.

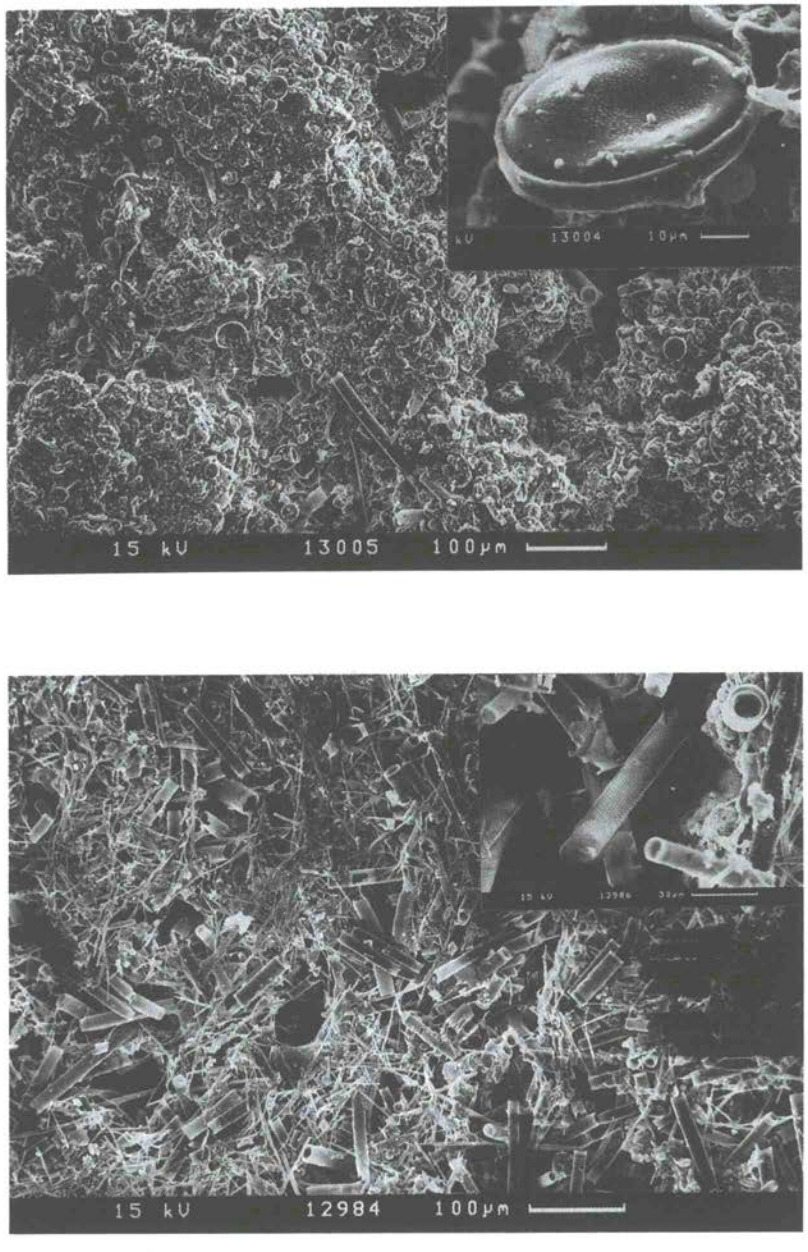

Figure 18.11 Scanning electron microscope pictures of the two principal diatoms contributing to extensive blooms in Lake Baikal: (a) *Stephanodiscus* sp. blooming in November and January/February and (b) *Melosira baikalensis* blooming in June.

18.5 CONCLUSIONS

Vertical particle fluxes in Lake Baikal have two maxima: one in winter and a smaller one in summer. The winter peak came as a surprise: it occurred while the lake is ice-covered. Both maxima occurred in the top and in the bottom trap, but the bottom trap received 5 times as much material. The composition of the intercepted material showed that the vertical particle flux in Lake Baikal had two sources: (i) resuspended sediment rich in lithogenics (45% of total) and opal (38%) and carrying an organic matter component (13%) which was relatively inert; and (ii) biogenic matter produced in the surface layer. This matter was dominated by organic matter (74%) and opal (25%) and was highly labile. Apparently a larger part of this material reached the floor of Lake Baikal during winter, when the organic matter in the lower trap released more nutrients and was apparently more labile, than in summer. SEM investigations showed that the particle flux can be differentiated into six seasons:

1. In autumn, material with a large percentage of organic matter of a very labile nature sinks. It may be associated with a bloom of flagellates.
2. In late autumn and early winter, a moderate particle flux peak is caused by a bloom of the diatom *Stephanodiscus* sp., which produced moderately high opal flux rates in the top trap in November.
3. In mid-winter, diatom contributions diminish and flagellates may become more dominant causing high overall fluxes in December and January.
4. In late winter (February), another *Stephanodiscus* bloom occurs, causing high opal and moderate organic matter fluxes. Apparently *Stephanodiscus* needs more light than other planktonic organisms which cause the mid-winter bloom, and is therefore most active at the beginning and end of the winter.
5. In spring (March-May), the flux is again dominated by organic matter and decreases from the overall flux peak in March to very low fluxes in May. This is the period when the ice cover finally breaks.
6. In summer (June-July), a secondary flux peak occurs, which is derived from a bloom of the diatom *Melosira baikalensis*. The settling particles carry very high opal concentration, and low amounts of organic matter. This bloom is most probably caused by the thermal stratification of Lake Baikal in summer.

The overall settling rate amounted to 11.5 g m^{-2} y^{-1} in the upper trap and to 57 g m^{-2} y^{-1} in the lower trap. The latter values (assuming a density of 2 g cm^{-3}) correspond to a sedimentation rate of roughly 0.03 mm y^{-1}. Assuming a porosity of 60% of the sediment weight (characteristic for the upper decimeters of sediment; see Wong et al., 1991) we find a sedimentation rate of 0.1 mm y^{-1} for the central basin of Lake Baikal. This is less than the geologically assumed rate of 0.3 mm y^{-1} (see above), but is in accordance with mass fluxes calculated from ^{137}Cs and ^{210}Pb measurements (Edington et al., 1991) which vary from 30 g m^{-2} y^{-1} (= 0.16 mm y^{-1}) to 180 g m^{-2} y^{-1} (= 0.74 mm y^{-1}) for basin stations.

Our data show that 7.6 times as much opal is intercepted by the lower trap than by the upper trap. Assuming opal to be a conservative tracer, (i.e., neglecting dissolution), resuspension must concentrate sediments from an area almost 8 times as large as the bottom of the lake because the flux at a depth of 400 m (and assumed to be representative of the new production of diatom frustrules) amounts to only 2.9 g m^{-2} y^{-1} compared to 22 g m^{-2} y^{-1} near the lake bottom. This large opal flux is in accordance with the common occurrence of diatomite layers in Lake Baikal sediments (e.g. Wong et al., 1991).

If the opal argument is accepted, then the organic matter intercepted by the lower trap must also derive from an at least 8 times larger area. As the organic matter fluxes between both traps is almost similar, one must conclude that only 1/8 of the organic matter passing the upper trap can reach the lower trap; i.e., roughly 1 g m^{-2} y^{-1} (or ca. 0.6 gC m^{-2} y^{-1}) - roughly 7 g m^{-2} y^{-1} (or ca. 4 gC m^{-2} y^{-1}) must respired in between. This is only a very tentative conclusion because it rests on the assumption that resuspension of organic matter follows the resuspension of opal at similar rates and that the carbon in the upper trap is representative of the real flux at that depth, neglecting the losses caused by intruding fish and CO_2 degassing and the possible input by trapped swimmers.

In comparison with the TOC concentrations measured in Lake Baikal sediments of between 1.1 and 3.2% (Wong et al., 1991), the sediment of the lower trap contained a higher proportion of organic carbon; i.e., ca. 7%. This suggests that some of the carbon which reaches the lake bottom is in fact still labile and can be respired within the time frame of bioturbation (i.e., within several years to decades). The C/N values of the sediments range from 6 to 7 in the central basin (Wong et al., 1991); i.e., they match the range of C/N ratios of between 6.6 and 8.9 in the lower trap.

It is interesting to note that $CaCO_3$ is present in the settling sediments in spite of the large pCO_2 especially in the top trap. $CaCO_3$ amounts to 7.8% of the flux in the upper trap and to 2% in the lower trap with very similar total flux rates. For comparison, Wong et al. (1991) commonly found $CaCO_3$ concentrations in sediments of between mostly 1–2% (always < 10%). They suggest that this carbonate is clastic in origin. One could argue that this may not be true because carbonate should behave like opal and lithogenic matter; i.e., we should find higher fluxes in the lower trap than in the top trap. Because of the significant carbonate fluxes in the top trap, one could alternatively assume that it is formed in the water column. This could occur at a rate of 0.9 g m^{-2} y^{-1} of which 0.36 g m^{-2} y^{-1} would be calcium. Therefore as much as 11000 t Ca y^{-1} could be extracted in the entire lake. This compares with a total Ca input of (compare concentrations in Table 18.2) 1.15 10^6 t y^{-1}. Thus the present $CaCO_3$ settling rate would extract only roughly 1% of the available Ca and would not be noticed in overall budget calculations. At present, we therefore cannot finally conclude what the source or the sources of the $CaCO_3$ in the Lake Baikal sediments are.

18.6 ACKNOWLEDGMENTS

This investigation was funded by the Federal German Ministry for Education, Science, Research and Technology (BMBF, Bonn, MFG 0081/6). The deployment and recovery operations were supervised by H. K. Wong in cooperation with G. Liebezeit, W. von Haugwitz and others. The cooperation of the captain and crew of the R/V *Vereshagin* is gratefully acknowledged.

18.7 REFERENCES

Alldredge, A. L. and M. W. Silver (1988) "Characteristics, dynamics and significance of marine snow", *Prog. Oceanogr.*, **20**, 41–82.

Artyoshkov, E. V., F. A. Letnikov and V. V. Ruzhich (1990) "The mechanisms of formation of the Baikal Basin", *J. Geodynamics*, **11**, 277–291.

Asper, V. L (1987) "Measuring the flux and sinking speed of marine snow aggregates", *Deep-Sea Res.*, **34**, 1–17.

Belova, N. A., B. F. Lut, L. P. Loginova and G. K. Khusevich (1983) "Sediment formation in Lake Baikal", *Hydrobiologia*, **103**, 281–285.

Chen, C. T. and F. J. Millero (1986) "Precise thermodynamic properties for natural waters, covering only the limnological range", *Limnol. Oceanogr.*, **31**, 657–662.

Degens, E. T., S. Kempe, A. Lein and Y. Sorokin (eds) (1992) *Interactions of Biogeochemical Cycles in Aqueous Systems*, Mitt. Geol.-Paläont. Inst. Univ. Hamburg No. 72, 289 pp.

Edington, D. N., J. V. Klump, J. A. Robbins, Y. S. Kusner, V. D. Pampura and I. V. Sandimirov (1991) "Sedimentation rates, residence times and radionuclide inventories in Lake Baikal from ^{137}Cs and ^{210}Pb in sediment cores", *Nature*, **350**, 601–604.

Eklund, H. (1965) "Stability of lakes near the temperature of maximum density", *Science*, **149**, 632–633.

Falkner, K. K., C. I. Measures, S. E. Herbelin and J. M. Edmond (1991) "The major and minor element geochemistry of Lake Baikal", *Limnol. Oceanogr.*, **36**, 413–423.

Gardner, W. D., K. R. Hinga and J. Marra (1983) "Observation on the degradation of biogenic material in the deep ocean with implications on accuracy of sediment trap fluxes", *J. Mar. Res.*, **41**, 195–214.

Grasshoff, K. (1983) "Determination of nitrite", in K. Grasshoff, M. Ehrhardt and K. Kremling (eds) *Methods of Seawater Analysis*, 2. ed., Verlag Chemie, Weinheim, 139–142.

Honjo, S. (1980) "Material fluxes and modes of sedimentation in the mesopelagic and bathypelagic zones", *J. Mar. Res.*, **38**, 53–97.

Honjo, S. and K. W. Doherty (1988) "Large aperture time-series sediment traps: design objectives, construction and application", *Deep-Sea Res.*, **35**, 133–149.

Ittekkot, V., R. R. Nair, S. Honjo, V. Ramaswamy, M. Bartsch, S. J. Manganini and B. N. Desai (1991) "Enhanced particle fluxes in Bay of Bengal induced by injection of water", *Nature*, **351**, 385–387.

Kempe, S. (1975) "A computer program for hydrochemical problems in karstic water", Ann. de Spéléologie, **30**/4, 699–702.

Koroleff, F. (1983a) "Determination of phosphorus", in K. Grasshoff, M. Ehrhardt and K. Kremling (eds) *Methods of Seawater Analysis*, 2. ed., Verlag Chemie, Weinheim, 125–139.

Koroleff, F. (1983b) "Determination of ammonia", in K. Grasshoff, M. Ehrhardt and K. Kremling (eds) *Methods of Seawater Analysis*, 2. ed., Verlag Chemie, Weinheim, 150–157.

Koroleff, F. (1983c) "Determination of silicon", in K. Grasshoff, M. Ehrhardt and K. Kremling (eds) *Methods of Seawater Analysis*, 2. ed., Verlag Chemie, Weinheim, 174–187.

Kozhov, M. M. (1963) *Lake Baikal and its Life*, W. Junk, Publishers, Den Haag, 344 pp.

Liebezeit, G. (1992) "Water and porewater chemistry of Lake Baikal Central Basin Station" in E. T. Degens, S. Kempe, A. Lein and Y. Sorokin (eds) *Interactions of Biogeochemical Cycles in Aqueous Systems*, Mitt. Geol.-Paläont. Inst. Univ. Hamburg No. 72, 41–52

Logatchev, N. A. and Y. A. Zorin (1987) "Evidence and causes of two stage-development of the Baikal-Rift", *Tectonophysics*, **143**, 225–234.

Mortlock, R. A. and P. N. Froelich (1989) "A simple method for the rapid determination of biogenic opal in pelagic marine sediments", *Deep-Sea Res.*, **36**, 1415–1426.

Müller, P. J., E. Suess and C. A. Ungerer (1986) "Amino acids and amino sugars of surface particulate and sediment trap material from waters of the Scotia Sea", *Deep-Sea Res.*, **33**, 819–838.

National Geographic, (1981) *Atlas of the World*, Nat. Geogr. Soc., Washington, 383 pp.

Nikolaev, V. G., L. A. Vaniakin, V. V. Kalinin and V. Y. Milanovsky (1985) "The sedimentation section beneath Lake Baikal", *Int. Geol. Rev.*, **27**, 449–459.

Schaumburg, M. (1994) *Der vertikale Partikelfluß im Baikal See*, unpublished Diplom thesis, University of Hamburg, 78pp.

Scholz, C. A., K. D. Klitgord, D. R. Hutchinson, U. S. Ten Brink, L. P. Zonenshain, A. Y. Golmshtok and T. C. Moore (1993) "Results of 1992 seismic reflection experiment in Lake Baikal", *EOS*, 74(41), 465, 469–470.

Shanks, A. L. and J. D. Trent (1980) "Marine snow: Microscale nutrient patches", *Limnol. Oceanogr.*, **224**, 850–854.

Urrere, M. A. and G. A. Knauer (1981) "Zooplankton fecal pellet fluxes and vertical transport of particulate organic material in the pelagic environment", *J. Plankton Res.*, **3**, 369–387.

Votintsev, K. K. (1985) "Main features of the hydrochemistry of Lake Baikal water resource" engl. translat. *J. Vodnye Resurcy*, **12**, 106–116.

Wefer, G., E. Suess, W. Balzer, G. Liebezeit, P. J. Müller, C. A. Ungerer and W. Zenk (1982) "Fluxes of biogenic components from sediment trap deployment in circumpolar waters of the Drake Passage", *Nature*, **299**, 145–147.

Weiss, R. F., E. C. Carmack and V. M. Koropalov (1991) "Deep water renewal and biological production in Lake Baikal", *Nature*, **349**, 665–669.

Williams, J. D. H., J.-M. Jaquet and R. L. Thomas (1976) "Forms of phosphorus in surfical sediments of Lake Erie", *J. Fish. Res. Bd. Canada*, **33**, 413–429.

Wong, H. K., K. Anton, W. von Haugwitz, S. Kempe and W. Michaelis (1991) "Geologische Entwicklung und das rezente Sedimentationsregime im Baikalsee", Final Rep. Project MFG 0081/6 to the BMFT, unpublished, Hamburg, 192pp.

Zonenshain, L. P. and L. A. Savostin (1981) "Geodynamics of the Baikal Rift Zone (BRZ) and plate tectonics of Asia", *Tectonophysics*, **76**, 1–45.

18.8 APPENDIX

Table 18.A1 Data for cupwaters from the upper Lake Baikal trap (LB-T; 396 m depth).

Cup	pH	Cond. mS cm^{-1}	Loss* %	Si $\mu g\ l^{-1}$	P $\mu g\ l^{-1}$	NO_2 $\mu g\ l^{-1}$	NH_4 $mg\ l^{-1}$
T1	5.85	10.59	94.7	31.64	3.57	41.20	203
T2	5.95	3.76	98.2	9.97	3.43	8.12	184
T3	6.36	0.93	99.6	4.47	2.36	2.37	34.4
T4	6.27	2.79	98.7	21.59	2.17	9.44	125
T5	6.05	6.74	96.7	25.81	2.98	14.98	184
T6	6.25	3.78	98.2	14.37	2.23	8.52	162
T7	6.40	8.26	95.9	28.63	1.54	14.95	202
T8	6.45	3.43	98.3	18.18	2.96	11.00	161
T9	6.65	0.75	99.7	15.39	1.29	2.19	25
T10	6.94	1.74	99.2	20.68	2.85	5.21	124
T11	7.08	0.18	99.9	35.16	4.72	4.40	8.8
T12	7.31	0.35	99.9	0.26	3.33	4.43	122
T13	7.19	2.84	98.6	-	-	-	-
m	6.52	3.50	98.3	18.84	3.04	7.79	138

Table 18.A2 Data for cupwaters from the lower Lake Baikal trap (LB-B; 1582 m depth).

Cup	pH	Cond. mS cm^{-1}	Loss* %	Si $\mu g\ l^{-1}$	P $\mu g\ l^{-1}$	NO_2 $\mu g\ l^{-1}$	NH_4 $mg\ l^{-1}$
B1	7.97	1.36	99.4	67.7	0.41	0.006	0.63
B2	7.97	2.23	98.9	50.5	0.12	0.229	0.33
B3	7.15	1.53	99.3	51.0	0.16	0.131	4.18
B4	6.89	1.67	99.2	53.1	0.04	0.629	6.68
B5	7.04	0.74	99.7	55.5	0.04	0.160	14.13
B6	7.13	0.65	99.7	68.0	0.09	0.520	6.88
B7	7.33	1.48	99.3	49.8	0.32	0.142	5.17
B8	7.32	1.17	99.5	46.1	0.09	0.011	1.07
B9	6.87	2.03	99.0	66.5	0.06	-	0.05
B10	7.31	1.71	99.2	64.0	0.71	0.091	0.69
B11	7.17	1.85	99.1	68.5	0.08	0.252	0.45
B12	7.05	1.87	99.1	28.7	0.24	-	1.22
B13	8.04	0.125	100.0	-	-	-	-
m	7.33	1.42	99.3	55.77	0.19	0.363	3.13

Table 18.A3 Phosphorus and nitrogen fluxes and remineralization ratios for upper Lake Baikal trap (LB-T; 396 m depth).

Cup	P flux remin. mg m^{-2} d^{-1}	P flux part. mg m^{-2} d^{-1}	P rem. %	N flux NH_4+ NO_2 µmol m^{-2} d^{-1}	N flux part. µmol m^{-2} d^{-1}	N rem. %	N/P atomic ratio
T1	0.063	1.64	3.6	197.5	266.3	42.6	8.4
T2	0.062	0.64	8.8	185.9	228.0	44.9	18.3
T3	0.041	0.32	11.4	33.5	222.0	13.1	21.9
T4	0.038	1.22	3.0	126.0	184.2	40.6	7.6
T5	0.052	1.77	2.9	179.3	160.6	52.7	5.8
T6	0.041	1.27	3.1	163.4	31.1	84.0	4.6
T7	0.028	2.32	1.2	204.5	144.4	58.6	4.6
T8	0.054	1.44	3.6	163.2	173.2	48.5	7.0
T9	0.023	0.24	8.7	25.3	274.7	8.4	35.4
T10	0.052	0.72	6.7	125.3	154.0	44.9	11.2
T11	0.086	2.87	2.9	8.9	56.3	13.7	0.7
T12	0.061	0.30	16.9	123.0	110.3	52.7	10.0

Table 18.A4 Phosphorus and nitrogen fluxes and remineralization ratios for the lower Lake Baikal trap (LB-B; 1584 m depth).

Cup	P flux remin. mg m^{-2} d^{-1}	P flux part. mg m^{-2} d^{-1}	P rem. %	N flux NH_4+ NO_2 µmol m^{-2} d^{-1}	N flux part. µmol m^{-2} d^{-1}	N rem. %	N/P atomic ratio
B1	7.2	0.11	6.1	0.616	22.9	2.63	6.2
B2	2.2	0.11	2.0	0.423	25.2	1.65	7.1
B3	2.8	0.47	0.6	4.120	121.4	3.28	8.2
B4	0.7	0.51	0.14	6.748	142.1	4.53	9.0
B5	0.7	0.57	0.12	13.831	174.2	7.36	10.2
B6	1.6	0.55	0.29	7.155	138.4	4.92	8.2
B7	5.8	0.30	1.9	5.277	68.8	7.12	7.5
B8	1.6	0.19	0.84	1.085	44.4	2.38	7.4
B9	1.1	0.25	0.44	0.051	57.0	0.09	7.0
B10	12.9	0.34	3.6	0.733	71.8	1.01	6.4
B11	1.5	0.46	0.32	0.554	105.1	0.52	7.1
B12	4.4	0.38	1.14	1.233	83.7	1.45	6.9

Table 18.A5 Solid phase fluxes from the upper Lake Baikal trap (LB-T; 396 m depth).

Cup	Weight <1 mm mg	Total flux mg m^{-2} d^{-1}	Opal flux mg m^{-2} d^{-1}	Org. mat. flux mg m^{-2} d^{-1}	$CaCO_3$ flux mg m^{-2} d^{-1}	Lithogenics flux mg m^{-2} d^{-1}
T1	1104.5	77.5	0.58	79.90	7.68	-10.66
T2	263.5	19.17	1.39	17.35	1.76	-1.15
T3	78.3	5.49	5.38	4.22	0.83	-4.90
T4	364.4	25.57	4.34	13.66	3.01	4.70
T5	664.1	46.60	5.35	37.39	1.71	2.66
T6	356.3	25.93	17.07	21.97	3.00	-15.99
T7	766.0	55.74	4.08	46.48	5.62	-0.45
T8	469.9	34.19	2.27	30.50	1.65	-0.18
T9	57.5	4.19	1.01	2.42	0.23	0.55
T10	253.1	18.42	5.12	12.97	2.52	-1.02
T11	581.7	44.40	34.70	5.12	0.85	1.67
T12	296.8	21.60	14.90	6.67	0.68	-0.60

Table 18.A6 Solid phase fluxes from the lower Lake Baikal trap (LB-B; 1582 m depth).

Cup	Weight <1 mm mg	Total flux mg m^{-2} d^{-1}	Opal flux mg m^{-2} d^{-1}	Org. mat. flux mg m^{-2} d^{-1}	$CaCO_3$ flux mg m^{-2} d^{-1}	Lithogenics flux mg m^{-2} d^{-1}
B1	572.8	40.19	14.45	5.72	1.00	19.02
B2	486.8	35.44	11.67	5.50	2.57	15.64
B3	3072.5	215.58	67.00	30.27	1.79	116.51
B4	3389.6	237.83	89.86	32.88	2.78	112.34
B5	4081.5	286.84	106.87	37.50	18.62	123.86
B6	3242.3	235.90	91.36	33.97	1.57	109.00
B7	1509.3	109.80	40.12	16.47	1.65	51.58
B8	1077.3	78.39	27.80	11.57	1.76	37.25
B9	1301.0	94.67	31.34	13.89	0.63	48.76
B10	1835.5	133.60	51.22	19.30	2.45	60.55
B11	3081.6	222.20	96.17	26.43	0.93	100.70
B12	2612.0	190.05	100.67	22.52	2.70	63.96

Table 18.A7 Organic carbon and total nitrogen concentrations and ratios for the upper Lake Baikal trap (LB-T; 396 m depth).

Cup	C_{org} µmol m^{-2} d^{-1}	N_{part} µmol m^{-2} d^{-1}	C/N atomic ratio	N_{tot} µmol m^{-2} d^{-1}	C/N atomic ratio	C/N/P atomic ratio
T1	2661	266.3	10.0	463.8	5.7	48.1/8.4/1
T2	578	228.0	2.5	413.9	1.4	25.4/18.3/1
T3	141	222.0	0.6	255.5	0.6	12.1/21.9/1
T4	455	184.2	2.5	310.2	1.5	11.2/7.6/1
T5	1245	160.6	7.8	339.9	3.7	21.1/5.8/1
T6	732	31.1	23.5	194.5	3.8	17.3/4.6/1
T7	1548	144.4	10.7	348.9	4.4	20.5/4.6/1
T8	1016	173.2	5.9	336.4	3.0	21.1/7.0/1
T9	81	274.7	0.3	300.0	0.3	9.54/35.4/1
T10	432	154.0	2.8	279.3	1.6	17.4/11.2/1
T11	17	56.3	0.3	65.3	0.3	0.18/0.68/1
T12	222	110.3	2.0	233.3	1.0	19.0/20.0/1
						18.6/12.1/1

Table 18.A8 Organic carbon and total nitrogen concentrations and ratios for the lower Lake Baikal trap (LB-B; 1582 m depth).

Cup	C_{org} µmol m^{-2} d^{-1}	N_{part} µmol m^{-2} d^{-1}	C/N atomic ratio	N_{tot} µmol m^{-2} d^{-1}	C/N atomic ratio	C/N/P atomic ratio
B1	191	22.9	8.34	23.5	8.1	50.4/ 6.2/1
B2	183	25.2	7.29	25.6	7.2	50.7/ 7.1/1
B3	1008	121.4	8.31	125.5	8.0	66.0/ 8.2/1
B4	1095	142.1	7.71	148.8	7.4	66.2/ 9.0/1
B5	1249	174.2	7.17	188.0	6.6	67.7/10.2/1
B6	1131	138.4	8.18	145.5	7.8	63.6/ 8.2/1
B7	549	68.8	7.97	74.1	7.4	55.6/ 7.5/1
B8	385	44.4	8.68	45.5	8.5	62.3/ 7.4/1
B9	463	57.0	8.12	57.1	8.1	57.1/ 7.0/1
B10	643	71.8	8.95	72.5	8.9	56.4/ 6.4/1
B11	880	105.1	8.38	105.6	8.3	59.1/ 7.1/1
B12	750	83.7	8.97	84.9	8.8	60.6/ 6.9/1
						59.6/ 7.6/1

Table 18.A9 Free CO_2 in the Lake Baikal traps (LB-T: 392 m; LB-B: 1582 m depth).

Cup	PCO_2 ppmv	CO_2 µmol l^{-1}	CO_2 µmol/ m^{-2} d^{-1}	Cup	pCO_2 ppmv	CO_2 µmol l^{-1}	CO_2 µmol/ m^{-2} d^{-1}
T1	70000	4530	79.4	B1	526	34.3	0.60
T2	55600	3600	65.4	B2	526	34.3	0.62
T3	21600	1400	24.5	B3	3500	228.5	4.01
T4	26600	1720	30.2	B4	6370	416	7.29
T5	44200	2860	50.1	B5	4510	294	5.16
T6	27900	1800	32.8	B6	3660	239	4.35
T7	19700	1280	23.2	B7	2310	150	2.72
T8	17600	1140	20.7	B8	2360	154	2.80
T9	11100	717	13.0	B9	6670	436	7.93
T10	5680	368	6.7	B10	2418	150	2.72
T11	4120	266	4.8	B11	3340	218	3.97
T12	2420	156	2.8	B12	4400	288	5.24

ppmv: The pressure CO_2 exerts if the solution is exposed to air

CO_2 in µmol l^{-1}: the amount of free CO_2 in solution at the *in situ* temperatures of 3.5 and 3.2 °C in the upper and lower traps, respectively.

CO_2 flux = CO_2 µmol l^{-1} x 0.25 l / 0.509 m^2 / 28 (or 27) days

19 Particle Flux in the Ocean: Summary

V. ITTEKKOT

19.1 INTRODUCTION

The production of particles in the upper ocean and their removal to the deep sea determine the distribution of biogeochemical elements in seawater, fuel benthic life and is the source of sediments accumulating on the seafloor. The diagenetic alteration, decomposition and dissolution of particles during sinking control together with ocean circulation the distribution of oxygen, nutrients, CO_2 and many other trace constituents in seawater. Understanding the processes of particle formation in the upper ocean and of their transport and transformation throughout the water column is therefore crucial in determining the role of the oceans in global cycles of carbon and other associated elements.

The preceding chapters have addressed a wide range of issues related to the study of particle flux in the ocean including: (i) methods of marine particle flux studies, (ii) sources of marine particles and their variability, (iii) case studies of particle flux measurements using time-series sediment traps in different marine environments and (iv) the potential of long-term particle flux measurements to monitor global environmental and climatic changes. The focus is on settling particles in the ocean, their source, their mode of formation in the upper ocean and their transformation within the water column during sinking.

Direct measurements of fluxes of settling particles from the surface ocean to the deep sea and their spatial and temporal variability have become possible only with the advent of time-series sediment traps (Honjo, Chapter 7). Prior to this, studies on particles in the ocean were based on samples collected by conventional water samplers. This technique allowed the collection of suspended particles. Larger particles which constitute the bulk of particles settling to the seabottom often escaped sampling by these techniques. Sediment traps are specially designed instruments which can be moored at various depths in the sea and which allow the collection of settling particles at intervals of hours to years. Honjo (Chapter 7) gives an overview of the definitions, the units and the methods involved in the measurement of particle flux in the ocean and provides a global comparison of particle flux data based on information collected from a wide variety of environments during the last two decades.

Particle Flux in the Ocean
Edited by V. Ittekkot, P. Schäfer, S. Honjo and P. J. Depetris

19.2 PARTICLE SOURCES

The prime source of particles in the ocean is marine biological production. Particles are also introduced into the sea from the atmosphere and by the rivers. Dust inputs have been rarely measured directly due to problems associated with the measurements of dry deposition (Prospero, Chapter 3). Estimates based on aerosol data show dust inputs to be highly variable in space and time with most of the input occurring within very few precipitation events, as brief and infrequent pulses. They are a source of nutrients and essential elements (such as iron) to marine plankton. The atmospheric source is subject to anthropogenic perturbations.

Rivers introduce dissolved and particulate nutrients which stimulate biological particle production especially in coastal waters (Depetris, Chapter 4). The bulk of river-transported material is trapped in deltas and estuaries. A small fraction escapes to the ocean, especially in areas where rivers are connected to the deep sea by canyons. Episodic events such as floods enhance the transfer of river-derived material to deep basins. Small mountain streams are important in this connection. River inputs into the oceans are affected by human activities in the drainage basins such as deforestation which increases erosion and sediment transport, and the construction of dams and barrages which reduces sediment transport due to retention in reservoirs.

19.3 METHODS AND PROBLEMS

Asper (Chapter 5) and Honjo (Chapter 7) discuss the methods of investigation of particle flux in the ocean and the associated problems. The identified problems include: (i) hydrodynamic bias in the collection efficiency of sediment traps caused by the flow of water relative to the trap opening, (ii) artificial enhancement of particle collection by zooplankton which actively enter the trap and die (referred to as "swimmers") and, (iii) remineralization or degradation of the particles during the interval of time between their arrival in the trap and retrieval of the sample.

The potential of large hydrodynamic biases makes the collection of environmental data (e.g., ocean currents) extremely important during particle flux monitoring. Measurements of natural radionuclides in sediment-trap samples can provide useful limits on the degree of hydrodynamic bias during trap deployments (Bacon, Chapter 6). The degree of bias will be determined by the degree of agreement between the measured and the expected fluxes. Also here, the knowledge of the effects of horizontal transport and temporal variability of the balance between supply and removal of the reactive daughter nuclides is a prerequisite for data interpretation. The tracer results can be used to correct flux data where hydrodynamic bias occurs. Evidence based on ^{230}Th and ^{231}Pa suggests that properly designed sediment traps moored in quiescent conditions in the deep ocean (away

from boundary currents) can be considered accurate to within ± 25% or better whereas significant hydrodynamic biases may occur in traps deployed in the upper ocean. Further work is needed to delineate the conditions under which reliable results can be obtained.

The problem of swimmers is being dealt with in several ways. They include hand picking of the remains of the organisms out of the sample, the use of screens over trap mouth to prevent swimmers from entering the trap and the use of mechanical devices to exclude the swimmers.

The simplest way to prevent the decomposition of samples is the use of a preservative. The commonly used preservative is mercuric chloride, but others such as formalin and sodium azide have also been used depending on the type of the planned investigation. The analysis of the supernatant fluids associated with the sediment trap samples is useful to identify any decomposition that might have occurred and, to apply the necessary corrections to the measured particle fluxes.

The reliable interpretation of time-series data collected by sediment traps from the deep sea requires that simultaneous time-series information is available on atmospheric and upper ocean processes (Schlüssel, Chapter 2). This includes information on: (i) the flux of material from rivers, atmospheric dust inputs and marine biological production, and (ii) the physical parameters affecting the dynamics of the upper ocean such as wind, rainfall, sea surface temperature and the extent of sea ice. Observations from space provide extensive global collection of such information and represent probably the only source of synoptic information on large areas of the global atmosphere and ocean. The planned amendment and the replacement of the current operational satellites by orbiters carrying advanced and newly developed instruments will benefit research on particle flux in the ocean.

19.4 RESULTS FROM EXPERIMENTS

The results from the experiment in the Sargasso Sea were the first to show that the flux of material to the ocean's interior varies seasonally and in pulse with primary productivity in the surface layers (Deuser, Chapter 9). This seasonal pulse is discernible in each of the 16 years for which data are now available. An important aspect of the results are the observed periodicities of 2–6 months discerned from the data collected at biweekly sampling intervals.

In the temperate and subarctic North Atlantic more than half of the annual flux to the ocean's interior is related to plankton blooms in the surface layers (Honjo, Chapter 7). The propagation of the blooms from south to north was recorded in the delay in peak fluxes measured by traps moored at various locations.

The pattern of fluxes to the deep sea at two sites located close to each other in the eastern equatorial Atlantic (Fischer and Wefer, Chapter 10) was consistent

with the high spatial and temporal variability of the study area with respect to surface water properties, the extent of the upwelling area and atmospheric circulation (e.g., Inter Tropical Convergence Zone movements).

Few changes have been found in total particle flux to the deep equatorial Pacific Ocean over a year. However, biogenic silica and C_{org} fluxes showed an upwelling-related variability (Honjo, Chapter 7). Further results from the Pacific come from the Philippine and Caroline Basins in the region of the North Equatorial Current (NEC) and the Equatorial Counter Current (ECC), respectively (Kempe and Knaack, Chapter 17). Observations at both sites recorded low fluxes consistent with the prevailing nutrient regime in the area. A slight variability in fluxes was observed which was related to changes in the direction of water mass movements.

In regions of the western and eastern North Pacific such as the Gulf of Alaska, Bering Sea and in the Sea of Okhotsk, particle flux patterns were characterized by a succession of events (Honjo, Chapter 7) with high fluxes of biogenic silica with diatom frustules in spring and culminating with a $CaCO_3$ flux peak in autumn.

The relationship between upper ocean processes induced by the Asian monsoon and the particle flux to the deep sea is described by Haake et al. (Chapter 14) based on a record from three locations across the Arabian Sea in the northern Indian Ocean. All locations exhibited a bimodal flux pattern with peaks during the SW and NE monsoons. The temporal variability of particle flux to the deep sea during the monsoons reflected the changes in the upper ocean plankton community structure brought about by changes in the nutrient regime: high $CaCO_3$ fluxes related to coccolithophorid blooms were followed by high biogenic silica fluxes from diatom blooms.

Schäfer et al. (Chapter 15) report on the pattern of particle flux in the Bay of Bengal, a marine region which comes under the influence of some of the largest rivers of the world with their high fresh water and sediment inputs. While the total flux is largely determined by the amount of lithogenic material, its nature is determined by the seasonal changes in the upper ocean plankton community structure. So for example, the biogenic fluxes are characterized by low carbonate/opal ratios and, as a result, high organic carbon/carbonate-carbon ratios (C_{org}/$C_{Carbonate}$) during periods of high fresh water discharge. At locations away from the influence of rivers, wind-driven biological processes determine the nature and quantity of fluxes. Such river-induced effects are common for even a low sediment discharge river such as the São Francisco River, which influenced the production and sedimentation of organic matter along the Brazilian coastal margin (Jennerjahn et al., Chapter 11).

In the South China Sea the particle flux pattern was closely related to the monsoonal wind-regime and the associated oceanographic processes (Wiesner et al., Chapter 16). Spectacularly high fluxes were recorded in this area from the introduction of volcanic dust (9012 g m^{-2}) from the 1991 eruption of the Mount Pinatubo (Philippines). The high fluxes were recorded simultaneously in mid and deep water within less than 3 days after the release of the major eruption plume. Fur-

thermore, dissolved silicate released from volcanic ash affected the upper ocean plankton community structure in the following year, when biogenic silica was a major component of the flux of material to the deep sea.

Particle flux appears to be controlled not only by primary productivity in the surface ocean and the inputs from external sources but also by the primary producer-grazer relationship (Bathmann, Chapter 13). Evidence for this comes from the exceptionally low vertical flux, particularly in winter, in the central, seasonally ice covered Weddell Sea. This low flux is not related to a corresponding decrease in productivity but to intense grazing by an active population of zooplankton which thrive on the algae flushed from the ice during brine discharge. On the other hand, mass sedimentation resulting from blooms of phytoplankton was encountered in open ocean waters along the Polar Frontal zone in the absence of grazers (krill, calanoid copepods and salps).

Along continental margins, the general circulation of water masses, seasonal changes of continental inputs and marine productivity control the pattern of particle flux (Etcheber et al., Chapter 12). The results from the Atlantic and the Mediterranean show that particle fluxes decrease in an offshore direction. They increase with depth where particle injection into the ocean's interior from shelf and slope environments occurs. In the Mediterranean, fluxes are minimal in summer and maximal in winter. Seasonal variability is less pronounced along the Atlantic margin. An enrichment of C_{org} is also observed in these margins. The biogeochemical characteristics of this material are determined by inputs from marine and continental sources as well as by changes in the rates of decomposition.

Kempe and Schaumburg (Chapter 18) present data on particle flux within the largest and deepest fresh water body on earth, the Lake Baikal. The pattern of particle flux is bimodal with peaks in winter and summer. Resuspended sediments and biogenic material produced in the surface layer are the major particle sources.

19.5 ENVIRONMENTAL SIGNALS

Not all the material leaving the oceanic surface waters reaches the deep sea. Significant losses or decomposition have been found to occur in the biogenic components (Honjo, Chapter 7). The quantification of these losses, taking into account both the dissolved and particulate constituents, is just beginning to be attempted. In certain areas of the oceans such as the Atlantic only 30% silica, and about 1–3% organic matter, with regard to the initial amount leaving the surface reaches a water depth of 2000 m. Where increases have been found in the fluxes of lithogenic material with depth lateral transports are indicated.

Despite these losses or degradation, signals of processes in the surface layers of the sea can be recognized without much delay in settling particles sampled in the deep sea. This is recorded not just in the total and component fluxes but also in

the detailed chemical nature, and planktonic and stable isotopic composition of the settling material. Of special interest is the stable carbon and nitrogen isotopic composition (Curry et al., 1992; Altabet, Chapter 8). For example, seasonal variations have been observed in the stable nitrogen isotopic composition of settling particles in various oceanic environments, which are related to the nutrient situation in the surface layers. In certain marine regions such as the Arabian Sea, signals of denitrification are recorded in the nitrogen isotopic composition (Schäfer and Ittekkot, 1993). These signals are also preserved in bottom sediments, where they have been used to infer past changes in marine denitrification processes (Altabet et al., 1995).

19.6 PARTICLE FLUX AND CARBON STORAGE IN THE DEEP SEA

The rapid transfer of material to the deep sea from the surface layers occurs because most of the flux is in large aggregates with high settling rates. They include fecal pellets ejected by filter-feeding zooplankton and particle aggregates held together by organic matter ("marine snow") released from plankton. Fecal pellets and marine snow have high sinking rates (400 to > 1000 m d^{-1}) and can transit a 3 km water column in about a week (e.g., Alldredge and Silver, 1988; Honjo, Chapter 7). Both are susceptible to bacterial attack and decomposition in the water column, which will depend on how long the aggregates remain suspended there. Fecal pellets and macroaggregates are found to contain both biogenic and significant amounts of lithogenic material, including riverine and aeolian particles. The incorporation of mineral particles such as clays into large aggregates increase their settling rates (Fowler and Knauer, 1986) and, as a consequence, effect the rapid transfer of both minerals and the freshly produced organic matter to the deep ocean (Ittekkot et al., 1992). This organic-mineral interaction is of relevance to the removal of atmospheric CO_2 and its storage in the deep sea (Figure 19.1).

Time-series sediment trap experiments with seasonal resolution have shown that the material arriving at the sea floor during periods of high fluxes is enriched in labile organic matter (Haake et al., Chapter 14). During high abiogenic fluxes in the Arabian Sea, the intermediate layers are characterized by seasonal changes in C_{org} as well as in labile organic constituents such as amino acids (their abundances as well as their spectral distributions), which indicate a reduced degradation (Haake et al., 1992). Consequently, the deep ocean receives relatively higher quantities of fresh, labile material, which has the potential to be degraded at the sediment-water interface.

Information on the degradation of organic matter in the deep sea may be obtained in part by comparing the fluxes of C_{org} measured in deep-moored traps with accumulation rates in the underlying sediments. The C_{org} content of settling

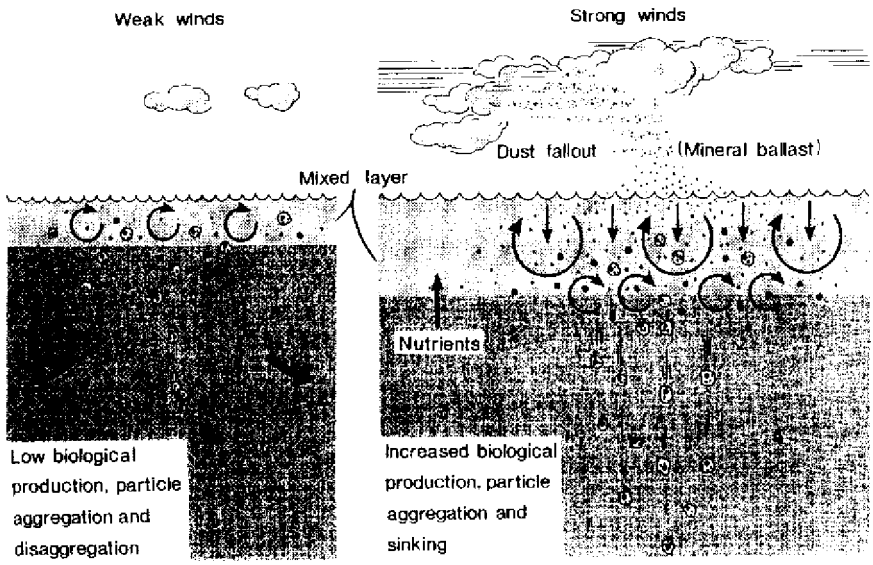

Figure 19.1 Schematic of processes that control organic matter production and removal to the deep sea. Dust particles deposited at the sea surface not only introduce essential trace nutrients such as iron (stimulating primary productivity), but also become incorporated into organic aggregates that form high-density particles (the ballast effect) with faster sinking rates - thus accelerating the transfer of newly fixed carbon dioxide to the deep sea. The efficiency of this transfer determines the storage of carbon in the deep sea (after Ittekkot, 1993).

material intercepted at water depths of 2000 to 3000 m is consistently higher than that of the underlying surface sediments by at least a factor of 5 (Sirocko and Ittekkot, 1992) suggesting significant losses of C_{org} between deep-moored traps and sediments. These losses appear to be proportional to total material flux to the ocean's interior. The ultimate effect is that with increasing fluxes there is an increase in the amount of organic matter being remineralized in the deeper parts of the oceans. In other words, the storage of carbon in the deep sea via remineralization of organic matter and the particle fluxes are coupled processes, whereby an increase in deep-sea fluxes leads to increased carbon storage and consequently to a decrease in atmospheric CO_2-content.

19.7 GENERAL CONCLUSIONS

Sediment traps are the best presently available tools for studying particle fluxes linking processes at the sea surface with transport to the seafloor. They can collect

samples continuously on hourly to yearly schedules. Fluxes measured during long-term experiments have recorded the signatures of all upper ocean conditions and processes. Potential problems to be addressed in association with sediment trapping are hydrodynamic bias, sample distortion by swimmers and decomposition. Use of natural tracers appears to be promising in resolving this issue.

The biogeochemical processes in the deep sea are coupled to atmospheric processes via particle flux in the ocean, the link being variations in the primary productivity in the upper ocean which exhibits strong spatial and temporal variability. To resolve the associated variability in the fluxes of biogeochemical elements to the oceans' interior, simultaneous long-term monitoring of the atmosphere and the surface ocean by satellite remote sensing, and of the deep sea by time-series devices such as sediment traps will be necessary.

The comprehensive elucidation of the factors controlling particle fluxes in the ocean further requires that investigations of oceanic processes be complemented with long-term data sets from the atmosphere and from the terrestrial environment. The latter exerts a strong influence on particle flux in the ocean both directly by providing particles and indirectly by stimulating marine biological processes. Investigations of dust fallout over the oceans, suspended matter and nutrient inputs from rivers and from continental margins have to be incorporated into programs designed to understand processes controlling particle flux in the oceans. The nature and magnitude of these inputs have been changing due to human activities. Also, they are likely to be affected by the projected regional and global climate changes.

The efficiency of the biological pump (organic carbon pump) in the ocean in sequestering atmospheric CO_2 is determined by the production and "rain ratio" of $C_{org}/C_{Carbonate}$. This, in turn, is determined by the production ratio of diatoms to coccolithophorids in the upper ocean. Increased diatom production tends to increase the ratios, and thus the efficiency of the biological pump. It is therefore important to understand the factors controlling the shifts in the upper ocean biological community structure and the variabilty of the component fluxes to the deep sea. Time-series measurements of particle flux in the ocean suggest that such shifts are related to the availability of silicate, the major limiting element for diatoms in the upper ocean. A better understanding of the interaction of the silica cycle with the cycles of other nutrient elements such nitrogen and phosphorus in the ocean will be crucial to assess the efficiency of the oceanic biological pump to sequester atmospheric CO_2.

Marine regions of interest for future research in this context are areas affected by nutrient inputs from upwelling water masses, continental margins, rivers and ice-melt. They receive an adequate supply not just of dissolved phosphate and nitrate but also of silicate. These are also regions which are likely to be affected by potential changes in ocean circulation, in precipitation and runoff, and in cryosphere components expected from a projected change in climate.

Particles settling to the seafloor carry environmental and climatic information to the deep sea. This information is likely to be modified and in some instances lost due to dissolution, decomposition and transformation reactions which occur during settling and/or at the sediment-water interface. The degree of preservation of these signals in sediments has to be investigated in order to assess their paleoceanographic use.

Particle flux in the ocean responds to climatic and environmental forcing. Therefore, oceanic particle flux studies have the potential to detect, monitor and help in reconstructing, global changes.

19.8 REFERENCES

Alldredge, A. L. and M. W. Silver (1988) "Characteristics, dynamics and significance of marine snow", *Prog. Oceanogr.*, **20**, 41–82.

Altabet, M. A. (1996) "Nitrogen and carbon isotopic tracers of the source and transformation of particles in the deep sea", in V. Ittekkot, P. Schäfer, S. Honjo and P. J. Depetris (eds) *Particle Flux in the Ocean*, SCOPE Report 57, John Wiley & Sons, Chichester, 155–184.

Altabet, M. A., R. Francois, D. W. Murray and W. L. Prell (1995) "Climate-related variations in denitrification in the Arabian Sea from sediment $^{15}N/^{14}N$ ratios", *Nature*, **373**, 506–509.

Asper, V. L. (1996) "Particle flux in the ocean: Oceanographic tools", in V. Ittekkot, P. Schäfer, S. Honjo and P. J. Depetris (eds) *Particle Flux in the Ocean*, SCOPE Report 57, John Wiley & Sons, Chichester, 71–84.

Bacon, M. P. (1996) "Evaluation of sediment traps with naturally occurring radionuclides", in V. Ittekkot, P. Schäfer, S. Honjo and P. J. Depetris (eds) *Particle Flux in the Ocean*, SCOPE Report 57, John Wiley & Sons, Chichester, 85–90.

Bathmann, U. (1996) "Abiotic and biotic forcing on vertical particle flux in the Southern Ocean", in V. Ittekkot, P. Schäfer, S. Honjo and P. J. Depetris (eds) *Particle Flux in the Ocean*, SCOPE Report 57, John Wiley & Sons, Chichester, 243–250.

Curry, W. B., D. R. Ostermann, M. V. S. Guptha and V. Ittekkot (1992) "Foraminiferal production and monsoonal upwelling in the Arabian Sea: Evidence from sediment traps", in C. P. Summerhayes, W. L. Prell and K. C. Emeis (eds) *Upwelling Systems: Evolution Since the Early Miocene*, Geological Society Special Publication No. 64, 93–106.

Depetris, P. J. (1996) "Riverine transfer of particulate matter to ocean systems", in V. Ittekkot, P. Schäfer, S. Honjo and P. J. Depetris (eds) *Particle Flux in the Ocean*, SCOPE Report 57, John Wiley & Sons, Chichester, 53–69.

Deuser, W. G. (1996) "Temporal variability of particle flux in the deep Sargasso Sea", in V. Ittekkot, P. Schäfer, S. Honjo and P. J. Depetris (eds) *Particle Flux in the Ocean*, SCOPE Report 57, John Wiley & Sons, Chichester, 185–198.

Etcheber, H., S. Heussner, O. Weber, A. Dinet, X. Durrieu de Madron, A. Monaco, R. Buscail and J. C. Miquel (1996) "Organic carbon fluxes and sediment biogeochemistry on the French Mediterranean and Atlantic margins", in V. Ittekkot, P. Schäfer, S. Honjo and P. J. Depetris (eds) *Particle Flux in the Ocean*, SCOPE Report 57, John Wiley & Sons, Chichester, 223–241.

Fischer, G. and G. Wefer (1996) "Seasonal and interannual particle fluxes in the eastern equatorial Atlantic from 1989 to 1991: ITCZ migrations and upwelling", in V. Ittekkot,

P. Schäfer, S. Honjo and P. J. Depetris (eds) *Particle Flux in the Ocean*, SCOPE Report 57, John Wiley & Sons, Chichester, 199–214.

Fowler, S. W. and Knauer, G. A. (1986) "Role of large particles in the Transport of elements and organic compounds through the oceanic water column. *Progr. Oceanogr.*, **16**, 147–194.

Haake, B., V. Ittekkot, V. Ramaswamy, R. R. Nair and S. Honjo (1992) "Fluxes of amino acids and hexosamines to the deep Arabian Sea", *Mar. Chem.*, **40**, 291–314.

Haake, B., T. Rixen, T. Reemtsma, V. Ramaswamy and V. Ittekkot (1996) "Processes determining seasonality and interannual variability of settling particle fluxes to the deep Arabian Sea", in V. Ittekkot, P. Schäfer, S. Honjo and P. J. Depetris (eds) *Particle Flux in the Ocean*, SCOPE Report 57, John Wiley & Sons, Chichester, 251–270.

Honjo, S. (1996) "Fluxes of particles to the interior of the open oceans", in V. Ittekkot, P. Schäfer, S. Honjo and P. J. Depetris (eds) *Particle Flux in the Ocean*, SCOPE Report 57, John Wiley & Sons, Chichester, 91–154.

Ittekkot, V. (1993) "The abiotically driven biological pump in the ocean and short-term fluctuations in atmospheric CO_2 contents", *Glob. Planet. Change*, **8**, 17–25.

Ittekkot, V., B. Haake, M. Bartsch, R. R. Nair and V. Ramaswamy (1992) "Organic carbon removal in the sea: The continental connection", in C. P. Summerhayes, W. L. Prell and K. C. Emeis (eds) *Upwelling Systems: Evolution Since the Early Miocene*, Geological Society Special Publication No. 64, 167–176.

Jennerjahn, T. C., V. Ittekkot and C. E. V. Carvalho (1996) "Preliminary data on particle flux off the São Francisco River, Eastern Brazil", in V. Ittekkot, P. Schäfer, S. Honjo and P. J. Depetris (eds) *Particle Flux in the Ocean*, SCOPE Report 57, John Wiley & Sons, Chichester, 215–222.

Kempe S. and H. Knaack (1996) "Vertical particle flux in the western Pacific below the North Equatorial Current and the Equatorial Counter Current", in V. Ittekkot, P. Schäfer, S. Honjo and P. J. Depetris (eds) *Particle Flux in the Ocean*, SCOPE Report 57, John Wiley & Sons, Chichester, 313–323.

Kempe S. and M. Schaumburg (1996) "Vertical particle flux in Lake Baikal", in V. Ittekkot, P. Schäfer, S. Honjo and P. J. Depetris (eds) *Particle Flux in the Ocean*, SCOPE Report 57, John Wiley & Sons, Chichester, 325–355.

Prospero, J. M. (1996) "The atmospheric transport of particles to the ocean", in V. Ittekkot, P. Schäfer, S. Honjo and P. J. Depetris (eds) *Particle Flux in the Ocean*, SCOPE Report 57, John Wiley & Sons, Chichester, 19–52.

Schäfer, P. and V. Ittekkot (1993) "Seasonal variability of $\delta^{15}N$ in settling particles in the Arabian Sea and its palaeogeochemical significance", *Naturwissenschaften*, **80**, 511–513.

Schäfer, P., V. Ittekkot, M. Bartsch, R. R. Nair and J. Tiemann (1996) "Fresh water influx and particle flux variability in the Bay of Bengal", in V. Ittekkot, P. Schäfer, S. Honjo and P. J. Depetris (eds) *Particle Flux in the Ocean*, SCOPE Report 57, John Wiley & Sons, Chichester, 271–292.

Schlüssel, P. (1996) "Remote sensing of parameters relevant to the particle flux in the ocean using meteorological satellites", in V. Ittekkot, P. Schäfer, S. Honjo and P. J. Depetris (eds) *Particle Flux in the Ocean*, SCOPE Report 57, John Wiley & Sons, Chichester, 7–17.

Sirocko, F. and V. Ittekkot (1992) "Organic carbon accumulation rates in the Holocene and glacial Arabian Sea: Implications for O_2-consumption in the deep-sea and atmospheric CO_2-variations", *Clim. Dynamics*, 7, 167–172.

Wiesner, M. G., L. Zheng, H. K. Wong, Y. Wang and W. Chen (1996) "Fluxes of particulate matter in the South China Sea", in V. Ittekkot, P. Schäfer, S. Honjo and P. J. Depetris (eds) *Particle Flux in the Ocean*, SCOPE Report 57, John Wiley & Sons, Chichester, 293–312.

Index

SCOPE 36: Acidification in Tropical Countries, 1988, 424 pp
SCOPE 37: Biological Invasions: A Global Perspective, 1989, 528 pp
SCOPE 38: Ecotoxicology and Climate with Special Reference to Hot and Cold Climates, 1989, 432 pp
SCOPE 39: Evolution of the Global Biogeochemical Sulphur Cycle, 1989, 224 pp
SCOPE 40: Methods for Assessing and Reducing Injury from Chemical Accidents, SGOMSEC 6, 1989, 320 pp
SCOPE 41: Short-Term Toxicity Tests for Non-Genotoxic Effects, SGOMSEC 4, 1990, 353 pp
SCOPE 42: Biogeochemistry of Major Worlds Rivers, 1991, 356 pp
SCOPE 43: Stable Isotopes: Natural and Anthropogenic Sulphur in the Environment, 1991, 472 pp
SCOPE 44: Introduction of Genetically Modified Organisms into the Environment, 1990, 224 pp
SCOPE 45: Ecosystem Experiments, 1991, 296 pp
SCOPE 46: Methods for Assessing Exposure of Human and Non-Human Biota, SGOMSEC 5, 1991, 448 pp
SCOPE 47: Long-term Ecological Research. An International Perspective, 1991, 312 pp
SCOPE 48: Sulphur Cycling on the Continents: Wetlands, Terrestrial Ecosystems and Associated Water Bodies, 1992, 345 pp
SCOPE 49: Methods to Assess Adverse Effects of Pesticides on Non-Target Organisms, SGOMSEC 7, 1992, 264 pp
SCOPE 50: Radioecology After Chernobyl, 1993, 367 pp
SCOPE 51: Biogeochemistry of Small Catchments: A Tool for Environmental Research, 1993, 432 pp
SCOPE 52: Methods to Assess DNA Damage and Repair: Interspecies Comparisons, SGOMSEC 8, 1994, 257 pp
SCOPE 53: Methods to Assess the Effects of Chemicals on Ecosystems, SGOMSEC 10, 1995, 440pp
SCOPE 54: Phosphorus in the Global Environment: Transfers, Cycles and Management, 1995, 480pp
SCOPE 55: Functional Roles of Biodiversity: A Global Perspective, 1996, 496pp
SCOPE 56: Global Change: Effects on Coniferous Forests and Grasslands, 1996, 480pp
SCOPE 57: Particle Flux in the Ocean, 1996, 396pp

Funds to meet SCOPE expenses are provided by contributions from SCOPE Committees, an annual subvention from ICSU (and through ICSU, from UNESCO), an annual subvention from the French Ministère de l'Environnement, contracts with UN Bodies, particularly UNEP, and grants from Foundations and industrial enterprises.

SCOPE 57

PARTICLE FLUX IN THE OCEAN

Edited by
V. Ittekkot
Universität Hamburg, Germany

P. Schäfer
Universität Hamburg, Germany

S. Honjo
Woods Hole Oceanographic Institution, USA

P. J. Depetris
Universidad Nacional de Cordoba, Argentina

Particle flux in the ocean is coupled to biogeochemical processes in the upper ocean which are driven by the prevailing meteorological and oceanographic regimes. Planktonic organisms and their metabolic waste products are the key link between upper ocean and deep sea. They effectively package marine biogenic particles and particles introduced at the sea surface from rivers and atmospheric fallout onto large high density aggregates. These aggregates, because of their higher sinking speeds, are rapidly transported to the sea-bottom. This process effects the transfer of carbon dioxide fixed at the sea surface during photosynthesis to the deep sea and facilitates its storage there. This volume contains review articles as well as case studies on aspects of particle flux in the ocean contributed by scientists who are actively involved in particle flux research. They describe the tools that are available today for the simultaneous and continuous monitoring of atmospheric and surface ocean processes and ocean particle fluxes, the major sources and pathways of particles to the ocean, the general trends in ocean particle dynamics and variability as well as the environmental and climate signals embedded in settling particles in the ocean and their paleooceanographic utility.

The cover photograph shows RIV Sonne *and is reproduced courtesy of Jörg Tiemann.*

ICSU

UNEP

ISBN 0-471-96073-X

9 780471 960737

JOHN WILEY & SONS
Chichester · New York · Brisbane · Toronto · Singapore